Stereoselective ring-opening polymerization of functional β-lactones : access to original polyhydroxyalkanoates

Hui Li

▶ **To cite this version:**

Hui Li. Stereoselective ring-opening polymerization of functional β-lactones : access to original polyhydroxyalkanoates. Polymers. Université de Rennes; Université de Rennes 1, 2022. English. NNT : 2022REN1S077 . tel-04812759

HAL Id: tel-04812759

https://theses.hal.science/tel-04812759v1

Submitted on 1 Dec 2024

HAL is a multi-disciplinary open access archive for the deposit and dissemination of scientific research documents, whether they are published or not. The documents may come from teaching and research institutions in France or abroad, or from public or private research centers.

L'archive ouverte pluridisciplinaire **HAL**, est destinée au dépôt et à la diffusion de documents scientifiques de niveau recherche, publiés ou non, émanant des établissements d'enseignement et de recherche français ou étrangers, des laboratoires publics ou privés.

UNIVERSITÉ DE RENNES 1

THESE DE DOCTORAT DE

L'UNIVERSITE DE RENNES 1

ECOLE DOCTORALE N° 596
Matière, Molécules, Matériaux
Spécialité: Chimie Moléculaire et Macromoléculaire

Par
Hui LI

Stereoselective Ring-Opening Polymerization of Functional β-Lactones: Access to Original Polyhydroxyalkanoates

Thèse présentée et soutenue à Rennes, le 30 novembre, 2022
Unité de recherche: Institut des Sciences Chimiques de Rennes − UMR CNRS 6226

Rapporteurs avant soutenance:

Mathias Destarac	Professeur, IMPCR, Université Toulouse III - Paul Sabatier
Philippe Zinck	Professeur, Université de Lille

Composition du Jury:

Président:	Mathias Destarac	Professeur, IMPCR, Université Toulouse III - Paul Sabatier
Examinateur:	Philippe Zinck	Professeur, Université de Lille
Directeur de thèse:	Jean-François Carpentier	Professeur, Université de Rennes 1
Directrice de thèse:	Sophie M. Guillaume	Directrice de Recherche CNRS, Université de Rennes 1

Membre Invitée:

Françoise Le Guen	Professeur, Université de Rennes 1

UNIVERSITÉ DE RENNES 1

Titre: Polymérisation Stéréosélective par Ouverture de Cycle de β-Lactones Fonctionnelles: Accès à des Polyhydroxyalcanoates Originaux

Mots clés: Polythioesters; Polymérisation par ouverture de cycle; Catalyse stéréosélective; Yttrium; β-(Thio)lactone

Résumé: Les polymères synthétiques conventionnels sont omniprésents dans la société moderne en raison de leurs nombreuses caractéristiques avantageuses: légèreté, coût relativement faible, durabilité et diverses propriétés thermomécaniques. Il est largement reconnu que l'utilisation de polymères d'origine fossile est à l'origine de problèmes environnementaux majeurs d'origine anthropique, tels que la pollution plastique et le changement climatique. Une alternative intéressante aux plastiques classiques (polyoléfines) issus de ressources fossiles est l'utilisation de plastiques (bio)dégradables, notamment ceux issus de ressources naturelles renouvelables. Parmi ces polymères (bio)dégradables, les poly(β-hydroxyalcanoate)s (PHAs), qui peuvent être préparés chimiquement par polymérisation par ouverture de cycle (ROP) des β-lactones correspondantes, présentent un intérêt tout particulier. Cependant, l'inconvénient intrinsèque des PHAs, à savoir leur manque de diversité fonctionnelle, limite leur gamme d'application. Les modifications des PHAs au niveau de leurs groupements pendants et de leur squelette, permettent d'accéder à des polymères présentant des propriétés physico-chimiques différentes et ajustables, offrant ainsi diverses stratégies pour élargir leur champ d'applications.

Dans la première partie bibliographique de ce manuscrit, la préparation de poly(thio)esters stéréoréguliers par ROP des monomères correspondants, telle que rapportée dans la litérature, est résumée de manière approfondie et systématique. Par la suite, sur la base des travaux précédents réalisés dans le groupe et pour mieux comprendre les facteurs qui contrôlent la stéréosélectivité, nous avons conçu une nouvelle β-lactone fonctionnelle racémique, à savoir la 4-(2-(benzyloxy)éthyl)oxétan-2-one qui diffère "simplement" de la 4-benzyloxyméthyl-β-propiolactone racémique monomère étudiée précédemment par le remplacement dans le groupe latéral (exocyclique) de l'entité méthylènyle par un éthylènyle, afin d'évaluer la ROP stéréosélective médiée par l'utilisation de complexes d'yttrium. Les meilleures activités catalytiques ont été atteintes en utilisant les complexes d'yttrium avec les substituants "encombrés" installés sur le ligand bisphénolate (par ex, *t*Bu, CMe_2Ph), donnant des polymères syndiotactiques enrichis (P_r jusqu'à 0,86), tandis que les complexes d'yttrium incorporant un ligand halogéné "non encombré", tel que Cl, ont conduit à des polymères atactiques, suggérant que les "interactions non covalentes" n'étaient pas en jeu pendant la polymérisation, contrairement à ce qui a été observé dans nos études précédentes.

De plus, l'introduction d'atomes de soufre dans le squelette du plus simple des PHAs, le poly(3-hydroxybutyrate) (P3HB), a également été étudiée au travers de la ROP de la β-thiobutyrolactone racémique (rac-TBL) avec une variété d'amorceurs/catalyseurs de type anionique. Parmi ceux-ci, les complexes tétradentés de type amino-alkoxy-bis(phénolate) d'yttrium ont donné les résultats les plus prometteurs en termes d'activité et de contrôle de la microstructure macromoléculaire, notamment en termes de stéréosélectivité. Il s'agit du premier exemple d'une ROP hautement stéréosélective d'une thiolactone chirale racémique offrant sélectivement des polymères (poly(3-thiobutyrate, P3TB) cycliques, soit hautement isotactiques, soit hautement syndiotactiques. Enfin, des résultats préliminaires sur des essais de copolymérisation par ouverture de cycle entre le rac-TBL et la rac-β-butyrolactone catalysée par des complexes d'yttrium et sur la ROP de rac-TBL initiée par des organocatalyseurs de type phosphazène sont également documentés.

Title: Stereoselective Ring-Opening Polymerization of Functional β-Lactones: Access to Original Polyhydroxyalkanoates

Keywords: Polythioesters; Ring-opening polymerization; Stereoselective catalysis; Yttrium; β-(Thio)lactone

Abstract: Conventional synthetic polymers are ubiquitous in modern society due to their many valuable characteristics such as light weight, relatively low cost, durability, and diverse thermomechanical properties. It is widely recognized that the use of fossil-based polymers is leading to major anthropogenic environmental issues, such as plastics pollution and global climate change. An attractive alternative to fossil resources-based plastics (typically polyolefins…) is the use of (bio)degradable plastics, especially those derived from natural, renewable resources. Among those (bio)degradable polymers, poly(β-hydroxyalkanoate)s (PHAs) which can be chemically prepared by ring-opening polymerization (ROP) of the corresponding β-lactones, are of particular interest. However, the intrinsic drawback of PHAs, that is the lack of functional diversity, limits their range of applications. The modifications of PHAs in terms of pendent group and the backbone, enables to access to diverse PHAs and to polymers with different and tunable physicochemical properties, thereby becoming powerful strategies to widen the scope of their applications.

At the outset of this manuscript, the preparation of stereoregular poly(thio)esters by ROP of the corresponding cyclic monomers, as described in the literature, is in-depth described. Subsequently, on the basis of previous works conducted in our group and to gain further insights into the factors that control the stereoselectivity in the ROP of chiral racemic β-lactones, we designed another such monomer, namely 4-(2-(benzyloxy)ethyl)oxetan-2-one, which "simply" differs from the former studied racemic 4-benzyloxymethyl-β-propiolactone by replacement in the pendant (exocyclic) group of methylenyl by an ethylenyl moiety. This new monomer was subjected to stereoselective ROP mediated by discrete yttrium complexes. The best catalytic activities were reached using the yttrium complexes with the "crowded" substituents installed on the bisphenolate ligand (e.g., *t*Bu, CMe_2Ph), giving syndiotactic-enriched polymers (P_r up to 0.86), while the yttrium complexes incorporating halogenated "uncrowded" ligand, such as Cl, led to atactic polymers, suggesting "non-covalent interactions" were not at play during polymerization in contrast to what was observed in our previous studies.

Additionally, the introduction of sulfur atoms into the backbone of the simplest asymmetric PHAs, poly(3-hydroxybutyrate) (P3HB), by ROP of the corresponding racemic β-thiobutyrolactone (rac-TBL) promoted by a variety of anionic-type initiators/catalysts was also demonstrated in this PhD work, Among the variety of catalysts investigated, tetradentate bis(phenolate) yttrium complexes gave the most promising results in terms of activity, control over the polymerization and especially in terms of stereoselectivity. This is the first report of a highly stereoselective ROP of a racemic chiral thiolactone to afford either highly isotactic or highly syndiotactic *cyclic* poly(3-thiobutyrate) (P3TB). Lastly, preliminary results on attempts to ring-opening copolymerize rac-TBL and rac-β-butyrolactone catalyzed by yttrium complexes and on the ROP of rac-TBL initiated by phosphazene-type organocatalysts are also documented.

Stereoselective Ring-Opening Polymerization of Functional β-Lactones: Access to Original Polyhydroxyalkanoates

Hui LI

A thesis submitted for the degree of Doctor of Philosophy

Institut des Sciences Chimiques de Rennes − UMR CNRS 6226

Université de Rennes 1

September 2022

Table of Contents

Acknowledgments

First, I would like to thank my supervisors Prof. Jean-François Carpentier and Dr. Sophie M. Guillaume for this excellent opportunity to join the group. I consider myself extremely lucky that they allowed me the flexibility to undertake my Ph.D. project. Jean-François always encouraged me to insist when my work was not going smoothly. I am impressed by the meticulous and rigorous scholarship from Sophie. Thank you very much for your guidance and for being supportive of my research work.

I would also like to thank the members of the jury, Prof. Philippe Zinck, Prof. Mathias Destarac, and Prof. Françoise Le Guen for accepting to review for my work and examine the progress I have made over the past several years.

I am thankful to those behind this work, especially Philippe Jehan for mass spectrometry, Jérôme Ollivier for DCS, TGA and mass spectrometry analyses, Dr. Elsa Caytan for NMR analyses, Dr. Evgueni Kirillov for his advice of my work, and Marielle Blot for chiral HPLC analyses. Without their help, my chemistry could not have arrived here.

Valérie, Joanna, and Dimitra, I am truly lucky that we are in the same lab. All of you are kind and always willing to help me without hesitation, and I appreciate that.

I would like to express my gratitude from my heart to all the other members of the JFC group. I have been so lucky enough to share the unforgettable time with these wonderful people: Orlando, Peter, Kana, Rama, Abdallah, Thierry, Raghu, Yann, Liye, Wei-Heng, Vishal, Vyshakh, Xavier, Albert, Sary, Miguel, Ekaterina, Ali, Julien, and so on.

Thank you to all my fellow Chinese who were in Rennes. We had many beautiful moments together in France: Zhuan, Bing, Meng-Da, Yue, Min, Linhao, Liwei, Jiajun, Jian, and so on.

Special gratitude to Prof. Pierre H. Dixneuf, who knows my former supervisors well in China, makes me feel at home in Rennes.

Finally, thank you to all my family members: my grandfather, my parents, my sister, my brother-in-law, and my niece. If they had not supported me to train on the other side of the world, I would not have been in France, such a peaceful and lovely country. I am grateful for all the sacrifices you all have made for me and the encouragement throughout my studies.

I am grateful to the financial support provided by the China Scholarship Council.

Words are powerless to express my gratitude to all of you!

Abstract

Conventional synthetic polymers are ubiquitous in modern society due to their many valuable characteristics such as light weight, relatively low cost, durability, and diverse thermomechanical properties. It is widely recognized that the use of fossil-based polymers is leading to major anthropogenic environmental issues, such as plastics pollution and global climate change. An attractive alternative to fossil resources-based plastics (typically polyolefins…) is the use of (bio)degradable plastics, especially those derived from natural, renewable resources. Among those (bio)degradable polymers, poly(β-hydroxyalkanoate)s (PHAs) which can be chemically prepared by ring-opening polymerization (ROP) of the corresponding β-lactones, are of particular interest. However, the intrinsic drawback of PHAs, that is the lack of functional diversity limits their range of applications. The modifications of PHAs in terms of pendent group and the backbone, enables to access to diverse PHAs and to polymers with different and tunable physicochemical properties, thereby becoming powerful strategies to widen the scope of their applications.

At the outset of this manuscript, the preparation of stereoregular poly(thio)esters by ROP of the corresponding cyclic monomers, as described in the literature, is in-depth described. Subsequently, on the basis of previous works conducted in our group and to gain further insights into the factors that control the stereoselectivity in the ROP of chiral racemic β-lactones, we designed another such monomer, namely 4-(2-(benzyloxy)ethyl)oxetan-2-one, which 'simply' differs from the former studied racemic 4-benzyloxymethyl-β-propiolactone by replacement in the pendant (exocyclic) group of methylenyl by an ethylenyl moiety. This new monomer was subjected to stereoselective ROP mediated by discrete yttrium complexes. The best catalytic activities were reached using the yttrium complexes with the 'crowded' substituents installed on the bisphenolate ligand (*e.g.*, *t*Bu, CMe_2Ph), giving syndiotactic-enriched polymers (P_r up to 0.86), while the yttrium complexes incorporating halogenated "uncrowded" ligand, such as Cl, led to atactic polymers, suggesting 'non-covalent interactions' were not at play during polymerization in contrast to what was observed in our previous studies.

Additionally, the introduction of sulfur atoms into the backbone of the simplest asymmetric PHAs, poly(3-hydroxybutyrate) (P3HB), by ROP of the corresponding racemic β-thiobutyrolactone (*rac*-TBL) promoted by a variety of anionic-type initiators/catalysts was also demonstrated in this PhD work, Among the variety of catalysts investigated, tetradentate bis(phenolate) yttrium complexes gave the most promising results in terms of activity, control over the polymerization and especially in terms of stereoselectivity. This is the first report of a highly stereoselective ROP of a racemic chiral thiolactone to afford either highly isotactic or highly syndiotactic *cyclic* poly(3-thiobutyrate) (P3TB). Lastly, preliminary results on attempts to ring-opening copolymerize *rac*-TBL and *rac*-β-butyrolactone catalyzed by yttrium complexes and on the ROP of *rac*-TBL initiated by phosphazene-type organocatalysts are also documented.

Key words: Polythioesters; Ring-opening polymerization; Stereoselective catalysis; Yttrium; β-(Thio)lactone

Résumé

Les polymères synthétiques conventionnels sont omniprésents dans la société moderne en raison de leurs nombreuses caractéristiques avantageuses: légèreté, coût relativement faible, durabilité et diverses propriétés thermomécaniques. Il est largement reconnu que l'utilisation de polymères d'origine fossile est à l'origine de problèmes environnementaux majeurs d'origine anthropique, tels que la pollution plastique et le changement climatique. Une alternative intéressante aux plastiques classiques (polyoléfines) issus de ressources fossiles est l'utilisation de plastiques (bio)dégradables, notamment ceux issus de ressources naturelles renouvelables. Parmi ces polymères (bio)dégradables, les poly(β-hydroxyalcanoate)s (PHAs), qui peuvent être préparés chimiquement par polymérisation par ouverture de cycle (ROP) des β-lactones correspondantes, présentent un intérêt tout particulier. Cependant, l'inconvénient intrinsèque des PHAs, à savoir leur manque de diversités fonctionnelle, limite leur gamme d'application. Les modifications des PHAs au niveau de leurs groupements pendants et de leur squelette, permettent d'accéder à des polymères présentant des propriétés physico-chimiques différentes et ajustables, offrant ainsi diverses stratégies pour élargir leur champ d'applications.

Dans la première partie bibliographique de ce manuscrit, la préparation de poly(thio)esters stéréoréguliers par ROP des monomères correspondants, telle que rapportée dans la littérature, est résumée de manière approfondie et systématique. Par la suite, sur la base des travaux précédents réalisés dans le groupe et pour mieux comprendre les facteurs qui contrôlent la stéréosélectivité, nous avons conçu une nouvelle β-lactone fonctionnelle racémique, à savoir la 4-(2-(benzyloxy)éthyl)oxétan-2-one qui diffère "simplement" de la 4-benzyloxyméthyl-β-propiolactone racémique monomère étudiée précédemment par le remplacement dans le groupe latéral (exocyclique) de l'entité méthylènyle par un éthylènyle, afin d'évaluer la ROP stéréosélective médiée par l'utilisation de complexes d'yttrium. Les meilleures activités catalytiques ont été atteintes en utilisant les complexes d'yttrium avec les substituants "encombrés" installés sur le ligand bisphénolate (par ex, *t*Bu, CMe_2Ph), donnant des polymères syndiotactiques enrichis (P_r jusqu'à 0,86), tandis que les complexes d'yttrium incorporant un ligand halogéné "non encombré", tel que Cl, ont conduit à des polymères atactiques, suggérant que les "interactions non covalentes" n'étaient pas en jeu pendant la polymérisation, contrairement à ce qui a été observé dans nos études précédentes.

De plus, l'introduction d'atomes de soufre dans le squelette du plus simple des PHAs, le poly(3-hydroxybutyrate) (P3HB), a également été étudiée au travers de la ROP de la β-thiobutyrolactone racémique (*rac*-TBL) avec une variété d'amorceurs/catalyseurs de type anionique. Parmi ceux-ci, les complexes tétradentés de type amino-alkoxy-bis(phénolate) d'yttrium ont donné les résultats les plus prometteurs en termes d'activité et de contrôle de la microstructure macromoléculaire, notamment en termes de stéréosélectivité. Il s'agit du premier exemple d'une ROP hautement stéréosélective d'une thiolactone chirale racémique offrant sélectivement des polymères (poly(3-thiobutyrate, P3TB)

cycliques, soit hautement isotactiques, soit hautement syndiotactiques. Enfin, des résultats préliminaires sur des essais de copolymérisation par ouverture de cycle entre le *rac*-TBL et la *rac*-β-butyrolactone catalysée par des complexes d'yttrium et sur la ROP de *rac*-TBL initiée par des organocatalyseurs de type phosphazène sont également documentés.

Mots clés: Polythioesters; Polymérisation par ouverture de cycle; Catalyse stéréosélective; Yttrium; β-(Thio)lactone.

Abbreviations

BDI	β-Diketiminate
CO	Carbon monoxide
cumyl	α,α-dimethylbenzyl
CEC	Chain-end control
CL	Caprolactone
$Đ_M$	Dispersity
DL	Diolide
DCM	Dichloromethane
DSC	Differential scanning calorimetry
DFT	Density-functional theory
DBU	1,8-Diazabicyclo(5.4.0)undec-7-ene
DME	1,2-Dimethoxyethane
ESI	Electrospray ionization
equiv.	Equivalent
HPLC	High-performance liquid chromatography
*i*PrO	Isopropyl
LA	Lactide
M_n	Number-average molar mass
M_w	Weight-average molar mass
MALDI-ToF	Matrix-assisted laser desorption ionization time-of-flight
MS	Mass spectrometry
Me	Methyl
NMR	Nuclear magnetic resonance
PHA	Poly(hydroxyalkanoate)
P3HB	Poly(3-hydroxybutyrate)
P3TB	Poly(3-thiobutyrate)
PTE	Polythioester
PLA	Polylactide
PCL	Polycaprolactone
P_r	Probability of forming a *racemic* dyad
P_m	Probability of forming a *meso* dyad
pK_a	Acid dissociation constant (log)
Ph	Phenyl
rac	*racemic*

BL	β-Butyrolactone
BPL^{OR}	4-Alkoxymethylene-β-propiolactone
MLA^{R}	Malolactonates
TBL	β-Thiobutyrolactone
r.t.	Room temperature
ROP	Ring-opening polymerization
ROCOP	Ring-opening copolymerization
SEC	Size-exclusion chromatography
T_m	Melting temperature
T_g	Glass transition temperature
T_d	Degradation temperature
TOF	Turnover frequency
*t*Bu	*tert*-Butyl
THF	Tetrahydrofuran
TGA	Thermogravimetric analysis
Tol	Toluene

Research Background and Objective

Fossil-based plastics, such as polyolefins, and poly(ethylene terephthalate) (PET), have been integral to the many impactful societal advancements of the 20th century, which have greatly improved the quality of human life due to their characteristics of light weight, relatively low cost, durability, and diverse properties. However, the phenomenal durability of commodity plastics has led to their widespread use, which produces millions of metric tons of plastic waste every year and subsequently accumulates in the environment. In fact, plastic debris in marine environments are now widely recognized as an enormous environmental problem, which will weigh as much as fish by 2050 if plastic handling and waste management are not improved.[1-3] Three major conventional approaches exist to deal with plastic waste: landfill, incineration, and recycling. Alarmingly, as of 2019, it was estimated that of all post-consumer waste plastics that has been generated, only around 9% had been successfully recycled, and 69% remained in landfills or in the environment. However, landfill always suffers from non-degradability or from extremely slow degradation rate of most polymer wastes.[4] An attractive alternative to petroleum-based plastics is the use of (bio)degradable plastics, which may aid in reducing dependence on and in the use of non-renewable fossil fuels for plastic production.

(Bio)degradable polymers containing chemically weak covalent bonds in the main chain, such as esters, acetals, and carbonate groups, can be triggered to degrade by different degradation pathways, *e.g.*, hydrolytic, enzymatic, or redox. Various kinds of (bio)degradable polymers have been extensively investigated, which have been mainly focused on natural and synthetic polymers. Natural polymers, are available from renewable sources, and include polysaccharides, proteins, peptides, starch, *etc.* However, some disadvantages associated with natural polymers include a great level of variability depending on their sources, complex structures, and complicated and costly extraction processes. In comparison, synthetic degradable polymers can be tailored at the molecular level to modulate the properties of the resulting materials. Therefore, polymer chemists are particularly interested in the development of chemically synthesized (bio)degradable polymer materials, especially from natural (biomass) resources.[5-7]

According to the latest market data compiled by European Bioplastics, bioplastics, produced from renewable biomass sources, accounted for less than one percent of the more than 367 million tonnes of plastic produced annually. Among those bio-based plastics, poly(butylene-adipate-*co*-terephthalate) (PBAT) and polylactide (PLA), have the highest market share. PBAT, a random copolymer prepared by polycondensation of butanediol (BDO), adipic acid (AA) and terephthalic acid (PTA), is the highest consumption volume of bioplastic (Chart 1), which is a fully (bio)degradable alternative to low-density polyethylene.[8] Yet, the removal of small-molecule by-product, such as water, from the reactions necessitates the use of high temperatures (usually > 190 ℃) and/or under vacuum conditions, making

this approach very energy-intensive. Additionally, their relatively lower mechanical properties compared with conventional plastics have limited their use in a broader range of applications.

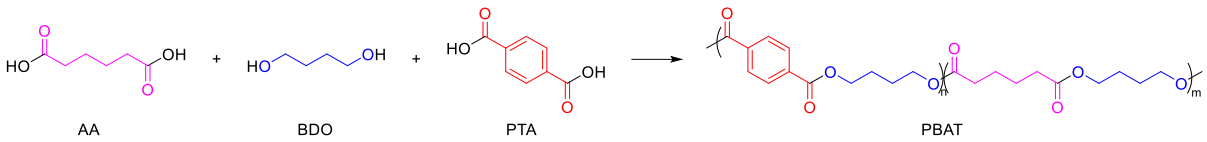

Chart 1. The synthetic procedure towards poly(butylene-adipate-*co*-terephthalate).[8]

PLA, usually prepared by the ring-opening polymerization (ROP) of lactide (Chart 2), is a biomass and (bio)degradable polyester.[9,10] It is considered as one of the most commercially promising bioplastics, due to its good mechanical properties, processability, renewability, and non-toxicity, which can find applications in disposable packaging products, such as food packaging, and medical devices. However, PLA can only degrade in industrial composting systems (usually at a high temperature, around 58 °C) and anaerobic digestion. If products made from these plastics are discarded into conventional waste streams such as landfill, or find their way into the open environment, such as rivers and oceans, potential environmental benefits will not be realized and this may worsen, rather than reduce, the problem of plastic pollution.

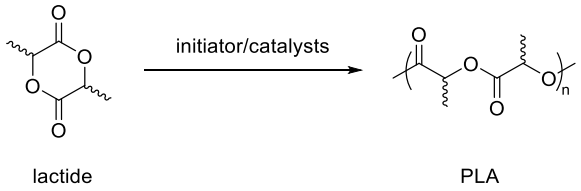

Chart 2. The common synthetic pathway towards polylactide (PLA) by ring-opening polymerization of lactide.[11]

Poly(hydroxyalkanoate)s (PHAs), an important family of (bio)degradable polymer family which are expected to witness impressive growth in the next few years, are able to (bio)degrade in ambient environments, even in the ocean. These materials combine the film-barrier properties of polyesters with the mechanical performances of petroleum-based polyethylene and polypropylene. PHAs differ one from another by the side chain at the β-position of the repeating units along the backbone.

Among the large variety of PHAs, poly(3-hydroxybutyrate) (P3HB) stands out. When prepared by fermentation of naturally occurring biomass-derived sugars (*e.g.*, sucrose, glucose) with microorganisms, it is a purely (*R*)-isotactic, highly crystalline thermoplastic.[12,13] However, the melting temperature (T_m = 180 °C) of the perfectly isotactic P3HB is very close to its decomposition temperature (T_d = 180−200 °C), which leads to thermal degradation by ester pyrolysis during melt processing, thereby making the final products difficult to process. Alternatively, P3HB can be prepared chemically by the ROP of racemic β-butyrolactone (*rac*-BL) or diolide (*rac*-DL), where the relief of ring-strain is the driving force for polymerization.[14,15] Highly isotactic (*R*)- or (*S*)-P3HB can be obtained when

optically pure (*R*)- or (*S*)-BL is involved, while the use of a racemic mixture of BL can give rise to either atactic, isotactic or syndiotactic materials,† depending on the nature of the catalyst used.[16] Distinct types of metal catalysts, such as yttrium, zinc, lanthanides, magnesium, indium, aluminum, bearing different supporting ligands have been employed for the ROP of *rac*-BL to obtain P3HBs with a good control over molar mass and dispersity. Among them, rare earth complexes of the type of 'Ln{ONXO^{R1,R2}}(Nu)(L)$_n$' (Nu = nucleophilic moiety initiating the ring opening = alkyl, amide, alkoxide; L = donor or solvent molecules such as THF; n = 0, 1), most especially yttrium ones, constitute a 'privileged class' of initiators/catalysts for the ROP of *rac*-BL and of its higher and functional derivatives (Chart 3), as they afford high activity and special stereocontrol abilities.[17] Our group reported that yttrium catalysts stabilized by tetradentate amino alkoxy- or diamino-bis(phenolate) ligands {ONXO^{R1,R2}}$^{2-}$ (X = O, N) provide access to highly syndiotactic P3HB with a probability for *racemic* enchainment (P_r) up to 0.96 by a chain-end control mechanism, provided that bulky aryl-containing R^1 substituents are installed at the *ortho* positions of the phenolate platform.[18]

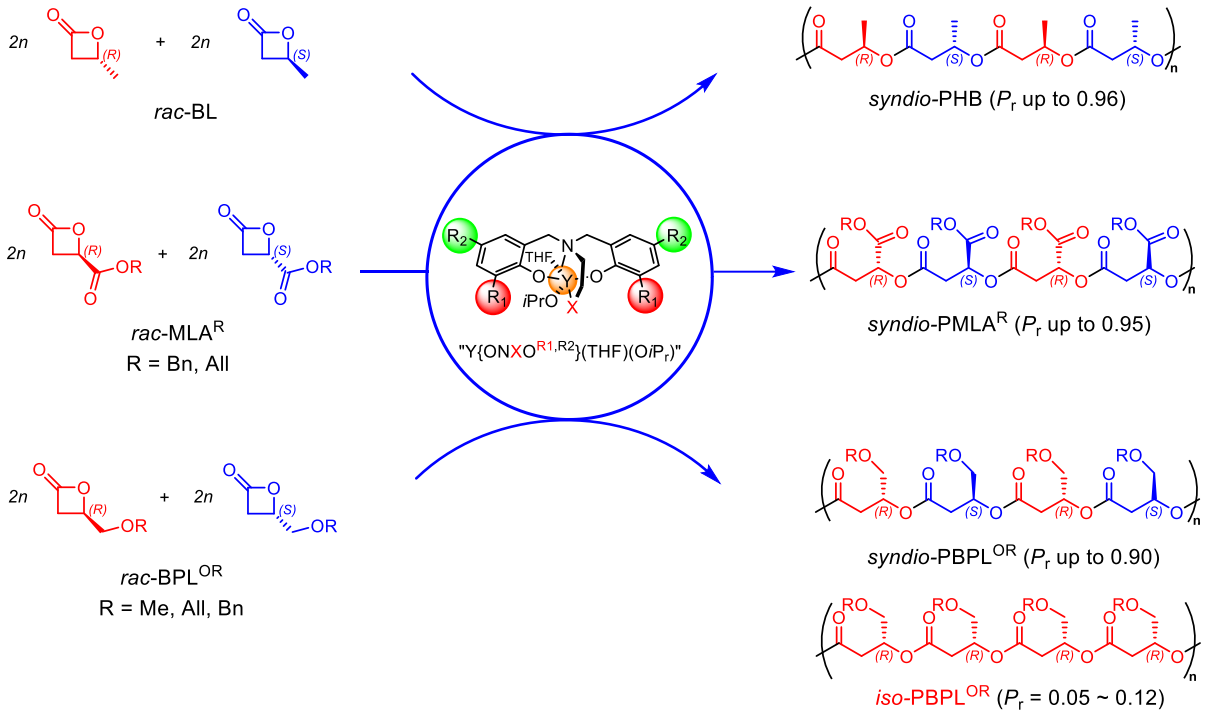

Chart 3. Chemical preparation of simple and functional poly(3-hydroxyalkanoate)s (PHAs) as syndiotactic or isotactic (as 1:1 mixture of enantiomeric chains) polyesters by ROP of racemic β-lactones with yttrium-based catalysts.[19-21]

Introduction of a pendant functional group along the polyester chains enables to access to chemically reactive PHAs and to polymers with different and tunable physicochemical properties, thereby widening their range of applications.[22,23] The above-mentioned stereoselective yttrium-based

† Several parameters have been reported to influence the mechanical properties of P3HB; the most important factors are the molar mass and dispersity, the crystallinity and, perhaps more decisively, the microstructure of the polymer.

ROP catalysis was then extended to racemic functional or higher β-lactones, in particular to racemic β-malolactonates (*rac*-4-alkoxycarbonyl-β-propiolactones, *rac*-MLA^{R}; R = allyl, benzyl), which are of high interest because of the readily tunable/transformable pendant carboxylate moieties (Chart 3).[24,25] Surprisingly enough, for this class of β-lactones, only yttrium catalysts with an uncrowded *ortho*-substituted {ONXO^{R1,R2}}$^{2-}$ ligand, *e.g.*, R^{1} = Me or Cl, allowed for highly syndiotactic polymerizations (P_r > 0.95). Catalysts with sterically crowded R^{1} alkyl/aryl *ortho*-substituents on the {ONXO^{R1,R2}}$^{2-}$ ancillary afforded only modest syndioselectivity.

Driven by our interest to expand on this chemistry and to address the preparation of functional PHAs, such stereoselective ROP by yttrium complexes was extended to *rac*-4-alkoxymethylene-β-propiolactones (*rac*-BPL^{OR}s; R = methyl, allyl, benzyl) (Chart 3).[24,26] Interestingly, the simple modification of the *ortho* R^{1} substituents on the {ONXO^{R1,R2}}$^{2-}$ platform of the yttrium catalyst induced a complete switch from syndioselective to isoselective polymerization of this specific class of *rac*-BPL^{OR}s: an yttrium complex bearing an *o,p*-dihalogen (F, Cl, Br)-substituted ligand generated highly isotactic polyesters (probability for *meso* enchainment, $P_m = 1 - P_r$ up to 0.95), while complexes with bulky *tert*-butyl and cumyl (CMe_2Ph) -substituted R^{1} ligands gave syndio-enriched PBPL^{OR}s (P_r = 0.90). DFT computations performed for the first elementary steps of the ROP of *rac*-BPL^{OR} suggested that the origin of the isoselectivity could be traced back to attractive C–H···X 'non-covalent interactions' between hydrogen from the alkoxymethylene group in the last ring-opened monomer unit in the growing chain and the *ortho*-halogen substituents of the ligand platform.

The (bio)degradability of PHAs has attracted increasing attention, yet the functionality of PHAs limits their range of applications. In this regard, the modification of PHAs in terms of pendent group is a strategy to modify their performance. *Chapter 1* thus summaries the eminent advances that have been made in the field of the preparation of aliphatic polythioesters, the sulfur analogues of aliphatic polyesters, and of the stereoregular polyesters, by ROP of the corresponding monomer mediated by well-defined metal-based complexes, especially yttrium ones, and also promoted by organic molecules.

Based on our previous work and to gain further insights into the factors that control the stereoselectivity, we designed in *Chapter 2*, another racemic functional β-lactone namely 4-(2-(benzyloxy)ethyl)oxetan-2-one (*rac*-BPL^{CH2CH2OBn}), to assess the stereoselective ROP mediated by using yttrium complexes. The *rac*-BPL^{CH2CH2OBn} 'simply' differs from *rac*-BPL^{OBn} by replacement in the pendant (exocyclic) group of methylene (−**CH$_2$**OBn) by an ethylene moiety (−**CH$_2$CH$_2$**OBn), which shall enable us to assess the influence of the arm length and possible implication of the other −CH_2− from the pendant group (−CH_2**<u>CH$_2$</u>**OBn) on the catalytic ROP process.

Additionally, the modification of backbone of P3HB can endow polymers with differentiated, sometimes enhanced properties, such as improved thermal, mechanical and optical properties, thereby further widening the application scope of PHAs.[27-29] Hence, polythioesters (PTEs), that is polyester counterparts with thioester linkages ((C=O)- S) within the backbone, are of great interest due to their biocompatibility and degradability properties, which have been drawing increasing attention in the past

half-decade. However, the ROP of racemic β-thiobutyrolactone (*rac*-TBL) towards poly(3-thiobutyrate) (P3TB), the thioester analogue of the ubiquitous P3HB, was never documented. *Chapter 3* then investigates the chemical synthesis of P3TB via ROP of the corresponding *rac*-TBL with anionic-type initiators/catalysts. In addition, preliminary attempts in ring-opening copolymerization (ROCOP) of *rac*-TBL and *rac*-BL mediated by yttrium catalyst are also described.

Apart from metal-based catalyzed ROP, catalysis mediated by organic molecules has been more recently revealed as another appealing approach for ROP, especially as a metal-free approach, within the context of polyesters designed for electronics and biomedical applications.[30,31] Polymerization based on simple organic molecules is thus currently of topical interest for their high chemical stability, long shelf life, low cost, easy availability, and ease of handling. In this context, preliminary attempts in the ROP of *rac*-TBL promoted by phosphazene-based initiators/catalysts are documented in *Chapter 4*.

Finally, at the end of this manuscript, the conclusion is drawn from the progress of this project, and some perspectives are also mentioned.

References

[1] C. Jehanno, J. W. Alty, M. Roosen, S. De Meester, A. P. Dove, E. Y. Chen, F. A. Leibfarth, H. Sardon, Critical Advances and Future Opportunities in Upcycling Commodity Polymers. *Nature* **2022**, *603*, 803-814.

[2] J. M. Garcia, M. L. Robertson, The Future of Plastics Recycling. *Science* **2017**, *358*, 870-872.

[3] R. Geyer, J. R. Jambeck, K. L. Law, Production, Use, and Fate of All Plastics ever Made. *Sci. Adv.* **2017**, *3*, e1700782.

[4] M. Hong, E. Y. X. Chen, Chemically Recyclable Polymers: A Circular Economy Approach to Sustainability. *Green Chem.* **2017**, *19*, 3692-3706.

[5] O. Santoro, L. Izzo, F. Della Monica, Recent Advances in RO(CO)P of Bio-Based Monomers. *Sustain. Chem.* **2022**, *3*, 259-285.

[6] Q. Zhang, M. Song, Y. Xu, W. Wang, Z. Wang, L. Zhang, Bio-Based Polyesters: Recent Progress and Future Prospects. *Prog. Polym. Sci.* **2021**, *120*, 101430.

[7] C. Vilela, A. F. Sousa, A. C. Fonseca, A. C. Serra, J. F. J. Coelho, C. S. R. Freire, A. J. D. Silvestre, The Quest for Sustainable Polyesters – Insights into the Future. *Polym. Chem.* **2014**, *5*, 3119-3141.

[8] J. Jian, Z. Xiangbin, H. Xianbo, An Overview on Synthesis, Properties and Applications of Poly(butylene-adipate-co-terephthalate)–PBAT. *Advanced Industrial and Engineering Polymer Research* **2020**, *3*, 19-26.

[9] M. J. Tschan, R. M. Gauvin, C. M. Thomas, Controlling Polymer Stereochemistry in Ring-Opening Polymerization: a Decade of Advances Shaping the Future of Biodegradable Polyesters. *Chem. Soc. Rev.* **2021**, *50*, 13587-13608.

[10] M. J. Stanford, A. P. Dove, Stereocontrolled Ring-Opening Polymerisation of Lactide. *Chem. Soc. Rev.* **2010**, *39*, 486-494.

[11] O. Dechy-Cabaret, B. Martin-Vaca, D. Bourissou, Controlled Ring-Opening Polymerization of Lactide and Glycolide. *Chem. Rev.* **2004**, *104*, 6147-6176.

[12] A. Z. Naser, I. Deiab, B. M. Darras, Poly(lactic acid) (PLA) and Polyhydroxyalkanoates (PHAs), Green Alternatives to Petroleum-Based Plastics: A Review. *RSC Adv.* **2021**, *11*, 17151-17196.

[13] A. T. Adeleye, C. K. Odoh, O. C. Enudi, O. O. Banjoko, O. O. Osiboye, E. Toluwalope Odediran, H. Louis, Sustainable Synthesis and Applications of Polyhydroxyalkanoates (PHAs) from Biomass. *Process Biochem.* **2020**, *96*, 174-193.

[14] X. Tang, E. Y.-X. Chen, Chemical Synthesis of Perfectly Isotactic and High Melting Bacterial Poly(3-hydroxybutyrate) from Bio-sourced Racemic Cyclic Diolide. *Nat. Commun.* **2018**, *9*, 2345.

[15] L. R. Rieth, D. R. Moore, E. B. Lobkovsky, G. W. Coates, Single-Site β-Diiminate Zinc Catalysts for the Ring-Opening Polymerization of β-Butyrolactone and β-Valerolactone to Poly(3-hydroxyalkanoates). *J. Am. Chem. Soc.* **2002**, *124*, 15239-15248.

[16] C. G. Jaffredo, J. F. Carpentier, S. M. Guillaume, Controlled ROP of β-Butyrolactone Simply Mediated by Amidine, Guanidine, and Phosphazene Organocatalysts. *Macromol. Rapid Commun.* **2012**, *33*, 1938-1944.

[17] J.-F. Carpentier, Rare-Earth Complexes Supported by Tripodal Tetradentate Bis(phenolate) Ligands: A Privileged Class of Catalysts for Ring-Opening Polymerization of Cyclic Esters. *Organometallics* **2015**, *34*, 4175-4189.

[18] A. Amgoune, C. M. Thomas, S. Ilinca, T. Roisnel, J.-F. Carpentier, Highly Active, Productive, and Syndiospecific Yttrium Initiators for the Polymerization of Racemic β-Butyrolactone. *Angew. Chem. Int. Ed.* **2006**, *45*, 2782-2784.

[19] H. Li, R. M. Shakaroun, S. M. Guillaume, J.-F. Carpentier, Recent Advances in Metal-Mediated Stereoselective Ring-Opening Polymerization of Functional Cyclic Esters towards Well-Defined Poly(hydroxy acid)s: From Stereoselectivity to Sequence-Control. *Chem. Eur. J.* **2020**, *26*, 128-138.

[20] R. Ligny, M. M. Hanninen, S. M. Guillaume, J.-F. Carpentier, Steric *vs.* Electronic Stereocontrol in Syndio- or Iso-selective ROP of Functional Chiral β-Lactones Mediated by Achiral Yttrium-Bisphenolate Complexes. *Chem. Commun.* **2018**, *54*, 8024-8031.

[21] J. S. Klitzke, T. Roisnel, E. Kirillov, O. d. L. Casagrande, J.-F. Carpentier, Yttrium– and Aluminum–Bis(phenolate)pyridine Complexes: Catalysts and Model Compounds of the Intermediates for the Stereoselective Ring-Opening Polymerization of Racemic Lactide and β-Butyrolactone. *Organometallics* **2013**, *33*, 309-321.

[22] R. M. Shakaroun, H. Li, P. Jéhan, M. Blot, A. Alaaeddine, J.-F. Carpentier, S. M. Guillaume, Stereoselective Ring-Opening Polymerization of Functional β-Lactones: Influence of the Exocyclic Side-Group. *Polym. Chem.* **2021**, *12*, 4022-4034.

[23] C. G. Jaffredo, S. M. Guillaume, Benzyl β-Malolactonate Polymers: A Long Story with Recent Advances. *Polym. Chem.* **2014**, *5*, 4168-4194.

[24] R. Ligny, M. M. Hanninen, S. M. Guillaume, J.-F. Carpentier, Highly Syndiotactic or Isotactic Polyhydroxyalkanoates by Ligand-Controlled Yttrium-Catalyzed Stereoselective Ring-Opening Polymerization of Functional Racemic β-Lactones. *Angew. Chem. Int. Ed.* **2017**, *56*, 10388-10393.

[25] C. G. Jaffredo, Y. Chapurina, E. Kirillov, J.-F. Carpentier, S. M. Guillaume, Highly Stereocontrolled Ring-Opening Polymerization of Racemic Alkyl β-Malolactonates Mediated by Yttrium [Amino-alkoxy-bis(phenolate)] Complexes. *Chem. Eur. J.* **2016**, *22*, 7629-7641.

[26] R. Ligny, S. M. Guillaume, J.-F. Carpentier, Yttrium-Mediated Ring-Opening Copolymerization of Oppositely Configurated 4-Alkoxymethylene-β-Propiolactones: Effective Access to Highly Alternated Isotactic Functional PHAs. *Chem. Eur. J.* **2019**, *25*, 6412-6424.

[27] H. Li, S. M. Guillaume, J. F. Carpentier, Polythioesters Prepared by Ring-Opening Polymerization of Cyclic Thioesters and Related Monomers. *Chem. Asian J.* **2022**, *17*, e202200641.

[28] T.-J. Yue, L.-Y. Wang, W.-M. Ren, The Synthesis of Degradable Sulfur-Containing Polymers: Precise Control of Structure and Stereochemistry. *Polym. Chem.* **2021**, *12*, 6650-6666.

[29] S. Aksakal, R. Aksakal, C. R. Becer, Thioester Functional Polymers. *Polym. Chem.* **2018**, *9*, 4507-4516.

[30] W. N. Ottou, H. Sardon, D. Mecerreyes, J. Vignolle, D. Taton, Update and Challenges in Organo-Mediated Polymerization Reactions. *Prog. Polym. Sci.* **2016**, *56*, 64-115.

[31] A. P. Dove, Organic Catalysis for Ring-Opening Polymerization. *ACS Macro Lett.* **2012**, *1*, 1409-1412.

Chapter 1

The Synthesis of Stereoregular Polythioesters and Polyesters by Ring-Opening Polymerization of the Corresponding Monomers: State of the Art‡

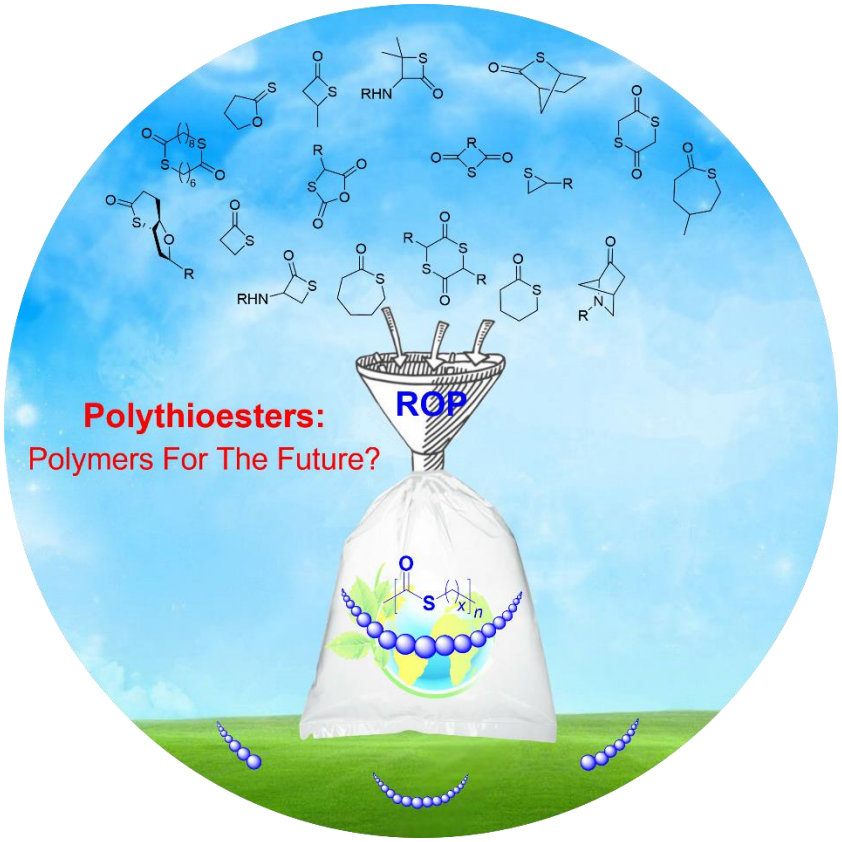

‡ Part of this chapter has appeared in print, see:

[1] H. Li, R. M. Shakaroun, S. M. Guillaume, J.-F. Carpentier, Recent Advances in Metal-Mediated Stereoselective Ring-Opening Polymerization of Functional Cyclic Esters towards Well-Defined Poly(hydroxy acid)s: From Stereoselectivity to Sequence-Control. *Chem. Eur. J.* **2020**, *26*, 128-138.

[2] H. Li, S. M. Guillaume, J. F. Carpentier, Polythioesters Prepared by Ring-Opening Polymerization of Cyclic Thioesters and Related Monomers. *Chem. Asian J.* **2022**, *17*, e202200641.

1.1 Introduction

Polyesters are a ubiquitous class of (bio)degradable polymers that can be broadly divided into semi-aromatic and aliphatic polyesters. Semi-aromatic polyesters, such as poly(ethylene terephthalate) and poly(butylene terephthalate), are widely applied engineering thermoplastics that have good mechanical strength, and excellent chemical resistance and electrical insulation properties.[1,2] Aliphatic polyesters have received much more attention as appealing, potentially sustainable alternatives to petroleum-based polymers due to their numerous renewable sources, facile hydrolytic degradation to typically benign products, and high biocompatibility.[3]

Aliphatic polyesters can be prepared from polycondensation reactions of diols and diacids (or diesters) or hydroxyl acids, which is the common route to polyesters in industry. However, the removal from the reaction medium of small-molecule by-products, such as water or alcohol, necessitates the use of high temperatures, making this approach very energy-intensive. An alternative route to aliphatic polyesters is the ring-opening copolymerization (ROCOP) of epoxides and cyclic anhydrides, which is now also an important methodology to produce polyesters with well-defined microstructure, although no stereocontrolled ROCOP has been documented to date.[4] The application of ROCOP and polycondensation approaches allow access to a broader range of polymer structures, yet the most convenient and efficient method to access polyesters with a good control over the macromolecular parameters: molar mass, dispersity, end-group fidelity, and even stereoselectivity, is arguably the ring-opening polymerization (ROP) of heterocyclic monomers, especially when performed with discrete metal-based catalysts.[5] Various well-defined metal-based catalysts are operative via a so-called 'coordination−insertion' mechanism, which enables a good control over the molecular parameters of the resulting polymer. Critical initiator criteria are sufficient Lewis acidity to enable binding and activation of the monomer unit and a labile metal alkoxide (or amide) bond so as to enable efficient insertion.[6] Additionally, owing to increasing demand for metal-free polymers in biomedical and microelectronic applications, organocatalyzed polymerization has also attracted considerable attention and achieved remarkable advances in the past two decades. Besides many intrinsic merits, for example, relatively low toxicity, good solubility in common organic solvents, tolerant to air and moisture, organocatalysts exhibit great potential for ROP of heterocycles monomers in terms of activity, topology, even in stereoselectivity.[7-11] It is worth nothing that, in contrast to organometallic catalysts, the polymerization mechanism at play in organocatalyzed ROP strongly depends on the chemical nature of the monomer, catalyst, and/or initiator.

Poly(hydroxyalkanoate)s (PHAs) are a class of aliphatic polyesters that find a variety of packaging, agricultural, biomedical and pharmaceutical applications, thanks to their biocompatibility and (bio)degradability (Figure 1.1).[12] PHAs feature different side-chain substituents along the backbone, thereby imparting chirality to each repeating units. The chemical nature of these side-groups and the successive enchainment of the chiral monomer units along the macromolecules, especially the

regularity of stereocenters along the polymer chain, both dictate and modulate the physical, mechanical properties of the resulting polymer materials. Side-chain functionality along the backbone of PHAs is highly desirable since, besides providing a way to influence the thermal and mechanical properties, it offers a handle to chemically modify the scope of the polymer materials through post-polymerization modification of the side chain.

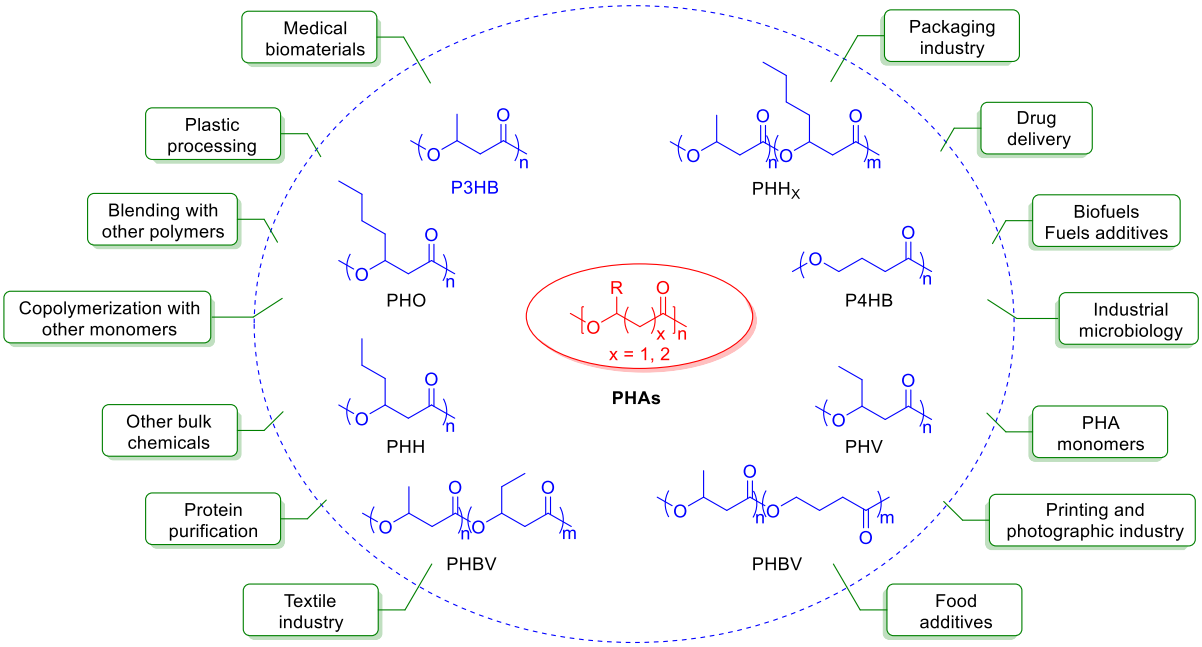

Figure 1.1. General structure, specific examples and common applications of poly(hydroxyalkanoate)s.[12]

In addition to modify the pendant group of PHAs, the modification of the PHAs backbone can also endow polymers with differentiated, sometimes enhanced properties, such as improved thermal, mechanical and optical properties, thereby further widening the application scope of PHAs. In fact, polythioesters (PTEs) (featuring the (C=O)- S linkage) exhibit valuable properties different from those of their oxoester analogues (*i.e.*, polyesters with (C=O)- O linkage), including high refractive index and improved crystallinity. Another much significant characteristic of PTEs is the weak (C=O)−S bond and its intrinsic reactivity; hence, PTEs, in comparison to their corresponding polyester analogues, possess greater potential as dynamic and responsive materials. Although PTEs have not been extensively studied thus far, the synthetic approach towards polyesters and polythioesters are often the same in light of the similarity of their chemical structures.[13]

This chapter mainly focuses on recent developments on the preparation of PTEs by ROP of the corresponding cyclic thiolactone, *S*-carboxyanhydrides and thionolactones, as a function of their ring size (section 1.2), and on the synthesis of aliphatic polyesters with controlled tacticity by stereoselective ROP of chiral racemic heterocyclic monomers meditated by well-defined metal-based catalysts, especially yttrium ones, and organocatalysts (section 1.3).

1.2 The Preparation of Aliphatic Polythioesters from Thiolactones and Related Monomers − State of the Art

Aliphatic polythioesters (PTEs) can be prepared from the polycondensation of thiocarboxylic acids (–C(=O)SH) by removal of water under azeotropic distillation conditions. Yet, ring-opening polymerization (ROP) of thiolactones (–C(=O)–S–) is commonly favoured because it enables the formation of higher molar mass PTEs under milder reaction conditions. Also, ROP of thiolactones, a chain growth process, allows the preparation of linear aliphatic PTEs better controlled in terms of molecular parameters than the aforementioned step-growth process.

1.2.1 Ring-Opening Polymerization of 4-Membered β-Propiothiolactones and Higher Derivatives

Poly(β-propiothiolactone), the in-chain sulfur analogue of poly(3-hydroxypropionate), is often observed as the by-product or even the main compound incidental to the synthesis of β-propiothiolactone. For example, the group of Knunyants reported that poly(ɓ-thioester) (PβTE) formed exclusively from the reaction of β-thiohydroxy-propionic acid with a chloroformate in the presence of triethylamine, even in dilute aqueous solution (Figure 1.2, top).[14] The chemical structure of the recovered polymer was supported by the formation of the corresponding amides and esters of β-thiohydroxy-propionic acid upon its reaction with either amines or alcohols, respectively. β-Propiothiolactone is also obtained from the reaction of 3-chloropropionyl chloride with hydrogen sulfide in the presence of an excess of triethylamine in methylene chloride, yet, alongside poly(β-propiothiolactone) as the major product.

β-Propiothiolactone is briefly reported to "readily polymerize in the presence of small amounts of NaOH in dilute aqueous solution", giving rise to the corresponding PβTE (Figure 1.2, bottom).[14] Yet, the topology (linear or cyclic) and the nature of the terminal groups of the resulting PβTE remain undocumented. The returned PβTE can be easily cleaved by amines giving the corresponding amides of β-thiohydroxy-propionic acid, thereby providing a chemical degradation pathway. To our knowledge, the thermal properties of chemically synthesized PβTEs have never been documented. Microbial PβTE, as produced from *E. Coli*. cultured with thioalkanoic acids, melts at 170 °C, a temperature much higher (*ca*. +93 °C) than that of the *O*-analogous polymer, namely poly(3-hydroxypropionate).[15,16]

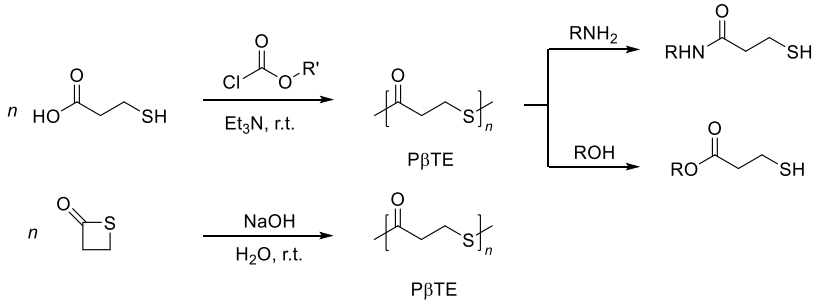

Figure 1.2. Chemical synthesis of poly(β-propiothiolactone) (PβTE) from β-propiothiolactone.[14]

To date, very few results have been published concerning the preparation and properties of PTEs derived from β-propiothiolactone derivatives. Early examples tracing back to the 1960s reported the ROP of (*S*)-α-*p*-toluenesulfonamido-β-propiothiolactone (NTs-PTL) either in bulk (*i.e.*, under neat conditions) at a temperature slightly above its melting point, initiated by small amounts (1 mol%) of water or benzyl thioalcohol, or in DMF in the presence of various nucleophilic initiators such as dimethylamine, or even thermally (100 °C) without any initiator, to produce the corresponding optically active poly(NTs-PTL) (Figure 1.3).[17] However, these polythioesters showed low molar mass values (typically 2,600–12,700 g mol^{-1}), as determined from iodometric titration in DMF solution. This analytical technique did not enable to gain further information on terminal groups fidelity of or dispersity.

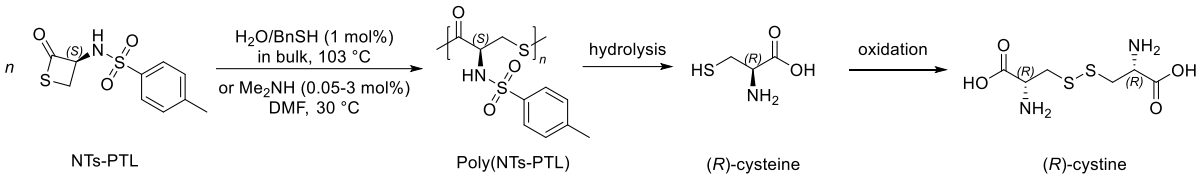

Figure 1.3. ROP of NTs-PTL towards optically active PTE.[17]

The authors proposed a mechanism (Figure 1.4) involving the nucleophilic attack (*e.g.*, amine) onto the electrophilic carbonyl carbon atom of NTs-PTL monomer (II), thereby opening the ring to form a zwitterionic thiolate-type intermediate (III); the latter is a strong nucleophile that can further react with additional monomer upon propagation, eventually giving linear PTE. Hydrolysis of the resulting poly(NTs-PTL) led to (*R*)-cysteine which was subsequently oxidized to (*R*)-cystine of the same optical/enantiomeric purity, indicating that such polymerization conditions do not induce racemization of the monomer. It further demonstrates that this class of PβTE can readily degrade into small molecules from which the initial NTs-PTL monomer can be resynthesized. In light of the pendant reactive amino group, these poly(NTs-PTL)s raised great interest to introduce different functional groups along the PTE backbone, upon chemical modification. Also, non-amide-bonded polycysteines containing thioester groups in the main chain are known to play an important role in acylation reactions in biological systems as well.

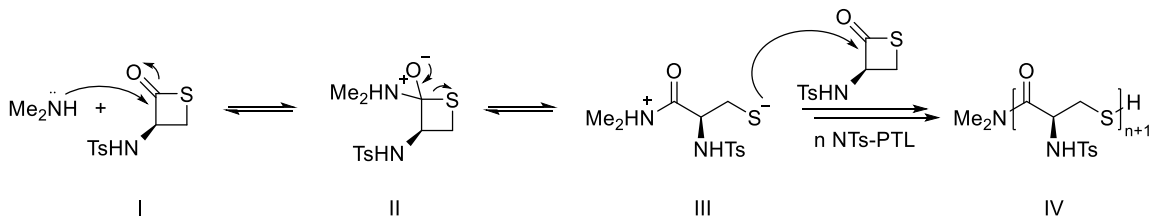

Figure 1.4. Proposed mechanism for the Me_2NH-initiated ROP of NTs-PTL.[17]

Further studies conducted by the same group evidenced the great impact of the NTs functional groups on their rate of polymerization. A series of α-(*para*-substituted-benzenesulfonamido)-β-propiothiolactones NTs^{R}-PTL were subjected to ROP initiated by benzyl mercaptan, thereby investigating the electronic contribution of the R *para* substituent (Figure 1.5).[18] Kinetic analysis, by measuring the change of specific rotation as a function of time, indicated that the ROP at room temperature is first order in monomer with k_{OMe} = 2.555, k_{Me} = 2.22, k_{H} = 2.028; k_{Cl} = 1.611, and k_{NO2} = 0.533 mL g^{-1} h^{-1}. It was then proposed that the proton on the nitrogen atom, which acidity is modulated by the *para* substituent, plays a significant role.

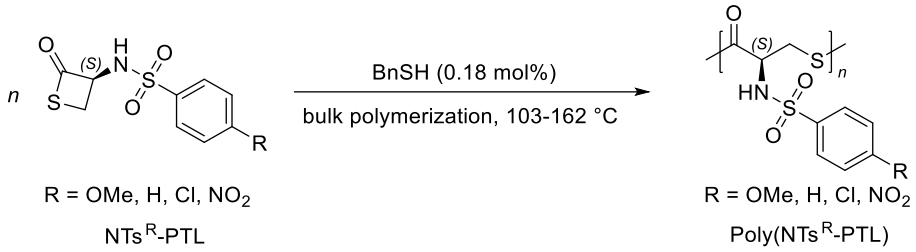

Figure 1.5. ROP of various α-acylamino-β-thiolactones NTs^{R}-PTLs.[18]

To gain further insights into the contribution of this proton to the rate of polymerization through hydrogen bonding, the polymerizability of a set of *N*,*N*-disubstituted β-thiolactones was compared with that of *N*-monosubstituted analogues.[19] The rates of conversion, as determined by monitoring the change of specific rotation with time, indicated that the *N*-tosylamino derivative polymerizes much faster than *N*-methyl-*N*-tosylamino-β-thiolactone. The other examples further illustrated the higher polymerizability of *N*-monosubstituted *vs*. *N*,*N*-disubstituted β-thiolactones and showed that the rate of the initiating and propagating steps of the ROP of *para*-substituted benzenesulfonamido-β-thiolactones are strongly improved by hydrogen bonding.

More recently, the group of Matsuoka insightfully revisited the ROP of a *N*-Boc-cysteine-derived β-thiolactone (*N*^{Boc}-PenTL) initiated by *N*-Boc-*L*-cysteine methyl ester in *N*-methyl-2-pyrrolidone (NMP) (Figure 1.6).[20] Both NMR spectroscopy and matrix-assisted laser desorption ionization time-of-flight (MALDI-ToF) mass spectrometry (MS) analyses of the resulting polymer corroborated the formation of *α*-OMe,*ω*-SH end-capped PβTE. The molar mass of the PβTEs measured by SEC and ^{1}H NMR analyses, yet relatively low (M_n < 10,000 g mol^{-1}), was, to some extent, controlled by the monomer-to-initiator feed ratio (up to 100:1). However, the dispersity was relatively broad ($Đ_M$ ≈ 1.6–2.4), in part due to extensive transthioesterification reactions concomitant to the ROP. This easy thiol−thioester exchange, often referred to as 'dynamic nature of β-thioesters', also limits reaching high molar mass polymers. Due to the higher solubility of this PβTE in THF, the latter solvent was also examined as a reaction medium. However, the ROP of *N*^{Boc}-PenTL proved ineffective in THF, even under reflux, suggesting that NMP is essential for the polymerization to proceed. The authors proposed that the high polarity and low basicity of NMP increase the nucleophilicity of the thiol group of the

initiator. Some mechanistic studies revealed that the propagating chain-end is indeed the thiol group that attacks the carbonyl moiety to open the monomer ring by C(=O)−S bond scission. This is reminiscent of the anionic ROP of β-lactones which can proceed via C(=O)−O bond 'acyl' cleavage leading to alkoxy propagating species and eventually an alcohol chain-end (after final workup) (the other mode being C_β- O(C(=O)) bond 'alkyl' cleavage, leading to carboxylate propagating species and eventually a carboxylic chain-end).[21]

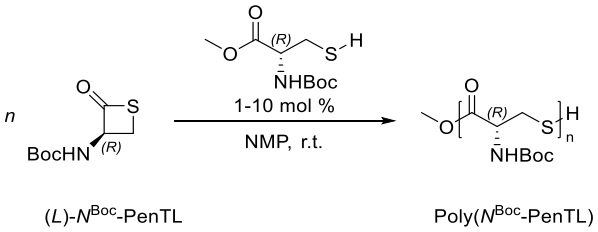

Figure 1.6. ROP of a *N*-Boc-cysteine derived β-thiolactone (N^{Boc}-PenTL).[20]

Noteworthy, the thiol group exhibits a unique reactivity as compared to amino and hydroxyl groups. A famous example is the thiol-ene click reaction which can be applied to modify thiol-functionalized PTEs.[22] Hence, reaction of the PβTE recovered from the ROP of the cysteine-derived β-thiolactone with a norbornene-terminated PEG, using DMAP as radical photoinitiator, quantitatively afforded the corresponding PTE-*b*-PEG block copolymer (Figure 1.7, top). SEC monitoring showed the shift of the unimodal elution profiles to higher molar mass values throughout the reaction. Another valuable reaction is the intramolecular *S*-to-*N* acyl migration in the cysteine skeleton, triggered by the deprotection of the pendant *N*-Boc groups, leading to the PβTE main chain transformation to polycysteine (Figure 1.7, bottom). Surprisingly, the returned polycysteine displayed a higher molar mass than the starting PβTE, in spite of the abstraction of Boc groups that should ultimately decrease the value. The rationalization proposed relies on the higher rigidity of polycysteine - as the amide is more rigid than the thioester group due to the larger resonance between the carbonyl and the nitrogen- , leading to a larger conformational shape of the macromolecules. Another suggestion, perhaps more likely, is the intermolecular bonding of polycysteines through the formation of S−S bonds.

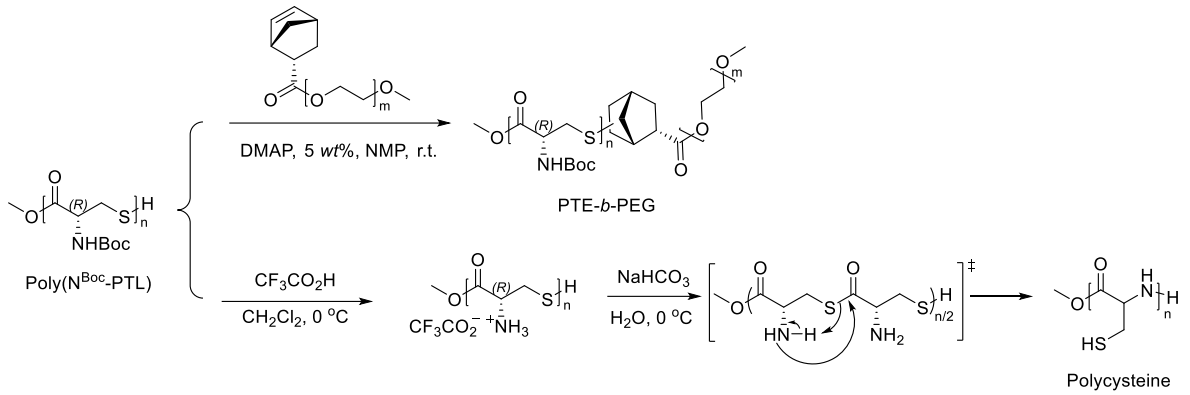

Figure 1.7. Post-polymerization functionalization of a poly(ɓ-thioester) obtained from the ROP of a cysteine-derived β-thiolactone.[20]

To alleviate transthioesterification and tune more favourably the thermodynamics closer to equilibrium, the group of Lu recently modified the cysteine-derived β-thiolactone structure by introducing a geminal dimethyl group on the β position of the four-membered ring (N^{R}-PenTL).[23] This monomer is easily synthesized from the naturally occurring amino acid *D*-penicillamine in a one-pot process and, notably, it can be tailored with different side-chains. The bulk polymerization of N^{ene}-PenTL promoted by a weakly basic organocatalyst such as triethylamine, was investigated in the presence of benzylthiol as co-initiator at room temperature (Figure 1.8). At a $[N^{ene}\text{-PenTL}]_0/[NEt_3]_0/[BnSH]_0$ feed ratio of 100:1:1, 61% monomer conversion was achieved within 72 h, affording the corresponding PβTE with a considerably higher molar mass and narrower dispersity (M_n = 19,400 g mol^{-1}, $Đ_M$ = 1.10) than the related PβTEs previously reported by the group of Matsuoka (same feed ratio; *vide supra*). Replacing triethylamine with the more basic 1,8-diazabicyclo(5.4.0)undec-7-ene (DBU) accelerated the ROP with 59% monomer conversion being achieved within 6 h. Noteworthy, when the ROP of N^{ene}-PenTL was quenched with iodoacetamide, MALDI-ToF MS analysis revealed the formation of poly(N^{ene}-PenTL) bearing $PhCH_2S$– and –CH_2CONH_2 chain-end groups, further confirming that thiolate is the propagating species. The molar mass of the poly(N^{ene}-PenTL)s increased linearly from low (M_n = 6,400 g mol^{-1}, $Đ_M$ = 1.11) to medium (M_n = 18,500 g mol^{-1}, $Đ_M$ = 1.14) upon raising the feed ratio from 30:1:0.1 to 100:1:0.1. The M_n values also displayed a linear relationship with monomer conversion along with narrow dispersity, all supporting the controlled living character of the DBU-catalyzed ROP of N^{ene}-PenTL. The ROP of N^{C8}-PenTL and N^{EG4}-PenTL showed a similar control. The use of the more basic *t*BuP_4 phosphazene superbase, allowed preparing higher molar mass poly(N^{C8}-PenTL) (M_n up to 70,600 g mol^{-1} using a feed ratio of 350:1:1), still maintaining a fairly narrow dispersity ($Đ_M$ = 1.23). This provides a pathway to high molar mass PβTEs, which remains a bottleneck due to the dynamic nature of β-thioesters.

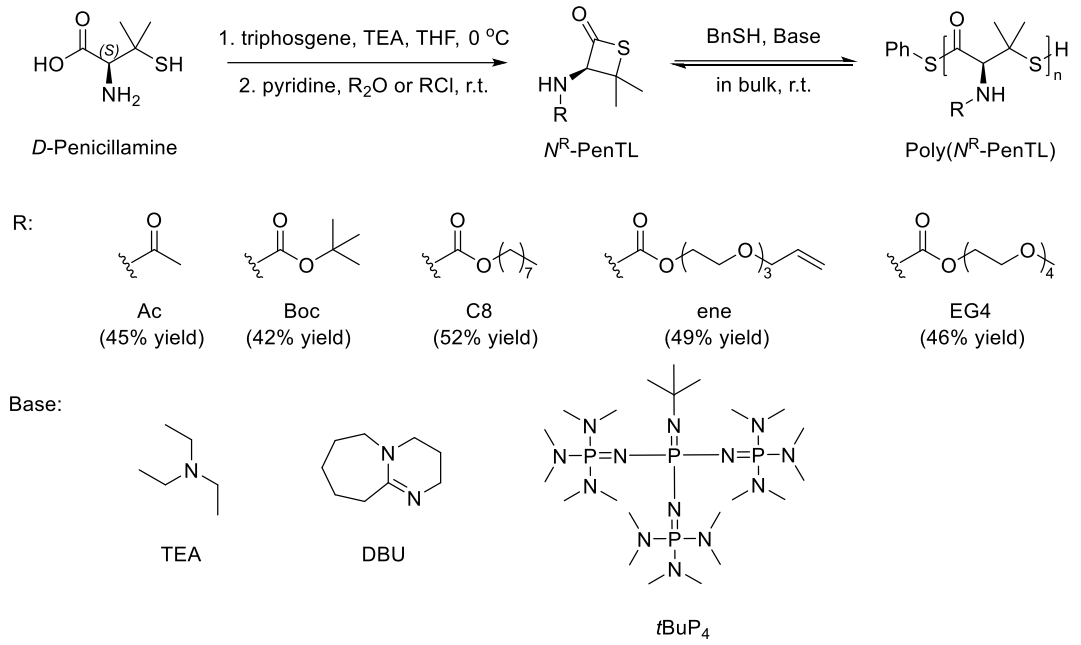

Figure 1.8. Synthesis and ROP of various N^{R}-PenTL type β-thiolactones.[23]

The introduction of a geminal dimethyl group on the lactone ring, as a result of the Thorpe-Ingold effect, considerably lowers the ring strain of otherwise highly strained β-thiolactone and makes the recyclability of PβTEs based on such cysteine-derived thiolactones possible. Hence, when the isolated α-PhCH$_2$S,ω-SH-poly(N^{R}-PenTL) was treated with DBU at 65 °C, gradual depolymerization was confirmed by NMR and SEC analyses (Figure 1.9). Yet, evaluation of the optical rotation of the recovered monomer revealed significant racemization upon depolymerization. More interestingly, at lower temperatures (such as room temperature), poly(N^{R}-PenTL) could be completely depolymerized (> 95% conversion) into the enantiopure monomers, revealing that a reduced temperature prevents racemization. On the other hand, α-PhCH$_2$S,ω-CH$_2$CONH$_2$-poly(N^{R}-PenTL) obtained by reaction of the original polymer with iodoacetamide, remained unchanged upon treatment with DBU even after 12 h at room temperature. More interestingly, poly(N^{R}-PenTL)s ω-terminated with either –CH$_2$CONH$_2$ or –SH could be completely depolymerized into the N^{R}-PenTL monomers when treated with PhSNa at ambient temperature. Hence, this class of monomers offers an appealing platform for environmentally-friendly recyclable plastic materials within a circular economy.[24,25]

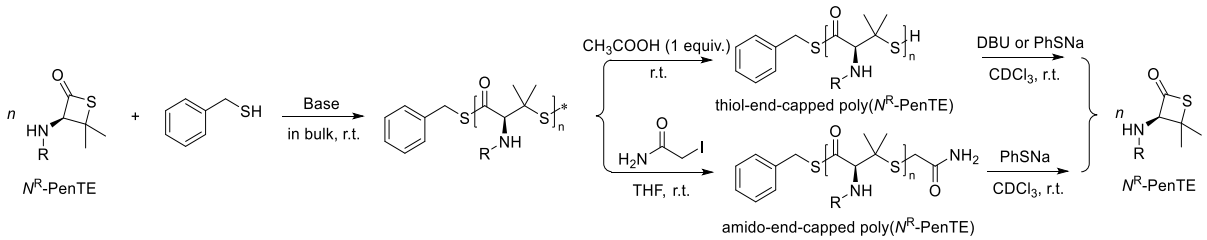

Figure 1.9. Facile chain-end functionalization of various PTEs and subsequent depolymerization into N^{R}-PenTE.[23]

1.2.2 Ring-Opening Polymerization of 5-Membered Fused Bicyclic γ-Thiolactones

In 2019, the group of Lu reported the controlled ROP of chiral *N*-substituted *cis*-4-thia-*L*-proline thiolactone (N^{R}-PTL, R = Boc, Cbz, or ene), initially synthesized from *trans*-4-hydroxy-*L*-proline (4-Hyp), an abundant biosourced feedstock (Figure 1.10).[26] The authors rationalized the reactivity (TOF *ca*. 30 h^{-1} at room temperature) of this monomer by the high strain of the fused bicyclic thioester ring, as similarly observed for the bridged bicyclic γ-butyrolactone. The ROP of N^{Boc}-PTL performed by KO*t*Bu in highly polar solvents (*e.g.*, acetonitrile, DMF or NMP) is uncontrolled and returned mixtures of both linear and small cyclic chains. Less polar solvents, such as chloroform and dichloromethane, suppress back-biting reactions, achieving controlled ROP of N^{Boc}-PTL at ambient temperature when using benzylthiol or triethylamine as the initiator and a catalyst, respectively. This afforded well-defined poly(N^{Boc}-PTL)s with narrow dispersity (typically $Đ_M$ = 1.03–1.10) and predictable molar mass values (M_n up to 20,100 g.mol^{-1}) dictated by the monomer-to-initiator feed ratio. These observations support a relatively fast initiation (as compared to propagation) along with limited undesirable side reactions (classically inter- and intra-molecular transthioesterification reactions). Evidence of the terminal thiol group of the poly(N^{Boc}-PTL)s was indirectly gained from its subsequent reaction with the iodoacetamide reagent, which returned α-$PhCH_2S$,ω-CH_2CONH_2-poly(N^{Boc}PTE) as revealed by MALDI-ToF MS analysis. Switching the catalyst from triethylamine to the more basic 1,8-diazabicyclo[5.4.0]undec-7-ene (DBU) significantly accelerated the polymerization, thereby precluding kinetics monitoring. The ROP of N^{Cbz}-PTL and N^{ene}-PTL proceeded similarly to that of N^{Boc}-PTL, highlighting the versatility of this polymerization.

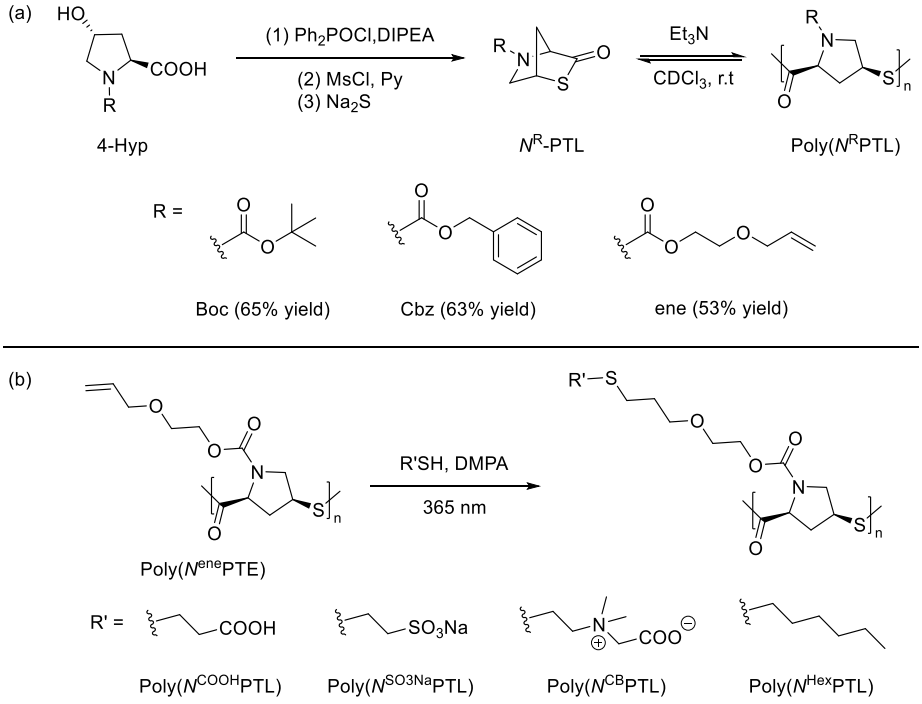

Figure 1.10. Synthesis and ROP of N^{R}-PTL and subsequent post-polymerization functionalization of poly(N^{R}PTL). [26]

The side-chain allyl group of poly(N^{ene}PTL) can be easily modified upon reaction with various functional thiols under UV irradiation to give a set of chemically diverse PgTEs including carboxylic, sulfonate, zwitterionic, or alkyl groups.[26] On the other hand, functionalization of poly(N^{Boc}PTL) with various thiols in the presence of triethylamine at room temperature did not proceed at the expense of smooth depolymerization back to the initial monomer (with quantitative regeneration of the monomer). This mild ROP/depolymerization chemistry may pave the way to sustainable recyclable materials. However, such PgTEs exhibit relatively low thermal stability and did not feature a melting temperature (T_m) despite their chiral microstructure.

To offer better promise to such PgTEs, *e.g.*, to impart them with high crystallinity for targeted applications and also for better chemical recyclability, a bridged bicyclic thiolactone, namely 2-thiabicyclo[2.2.1]heptan-3-one ($^{[221]}$BTL) was designed (Figure 1.11).[27] This latter monomer can be prepared in a racemic form from a bio-based olefin carboxylic acid. The ROP of *rac*-$^{[221]}$BTL was first conducted effectively with four different catalyst systems: La{N(TMS)$_2$}$_3$, DBU and *t*BuP$_4$ in the presence of benzyl alcohol (BnOH) as co-initiator. Stereoregularity of these reactions yet significantly depended on the monomer concentration, reaction solvent polarity and monomer-to-initiator ratio. In toluene solution with [$^{[221]}$BTL]$_0$ < 1.6 g mL^{-1} and [$^{[221]}$BTL]$_0$/[BnOH]$_0$ < 300:1, at room temperature, all reactions gave stereo-disordered PBTLs (P_r ~ 0.21–0.46), regardless of the catalyst used. Unexpectedly, under these operating conditions, all these PBTLs exhibit a high crystallinity with T_m values typically in the range 166–176 °C. Increasing the monomer concentration ([$^{[221]}$BTL]$_0$ > 2.4 g mL^{-1}) and decreasing the catalyst loading ([$^{[221]}$BTL]$_0$/[*t*BuP$_4$]$_0$ > 1000:1) returned essentially perfectly isotactic PBTL (P_r ~ 1), as further corroborated by a high T_m of 213 °C. Moving to *N*-heterocyclic carbene (NHC), namely1,3-bis(2,4,6-trimethylphenyl)imidazol-2-ylidene (IMes), enabled to increase the feed ratios ([$^{[221]}$BTL]$_0$/[IMes]$_0$/[BnOH]$_0$) up to 5000:1:1, and gave a highly stereoregular (P_r = *ca.* 1), high molar mass ($M_{n,SEC}$ = 48,300 g mol^{-1}), and crystalline PBTL with T_m = 213 °C. In line with previous observations by Waymouth[28] which showed that, with the help of an alcohol, NHCs are able to promote ROP of cyclic esters to produce linear polyesters, the ROP of $^{[221]}$BTL mediated by IMes in the presence of alcohol initiators generated well-defined linear PTEs. Remarkably, the ROP of $^{[221]}$BTL by NHC without alcohol gives cyclic PBTLs, as evidenced by MALDI-ToF MS analysis, and further demonstrated by its lower intrinsic viscosity compared with its linear counterpart (typically [μ]$_{cyclic}$/[μ]$_{linear}$ = *ca.* 0.7). The melting temperature of PBTLs increases monotonously and linearly with the tacticity (T_m = 54.8 × P_r + 157.4 °C with P_r ranging from 0.47 to 1). These results show that these PTEs exhibit a singular ability to crystallize, even with a high degree of stereochemical disorder. In addition, the thermal stability of cyclic PBTL is about 7 °C higher than that its linear counterpart (T_d = 321 °C), which is consistent with the fact that the thermal stability of cyclic polymers is generally higher than that of the linear analogues. This provides a valuable thermal processing window of more than 100 °C for PBTL (above the T_m and below the T_d).

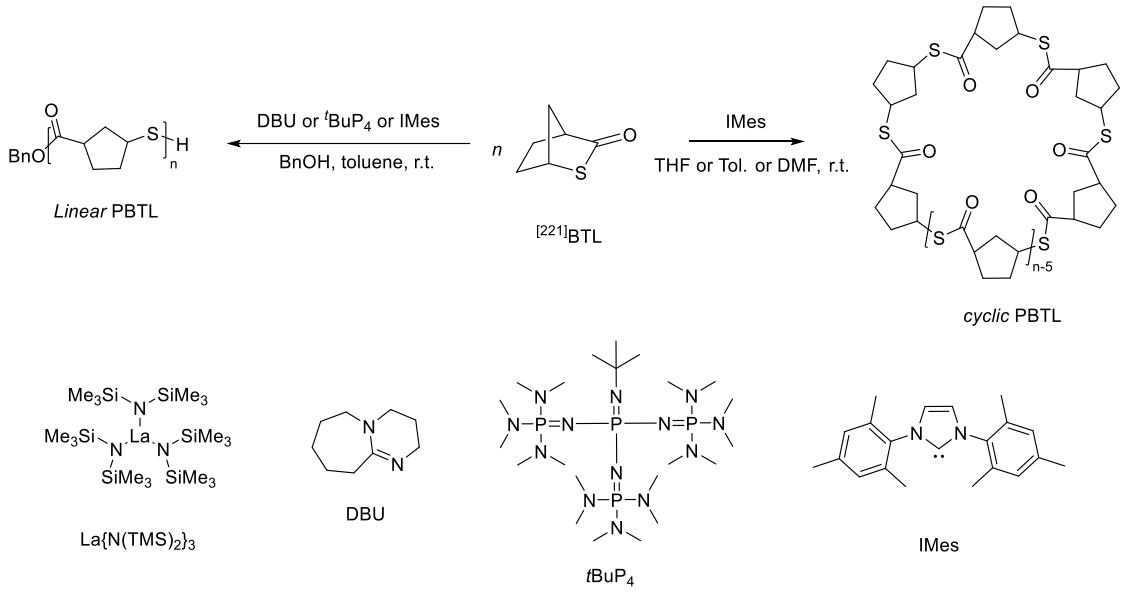

Figure 1.11. ROP of the bicyclic γ-thiolactone [221]BTL. [27]

Another valuable property of these PBTLs is their intrinsic chemical recyclability for a closed-loop life cycle.[27] When cyclic PBTL was treated with either La{N(TMS)$_2$}$_3$ at 100 °C in bulk, or with IMes (2 M toluene solution) at room temperature, depolymerization occurred quantitatively giving back the monomer without isomerization. The recycled [221]BTL can then be directly repolymerized into PBTL; this was assessed on one cycle but can, in principle, be extended to multiple recycling. No information was provided on the possibility to depolymerize/recycle the linear polymer. Overall, these PBTL polythioesters possess a unique set of desired properties, such as tunable tacticity from atactic to perfect stereoregularity, intrinsic tacticity-independent crystallinity, high thermal stability and chemical recyclability.

1.2.3 Ring-Opening Polymerization of 6-Membered δ-Thiolactones and Derivatives

Early attempts on ROP of the 6-membered δ-thiovalerolactone (TVL) date back to 1968 (Figure 1.12); yet, the monomer conversion was extremely low (*ca*. 21%) and molar mass and dispersity data of the resulting PTVL remained limited, at that time.[29] The authors hypothesized that there is a monomer/polymer equilibrium (that is quite usual in the field of heterocyclics ROP), leading to a limited molar mass.

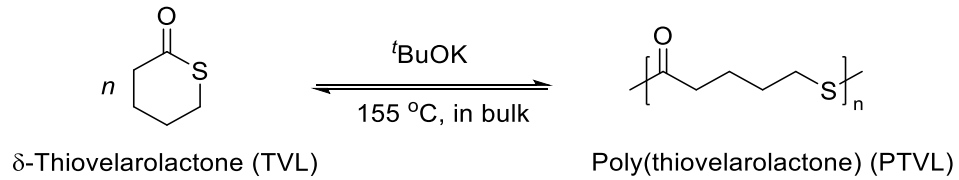

Figure 1.12. Early attempts at ROP of δ-thiovalerolactone.[29]

The group of Matsuoka reported the formation of polythiolactide (PTLA), an attractive analogue of the ubiquitous polylactide (PLA) – an extensively studied renewable and biodegradable polymer (Figure 1.13, top).[30] *Racemic* thiolactide (*rac*-TLA) was synthesized analogously to lactide prior to this work, that is by condensation of the material obtained from thermolysis of PTLA, while cyclization reaction from α-mercapto acid was implemented in this contribution similar to that of Tao's findings (*vide infra*).[31] The isolated TLA consists of the *racemic* and *meso* forms at a ratio of 98:2–95:5. DFT calculations combined to the condensation of cyclic (*R*)-thiolactide acid suggested that the *racemic* form is much more stable than the *meso* isomer, as also demonstrated by the group of Tao (*vide infra*).[31] The ROP of *rac*-TLA examined with a thiol/DBU combination at room temperature showed first that the conversion of the monomer remained limited to 25%, even in concentrated solutions, or by extension of the reaction time or by increasing the reaction temperature. The monomer conversion reached about 50% when performing the ROP in bulk, but still did not increase upon prolonging the reaction time. Also, decreasing the amount of the initiator increased the molar mass of the PTLA at constant monomer conversion. These findings suggest that the ROP of TLA reaches an equilibrium between monomer and polymer, which was further confirmed by three different post-polymerization treatments: i) additional feeding of *rac*-TLA resulted in the same ceiling conversion along with an increase of the molar mass of the resulting PTLA, ii) heating to 60 °C led to a decrease of the monomer conversion, and iii) addition of CH_2Cl_2 gave rise to partial depolymerization to TLA. Surprisingly, sterically hindered bases, such as diisopropylethylamine or 1,2,2,6,6-pentamethylpiperidine, were found to promote ROP without addition of an initiator, while a weaker amine, such as pyridine, was unable to do so. The authors presumed that these non-nucleophilic amines enable deprotonation at the α-position of the thioester carbonyl group thus initiating the polymerization (Figure 1.13, bottom); this further suggests that thioester has a more acidic carbonyl α-proton than its oxoester analogue. PTLA was always isolated as a mixture of linear and cyclic polymers, as verified by MALDI-ToF MS analysis. In fact, intra- and intermolecular thiol-thioester exchange reactions occur during the ROP.

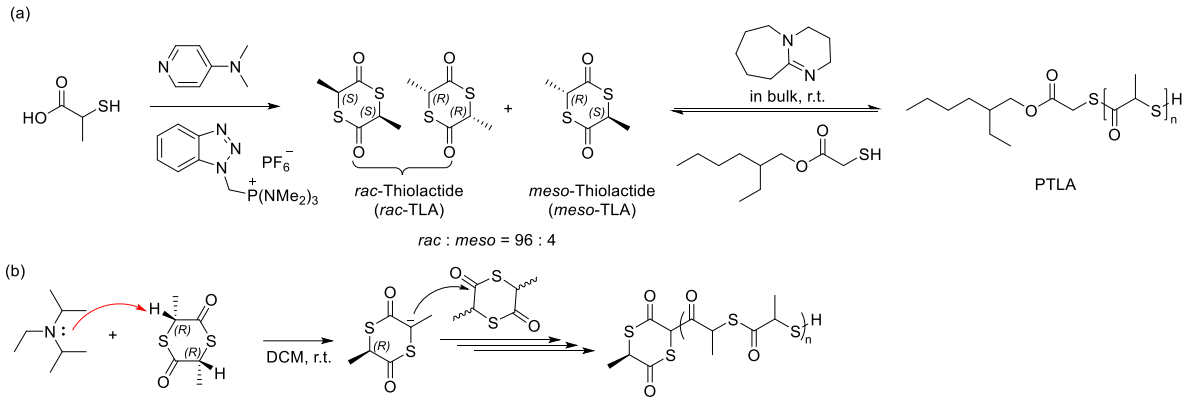

Figure 1.13. (a) The synthesis of *rac*-thiolactide and its ROP by a basic organocatalyst; (b) ROP of *rac*-TLA initiated by a non-nucleophilic amine.[30]

The copolymerization of *rac*-thiolactide (TLA) with thioglycolide (TGL) was also briefly studied (Figure 1.14).[30] Prior investigation of the homopolymerization of TGL using a combination of thiol and DBU also reached an equilibrium as observed in the ROP of *rac*-TLA. The ring-opening copolymerization of TGL with *rac*-TLA proceeds with higher conversions of both monomers as compared to those reached in the corresponding homopolymerizations; no detail on reactivity ratios, microstructure and properties of these copolymers were however reported.

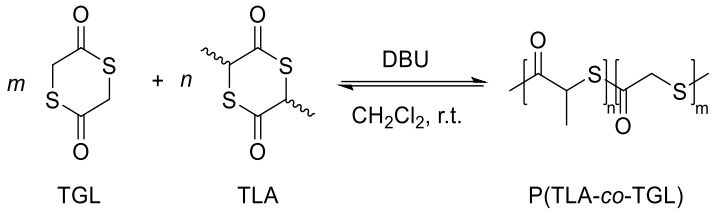

Figure 1.14. Ring-opening copolymerization of thioglycolide and thiolactide. [30]

In 2021, the group of Tao revisited the chemistry of PTLA, also expanding the monomer scope to different substituted 6-membered thiolactones (Figure 1.15).[31] The latter monomers bearing different side chains were efficiently synthesized by cyclization reaction from α-mercapto acid in good yields. Yet, the isomeric (*rac*/*meso*) ratio of the monomers was not documented. Investigation of the thermodynamics of the ROP of *rac*-TLA indicated that the ceiling temperature is –67 °C, and 197 °C for an initial monomer concentration of 1.0 and 5.0 M, respectively; this suggests that ROP of *rac*-TLA should reach complete conversion rather easily when conducted at high concentration. In fact, the ROP of *rac*-TLA promoted by a basic organocatalyst such as 4-(*N*,*N*-dimethylamino) pyridine (DMAP), in the presence of benzyl thiol as co-initiator, proceeds rapidly in a controlled fashion at 25 °C in dichloromethane at high monomer concentration ($[TLA]_0$ = 5.9 M), achieving 58% conversion in 10 min. The ROP reaction under these conditions is rather well-controlled, as confirmed by the linear growth of the experimental molar masses ($M_{n,SEC}$) as a function of monomer conversion, coupled with rather narrow dispersities ($Đ_M$ < 1.40). The presence of a terminal thiol moiety was demonstrated by the end-capping with iodoacetamide, which afforded a PTLA bearing $PhCH_2S$– and $–CH_2CONH_2$ chain-end groups. However, inevitable transthioesterification side reactions occurred during polymerization, as demonstrated by MALDI-ToF MS analysis (observation of half TLA repeating units). Of note, the ROP of *rac*-TLA using DMAP or benzyl thiol alone, under comparable conditions, was ineffective. Collectively, all these results suggest an activation mechanism where DMAP activates the benzyl thiol initiator or thiol chain-end. Switching the DMAP catalyst to triethylamine or stronger bases, namely 1,5,7-triazabicyclo[4.4.0]dec-5-ene (TBD, pK_a^{CH3CN} = 26.0) or a phosphazene such as *t*BuP_2 (pK_a^{CH3CN} = 33.5), improved the polymerization rate but in an uncontrolled manner ($Đ_M$ > 1.50); this corroborates that extensive transthioesterification competes with chain propagation with such strongly basic organocatalysts.

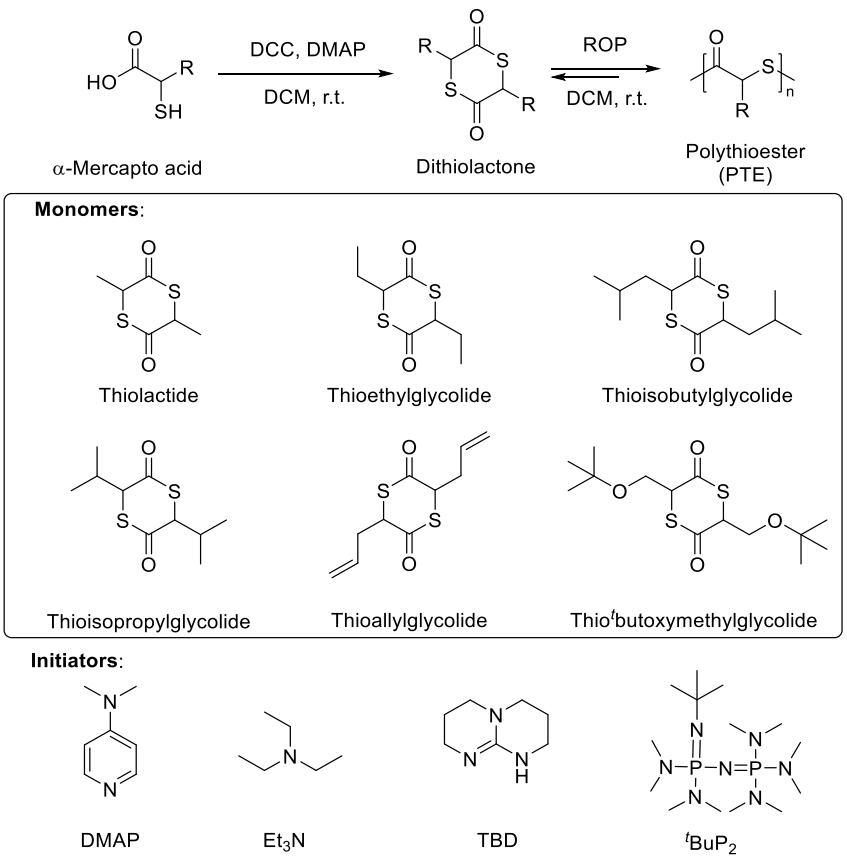

Figure 1.15. Synthetic route and ROP of dithiolactones by basic organocatalysts.[31]

As aforementioned, a remarkable feature of the obtained PTLA is its chemical recyclability due to its low ceiling temperature.[31] The group of Tao further evidenced quantitative recovery of the TLA monomer in high selectivity within a few minutes at room temperature via ring-closing depolymerization, with or without solvent. It returned a mixture of *rac*/*meso*-TLA in a *ca.* 98:2 ratio, in line with works and DFT calculations from the group of Matsuoka, irrespective of the severe extent of transthioesterification reactions; pure *rac*-TLA could be further separated by recrystallization in 95% isolated yield. Collectively, owing to the large energy difference between the *rac* and *meso* isomers of TLA, coupled with the increased acidity of the α-carbonyl H (as compared to the parent lactide), depolymerization of PTLA is accompanied by the simultaneous quantitative *meso*-to-*rac*-TLA conversion, thereby ensuring high depolymerization selectivity.

Another notable contribution from the group of Tao is to provide opportunities to implement ROP of related 6-membered dithiolactones bearing different side chains; this enabled tailoring of physical, mechanical and biological properties of the resulting PTE materials.[31] The ROP of these functional dithiolactones was successfully achieved under the reaction conditions established for TLA, and proceeded in a controlled manner. All the resulting PTLAs could be depolymerized into the corresponding monomers. The thermal properties of these polythioesters spanned a broad glass transition and degradation temperature range (T_g = –19.2 to +1.9 °C and $T_d^{5\%}$ = 182–254 °C; $T_d^{5\%}$ defined as the temperature for 5% weight loss, respectively); unexpectedly, the atactic

poly(thioisopropylglycolide) is semicrystalline with a T_m of 115.6 °C. Interestingly, a random copolythioester made from *rac*-TLA and *rac*-thioethylgylcolide was found to depolymerize easily as well, yet providing, as expected, a mixture of symmetrical and asymmetrical dithiolactone monomers. Hence, overall, the DMAP-catalyzed ROP of dithiolactones paves a new way towards functional, recyclable PTEs from readily available feedstock, foreseeing the development of new polymer materials.

In 2018, the group of Bowman reported the ROP of 6-membered δ-thiovalerolactones functionalized with natural nucleosides into the corresponding functional poly(δ-thiovalerolactone)s (Figure 1.16).[32] Due to the structural and stereochemical similarity to DNA of this latter linked-DNA thioester, this non-natural polymer is anticipated to tightly bind to its native complement (i.e., native DNA); it thus constitutes a first step towards a platform that is expected to culminate in the synthesis of sequence-controlled polymers via dynamic-template-directed synthesis. The targeted δ-thiolactones, that is thymine-based thiovalerolactone (TTVL) and deoxyuridine-based thiovalerolactone (DTVL), were synthesized in multiple steps, and subsequently subjected to ROP mediated by basic organocatalysts. TTVL, used as a model monomer, undergoes ROP in the presence of *N*,*N*-diisopropylethylamine (DIPEA) as catalyst and 1-octanethiol as initiator, in THF at room temperature. The highest molar mass (up to 5,700 g mol^{-1}) of PTTVL was achieved at a monomer-to-initiator ratio of 100:1:1 over prolonged reaction time (6 h); yet, the monomer conversion was relatively low (*ca.* 27 %). *In situ* end-capping of these polymers following the ROP reaction was found to be critical, likely due to their low ceiling temperature; otherwise, significant degradation or inconsistent results were noted, indicating that such system exhibits an intrinsic reversible monomer-polymer equilibrium. The optimized ROP conditions were extended to DTVL, giving a PDTVL oligomer ($M_{n,SEC}$ up to 2,700 g mol^{-1}). These general conditions also provided low molar mass copolymers of TTVL and DTVL (M_n = 3,700 g mol^{-1}, $Đ$ = 1.45). Interestingly, the thiol-thioester exchange reaction was demonstrated by (i) the reaction of 1-octanethiol with the isolated PδTE, and by (ii) the coalescing of two uncapped homopolymers of different chemical composition into a single copolymer; these observations strongly support the dynamic and responsive behaviour of PTEs.

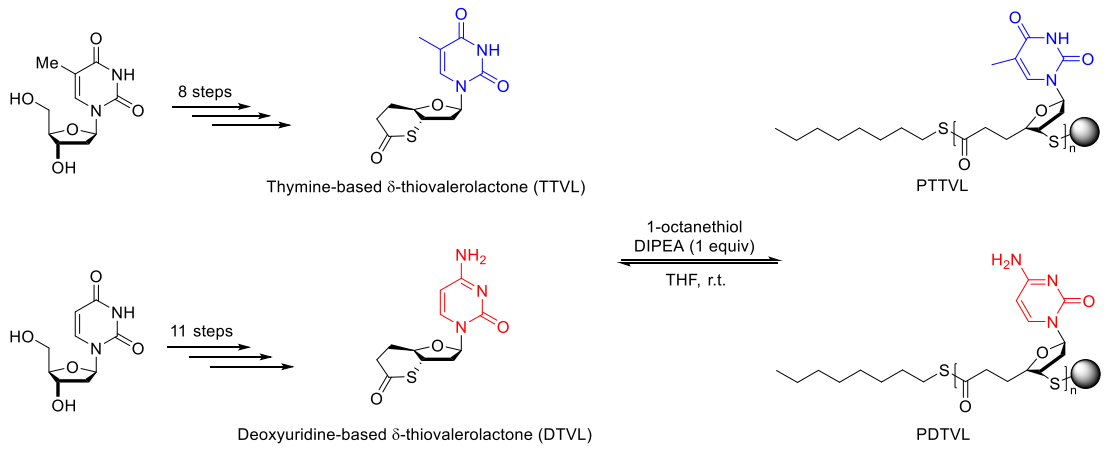

Figure 1.16. ROP of nucleobase-functionalized δ-thiolactones.[32]

Overall, although the scope of 6-membered thioesters has not been extensively studied, these few examples demonstrate its large potential as recyclable materials due to the low ceiling temperature.[33]

1.2.4 Ring-Opening Polymerization of 7-Membered ε-Thiocaprolactone

The initial report of the ROP of ε-thiocaprolactone (TCL) and β/γ-methyl-substituted ε-thiocaprolactone dates back to 1964 (Figure 1.17).[29,34,35] These early polymerizations were promoted by inorganic bases such as *t*BuOK, *n*BuLi, Na dispersion, and they were most likely uncontrolled with limited information on molar mass and dispersity.

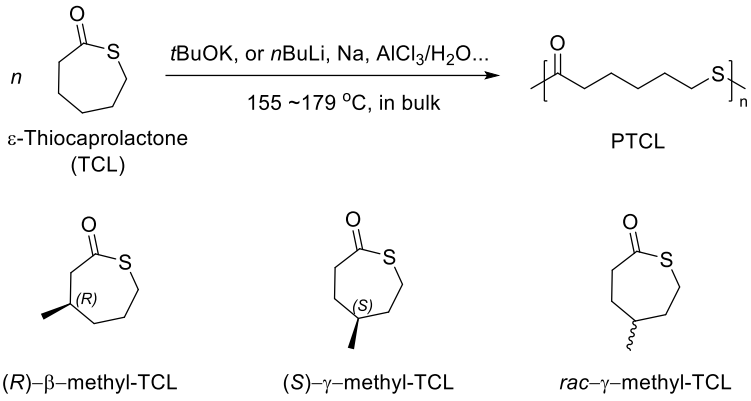

Figure 1.17. ROP of ε-thiocaprolactone (TCL) initiated by inorganic bases.[29,34,35]

In 2015, the group of Kiesewetter described the synthesis of well-controlled PTCL by ROP of TCL using organocatalysts (Figure 1.18).[36] In the absence of an H-bond donor, a series of bases such as tris[2-(dimethylamino)ethyl]-amine (Me_6TREN), (2-*tert*-butylimino-2-diethylamino-1,3-dimethyl-perhydro-1,3,2-diazaphosphorine (BEMP), (4-(dimethylamino)pyridine (DMAP), 7-methyl-1,5,7-triazabicyclo[4.4.0]dec-5-ene (MTBD) and 1,8-diazabicyclo[5.4.0]undec-7-ene (DBU), were screened in $CHCl_3$ at ambient temperature. Among them, MTBD and DBU were the most effective ones, promoting ROP in a controlled manner. This was confirmed by the linear growth of the experimental molar mass ($M_{n,SEC}$ up to 32,000 g mol^{-1}) as a function of monomer conversion, while dispersities remained relatively narrow ($Đ_M$ = 1.40–1.67); yet, these values broadened with increased reaction time, an indirect evidence of easy and fast transthioesterification reactions. The high activity of DBU and MTBD coupled with the observation that, on the other hand, the considerably basic but non-nucleophilic BEMP is inoperative, revealed that the ROP of TCL likely follows a nucleophilic mechanism (Figure 1.19): DBU and MTBD are not acting as general bases but rather promote ROP via nucleophilic attack at the thioester moiety.

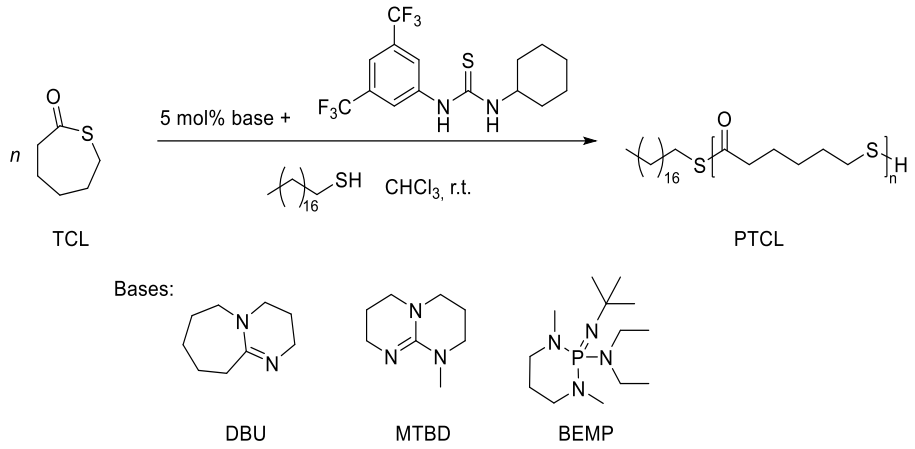

Figure 1.18. ROP of ε-thiocaprolactone (TCL) promoted by a basic organocatalyst and eventual addition of a thiourea.[36]

A two-component organocatalytic system featuring a H-bond donor and a H-bond acceptor moieties, has been demonstrated as a powerful strategy for the controlled ROP of cyclic esters.[9,10,37] Thus, thiourea (a H-bond donor) was investigated in the ROP of TCL. An NMR titration of TCL and thiourea revealed minimal activation of the monomer by thiourea, with a binding constant (K_{eq} = 2.7) much smaller than that of the parent oxo-CL (K_{eq} = 42). DFT calculations further supported these NMR observations. Despite the small binding constant between TCL and thiourea, the H-bond donor exhibits a marked effect on the ROP. The polymerization rate drastically increased upon addition of one equivalent of thiourea; on the other hand, the dispersity became somehow narrower (from $Đ_M$ = 1.67 to 1.47), suggesting that monomer activation by thiourea may be operative despite the low binding constant. The linear growth of the experimental molar mass ($M_{n,SEC}$) as a function of monomer conversion revealed a controlled character. When initiated in the presence of pyrenebutanol, the ROP of TCL catalyzed by this MTBD/thiourea combination featured similar ring-opening kinetics, as when initiated from octadecanethiol; the resulting polymers exhibited overlapping RI and UV SEC traces, consistent with high end-group fidelity. NMR studies were consistent with a chain-end activation mechanism where the base activates the thiol proton by nucleophilic attack (Figure 1.19); this contrasts with the traditional ROP organocatalysis towards polyesters wherein the chain-end is activated through strong H-bonding.

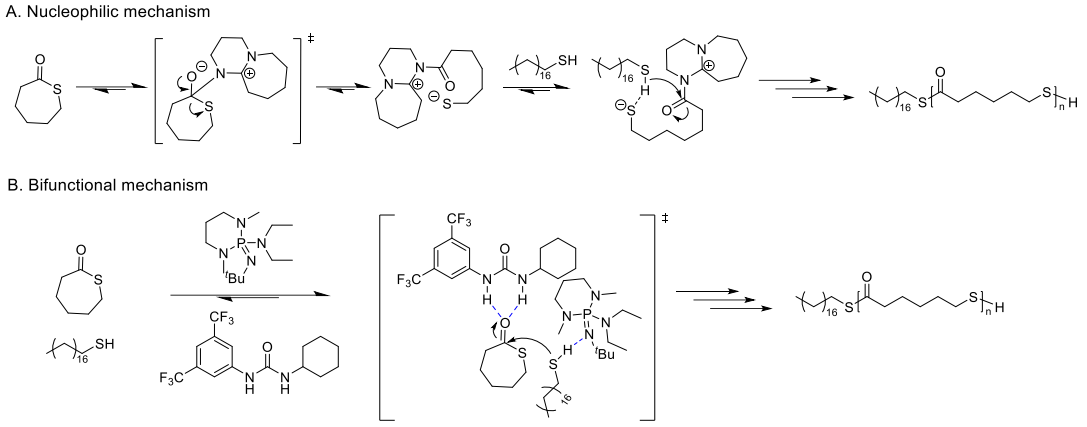

Figure 1.19. Proposed mechanisms for ROP of TCL.[36]

On the other hand, high molar mass PTCL (M_n = 30,000 g mol^{-1}) was also prepared by lipase-catalyzed polymerization of 6-mercaptohexanoic acid.[38] As expected, it was found that the T_m of the resulting PTCL (*ca.* 102 °C) was much higher than that of the corresponding oxo analogue PCL (T_m = *ca.* 60 °C). More interestingly, the obtained PTCL was observed to degrade nearly quantitatively by the same lipase in toluene at 100 °C after 8 days to produce cyclic oligomers, mainly consisting of TCL and the dimer of TCL, which could reproduce the PTCL with nearly the same molar mass as the initial PTCL, providing another opportunity to develop recyclable plastics.

In 2017, the group of Avérous reported the enzymatic ROP of ε-thiocaprolactone mediated by Novozyme 435, yielding the corresponding PTEs with low molar mass (M_n = 4,400 g mol^{-1}) and narrow dispersity ($Đ_M$ = 1.10) (Figure 1.20).[39] The methodology was extended to the ROCOP of ε-thiocaprolactone and ε-caprolactone by the same lipase in toluene at 70 °C in one-step or two-step copolymerization strategies, giving rise to relatively low molar mass copolymers (M_n = 2,900-10,800 g mol^{-1}). The copolymers resulting from the two strategies were apparently statistical in both cases (as determined by NMR and MALDI-ToF MS); they featured T_m values in the range of 31–56 °C that are lower than those of the corresponding homopolymers (T_m = 61 °C for PTC and T_m = 55 °C for PTCL, respectively).

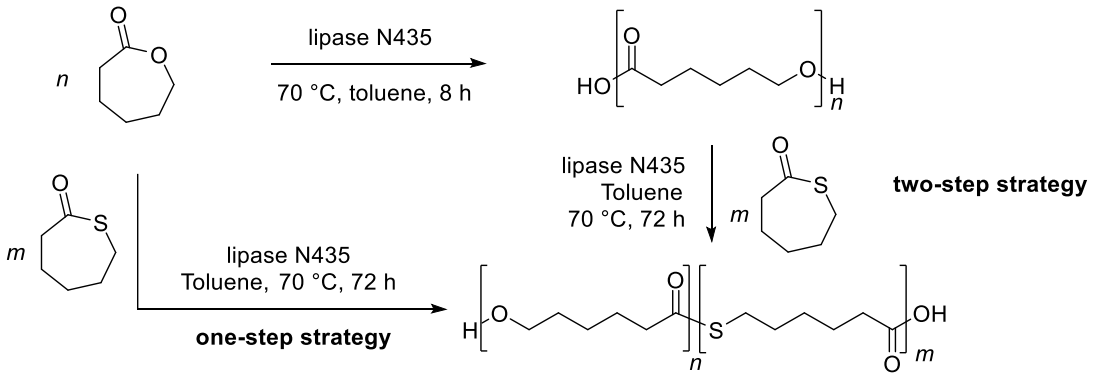

Figure 1.20. One- and two-step strategies for copolymerization of ε-thiocaprolactone and ε-caprolactone.[39]

In 2007, the group of Matsumura reported the enzymatic ROP of a cyclic (hexanedithiol-sebacate) thioester mediated by a lipase (Figure 1.21).[40] The cyclic (hexanedithiol-sebacate) monomer was synthesized from hexane-1,6-dithiol and dimethyl sebacate in the presence of immobilized lipase CA, yet in a low isolated yield (16%), as customary of macrocyclic monomers. The ROP reaction produced PTEs with high molar mass (M_w = 120,000 g mol^{-1}), significantly higher than that of the PTE obtained by direct polycondensation of the dithiol and diacid. The molar mass of the PTEs was influenced by the reaction conditions, such as reaction temperature, enzyme concentration, and reaction time. The resulting poly(hexanedithiol-sebacate) had a higher melting temperature (T_m = 108.8 °C) than the corresponding ester analogue (T_m = 74.8 °C).

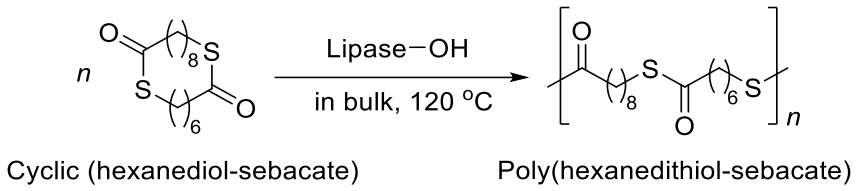

Figure 1.21. Lipase-catalyzed ROP of a large cyclic thioester.[40]

1.2.5 Ring-Opening Polymerization of *S*-Carboxyanhydrides

In 2021, the group of Tao reported the formation of PTEs from *S*-carboxyanhydrides (SCA) which can be synthesized from α-amino acids in good yields (Figure 1.22).[41] A series of catalysts/initiators, such as TEA, DMAP, dodecyltrimethylammonium bromide (DTMeAB), tetraoctylammonium bromide [(Oct)$_4$Br], and PPNCl ([PPN] = bis(triphenylphosphine)iminium), were used to promote the ROP of *D*-SerSCA. Among these, TEA- and DMAP-based systems gave oligomers with molar mass lower than the theoretical values; the DTMeAB, (Oct)$_4$Br, and PPNCl systems mediated a poorly controlled ROP, as the observed molar mass values were significantly higher than the predicted ones. Surprisingly, the introduction of an acidic chain transfer agent (CTA) markedly favored the control of the molar mass of the resulting PTE, delivering ultrafast polymerization (TOF = *ca*. 1,500 min^{-1}) and PTEs with narrow dispersity. The controlled nature of these ROPs was confirmed by the quite good agreement between the experimental molar masses and the theoretical ones calculated from the conversion and $[SCA]_0/[CTA]_0$ ratios, the linear growth of the experimental molar masses as a function of monomer conversion coupled with narrow dispersities ($Đ_M$ < 1.3), and the chain extension experiment (*i.e.*, upon addition of extra monomer).

Most importantly, the stereoregularity of the isolated PTE prepared with the PPNOBz/BzOH system was retained, indicating that this system does not promote racemization of SCAs nor of the resulting PTEs.

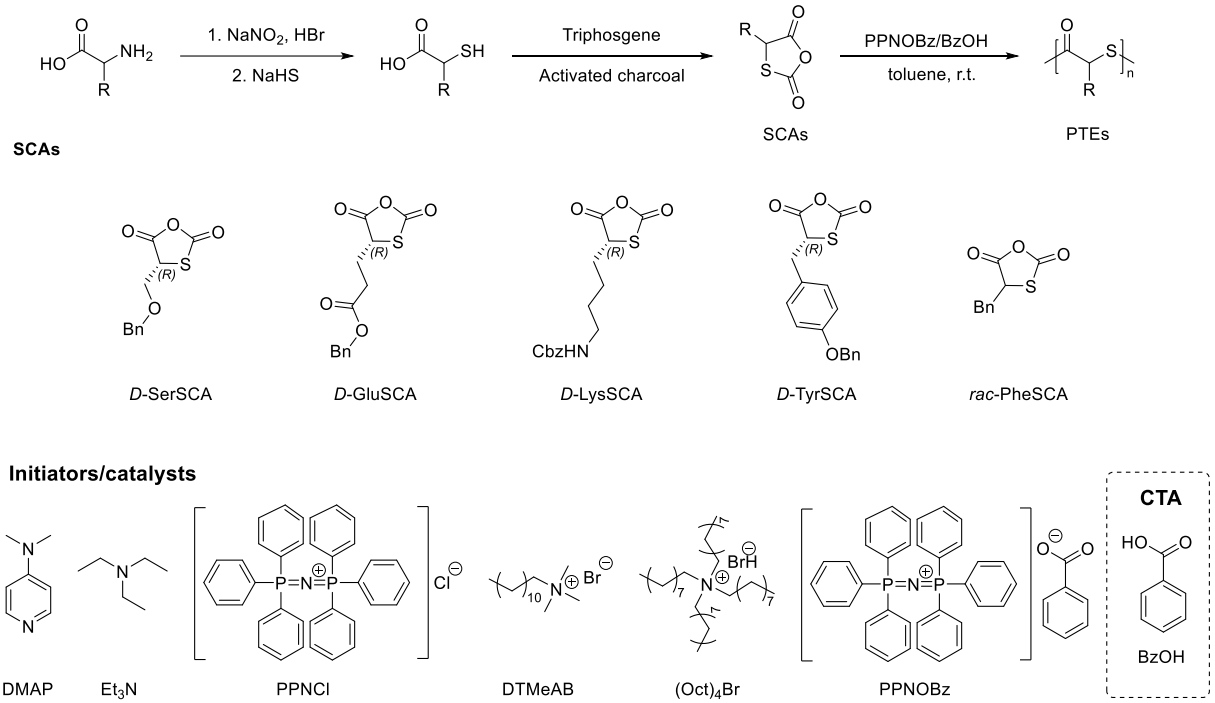

Figure 1.22. Typical synthesis of *S*-carboxyanhydrides and their subsequent ROP using organocatalysts and a chain-transfer agent (CTA).[41]

A remarkable feature of this approach is its versatile functionality due to the diverse structures of starting α-amino acids. Hence, this chemistry was successfully extended to the ROP of *D*-GluSCA, *D*-LysSCA, *D*-TyrSCA, and *rac*-PheSCA (Figure 1.22).[41] All polymerizations were rapid and controlled, similarly to the ROP of *D*-SerSCA. A random or sequential copolymerization of *D*-SerSCA and *D*-GluSCA gave a well-defined random or block copolymer, respectively. Valuably, the ROP reaction is water-insensitive and proceeds smoothly under air. Overall, these ROPs of SCA monomers offer control and tuning of molar mass, dispersity, stereoregularity, and side-chain functionalities. Similarly to polydithiolactones, preliminary studies showed that these isolated PTEs prepared from SCAs feature good depolymerization ability under mild conditions (triethylamine as the catalyst in $CDCl_3$ at room temperature), giving a quantitative recovery of the corresponding cyclic dithioester monomers.

DFT computations supported that the selectivity towards monomer propagation over transthioesterification is a consequence of the high polymerizability of SCAs.[41] Also, the calculated energy barrier for chain back-biting involving nucleophilic attack onto the terminal anhydride is higher than that of chain propagation. Based on these results, a plausible mechanism for the ROP of SCAs was proposed, as modelled with PPNOBz (the best initiator established experimentally) (Figure 1.23). The reaction starts with the nucleophilic attack of PPNOBz onto the highly reactive monomer, with concomitant release of CO_2. Then, the formed thiolate is protonated by the carboxylic acid used as CTA, generating a thiol and another carboxylate. This initiation step proceeds iteratively until all carboxylic acid is consumed. After that, proton transfer between dormant (thiol) and active chain-ends (thiolate)

enables propagation. Owing to the large acidity discrepancy between the initiating and propagating species, chain growth shows an induction period, as evidenced by experimental kinetic studies.

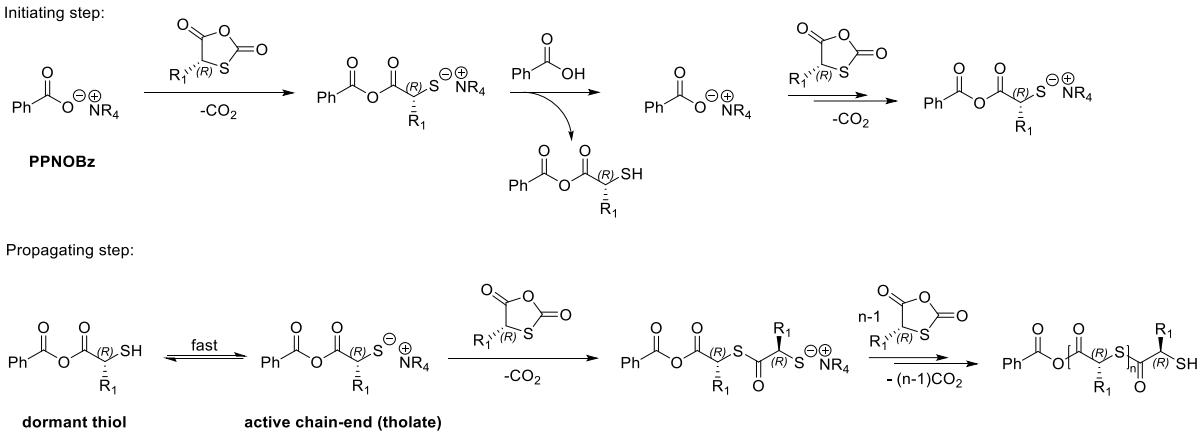

Figure 1.23. Plausible mechanistic pathway for the PPNOBz/BzOH-mediated ROP of SCAs based on DFT calculations.[41]

1.2.6 Isomerizing Ring-Opening Polymerization of 5-Membered Thionolactones

Thionolactones are another category of sulfur-containing monomer for synthesizing PTEs. The advantage of these monomers is that they can be, as a comonomer, incorporated into polyacrylates or polyolefins by radical ring-opening polymerization, which combines the advantages of both radical polymerization and ROP, to produce biodegradable polymers for biomedical applications.[42-46] Those reactions are yet out of the scope of the present review and, although thionolactones have attracted much attention over the past few years in polymer science, only salient homopolymers obtained from the ROP of thionolactones are discussed herein.

A recent contribution by the group of Hong reports the formation of sustainable and degradable poly(γ-thionobutyrolactone)s (PgTBLs) by polymerization of challenging five-membered γ-thionolactones (Figure 1.24).[47] The reaction is thermodynamically driven by the S/O isomerization instead of ring-strain relief, and thus referred to as isomerization ROP (IROP). The controlled IROP of TnBL takes place in the presence of the strongly basic phosphazene $^{t}BuP_4$ and Ph_2CHOH; it was typically performed in highly concentrated toluene solution, the high monomer concentration being a critical factor for driving the IROP, at 80 °C within a few hours, forming PTBLs with high selectivity (up to 97%). The controlled nature of this IROP was confirmed by the linear growth of the experimental molar mass as a function of monomer feed ratio (at full monomer conversions), along with relatively narrow dispersity ($Đ_M$ <1.6). $M_{n,SEC}$ as high as 162,600 g mol^{-1} could be reached, while the previously reported cationic ROP of γ-thionobutyrolactone generated oligomers with molar mass values that did not exceed 6,300 g mol^{-1} along with broad dispersity ($Đ_M$ > 2.2).[48]

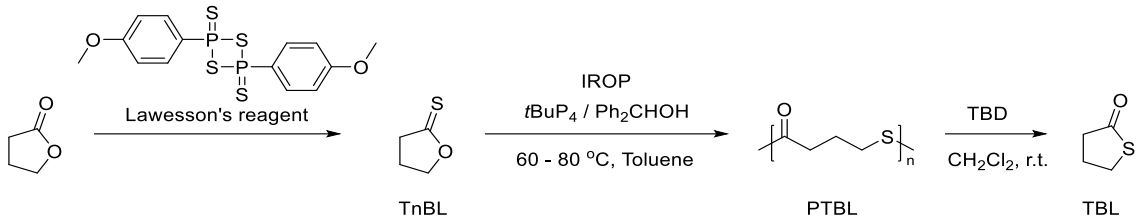

Figure 1.24. Synthesis and isomerizing ROP of γ-thionolactones.[47]

The high molar mass PTBL obtained revealed a semicrystalline thermoplastic with high melting and degradation temperatures (T_m = 100 °C; $T_d^{5\%}$ = 230 °C), which exhibits good mechanical and hydrophilic performance (M_n = 162.6 kg mol^{-1}: Young's modulus, E = 296.5 MPa; yield strength, σ_y = 15.7 MPa; tensile strength, σ_b = 29.8 MPa; elongation at break, ϵ_B = 412.5%; and static contact angle, θ = 78.4°). This kind of PγTE features thermal and mechanical properties that are competitive with commercial low-density polyethylene (aka LDPE: $T_m \approx$ 105 °C, $E \approx$ 280 MPa, $\sigma_y \approx$ 8 MPa, $\sigma_b \approx$ 10 MPa, $\epsilon_B \approx$ 200%, $\theta \approx$ 102°).[49] This suggests the utility of PTBL as an alternative to petroleum-based non-degradable plastics. In fact, the organocatalyst 1,5,7-triazabicyclo[4.4.0]dec-5-ene (TBD) efficiently promotes the degradation of PTBL, quantitatively converting it into its γ-thiobutyrolactone, bestowing a valuable end-of-life to such polymers.

The generality of the above IROP strategy was extended to methyl-substituted TnBL derivatives (Figure 1.25); this included α-methyl-γ-thionobutyrolactone (α-MeTnBL), β-methyl-γ-thionobutyrolactone (β-MeTnBL) and γ-methyl-γ-thionobutyrolactone (γ-MeTnBL), which can be prepared via one-step sulfurization of the corresponding methyl-substituted γ-butyrolactones. Under the optimized conditions established for the IROP of TnBL, rapid and selective polymerizations of α-MeTnBL and β-MeTnBL were also achieved by the combination of *t*BuP$_4$ and Ph$_2$CHOH, providing the corresponding PγTEs with high molar mass. However, when switching to γ-MeTnBL, the use of the above catalytic system only formed the dimer of γ-MeTnBL.

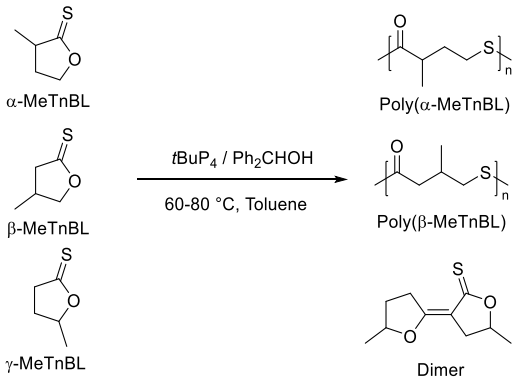

Figure 1.25. Generalization of the IROP strategy to related γ-thionolactones.[47]

Further mechanistic insights were gained from DFT computational studies (Figure 1.26). The calculated energy profile showed that the energy barrier of the proton-transfer pathway facilitated by

Ph_2CHOH-mediated deprotonation is substantially lower than that of the nucleophilic pathway. This clearly suggests that the polymerization is selectively initiated through the kinetically favourable proton transfer pathway; this is supported by the observation of the HS- end-group of low molar mass PTBL analyzed by electrospray ionization mass spectrometry (ESI MS). Noteworthy, not only does Ph_2CHOH play an important role in facilitating the deprotonation process, it also effectively suppresses backbiting side-reactions during propagation by acting as an H-bonding donor to stabilize the $–C(O)S^-$ propagation species along with $[t\text{BuP}_4\text{H}]^+$, thereby accounting for the controlled IROP of such TnBLs. Four different TBL ring-opening modes, namely paths A, B, C and D, were considered (Figure 1.26): the formed enolate anion active species ([Int.]) could attack another TBL monomer via two reactive sites, site 1 and site 2, by either enolate-S^- (site A) or enolate-C^- (site B).The energy profile of these four ring-opening modes (propagating step), and in particular the much lower energy barrier of path C, revealed the origin of the thermodynamically advantageous S/O isomerization product: the exclusive cleavage of the O−alkyl bond of TnBL (path C) rather than of the more commonly opened O−acyl bond (paths A and B) provides an overall thermodynamic driving force for the ROP of non-strained γ-thionobutyrolactones at room temperature or above towards PTE.

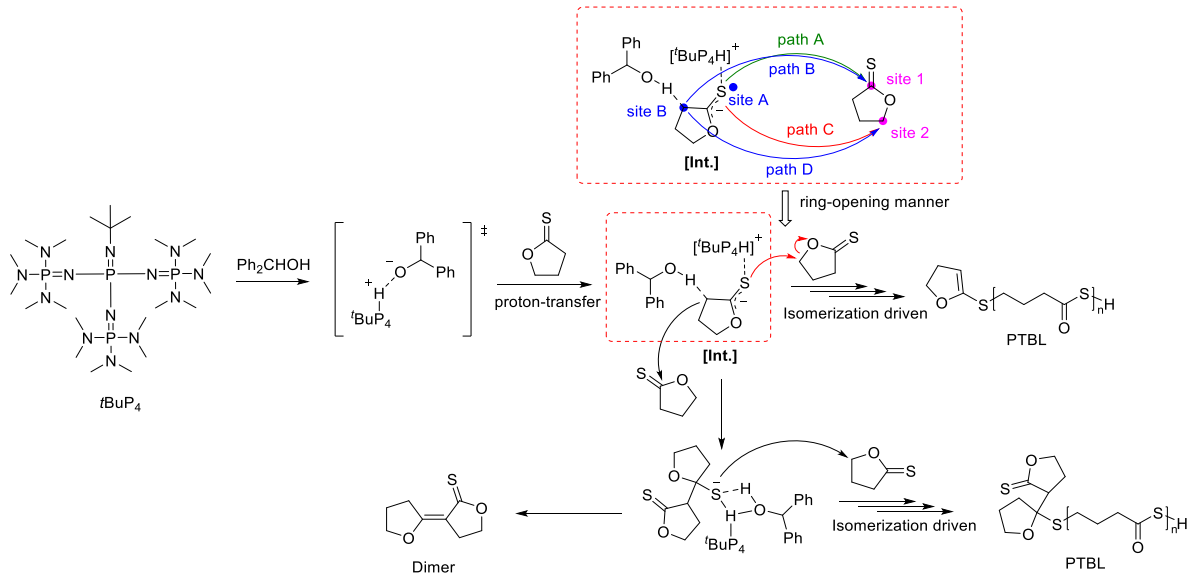

Figure 1.26. Possible mechanistic pathway for the isomerizing ROP of TnBL.[47]

Although advances have been made in the field of PTEs, all of these examples returned atactic polymers, unless starting from enantiomerically pure monomers. Compared with PTEs, the formation of stereoregular polyesters, has made impressive progress over the past two decades through the ROP of the corresponding chiral racemic heterocyclic monomers mediated by well-defined metal-based complexes or organocatalysts. Control of stereoselectivity, when the chiral racemic monomer is used, provides materials with finely tuned properties for specific applications.

1.3 Aliphatic Polyesters with Controlled Tacticity Prepared by Stereoselective Ring-Opening Polymerization of Chiral Racemic Heterocyclic Monomers

This section covers the contributions of the last two decades concerning the stereoselective ring-opening polymerization (ROP) of racemic heterocyclic monomers towards stereoregular polyesters. Only salient examples of high stereocontrolled catalysts (P_m, P_r or $\alpha > 0.80$) and new chiral monomers will be discussed.

1.3.1 Metal-Mediated Stereoselective Ring-Opening Polymerization of Chiral Racemic Heterocyclic Monomers

Among all chiral monomers, the stereoselective ROP of *racemic* lactide (*rac*-LA) has been the most extensively studied over the past two decades due to the attractive applications of the resulting polymers.

1.3.1.1 Stereoselective Ring-Opening Polymerization of *rac*-Lactide

Polylactides (PLAs) with different kinds of stereosequences (isotactic, heterotactic, stereoblock) and sometimes self-assembled (stereocomplexed PLA) have been successfully prepared by well-defined metal-based complexes (Figure 1.27).[5,50-54] Studies of the resulting PLAs have shown a strong correlation between the thermal properties of PLAs and their stereosequences; specifically, the melting point (T_m) of homochiral PLLA or PDLA is *ca.* 180 °C, while that of a stereocomplex (double strained polymer formed from a 1:1 mixture of PLLA and PDLA) is *ca.* 50 °C higher than that of the homochiral polymers. Because PLA starts to decompose when heated above its T_m, the formation of such stereocomplex is an attractive technique to improve its thermal stability.

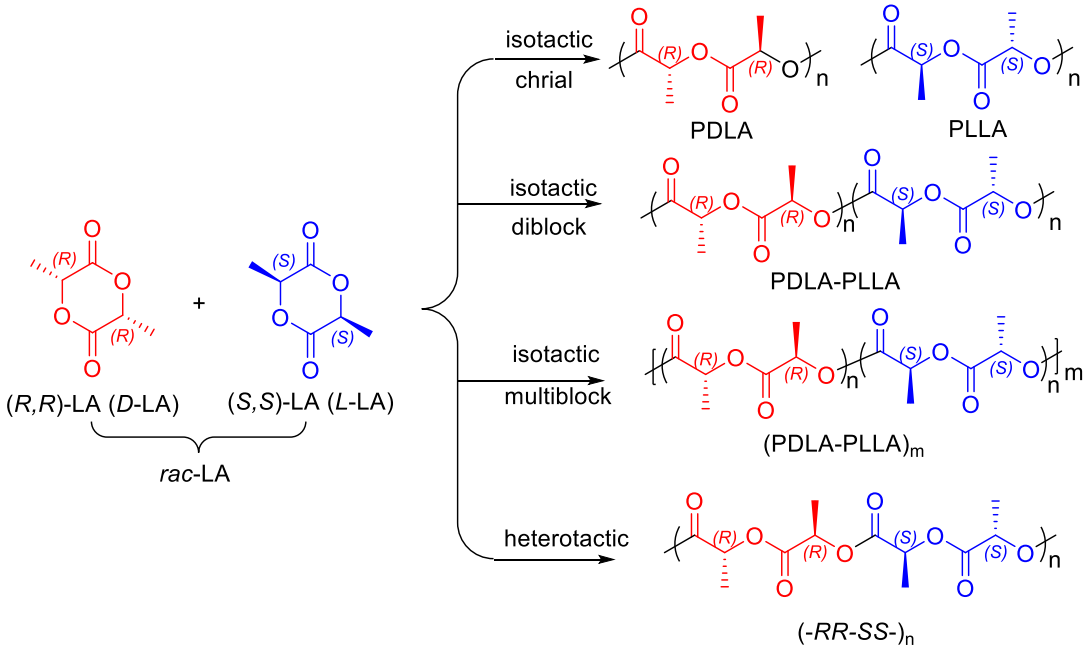

Figure 1.27. Polylactide (PLA) microstructures.[55]

Among the variety of catalysts/initiators that have been used for this purpose, of particular note are undoubtedly rare-earth complexes, especially yttrium ones in terms of activity and stereoselectivity. In this section, special emphasis will be placed on these systems.

Our group was the first to report the formation of heterotactic PLA by using yttrium complexes bearing tripodal tetradentate bis(phenoxy) ligands (Figure 1.28); these have now been widely investigated.[56] Manipulation of the substituents on the phenoxy rings allowed access to PLAs with different levels of heterotacticity (P_r values in the range 0.56−0.96).§ The more sterically hindered substituents at the *ortho*-position (R^1), the higher the heterotacticity [Cl (P_r = 0.56) < CMe_3 (P_r = 0.80) < CMe_2Ph (P_r = 0.90) < CMe_2 (4-CF_3-Ph) (P_r = 0.93–0.94) < CMe_2*t*Bu (P_r = 0.94–0.95) < CPh_3 (P_r = 0.95–0.96)].[57,58] The electronic nature of the substituents appears to exert much less influence, indicating that the reaction is under steric control; this is consistent with usual hypothesis for a "chain-end control" (CEC) mechanism. Another important factor in these *rac*-LA ROP reactions is the solvent. High heterotacticities were observed by using THF as the solvent, while with toluene or dichloromethane, much lower stereoselectivities were found (*e.g.*, P_r = 0.65 in toluene vs. P_r =0.90 in THF).

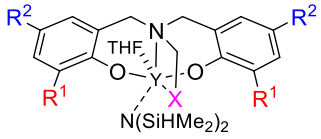

"Y{ONXO^{R1,R2}}{N(SiHMe$_2$)$_2$}(THF)"

Y-1

Carpentier, 2004, 2006, 2011

X =	CH_2NMe_2	CH_2OMe
R^1 = R^2 = *t*Bu	**a**	**b**
R^1 = R^2 = CMe_2Ph	-	**c**
R^1 = R^2 = Me	-	**d**
R^1 = R^2 = Cl	-	**e**
R^1 = CPh_3, R^2 = Me	-	**f**
R^1 = CMe_2*t*Bu, R^2 = Me	-	**g**
R^1 = CMe_2(4-$CF_3C_6H_4$), R^2 = Me	-	**h**
R^1 = CMe_2Ph, R^2 = Me	**i**	**j**
R^1 = CMe_2(*p*Cl-Ph), R^2 = Me	-	**k**

Figure 1.28. Yttrium-based complexes used for the stereoselective ROP of *rac*-LA.[56-60]

Okuda and coworkers have investigated a series of yttrium, scandium, and lutetium complexes supported by *1,ω*-dithiaalkanediyl-bridged bis(phenolate) ligands for the ROP of *rac*-LA (Figure 1.29).[61,62] Again, the ancillary ligand proved critical for stereoselectivity. Indeed, the stereoselectivity of these group 3 complexes increased with the size of the bisphenoxy ligands. However, the influence of the bridge turned out to be even more pronounced. The most notable surge in heterotacticity was observed with the extension of the bridging unit from C_2 to C_3 along with the bulkiness of the *ortho*-substituent (R^1) on the phenoxy groups; a further increase in the length of the bridging unit to a C_4

§ P_m and P_r probabilities are synonymous with the dyad tactic fraction (*m*) and (*r*). In the ROP of chiral cyclic monomers, the degree of stereoregularity is commonly expressed as the probability of *racemic* or *meso* enchainment (probability of generating a next *racemic* (syndiotactic) or *meso* (isotactic) dyad), P_r and P_m (P_m =1–P_r), respectively. P_r = P_m =0.50 describes a completely atactic polymer; P_m = 1.00 (*i.e.*, P_r = 0.00) and P_m = 0.00 (*i.e.*, P_r = 1.00) describe perfectly isotactic and syndiotactic polymers, respectively. These parameters can be calculated from the deconvoluted homonuclear decoupled ^{1}H NMR and/or quantitative ^{13}C NMR spectra (more details, see Appendices).

bridge did not bring any further improvement in heteroselectivity. The scandium complex led to the highest degree of heteroselectivity (P_r as high as 0.95), while the yttrium complex led to PLAs with the P_r values ranging from 0.84 to 0.88. This increased heteroselectivity for the scandium complexes is attributed to its small ionic radius, enabling the ancillary ligand to exert a more significant steric effect.

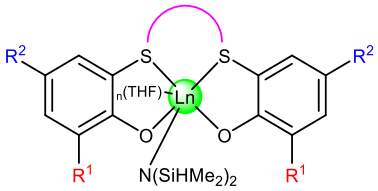

"Ln{OSSO^{R1,R2}}(THF)$_n${N(SiHMe$_2$)$_2$}"

Ln-2

Okuda, 2006, 2008

	Bridge	R^1	R^2	P_r		
				Sc	Y	Lu
C_2	-$(CH_2)_2$-	*t*Bu	Me	0.78	0.68	0.64
	-$(CH_2)_2$-	*t*Bu	*t*Bu	0.80	0.71	-
		*t*Bu	Me	0.82	0.72	0.67
C_3	-$(CH_2)_3$-	*t*Bu	Me	0.95	-	-
	-$(CH_2)_3$-	*t*Bu	*t*Bu	-	0.84	-
C_4		*t*Bu	Me	0.94	0.85	0.82
		CMe_2Ph	CMe_2Ph	-	0.86	-
		1-adamantyl	Me	0.93	-	-
		*t*Bu	Me	0.94	0.88	-

Figure 1.29. Group 3 complexes were reported by Okuda and coworkers for the stereoselective ROP of *rac*-LA.[61,62]

The authors proposed that the stereochemistry is controlled by a dynamic monomer recognition process involving interconversion of the ligand configuration, as illustrated in Figure 1.30. There are two enantiomers of the complex, **Λ** and **Δ**, each showing a particular selectivity for a certain enantiomer of *rac*-LA. After the insertion of either enantiomer of *rac*-LA in the initiating step, the bulky chiral environment around the metal centre generated by the ligand framework enables one of the enantiomers to approach and coordinate onto the metal centre. After the ring opening of the coordinated monomer, steric repulsion between the *S*-methyl group of the ring opened LA unit and the *ortho*-substituent of the ligand induces a transformation between **Λ** and **Δ**. The **Δ** enantiomer selectively attacks (*R*,*R*)-LA, eventually leading to the formation of highly heterotactic PLA. Other groups have subsequently been referred this type of mechanism (*vide infra*).

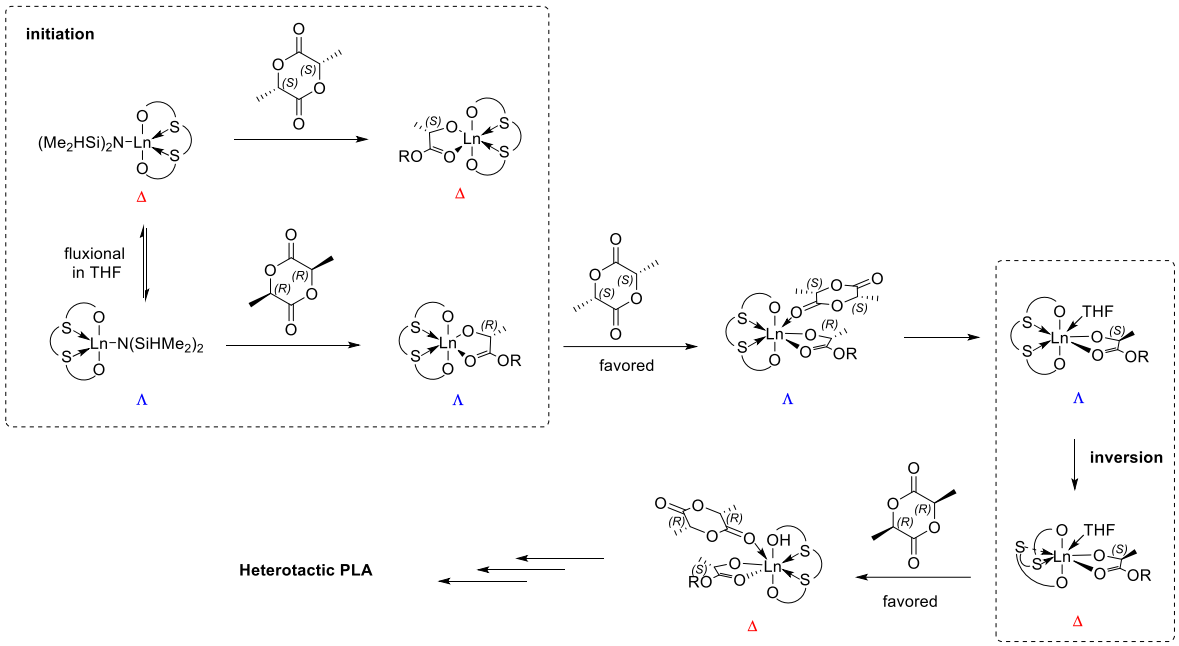

Figure 1.30. Proposed "dynamic monomer-recognition process" in heteroselective ROP of *rac*-LA.[62]

Williams and coworkers reported yttrium complexes supported by achiral phosphasalen ligands producing heterotactic PLAs with excellent rates (TOF > 11.5 s^{-1}) and high stereoselectivity (P_r up to 0.90) at r.t. (Figure 1.31).[63,64] It is well-known that modifying the length and nature of the bridging group between the phenoxy moieties of the related salen ligands can influence the catalytic behaviour. Indeed, phosphasalen yttrium complexes with C_2 bridge groups are much more active than those with C_3-bridged ligands; this contrasts with previous results reported by Nomura (*see above*), where C_3-bridged complexes were significantly faster and had more stereoselectivity than C_2-bridged analogues. It turned out that the more electron-donating ligand induces higher rate; conventionally, increased activity has been expected upon substitution of Lewis acidic complexes with electron-deficient groups.[6,65] On the other hand, the degree of heteroselectivity decreases according to the nature of the diimine linker group of the complexes in the order ethylene > cyclohexylene > phenylene > propylene. Thereby, the fastest phosphasalen yttrium complex shows the highest heteroselectivity. It is worth noting here that such heteroselectivity is relatively rare for this type of yttrium complex, as the related salen/salan yttrium initiators show little or no heteroselectivity (P_r < 0.7); this may be related to their excellent electron-donating abilities (strong σ- and π- donor abilities) and the increased steric shielding of the active site, in particular from the two phenyl substituents on the phosphorus atoms. The selection of solvent is also a crucial factor for achieving high heteroselectivity (*e.g.*, P_r = 0.67 in toluene *vs.* P_r = 0.84 in THF, for yttrium complex bearing phenylene-bridged phosphasalen ligand) in line with previous reports by our group, although the exact reason for this solvent effect remains obscure.

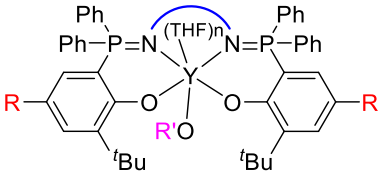

Y-3
Williams, Auffrant, 2012, 2013

	Linker	R	R'	n
C_2		*t*Bu	*t*Bu	0
		OMe	*t*Bu	0
		*t*Bu	*t*Bu	1
		*t*Bu	*t*Bu	1
		*t*Bu	*t*Bu	1
C_3		*t*Bu	*t*Bu	1
		*t*Bu	*t*Bu	1
		*t*Bu	EtO	1

Figure 1.31. Yttrium phosphasalen complexes used for heteroselective ROP of *rac*-LA.[63-65]

To investigate further the electronic influence of the yttrium phosphasalen complexes on ROP of *rac*-LA, Williams and coworkers targeted a novel phosphasalen ligand with an extra NH-donor in the bridging group (Figure 1.32, left).[65] Such hexacoordinate complex shows excellent activity (TOF ~ 870 h^{-1}) and good isoselectivity for *rac*-LA polymerization (P_m = 0.72−0.77), at 25 °C in THF, in a controlled manner. Upon decreasing the reaction temperature to -15 °C, the level of isoselectivity was improved with P_m values in the range 0.81−0.84. Careful analysis of the microstructures of the obtained PLAs revealed that the stereocontrol occurs by a CEC mechanism, implying that the coordination chemistry of the growing polymer chain plays a significant role in influencing the overall stereochemistry, in contrast to the former pentacoordinate yttrium complexes giving heterotactic PLAs (Figure 1.31).

In 2014, Williams and coworkers studied the influence of the nature of the metal center on the stereochemical outcome in ROP of *rac*-LA (Figure 1.32, right).[66] Combined with a "smaller" metal center, such as lutetium, such phosphasalen complex shows enhanced isoselectivity (P_m = 0.82 at 25 °C) compared to the parent yttrium complex (P_m = 0.72−0.77 at 25 °C). It was also possible to completely switch the stereoselectivity by coordinating a "larger" metal centre, *e.g.*, lanthanum, resulting in heterotactic PLA (P_r = 0.72, at 25 °C). Such contrasted behaviours were explained by a more sterically congested metal coordination sphere with reduced fluxionality of the phosphorus substituents in the case of yttrium and lutetium. In contrast, a more open coordination geometry and fluxionality of the phosphorus substituents accounted for the heteroselectivity in the case of a larger metal centre such as lanthanum.

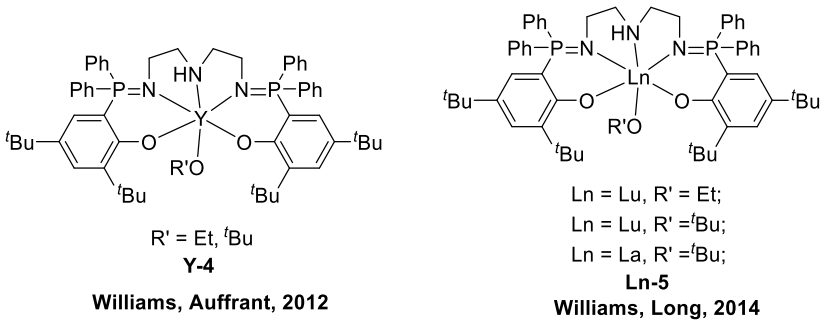

Figure 1.32. Group 3 phosphasalen complexes used for the stereoselective ROP of *rac*-LA.[65,66]

In 2018, Xu and coworkers developed highly active yttrium complexes stabilized by achiral bis(phenoxy) ether ligands to give stereoblock isotactic PLAs with P_m value up to 0.90 at -15 °C in DCM (Figure 1.33).[67] The isoselectivity of yttrium complexes improves as the size of the bis(phenoxy) ligand increases; the *tert*-butyl substituted yttrium complexes, irrespective of the nature of the bridging group, afford isotactic PLA (P_m = 0.83~0.84 at room temperature), while H-substituted ones lead to atactic PLAs. Kinetic studies revealed that chain-end chirality differentiates an enantiomer with the same chiral sense from *rac*-LA, indicating a CEC mechanism is operative in this catalytic system; this was further demonstrated by DFT calculations.

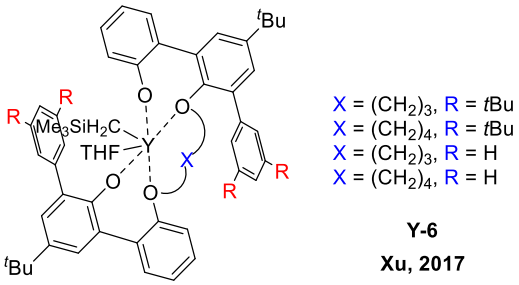

Figure 1.33. Yttrium bis(phenoxy) ether complexes for isoselective ROP of *rac*-LA.[67]

1.3.1.2 Stereoselective Ring-Opening Polymerization of Racemic Lactones

Another important bioderived and biodegradable synthetic plastic on the market is poly(β-hydroxybutyrate) (P3HB). P3HB is naturally produced by various bacteria and other living organisms, with perfect isotacticity. On the other hand, chemical synthesis of the corresponding racemic cyclic ester, namely *rac*-β-butyrolactone (*rac*-BL), provides a way to access P3HB by ROP with various microstructures (Figure 1.34).

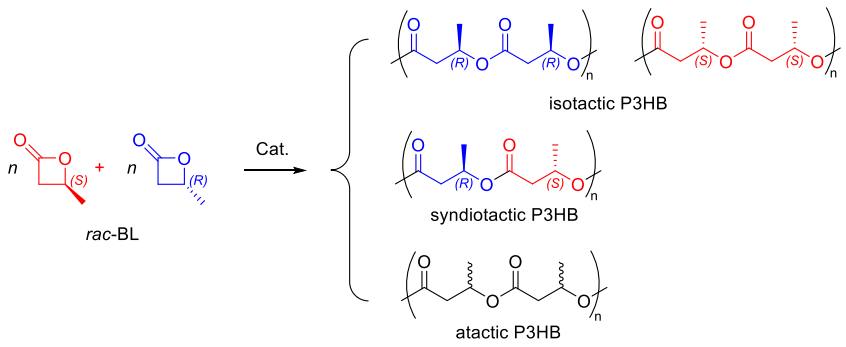

Figure 1.34. Chemically prepared P3HBs from ROP of β-butyrolactone (*rac*-BL).[21,68-70]

Although most catalytic systems effective towards *rac*-LA are extremely sluggish toward *rac*-BL and produce low molar mass P3HB, Coates and coworkers first reported that β-diiminate zinc alkoxide complexes (Figure 1.35) can efficiently polymerize *rac*-BL under mild conditions to give P3HB in a controlled manner.[71] However, all the P3HBs produced were found to be atactic. Despite advances in stereoselective ROP of β-lactones, stereospecific metal-based initiators remain rare.[21,68-70]

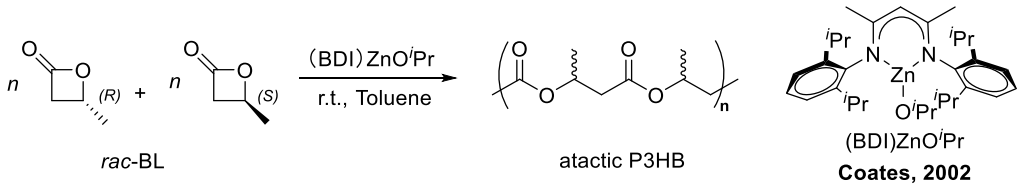

Figure 1.35. β-Diiminate zinc alkoxide complex used for ROP of *rac*-β-butyrolactone (*rac*-BL).[71]

The first example of stereocontrolled ROP of *rac*-BL was reported by Spassky and coworkers, using a chiral initiator obtained from the reaction of simple group 12/13 alkyl metals ($ZnEt_2$, $AlEt_3$, $CdMe_2$) with (*R*)-3,3-dimethyl-1,2-butanediol (Figure 1.36).[72] With the zinc- and aluminum-based initiators, the (*R*)-enantiomer of *rac*-BL was preferentially incorporated in the polymer chain with stereoselectivity ratios k_R/k_S of 1.6 and 1.1, respectively. On the contrary, the cadmium-based initiator polymerizes the (*S*)-enantiomer with a stereoselectivity ratio k_S/k_R of 1.01. The zinc-based initiator was the most isoselective system; fractionation of the resulting polymer gave a crystalline, predominantly isotactic part (P_m = *ca.* 0.8, insoluble in MeOH) and an amorphous atactic part (soluble in MeOH).

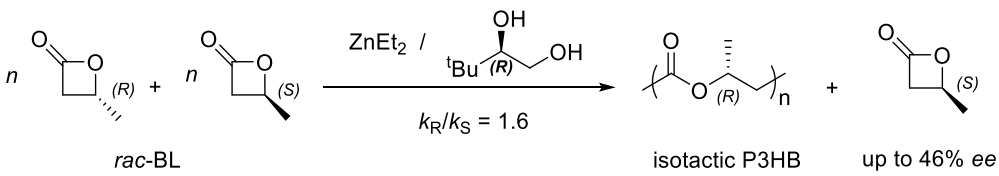

Figure 1.36. Isoselective ROP of *rac*-BL *via* kinetic resolution.[72]

Chromium(III) salophen complexes reported by Rieger and coworkers featured modest activity (TOF = 162 h^{-1} at 100 °C) and allowed the formation of high molar mass P3HB ($M_{n,SEC}$ up to 780 kg

mol^{-1}), yet with extremely broad dispersities ($Đ_M$ = 5.2~9.6), and only an isotactic-bias structure (P_m = 0.63-0.66) (Figure 1.37).[73]

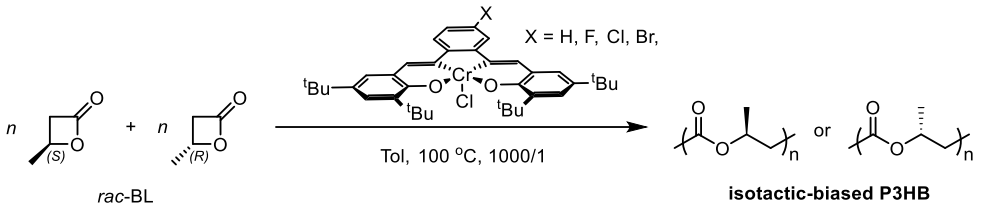

Figure 1.37. Access to isotactic-biased P3HB by ROP of *rac*-BL using chromium(III) salophen complexes.[73]

In 2006, our group showed that the aforementioned yttrium complexes (Figure 1.38) can achieve syndioselective ROP of *rac*-BL, with unprecedented catalytic performances under mild conditions (r.t.): high polymerization activity (TOF ~ 340−22,000 h^{-1}), excellent polymerization control, and high syndiotacticity (P_r up to 0.94).[57,74] The nature of the *ortho*-substituents on the phenoxy groups of the ligand (R^1) profoundly impacts the stereoselectivity. Less crowded substituents, such as methyl (**Y-1c**), led to atactic P3HBs (P_r = 0.56), while yttrium complexes with sterically hindered substituents, such as -CMe_2Ph (cumyl, **Y-1i**) or -CPh_3 (trityl, **Y-1e**), generate highly syndiotactic P3HBs (P_r values of 0.90 and 0.94, respectively). Nevertheless, not all bulky substituted complexes gave a similar level of syndioselectivity: the aliphatic CMe_2*t*Bu (**Y-1f**), having a similar steric bulkiness to that of cumyl, gave syndio-enriched P3HBs with a P_r of 0.70, actually much lower than that achieved with the less sterically crowded ^{t}Bu-substituted yttrium complex (P_r = 0.81, **Y-1a**). On the other hand, the yttrium complex (**Y-1g**) bearing the extra electron-withdrawing groups on cumyl groups (-CMe_2(*p*-CF_3-Ph)) is significantly less syndioselective than the parent cumyl-substituted complex (P_r = 0.83 vs. 0.91, respectively). Hence, both steric and electronic considerations seem to be operative in these stereocontrolled reactions. DFT calculations on the model intermediates revealed that the stabilizing interactions (−CH_2···π phenyl interactions) between a hydrogen from a methylene group of the last inserted BL unit and the aryl rings present in *ortho*-substituents of the ligand, account for the formation of high syndiotactic P3HBs.[57] When bulky substituted ligands (such as *t*Bu) are combined with various lanthanide metals (such as Yb, Er, Sm), no pronounced effect on the stereoselectivity for *rac*-BL polymerization was observed; this is quite different from the ROP of *rac*-LA.[75]

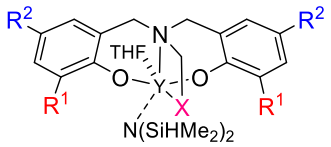

"Y{ONXO^{R1,R2}}{N(SiHMe$_2$)$_2$}(THF)"

Y-1

Carpentier, Thomas, 2006
Carpentier, 2003, 2004, 2011
Carpentier, Kirillov, 2014

X =	CH_2NMe_2	CH_2OMe
$R^1 = R^2 = t$Bu	-	**a**
$R^1 = R^2 = CMe_2Ph$	-	**b**
$R^1 = R^2 = Me$	-	**c**
$R^1 = R^2 = Cl$	-	**d**
$R^1 = CPh_3$, $R^2 = Me$	-	**e**
$R^1 = CMe_2t$Bu, $R^2 = Me$	-	**f**
$R^1 = CMe_2(4\text{-}CF_3C_6H_4)$, $R^2 = Me$	-	**g**
$R^1 = CMe_2Ph$, $R^2 = Me$	**h**	**i**
$R^1 = CMe_2(p$Cl-Ph), $R^2 = Me$	-	**j**

Figure 1.38. Amino-alkoxy-bis(phenoxy) yttrium complexes used for stereoselective ROP of *rac*-BL.[57,59,74]

^{13}C NMR spectroscopic studies of P3HBs with different levels of syndiotacticity enabled a detailed assignment of carbonyl, methylene, and methine resonances at the dyad and triad levels.[76] On this ground, a statistical Bernoulli analysis confirmed that syndioselectivity originates from a CEC mechanism. In addition, a relatively strong solvent-dependence of stereoselectivity was observed in the reaction, P_r values in toluene are much higher than those in THF (*e.g.*, P_r = 0.83 in THF *vs.* 0.94 in toluene for **Y-1i**, respectively). It is noteworthy that the reverse trend, *i.e.* better stereoselectivity in THF than that in toluene, was observed in ROP of *rac*-LA with the same yttrium complexes.[56] Out of the expectation, switching the metal center from yttrium to scandium stabilized by the same bulky ligands, such as ***b***, ***h-j***, the complexes are inactive for *rac*-BL under similar conditions.[59]

In 2008, our group in collaboration with Trifonov and coworkers reported a series of new bis(guanidinate) alkoxide group 3 metal complexes (Figure 1.39).[77] These complexes are moderately active catalysts/initiators for *rac*-BL living polymerization with TOF up to 30 h^{-1} at room temperature in toluene, giving syndiotactic-enriched P3HBs (P_r up to 0.84).

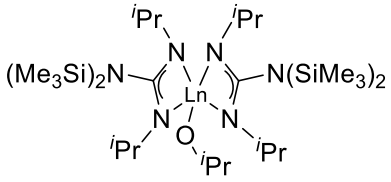

Ln = Y; Lu

Ln-7

Trifonov, Carpentier, 2008

Figure 1.39. Bis(guanidinate) alkoxide group 3 metal complexes used for stereoselective ROP of *rac*-BL.[77]

In 2010, our group reported a series of scandium, yttrium and lanthanum amido complexes supported by tridentate bis(*ortho*-silyl-substituted naphtholate) ligands (Figure 1.40).[78] These complexes based on *o*-$SiPh_3$ substituted ligands converted *rac*-BL at 20−50 °C into P3HBs with TOF up to 720 h^{-1}, while complexes having *o*-$SiMe_2{}^t$Bu substituents on the naphtholate rings were found inactive towards *rac*-BL polymerization, regardless of the metal centre. In line with our previous work

on stereoselective ROP of *rac*-BL with amino-alkoxy-bis(phenolate) yttrium systems,[57] a strong solvent-dependence of stereoselectivity was observed in this catalytic system as well: syndiotactic-enriched P3HB (P_r up to 0.87) was obtained when using toluene as solvent, while atactic P3HB was obtained in THF. The degree of stereocontrol in these polymerizations of *rac*-BL is significantly affected by the nature (and ionic radius) of the metal centre (Sc, Y, La), the central linker in the ligand framework (pyridine, thiophene), and the *ortho*-silyl substituent ($SiPh_3$, $SiMe_2tBu$), thereby providing a way to manipulate the ligand to obtain higher stereoregular P3HBs. However, no clear trends for predicting the structure/property relationships have been identified so far.

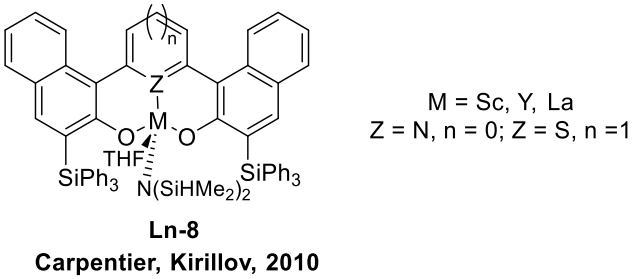

Figure 1.40. Syndiospecific ROP of *rac*-BL promoted by tridentate bis(naphtholate) based amido complexes.[78]

In 2013, our group reported the synthesis of yttrium complexes supported by original pyridine-bis(phenoxy) ligands and explored their behaviour in ROP of *rac*-BL (Figure 1.41).[79] Their performances (activity, tacticity) are much affected by the nature of the solvent. The ROP of *rac*-BL promoted by yttrium amido complex **Y-9a** allowed the formation of poorly (P_r values of *ca.* 0.60 for those obtained in pyridine, TOF: 492 h^{-1}) to highly syndiotactic P3HBs (P_r values of *ca.* 0.80 for those produced in toluene, TOF: 65 h^{-1}). Surprisingly, when five equivalents of pyridine were added to the reaction medium that preformed in toluene, the catalyst performance was dramatically amplified (TOF: 12,000 h^{-1}, $P_r \sim 0.86$). The origin of these effects remains unclear; yet, one possibility is a *trans* influence occurring through coordination of pyridine onto the yttrium centre. Such neutral donor improving catalytic behaviour in the stereoselective ROP of *rac*-BL is not an exception (*vide infra*); this seems to provide a simple and inexpensive way to modulate catalyst performance further.[80]

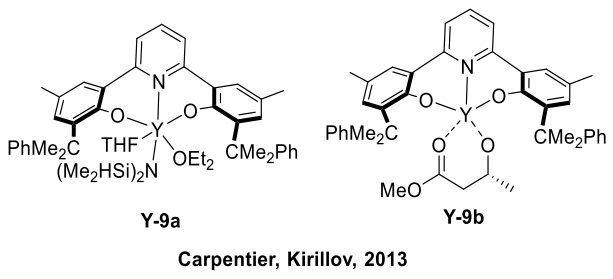

Figure 1.41. Syndiospecific ROP of *rac*-BL promoted by pyridine-bis(phenoxy) yttrium amido complexes.[79]

Yttrium complexes proved to be the most efficient initiator for stereoselective ROP of *rac*-BL to give highly syndiotactic P3HB (P_r up to 0.94). Thomas and coworkers expanded the scope of the ligand to salan (Figure 1.42), which has already shown impressive performance in aluminium-based stereoselective ROP of *rac*-LA.[81,82] With reasonable polymerization control, such a catalytic system led to highly syndiotactic P3HBs (P_r up to 0.90). DFT investigations on the stereoselectivity of the first two monomers insertion are fully consistent with the experimentally observed tacticity, which originates from a CEC mechanism.[81]

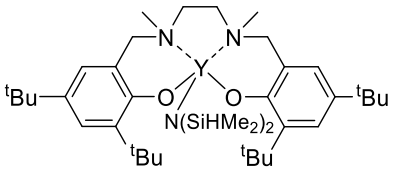

Y-10
Thomas, 2009, 2013

Figure 1.42. ROP of *rac*-BL by using salan-yttrium complex.[81]

In 2018, Yao and coworkers revisited rare-earth metal salan complexes by tuning the substituents on the *N* atoms of the salan ligand framework and subsequently using these complexes for the ROP of *rac*-BL (Figure 1.43).[83] Regardless of the nature of the metal centre, the tacticity of the resulting P3HBs is drastically affected by the substituents on the bridging *N* atoms: phenyl groups induce the formation of isotactic-enriched P3HB (P_m up to 0.77), and *t*Bu groups give rise to atactic P3HB (P_m= 0.52~0.54). In contrast, cyclohexyl substituents lead to syndiotactic-enriched P3HB (P_r up to 0.78). Although the tacticity values remain low (P_m value typically ranges from 0.22 to 0.77), these results provide a remarkable example that solely tuning the substituents on the *N* atoms of the ligand frameworks can induce a switch of the polymerization stereoselectivity. However, the nature of the stereocontrol mechanism was not yet established. One can postulate that, since both substituents on the bridging *N* atoms on the ligands eclipse central metal atoms, the backbone substituents can closely approach the site of polymer chain growth and thereby influence monomer selectivity.

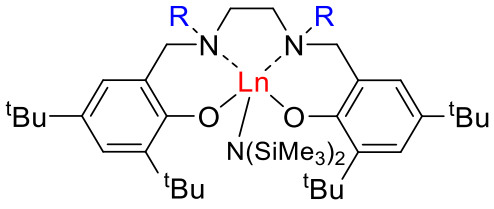

Ln =	Y	Yb
R = Ph	10a	11a
R = Cy	10b	11b
R = *t*Bu	10c	11c

Yao, Wang, Luo, 2018

Figure 1.43. Salan-yttrium complexes used for the stereoselective ROP of *rac*-BL.[83]

Recently, Robison and coworkers discovered that replacing the capping donor group of tetradentate amino alkoxy bisphenoxy ligand (*see above*) with a non-coordinating *N*-benzyl substituent,

generated six-coordinated lanthanum amide complex **La-12** which catalytic performance towards *rac*-BL could be amplified by an exogenous neutral donor ligand (Figure 1.44).[84] Compared with the parent complex **Y-1a**, the ROP of *rac*-BL promoted by this lanthanum complex **La-12** was sluggish (TOF = 42 h^{-1}). Surprisingly, isotactic-biased P3HB (P_m = 0.57) was generated, which is the opposite tendency as compared to other Group 3 catalysts (*see above*) which in most cases return syndiotactic P3HB. When two equivalents of hard, monodentate phosphine oxide (OPR_3, R = nC_8H_{17}, Ph, NMe_2) were added into the catalytic system, the catalytic performance were enhanced (TOF ~ 194 h^{-1}, P_m = 0.71−0.75). The most robust donor, $OP(nC_8H_{17})_3$, generated the most active, isoselective catalyst for *rac*-BL (0 °C: TOF = 200 h^{-1}, P_m = 0.80). Structural comparisons of **La-12** with the structurally related tethered-donor complex **Y-1a** revealed that the opposite stereoselectivity origins from increased axial steric pressure exerted by the bulky exogenous neutral donor. Initial mechanistic studies with $OPPh_3$ showed that neutral donors impact several fundamental catalyst equilibria associated with propagation, stereocontrol, and catalyst deactivation. In their follow-up work, the stereoselectivity of this complex was found to be nearly independent of the donor strength and steric profile, despite the presence of a neutral donor being crucial to the observed isoselectivity.[85]

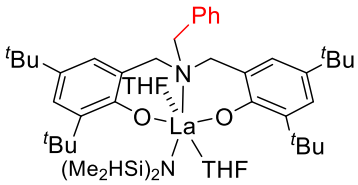

La-12
Robinson, 2020, 2022

Figure 1.44. Benzyl-amino-bisphenolate lanthanum complex used for isoselective ROP of *rac*-BL.[84]

Chen and coworkers realized an exciting breakthrough in the formation of perfectly isotactic P3HB using a different strategy (Figure 1.45).[86] A racemic cyclic dimer of 3-hydroxybutyrate, namely the eight-membered cyclic diolide (*rac*-DL), was used to form perfectly isotactic P3HB. The best catalyst proved to be chiral yttrium salcy species **Y-15d**, featuring trityl groups installed at the *ortho*-phenoxy positions (R^1) of the salen-type ligand; it produced purely isotactic P3HB (P_m > 0.99, [*mm*] > 99%) in a controlled manner with a high T_m of up to 171 °C, M_n of up to 154 kg mol^{-1}, and low dispersity ($Đ_M$ = 1.01) under ambient conditions. The stereoselective ROP of *rac*-DL with enantiomeric catalysts **(*R*,*R*)-Y-15d** and **(*S*,*S*)-Y-15d** automatically stops at 50% conversion and yields enantiopure (*R*,*R*)-DL and (*S*,*S*)-DL with > 99% *ee*.

The corresponding poly[(*S*)-BL] and poly[(*R*)-BL] generated by enantiomeric catalysts, **(*R*,*R*)-Y-15d** and **(*S*,*S*)-Y-15d**, respectively, have a high T_m of 175 °C, which is higher (by 5−7 °C) than that of 1:1 mixture of poly[(*R*,*R*)-BL] and poly[(*S*,*S*)-BL], indicating no stereocomplexation between two enantiomeric P3HB chains. MALDI-ToF MS investigations revealed that when using ***rac*-Y-15** for *rac*-

DL polymerization, the resulting polymer is predominately a mixture of poly[(*S*)-BL] and poly[(*R*)-BL]; trace amounts of the stereoblock polymer poly[(*S*)-BL-*b*-(*R*)-BL] were formed; these result from transesterification as evidenced by the higher dispersity upon longer reaction time and the appearances of molecular ion peaks with the spacing between the neighbouring peaks being that of the half molar mass of the repeat unit. Yet, the latter side reaction can be inhibited by limiting the reaction time and/or reducing the monomer-to-catalyst feed ratio. DFT calculations revealed that the operating stereo-inducing mechanism was a enantiomorphic-site control (ESC) mechanism.[87] This approach was extended to other members of this diolide family, such as the ethyl, butyl, and benzyl derivatives (*rac*-DL^{Et}, *rac*-DL^{Bu}, and *rac*-DL^{Bn}, respectively), which were also polymerized using similar catalytic systems.[87,88]

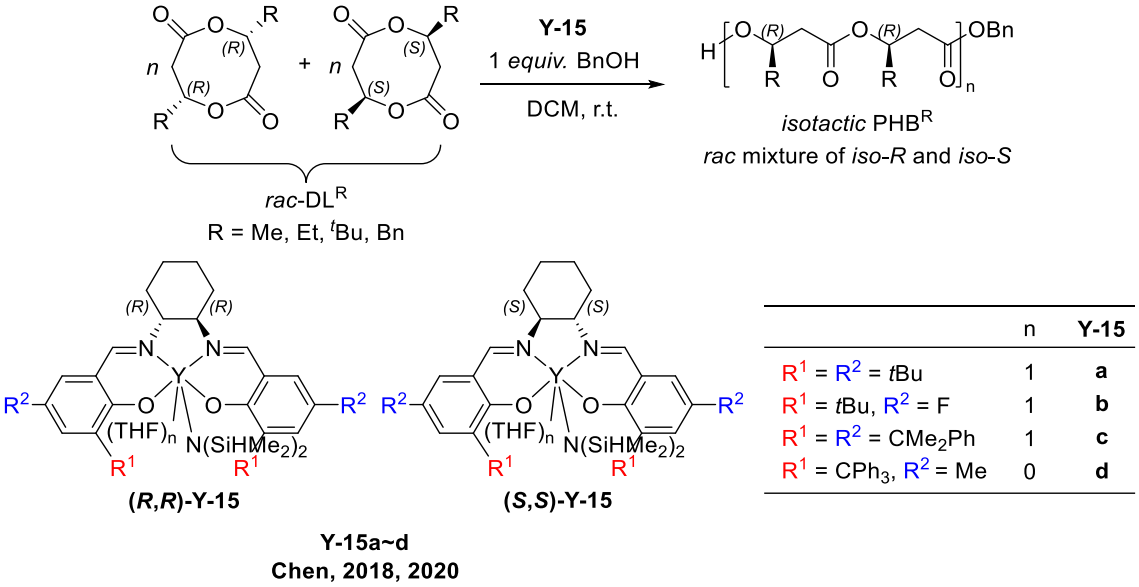

Figure 1.45. Access to highly isotactic P3HB from the stereoselective ROP of *rac*-DL^{R} with chiral yttrium-salen complexes.[86]

However, although P3HB is biorenewable, biodegradable, and biocompatible and exhibits desirable physical properties (high T_m and crystallinity) and film-barrier properties (as excellent packaging material), it is mechanically brittle (~3% elongation at break), and its stiffness and hydrophobicity often impede their direct use.[89] On the other hand, naturally occurring PHAs feature different side-chain substituents along the backbone. The chemical nature of these side-groups and the successive enchainment of the chiral monomer units along the macromolecules both modulate the physical, mechanical and biological properties of the resulting polymer materials.[90] Therefore, introduction of various functional pendant groups into PHA has become a field of research to possibly widen their applications. In this regard, poly(benzyl β-malolactonate) (PMLA^{Bn}), a hydrophobic PHA which can be easily converted into a hydrophilic poly(β-malic acid), has drawn much interest over the past two decades.[91] Although various catalysts/initiators have been studied for the ROP of racemic β-malolactonates (*rac*-MLA^{R}, R = benzyl, allyl), few of them have shown significant stereoselectivity.

Our group realized the stereoselective ROP of *rac*-MLA^{R}s by using aforementioned yttrium complexes **Y-1**, generating syndiotactic poly(β-malic acid) derivatives (PMLA^{R}s) in a controlled fashion (Figure 1.46).[92] In line with their performance in ROP of *rac*-BL, yttrium complexes show high activity for *rac*-MLA^{R}s. High stereoselectivity was also observed, but with marked differences concerning the stereocontrol parameters. Yttrium complexes bearing highly sterically bulky R^{1} substituents on the ligand lead only to syndio-biased/enriched PMLA^{R}s (for R^{1} = cumyl (**Y-1h**), P_r = 0.68; for R^{1} = CPh$_3$ (**Y-1e**), P_r = 0.81; for R^{1} = CMe$_2$^{t}Bu (**Y-1f**), P_r = 0.86). Surprisingly, high syndioselectivity (P_r > 0.95) was observed for the complexes (**Y1-d/l**) incorporating ligand with *o*,*p*-dichloro-substituents installed in the phenoxy rings. It is worth noting that *o*,*p*-dichloro-substituted complex is non stereoselective in the ROP of *rac*-BL (P_r = 0.42−0.45). It is only via recent studies which have investigated complexes bearing "uncrowded" substituted, such as (Br, F, Me), ligands in the ROP of *rac*-MLA^{R}s, that these proved as syndioselective as the dichloro-substituted complex (P_r > 0.92). Hence, in contrast with *rac*-BL, the ROP of *rac*-MLA^{R}s is also, in part, controlled by steric factors but requires small substituents to afford high syndiotacticity.

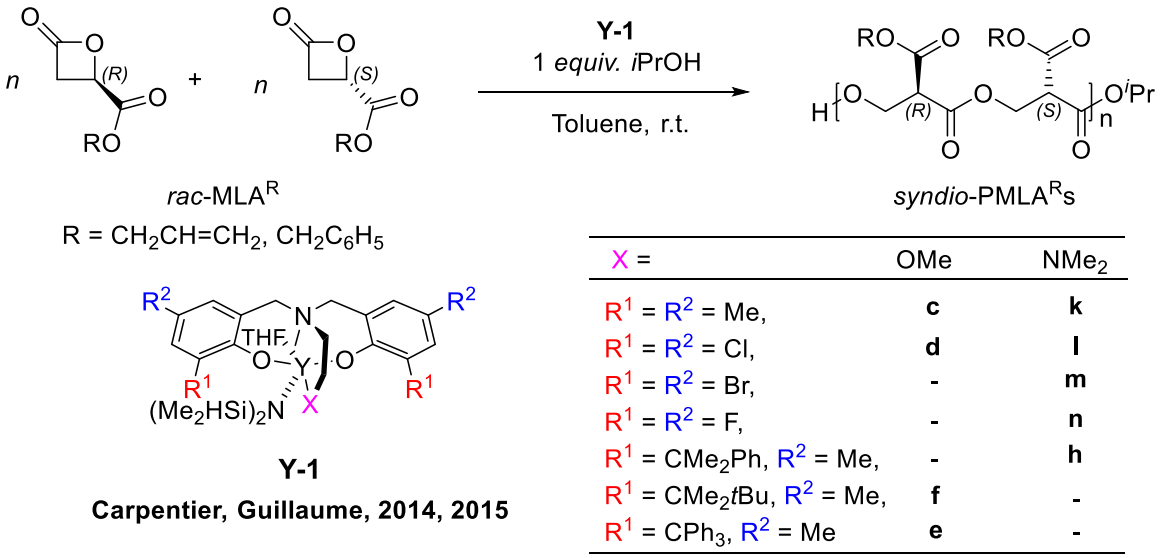

X =	OMe	NMe$_2$
R^{1} = R^{2} = Me,	**c**	**k**
R^{1} = R^{2} = Cl,	**d**	**l**
R^{1} = R^{2} = Br,	-	**m**
R^{1} = R^{2} = F,	-	**n**
R^{1} = CMe$_2$Ph, R^{2} = Me,	-	**h**
R^{1} = CMe$_2$^{t}Bu, R^{2} = Me,	**f**	-
R^{1} = CPh$_3$, R^{2} = Me	**e**	-

Figure 1.46. Access to syndiotactic PMLA^{R} from the stereoselective ROP of *rac*-MLA^{R} with yttrium complexes.[69,92,93]

In 2017, our group investigated the yttrium-catalyzed stereoselective ROP of *rac*-4-alkoxymethylene-β-propiolactones (*rac*-BPL^{OR}s, R = methyl, allyl, benzyl, *et al.*) which ''simply'' differ from *rac*-MLA^{R}s (*see above*) by replacement in the pendant (exocyclic) group of a carbonyl by a methylene moiety. This led to an interesting observation of stereoselectivity change from syndio- to isoselective polymerization when yttrium complexes bearing sterically bulky ligands (**Y-1b/p**) switch to *halogen*-substituted ones (**Y-1d/l**) (Figure 1.47).[94] High syndioselective (P_r = 0.85-0.90) ROP of *rac*-BPL^{OR} was achieved by yttrium complexes incorporating bulky *ortho*-substituents (such as R^{1} = CMe$_2$Ph, *t*Bu) on the phenoxy rings. The dimethyl-substituted yttrium complexes (**Y-1c/k**) gave atactic

PBPL^{OR}s, demonstrating that syndiotactic ROP is under steric control. On the other hand, yttrium complexes bearing "uncrowded" *ortho*-substituents on the phenoxy rings, such as fluoro, chloro or bromo-substituents, induced the formation of highly isotactic PBPL^{OR}s (likely as a racemic mixture of iso-(*R*)-PBPL^{OR} and iso-(*S*)-PBPL^{OR}). These results indicate that sterics are not the main factor controlling the isoselectivity of this class of β-lactones. DFT studies reveal that isoselectivity arose from the attractive interactions between methylene hydrogens of the last inserted monomer within the growing polymer chain and the halogen *ortho*-substituents installed in the phenoxy rings.

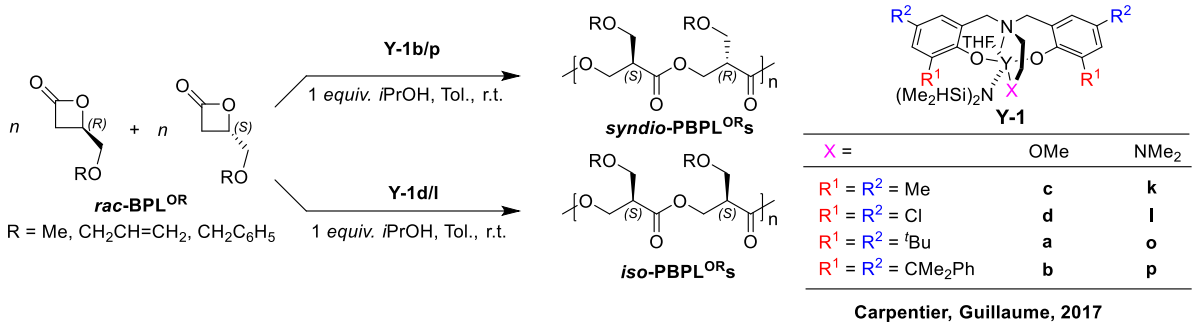

Figure 1.47. Access to syndiotactic or isotactic PBPL^{OR}s from the stereoselective ROP of *rac*-BPL^{OR}s.[94]

The above-mentioned versatility of the yttrium complexes was further documented by Chen and coworkers.[95] Their search for high-performance polymer materials led them to investigate the ROP of racemic *trans*-cyclohexyl-ring fused γ-butyrolactone (*rac*-GBL) (Figure 1.48). Screening of various catalysts ended up in identifying yttrium complexes (**Y-1'**). The nature of the X moiety within the ligand's side-arm was found to play a decisive role in determining the tacticity of the resulting PCBLs. In fact, the yttrium complexes bearing *t*Bu-substituted ligand with a −OMe side arm donor (**Y-1'd**) afforded moderately heterotactic PCBLs (P_r up to 0.75) under optimized conditions (DCM as a solvent, at -65 °C, without coinitiator). On the other hand, upon tuning the −X capping moiety of the tripodal tetradentate bis(phenoxy) ligand, *rac*-GBL polymerization can be changed into isoselectivity. Only the highly sterically crowded trityl-substituted yttrium complex (**Y-1'j**) features a significant isoselectivity at room temperature (P_m = 0.77); all the other complexes incorporating a less bulky *ortho*-substituent, such as $CMePh_2$, CMe_2Ph or *tert*-butyl, lead to isotactic-biased or atactic PCBLs (P_m = 0.50−0.65). Upon decreasing the temperature to −65 °C, the **Y-1'j** complex remains active, affording the corresponding PBCLs with more pronounced stereoselectivity with P_m up to 0.95. Microstructure statistical analysis and Bernoulli model triad test indicated that both heteroselectivity and isoselectivity originate from a CEC mechanism, though the reversal of stereoselectivity upon changing the X capping group still has not been rationalized so far. Another interesting point of this study is the formation of a stereocomplex between the blocks of *R*- and *S*- units within the isotactic PCBLs chain, providing superior thermal performance (T_m = 175 °C) compared to their respective enantiomeric polymers (T_m = 127 °C).[96]

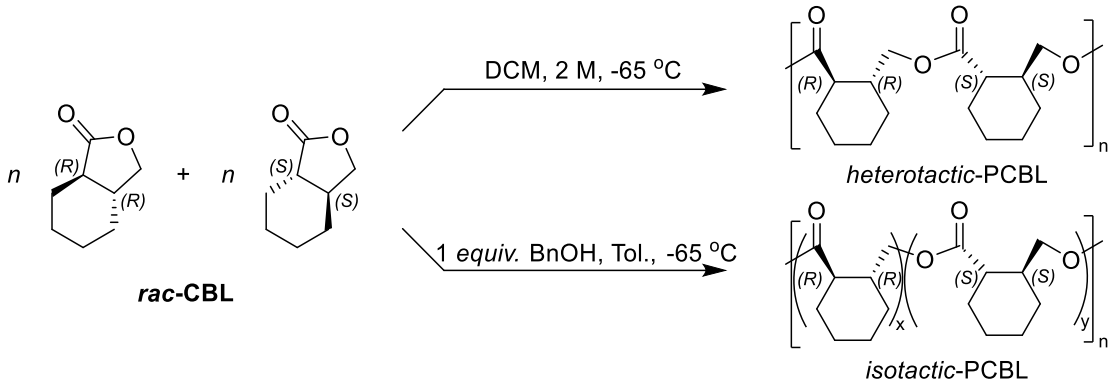

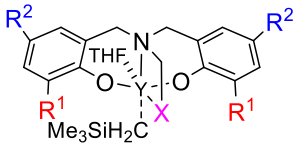

Y-1'
Chen, 2019

X =	CH_2OMe	CH_2NMe_2	CH_2NEt_2
$R^1 = R^2 = Me$	**a**	-	-
$R^1 = R^2 = Cl$	**b**	**c**	-
$R^1 = R^2 = {}^t Bu$	**d**	**e**	-
$R^1 = R^2 = CMe_2Ph$	**f**	**g**	**h**
$R^1 = CMePh_2$, $R^2 = Me$	-	**i**	-
$R^1 = CPh_3$, $R^2 = Me$	-	**j**	-

Figure 1.48. Stereoselective ROP of *trans*-cyclohexyl-ring-fused γ-butyrolactone (*rac*-CBL) by yttrium complexes.[95]

As a final salient example of stereoselective ROP of asymmetric lactones in this section, Zhu and coworkers explored the development of polymers with desirable thermal and mechanical properties by monomer design when addressing the intrinsic limitation (that is, the relatively low melting point $T_m \approx$ 60 °C) of polycaprolactone, thereby two monomers, *trans*-cyclohexyl-ring-fused 1,5-dioxepan-2-one (*rac*-CDXO) and 1,4-oxathiepan-7-one (*rac*-COTO), being designed (Figure 1.49).[97] A series of catalytic systems, such as yttrium alkyl complex stabilized by nonchiral tetradentate amino alkoxy bisphenoxy ligand (**Y-1'e**), yttrium silylamido complex supported by *N*,*N*'-bis(salicylidene)cyclohexanediimine (**Y-15a**), and zinc complexes ligated by bulky β-diiminate ligands ($(BDI^{Et})Zn\{N(TMS)_2\}$ and $(BDI^{iPr})Zn\{N(TMS)_2\}$), were screened for stereoselective ROP of *rac*-CDXO and *rac*-COTO, respectively. Among them, zinc complexes proved to be the most efficient, exhibiting good stereoselectivity. The zinc complex with a bulky ligand, $(BDI^{iPr})Zn\{N(TMS)_2\}$, gave rise to PCDXO and PCOTO with P_r values of 0.92 and 0.91, respectively, under optimized conditions. However, the nature of the stereocontrolled mechanism operative with this system has not been established so far. When PCOTO was treated with oxidants, such as 3-chloroperbenzoic acid (*m*CPBA), in DCM at 0 °C, it converted into a pure oxidized product SO_2-PCOTO, which exhibited a significant improvement in glass transition temperature (T_g) from 18 °C to 112 °C in comparison with the parent PCOTO.

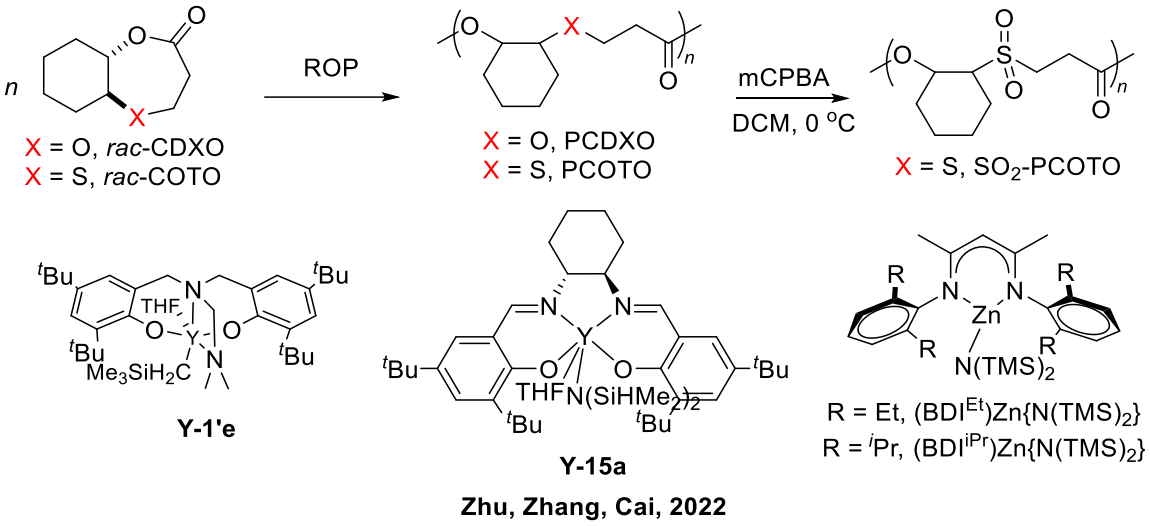

Figure 1.49. the stereoselective ROP of *trans*-cyclohexyl-ring-fused 1,5-dioxepan-2-one (CDXO) and 1,4-oxathiepan-7-one (COTO).[97]

1.3.1.3 Stereoselective Ring-Opening Polymerization of *O*-Carboxyanhydrides

Tremendous efforts have been paid to introduce functionality to regulate the physicochemical performances of polyesters and to extend their applications.[98] Although the ring-opening copolymerization (ROCOP) of epoxides and cyclic anhydrides has the potential to give a wide range of polyesters with various side-arms, the synthesis of stereoregular polyesters with side-chain functional groups remains challenging.[4] In this regard, *O*-carboxyanhydrides (OCAs) are alternative monomers that can be easily synthesized and polymerized to prepare stereoregular polyesters.

Compared with other heterocyclic monomers, the development of organometallic catalysts for ROP of OCAs is relatively slow. Many organometallics that successfully mediated the ROP of LA and lactones failed to induce the ROP of OCAs, not to mention stereoselective polymerization. A breakthrough in this field was achieved by Wu and coworkers in 2017.[99] Using the zirconium/hafnium amino-tris(phenolate) alkoxide complexes, the high syndioselective ROP of *rac*-OCA^{R}s (R= Me, Bn, *p*-$CH_2C_6H_4OBn$) was achieved (Figure 1.50). It turned out that both Zr- and Hf-lactate complexes gave better catalytic performance, such as activities and control of molar masses as compared with their corresponding isopropoxide analogues. The Hf complexes induce a slightly better syndiotacticity than the Zr ones, but the P_r values remain modest for polyOCA^{Lac}s (0.80−0.84); they can reach up to 0.93−0.95 for polyOCA^{R}s derived from the bulkier *rac*-OCA^{Phe} and *rac*-OCA$^{Tyr(OBn)}$ monomers. ^{13}C NMR analysis of the resulting polymer is consistent with a CEC mechanism.

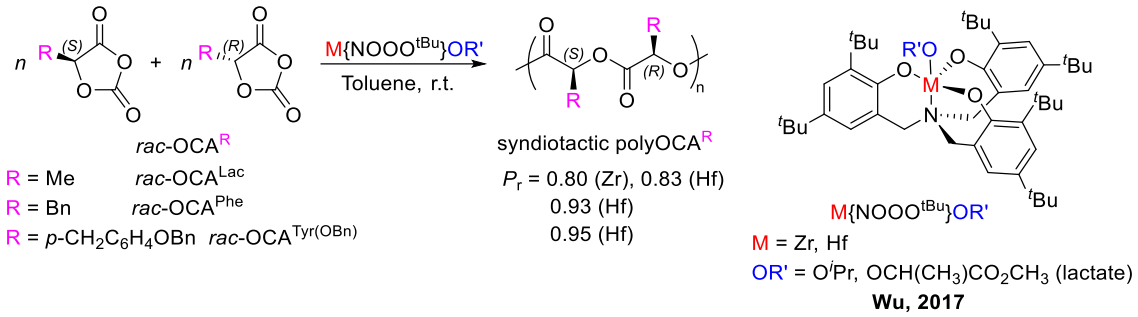

Figure 1.50. Access to syndiotactic poly(*rac*-OCA^{R})s from the ROP of *racemic O*-carboxyanhydrides (*rac*-OCA^{R}s).[99]

However, using *rac*-OCA^{Lac} as monomer and decreasing the reaction temperature, the syndioselectivity drops from 0.83 at 25 °C, to 0.75 at −40 °C, and further decreases to 0.72 at −60 °C. This is inconsistent with a CEC mechanism. A stereocontrol mechanism, referred to as "enhanced" chain-end control, as initially suggested by Davidson and coworkers, was proposed to account for this unusual behaviour.[100] This mechanism involves the inversion of the two diastereomers, (*S*)-(*M*)-Hf and (*S*)-(*P*)-Hf), due to the axial chirality of the metal centre. One of the two diastereomers is supposed to be more syndioselective and more active than the other one. For example, (*S*)-(*M*)-Hf selectively opens *R*-OCA^{R} to form a less active and less syndioselective intermediate of (*S*)-(*R*)-(*M*)-Hf, which can be inverted to active and highly syndioselective (*S*)-(*R*)-(*P*)-Hf to further selectively open next *S*-OCA^{R}; then syndiotactic propagation can proceed (Figure 1.51). Because interconversion between the two diastereomers is slower at lower temperatures, the less active and less syndioselective species accumulate and eventually decrease the syndioselectivity.

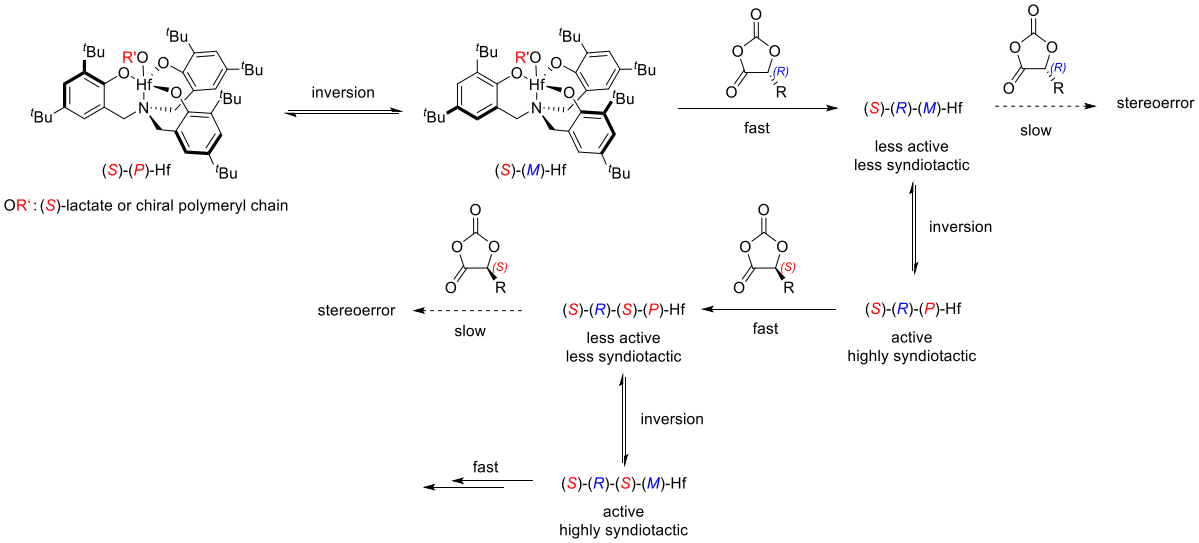

Figure 1.51. The "enhanced" chain-end control mechanism possibly operative in the stereoselective ROP of *rac*-OCA^{R}s with Hf{NOOO^{tBu2}} complex.[99]

Inspired by the high heteroselectivity of the related zinc alkoxide in the ROP of *rac*-LA with a P_r of 0.96 reported by Chisholm,[101] Wu and coworkers recently identified a zinc complex

(TMPZn(lactate)) stabilized by a dipyrrin ligand which could meditate the isoselective ROP of *rac*-OCA^{R}s (R = Me, Bn, *p*-(benzyloxy)benzyl) with P_m up to 0.95 (Figure 1.52).[102] The ROP of 100 equiv. of *L*-OCA^{Lac}, *L*-OCA^{Phe}, *L*-OCA$^{Tyr(OBn),}$ and *L*-OCA^{Ph} meditated by *L*-TMPZn(lactate), is completed within 1 min in THF at 0 ℃ without epimerization; on the other hand, the conversion of *L*-OCA^{Ph} reaches less than 5 %, even after 24 h accompanied by significant epimerization. The authors attributed these results to both the polymerization rate and the slightly low acidity of methine in monomers of *L*-OCA^{Lac}, *L*-OCA^{Phe}, *L*-OCA$^{Tyr(OBn)}$, leading to the retention of the chiral centres, while the slow rate of polymerization and the high acidity of methine in *L*-OCA^{Ph} (due to the electron-withdrawing effect of the phenyl group), should play essential roles in epimerization reaction.

The controlled isoselective ROP of *rac*-OCA^{Lac} was achieved by *rac*-TMPZn(lactate) with a P_m of 0.92 in THF at 0 ℃. Upon lowering the reaction temperature down to −70 ℃, the level of isoselectivity dramatically increased (P_m up to 0.97). The stereoselective ROP of *rac*-OCA^{Bn} promoted by *rac*-TMPZn(lactate) further demonstrates the potential versatility of this catalytic system. The experimental results revealed that the ROP of *rac*-OCA^{Bn} was relatively controlled, yet the dispersities ($Đ_M$ = 1.06~1.50) of the resulting polymers were a little broader than that of polyOCA^{Lac}s ($Đ_M$ = 1.06~1.25). MALDI-ToF MS analysis of the resulting polyOCA^{Phe}s reveals that the polymers are a mixture of linear and cyclic polymers. To suppress side reactions, the ROP of *rac*-OCA^{Phe} was conducted at −70 ℃, leading to experimental molar masses consistent with the theoretical ones along with narrow dispersities; also, as expected, the level of isoselectivity increased from 0.86 to 0.96. When the monomer was extended to *rac*-OCA$^{Tyr(OBn)}$, the ROP reaction exhibited a high level of isoselectivity at −70 ℃ with a P_m of 0.95. Using enantiopure *L*-TMPZn(lactate) as an initiator, similar kinetics for the ROP of *L*- and *D*-OCA^{Phe} suggested that the isoselective mechanism originates from a CEC mechanism.

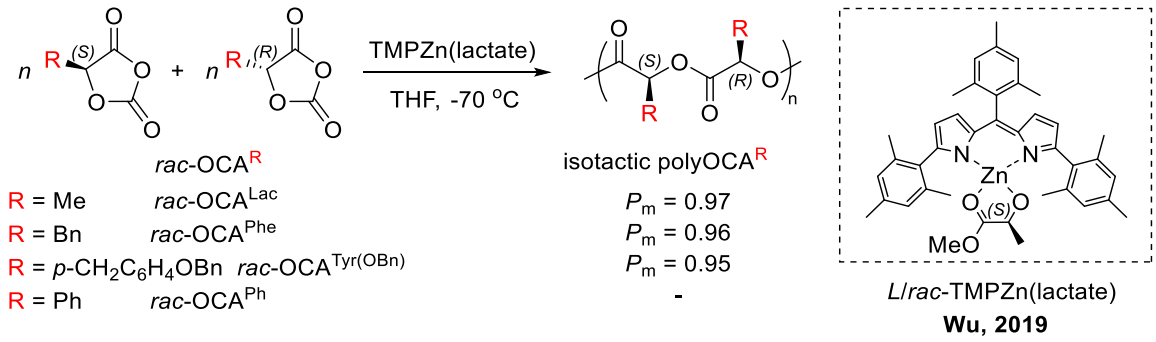

Figure 1.52. Isoselective ROP of *rac*-OCA^{R}s by zinc complexes.[102]

The same group demonstrated that an aminobisphenolate Zn complex paired with 3-fluoropyridine, as weak Lewis pairs, along with *rac*-(methyl mandelate) as an initiator, could mediate the isoselective ROP of *rac*-OCA^{Ph} with a high P_m of 0.92 at −50 ℃ in toluene (Figure 1.53).[103] A weak Lewis pair and an initiator are found to be vital to eliminate epimerization and accelerate the reaction, respectively. The weak interaction between 3-fluoropyridine and the zinc complex could easily be substituted by

OCA^{Ph} monomer. Based on these facts, the authors proposed a cooperatively bifunctional mechanism depicted in Figure 1.54.

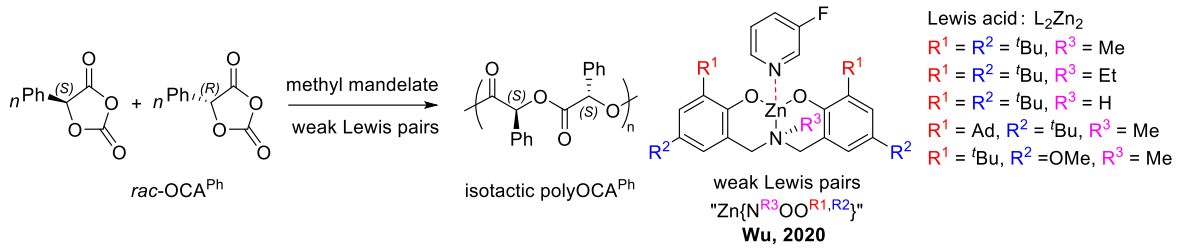

Figure 1.53. Isoselective ROP of *rac*-OCA^{Ph} by weak Lewis pairs.[103]

Zinc complexes stabilized by *t*Bu-substituted aminobisphenolate ligands, "Zn{N^{Me}OO^{tBu,tBu}}", gave the highest isoselectivity with a P_m of 0.92 in toluene at −50 °C. It is worth noting that the T_m value of a 1:1 mixture of enantiopure poly(*L*-OCA^{Ph}) and poly(*D*-OCA^{Ph}) can reach 173 °C, which is much higher than their corresponding isotactic polyOCA^{Ph} (T_m = 116 °C), respectively, implying the formation of a stereocomplex.

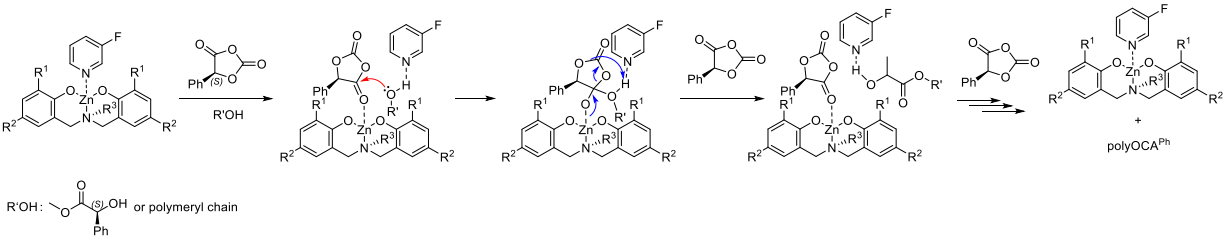

Figure 1.54. Proposed mechanism for the stereoselective ROP of OCA^{Ph} using weak Lewis pairs.[103]

In 2018, Tong and coworkers disclosed a powerful strategy to achieve stereoselective ROP of *rac*-OCA^{R}s.[104] A catalytic system made of photoredox-active (bpy)Ni(COD)/[Ir] catalysts along with a Zn complex, {NOO^{R}}ZnEt, stabilized by tridentate Schiff base ligand, was identified to mediate controlled ROP of *rac*-OCA^{R}s without epimerization, affording high isotactic poly(*rac*-OCA^{R})s (P_m = 0.88−0.97) with high molar mass (up to 80 kg mol^{-1}) and narrow dispersities ($Đ_M$ < 1.10) (Figure 1.55). All the components of this catalytic system are necessary for the controlled polymerization results: the photoredox (bpy)Ni(COD)/[Ir] systems are responsible for decarboxylation; while the zinc complex is crucial for chain propagation.[105] They further demonstrated that the substituent of the {NNO^{R}}ZnEt complex is vital to the level of stereoselectivity; the highest isoselective poly(*rac*-OCA^{Phe})s (P_m = 0.93–0.97) was obtained by Zinc complex with R electron-donating and bulky group, {NNO^{tBu}}ZnEt. On the other hand, replacing {NNO^{tBu}}ZnEt by Zn(N(SiMe$_3$)$_2$)$_2$ affords poly(*rac*-OCA^{R})s with a modest P_m of 0.66. Based on detailed kinetic studies, they concluded that the resulting polymer is stereoblock, and spectroscopic analyses suggest a CEC mechanism.

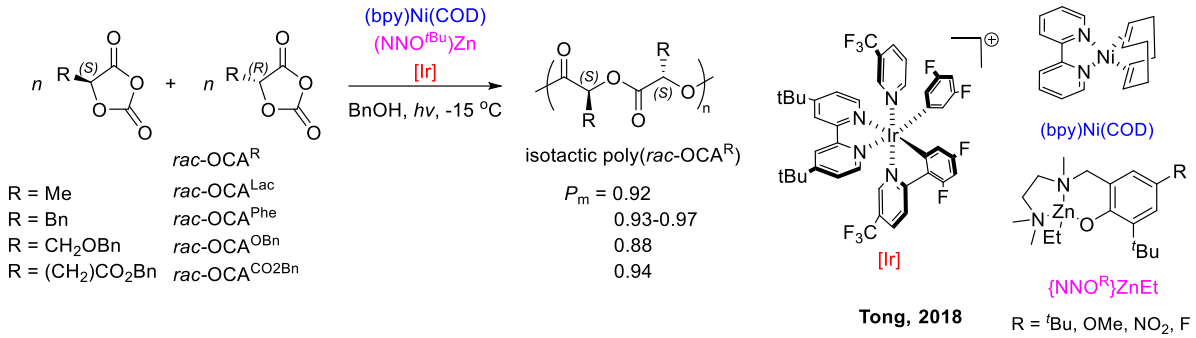

Figure 1.55. Access to isotactic stereoblock poly(*rac*-OCA^{R})s from the stereoselective ROP of *rac*-*O*-carboxyanhydrides (OCA^{R}s) with the {NNO^{tBu}}ZnEt/BnOH/Ni/Ir system.[104]

Tong and coworkers unveiled a new electrochemical pathway to achieve the stereoselective ROP of *rac*-OCA^{R}s (Figure 1.56).[106] When a current was applied, the "**{Co}-1/{Zn}-1**" catalytic system provided highly *isotactic* poly(*rac*-OCA^{Phe}) with a high P_m value of 0.95 and a molar mass of 67.6 kg mol^{-1} coupled with narrow dispersity ($Đ_M$ < 1.10) at a feed ratio of 300 at 0 °C in THF. On the contrary, the **{Co}-2/{Zn}-2** system led to *syndiotactic* poly(*rac*-OCA^{Phe}) with a molar mass of 46.2 kg mol^{-1} and a P_r value of 0.79. Yet, such a switch of stereoselectivity was not observed in the electrochemical polymerizations of other *rac*-OAC^{R}s (R = Me, $(CH_2)_2CO_2Bn$) since both of the "**{Co}-1/{Zn}-1** and **{Co}-2/{Zn}-2**" catalytic systems afford isotactic stereoblock poly(*rac*-OCA^{R})s. This indicates that the side-chain functionalities of *rac*-OCA monomers influence the stereoselectivity. However, the operating mechanism of these catalytic systems is still unknown.

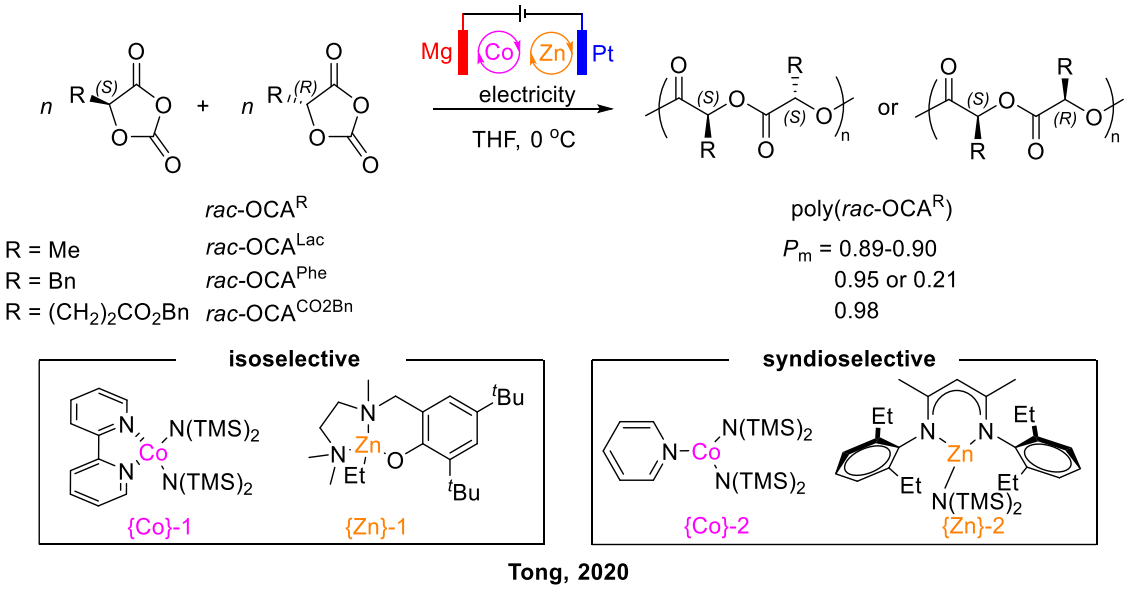

Figure 1.56. Co/Zn complexes-mediated electrochemical ROP of *rac*-OCA^{R}s.[106]

Despite significant advances in the stereoselective ROP of chiral racemic heterocyclic monomers by metal-based catalysts, inevitable contamination of the resulting polymer by trace metal residues may have non-negligible impacts on the overall quality of the final products, especially when they are

applied to biomedical or microelectronic fields. Over the last two decades, organocatalysis has become a potent tool in polymer chemistry.[9] Most organocatalysts are water and air-tolerant, affording polymers that are free of residual metal contaminates, which have become attractive alternatives to organometallic catalysts.

1.3.2 Organocatalytic Stereoselective Ring-Opening Polymerization of Chiral Racemic Heterocyclic Monomers

To date, only a handful of studies of the stereocontrolled ROP of *rac*-LA and seven-membered lactone using either chiral or achiral organic catalysts have been reported.

1.3.2.1 Organocatalytic Stereoselective Ring-Opening Polymerization of *rac*-Lactide

In 2005, Hedrick and coworkers reported sterically encumbered *N*-heterocyclic carbenes (NHCs), catalyzed *rac*-LA polymerization, leading to highly isotactic PLAs (Figure 1.57).[107] The activity of achiral and chiral NHC, **NHC-1** and **(*R,R*)-NHC-2**, are remarkably high, enabling to perform the polymerization at low temperatures (such as -70 °C) to generate a highly isotactic PLA (P_m = 0.88−0.90 *vs.* P_m = 0.59 at r.t. in DCM). When ***rac*-NHC-2** was used to initiate *rac*-LA polymerization, no significant enhancement of isotacticity was found under identical conditions, and the activity of the NHCs remained the same, suggesting that the dominating factor determining stereoselectivity is the steric congestion of the active site, despite of the chirality of the catalyst. Moreover, ROP of *meso*-LA promoted by **(*R,R*)-NHC-2**, produced heterotactic PLA. Collectively, these results proved that the mechanism for both achiral and chiral NHCs are consistent with a CEC mechanism.

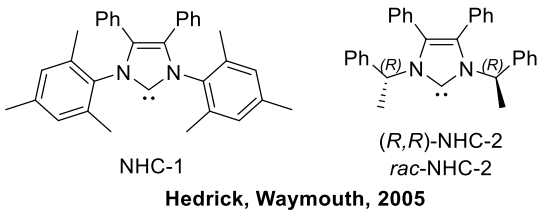

Figure 1.57. *N*-heterocyclic carbenes (NHCs) used for the stereoselective ROP of *rac*-LA.[107]

In 2007, Wade and coworkers employed a dimeric phosphazene base, 1-*tert*-butyl-2,2,4,4,4-pentakis(dimethylamino)-2Λ,^{5}4Λ^5-catenadi(phosphazene) (*t*BuP$_2$), as a catalyst to produce isotactic stereoblock PLA.[108] This phosphazene base exhibits excellent activity (TOF = 28 min^{-1}) for the ROP of *rac*-LA at room temperature in toluene, affording isotactic-biased PLA with a P_m value of 0.72. Upon lowering the temperature to −70 °C, the level of stereoselectivity was dramatically improved to 0.95 while still maintaining relatively high activity (TOF = 33.4 h^{-1}). Stoichiometric reaction revealed that an intramolecular hydrogen bond occurred between the alcohol initiator and *t*BuP$_2$, thus turning the initiator or the growing chain-end into a stronger nucleophile for the ring-opening event. The authors believe that the alcohol-activated mechanism accounts for such a stereocontrol (Figure 1.58). At the

initiation step, the alcohol initiator was activated by *t*BuP$_2$ through H-bonds; the activated alcohol would open the ring of *D*-LA and *L*-LA with equal possibility, leading to ring-opened units, and meanwhile, the ^{t}BuP$_2$ could interact with the terminal alkoxide by H-bonds, which presumably influences the steric hindrance around the active site, thereby improving the stereoselectivity. Subsequently, the ring-opened units selectively attack the same enantiomeric monomers leading to isotactic enchainment. When an active polymer chain mistakenly opens an opposite enantiomeric monomer, the following growth of the polymer chain is controlled by the last inserted monomer, accounting for the formation of isotactic stereoblock microstructures.

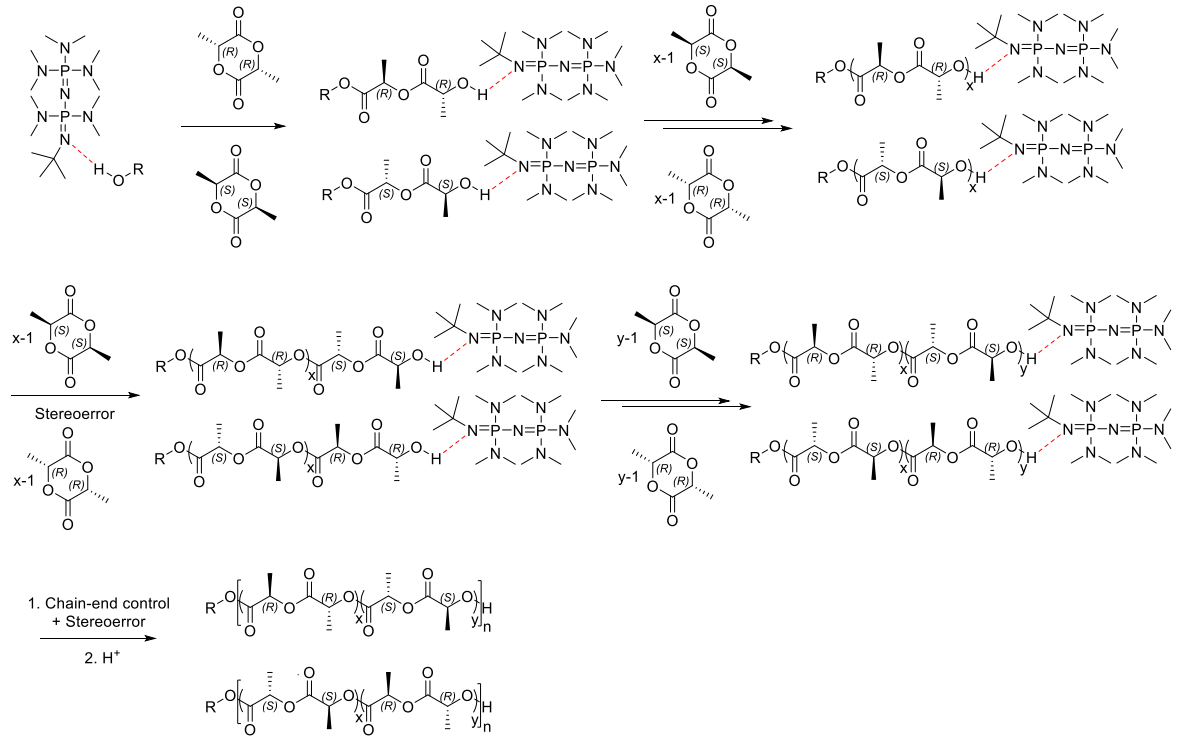

Figure 1.58. Proposed mechanism for the stereoselective ROP of *rac*-LA by *t*BuP$_2$.[108]

Inspired by the contribution of Wade,[108] Li and coworkers explored a novel cyclic trimeric phosphazene base (CPTB) having a spherical structure with a larger diameter (about 1.4 nm) as compared to that of *t*BuP$_2$, in the stereoselective ROP of *rac*-LA, affording highly isotactic stereoblock PLA with a P_m value of 0.92 at −75 °C (Figure 1.59).[109] In fact, the CPTB catalysed *rac*-LA polymerization, affording atactic PLA (P_m = 0.52) at r.t. in toluene with high activity (TOF = 600 h^{-1}). Upon decreasing the reaction temperature to −75 °C, the degree of isoselectivity was strikingly increased to P_m = 0.92. Since the molecule of CTPB is symmetrical, the chain-end control mechanism was proposed to explain the formation of isotactic stereoblock PLA, which was further supported by kinetic studies. The high stereoselectivity of CTPB is mainly attributed to the encumbered surroundings at the propagation chain-end derived from the large CTPB molecule, which is similar to that of *t*BuP$_2$ (*see above*).[8]

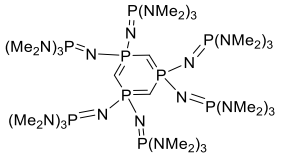

Figure 1.59. Cyclic trimeric phosphazene base used for stereoselective ROP of *rac*-LA.[109]

Coulembier and coworkers investigated a non-sterically encumbered and achiral base, *e.g.*, 1,5,7-triazabicyclo[4.4.0]dec-5-ene (TBD), meditated stereoselective ROP of *rac*-LA at cryogenic temperature (Figure 1.60).[110] Indeed, such ROP reaction gave high isotactic PLAs (P_m = 0.80−0.84) under identical conditions as *t*BuP$_2$ did. On the other hand, stereoselective ROP of *meso*-LA at −75 °C in toluene catalysed by TBD, gave heterotactic PLA with a P_r of 0.80, demonstrating that the propagating chain end has an essential impact on the propagating step. DFT calculations revealed that the stereocontrol ROP of *rac*-LA originates from a perfect imbrication of both chiral LA and the propagating chiral end-group interacting with the achiral TBD catalyst, which is facilitated at low temperatures.

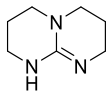

Figure 1.60. Non-sterically encumbered achiral TBD base used for the stereocontrolled ROP of *rac*-LA.[110]

Although excellent stereocontrol can be achieved by achiral organocatalysts, ROP reactions are generally conducted at low temperatures. In this context, Taton and coworkers have recently reported that Takemoto's organocatalysts could promote the high stereocontrolled ROP of *rac*-LA, yielding isotactic-enriched PLA with a P_m value up to 0.90 in toluene at room temperature (Figure 1.61).[111] Despite excellent stereocontrol ROP reactions have shown a relatively poor catalytic activity (TOF ≈ 0.14 h^{-1}) at room temperature. Yet, upon increasing the reaction temperature, transesterification reactions were detected, giving rise to poor stereocontrol (P_m = 0.72 at 85 °C *vs.* P_m = 0.67 at 150 °C). Related kinetics and NMR studies have evidenced the concomitant occurrence of both the CEC and ESC mechanisms, which is further supported by the formation of atactic PLA from *meso*-LA mediated by (*R*,*R*)-TUC.

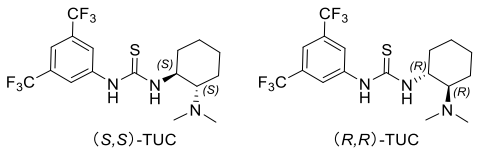

Figure 1.61. Takemoto's catalyst used for the stereocontrolled ROP of *rac*-LA.[111]

In their subsequent contribution, Taton and coworkers reported a binary organocatalytic system, the chiral Takemoto's catalyst and an organic phosphazene base (*t*BuP$_1$ or *t*BuP$_2$), with both relatively high activity (TOF ranging from 30 to 67 h^{-1} at room temperature) and high stereoselectivity (P_m up to 0.96), that provides highly crystalline PLA materials (T_m up to 187 °C) from *rac*-LA (Figure 1.62).[112] Interestingly, the weaker phosphazene base *t*BuP$_1$ (pK_a = 26.7 in MeCN) promotes stereocontrol, probably via an associated mechanism involving H-bonding, while the stronger phosphazene base *t*BuP$_2$ (pK_a = 33.5 in MeCN), provides faster polymerization but less stereocontrol via a phosphazenium thioimidate ion pair. Kinetics studies revealed that the controlled nature of *rac*-LA polymerization and the ESC mechanism is dominant over the ROP process.

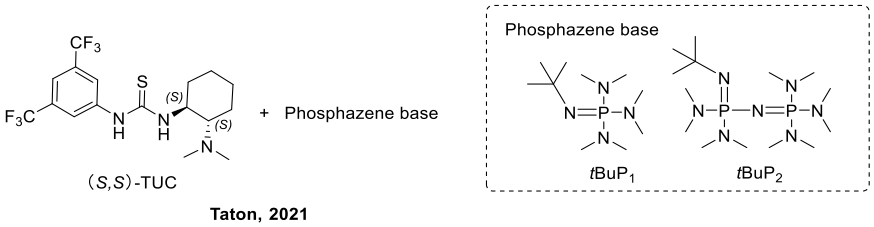

Figure 1.62. A binary organocatalysts (composed of Takemoto's catalyst and a phosphazene base) was used for the stereocontrolled ROP of *rac*-LA.[112]

In 2011, Chen and coworkers initially investigated the stereoselective ROP of *rac*-LA by using cinchona alkaloids (***β*-ICD**). ***β*-ICD** afforded a crystalline isotactic-enriched PLA with a P_m value of 0.75.[113] Encouraged by these results, they redesigned a series of multifunctional chiral organocatalysts, involving a core of cinchona alkaloids with thiourea and chiral binaphthyl-amine (BINAM) moieties, to develop a high enantioselective *rac*-LA polymerization (Figure 1.63).[114] The ROP of *rac*-LA mediated by **(*R*)-1** in *o*-difluorobenzene at r.t. afforded isotactic PLA with a P_m of 0.88 at 51% conversion and the highest enantioselectivity factor to date ($s = k_S/k_D = 53$). Surprisingly, when the conversion of *rac*-LA reached 83%, the level of isoselectivity drops to 0.82, suggesting the system loses enantioselectivity when the reaction reaches a high conversion.

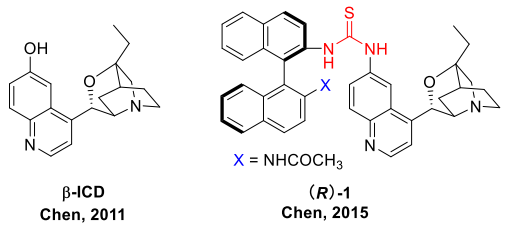

Figure 1.63. Bifunctional chiral catalysts used for the stereoselective ROP of *rac*-LA.[113,114]

In 2019, Williams and coworkers reported a new strategy to perform the isoselective ROP of *rac*-LA by exploiting the conformational dynamism of rotaxanes.[115] The rotaxanes comprise a crown ether macrocycle and an axle, the latter containing both an ammonium and a thiourea or triazole group(Figure 1.64). When the ether macrocycle resides over the protonated ammonium group by strong

intramolecular H-bonding, the rotaxanes are inactive for *rac*-LA polymerization in the presence of benzyl alcohol. Yet, when one equimolar of the strong base was added, the catalytic system became moderately active for *rac*-LA polymerization (TOF ≈ 0.42 h^{-1}), yielding isotactic PLAs with P_m values ranging from 0.66 to 0.81. NMR studies revealed that the amine interacts weakly with the macrocycle, allowing, upon deprotonation, its free movement along the axle. The accessibility of thiourea was found to be essential; when replacing the thiourea group of rotaxane-1 with the weaker hydrogen bond-donating triazole (rotaxane-2) or with the bulkier group (rotxane-3), the rotaxane significantly reduces stereocontrol (P_m = 0.81 for rotaxane-1 *vs.* P_m = 0.66 for rotaxane-2; P_m = 0.77 for rotaxane-3, respectively). This original system could be considered as a bulky amine–thiourea catalytic system: neutral rotaxane features thiourea/triazole groups activate the LA monomer and amine groups to activate benzyl alcohol, respectively. Subsequently, the activated benzyl alcohol attacks the coordinated lactide forming an *α*-hydroxyl-*ω*-ester which is subsequently (re)activated and attacks another LA monomer.

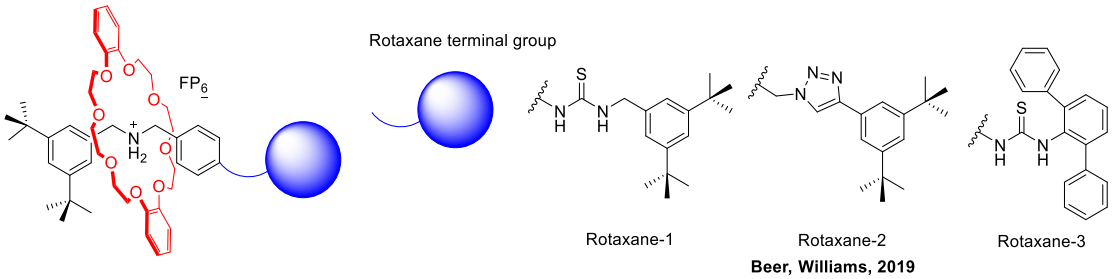

Figure 1.64. [2]Rotaxane catalysts used for isoselective ROP of *rac*-LA.[115]

Cossio and coworkers reported the first example of chiral amino acids bearing multiple chiral centres in the stereoselective ROP of *rac*-LA.[116] Chiral amino acids, (2*S*,3*R*,4*S*,5*S*)-1-methyl-4-nitro-3,5-diphenyl-pyrrolidine-2-carboxylic acid (*endo*-N^{Me}-Pro) and (2S,3S,4R,5S)-1-methyl-4-nitro-3,5-diphenyl-pyrrolidine-2-carboxylic acid (*exo*-N^{Me}-Pro), in the presence of strong base, such as DBU, afforded highly isotactic PLA (P_m > 0.90) under mild conditions (Figure 1.65). Both *endo* and *exo* chiral amino acids showed an opposite preference for enantiomers. Indeed, *endo* chiral amino acid selectively polymerized *D*-LA, whereas *exo* chiral amino acid preferentially reacted with *L*-LA. The influence of the densely substituted amino acids upon the enantioselectivity was further evidenced by DFT calculations.

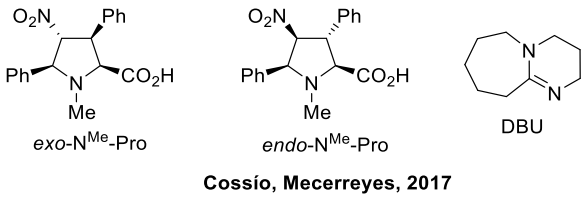

Figure 1.65. *Exo*-densely substituted *L*-proline and *endo*-densely substituted *L*-proline combined with DBU used for kinetic resolution ROP of *rac*-LA.[116]

Satoh and coworkers described the first chiral BINOL-derived phosphoric acids mediated stereoselective ROP of *rac*-LA in the presence of 3-phenyl-1-propanol, affording isotactic PLA with a P_m value of 0.86 (Figure 1.66).[117] Yet, the catalytic systems exhibit a poor activity (TOF = 1.36 h^{-1} with ***(R)-a*** at 75 ℃ in toluene) and a low degree of polymerization (*DP* up to 50). **(*R*)-a** preferentially reacted with *D*-LA at 75 ℃ with a k_D/k_L value of 28.3 at a monomer conversion of 49%. Polymerization reaction was found to proceed through the dual activation of the carbonyl group of the monomer and of the hydroxyl group of the propagating chain-end due to the acid and base dual function of the −OH group and the phosphoryl oxygen of the chiral phosphoric acid catalysts, respectively.

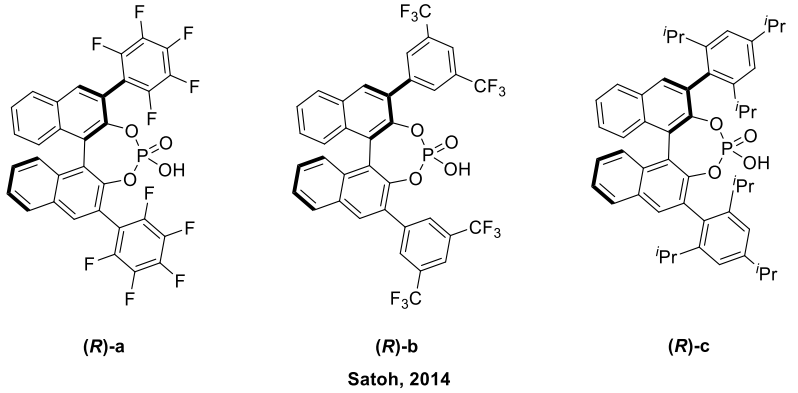

Figure 1.66. Chiral BINOL-derived monophosphoric acids used for the enantiomer-selective ROP of *rac*-LA.[117]

1.3.2.2 Organocatalytic Stereoselective Ring-Oping Polymerization of Racemic Lactones

Wang and coworkers explored the stereoselective ROP of racemic 6-aryl-*ε*-caprolactones by chiral phosphoric acids, affording stereogradient polycaprolactones (PCL^R) with the enantioselectivity factor up to 4.1 at 44% conversion (Figure 1.67).[118] The stereoselective ROP of 6-phenyl-*ε*-caprolactone promoted by **(*S*)-CPA-5** despite the poor activity (TOF ≈ 1−2 h^{-1} at 90 ℃), gave PCL^{Ph} with the highest stereoselectivity factor ($s = k_S/k_R = 2.6$). With the sterically hindered monomer, $CL^{p\text{-tBu-Ph}}$, the activity of **(*S*)-CPA-5** dramatically decreased (TOF = 0.14 h^{-1}), yet the stereoselectivity factor remained (s = 2.5). Surprisingly, with *chloro*-substituted monomer, $CL^{p\text{-Cl-Ph}}$, **(*S*)-CPA-5** afforded the highest enantioselectivity (s = 4.1). Chiral HPLC revealed a decrease of one enantiomer and an increase of the other enantiomer during the polymerization process, suggesting the formation of a stereogradient PCL^R. In their subsequent work, Wang and coworkers described the stereoselective ROP of *rac*-CL^{Me} polymerization.[119] The kinetic studies revealed the activity of (*R*)-CL^{Me} was ten times faster than of (*S*)-CL^{Me} when using **(*R*)-CPA-2** as the catalyst. Chiral HPLC revealed that the *s*-factor remains at 4.4 at 50% conversion; upon decreasing the reaction temperature to 0 ℃, the *s*-factor dramatically improved to 7.3.

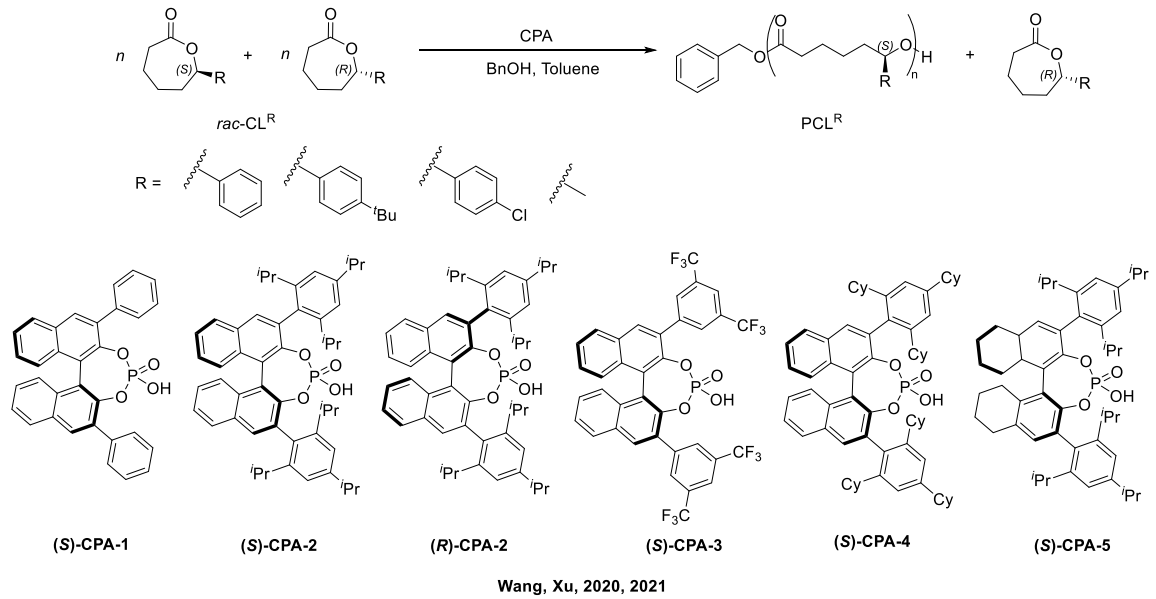

Figure 1.67. Asymmetric kinetic resolution polymerization of racemic 6-substituted-ε-caprolactones.[118,119]

Organocatalysts have the advantage of being water and air-tolerant and provide polymers free of residual metal contaminants, which is attractive for some applications. Yet, such initiators as mentioned above generally exhibit high stereoselectivities, but low catalytic activities, resulting in the formation of low molar mass aliphatic polyesters. To obtain more efficient organocatalysts, it will be essential to improve the activity of organocatalysts in future systems.

References

[1] L. Peña Carrodeguas, C. Martín, A. W. Kleij, Semiaromatic Polyesters Derived from Renewable Terpene Oxides with High Glass Transitions. *Macromolecules* **2017**, *50*, 5337-5345.

[2] J. Wu, P. Eduard, S. Thiyagarajan, B. A. Noordover, D. S. van Es, C. E. Koning, Semi-Aromatic Polyesters based on a Carbohydrate-Derived Rigid Diol for Engineering Plastics. *ChemSusChem* **2015**, *8*, 67-72.

[3] R. Tong, New Chemistry in Functional Aliphatic Polyesters. *Ind. Eng. Chem. Res.* **2017**, *56*, 4207-4219.

[4] J. M. Longo, M. J. Sanford, G. W. Coates, Ring-Opening Copolymerization of Epoxides and Cyclic Anhydrides with Discrete Metal Complexes: Structure-Property Relationships. *Chem. Rev.* **2016**, *116*, 15167-15197.

[5] M. J. Tschan, R. M. Gauvin, C. M. Thomas, Controlling Polymer Stereochemistry in Ring-Opening Polymerization: a Decade of Advances Shaping the Future of Biodegradable Polyesters. *Chem. Soc. Rev.* **2021**, *50*, 13587-13608.

[6] A. Buchard, C. M. Bakewell, J. Weiner, C. K. Williams In *Top. Organomet. Chem.*; Springer: Berlin, 2012; Vol. 39.

[7] A. Khalil, S. Cammas-Marion, O. Coulembier, Organocatalysis Applied to the Ring-Opening Polymerization of β-Lactones: A Brief Overview. *J. Polym. Sci., Part A: Polym. Chem.* **2019**, *57*, 657-672.

[8] S. Liu, C. Ren, N. Zhao, Y. Shen, Z. Li, Phosphazene Bases as Organocatalysts for Ring-Opening Polymerization of Cyclic Esters. *Macromol. Rapid. Commun.* **2018**, *39*, e1800485.

[9] W. N. Ottou, H. Sardon, D. Mecerreyes, J. Vignolle, D. Taton, Update and Challenges in Organo-Mediated Polymerization Reactions. *Prog. Polym. Sci.* **2016**, *56*, 64-115.

[10] C. Thomas, B. Bibal, Hydrogen-Bonding Organocatalysts for Ring-Opening Polymerization. *Green Chem.* **2014**, *16*, 1687-1699.

[11] M. Fevre, J. Pinaud, Y. Gnanou, J. Vignolle, D. Taton, N-Heterocyclic Carbenes (NHCs) as Organocatalysts and Structural Components in Metal-Free Polymer Synthesis. *Chem. Soc. Rev.* **2013**, *42*, 2142-2172.

[12] F. H. Isikgor, C. R. Becer, Lignocellulosic Biomass: a Sustainable Platform for the Production of Bio-based Chemicals and olymers. *Polym. Chem.* **2015**, *6*, 4497-4559.

[13] H. R. Kricheldorf, G. Schwarz, Poly(thioester)s. *J. Macromol. Sci. A: Pure Appl. Chem.* **2007**, *44*, 625-649.

[14] I. L. Knunyants, N. D. Kuleshova, M. G. Lin'kova, β-Propiothiolactone. *Bull. Acad. Sci. USSR, Div. Chem. Sci.* **1965**, *14*, 1043-1045.

[15] D. Y. Kim, T. Lutke-Eversloh, K. Elbanna, N. Thakor, A. Steinbuchel, Poly(3-mercaptopropionate): a nonbiodegradable biopolymer? *Biomacromolecules* **2005**, *6*, 897-901.

[16] T. Lutke-Eversloh, A. Fischer, U. Remminghorst, J. Kawada, R. H. Marchessault, A. Bogershausen, M. Kalwei, H. Eckert, R. Reichelt, S. J. Liu, A. Steinbuchel, Biosynthesis of Novel Thermoplastic Polythioesters by Engineered *Escherichia Coli*. *Nat. Mater*. **2002**, *1*, 236-240.

[17] D. Fleš, V. Tomašić, Preparation of Poly-(*S*)(-)-[α-(*para*-toluenesulfonamido)-β-propiothiolactone]. *J. Polym. Sci. Part B: Polym. Lett.* **1968**, *6*, 809-813.

[18] V. Jarm, D. Fleš, Polymerization and Properties of Optically Active α-(*para*-Substituted Benzenesulfonamido)-β-Lactones. *J. Polym. Sci., Part A: Polym. Chem.* **1977**, *15*, 1061-1071.

[19] B. Jerman, D. Fleš, Synthesis and Polymerization of (*R*)-(+)-2-Methyl-2-Ethyl-3-Propiothiolactone. *J. Polym. Sci., Part A: Polym. Chem.* **1976**, *14*, 1117-1125.

[20] M. Suzuki, K. Makimura, S. Matsuoka, Thiol-Mediated Controlled Ring-Opening Polymerization of Cysteine-Derived β-Thiolactone and Unique Features of Product Polythioester. *Biomacromolecules* **2016**, *17*, 1135-1141.

[21] J.-F. Carpentier, Discrete Metal Catalysts for Stereoselective Ring-Opening Polymerization of Chiral Racemic β-Lactones. *Macromol. Rapid. Commun.* **2010**, *31*, 1696-1705.

[22] J. C. Worch, A. P. Dove, Click Step-Growth Polymerization and E/Z Stereochemistry Using Nucleophilic Thiol-yne/-ene Reactions: Applying Old Concepts for Practical Sustainable (Bio)Materials. *Acc. Chem. Res.* **2022**. *55*, 2355–2369

[23] W. Xiong, W. Chang, D. Shi, L. Yang, Z. Tian, H. Wang, Z. Zhang, X. Zhou, E.-Q. Chen, H. Lu, Geminal Dimethyl Substitution Enables Controlled Polymerization of Penicillamine-Derived β-Thiolactones and Reversed Depolymerization. *Chem* **2020**, *6*, 1831-1843.

[24] J. G. Rosenboom, R. Langer, G. Traverso, Bioplastics for a Circular Economy. *Nat. Rev. Mater.* **2022**, *7*, 117-137.

[25] G. W. Coates, Y. D. Y. L. Getzler, Chemical Recycling to Monomer for an Ideal, Circular Polymer Economy. *Nat. Rev. Chem.* **2020**, *5*, 501-516.

[26] J. Yuan, W. Xiong, X. Zhou, Y. Zhang, D. Shi, Z. Li, H. Lu, 4-Hydroxyproline-Derived Sustainable Polythioesters: Controlled Ring-Opening Polymerization, Complete Recyclability, and Facile Functionalization. *J. Am. Chem. Soc.* **2019**, *141*, 4928-4935.

[27] C. Shi, M. L. McGraw, Z. C. Li, L. Cavallo, L. Falivene, E. Y.-X. Chen, High-Performance Pan-Tactic Polythioesters with Intrinsic Crystallinity and Chemical Recyclability. *Sci. Adv.* **2020**, *6*, eabc0495.

[28] H. A. Brown, R. M. Waymouth, Zwitterionic Ring-Opening Polymerization for the Synthesis of High Molecular Weight Cyclic Polymers. *Acc. Chem. Res.* **2013**, *46*, 2585-2596.

[29] C. G. O. J. K. Weise, Anionic Ring-Opening Polymerization of Thiolactones. *J. Am. Chem. Soc.* **1968**, *90*, 3353-3357.

[30] M. Suzuki, A. Watanabe, R. Kawai, R. Sato, S.-i. Matsuoka, S. Kawauchi, Ring-opening polymerization of thiolactide by using thiol-amine combination. *Polymer* **2021**, *215*, 123386.

[31] Y. Wang, M. Li, J. Chen, Y. Tao, X. Wang, O-to-S Substitution Enables Dovetailing Conflicting Cyclizability, Polymerizability, and Recyclability: Dithiolactone vs. Dilactone. *Angew. Chem. Int. Ed.* **2021**, *60*, 22547-22553.

[32] S. Mavila, B. T. Worrell, H. R. Culver, T. M. Goldman, C. Wang, C. H. Lim, D. W. Domaille, S. Pattanayak, M. K. McBride, C. B. Musgrave, C. N. Bowman, Dynamic and Responsive DNA-like Polymers. *J. Am. Chem. Soc.* **2018**, *140*, 13594-13598.

[33] K. A. Stellmach, M. K. Paul, M. Xu, Y. L. Su, L. Fu, A. R. Toland, H. Tran, L. Chen, R. Ramprasad, W. R. Gutekunst, Modulating Polymerization Thermodynamics of Thiolactones Through Substituent and Heteroatom Incorporation. *ACS Macro Lett.* **2022**, *11*, 895-901.

[34] C. G. O. J. K. Weise, Optical Rotatory Dispersion Studies of Asymmetric Poly(thiol esters). *J. Am. Chem. Soc.* **1968**, 3538-3543.

[35] C. G. Overberger, J. Weise, A Polythioester by Ring-Opening Polymerization. *J. Polym. Sci. Part B: Polym. Lett.* **1964**, *2*, 329-331.

[36] T. J. Bannin, M. K. Kiesewetter, Poly(thioester) by Organocatalytic Ring-Opening Polymerization. *Macromolecules* **2015**, *48*, 5481-5486.

[37] A. P. Dove, Organic Catalysis for Ring-Opening Polymerization. *ACS Macro Lett.* **2012**, *1*, 1409-1412.

[38] K. Shimokawa, M. Kato, S. Matsumura, Enzymatic Synthesis and Chemical Recycling of Polythiocaprolactone. *Macromol. Chem. Phys.* **2011**, *212*, 150-158.

[39] S. W. Duchiron, E. Pollet, S. Givry, L. Avérous, Enzymatic Synthesis of Poly(ε-caprolactone-co-ε-thiocaprolactone). *Eur. Polym. J.* **2017**, *87*, 147-158.

[40] M. Kato, K. Toshima, S. Matsumura, Enzymatic Synthesis of Polythioester by the Ring-Opening Polymerization of Cyclic Thioester. *Biomacromolecules* **2007**, *8*, 3590-3596.

[41] Y. Wang, M. Li, S. Wang, Y. Tao, X. Wang, S-Carboxyanhydrides: Ultrafast and Selective Ring-Opening Polymerizations Towards Well-defined Functionalized Polythioesters. *Angew. Chem. Int. Ed.* **2021**, *60*, 10798-10805.

[42] G. R. Kiel, D. J. Lundberg, E. Prince, K. E. L. Husted, A. M. Johnson, V. Lensch, S. Li, P. Shieh, J. A. Johnson, Cleavable Comonomers for Chemically Recyclable Polystyrene: A General Approach to Vinyl Polymer Circularity. *J. Am. Chem. Soc.* **2022**. *144*, 12979–12988

[43] C. M. Plummer, N. Gil, P.-E. Dufils, D. J. Wilson, C. Lefay, D. Gigmes, Y. Guillaneuf, Mechanistic Investigation of ε-Thiono-Caprolactone Radical Polymerization: An Interesting Tool to Insert Weak Bonds into Poly(vinyl esters). *ACS Appl. Polym. Mater.* **2021**, *3*, 3264-3271.

[44] T. Pesenti, J. Nicolas, 100th Anniversary of Macromolecular Science Viewpoint: Degradable Polymers from Radical Ring-Opening Polymerization: Latest Advances, New Directions, and Ongoing Challenges. *ACS Macro Lett.* **2020**, *9*, 1812-1835.

[45] N. M. Bingham, Q. u. Nisa, S. H. L. Chua, L. Fontugne, M. P. Spick, P. J. Roth, Thioester-Functional Polyacrylamides: Rapid Selective Backbone Degradation Triggers Solubility Switch Based on Aqueous Lower Critical Solution Temperature/Upper Critical Solution Temperature. *ACS Appl. Polym. Mater.* **2020**, *2*, 3440-3449.

[46] R. A. Smith, G. Fu, O. McAteer, M. Xu, W. R. Gutekunst, Radical Approach to Thioester-Containing Polymers. *J. Am. Chem. Soc.* **2019**, *141*, 1446-1451.

[47] P. Yuan, Y. Sun, X. Xu, Y. Luo, M. Hong, Towards High-Performance Sustainable Polymers via Isomerization-Driven Irreversible Ring-Opening Polymerization of Five-Membered Thionolactones. *Nat. Chem.* **2022**, *14*, 294-303.

[48] H. Kikuchi, N. Tsubokawa, T. Endo, First Example of Cationic Ring-Opening Polymerization of γ-Thionobutyrolactone. *Chem. Lett.* **2005**, *34*, 376-377.

[49] F. M. Haque, S. M. Grayson, The Synthesis, Properties and Potential Applications of Cyclic Polymers. *Nat. Chem.* **2020**, *12*, 433-444.

[50] P. J. Dijkstra, H. Z. Du, J. Feijen, Single Site Catalysts for Stereoselective Ring-Opening Polymerization of Lactides. *Polym. Chem.* **2011**, *2*, 520-527.

[51] C. M. Thomas, Stereocontrolled Ring-Opening Polymerization of Cyclic Esters: Synthesis of New Polyester Microstructures. *Chem. Soc. Rev.* **2010**, *39*, 165-173.

[52] R. Platel, L. Hodgson, C. Williams, Biocompatible Initiators for Lactide Polymerization. *Polym. Rev.* **2008**, *48*, 11-63.

[53] O. Dechy-Cabaret, B. Martin-Vaca, D. Bourissou, Controlled Ring-Opening Polymerization of Lactide and Glycolide. *Chem. Rev.* **2004**, *104*, 6147-6176.

[54] M. J. Stanford, A. P. Dove, Stereocontrolled Ring-Opening Polymerisation of Lactide. *Chem. Soc. Rev.* **2010**, *39*, 486-494.

[55] T. M. Ovitt, G. W. Coates, Stereochemistry of Lactide Polymerization with Chiral Catalysts: New Opportunities for Stereocontrol Using Polymer Exchange Mechanisms. *J. Am. Chem. Soc.* **2002**, *124*, 1316-1326.

[56] C. X. Cai, A. Amgoune, C. W. Lehmann, J.-F. Carpentier, Stereoselective Ring-Opening Polymerization of Racemic Lactide Using Alkoxy-Amino-Bis(phenolate) Group 3 Metal Complexes. *Chem. Commun.* **2004**, 330-331.

[57] M. Bouyahyi, N. Ajellal, E. Kirillov, C. M. Thomas, J.-F. Carpentier, Exploring Electronic versus Steric Effects in Stereoselective Ring-Opening Polymerization of Lactide and β-Butyrolactone with Amino-alkoxy-bis(phenolate)-yttrium Complexes. *Chem. Eur. J.* **2011**, *17*, 1872-1883.

[58] A. Amgoune, C. M. Thomas, T. Roisnel, J.-F. Carpentier, Ring-Opening Polymerization of Lactide with Group 3 Metal Complexes Supported by Dianionic Alkoxy-Amino-Bisphenolate Ligands: Combining High Activity, Productivity, and Selectivity. *Chem. Eur. J.* **2005**, *12*, 169-179.

[59] Y. Chapurina, J. Klitzke, L. Casagrande Ode, Jr., M. Awada, V. Dorcet, E. Kirillov, J.-F. Carpentier, Scandium *versus* Yttrium{amino-alkoxy-bis(phenolate)} Complexes for the Stereoselective Ring-Opening Polymerization of Racemic Lactide and β-Butyrolactone. *Dalton. Trans.* **2014**, *43*, 14322-14333.

[60] C.-X. Cai, L. Toupet, C. W. Lehmann, J.-F. Carpentier, Synthesis, Structure and Reactivity of New Yttrium Bis(dimethylsilyl)amido and Bis(trimethylsilyl)methyl Complexes of a Tetradentate Bis(phenoxide) Ligand. *J. Organomet. Chem.* **2003**, *683*, 131-136.

[61] H. Ma, T. P. Spaniol, J. Okuda, Rare-Earth Metal Complexes Supported by 1,ω-Dithiaalkanediyl-bridged Bis(phenolato) Ligands: Synthesis, Structure, and Heteroselective Ring-Opening Polymerization of *rac*-Lactide. *Inorg. Chem.* **2008**, *47*, 3328-3339.

[62] H. Ma, T. P. Spaniol, J. Okuda, Highly Heteroselective Ring-Opening Polymerization of *rac*-Lactide Initiated by Bis(phenolato)scandium Complexes. *Angew. Chem. Int. Ed.* **2006**, *45*, 7818-7821.

[63] C. Bakewell, T.-P.-A. Cao, X. F. Le Goff, N. J. Long, A. Auffrant, C. K. Williams, Yttrium Phosphasalen Initiators for rac-Lactide Polymerization. *Organometallics* **2013**, *32*, 1475-1483.

[64] T. P. Cao, A. Buchard, X. F. Le Goff, A. Auffrant, C. K. Williams, Phosphasalen yttrium complexes: highly active and stereoselective initiators for lactide polymerization. *Inorg. Chem.* **2012**, *51*, 2157-2169.

[65] C. Bakewell, T. P. Cao, N. Long, X. F. Le Goff, A. Auffrant, C. K. Williams, Yttrium Phosphasalen Initiators for *rac*-Lactide Polymerization: Excellent Rates and High Iso-Selectivities. *J. Am. Chem. Soc.* **2012**, *134*, 20577-20580.

[66] C. Bakewell, A. J. White, N. J. Long, C. K. Williams, Metal-Size Influence in Iso-Selective Lactide Polymerization. *Angew. Chem. Int. Ed.* **2014**, *53*, 9226-9030.

[67] T.-Q. Xu, G.-W. Yang, C. Liu, X.-B. Lu, Highly Robust Yttrium Bis(phenolate) Ether Catalysts for Excellent Isoselective Ring-Opening Polymerization of Racemic Lactide. *Macromolecules* **2017**, *50*, 515-522.

[68] H. Li, R. M. Shakaroun, S. M. Guillaume, J.-F. Carpentier, Recent Advances in Metal-Mediated Stereoselective Ring-Opening Polymerization of Functional Cyclic Esters towards Well-Defined Poly(hydroxy acid)s: From Stereoselectivity to Sequence-Control. *Chem. Eur. J.* **2020**, *26*, 128-138.

[69] R. Ligny, M. M. Hanninen, S. M. Guillaume, J.-F. Carpentier, Steric *vs.* Electronic Stereocontrol in Syndio- or Iso-selective ROP of Functional Chiral β-Lactones Mediated by Achiral Yttrium-Bisphenolate Complexes. *Chem. Commun.* **2018**, *54*, 8024-8031.

[70] J.-F. Carpentier, Rare-Earth Complexes Supported by Tripodal Tetradentate Bis(phenolate) Ligands: A Privileged Class of Catalysts for Ring-Opening Polymerization of Cyclic Esters. *Organometallics* **2015**, *34*, 4175-4189.

[71] L. R. Rieth, D. R. Moore, E. B. Lobkovsky, G. W. Coates, Single-Site β-Diiminate Zinc Catalysts for the Ring-Opening Polymerization of β-Butyrolactone and β-Valerolactone to Poly(3-hydroxyalkanoates). *J. Am. Chem. Soc.* **2002**, *124*, 15239-15248.

[72] A. Le Borgne, N. Spassky, Stereoelective Polymerization of β-Butyrolactone. *Polymer* **1989**, *30*, 2312-2319.

[73] M. Zintl, F. Molnar, T. Urban, V. Bernhart, P. Preishuber-Pflugl, B. Rieger, Variably Isotactic Poly(hydroxybutyrate) from racemic β-Butyrolactone: Microstructure Control by Achiral Chromium(III) Salophen Complexes. *Angew. Chem. Int. Ed.* **2008**, *47*, 3458-3460.

[74] A. Amgoune, C. M. Thomas, S. Ilinca, T. Roisnel, J.-F. Carpentier, Highly Active, Productive, and Syndiospecific Yttrium Initiators for the Polymerization of Racemic β-Butyrolactone. *Angew. Chem. Int. Ed.* **2006**, *45*, 2782-2784.

[75] K. Nie, L. Fang, Y. Yao, Y. Zhang, Q. Shen, Y. Wang, Synthesis and Characterization of Amine-Bridged Bis(phenolate)lanthanide Alkoxides and Their Application in the Controlled Polymerization of *rac*-lactide and *rac*-β-butyrolactone. *Inorg. Chem.* **2012**, *51*, 11133-11143.

[76] N. Ajellal, M. Bouyahyi, A. Amgoune, C. M. Thomas, A. Bondon, I. Pillin, Y. Grohens, J.-F. Carpentier, Syndiotactic-Enriched Poly(3-hydroxybutyrate)s via Stereoselective Ring-Opening Polymerization of Racemic β-Butyrolactone with Discrete Yttrium Catalysts. *Macromolecules* **2009**, *42*, 987-993.

[77] N. Ajellal, D. M. Lyubov, M. A. Sinenkov, G. K. Fukin, A. V. Cherkasov, C. M. Thomas, J.-F. Carpentier, A. A. Trifonov, Bis(guanidinate) Alkoxide Complexes of Lanthanides: Synthesis, Structures and Use in Immortal and Stereoselective Ring-Opening Polymerization of Cyclic Esters. *Chem. Eur. J.* **2008**, *14*, 5440-5448.

[78] E. Grunova, E. Kirillov, T. Roisnel, J.-F. Carpentier, Group 3 Metal Complexes Supported by Tridentate Pyridine- and Thiophene-Linked Bis(naphtholate) Ligands: Synthesis, Structure, and Use in Stereoselective Ring-Opening Polymerization of racemic Lactide and β-Butyrolactone. *Dalton. Trans.* **2010**, *39*, 6739-6752.

[79] J. S. Klitzke, T. Roisnel, E. Kirillov, O. d. L. Casagrande, J.-F. Carpentier, Yttrium– and Aluminum–Bis(phenolate)pyridine Complexes: Catalysts and Model Compounds of the Intermediates for the Stereoselective Ring-Opening Polymerization of Racemic Lactide and β-Butyrolactone. *Organometallics* **2013**, *33*, 309-321.

[80] X. Dong, J. R. Robinson, The Versatile Roles of Neutral Donor Ligands in Tuning Catalyst Performance for the Ring-Opening Polymerization of Cyclic Esters. *New J. Chem.* **2022**, *46*, 444-453.

[81] J. Fang, M. J. L. Tschan, T. Roisnel, X. Trivelli, R. M. Gauvin, C. M. Thomas, L. Maron, Yttrium catalysts for syndioselective β-butyrolactone polymerization: on the origin of ligand-induced stereoselectivity. *Polym. Chem.* **2013**, *4*, 360-367.

[82] J. W. Kramer, D. S. Treitler, E. W. Dunn, P. M. Castro, T. Roisnel, C. M. Thomas, G. W. Coates, Polymerization of Enantiopure Monomers Using Syndiospecific Catalysts: A New Approach to Sequence Control in Polymer Synthesis. *J. Am. Chem. Soc.* **2009**, *131*, 16042-16044.

[83] Z. Zhuo, C. Zhang, Y. Luo, Y. Wang, Y. Yao, D. Yuan, D. Cui, Stereo-Selectivity Switchable ROP of rac-β-Butyrolactone Initiated by Salan-Ligated Rare-Earth Metal Amide Complexes: the Key Role of the Substituents on Ligand Frameworks. *Chem. Commun.* **2018**, *54*, 11998-12001.

[84] X. Dong, J. R. Robinson, The Role of Neutral Donor Ligands in The Isoselective Ring-Opening Polymerization of rac-β-Butyrolactone. *Chem. Sci.* **2020**, *11*, 8184-8195.

[85] X. Dong, A. M. Brown, A. J. Woodside, J. R. Robinson, N-Oxides Amplify Catalyst Reactivity and Isoselectivity in the Ring-Opening Polymerization of *rac*-β-Butyrolactone. *Chem. Commun.* **2022**, *58*, 2854-2857.

[86] X. Tang, E. Y.-X. Chen, Chemical Synthesis of Perfectly Isotactic and High Melting Bacterial Poly(3-hydroxybutyrate) from Bio-sourced Racemic Cyclic Diolide. *Nat. Commun.* **2018**, *9*, 2345.

[87] X. Tang, A. H. Westlie, L. Caporaso, L. Cavallo, L. Falivene, E. Y.-X. Chen, Biodegradable Polyhydroxyalkanoates by Stereoselective Copolymerization of Racemic Diolides: Stereocontrol and Polyolefin-Like Properties. *Angew. Chem. Int. Ed.* **2020**, *59*, 7881-7890.

[88] A. H. Westlie, E. Y.-X. Chen, Catalyzed Chemical Synthesis of Unnatural Aromatic Polyhydroxyalkanoate and Aromatic-Aliphatic PHAs with Record-High Glass-Transition and Decomposition Temperatures. *Macromolecules* **2020**, *53*, 9906-9915.

[89] X. Tang, A. H. Westlie, E. M. Watson, E. Y.-X. Chen, Stereosequenced Crystalline Polyhydroxyalkanoates from Diastereomeric Monomer Mixtures. *Science* **2019**, *366*, 754-758.

[90] J. C. Worch, H. Prydderch, S. Jimaja, P. Bexis, M. L. Becker, A. P. Dove, Stereochemical Enhancement of Polymer Properties. *Nat. Rev. Chem.* **2019**, *3*, 514-535.

[91] C. G. Jaffredo, S. M. Guillaume, Benzyl β-Malolactonate Polymers: A Long Story with Recent Advances. *Polym. Chem.* **2014**, *5*, 4168-4194.

[92] C. G. Jaffredo, Y. Chapurina, S. M. Guillaume, J.-F. Carpentier, From Syndiotactic Homopolymers to Chemically Tunable Alternating Copolymers: Highly Active Yttrium Complexes for Stereoselective Ring-Opening Polymerization of β-Malolactonates. *Angew. Chem. Int. Ed.* **2014**, *53*, 2687-2691.

[93] C. G. Jaffredo, Y. Chapurina, E. Kirillov, J.-F. Carpentier, S. M. Guillaume, Highly Stereocontrolled Ring-Opening Polymerization of Racemic Alkyl β-Malolactonates Mediated by Yttrium [Amino-alkoxy-bis(phenolate)] Complexes. *Chem. Eur. J.* **2016**, *22*, 7629-7641.

[94] R. Ligny, M. M. Hanninen, S. M. Guillaume, J.-F. Carpentier, Highly Syndiotactic or Isotactic Polyhydroxyalkanoates by Ligand-Controlled Yttrium-Catalyzed Stereoselective Ring-

Opening Polymerization of Functional Racemic β-Lactones. *Angew. Chem. Int. Ed.* **2017**, *56*, 10388-10393.

[95] J. B. Zhu, E. Y.-X. Chen, Catalyst-Sidearm-Induced Stereoselectivity Switching in Polymerization of a Racemic Lactone for Stereocomplexed Crystalline Polymer with a Circular Life Cycle. *Angew. Chem. Int. Ed.* **2019**, *58*, 1178-1182.

[96] J. B. Zhu, E. M. Watson, J. Tang, E. Y.-X. Chen, A Synthetic Polymer System with Repeatable Chemical Recyclability. *Science* **2018**, *360*, 398-403.

[97] X. Yang, W. Zhang, H.-Y. Huang, J. Dai, M.-Y. Wang, H.-Z. Fan, Z. Cai, Q. Zhang, J.-B. Zhu, Stereoselective Ring-Opening Polymerization of Lactones with a Fused Ring Leading to Semicrystalline Polyesters. *Macromolecules* **2022**, *55*, 2777–2786.

[98] J. Wang, Y. Tao, Synthesis of Sustainable Polyesters via Organocatalytic Ring-Opening Polymerization of *O*-Carboxyanhydrides: Advances and Perspectives. *Macromol. Rapid. Commun.* **2021**, *42*, e2000535.

[99] Y. Sun, Z. Jia, C. Chen, Y. Cong, X. Mao, J. Wu, Alternating Sequence Controlled Copolymer Synthesis of α-Hydroxy Acids via Syndioselective Ring-Opening Polymerization of O-Carboxyanhydrides Using Zirconium/Hafnium Alkoxide Initiators. *J. Am. Chem. Soc.* **2017**, *139*, 10723-10732.

[100] A. J. Chmura, M. G. Davidson, C. J. Frankis, M. D. Jones, M. D. Lunn, Highly active and stereoselective zirconium and hafnium alkoxide initiators for solvent-free ring-opening polymerization of rac-lactide. *Chem. Commun.* **2008**, 1293-1295.

[101] V. Balasanthiran, M. H. Chisholm, K. Choojun, C. B. Durr, P. M. Wambua, TMPZnN($SiMe_3$)$_2$, [TMPZn(μ-O^{i}Pr)]$_2$ and TMPZn[$OCMe_2C(O)OEt$]. Their Role in the Ring-Opening of *rac*-Lactide and ε-Caprolactone where TMP = 1,5,9-trimesityldipyrromethene. *J. Organomet. Chem.* **2016**, *812*, 56-65.

[102] Y. Cui, J. Jiang, X. Pan, J. Wu, Highly Isoselective Ring-Opening Polymerization of *rac*-*O*-Carboxyanhydrides Using a Zinc Alkoxide Initiator. *Chem. Commun.* **2019**, *55*, 12948-12951.

[103] J. X. Jiang, Y. Q. Cui, Y. G. Lu, B. Zhang, X. B. Pan, J. C. Wu, Weak Lewis Pairs as Catalysts for Highly Isoselective Ring-Opening Polymerization of Epimerically Labile *rac*-*O*-Carboxyanhydride of Mandelic Acid. *Macromolecules* **2020**, *53*, 946-955.

[104] Q. Feng, L. Yang, Y. Zhong, D. Guo, G. Liu, L. Xie, W. Huang, R. Tong, Stereoselective Photoredox Ring-Opening Polymerization of *O*-Carboxyanhydrides. *Nat. Commun.* **2018**, *9*, 1559.

[105] Q. Feng, R. Tong, Controlled Photoredox Ring-Opening Polymerization of *O*-Carboxyanhydrides. *J. Am. Chem. Soc.* **2017**, *139*, 6177-6182.

[106] Y. L. Zhong, Q. Y. Feng, X. Q. Wang, J. Chen, W. J. Cai, R. Tong, Functionalized Polyesters via Stereoselective Electrochemical Ring-Opening Polymerization of *O*-Carboxyanhydrides. *ACS Macro Lett.* **2020**, *9*, 1114-1118.

[107] A. P. Dove, H. Li, R. C. Pratt, B. G. Lohmeijer, D. A. Culkin, R. M. Waymouth, J. L. Hedrick, Stereoselective Polymerization of *rac*- and *meso*-Lactide Catalyzed by Sterically Encumbered N-heterocyclic Carbenes. *Chem. Commun.* **2006**, 2881-2883.

[108] L. Zhang, F. Nederberg, J. M. Messman, R. C. Pratt, J. L. Hedrick, C. G. Wade, Organocatalytic stereoselective ring-opening polymerization of lactide with dimeric phosphazene bases. *J. Am. Chem. Soc.* **2007**, *129*, 12610-12611.

[109] S. Liu, H. Li, N. Zhao, Z. Li, Stereoselective Ring-Opening Polymerization of rac-Lactide Using Organocatalytic Cyclic Trimeric Phosphazene Base. *ACS Macro Lett.* **2018**, *7*, 624-628.

[110] S. Moins, S. Hoyas, V. Lemaur, B. Orhan, K. Delle Chiaie, R. Lazzaroni, D. Taton, A. P. Dove, O. Coulembier, Stereoselective ROP of *rac*- and *meso*-Lactides Using Achiral TBD as Catalyst. *Catalysts* **2020**, *10*, 620-627.

[111] B. Orhan, M. J. L. Tschan, A.-L. Wirotius, A. P. Dove, O. Coulembier, D. Taton, Isoselective Ring-Opening Polymerization of *rac*-Lactide from Chiral Takemoto's Organocatalysts: Elucidation of Stereocontrol. *ACS Macro Lett.* **2018**, *7*, 1413-1419.

[112] M. S. Zaky, A. L. Wirotius, O. Coulembier, G. Guichard, D. Taton, A Chiral Thiourea and a Phosphazene for Fast and Stereoselective Organocatalytic Ring-Opening Polymerization of Racemic Lactide. *Chem. Commun.* **2021**, *57*, 3777-3780.

[113] G. M. Miyake, E. Y.-X. Chen, Cinchona Alkaloids as Stereoselective Organocatalysts for the Partial Kinetic Resolution Polymerization of *rac*-Lactide. *Macromolecules* **2011**, *44*, 4116-4124.

[114] J. B. Zhu, E. Y. Chen, From *meso*-Lactide to Isotactic Polylactide: Epimerization by B/N Lewis Pairs and Kinetic Resolution by Organic Catalysts. *J. Am. Chem. Soc*. **2015**, *137*, 12506-12509.

[115] J. Y. C. Lim, N. Yuntawattana, P. D. Beer, C. K. Williams, Isoselective Lactide Ring Opening Polymerisation using [2]Rotaxane Catalysts. *Angew. Chem. Int. Ed.* **2019**, *58*, 6007-6011.

[116] A. Sanchez-Sanchez, I. Rivilla, M. Agirre, A. Basterretxea, A. Etxeberria, A. Veloso, H. Sardon, D. Mecerreyes, F. P. Cossio, Enantioselective Ring-Opening Polymerization of rac-Lactide Dictated by Densely Substituted Amino Acids. *J. Am. Chem. Soc.* **2017**, *139*, 4805-4814.

[117] K. Makiguchi, T. Yamanaka, T. Kakuchi, M. Terada, T. Satoh, Binaphthol-Derived Phosphoric Acids as Efficient Chiral Organocatalysts for the Enantiomer-Selective Polymerization of *rac*-Lactide. *Chem. Commun.* **2014**, *50*, 2883-2885.

[118] C. Lv, G. Xu, R. Yang, L. Zhou, Q. Wang, Chiral Phosphoric Acid Catalyzed Asymmetric Kinetic Resolution Polymerization of 6-Aryl-ε-caprolactones. *Polym. Chem.* **2020**, *11*, 4203-4207.

[119] C. Lv, G. Xu, R. Yang, L. Zhou, Q. Wang, Stereogradient polycaprolactones formed by asymmetric kinetic resolution polymerization of 6-methyl-ε-caprolactone. *Polym. Chem.* **2021**, *12*, 4856-4863.

Chapter 2

Influence of the Exocyclic Side-Group in the Stereoselective Ring-Opening Polymerization of Functional β-Lactones: ROP of 4-Ethylenylalkoxy vs. Methylenealkoxy-β-Butyrolactones[††]

Previous work by Ligny *et al. Angew. Chem. Int. Ed.* **2017**, *56*, 10388-10393:

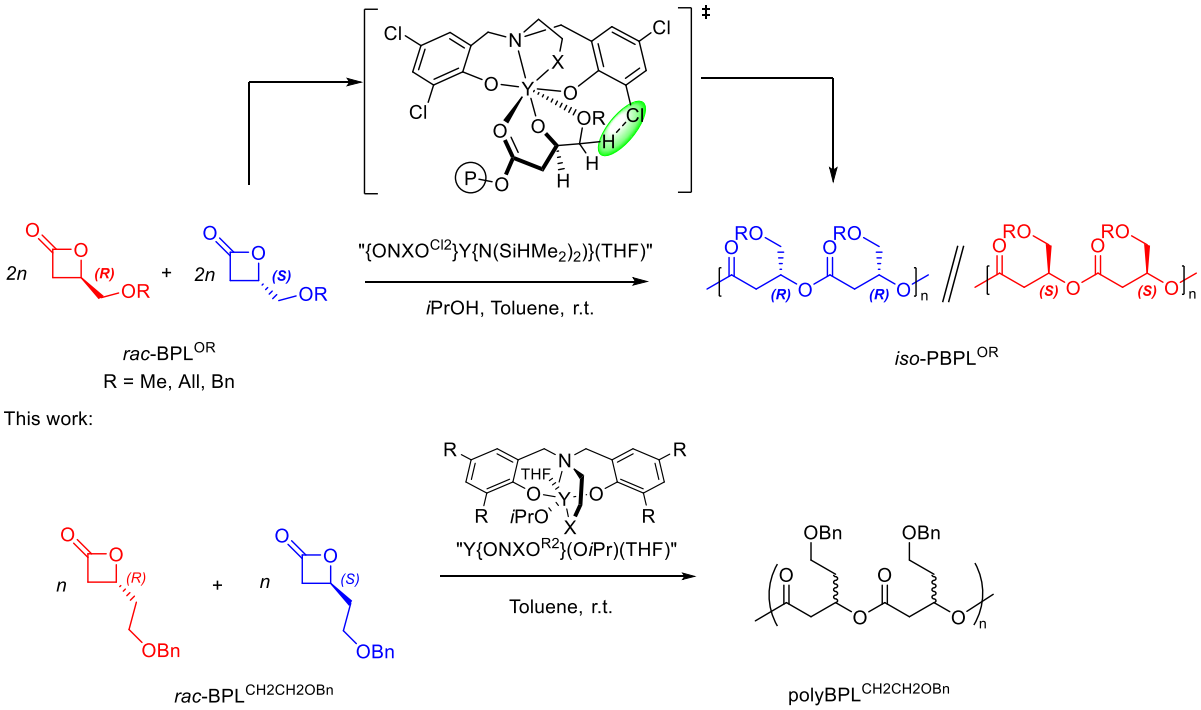

[††] Part of this chapter has appeared in print, see:

R. M. Shakaroun, H. Li, P. Jéhan, M. Blot, A. Alaaeddine, J.-F. Carpentier, S. M. Guillaume, Stereoselective Ring-Opening Polymerization of Functional β-Lactones: Influence of the Exocyclic Side-Group. *Polym. Chem.* **2021**, *12*, 4022-4034.

2.1 Introduction

In 2017, our group reported the first stereoselective ring-opening polymerization (ROP) of *rac*-4-alkoxymethylene-β-propiolactones (*rac*-BPL^{OR}s) by tripodal tetradentate bisphenolate yttrium complexes, "Y{ONXO^{R1,R2}}(N(SiHMe$_2$)(THF)", featuring both an excellent catalytic activity and a high degree of control over the molar mass of the resulting PBPL^{OR}s (Figure 2.1).[1] It was shown that a simple modification of the *ortho*-substituents R^1 on the {ONXO^{R1,R2}}$^{2-}$ platform of the yttrium catalyst results in a complete switch from syndioselective to isoselective polymerization of this specific class of β-lactones. In fact, highly syndioselective (P_r = 0.85-0.90) ROP of *rac*-BPL^{OR} was achieved by yttrium complexes incorporating bulky *ortho*-substituents (such as R^1 = CMe$_2$Ph, *t*Bu) on the phenoxy rings. The dimethyl-substituted yttrium complexes gave atactic PBPL^{OR}s, demonstrating that syndiotactic ROP is under steric control. On the other hand, yttrium complexes bearing "uncrowded" *ortho*-substituents on the phenoxy rings, such as fluoro, chloro or bromo-substituents, induced the formation of highly isotactic PBPL^{OR}s (likely as a racemic mixture of *iso*-(*R*)-PBPL^{OR} and *iso*-(*S*)-PBPL^{OR}). These results indicate that sterics are not the main factor controlling the isoselectivity of this class of β-lactones but that electronic factors must also be at play.

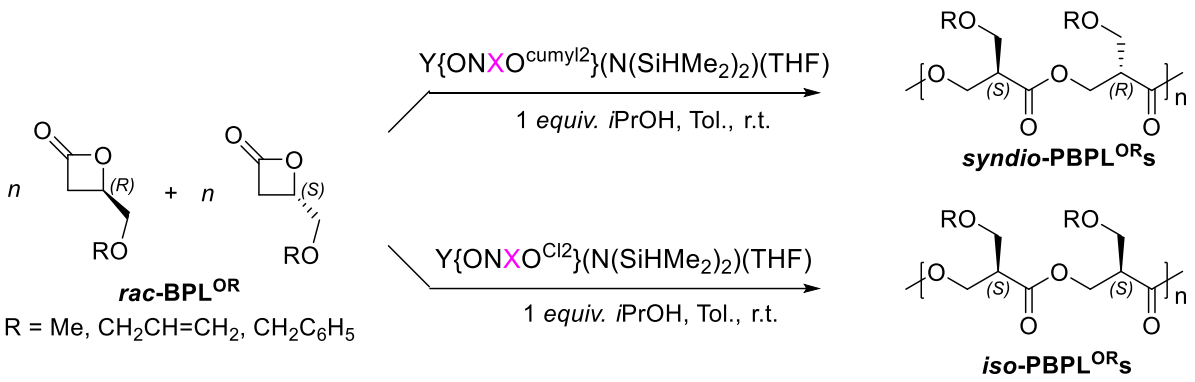

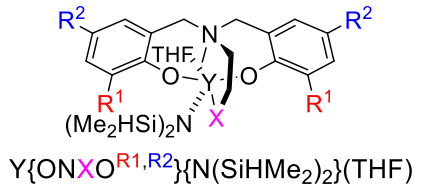

X =	NMe$_2$	OMe
R^1 = R^2 = Me	**a**	**b**
R^1 = R^2 = Cl	**c**	**h**
R^1 = R^2 = *t*Bu	**d**	**e**
R^1 = R^2 = CMe$_2$Ph	**f**	**g**

Figure 2.1. Access to syndiotactic or isotactic PBPL^{OR}s from the stereoselective ROP of *rac*-BPL^{OR}s with yttrium catalysts.[1-3]

DFT computations were performed for the elementary steps of the ROP of *rac*-BPL^{OR} and revealed that the origin of the isoselectivity was traced back to relatively strong C−H···Cl attractive interactions between hydrogen from the alkoxymethylene group of the pendant chain in the ring-opened monomer and the *chloro para*-substituents of the ligand (Figure 2.2).[1]

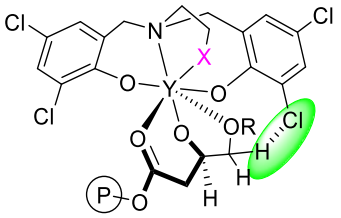

Figure 2.2. "Non-covalent interactions" at work in stereoselective ROP of *rac*-BPL^{OR}.[1]

To further support these DFT results, we designed two other functional *rac*-β-lactones (Figure 2.3), namely 4-(2-(benzyloxy)ethyl)oxetan-2-one (*rac*-BPL^{CH2CH2OBn}) and 4-[[(methylsulfonyl)oxy]methyl]-2-oxetanone (*rac*-BPL^{OSO2R}), to assess the stereoselective ROP by using the same class of yttrium complexes. The former *rac*-BPL^{CH2CH2OBn} 'simply' differs from *rac*-BPL^{OBn} by replacement in the pendant (exocyclic) group of methylene by an ethylene moiety, which shall enable us to assess the influence of the arm length and possible implication of the other $-CH_2-$ from the pendant group ($-CH_2\mathbf{\underline{CH_2}}OBn$) on the catalytic ROP process; indeed, this is much likely to affect the interaction between the side-arm group ($-CH_2CH_2OBn$) with the catalyst. The second lactone shall enable to assess the input of the pendant sulfonated group on the stereocontrol to be compared with previously investigated ether and alkoxycarbonyl functional groups.[4,5]

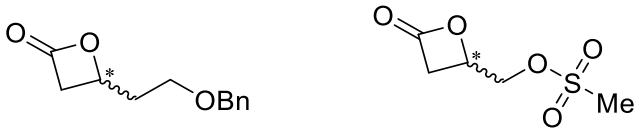

rac-BPL^{CH2CH2OBn} *rac*-BPL^{OSO2Me}

Figure 2.3. Functional β-lactones investigated in this chapter.

2.2 Carbonylation of Epoxides towards Functional β-Lactones

2.2.1 Carbonylation of Epoxides: State of the Art

The introduction of carbonyl functional groups using transition-metal-catalyzed carbon monoxide (CO) insertion ("carbonylation reaction") is a synthetically valuable transformation.[6] Application of this methodology, in conjunction with readily available epoxide substrates, provides facile access to β-lactones, that are useful precursors for synthesizing polymers, such as poly(3-hydroxyalkanoates). In 2001, Alper and coworkers reported an effective catalytic system made of neutral Lewis acids (such as BF_3 ¶Et_2, $SnCl_4$) with $[PPN]^+[Co(CO)_4]^-$ ($[PPN]^+$ = bis(triphenylphosphine)iminium) that can catalyze the ring-expansion carbonylation of a range of simple and functional epoxides (Figure 2.4).[7] Although this system required long reaction times (typically 24−48 h), it produced several β-lactones in good yields with retention of their configuration.

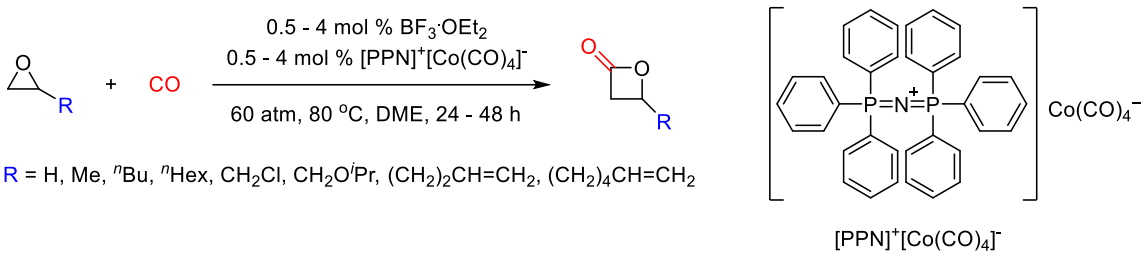

Figure 2.4. Alper's carbonylation of epoxides to β-lactones.[7]

Based on Alper's contribution, Coates and coworkers next reported a well-defined aluminium catalyst, $[(salph)Al(THF)_2]^+[Co(CO)_4]^-$ (salph = *N,N'-o*-phenylenebis(3,5-di-*tert*-butylsalicylideneimine)), also active for carbonylation of epoxides (Figure 2.5).[8] Yet, the high pressure of CO (60 bars) necessary for an efficient and selective carbonylation limits the use of these catalysts to laboratory applications. Thus, an efficient catalyst under mild conditions and low pressure of CO would be a significant advance, enabling the widespread use of epoxide carbonylation as a route to β-lactones. In 2006, the same group reported that $[(salph)Cr(THF)_2]^+[Co(CO)_4]^-$ carbonylated a range of epoxides to form selectively β-lactones at CO pressures as low as 1 atm.[9]

The authors proposed a catalytic cycle for the epoxide carbonylation by this Lewis acid/tetracarbonylcobaltate catalyst system (Figure 2.5).[6] It includes four steps: (1) activation of the epoxide by coordination to the Lewis acid; (2) attack of $[Co(CO)_4]^-$ on the activated epoxide occurring at the less hindered carbon of the epoxide, resulting in CO insertion adjacent to this center; the attack proceeds *via* a S_N2 pathway, resulting in inversion of stereochemistry at the *α* carbon and the concomitant reversal of *cis*/*trans* stereochemistry; (3) insertion of CO into the new cobalt-carbon bond, and the subsequent uptake of CO; and (4) metal alkoxide intramolecular attack of the acyl carbon to give the corresponding β-lactone and regenerate the original catalyst.

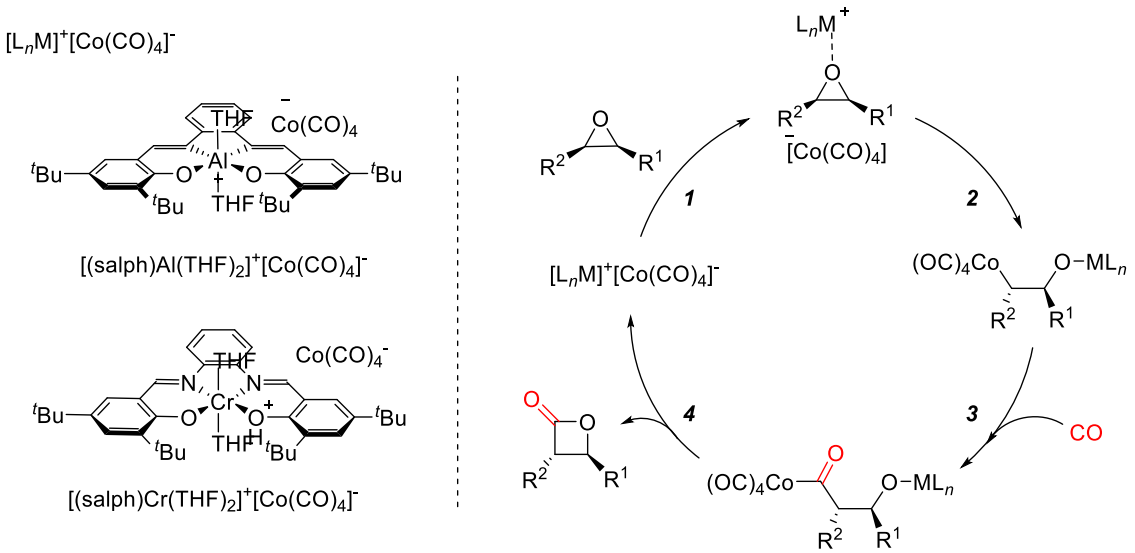

Figure 2.5. Proposed catalytic cycle for the carbonylation of epoxides.[6,9]

2.2.2 Synthesis and Characterization of *rac*-BPL^{CH2CH2OBn} and (*S*)-BPL^{CH2CH2OBn} and Attempts to Synthesize *rac*-BPL^{OSO2Me}

Synthesis of *rac*-4-(2-(benzyloxy)ethyl)oxetan-2-one (*rac*-BPL^{CH2CH2OBn})

Rac-2-[2-(benzyloxy)ethyl]oxirane was prepared in moderate overall yield (54%) on a multi-gram scale (*ca.* 4 g) from commercially available 3-buten-1-ol. Upon treatment with sodium hydride and benzyl bromide in THF at room temperature overnight, the starting reagent was converted into 1-benzyloxybut-3-ene in good isolated yield (85%). The intermediate was reacted with *meta*-chloroperoxybenzoic acid (m-CPBA) in CH_2Cl_2 at 0 °C for 16 h, leading to a racemic mixture of the corresponding epoxide in 63% yield (Figure 2.6).[10]

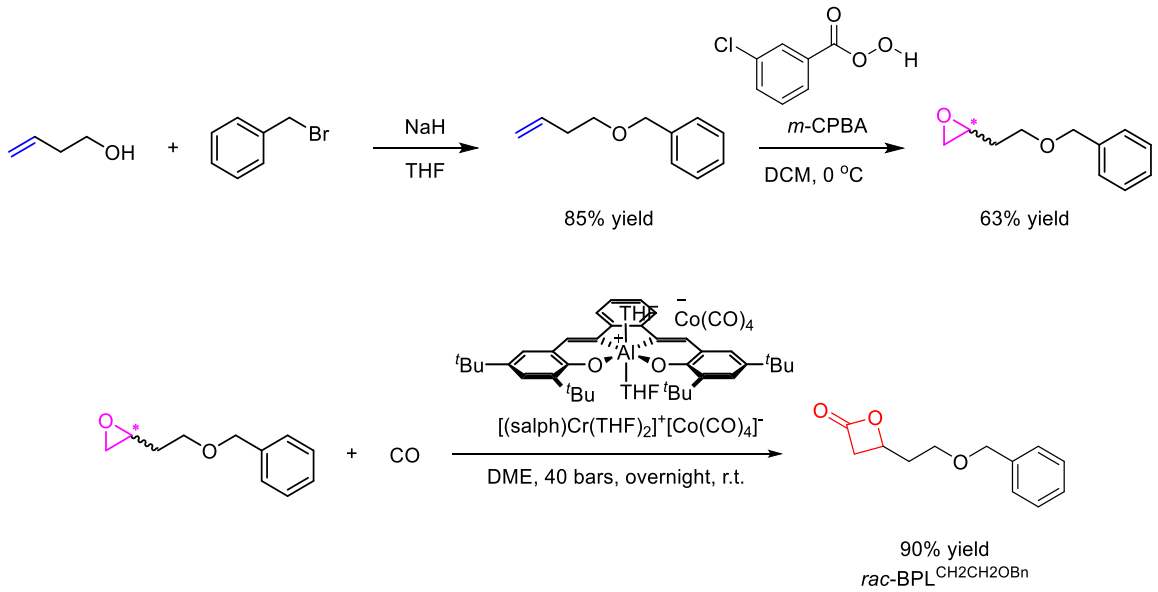

Figure 2.6. The synthetic pathway towards *rac*-4-(2-(benzyloxy)ethyl)oxetan-2-one (*rac*-BPL^{CH2CH2OBn}).[10]

Subsequently, the isolated *rac*-2-((benzyloxy)methyl)oxirane was subjected to carbonylation by Coates' chromium-tetrabonylcobaltate catalyst, $[(salph)Cr(THF)_2]^+[Co(CO)_4]^-$, using a modified literature procedure (the reaction was conducted at higher pressure, *i.e.* 40 bars instead of 1 bar), giving rise to the desired *rac*-4-(2-(benzyloxy)ethyl)oxetan-2-one (*rac*-BPL^{CH2CH2OBn}) in good yield (90%). The resulting *rac*-BPL^{CH2CH2OBn} was fully characterized by NMR, MS, and chiral HPLC (see Experimental section).

Synthesis of (*S*)-4-(2-(benzyloxy)ethyl)oxetan-2-one ((*S*)-BPL^{CH2CH2OBn})

The enantiopure (*S*)-BPL^{CH2CH2OBn} was synthesized following the synthetic pathway described above for racemic one. The hydrolytic kinetic resolution (HKR) of *rac*-2-[2-(benzyloxy)ethyl]oxirane catalyzed by a chiral (salen)Co complex led to enantiopure (*S*)-2-[2-(benzyloxy)ethyl]oxirane (Figure 2.7).[11] Subsequently, the obtained (*S*)-2-[2-(benzyloxy)ethyl]oxirane underwent the carbonylation

reaction, giving the desired (*S*)-BPL^{CH2CH2OBn} in 90% yield, which was characterized by NMR and chiral HPLC (see Experimental section).

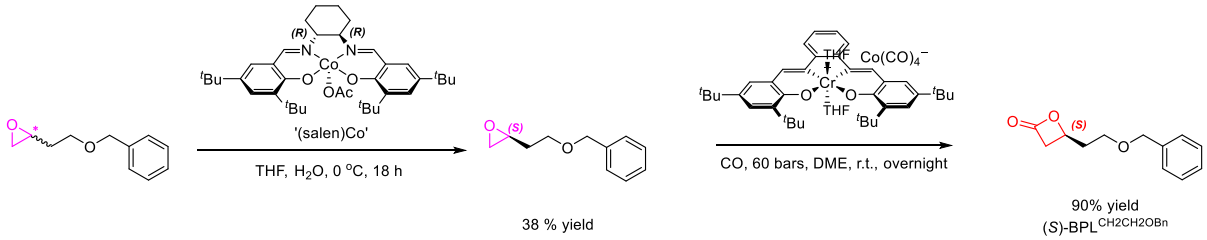

Figure 2.7. The synthetic procedure towards (*S*)-BPL^{CH2CH2OBn}.

Attempted synthesis of *rac*-BPL^{OSO2Me}

Rac-glycidyl methylene sulfonate (*rac*-GMS) was initially synthesized by a nucleophilic substitution reaction between glycidol and methylsulfonyl chloride. According to the patent procedure, carbonylation of *rac*-GMS by (salph)Cr-based catalyst was supposed to give *rac*-BPL^{OSO_2Me}.[12] Yet, the desired *rac*-BPL^{OSO_2Me} was not observed in the reaction mixture, while the patent authors reported 37% conversion of *rac*-GMS after 6 h. We suspected that the presence of impurities within *rac*-GMS, presumably methane sulfuric acid, may deactivate the catalyst (Figure 2.8). In this regard, the purification of *rac*-GMS should be essential for achieving a successful carbonylation reaction. When the purified *rac*-GMS (dried by CaH_2 and followed by distillation) was subjected to carbonylation reaction, a similar inefficient carbonylation reaction was observed, even at the [*rac*-GMS]$_0$/[Cat.]$_0$ feed ratio of 25:1 and at 50 bars. The other carbonylation catalyst [PPN]$^+$[Co(CO)$_4$]$^-$ also revealed inactive.

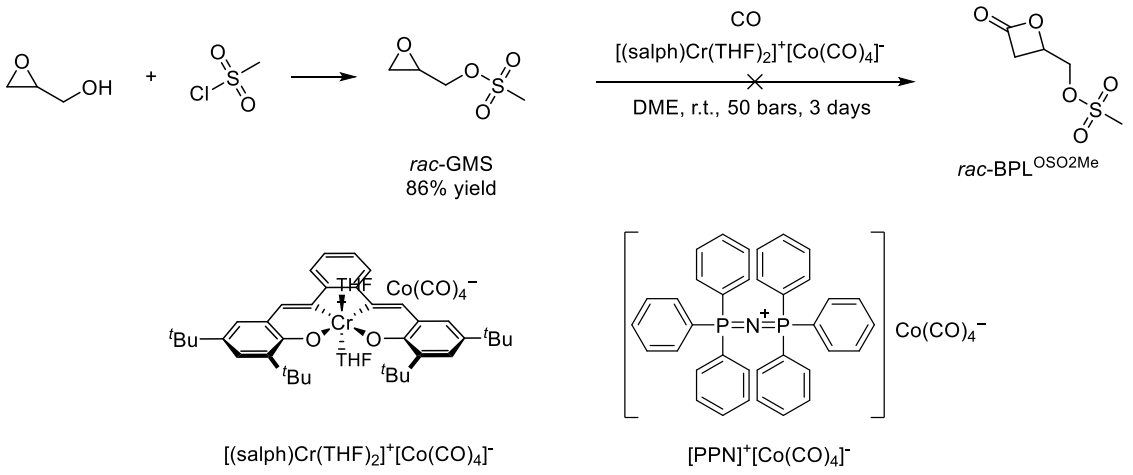

Figure 2.8. Attempted synthesis of *rac*-BPL^{OSO2Me}.

To assess why the carbonylation of *rac*-GMS was not successful, a control experiment was conducted, that is, the carbonylation of *rac*-GMS in the presence of *rac*-2-((allyloxy)methyl)oxirane (Figure 2.9). *Rac*-2-((allyloxy)methyl)oxirane was converted to *rac*-BPL^{OAll} (15% conversion after 3 days), while *rac*-GMS remained unreacted. In comparison, the carbonylation of *rac*-2-

((allyloxy)methyl)oxirane proceeds in 63% yield under identical conditions. We suspect the mesylate group may coordinate with the active site of the catalyst competing with the epoxide, and that this coordination would be stronger than the epoxide bond to the catalyst.

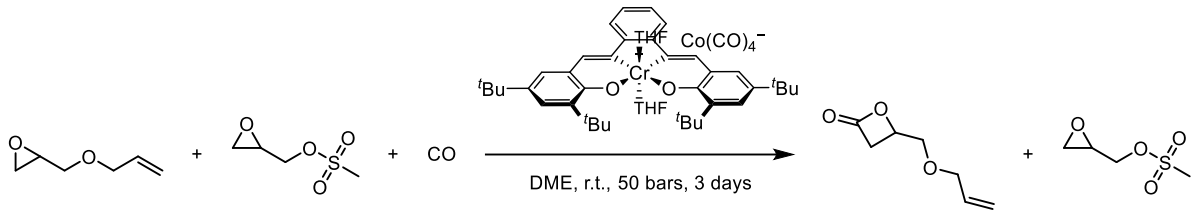

Figure 2.9. Attempted carbonylation of *rac*-GMS in the presence of *rac*-2-((allyloxy)methyl)oxirane.

2.3 Ring-Opening Polymerization of *rac*-BPL^{CH2CH2OBn} Promoted by Yttrium Catalysts: Activity and Kinetic Study

Initially, the stereoselective ROP of *rac*-BPL^{CH2CH2OBn} was investigated at room temperature in toluene, using the diamino- or aminoalkoxy-bis(phenolate) yttrium catalytic systems "Y{ONXO^{R1,R2}}(N(SiHMe$_2$)(THF)" (**a**–**g**) which differ in terms of the substituents installed on the phenolate ligand; the latter systems were selected in light of our previous work on the ROP of *rac*-BPL^{OR} (R = methyl, allyl, benzyl).[1] Note that the influence of the *para*-substituents on the phenolate ligand of yttrium complexes (**a**–**g**) has been found to exert little impact on the performance (especially the stereoselectivity) of the yttrium catalysts;[2] in this regard, they were not considered further in the present studies, although *para*-substituents affect the electronic properties of the complexes, which influence the catalytic activity. As implemented in our earlier studies, more reactive yttrium isopropoxide catalysts/initiators were conveniently generated *in situ* by the addition of 1 equivalent of *i*PrOH to the yttrium amido precursors **a**–**g**, respectively, which differ in terms of the substituents installed on the phenolate ligand.[1]

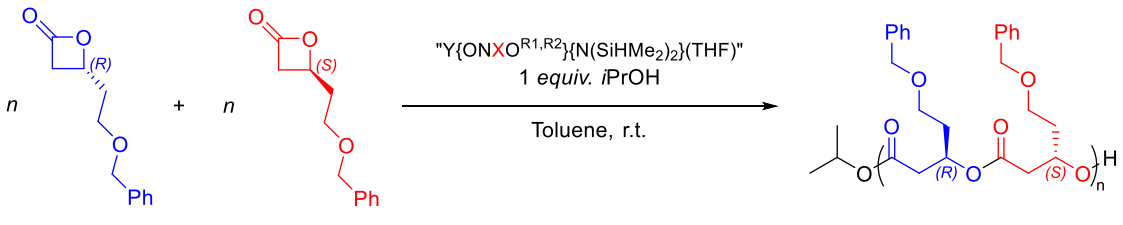

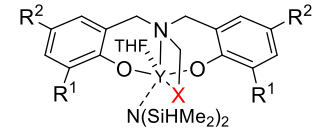

X =	CH_2NMe_2	CH_2OMe
$R^1 = R^2$ = Me	**a**	**b**
$R^1 = R^2$ = Cl	**c**	-
$R^1 = R^2$ = ^{t}Bu	**d**	**e**
$R^1 = R^2$ = CMe_2Ph	**f**	**g**

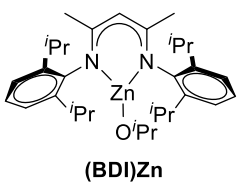

Scheme 2.1. Synthesis of syndiotactic-enriched polyBPL^{CH2CH2OBn} from the stereoselective ROP of *rac*-BPL^{CH2CH2OBn} mediated by yttrium catalysts and (BDI)Zn complex.

ROP of *rac*-BPL^{CH2CH2OBn} with yttrium catalysts based on ligands with small Me or Cl *ortho*-phenolate substituents (**a**−**c**) in the presence of *i*PrOH, proved to be somewhat sluggish regardless of the nature of the capping group (X moiety), presumably due to the aggregated/dimeric nature of these metal complexes.[13] For example, the Me-substituted catalyst systems (**a** and **b**) enabled near complete conversion of 25 equivalent of *rac*-BPL^{CH2CH2OBn} monomer within 7.5 h (Table 2.1, entries HL 259, HL177, and HL260), while the Cl-substituted one, **c**, was unable to complete monomer consumption; even with an extended reaction time up to 14 h only 65−78% conversion of monomer at the [*rac*-BPL^{CH2CH2OBn}]$_0$/[Cat.]$_0$/[*i*PrOH]$_0$ feed ratio of 25:1:1 was achieved at room temperature (Table 2.1, entries HL155 and HL261). The catalytic activity achieved by these catalysts (**a**, **b**, and **c**) as expressed by turnover frequency (TOF) values was rather poor: TOF$_{\mathbf{a}}$ = 3.7 h^{-1} (entry HL271), TOF$_{\mathbf{b}}$ = 4.8 h^{-1} (entry HL272) *vs.* TOF$_{\mathbf{c}}$ = 1.4 h^{-1} (entry HL261), respectively. It is noteworthy that, in contrast, these catalyst systems were quite active towards *rac*-BPL^{OR}s (R = Me, All, Bn), typically giving quantitative conversion of about 50 equivalent of *rac*-BPL^{OR} monomer within 2 h (TOF$_{\mathbf{b}}$ = 23 h^{-1} for *rac*-BPL^{OBn}) under the similar conditions.[1] In comparison, the zinc β-diketiminate complex, (BDI)ZnO*i*Pr, quite an active catalyst towards racemic β-butyrolactone (*rac*-BL),[14] only allowed complete conversion of 25 equiv. of *rac*-BPL^{CH2CH2OBn} monomer into polyBPL^{CH2CH2OBn} within 6 h under the same conditions (TOF ≈ 4.2 h^{-1}; Table 2.1, entry HL263).

Table 2.1. Polymerization results of ROP of *rac*-BPL^{CH2CH2OBn} mediated by yttrium catalysts.[a]

Entry	Cat.	$[BPL]_0/[Cat.]_0$ /$[i\text{PrOH}]_0$[b]	t[c] (min)	*Conv.*[d] %	$M_{n,theo}$[e] kg mol^{-1}	$M_{n,NMR}$[f] kg mol^{-1}	$M_{n,SEC}$[g] kg mol^{-1}	$Đ_M$[g]	P_r[h]
HL259	***a***	25:1:1	7.5	99	5.2	5.4	4.4	1.43	0.47
HL271	***a***	50:1:1	9	67	7.0	8.6	7.0	1.23	0.49
HL177	***b***	25:1:1	7.5	99	5.2	5.4	4.3	1.48	0.49
HL260	***b***	25:1:1	7.5	99	5.2	5.5	4.7	1.06	0.49
HL272	***b***	50:1:1	9	87	9.1	9.6	8.0	1.06	0.52
HL261	***c***	25:1:1	14	78	4.1	5.2	4.2	1.15	0.49
HL155	***c***	25:1:1	14	63	3.3	3.0	3.0	1.15	0.44
HL142	***d***	25:1:1	5	99	5.2	6.4	6.7	1.12	0.85
HL255	***d***	25:1:1	5	99	5.2	3.8	3.6	1.08	0.83
HL140	***e***	25:1:1	5	99	5.2	5.1	6.8	1.21	0.80
HL143	***f***	25:1:1	3	99	5.2	5.4	4.4	1.09	0.77
HL257	***f***	100:1:1	10	98	20.2	-	19.2	1.05	0.77
HL141	***g***	25:1:1	3	99	5.2	5.6	4.9	1.08	0.85
HL258	***g***	25:1:1	3	99	5.2	6.6	5.4	1.19	0.86
HL300	***g***	50:1:1	3	99	10.3	-	8.5	1.12	0.81
HL293	***g***	100:1:1	6	99	20.5	-	20.6	1.07	0.85
HL298	***g***	150:1:1	15	99	31.0	-	29.8	1.08	0.82
HL266[i]	***d***	25:1:1	3	99	5.2	5.9	3.6	1.08	< 0.05
HL284[i]	***d***	60:1:1	3	99	12.4	9.1	8.4	1.15	< 0.05
HL149	**(BDI)Zn**	25:1:0	180	52	2.7	2.6	2.4	1.07	0.62
HL263	**(BDI)Zn**	25:1:0	360	99	5.2	4.4	3.8	1.09	-

[a] Polymerization performed at room temperature, in toluene, $[rac\text{-BPL}^{CH2CH2OBn}]_0 = [M]_0 = 0.75$ M; [b] catalyst denoted by Cat.; [c] the reaction time was not optimized; [d] conversion of *rac*-BPL^{CH2CH2OBn} as determined by ^{1}H NMR analysis of the crude polymerization mixture; [e] molar mass calculated according to $M_{n,theo} = [BPL^{CH2CH2OBn}]_0/[Cat.]_0 \times Conv._{monomer} \times M_{monomer} + M_{iPrOH}$ ($M_{monomer} = 206$ g mol^{-1}; $M_{iPrOH} = 60$ g mol^{-1}); [f] molar mass as determined by ^{1}H NMR analysis of the isolated polyBPL^{CH2CH2OBn}, from the resonances of the terminal O*i*Pr group (refer to Experimental section); [g] number-average molar mass ($M_{n,SEC}$) and dispersity ($Đ_M$) as determined by SEC analysis in THF at 30 °C *vs.* polystyrene standards (uncorrected values); [h] P_r is the probability of *racemic* enchainment between BLP^{CH2CH2OBn} monomer units as determined by ^{13}C{^{1}H} NMR analysis of the isolated polyBPL^{CH2CH2OBn}; [i] monomer is enantiopure (*R*)-BPL^{CH2CH2OBn}.

On the other hand, yttrium catalyst systems with ancillary ligands bearing bulky substituents, such as *t*Bu, cumyl (**d**–**g)**, revealed quite active for the ROP of *rac*-BPL^{CH2CH2OBn}, allowing nearly quantitative conversion of 25–150 equivalents of *rac*-BPL^{CH2CH2OBn} within 3–15 min. More specifically, the yttrium complexes bearing *t*Bu-substituted ligands (**d** and **e**), no matter the nature of the side-arm group (X donor group), could achieve complete conversion of 25 equivalents of *rac*-BPL^{CH2CH2OBn} monomer in 5 min, leading to the corresponding polyBPL^{CH2CH2OBn}, that is with TOF values > 300 h^{-1}

(Table 2.1, entries HL142, HL255, and HL140). The yttrium complexes incorporating more sterically bulky substituents, such as $CMePh_2$ (cumyl), were even more active, allowing to convert 25 equivalents of *rac*-$BPL^{CH2CH2OBn}$ into polymer within 3 min (Table 2.1, entries HL143, HL141, and HL258). Eventually, the highest TOF value obtained for the ROP of *rac*-$BPL^{CH2CH2OBn}$ promoted by the catalytic system **g** (TOF > 1000 h^{-1}) was significantly higher than those reported for the related *rac*-BPL^{OR}s (R = Bn, All) similarly polymerized by these same yttrium catalytic systems (TOF > 26 h^{-1}).[4] We also noted that precatalyst systems with an $-NMe_2$ cap (X) on the ligand (**b** and **g**) are systematically more active than their OMe-capped counterparts (**a** and **f**), respectively, regardless of the *ortho* and *para* substituents, in line with our previous findings from *rac*-BPL^{OR}s.[1,2]

Overall, the yttrium complexes with $\{ONXO^{R1,R2}\}^{2-}$ ligand bearing sterically 'uncrowded' R^1 substituents, such as Me, Cl, are less active than those with sterically 'crowded' R^1 substituents, such as *t*Bu, cumyl, similarly to the previously reported ROP of *rac*-BL and its higher derivatives (*rac*-MLA^R, *rac*-BPL^{OR}). This observation is peculiar and might appear counterintuitive based on steric features as the approach of the monomer is anticipated to be favoured with reduced bulkiness around the metal center.

Detailed kinetic monitoring of NMR-scale reactions performed with *rac*-$BPL^{CH2CH2OBn}$ at room temperature with the catalyst systems **a**, **c**, **d**, and **f**, in toluene in the presence of 1 equivalent of *i*PrOH at the $[rac\text{-}BPL^{CH2CH2OBn}]_0/[Cat.]_0/[i\text{PrOH}]_0$ feed ratio of 60:1:1, confirmed the trends derived from batch experiments (Table 2.2). Linear semi-logarithmic plots established that the reactions are first order in the monomer (apparent constant rate: k_{app} = 6.69 ± 0.61 min^{-1}, **a**; k_{app} = 4.25 ± 0.43 min^{-1}, **c**; k_{app} = 67.3 ± 3.1 min^{-1}, **d**; k_{app} = 15.05 ± 0.38 min^{-1}, **f**; Figure 2.10).

Table 2.2. Kinetic data for the monitoring of the ROP of *rac*-BPL^{CH2CH2OBn} with various yttrium catalytic systems ([*rac*-BPL^{CH2CH2OBn}]$_0$/[Cat.]$_0$/[*i*PrOH]$_0$ = 60:1:1).[a]

Entry	Cat.	time (min)	Conv.[b] (%)	ln([BPL]$_0$/[BPL]$_t$)	$M_{n,theo}$[c] kg mol^{-1}	$M_{n,NMR}$[d] kg mol^{-1}	$M_{n,SEC}$[e] kg mol^{-1}	$Đ_M$[e]
HL492	***a***	60	11	0.118	1.4	1.3	1.4	1.05
		120	19	0.213	2.4	2.2	2.0	1.07
		180	27	0.311	3.3	3.2	2.7	1.07
		240	31	0.375	3.9	3.4	3.1	1.07
		540	46	0.625	5.8	5.5	4.3	1.07
HL493	***c***	60	8	0.081	1.0	1.1	1.3	1.08
		120	13	0.143	1.7	1.6	2.1	1.08
		180	19	0.211	2.4	2.5	2.6	1.09
		240	21	0.234	2.6	2.7	2.8	1.09
		540	33	0.402	4.1	3.9	3.7	1.13
HL494	***d***	0.5	35	0.439	4.4	4.0	3.6	1.08
		1	66	1.07	8.2	7.6	6.6	1.09
		2	90	2.31	11.2	11.0	8.7	1.07
		3	96	3.27	11.9	11.2	9.4	1.07
		5	100	-	12.4	11.9	9.4	1.08
HL495	***f***	0.5	8	0.088	1.1	1.0	1.6	1.07
		1	17	0.19	2.2	2.0	2.3	1.09
		2	35	0.428	4.3	4.1	3.8	1.09
		3	50	0.687	6.2	5.6	4.9	1.08
		4	61	0.952	7.6	7.2	6.2	1.08
		5	71	1.25	8.9	8.1	7.2	1.08

[a] Polymerization performed at room temperature, in toluene, [*rac*-BPL^{CH2CH2OBn}]$_0$ = [BPL] = 1.0 M; [b] conversion of *rac*-BPL^{CH2CH2OBn} as determined by ^{1}H NMR analysis of the crude polymerization mixture; [c] molar mass calculated according to $M_{n,theo}$ = [BPL^{CH2CH2OBn}]$_0$/[Cat.]$_0$ × *Conv.*$_{monomer}$ × $M_{monomer}$ + M_{iPrOH} ($M_{monomer}$ = 206 g mol^{-1}; M_{iPrOH} = 60 g mol^{-1}); [d] molar mass as determined by ^{1}H NMR analysis of the isolated polyBPL^{CH2CH3OBn}, from the resonances of the terminal O*i*Pr group (refer to Experimental section); [e] number-average molar mass ($M_{n,SEC}$) and dispersity ($Đ_M$) as determined by SEC analysis in THF at 30 °C *vs.* polystyrene standards (uncorrected values).

The reactions proceeded with good control over the polyBPL^{CH2HC2OBn} molar mass. All the polyBPL^{CH2CH2OBn} isolated exhibited, no matter the catalytic system used, a pretty good agreement between the theoretical molar mass values ($M_{n,theo}$) and the experimental values determined by NMR ($M_{n,NMR}$) and by SEC ($M_{n,SEC}$) analyses. The experimental molar mass values of the polyBPL^{CH2CH2OBn} increased linearly with the *rac*-BPL^{CH2CH2OBn} monomer loading up to a degree of polymerization of 150, as illustrated in Figure 2.11 (left). The dispersities of all polyBPL^{CH2CH2OBn} remained generally narrow ($Đ_M$ = 1.05–1.21), supporting a relatively fast initiation (compared to propagation) along with limited

undesirable side reactions, such as intra- and intermolecular transesterification reactions. Such dispersity values fell within the range of those typically obtained from the ROP of *rac*-BL and its related higher derivatives under similar conditions. Moreover, the molar mass of the resulting polyBPL^{CH2CH2OBn} increased linearly with the monomer conversion regardless of the nature of the yttrium catalytic systems (Table 2.1, Figure 2.11 (right)). All these characteristics highlighted the controlled feature and, to some extent, the livingness of the ROP of *rac*-BPL^{CH2CH2OBn} mediated by yttrium catalyst systems.

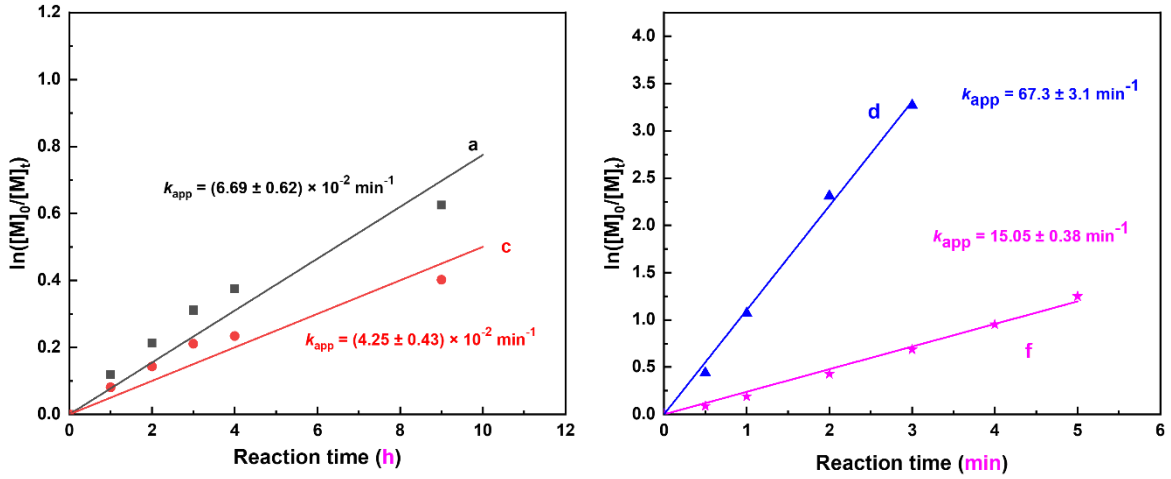

Figure 2.10. Semi-logarithmic first-order plots for ROP of *rac*-BPL^{CH2CH2OBn} mediated by Cat. **a** and **c** (left, Table 2.2, entries HL492 and HL493) and mediated by Cat. **d** and **f** (right, Table 2.2, entries HL494 and HL495).

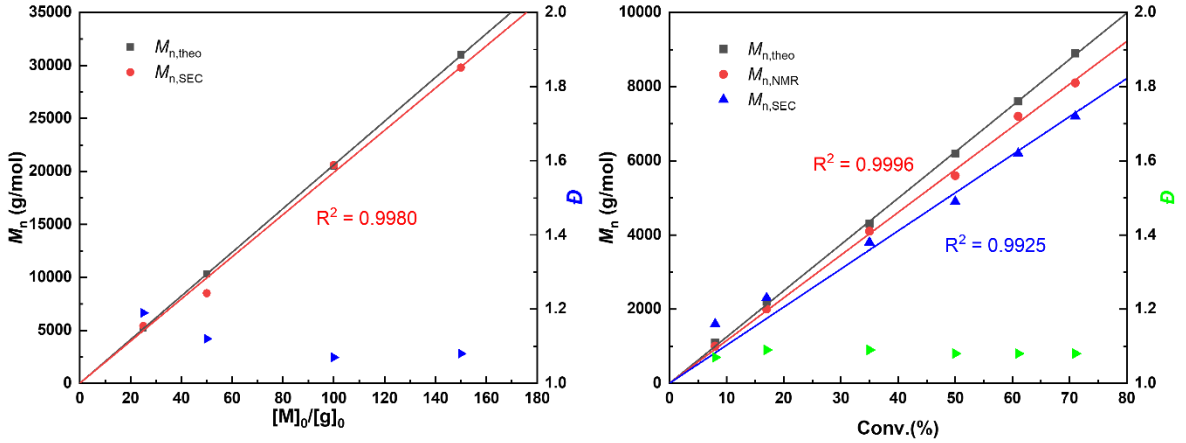

Figure 2.11 (left) variation of molar mass values of polyBPL^{CH2CH2OBn} prepared from the ROP of *rac*-BPL^{CH2CH2OBn} mediated by **g**/(*i*PrOH) (1:1) catalytic system as a function of the *rac*-BPL^{CH2CH2OBn} monomer loading ratio (Table 2.1, entries HL258, HL300, HL293, and HL298); (right) variation of molar mass values of polyBPL^{CH2CH2OBn} prepared from the ROP of *rac*-BPL^{CH2CH2OBn} mediated by **a**/(*i*PrOH) (1:1) catalytic system as a function of the monomer conversion (Table 2.2, entry HL492).

2.4 Macromolecular Characterizations of PolyBPL^{CH2CH2OBn} Synthesized by ROP of *rac*-BPL^{CH2CH2OBn}

The isolated polyBPL^{CH2CH2OBn}s were characterized and unambiguously authenticated by ^{1}H, ^{13}C NMR spectroscopy and matrix-assisted laser desorption/ionization time-of-flight mass spectrometry (MALDI-ToF MS). All ^{1}H spectra clearly displayed the characteristic signals corresponding to the BPL^{CH2CH2OBn} repeat units, especially the backbone methine (δ 5.25−5.35 ppm) and methylene (δ 2.47−2.57 ppm) signals, and the typical pendant $CH_2CH_2OCH_2Ph$ moieties (δ (ppm): 1.80–1.90, –C***H***$_2$CH$_2$OCH$_2$Ph; 3.38–3.47, –CH$_2$C***H***$_2$OCH$_2$Ph; 4.39–4.46, –CH$_2$CH$_2$OC***H***$_2$Ph; 7.20–7.31, –CH$_2$CH$_2$OCH$_2$***Ph***), respectively (Figure 2.12). The distinctive isopropoxycarbonyl chain-end group resonances were also clearly observed (δ (ppm): *ca.* 4.95 (CH$_3$)$_2$C***H***O–, *ca.* 1.17 (C***H***$_3$)$_2$CHO–), supporting the propagation from the 'Y{ONXO^{R1,R2}}'/(*i*PrOH) active species and further revealing the chain-end group fidelity. Similarly, ^{13}C{^{1}H} NMR spectra of the polyBPL^{CH2CH2OBn}s displayed the characteristic signals corresponding to BPL^{CH2CH2OBn} repeat units as well (Figure 2.13): δ (ppm) 169.22, –***C***O–; 138.11, 128.37, 127.64, 127.57, –***C***$_6$H$_5$; 72.92, –CH$_2$CH$_2$O***C***H$_2$Ph; 68.66, –***C***H=; 66.18, –CH$_2$***C***H$_2$OCH$_2$Ph; 39.02, –***C***H$_2$–; 33.82, –***C***H$_2$CH$_2$OCH$_2$Ph. Moreover, the terminal group resonances also appeared in ^{13}C{^{1}H} NMR spectra: δ (ppm): 68.04 (CH$_3$)$_2$***C***HO–, 1.17 (***C***H$_3$)$_2$CHO–). It is worth noting that *trans*-crotonate groups are not observed in the NMR spectroscopy, evidencing that these catalytic systems did not induce the elimination reaction of a molecule of H_2O from the terminal group on the polyBPL^{CH2CH2OBn} backbone, which is often observed in ROP of four-membered β-lactone, especially β-butyrolactone, but more generally with basic organocatalysts and not organometallic.[14]

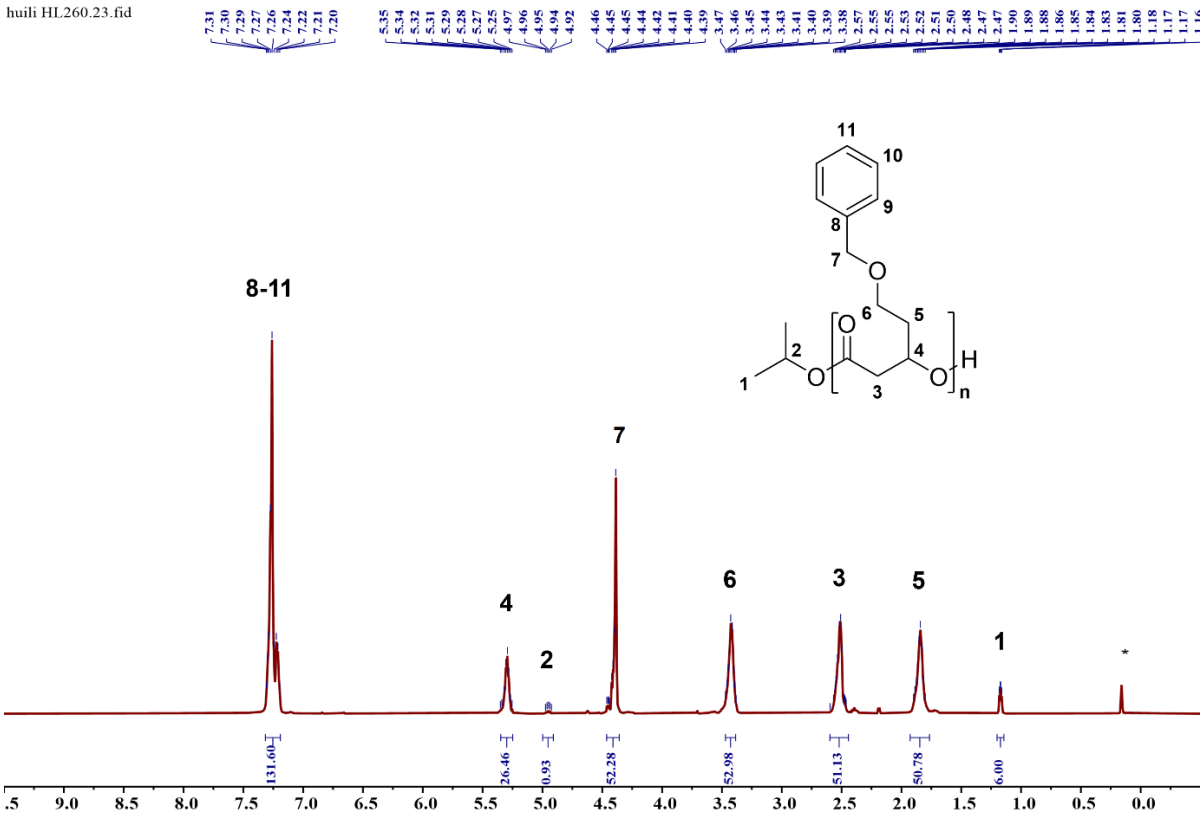

Figure 2.12. ^{1}H NMR spectrum (500 MHz, $CDCl_3$, 25 °C) of an atactic polyBPL^{CH2CH2OBn} prepared by ROP of *rac*-BPL^{CH2CH2OBn} with Cat. **b** in the presence of *i*PrOH (Table 2.1, entry HL260).

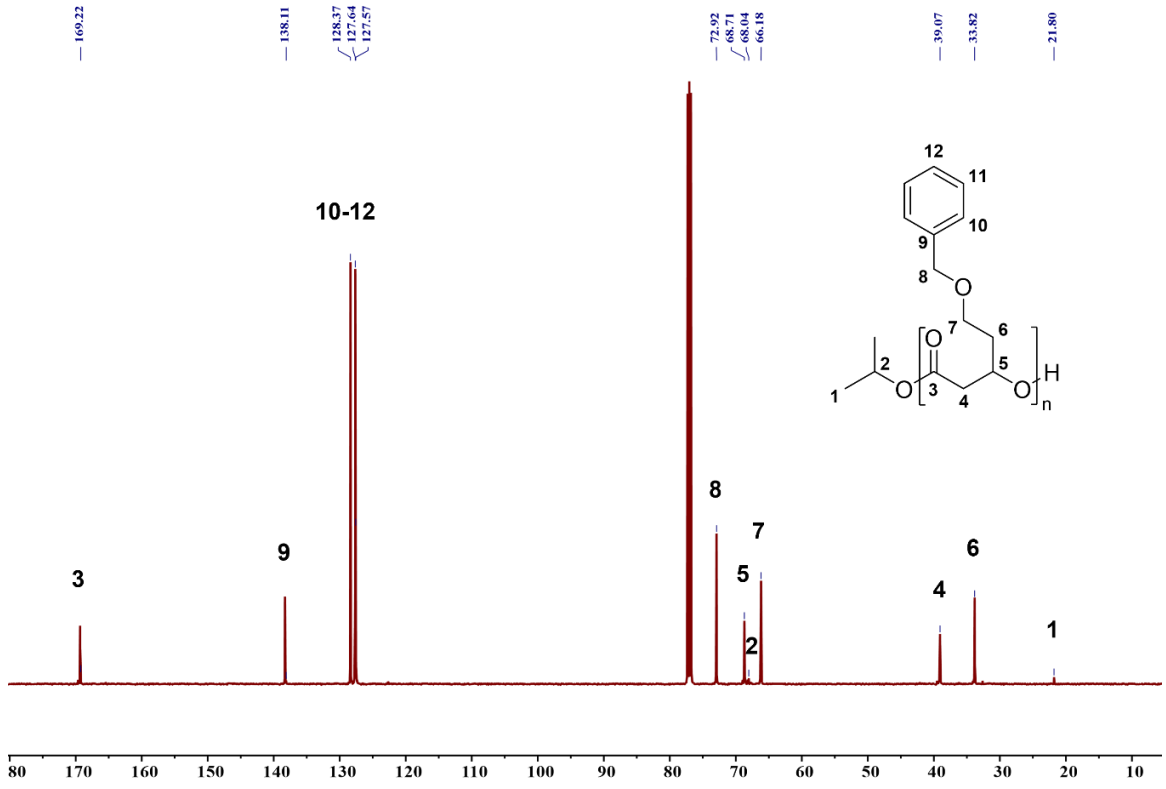

Figure 2.13 $^{13}C\{^{1}H\}$ NMR spectrum (125 MHz, $CDCl_3$, 25 °C) of an atactic polyBPL^{CH2CH2OBn} prepared by ROP of *rac*-BPL^{CH2CH2OBn} with Cat. **b** in the presence of *i*PrOH (Table 2.1, entry HL260).

Further evidence for the macromolecular structure of the prepared polyBPL^{CH2CH2OBn} was gained from MALDI-ToF mass spectrometry analysis (Figure 2.14). The spectrum was recorded for a low molar mass sample of polyBPL^{CH2CH2OBn} prepared with Cat. **f**/*i*PrOH catalytic system (Table 2.1, entry HL257), and showed two populations of macromolecules with a repeat unit of *m/z* = 206. The main population corresponds to *α*-isopropoxy,*ω*-hydroxy telechelic polyBPL^{CH2CH2OBn} chains ionized by Na^+, which was unequivocally confirmed by the close match with the corresponding isotopic simulations, as illustrated in Figure 2.15; for example, calculated *m/z* = 3174.493 *vs.* found *m/z* = 3174.461 for *n* = 15 ([*i*PrO−(COCH$_2$CH(C$_2$H$_4$OBn)O)$_n$−H]Na^+). The second minor population observed corresponds to α-isopropoxy,ω-dehydrated (*i.e.*, *ω*-crotonate) telechelic polyBPL^{CH2CH2OBn} chains ionized by Na^+, as also unambiguously confirmed by the close match with the corresponding isotopic simulation for [*i*PrO−(COCH$_2$CH(C$_2$H$_4$OBn)O)$_n$H-H$_2$O]Na^+; for example, calculated *m/z* = 3156.476 *vs.* found *m/z* 3156.451 for *n* = 15 ([*i*PrO−(COCH$_2$CH(C$_2$H$_4$OBn)O)$_n$H-H$_2$O]Na^+). However, such a crotonate group was undetectable in the NMR spectra of the prepared polyBPL^{CH2CH2OBn}, thereby suggesting that dehydration of the macromolecular chains likely occurred during the MALDI-ToF MS analysis or that it is a very minor population (overexpressed by MALDI analysis).

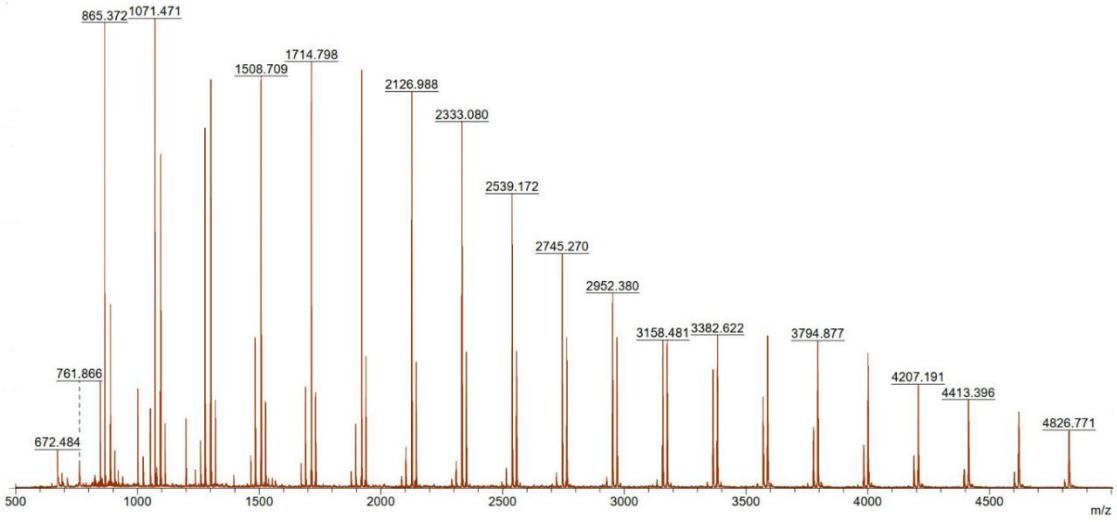

Figure 2.14. MALDI-ToF mass spectrum of a polyBPL^{CH2CH2OBn} prepared from ROP of *rac*-BPL^{CH2CH2OBn} with Cat. **f** in the presence of *i*PrOH in toluene (Table 2.1, entry HL 257).

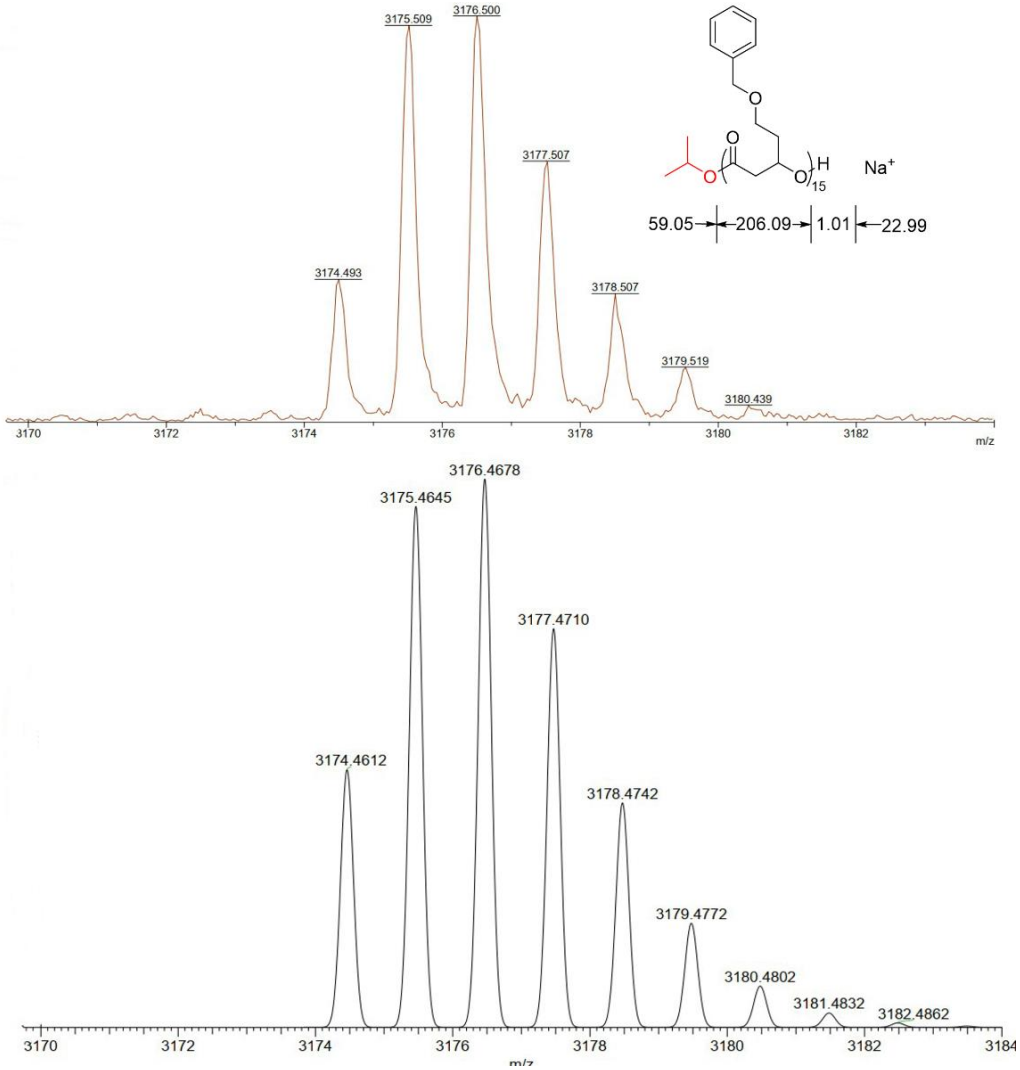

Figure 2.15. (Top). The zoomed MALDI-ToF MS spectrum of Figure 2.14 for *n*= 15, for {[*i*PrO−($COCH_2CH(C_2H_4OBn)O)_n$−H]+Na^+}; (bottom). the simulated MS spectrum of [*i*PrO−($COCH_2CH(C_2H_4OBn)O)_n$−H]+Na^+ for *n*= 15.

2.5 Microstructural Characterization of PolyBPL^{CH2CH2OBn}

Motivated by the outstanding stereoselectivity of the yttrium catalytic systems **a**–**g**/*i*PrOH in the ROP of chiral racemic β-lactones,[2] such as *rac*-BL, *rac*-MLA^R, *rac*-BPL^{OR}, the microstructures of the synthesized polyBPL^{CH2CH2OBn}s were closely examined. In most cases, the stereocontrol in the ROP of chiral cyclic esters mediated by these achiral yttrium catalytic systems originates from a chain-end control mechanism (CEM) (more details, refer to Appendices: the origin of stereoselectivity). Thus, syndiotactic polyesters are most often formed since the active species alternatively selects the enantiomer with the opposite configuration from racemic β-lactone during polymerization in order to minimize the steric bulkiness in the transition state.

The chemical shifts of some carbon atoms in a chiral polymer chain are sensitive to the relative stereochemistry of nearby stereocenters, which is particularly useful for investigating the microstructure of polymers.[15] In this regard, the tacticity of various isolated polyBPL^{CH2CH2OBn}s can be evaluated by

$^{13}C\{^{1}H\}$ NMR spectroscopy, one of the most common techniques for analyzing synthetic polymer tacticity. It is worth reminding that the *rac*-BPL^{CH2CH2OBn} monomer investigated in this chapter "simply" differs from the previously studied *rac*-BPL^{OBn} by replacing the methylene in exocyclic pendant group with an ethylene moiety; this 'minor' change may exert a significant influence on the microstructure of the resulting polymer.

At 125 MHz, only the carbonyl and the methylene groups along the main chain of the isolated polyBPL^{CH2CH2OBn}s exhibited resolved resonances, while the rest of the resonances only showed sharp singlets (Figure 2.16). Expansion of the carbonyl region of $^{13}C\{^{1}H\}$ NMR spectra of the polyBPL^{CH2CH2OBn}s (δ *ca.* 169.3–169.5 ppm) features four well-resolved resonances corresponding to triads. They form two (essentially non-overlapping) groups of two resonances, which are assigned, from high-to-low field to the four triads, *mr*, *rr*, *mm* and *rm*, respectively. Assignment of the *rm* and *mr* triad sequences was made assuming a relatively small chemical shift change between *m**m*** and *r**m***, as well as between *r**r*** and *m**r***, since there is a closer spatial proximity of the carbonyl carbon to the repeat unit which is linked to the methylene side of the carboxyl side observed in the stereosequence analysis.[16] The same triads distribution order was also observed in the carbonyl region (δ *ca.* 169.1 ppm) of the parent poly(3-hydroxybutyrate) (P3HB). The methylene region of $^{13}C\{^{1}H\}$ NMR spectra (δ *ca.* 39.0–39.4 ppm) features two broad, yet well-resolved resonances, the most downfield one being assigned to a *meso* (*m*, isotactic) dyad and the most upfield one to the *racemo* (*r*, syndiotactic) dyad. Careful deconvolution of these resonances allowed extracting P_r values. Definitive confirmation of these assignments was gained from the ^{13}C NMR spectrum of a perfectly isotactic polyBPL^{CH2CH2OBn} (Figure 2.16, a), prepared from the ROP of enantiopure (*R*)-BPL^{CH2CH2OBn} mediated by Cat. **d** (Table 2.1, entries HL284 and HL266).

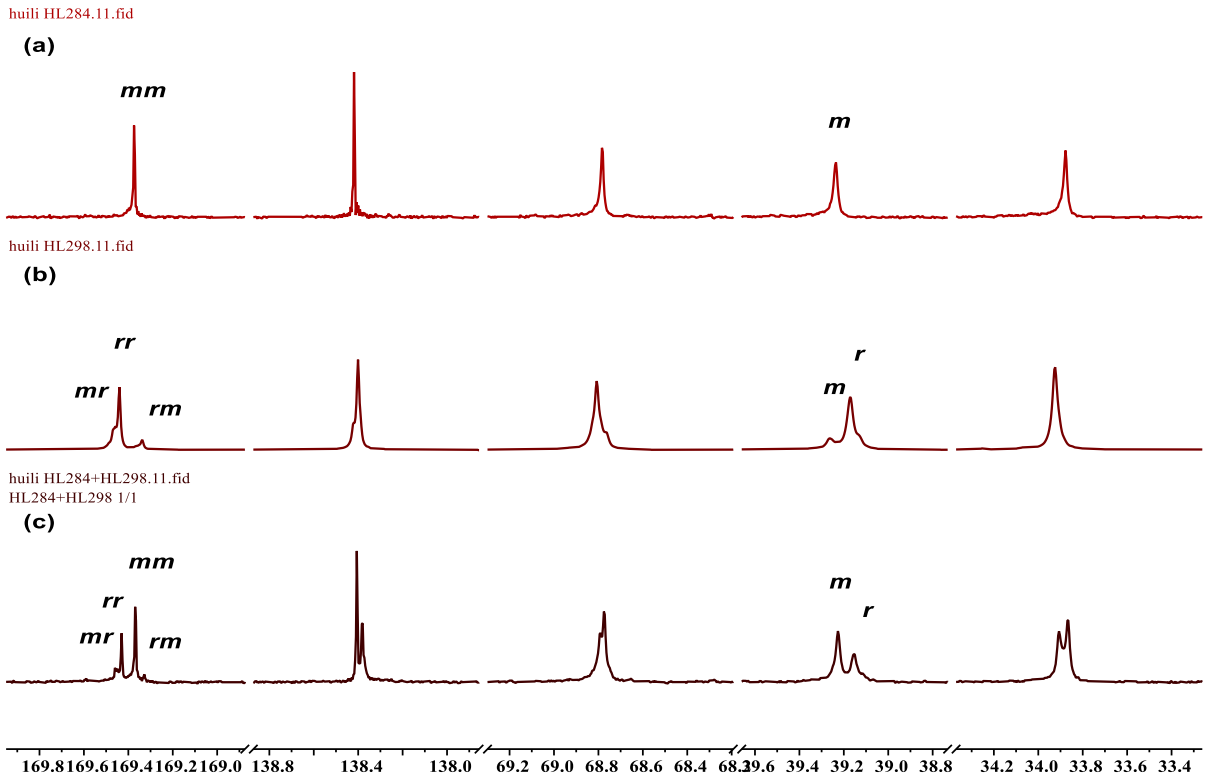

Figure 2.16. Regions (carbonyl, methylene in the backbone) of the $^{13}C\{^{1}H\}$ NMR spectra (125 MHz, $CDCl_3$, 25 °C) of: (a). perfectly isotactic polyBPL^{CH2CH2OBn} produced from enantiopure (*R*)-BPL^{CH2CH2OBn} ($P_r < 0.05$, Table 2.1, entry HL284); (b). an isolated syndiotactic-enriched polyBPL^{CH2CH2OBn} prepared by Cat. **f** (P_r = 0.82, Table 2.1, entry HL298); (c). a physical blend of perfectly isotactic and syndiotactic-enriched polyBPL^{CH2CH2OBn} (entry HL284+entryHL298).

Careful analysis of the $^{13}C\{^{1}H\}$ NMR spectra of polyBPL^{CH2CH2OBn} revealed that the isolated polymers were either syndiotactic-enriched or atactic, depending on the yttrium complexes used, namely **d**–**g** or **a**–**c**, respectively; none of them was isotactic-enriched (Figure 2.17). Moreover, no significant difference was observed in terms of tacticity upon variation of the X–donor group in the "capping" moiety of the $\{ONXO^{R1,R2}\}^{2-}$ ligand; this is similar to previous findings in the ROP of *rac*-β-butyrolactone and higher derivatives.[2,17] Yttrium complex incorporating bulky substituents at the *ortho*-positions of the phenolate rings (*t*Bu or cumyl groups, **d**–**g**) led to syndiotactic-enriched polyBPL^{CH2CH2OBn} ($P_r \approx 0.77$–0.86) (Table 2.1, entries HL143, HL257, HL141, HL258, HL300, HL293, HL298), in line with a CEM mechanism being at play. In comparison, similarly highly syndiotactic PBPL^{OBn} were reported from *rac*-BPL^{OBn} (P_r = 0.88–0.90) under the same conditions. More strikingly, the use of Cat. **c** bearing *ortho*-dichloro-substituted ligand gave atactic polyBPL^{CH2CH2OBn}s (P_r = 0.44–0.49) (Table 2.1, entries HL261 and HL155), while highly isotactic PBPL^{OBn}s were generated from *rac*-BPL^{OBn}. The similarly "uncrowded" catalysts **a**–**b** incorporated *ortho*-dimethyl-substituted ligand, returned atactic polyBPL^{CH2CH2OBn} with P_r values in the range of 0.49–052 (Table 2.1, entries HL259, HL271, HL155, HL260, and HL272), consistent with the previous observation in terms of stereoselectivity of P3HB and PBPL^{OBn}. In addition, as a benchmark reaction, (BDI)ZnO*i*Pr, a

nonstereoselective catalyst towards *rac*-BL, also generated almost atactic polyBPL^{CH2CH2OBn} (Table 2.1, entry HL149).

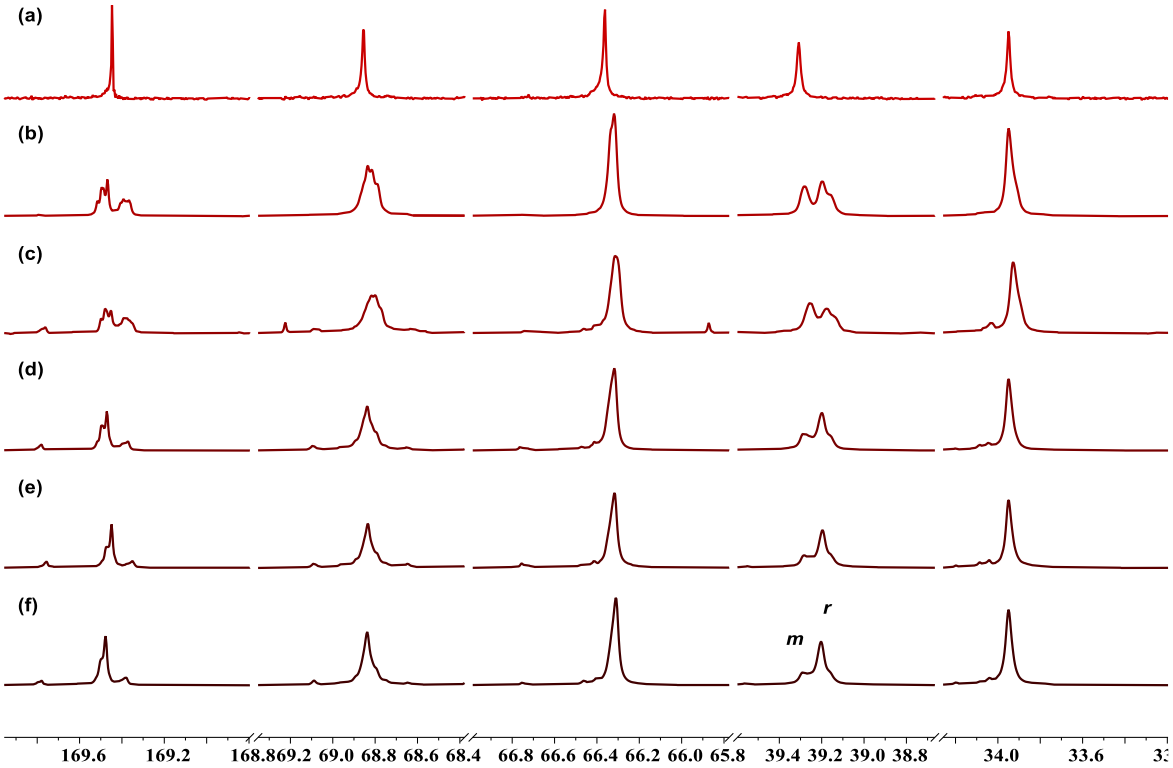

Figure 2.17. Regions (carbonyl, methylene in the backbone) of the $^{13}C\{^{1}H\}$ NMR spectra (125 MHz, $CDCl_3$, 25 °C) of: (a). perfectly isotactic polyBPL^{CH2CH2OBn} produced from enantiopure (*R*)-BPL^{CH2CH2OBn} mediated by Cat. **d** (P_r < 0.05, Table 2.1, entry HL284); (b). an isolated atactic polyBPL^{CH2CH2OBn} prepared by Cat. **a** (P_r = 0.49, Table 2.1, entry HL271); (c). an isolated atactic polyBPL^{CH2CH2OBn} prepared by Cat. **c** (P_r = 0.49, Table 2.1, entry HL261); (d). an isolated syndiotactic-biased polyBPL^{CH2CH2OBn} prepared by Cat. **f** (P_r = 0.77, Table 2.1, entry HL143); (e). an isolated syndiotactic-enriched polyBPL^{CH2CH2OBn} prepared by Cat. **d** (P_r = 0.83, Table 2.1, entry HL255); (f). an isolated syndiotactic-enriched polyBPL^{CH2CH2OBn} prepared by Cat. **g** (P_r = 0.86, Table 2.1, entry HL258).

Considering the yttrium catalyst flanked with a halogenated (Cl) uncrowded ancillary ligand, the presence of −C***H***$_2$− moiety within the pendant functional group (−C***H***$_2$OBn) in *rac*-BPL^{OBn}, was evidenced to be essential to afford highly isotactic PBPL^{OBn}. DFT calculations suggested that such rare isoselectivity arose from the presence of strong attractive Cl ẼH–C 'non-covalent interactions' between the *chloro* substituents and the alkoxymethylene group of the pendant chain in the ring-opened monomer. In comparison, for the ROP of *rac*-BPL^{CH2CH2OBn} mediated by Cat. **c**, 'simply' increasing the length of the pendent chain from alkoxymethylene "**CH$_2$**OBn" of *rac*-BPL^{OBn} to alkoxyethylene "**CH$_2$CH$_2$**OBn", seems to affect the Cl ẼH−C interactions. We assume this is possibly due to a different conformation in the monomer/active species interactions, and/or due to the decrease in acidity of the methylene moiety (–C***H***$_2$CH$_2$OBn) of the side-chain in –CH$_2$CH$_2$OBn *vs.* –CH$_2$OBn, ultimately

weakening the "noncovalent interactions" and leading to the loss of sterecontrol to afford atactic polymers, similarly to those obtained from yttrium catalyst incorporating dimethyl-substituent ligand.[1]

2.6 Thermal Signature of PolyBPL^{CH2CH2OBn}

The thermal behavior of the synthesized polyBPL^{CH2CH2OBn} was assessed by thermal gravimetry analysis (TGA) and differential scanning calorimetry (DSC). The TGA curve of polyBPL^{CH2CH2OBn} sample exhibits a sharp, one-step degradation profile (Figure 2.18). The polyBPL^{CH2CH2OBn} sample (M_n = 20.6 kg mol^{-1}, P_r = 0.85, Table 2.1, entry HL293) was found to thermally degrade at *ca.* 226 °C (T_d^{onset} = 226 °C, defined as the temperature for 5% weight loss), which is significantly lower than the one measured for the parent P3HB (T_d^{onset} = 256 °C).[18] Yet, the complete degradation signature of PBPL^{OBn} has not been established thus far.

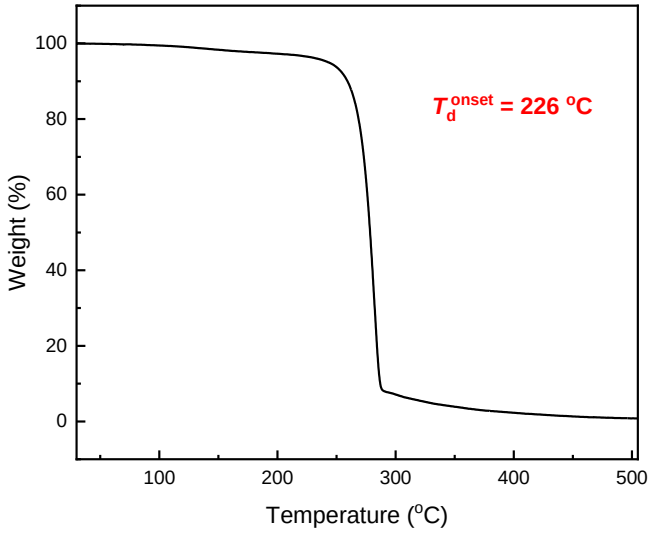

Figure 2.18. TGA thermograms of polyBPL^{CH2CH2OBn} produced from ROP of *rac*-BPL^{CH2CH2OBn} mediated by Cat. **f** in the presence of *i*PrOH (100:1:1, at room temperature, in toluene, M_n = 20.6 kg mol^{-1}, P_r = 0.85, Table 2.1, entry HL293). Heating rate = 10 °C.

DSC thermograms only showed the presence of a glass transition temperature (T_g); no melting temperature (T_m) was observed below 200 °C, regardless of the degree of the stereoregularity of the polymer, suggesting that the resulting polyBPL^{CH2CH2OBn}s are amorphous polyesters. This lack of crystallinity was similarly observed for the related syndiotactic or isotactic PBPL^{OBn}.

The glass transition temperature (T_g) values of the isolated polyBPL^{CH2CH2OBn}s are in the range of −15 ~ −9 °C. It is worth noting that the molar mass of the polyBPL^{CH2CH2OBn}s exerts little influence on the T_g values (T_g = −9 °C for M_n = 20.6 kg mol^{-1}, Table 2.1, entry HL293 *vs.* T_g = −11 °C for M_n = 6.4 kg mol^{-1}, Table 2.1, entry HL142). Moreover, no distinct tendency in T_g values of polyBPL^{CH2CH2OBn}s

associated with the stereoregularity was observed, which is not an uncommon observation (tacticity most usually does not affect T_g values).

2.7 Comparison of the Stereoselective Ring-Opening Polymerization of Functional β-Lactones Mediated by Yttrium Complexes

As mentioned above, the most valuable property of these yttrium complexes, 'Y{ONXO^{R1,R2}}', is undoubtedly their capability to control finely the stereochemistry of ROP reactions starting from racemic mixtures of functional β-lactones. In fact, it turned out that the stereoselectivity was strongly affected by both the nature of the *ortho*-substituents (R^1) installed on the phenolate ligands and the nature of the exocyclic functional group of the β-lactone monomer (Figure 2.19).

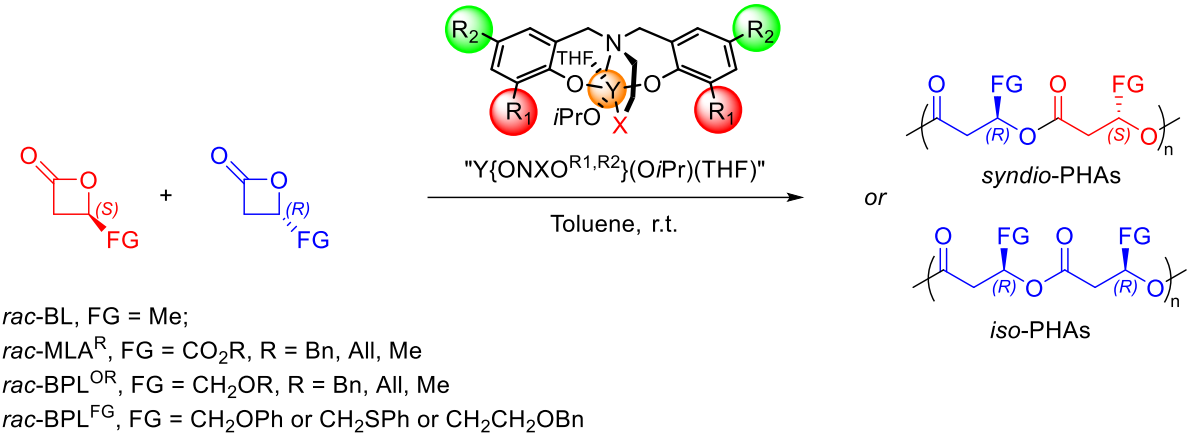

Figure 2.19. Stereoselective ROP of functional β-lactones towards stereoregular PHAs.[1-5,17,18]

The initial study conducted on the benchmark *rac*-BL monomer, revealed that the yttrium complexes incorporating "uncrowded" substituted ligand, such as R^1 = Me, Cl, generate atactic poly(3-hydroxybutyrate) (P3HB) (P_r = 0.56 (R^1 = Me), 0.45 (R^1 = Cl)).[19] Surprisingly, high syndioselectivity was observed from racemic β-malolactonates (*rac*-MLA^R, R = Bn, All, Me) for the ligand with 'uncrowded' substituents on the phenolate ring (P_r > 0.92 (R^1 = Me), > 0.95 (R^1 = Cl, F). In contrast to *rac*-BL and *rac*-MLA^R, for the ROP of *rac*-BPL^{OR} (R = Me, Bn, All) which differs from *rac*-MLA^{R}s by replacement in the pendant (exocyclic) group of a carbonyl by a methylene moiety, the dimethyl-substituted yttrium complex gives atactic PBPL^{OR}s (P_r = 0.49−0.51), while the use of yttrium complexes bearing ligands with halogens as *o,p*-substituents induced the formation of highly isotactic PBPL^{OR}s (P_r < 0.10).[4] It is worth pointing out that the *rac*-BPL^{FG}s (FG = CH_2OPh, CH_2SPh) "simply" differ from the previously studied *rac*-BPL^{OBn} by one less exocyclic methylene group in the phenoxide/phenylthiol moiety; yttrium complexes that incorporate "uncrowded" *ortho*-substituents on the phenolate rings, such as R^1 = Me, Cl, give the syndiotactic-biased polymers with P_r in the range of 0.74−0.79. In sharp contrast to *rac*-BPL^{FG}s, "uncrowded" *ortho*-substituted yttrium complexes return atactic polyBPL^{CH2CH2OBn} from *rac*-BPL^{CH2CH2OBn} (P_r = 0.49 (R^1 = Me, Cl)).[5]

As expected, the syndiotactic ROPs of all substituted β-lactones, *e.g.*, *rac*-BL, *rac*-MLA^{R}, *rac*-BPL^{OR}, and *rac*-BPL^{FG}, were observed with the yttrium complex incorporating bulky substituents at the *ortho*-positions of the phenolate rings (*t*Bu, cumyl, *etc*), indicating that these reactions are, to some extent, under steric control; this is consistent with the usual hypothesis for a chain-end stereocontrol mechanism in which crowding in the coordination sphere of the active metal center allows an optimal "transfer of the chiral information" from the growing macromolecular chain.[17] More specifically, the ROP of the simplest chiral β-lactone, *rac*-BL, affords highly syndiotactic P3HB; the syndiotacticity level basically increases with the steric bulkiness of the *ortho* substituent (R^1) on the ligand framework (P_r = 0.80 (R^1 = *t*Bu), 0.91 (R^1 = CMe_2Ph), 0.96 (R^1 = CPh_3)). In fact, not all bulky R^1 substituents do so: the purely aliphatic CMe_2*t*Bu, despite its bulkiness arguably comparable to the previous cumyl (CMe_2Ph), gave only syndio-enriched P3HB (P_r = 0.70). Also, yttrium complex bearing the electron-depleted ligand with R^1 = CMe_2(*p*-CF_3-Ph) is significantly less syndioselective than the parent cumyl-substituted ligand (P_r = 0.83 *vs.* 0.91, respectively), despite again their much similar bulkiness. Hence, not only steric but also electronic considerations appear to be at work in the stereocontrolled ROP of *rac*-BL. These yttrium catalyst systems with bulky *ortho*-substituents (R^1) on the ligand, such as CMe_2*t*Bu, CMe_2Ph, that proved highly syndioselective toward the ROP of *rac*-BL, afforded only syndiotactic-enriched PMLA^{R} (P_r = 0.82 (R^1 = CMe_2Ph), 0.87 (R^1 = CMe_2*t*Bu)) from *rac*-MLA^{R}; yet, the system based on the larger trityl proved less stereoselective than that with cumyl (P_r = 0.68 *vs.* 0.82, respectively). In contrast to the ROP of *rac*-BL, high syndiotacticity towards *rac*-BPL^{OR} (P_r *ca.* 0.80−0.90) can be achieved even with purely aliphatic bulky substituents. In comparison, the behaviour of these bulky complexes (R^1 = *t*Bu, cumyl, *etc*) towards *rac*-BPL^{FG} is similar to that observed with *rac*-MLA^{R}, that is yttrium complexes with *tert*-butyl and cumyl-substituted ligands lead to the similar levels of syndiotacticity (P_r in the range of 0.81−0.86).

The results described herein further highlight the strong dependence of the resulting PHA's stereocontrolled microstructure on the couple formed by the functional β-lactone and the yttrium catalyst, and more specifically on the chemical nature of the β-lactone side-arm and of the substituents on the metal surrounding ancillary.

2.8 Conclusion

New functional polyBPL^{CH2CH2OBn} homopolymers have been successfully prepared from the controlled ROP of the corresponding racemic 4-substituted-β-propiolactone *rac*-BPL^{CH2CH2OBn}, mediated by diamino- or amino-alkoxy-bis(phenolate) yttrium amido complexes **a**–**g** in the presence of isopropanol as co-initiator. All yttrium complexes revealed active, affording well-defined polyBPL^{CH2CH2OBn} with a good control of the polymerization in terms of molar mass values and limited undesirable side reactions (M_n up to 29.8 kg mol^{-1}, $Đ_M$ < 1.23).

The best catalytic activities reached by the yttrium complexes **d**–**g** with the 'crowded' substituents installed on the bisphenolate ligand (*e.g.*, *t*Bu, CMe_2Ph), in the ROP of *rac*-$BPL^{CH2CH2OBn}$ (TOF > 1000 h^{-1}), are higher than those achieved with the related *rac*-4-alkoxymethylene-β-propiolactones *rac*-BPL^{OBn} (TOF < 50 h^{-1}). On the other hand, catalysts with less-crowded phenolate substituents (*e.g.* Me, Cl) revealed significantly less active in the ROP of *rac*-$BPL^{CH2CH2OBn}$ (TOF < 5 h^{-1}).

Syndiotactic poly$BPL^{CH2CH2OBn}$s (P_r up to 0.86) were produced when the yttrium catalyst bears bulky substituents (such as, cumyl, *t*Bu); this is similar to syndiotactic $PBPL^{OBn}$ prepared by ROP of *rac*-BPL^{OBn}. On the other hand, the yttrium complexes incorporating halogenated "uncrowded" ligand, such as Cl, gave rise to atactic poly$BPL^{CH2CH2OBn}$, suggesting 'non-covalent interactions' were not at play during polymerization in contrast to what was observed in the synthesis of $PBPL^{OBn}$. In comparison, yttrium complexes with these small "uncrowded" substituents, such as Me, F, Cl, Br, generated highly syndiotactic $PMLA^{R}$. These results highlight that the combination of the metal's ligand framework featuring appropriate R^1 substituents in *ortho*-position of the phenolates, with the functional cyclic ester monomer, is the key to a successful and specific stereocontrol. Preparation and structural studies of the key intermediate evidencing non-covalent interactions between BPL^{OR} coordinated on (model) yttrium active site may offer further insights into the stereocontrolled ROP of these functional b-propiolactones.

Experimental Section

All syntheses and manipulations of air- and moisture-sensitive materials were carried out in flamed Schlenk-type glassware on a vacuum dual-manifold Schlenk line or in an argon-filled glovebox. HPLC-grade organic solvents were first purged extensively with nitrogen during filling 20 L-solvent reservoirs and then dried by passage through activated alumina [for dichloromethane] followed by passage through Q-5 supported copper catalyst [for toluene] stainless steel columns. *n*-Hexane, tetrahydrofuran (THF), and toluene were degassed and dried over sodium/benzophenone followed by distillation under argon. *iso*-Propanol (*i*PrOH), was purified by distillation over CaH_2. *meta*-Chloroperoxybenzoic acid (*m*CPBA) purchased from Aldrich and used as received. 3-butan-1-ol purchased from TCI and used as received.

In the glovebox, a Schlenk tube was charged with $[Y(N(SiHMe_2)_2)_3](THF)_2$ (40 μmol) and $\{ONXO^{R2}\}H_2$ (40 μmol), and toluene (0.50 mL) was added. To this solution, *i*PrOH (0.15 mL of a 2% (*v/v*) solution in toluene, 40 μmol) was added under stirring at room temperature. After 5 min of stirring, a solution of *rac*-$BPL^{CH2CH2OBn}$ (206 mg, 1 mmol, 25 *equiv.*) in toluene (0.50 mL) was added rapidly. After a desired period of time, the polymerization was quenched by addition of 2 mL of benzoic acid/$CHCl_3$ (10 mg mL^{-1}). A 0.2 mL of aliquot was taken from the reaction mixture and prepared for ^1H NMR analysis to obtain the percent monomer conversion data. The resulting mixture was concentrated to dryness under vacuum to obtain the crude polymer and then dissolved in DCM (*ca*.1 mL) and precipitated in pentane (*ca*. 100 mL). The final polymer was analyzed by NMR, and SEC analyses.

Synthesis of *rac*-4-(2-(benzyloxy)ethyl)oxetan-2-one (*rac*-$BPL^{CH2CH2OBn}$):

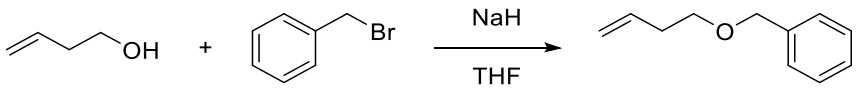

Scheme 2.2. Synthetic procedure towards 1-benzyloxybut-3-ene.

1-Benzyloxybut-3-ene was prepared according to the literature.[20] 3-Buten-1-ol (1.00 g, 13.9 mmol) was added dropwise to a suspension of NaH (0.74 g of a 50% dispersion in oil, washed twice with dry petroleum ether, 15.4 mmol) in dry THF (30 mL) at 0 °C under argon. After stirring at room temperature for l h, benzyl bromide (1.80 mL, 15.2 mmol) was added dropwise, and the resulting mixture left overnight. Saturated brine (15 mL) was added, and the mixture extracted with Et_2O (3 × 25 ml). The organic extracts were dried over $MgSO_4$, and the solvent removed under reduced pressure, to give crude 1-benzyloxybut-3-ene as a colourless oil (1.56 g, 69% yield).

^1H NMR (400 MHz, $CDCl_3$, 25 °C, Figure 2.20): δ 7.49 – 7.34 (m, 5H), 5.96 (ddt, J = 17.1, 10.2, 6.7, 1H), 5.27 – 5.12 (m, 2H), 4.62 (s, 2H), 3.63 (t, J = 6.7, 2H), 2.50 (qt, J = 6.7, 1.4, 2H).

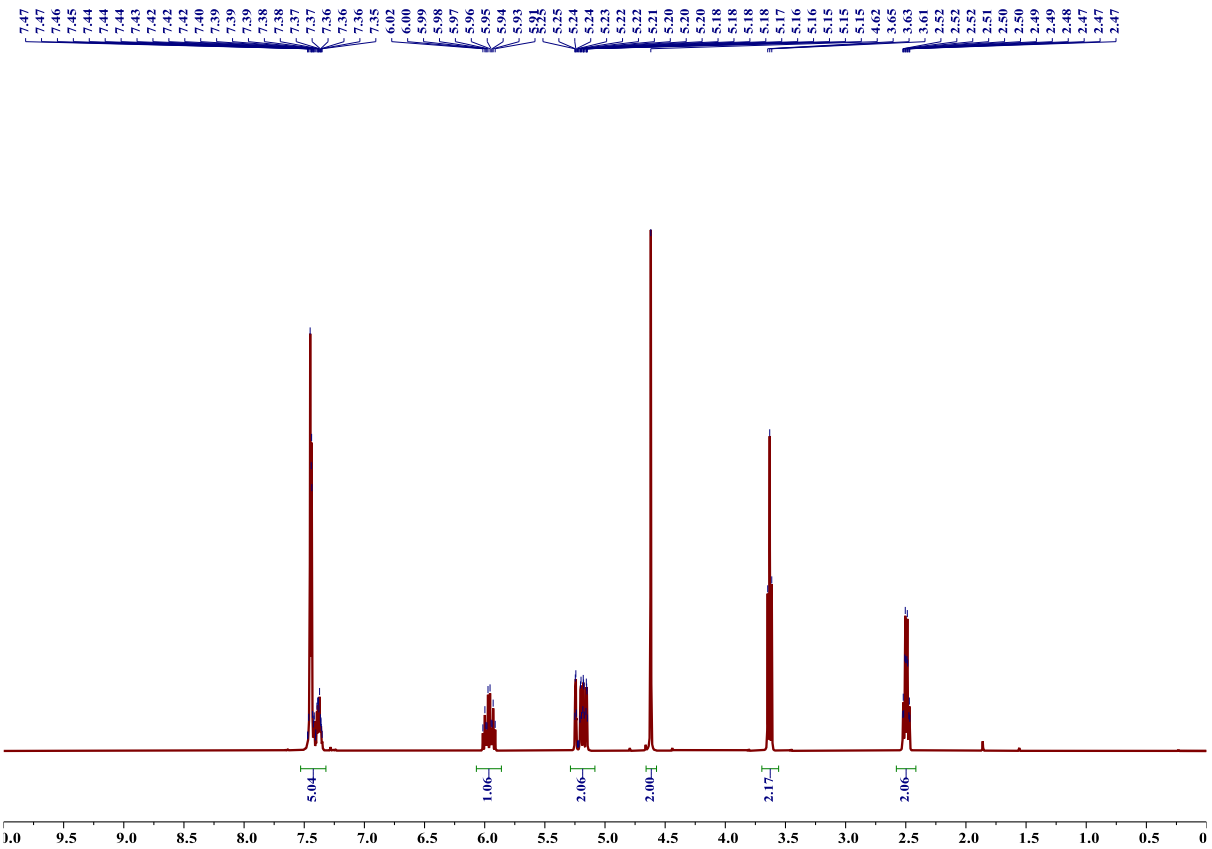

Figure 2.20. ^{1}H NMR spectrum (400 MHz, $CDCl_3$, 25 °C) of 1-benzyloxybut-3-ene.

Synthesis of Rac-2-[2-(Benzyloxy)ethyl]oxirane:

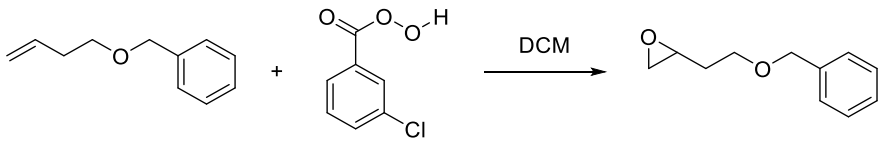

Scheme 2.3. Synthetic procedure of *rac*-2-[2-(benzyloxy)ethyl]oxirane.

Rac-2-[2-(Benzyloxy)ethyl]oxirane was prepared according to the literature.[10,20] 1-Benzyloxybut-3-ene (3.40 g, 20.9 mmol) was dissolved in dichloromethane (120 mL) and the solution was cooled to 0 °C. 75% *m*CPBA (9.40 g, 54.6 mmol) was added. The mixture was stirred at 0 °C for 1 h, and then at room temperature overnight and then was filtered through a Celite pad and concentrated under reduced pressure. The crude residue was dissolved in water (50 mL) and extracted with diethyl ether (3 × 50 mL). The combined organic layer was washed with 3 N NaOH (3 × 50 mL), brine (50 mL), dried over $MgSO_4$, and concentrated to give the crude epoxide as a colorless oil (63% yield).

^{1}H NMR (400 MHz, $CDCl_3$, 25 °C, Figure 2.21): δ 7.38 – 7.27 (m, 5H), 4.54 (s, 2H), 3.73 – 3.56 (m, 2H), 3.08 (dtd, J = 6.6, 4.3, 2.8, 1H), 2.79 (dd, J = 5.0, 4.0, 1H), 2.53 (dd, J = 5.0, 2.7, 1H), 1.92 (dddd, J = 14.4, 7.2, 6.1, 4.7, 1H), 1.79 (dq, J = 14.4, 6.0, 1H).

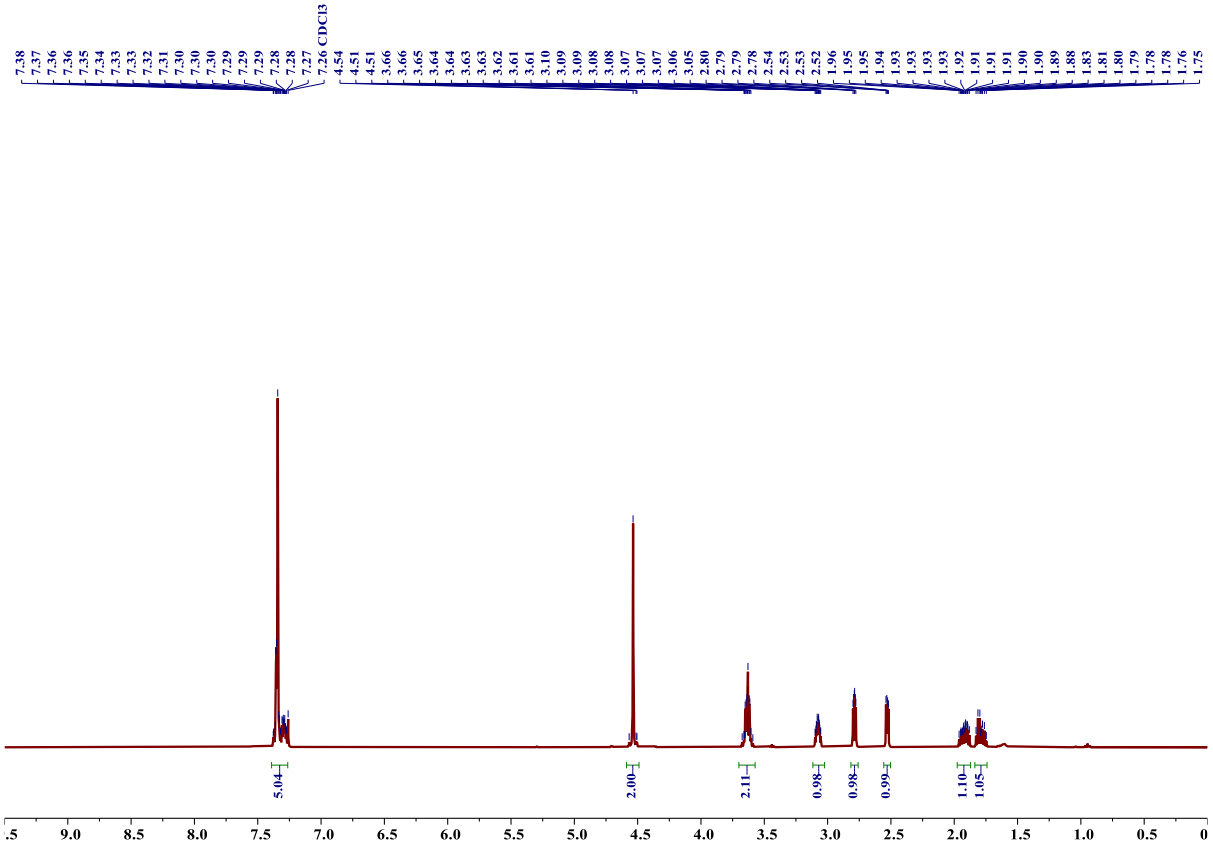

Figure 2.21. ^{1}H NMR spectrum (400 MHz, $CDCl_3$, 25 °C) of *rac*-2-[2-(benzyloxy)ethyl]oxirane.

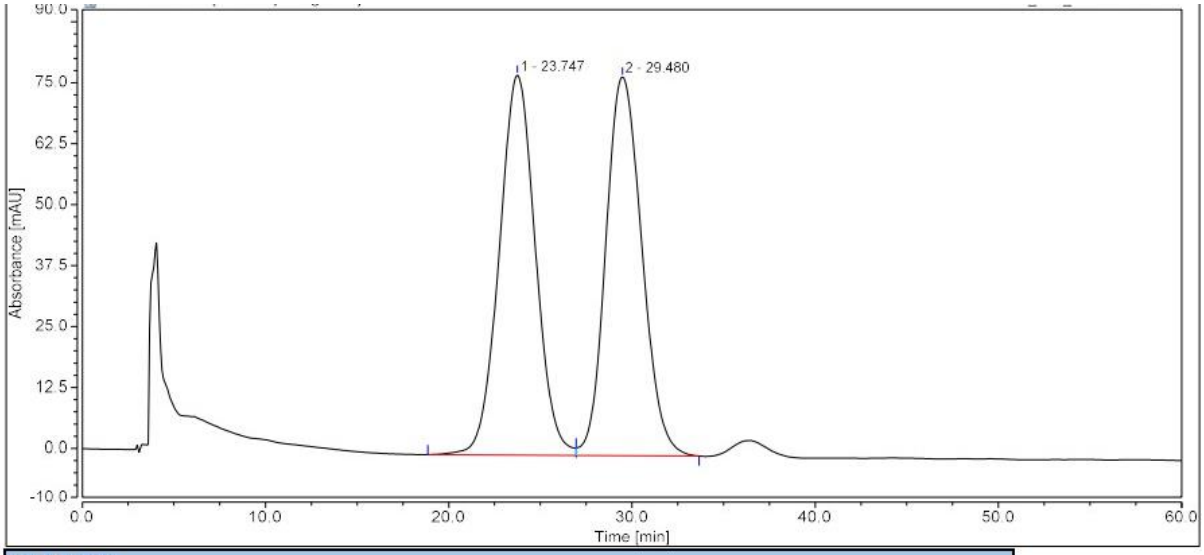

Peak Results						
No.	Peak Name	Retention Time min	Width (50%) min	Resolution (EP)	Asymmetry (EP)	Plates (EP)
1		23.747	2.103	1.60	1.03	706
2		29.480	2.135	n.a.	1.14	1057

Integration Results						
No.	Peak Name	Retention Time min	Area mAU*min	Height mAU	Relative Area %	Relative Height %
1		23.747	178.274	77.941	50.17	50.09
2		29.480	177.053	77.669	49.83	49.91
Total:			**355.328**	**155.609**	**100.00**	**100.00**

Figure 2.22. Chiral HPLC chromatogram (column Chiralcel-OD DAICEL; 250 mm × 4.6 mm, 5 µm; 20 °C with a UV detector at 214 nm) of *rac*-2-(2-(benzyloxy)ethyl)oxirane.

4-(2-(benzyloxy)ethyl)oxetan-2-one (*rac*-BPL^{CH2CH2OBn}):

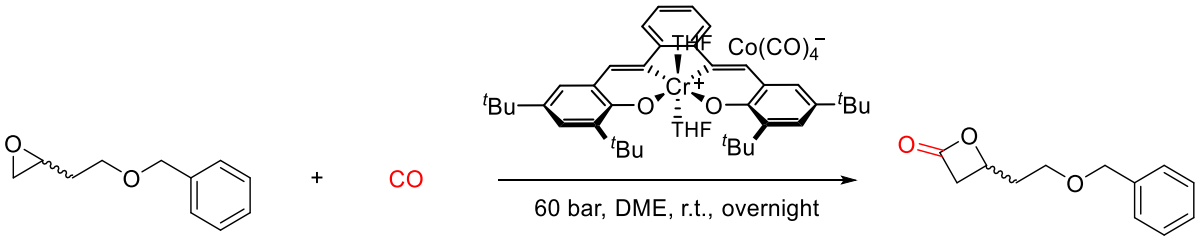

Scheme 2.4. The carbonylation of functional epoxide towards *rac*-BPL^{CH2CH2OBn}.

Rac-BPL^{C_2OBn} was prepared using a method adapted from the literature.[9] In the glovebox, an oven-dried Schlenk tube was charged with [salph(Cr(THF)$_2$)]$^+$[Co(CO)$_4$]$^-$ (540 mg, 0.5 mmol). On a vacuum line, dry DME (15 mL) was syringed in and the resulting solution was cannulated into a degassed high-pressure reactor which was pressurized with carbon monoxide to 30 bar, and stirred for 15 min before depressurization. A solution of 2-[2-(benzyloxy)ethyl]oxirane (50 mmol, 100 equiv.) in dry DME (15 mL) was transferred into the reactor which was then pressurized with CO to 60 bars. The reaction mixture was stirred for overnight. Then, the reactor was vented to atmospheric pressure, volatiles were removed under vacuum and the crude product was purified through alumina column using $CHCl_3$ as eluent. After evaporation of volatiles, the resulting *rac*-BPL^{CH2CH2OBn} was obtained (90% yield).

^{1}H NMR (500 MHz, $CDCl_3$, 25 °C, Figure 2.23**):** δ 7.28-7.37 (m, 5H), 4.71 (m, 1H), 4.51 (s, 2H), 3.62 (td, J = 5.30, 2.42 Hz, 2H), 3.53 (dd, J = 16.41, 5.86 Hz, 1H), 3.20 (dd, J = 16.41, 4.32 Hz, 1H), 2.11 (m, 2H).

^{13}C NMR (125 MHz, $CDCl_3$, 25 °C, Figure 2.24**):** δ 168.23, 138.18, 128.41, 127.74, 127.56, 73.13, 69.07, 65.73, 43.11, 34.66.

HRMS (ESI, Figure 2.25): calculated for $C_{12}H_{14}O_3Na^+$ ($[M+Na]^+$) m/z = 229.0835; found 229.0836.

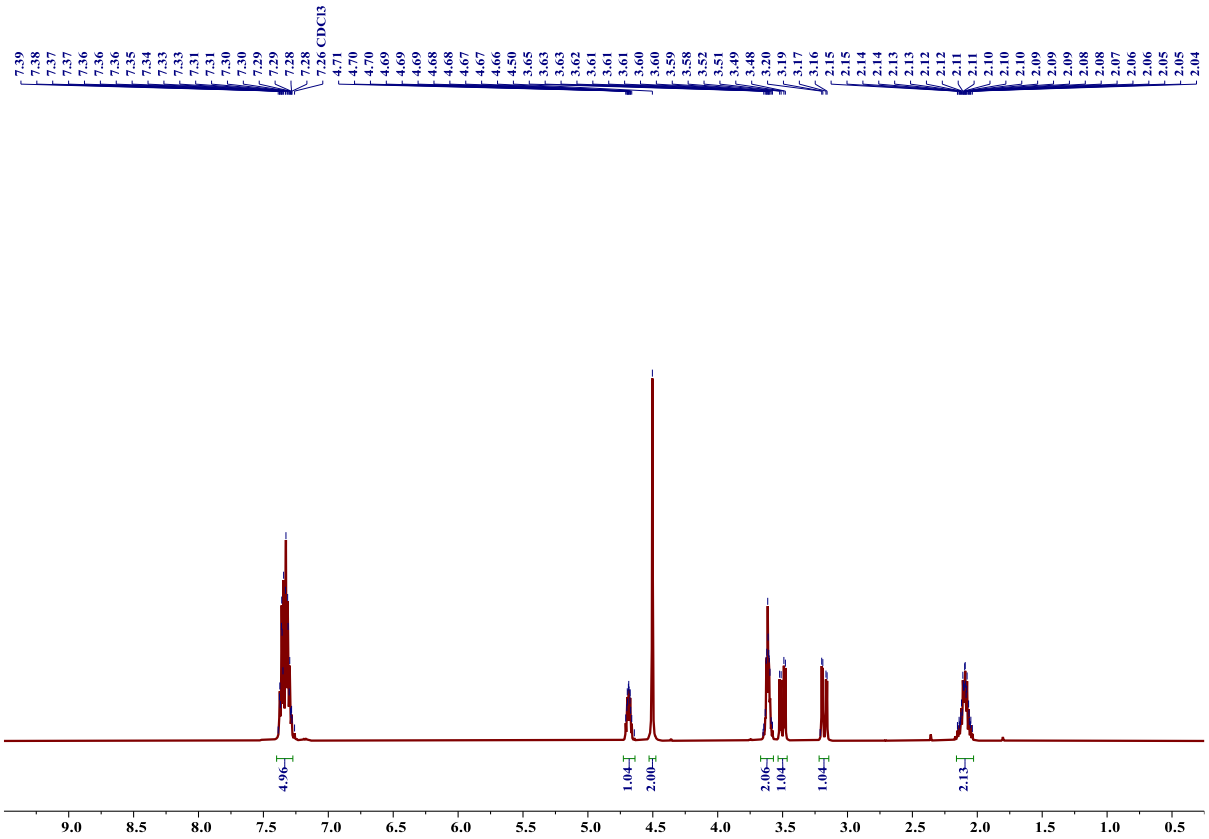

Figure 2.23. ^{1}H NMR spectrum (500 MHz, $CDCl_3$, 25 °C) of 4-(2-(benzyloxy)ethyl)oxetan-2-one.

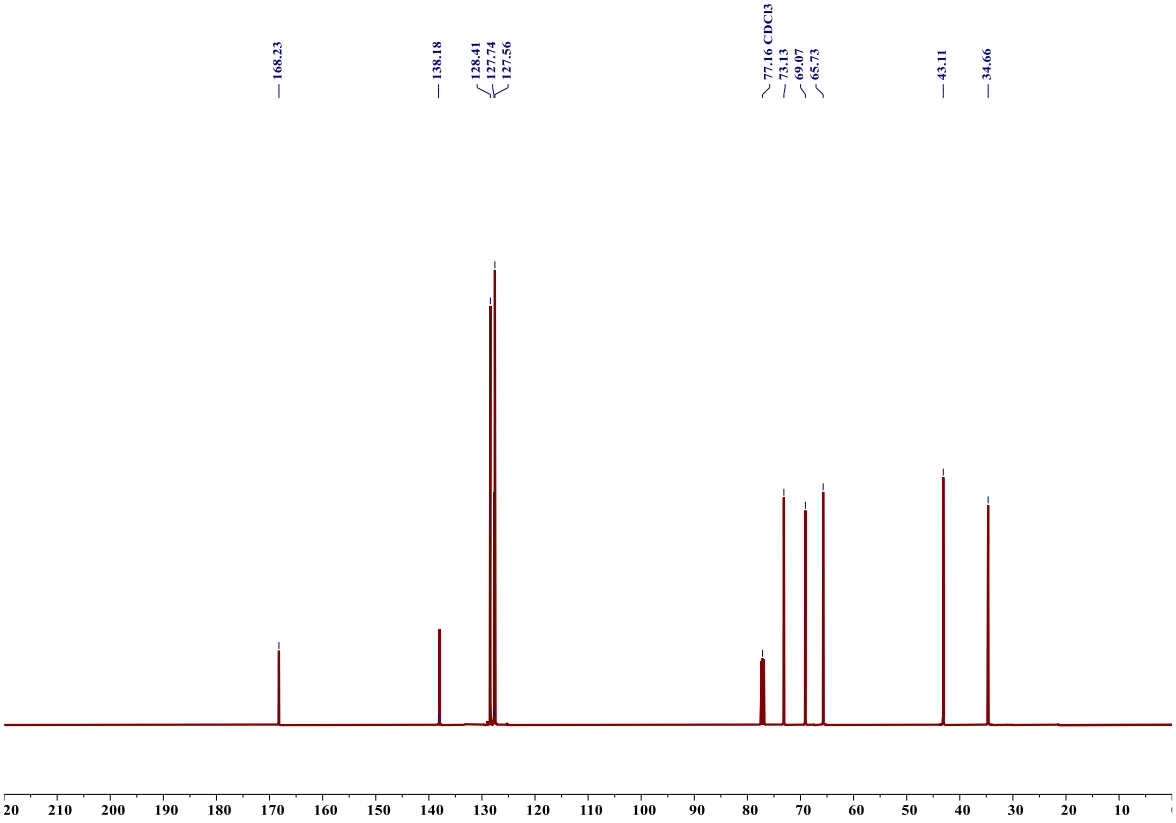

Figure 2.24 ^{13}C NMR spectrum (125 MHz, $CDCl_3$, 25 °C) of 4-(2-(benzyloxy)ethyl)oxetan-2-one.

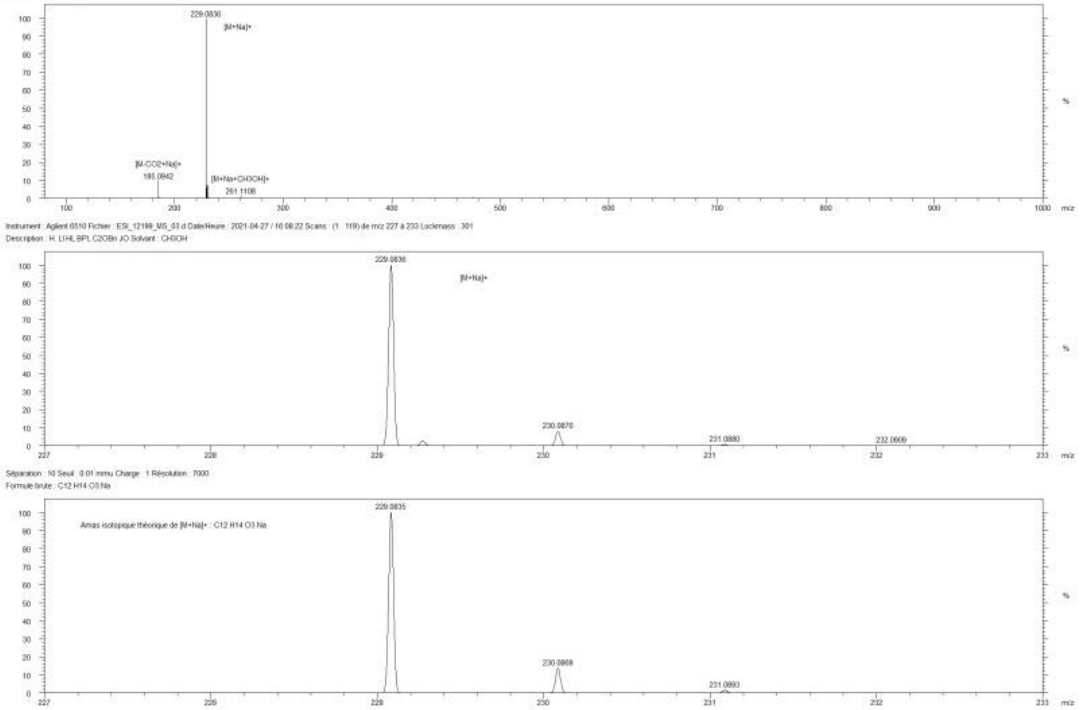

Figure 2.25. HRMS spectra of *rac*-BPL^{CH2CH2OBn}. Top: ESI mass spectrum of *rac*-BPL^{CH2CH2OBn}; middle: zoomed spectrum of top spectrum (*ca.* 230 *m*/*z*); bottom: simulated spectrum of *rac*-BPL^{CH2CH2OBn}.

(*S*)-(2-Phenylmethoxyethyl)oxirane:

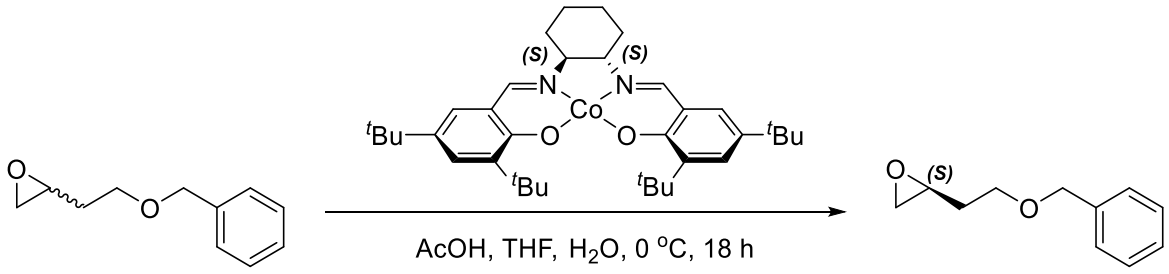

Scheme 2.5. Hydrolytic kinetic resolution (HKR) reaction of *rac*-(2-phenylmethoxyethyl)oxirane.

The catalyst ((*S*,*S*)-(salen)Co complex, 151 mg, 250 µmol, 0.005 *equiv.*) was dissolved in *rac*-(2-phenylmethoxyethyl)oxirane (8.90 g, 50.0 mmol), AcOH (57 µL, 1.0 mmol, 0.02 *equiv.*) and 0.5 mL THF. The solution was cooled to 0 °C, and treated with H_2O (495 µL, 27.5 mmol, 0.55 *equiv.*). After 18 h, (*S*)-(2-phenylmethoxyethyl) oxirane (3.50 g, 19.6 mmol, 39%) was isolated by vacuum distillation and the *ee* of the recovered epoxide was determined to be > 99% by chiral HPLC analysis (Figure 2.27).

^{1}H NMR (400 MHz, $CDCl_3$, 25 °C, Figure 2.26): δ 7.39 – 7.26 (m, 5H), 4.54 (s, 2H), 3.69 – 3.58 (m, 2H), 3.08 (dtd, J = 6.8, 4.4, 2.7, 1H), 2.79 (dd, J = 5.1, 4.0, 1H), 2.53 (dd, J = 5.1, 2.7, 1H), 1.92 (dddd, J = 14.4, 7.2, 6.1, 4.7, 1H), 1.79 (dq, J = 14.4, 6.0, 1H).

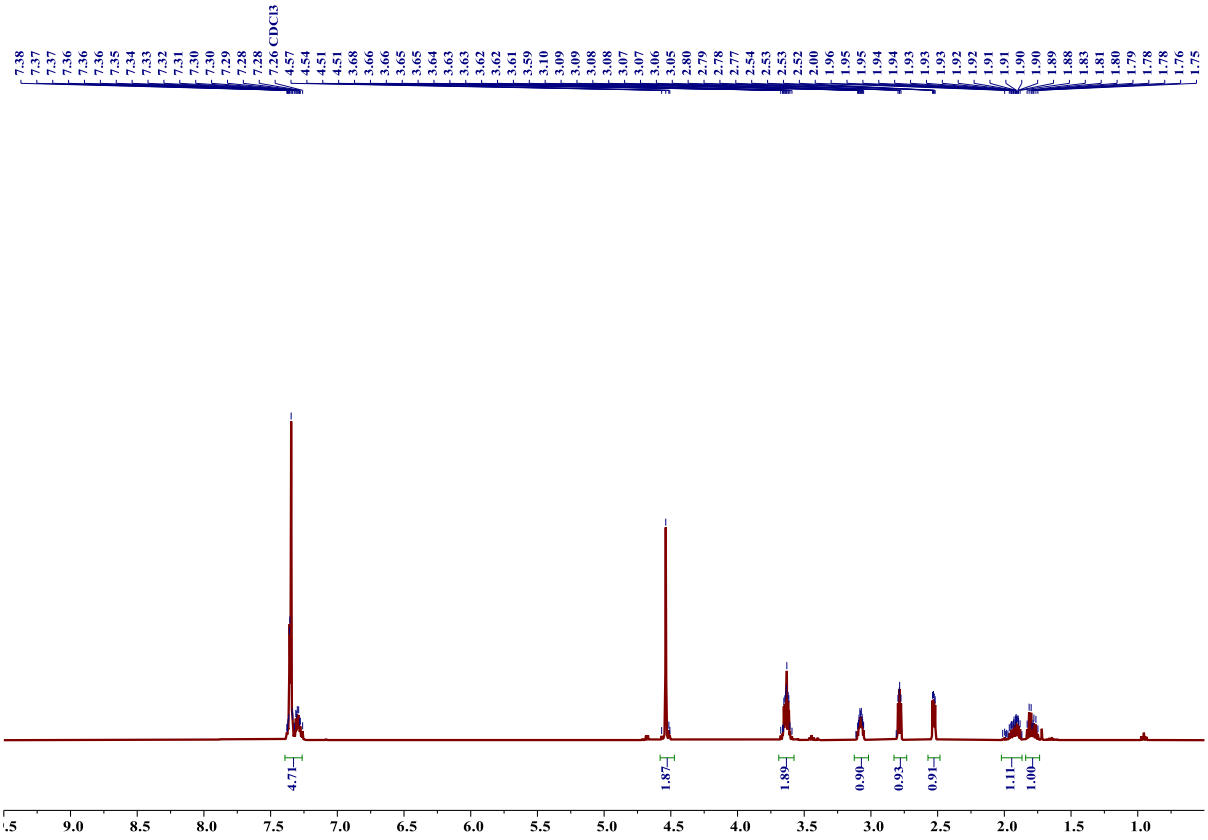

Figure 2.26. ^{1}H NMR spectrum (400 MHz, $CDCl_3$, 25 °C) of (*S*)-2-[2-(benzyloxy)ethyl]oxirane.

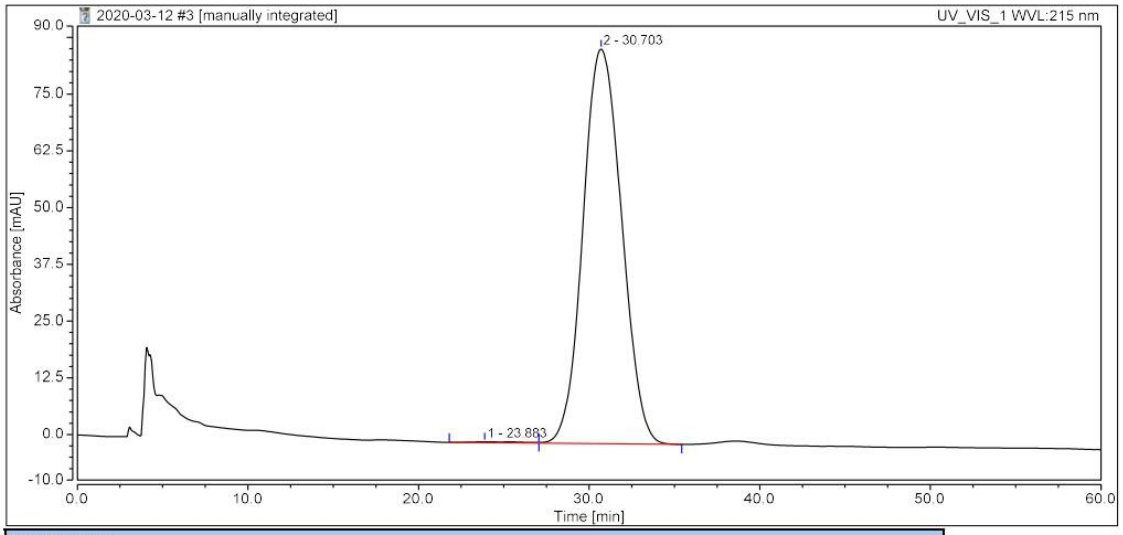

Peak Results						
No.	Peak Name	Retention Time min	Width (50%) min	Resolution (EP)	Asymmetry (EP)	Plates (EP)
1		23.883	n.a.	n.a.	n.a.	n.a.
2		30.703	2.488	n.a.	1.07	844

Integration Results						
No.	Peak Name	Retention Time min	Area mAU*min	Height mAU	Relative Area %	Relative Height %
1		23.883	0.713	0.196	0.31	0.23
2		30.703	228.145	86.946	99.69	99.77
Total:			**228.859**	**87.142**	**100.00**	**100.00**

Figure 2.27. Chiral HPLC chromatogram (column Chiralcel-OD DAICEL; 250 mm × 4.6 mm, 5 µm; 20 °C with a UV detector at 214 nm) of (*S*)-2-(2-(benzyloxy)ethyl)oxirane.

(*S*)-4-(2-(benzyloxy)ethyl)oxetan-2-one ((*S*)-BPL^{CH2CH2OBn}):

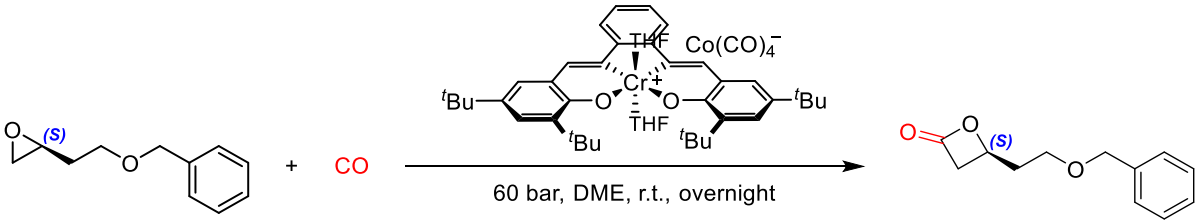

Scheme 2.6. The carbonylation of functional epoxide towards (*S*)-BPL^{CH2CH2OBn}.

(*S*)-BPL^{CH2CH2OBn} was prepared using a method adapted from the literature.[9] In the glovebox, an oven-dried Schlenk tube was charged with [salph(Cr(THF)$_2$)]$^+$[Co(CO)$_4$]$^-$ (270 mg, 0.25 mmol). On a vacuum line, dry DME (5 mL) was syringed in, and the resulting solution was cannulated into a degassed high-pressure reactor which was pressurized with carbon monoxide to 30 bar, and stirred for 15 min before depressurization. A solution of (*S*)-2-[2-(benzyloxy)ethyl]oxirane (19.6 mmol, 80 equiv.) in dry DME (15 mL) was transferred into the reactor which was then pressurized with CO to 60 bars. The reaction mixture was stirred for overnight. Then, the reactor was vented to atmospheric pressure, volatiles were removed under vacuum and the crude product was purified through alumina column using $CHCl_3$ as eluent. After evaporation of volatiles, the resulting (*S*)-BPL^{CH2CH2OBn} was obtained (90% yield).

^{1}H NMR (400 MHz, $CDCl_3$, 25 °C, Figure 2.28): δ 7.51 – 7.15 (m, 5H), 4.71 (dtd, J = 7.0, 6.0, 4.3, 1H), 4.51 (s, 2H), 3.68 – 3.57 (m, 2H), 3.53 (dd, J = 16.4, 5.9, 1H), 3.20 (dd, J = 16.4, 4.3, 1H), 2.22 – 2.03 (m, 2H).

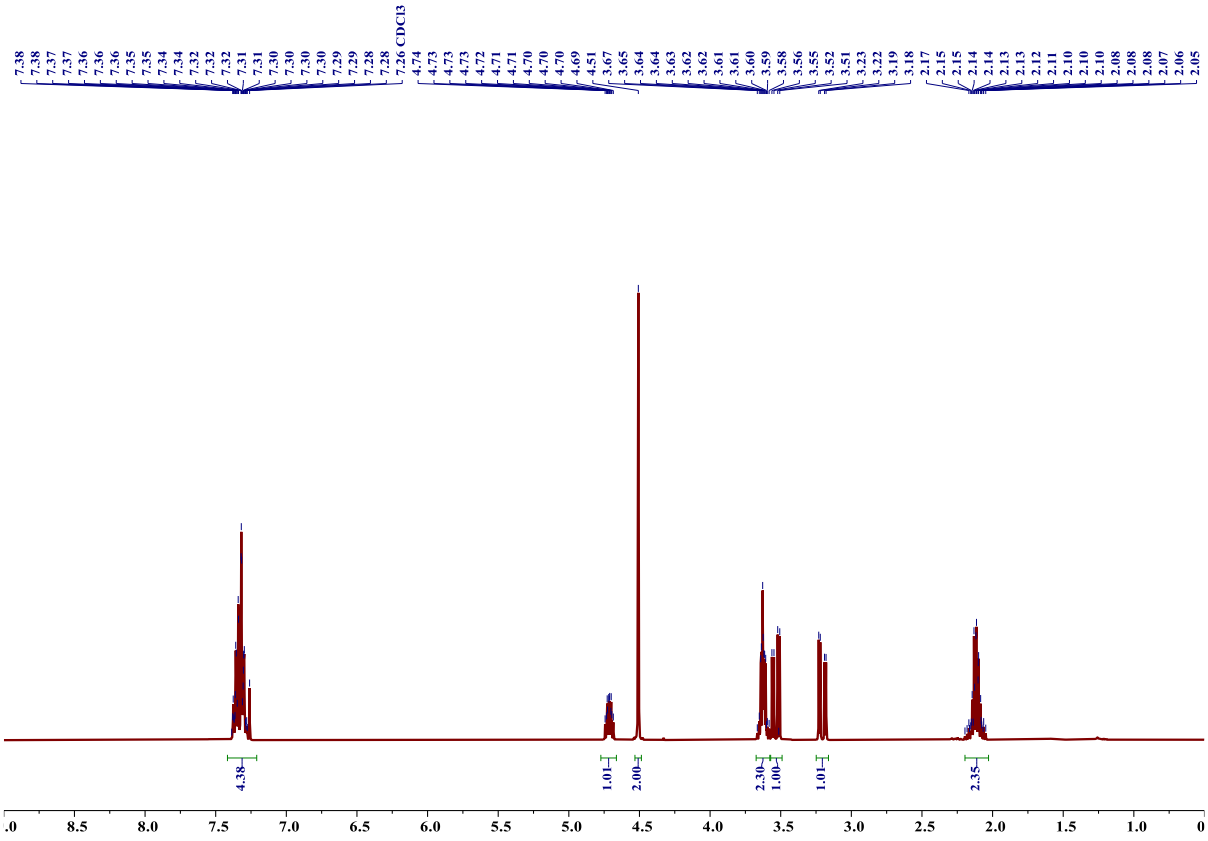

Figure 2.28. ^{1}H NMR spectrum (400 MHz, $CDCl_3$, 25 °C) of (*S*)-4-(2-(benzyloxy)ethyl)oxetan-2-one.

References

[1] R. Ligny, M. M. Hanninen, S. M. Guillaume, J.-F. Carpentier, Highly Syndiotactic or Isotactic Polyhydroxyalkanoates by Ligand-Controlled Yttrium-Catalyzed Stereoselective Ring-Opening Polymerization of Functional Racemic β-Lactones. *Angew. Chem. Int. Ed.* **2017**, *56*, 10388-10393.

[2] R. Ligny, M. M. Hanninen, S. M. Guillaume, J.-F. Carpentier, Steric *vs.* Electronic Stereocontrol in Syndio- or Iso-selective ROP of Functional Chiral β-Lactones Mediated by Achiral Yttrium-Bisphenolate Complexes. *Chem. Commun.* **2018**, *54*, 8024-8031.

[3] H. Li, R. M. Shakaroun, S. M. Guillaume, J.-F. Carpentier, Recent Advances in Metal-Mediated Stereoselective Ring-Opening Polymerization of Functional Cyclic Esters towards Well-Defined Poly(hydroxy acid)s: From Stereoselectivity to Sequence-Control. *Chem. Eur. J.* **2020**, *26*, 128-138.

[4] C. G. Jaffredo, Y. Chapurina, S. M. Guillaume, J.-F. Carpentier, From Syndiotactic Homopolymers to Chemically Tunable Alternating Copolymers: Highly Active Yttrium Complexes for Stereoselective Ring-Opening Polymerization of β-Malolactonates. *Angew. Chem. Int. Ed.* **2014**, *53*, 2687-2691.

[5] R. M. Shakaroun, H. Li, P. Jéhan, M. Blot, A. Alaaeddine, J.-F. Carpentier, S. M. Guillaume, Stereoselective Ring-Opening Polymerization of Functional β-Lactones: Influence of the Exocyclic Side-Group. *Polym. Chem.* **2021**, *12*, 4022-4034.

[6] T. L. Church, Y. D. Y. L. Getzler, C. M. Byrne, G. W. Coates, Carbonylation of Heterocycles by Homogeneous Catalysts. *Chem. Commun.* **2007**, 657-674.

[7] J. T. Lee, P. J. Thomas, H. Alper, Synthesis of β-Lactones by the Regioselective, Cobalt and Lewis Acid Catalyzed Carbonylation of Simple and Functionalized Epoxides. *J. Org. Chem.* **2001**, *66*, 5424-5426.

[8] Y. D. Y. L. Getzler, V. Mahadevan, E. B. Lobkovsky, G. W. Coates, Synthesis of β-Lactones: A Highly Active and Selective Catalyst for Epoxide Carbonylation. *J. Am. Chem. Soc.* **2002**, *124*, 1174-1175.

[9] J. W. Kramer, E. B. Lobkovsky, G. W. Coates, Practical β-Lactone Synthesis: Epoxide Carbonylation at 1 atm. *Org. Lett.* **2006**, *8*, 3709-3712.

[10] H. Choi, S. Y. Ham, E. Cha, Y. Shin, H. S. Kim, J. K. Bang, S. H. Son, H. D. Park, Y. Byun, Structure-Activity Relationships of 6- and 8-Gingerol Analogs as Anti-Biofilm Agents. *J. Med. Chem.* **2017**, *60*, 9821-9837.

[11] S. E. Schaus, B. D. Brandes, J. F. Larrow, M. Tokunaga, K. B. Hansen, A. E. Gould, M. E. Furrow, E. N. Jacobsen, Highly Selective Hydrolytic Kinetic Resolution of Terminal Epoxides Catalyzed by Chiral (Salen)Co(III) Complexes. Practical Synthesis of Enantioenriched Terminal Epoxides and 1,2-Diols. *J. Am. Chem. Soc.* **2002**, *124*, 1307-1315.

[12] G. W. Coates, J. W. Kramer, Low Pressure Carbonylation of Heterocycles. US7569709B22009.

[13] N. Ajellal, D. M. Lyubov, M. A. Sinenkov, G. K. Fukin, A. V. Cherkasov, C. M. Thomas, J.-F. Carpentier, A. A. Trifonov, Bis(guanidinate) Alkoxide Complexes of Lanthanides: Synthesis, Structures and Use in Immortal and Stereoselective Ring-Opening Polymerization of Cyclic Esters. *Chem. Eur. J.* **2008**, *14*, 5440-5448.

[14] L. R. Rieth, D. R. Moore, E. B. Lobkovsky, G. W. Coates, Single-Site β-Diiminate Zinc Catalysts for the Ring-Opening Polymerization of β-Butyrolactone and β-Valerolactone to Poly(3-hydroxyalkanoates). *J. Am. Chem. Soc.* **2002**, *124*, 15239-15248.

[15] E. Caytan, R. Ligny, J.-F. Carpentier, S. M. Guillaume, Evaluation of Band-Selective HSQC and HMBC: Methodological Validation on the Cyclosporin Cyclic Peptide and Application for Poly(3-hydroxyalkanoate)s Stereoregularity Determination. *Polymers* **2018**, *10*, 533-546.

[16] N. Ajellal, M. Bouyahyi, A. Amgoune, C. M. Thomas, A. Bondon, I. Pillin, Y. Grohens, J.-F. Carpentier, Syndiotactic-Enriched Poly(3-hydroxybutyrate)s via Stereoselective Ring-Opening Polymerization of Racemic β-Butyrolactone with Discrete Yttrium Catalysts. *Macromolecules* **2009**, *42*, 987-993.

[17] J.-F. Carpentier, Rare-Earth Complexes Supported by Tripodal Tetradentate Bis(phenolate) Ligands: A Privileged Class of Catalysts for Ring-Opening Polymerization of Cyclic Esters. *Organometallics* **2015**, *34*, 4175-4189.

[18] A. Amgoune, C. M. Thomas, S. Ilinca, T. Roisnel, J.-F. Carpentier, Highly Active, Productive, and Syndiospecific Yttrium Initiators for the Polymerization of Racemic β-Butyrolactone. *Angew. Chem. Int. Ed.* **2006**, *45*, 2782-2784.

[19] M. Bouyahyi, N. Ajellal, E. Kirillov, C. M. Thomas, J.-F. Carpentier, Exploring Electronic versus Steric Effects in Stereoselective Ring-Opening Polymerization of Lactide and β-Butyrolactone with Amino-alkoxy-bis(phenolate)-yttrium Complexes. *Chem. Eur. J.* **2011**, *17*, 1872-1883.

[20] B. Lygo, Stereoselective Synthesis of (±)-Methyl Homononactate and (±)-Methyl 8-*epi*-Homononactate. *Tetrahedron* **1988**, *44*, 6889-6896.

Chapter 3

Cyclic Poly(3-Thiobutyrate) Synthesized by Ring-Opening Polymerization of Racemic β-Thiobutyrolactone with Anionic-type Initiators/Catalysts: Control of Topology and Tacticity in Homopolymerization and Copolymerization Attempts[††]

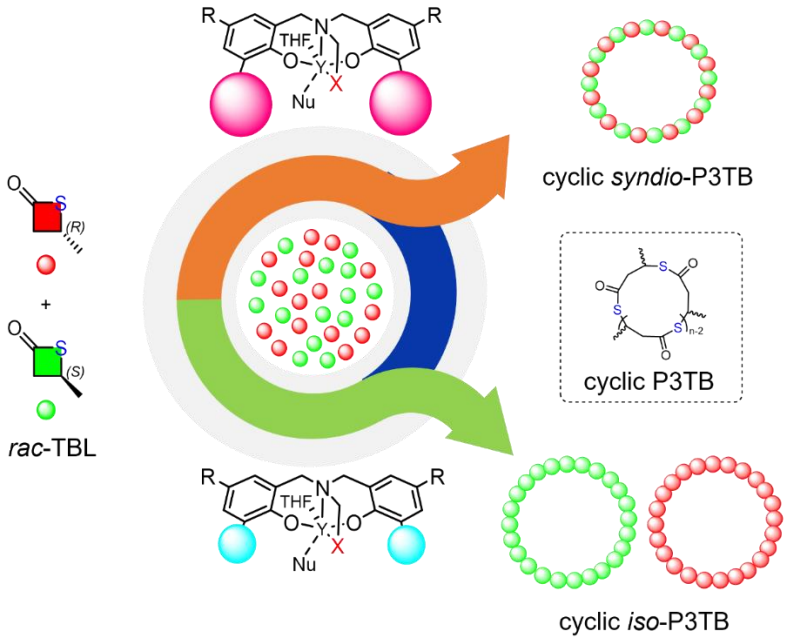

[††] Part of this chapter has appeared in print, see:

H. Li, J. Ollivier, S. M. Guillaume, J.-F. Carpentier, Tacticity Control of Cyclic Poly(3-Thiobutyrate) Prepared by Ring-Opening Polymerization of Racemic β-Thiobutyrolactone. *Angew. Chem. Int. Ed.* **2022**, *61*, e202202386.

3.1 Introduction

Poly(hydroxyalkanoate)s (PHAs) are a valuable class of polyesters, representing a possible alternative to controversial petrochemical-based plastics. PHAs combine the film-barrier properties of polyesters with the mechanical performance properties of petroleum-based polyethylene and polypropylene.[1] The most common natural PHA is poly(3-(*R*)-hydroxybutyrate) (*i*-P3HB), a perfectly isotactic, highly crystalline thermoplastic material, which is a biodegradable polymer with a high melting transition temperature (T_m = 180 °C). However, the melting point of *i*-P3HB is very close to its decomposition temperature (T_d = 180−200 °C), which leads to thermal degradation by ester pyrolysis during melt processing, thus making the final products difficult to process and expensive.

It is well-known that the introduction of sulfur atoms into the polymer backbone can endow polymers with enhanced properties, which are different from those of regular hydrocarbon-based polymer analogs. Therefore, as developed in Chapter 1, polythioesters (PTEs), polyester analogs with thioesters in the backbone, can be regarded as another paradigm of novel degradable polymers. although they have been gaining increasing attention over the past half-decade, PTEs are significantly less explored than their corresponding polyesters due to a lack of controlled ring-opening polymerization (ROP) methods enabling to convert thiolactones to high-molar-mass PTEs with narrow dispersity. Notable examples of ROP monomers for PTEs synthesis include β-thiolactone, dithiolactone, ε-thiocaprolactone (refer to the state of the art, Chapter 1).

Poly(3-thiobutyrate) (P3TB), the first biopolymer with thioester linkages in the backbone, was initially synthesized from a recombinant strain of *E. coli* two decades ago.[2] However, the fermentation approach can only generate P3TB with a difficultly controlled manner, very high molar mass of 176 kg mol^{-1} and a relatively broad dispersity ($Đ_M$ > 1.9). Additionally, the composition and mechanical performance of biosynthetic P3TB are difficult to adjust. On the other hand, it is well-known that chemical synthesis can be used to furnish polymers with varying and controlled molar mass, microstructures, and even topologies. Surprisingly enough, although PTEs are not that rare, the ROP of β-thiobutyrolactone towards P3TB was never documented prior to our works.

This chapter reports on the chemical synthesis of P3TB *via* ROP of the corresponding *rac*-β-thiobutyrolactone (*rac*-TBL) with anionic-type initiators/catalysts (Figure 3.1) (the organo-catalyzed ROP of *rac*-TBL is the subject of Chapter 4). The stability of *rac*-TBL makes this process challenging, and even more so if topology (linear vs. cyclic polymers) and stereoselectivity issues are simultaneously addressed. The ROP of *rac*-TBL was investigated by anionic-type systems, such as NaOMe, *t*BuOK, *n*BuLi, La{N(TMS)$_3$}$_3$, (BDI)ZnO*i*Pr, and "Y{ONXO^{R1,R2}}(N(SiHMe$_2$)$_2$)(THF)". Among them, tripodal tetradentate bis(phenolate) yttrium complexes gave the best promising results where the substituents installed on the phenolate rings induce switching from *iso*-enriched to *syndio*-biased P3TBs. This is the first report of a highly stereoselective ROP of a racemic chiral thiolactone. The resulting P3TBs were characterized by MALDI-ToF MS, NMR and TGA analyses, quite unexpectedly and

uniquely, revealing that pure cyclic PTBLs were generated. In addition, we describe attempts in ring-opening copolymerization (ROCOP) of *rac*-TBL and *rac*-β-butyrolactone (*rac*-BL) mediated by yttrium catalyst. However, likely due to the considerable difference in reactivity ratio between *rac*-BL and *rac*-TBL, these attempts gave rise to mixtures of cyclic P3TB and linear P3HB, as evidenced by NMR and MALDI-ToF MS analysis.

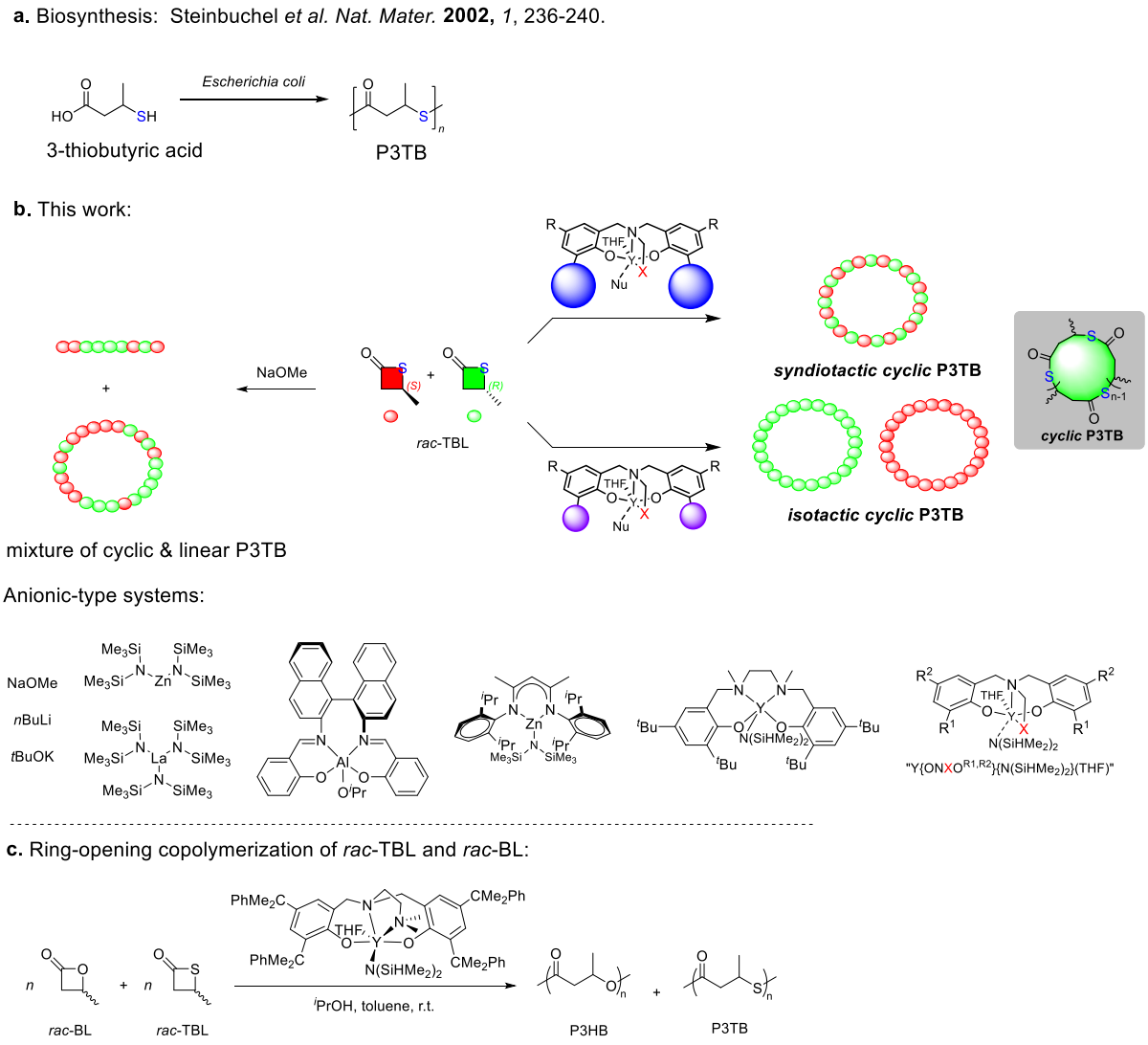

Figure 3.1. a) Fermentation approach towards P3TB; **b**) ROP of racemic 3-thiobutyrolactone (*rac*-TBL) mediated by anionic-type systems reported in our study; **c**) attempts at ROCOP of *rac*-TBL and *rac*-BL promoted by an yttrium catalyst.

3.2 The Synthesis of *rac*-β-Thiobutyrolactone and (*S*)-β-Thiobutyrolactone

The simplest and most efficient strategy for the preparation of b-thiolactones consists in the reaction between the acid chlorides of β-halogenocarboxylic acids with hydrogen sulfide in the presence of triethylamine (Figure 3.2). The yields of β-thiolactones are related to their stability, depending on the nature of the substituent. As in the case of g- and d-thiolactones, the stability of b-thiolactone ring

increases with the number of substituents.[3] So, the simplest chiral β-thiolactone, that is racemic b-thiobutyrolactone (or b-methyl-b-propiothiolactone herein denoted as *rac*-TBL), is theoretically very easy to decompose, as coped with during our study (see Experimental section).

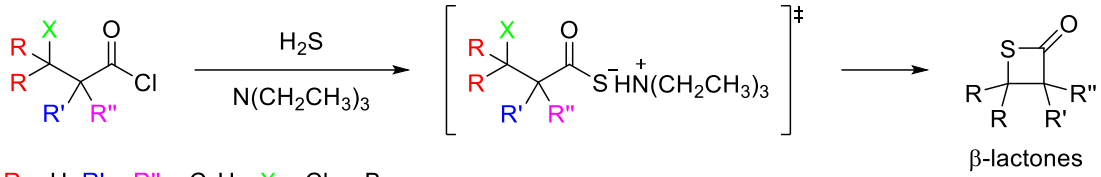

R = H, R' = R" = C_6H_5, X = Cl or Br;
R = H, R' = Me, R" = SCH_2CH_3, X = Cl;
R = H, R' = Me, R" = SCH_3, X = Cl;
R = Me, R' = R" = H, X = Br;

Figure 3.2. The common synthetic procedure towards β-lactones reported.

Half a century ago, Knunyants and coworkers reported the preparation of b-thiobutyrolactone (*rac*-TBL) through two strategies starting from b-bromobutyryl chloride and b-mercaptobutyric acid, respectively. The yield of *rac*-TBL starting from b-bromobutyryl chloride under these conditions is around 80%;[4] yet, in this case, hydrogen sulfide was used as the source of sulfur, which is a severe poison affecting the nervous system of human beings. Therefore, the second approach (Figure 3.3a) was preferentially employed to synthesize *rac*-TBL in our laboratory. After optimization of the reaction conditions, *rac*-TBL was finally obtained in 25% overall yield, initially starting from the electrophilic addition reaction of crotonic acid, a building block in the synthesis of copolymers with vinyl acetate, with thioacetic acid (Figure 3.3b). Subsequently, 3-mercaptobutyric acid (3MA) obtained from the first step underwent the ring-closing reaction, giving rise to the desired *rac*-TBL. The latter was fully characterized by NMR, HRMS, and chiral HPLC analyses (see the Experimental section).

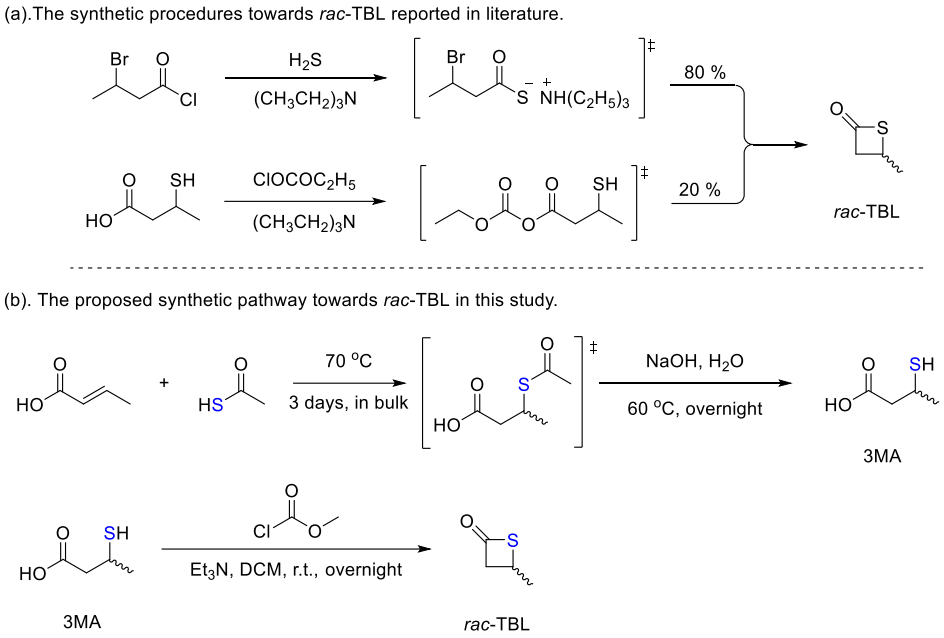

Figure 3.3. (a). The synthetic pathway towards *rac*-TBL previously reported; (b). the proposed pathway for *rac*-TBL developed in my work.

The synthesis of the thus far unreported enantiopure ɓ-thiobutyrolactone was relatively challenging. A German paper about the transformation of enantiopure β-butyrolactone[5] reported that enantiomerically pure thiobutyric acid can be obtained in good yield (47% isolated) by S_N2 ring-opening of enantiopure β-butyrolactone. Envisioning thiobutyric acid as a key intermediate, a synthetic pathway towards enantiopure β-thiobutyrolactone was designed (Figure 3.4**)**. Initially, (*R*)-butyrolactone ((*R*)-BL) was synthesized in low yield (the purification was not optimized) by carbonylation of enantiomerically pure (*R*)-propylene oxide. Subsequently, the obtained *R*-BL underwent a nucleophilic reaction with sodium hydrosulfide in water, leading to the formation of a mixture of (*S*)-thiobutyric acid and (*R*)-hydroxybutyric acid, as described in the literature.

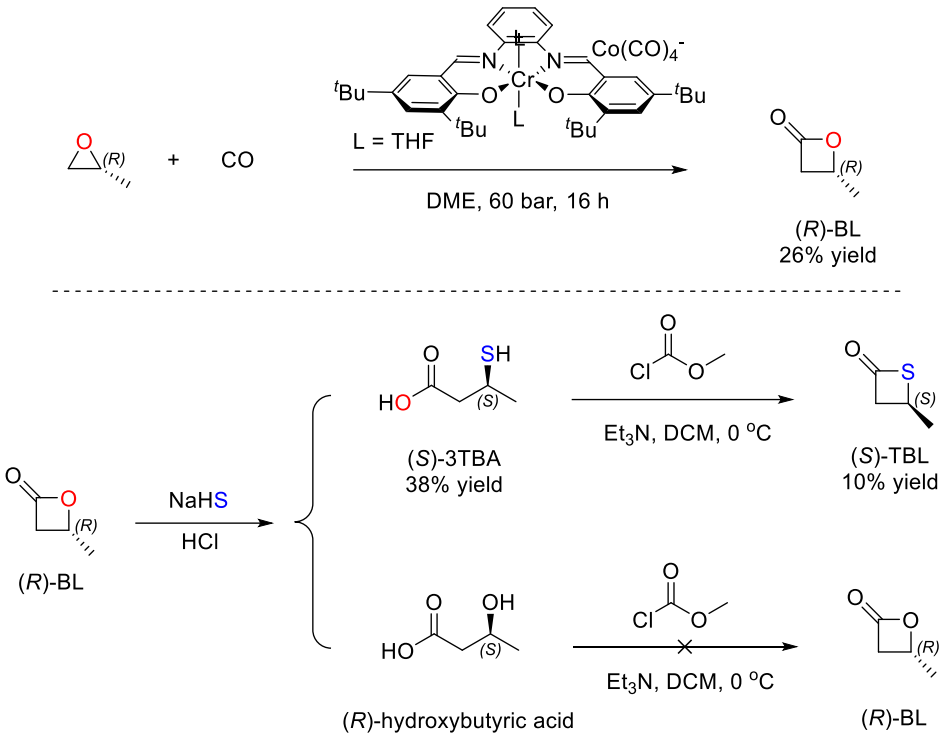

Figure 3.4. The synthetic pathway towards (*S*)-TBL starts from (*R*)-propylene oxide.

The resulting mixture (without purification) was directly subjected to the cyclization reaction using the same procedure established for the racemic one, that is in the presence of triethylamine and methyl chloroformate at 0 °C in DCM. It gave the corresponding enantiopure (*S*)-TBL in low yield (*ca.* 10%). This synthetic pathway has not been optimized thus far. The resulting (*S*)-TBL was characterized by ^{1}H NMR and chiral HPLC analyses (see the Experimental section).

In order to obtain *rac*-TBL in a higher yield, another synthetic strategy was attempted, that is the carbonylation of thiirane by using the ring-expansion carbonylation of functional epoxides as prototype (Figure 3.5). Introduction of carbonyl functional groups by using transition-metal-catalyzed carbon monoxide insertion is a synthetically useful transformation. The application of this methodology, in conjunction with readily available epoxide substrates, provides facile access to various functional β-lactones, valuable precursors for synthesizing polymers such as PHAs.[6] Even though the formation of β-thiolactone from propylene sulfide has never been documented, we envisioned that this type of catalyst could convert propylene sulfide into β-thiobutyrolactone by using carbonylation of epoxides as prototypes. At the outset, the reaction conditions used for carbonylation of epoxides, that is using DME as solvent at room temperature under 60 bars, were applied to this putative ring-expansion reaction of propylene sulfide (PS) (Table 3.1). However, none of the expected products were observed in an aliquot of the reaction mixture. Increasing the reaction temperature to 60 °C, switching to another catalytic system, $[PPN]^{+}Co(CO)_4^{-}$ or $Ru_3(CO)_{12}/Co_2(CO)_8$, resulted in the same observation

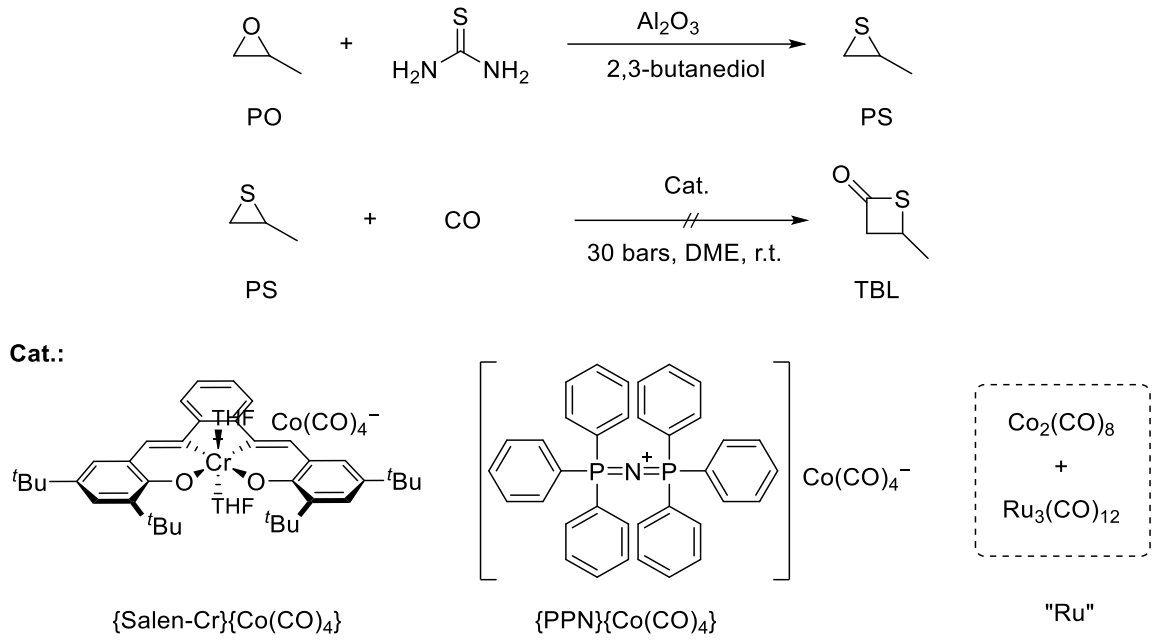

Figure 3.5. Attempted synthesis of *rac*-TBL from propylene oxide (PO) and propylene sulfide (PS).

Table 3.1. The attempts of carbonylation of thiirane.

Entry	Substrates	Cat.	[Substrate]:[Cat.]	Temp. (°C)	Pressure (bar)	Yield (%)
HL159	PS	'Salen-Cr'	25:1	r.t.	60	*n.o.*
-	PS	'Salen-Cr'	25:1	60	60	*n.o.*
HL162	PS	'[PPN]'	25:1	r.t.	60	*n.o.*
-	PS	'[PPN]'	25:1	60	60	*n.o.*
HL170	PS	'Ru'	25:1	125	60	*n.o.*

n.o. = the desired TBL was not observed or yield = 0 %

3.3 Activity and Selectivity of the Preliminary Catalyst Systems

The results of the preliminary screening of the ROP of *rac*-TBL with a variety of well-established metal-based catalysts/initiators (Figure 3.6) are summarized in Table 3.2. A series of simple, highly nucleophilic inorganic initiators, such as NaOMe, KO*t*Bu, *n*BuLi, active for the ROP of 'unstrained' γ-butyrolactone and methyl-substituted δ-valerolactones under harsh conditions,[7,8] enables the ROP of *rac*-TBL at room temperature. For example, NaOMe could initiate *rac*-TBL polymerization in C_6D_6 at ambient temperature at the $[rac\text{-TBL}]_0/[\text{NaOMe}]_0$ feed ratio of 23:1 with full conversion, giving rise to P3TB, yet with a molar mass value higher than the theoretical one and broad dispersity (Table 3.2, entry HL506). Using another common solvent, toluene, this system produced P3TB, again with a higher molar mass than the theoretical value (Table 3.2, entry HL654). The absence of control of the molar masses was further demonstrated by varying the feed ratio of $[rac\text{-TBL}]_0/[\text{NaOMe}]_0$, giving P3TB with a bimodal SEC trace. *n*BuLi, a more nucleophilic base, proved a less active initiator for the ROP of *rac*-TBL in THF as it allowed conversion of only 8% of 89 equiv. at −30 °C (Table 3.2, entry HL680). The

molar mass and dispersity values of the resulting P3TB indicated that the reaction proceeded also in an uncontrolled fashion.

Also, careful inspection of the microstructure of the resulting polymers formed from NaOMe, or *n*BuLi by ^{13}C NMR spectroscopy (*vide infra*) revealed the formation of essentially atactic P3TBs with P_m values ranging from 0.41 to 0.51.

Surprisingly, the zinc β-diketiminate complex (BDI)ZnO*i*Pr (**2a**), which is quite active for the polymerization of β-lactones and lactide, and the alternating copolymerization of carbon dioxide and epoxides,[9-12] turned out inactive towards *rac*-TBL polymerization at room temperature in toluene (Table 3.2, entry HL576). As a control experiment, no activity was also observed under the same conditions with $Zn[N(SiMe_3)_2]_2$ (**2b**), alone or with 2 equiv. of BnOH as co-initiator (Table 3.2, entries HL504 and HL651), the latter one being a well-established catalyst/initiator for the isoselective ROP of cyclic *O*-carboxyanhydrides.[13]

An enantiopure aluminum-salen complex with a binaphthyl backbone, (*R*)-(SalBinam)AlO*i*Pr (**1**), a highly effective catalyst for the stereoselective ROP of *rac* (*meso*)-lactide and the regioselective ROP of unsymmetrical cyclic diester, (*S*)-methyl glycolide,[14,15] allowed full conversion of 25 equiv. of *rac*-TBL at room temperature (Table 3.2, entry HL564). Yet, the recovered P3TB featured a M_n value as determined by SEC much higher than the theoretical one, suggesting a poor initiating efficiency and/or undesirable side-reactions, such as inter-, intra-transthioesterification, and back-biting reactions.

The lanthanum tris(amide), $La\{N(TMS)_2\}_3$ (**3**), the most earth-abundant and least expensive complex within the Ln series, also proved a quite active system for ROP of *rac*-TBL at room temperature, alone or in combination with an external protic co-initiator, yet again giving rise to ill-defined P3TB in terms of topology (*vide infra*). Again, careful inspection of the microstructure of the polymers formed with **1** or **3** by ^{13}C NMR spectroscopy (*vide infra*) revealed the formation of atactic P3TBs with P_m values of *ca.* 0.48−0.50 (Table 3.2, entries HL505 and HL368).

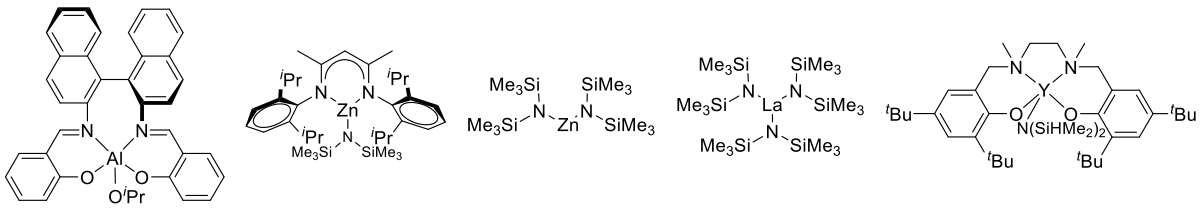

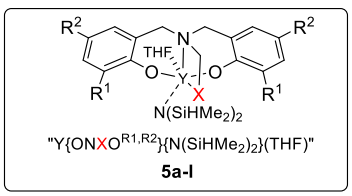

X =	CH_2NMe_2	CH_2OMe	CH_2NEt_2	2-pyridyl
$R^1 = R^2 = {}^t$Bu	**5a**	**5b**	-	-
$R^1 = R^2 = CMe_2Ph$	**5c**	**5d**	**5e**	**5f**
$R^1 = R^2 = Me$	**5g**	**5h**	**5i**	**5j**
$R^1 = R^2 = Cl$	**5k**	-	-	-
$R^1 = CPh_3$, $R^2 = Me$	**5l**	-	-	-

Figure 3.6. Structure of the catalysts/initiators used for the ROP of *rac*-TBL.

Table 3.2. Selected results of the preliminary screening of the ROP of *rac*-TBL.[a]

Ref.	Cat.	$[TBL]_0/[Cat.]/[I]_0$	I[b]	Solvent	time[c] (min)	Conv.[d] (%)	$M_{n,theo}$[e] (kg mol^{-1})	$M_{n,SEC}$[f] (kg mol^{-1})	$Đ_M$[f]	P_m[g]
HL506	-	23:0:1	NaOMe	C_6D_6	60	99	2.4	4.0	1.61	0.51
HL654	-	25:0:1	NaOMe	Tol	60	70	1.8	4.7	1.86	0.51
HL669	-	40:0:1	NaOMe	Tol	60	52	2.2	-	-	-
HL567	-	89:0:1	KO*t*Bu	THF	20	8	0.8	5.2	1.25	0.41
HL680[h]	-	50:0:1	*n*BuLi	THF	360	28	1.5	9.0	1.54	-
HL564	**1**	25:1:0	-	Tol	72	99	2.6	14.5	1.46	0.48
HL483	**2a**	50:1:1	*i*PrOH	Tol	120	0	-	-	-	-
HL504	**2b**	50:1:0	-	Tol	180	0	-	-	-	-
HL651	**2b**	50:1:2	BnOH	Tol	180	0	-	-	-	-
HL505	**3**	25:1:0	-	C_6D_6	< 1	99	2.6	5.2	1.53	0.50
HL368	**3**	100:1:3	BnSH	Tol	6	99	3.4	1.7	1.17	0.49
HL625	**4**	25:1:0	-	Tol	< 1	99	2.6	6.0	2.15	0.54
HL424	**4**	100:1:1	*i*PrOH	Tol	< 1	99	10.3	46.5	1.45	0.52
HL337	***5 a***	25:1:0	-	Tol	5	99	2.6	4.9	1.47	0.37
HL573	***5 a***	50:1:0	-	Tol	< 1	99	5.1	3.7	1.48	0.32
HL350	***5 a***	50:1:1	*i*PrOH	Tol	5	99	5.1	6.5	1.78	0.37
HL344	***5 a***	50:1:1	*i*PrOH	Tol	5	99	5.1	6.6	1.67	0.38
HL574	***5 a***	50:1:1	*i*PrOH	Tol	< 1	99	5.1	3.8	1.42	0.34
HL498	***5 a***	50:1:1	*i*PrSH	Tol	< 1	99	5.1	3.9	1.66	0.32
HL372	***5 a***	50:1:1	*i*PrSH	Tol	< 1	99	5.1	3.2	1.45	-
HL637	***5 a***	50:1:1	BnSH	Tol	< 1	99	5.1	3.5	1.65	0.32
HL348	***5 a***	100:1:1	BnSH	Tol	5	99	10.3	6.1	1.59	0.31

[a] Polymerization performed at room temperature, $[TBL]_0$ = 0.5 M; [b] co-initiator denoted as I; [c] the reaction time was not necessarily optimized; [d] conversion of *rac*-TBL was determined by ^{1}H NMR analysis of the crude polymerization mixture; [e] molar mass calculated according to $M_{n,theo} = [TBL]_0/[Cat.]_0 \times Conv._{TBL} \times M_{w,\,TBL}$; [f] number-average molar mass ($M_{n,SEC}$) and dispersity ($Đ_M$) as determined by SEC analysis in THF at 30 °C *vs.* polystyrene standards (uncorrected values); [g] P_m is the probability of *meso* enchainment between TBL units as determined by $^{13}C\{^1H\}$ NMR analysis of the isolated P3TBs.

As group 3 metal complexes, especially yttrium, have shown excellent performances in a variety of (stereoselective) ROPs of cyclic esters (refer to the state of the art, see Chapter 1), we next explored two different families of such achiral yttrium complexes. The amido yttrium-salan complex **4**, which produces – thanks to chain-end stereocontrol – highly alternating poly(3-hydroxyalkanoate) copolymers *via* ROP of equimolar mixtures of opposite enantiomers of different chiral β-lactones,[16] is very active for the ROP of *rac*-TBL: in toluene at ambient temperature, with or without a co-initiator (such as *i*PrOH), full conversion of 25-100 equiv. of the monomer proceeded within less than 1 min (Table 3.2, entries HL625 and HL424). The resulting P3TBs showed again molar mass values much higher than the theoretical ones. Moreover, the resulting polymers were also atactic, as assessed by ^{13}C NMR spectroscopy.

The most promising results were obtained with the discrete yttrium amido complex supported by a diamino-bis(phenolate) ligand bearing sterically bulky *t*Bu substituents, 'Y{ONNO^{tBu2}}(N(SiHMe$_2$)$_2$)(THF)' (**5a)**, that is a prototypical example among the family developed by our group since the early 2000s. The ROP of *rac*-TBL in toluene promoted by **5a**, without a protic co-initiator, proceeded very rapidly at ambient temperature as well (Table 3.2, entries HL337 and HL573). Although no detailed kinetics −due to the rapid reactions at room temperature with yttrium systems, kinetic monitoring by NMR was not possible −could be determined under these conditions, the turnover frequencies (TOF) exceed 3,000 h^{-1}; these values are at least comparable, possibly higher than those obtained in the ROP of the parent b-lactone *rac*-BL under the same conditions (TOF > 200 h^{-1}). ^{13}C NMR spectroscopy (*vide infra*) revealed that the resulting P3TBs are syndiotactic-enriched (P_m = 0.32−0.37), providing further opportunities in terms of stereocontrol improvement upon ligand tuning and optimization of the reaction conditions. On the other hand, the experimental molar mass values determined by SEC, $M_{n,SEC}$, did not vary proportionally with the values calculated from the monomer-to-initiator ratio; also the dispersity values were somewhat high ($Đ_M$, M_w/M_n = 1.47−1.48), and definitively higher than those typically observed ($Đ_M$ = 1.05−1.3) for P3HB obtained from ROP of *rac*-BL under similar conditions (*vide infra*).[17]

It is noteworthy that the yttrium-amide complexes themselves are excellent initiators for the ROP of *rac*-BL and its higher derivatives since they induce a good control over the molar mass (*i.e.*, narrow dispersities). Because the active propagating species in the ROP of cyclic esters is a metal alkoxide, isopropoxide yttrium complexes are highly desired, closely mimicking the putative propagating groups of the presumed active species. However, the chemistry of rare-earth alkoxides is much trickier than that of the corresponding amides. This is essentially due to the tendency of the highly oxophilic rare-earth elements to generate oxo species, which often collapse as multinuclear clusters and generate mixtures of compounds. Consequently, alkoxides are most often generated *in situ* or just prior the ROP. Yttrium isopropoxide catalysts/initiators were thus conveniently generated *in situ* by the addition of 1 equiv. of *i*PrOH to the mixture of the corresponding proligand and yttrium amide precursor, respectively; the use of an isopropoxide initiator is of further interest to analyze the terminal groups of the polymer, as the isopropoxycarbonyl group COO*i*Pr, in contrast to the bis(dimethylsilyl)amidocarbonyl group CON(SiHMe$_2$)$_2$, it is stable (upon isolation of the polymer under acidic conditions) and readily identified by NMR spectroscopy, hence enabling easy molar mass determination of linear polyesters. In this regard, the yttrium isopropoxide derived from **5a** was investigated in the ROP of *rac*-TBL in toluene at room temperature, allowing complete conversion of 50 equiv. of monomer within less than 1 min. Prolonging the reaction time to 5 min, the dispersities of the P3TBs formed became much broader than those recovered by quenching the polymerization less than 1 min ($Đ_M$ = 1,67−1.78 for 5 min, Table 3.2, entries HL350 and HL344 *vs.* $Đ_M$ = 1.42 for 1 min, entry HL574, respectively); this suggests that transesterification reactions occurred readily over the course of polymerization. In order to mimic the propagating species in the ROP of *rac*-TBL, thiols, such as, *i*PrSH and BnSH, were used as co-initiator

for yttrium-catalyzed ROP of *rac*-TBL under the same conditions as established before (Table 3.2, entries HL337 and HL573). It is apparent that the identity of the co-initiator slightly affects both the molar mass and the dispersities of the polymers, giving polymers with broader dispersities ($Đ_M$ = 1.45−1.66) and lower molar mass than theoretical values. We attributed these changes to the rate of initiation by the corresponding thioalkoxy yttrium species, being slower than the propagating rate of the polymerization.

3.4 Topology of the Isolated Poly(3-Thiobutyrate)

The returned P3TBs were characterized by NMR spectroscopy and matrix-assisted laser desorption/ionization time-of-flight mass spectroscopy (MALDI-ToF MS). The ^{1}H NMR spectra of the P3TBs isolated from catalysts **1−5a** clearly displayed the characteristic signals corresponding to TBL repeating units (Figure 3.7), especially the backbone methine (δ *ca.* 3.92 ppm) and methylene (δ *ca.* 2.84−2.88 and 2.68−2.70 ppm) signals, and the typical pendant methyl (δ *ca.* 1.32−1.34 ppm) moieties, respectively. Similarly, ^{13}C{^{1}H} NMR spectra of the P3TBs formed displayed the characteristic signals corresponding to TBL repeating units as well ((Figure 3.8). The chemical shift of carbonyl thioester group (−C(O)S−) of P3TB appears at *ca.* 195.60−195.84 ppm, which is at a much lower field than that of carbonyl oxoester (−CO_2−) of P3HB, also indicating that isomerization between thioester and thionoester (*δ* 225 ppm) is absent in this reaction, as the chemical resonance of thionoester (−C(S)O−) typically appears at $\delta > 225$ ppm.[18] In addition, because the electronegativity of the sulfur atom is much lower than that of the oxygen atom, the chemical shifts of the carbon of methine and methylene were distinct from those of P3HB.

The P3TB sample prepared from NaOMe (Table 3.2, entry HL506) showed a methoxycarbonyl end-group (*δ* 3.67 ppm) which was unambiguously observed by ^{1}H and ^{13}C NMR spectroscopy (Figure 3.9 and SI); yet, as discussed above, the molar mass estimated by NMR ($M_{n,NMR}$ = *ca.* 3,900 g mol^{-1}) was significantly higher than the theoretical one ($M_{n,theo}$ = *ca.* 2,400 g mol^{-1}), suggesting a poor initiation efficiency and/or unselective formation of linear and cyclic macromolecules under these conditions.

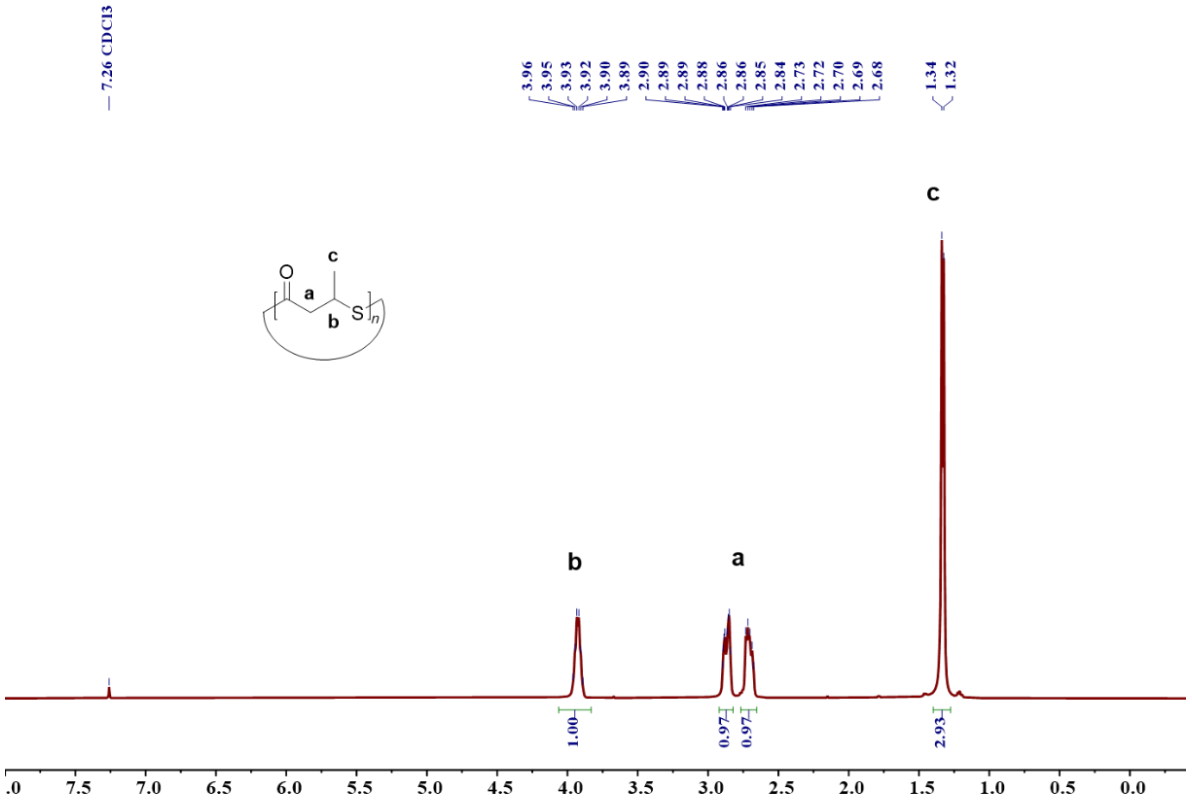

Figure 3.7. ^{1}H NMR spectrum (500 MHz, $CDCl_3$, 25 °C) of an isolated P3TB produced by the **5a**/*i*PrOH system (Table 3.2, entry 345).

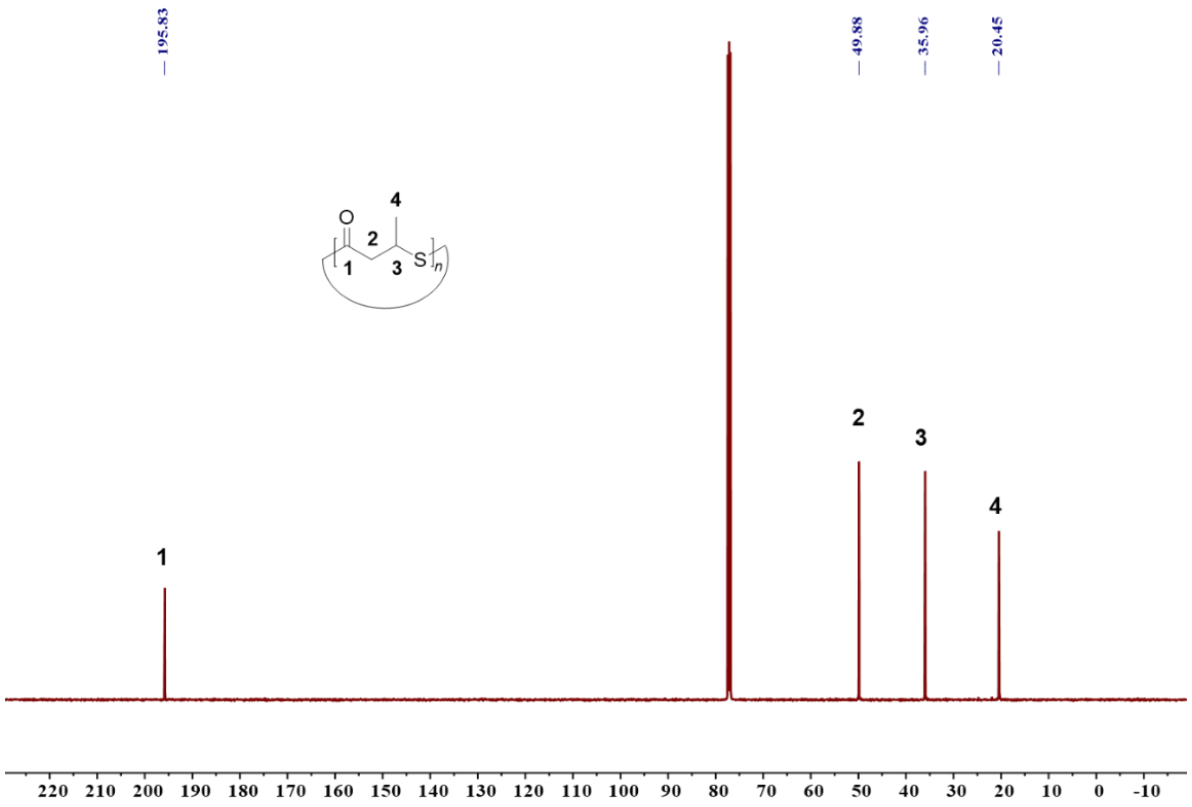

Figure 3.8. $^{13}C\{^{1}H\}$ NMR spectrum (126 MHz, $CDCl_3$, 25 °C) of an isolated P3TB produced by the **5a**/*i*PrOH system (Table 3.2, entry HL345).

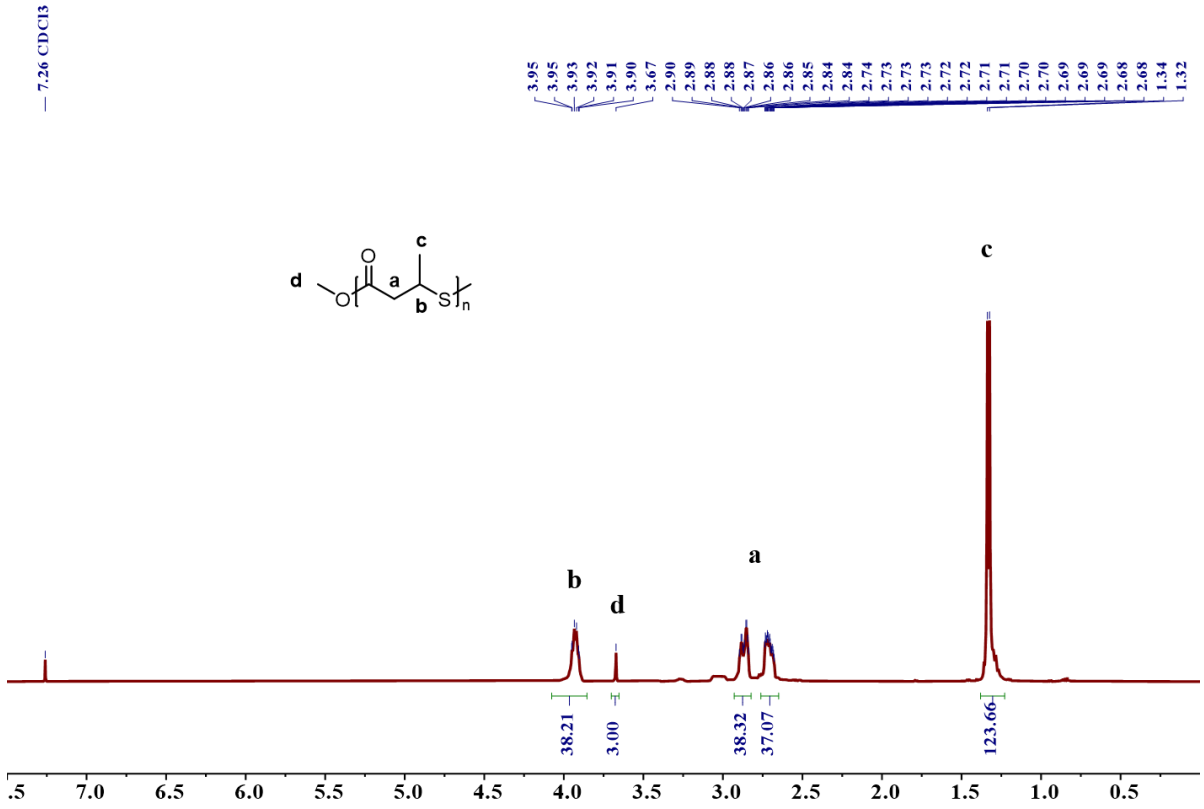

Figure 3.9. ^{1}H NMR spectrum (400 MHz, $CDCl_3$, 25 °C) of an isolated P3TB (at least in part linear) produced by NaOMe (Table 3.2, entry HL506).

Also, whether **5a** was used alone or in the presence of a co-initiator such as *i*PrOH, *i*PrSH, or BnSH, chain-end groups were not observed in the NMR spectra of the polymers. Similar observations were made from the NMR spectra of P3TBs prepared with *n*BuLi, the aluminium complex **1**, the trisamido lanthanum precursor **3**/BnOH (1:3) system, and the yttrium-salan complex **4**.

To get further insights into the mechanism of this polymerization, the chain initiation, the end-groups and the topology of the isolated P3TBs, the polymer samples were further investigated by MALDI-ToF MS.

In line with the above NMR data, analysis of P3TB samples prepared from NaOMe evidenced the formation of mixtures of linear MeO–$[C_4H_6SO]_n$–H and cyclic $[C_4H_6SO]_n$ macromolecules; these ROP experiments were hardly reproducible as small changes in the reactions conditions returned variable amounts of linear and cyclic structures, as assessed by mass spectrometry. For example, the MALDI-ToF mass spectrum of P3TB produced from NaOMe in C_6D_6 at room temperature at a feed ratio of 23:1, suggested that only linear macromolecules MeO–$[C_4H_6SO]_n$–H were formed ((Figure 3.10). However, the MALDI-ToF mass spectrum of the P3TB sample generated from NaOMe in toluene at ambient temperature revealed a mixture of linear and cyclic structures, indicating intramolecular back-biting (Experiment section, Figure 3.47). When increasing the reaction temperature to 30 °C, the mixture of linear and cyclic P3TB was also formed (Figure 3.11).

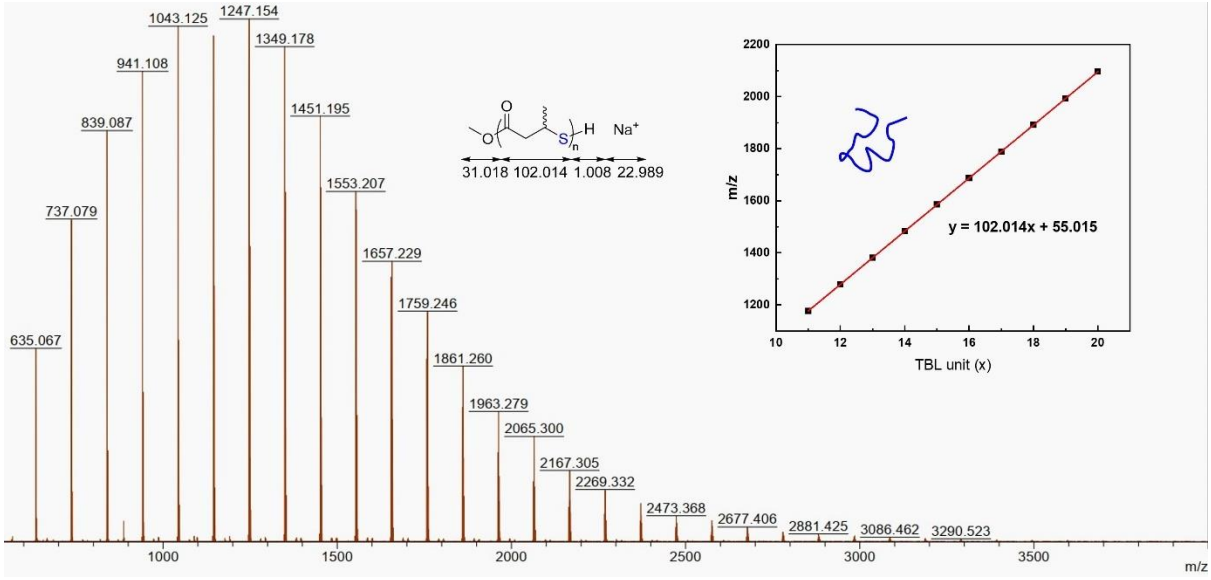

Figure 3.10. MALDI-ToF mass spectrum of an essentially linear P3TB produced by NaOMe in C_6D_6 (Table 3.2, HL506), with a plot of experimental *m/z* values vs. theoretical number of TBL repeating units.

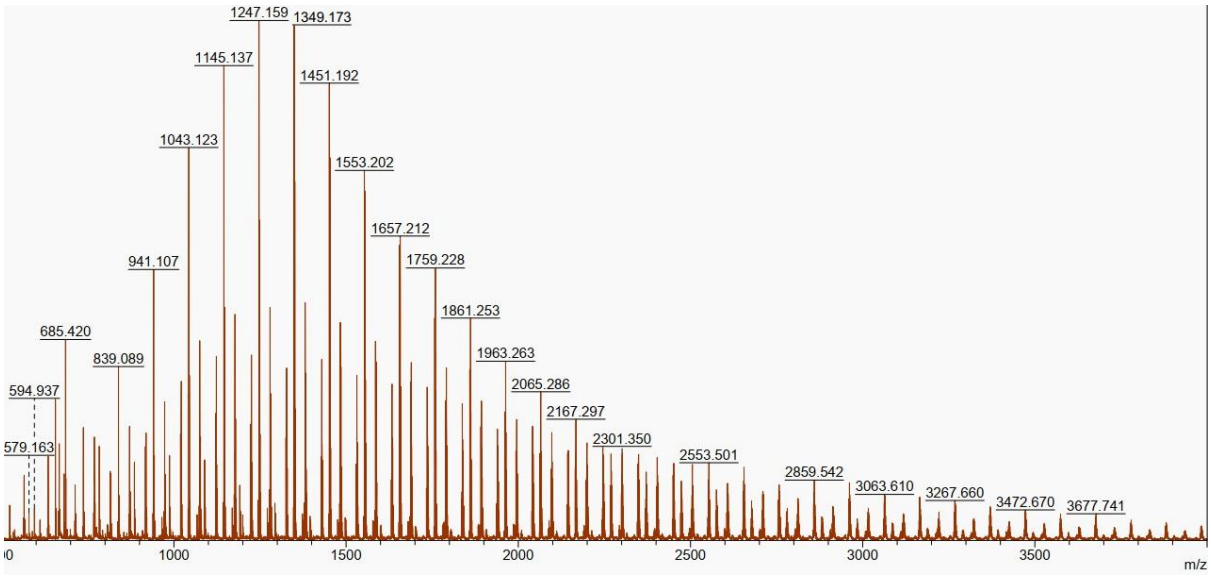

Figure 3.11. MALDI-ToF mass spectrum of a mixture of several populations of P3TB, including cyclic (major) and linear (less intense) P3TB, produced by the ROP of *rac*-TBL with NaOMe in toluene (40:1, toluene, 30 °C, 1 h, Table 3.2, entry HL669).

Conversely, the P3TBs resulting from the ROP of *rac*-TBL promoted by discrete complexes **1**, **4** or **5a** revealed a single population of cyclic macromolecules, *i.e.* without chain-end groups; for the latter complex, regardless of the use of a co-initiator (*i*PrOH, *i*PrSH, or BnSH, 1 equiv. vs. Y) (Figure 3.12, Figure 3.14 and Figure 3.15), no matter the nature of the ROP solvent (toluene or THF, Figure 3.12 and Figure 3.16) and of the substituents installed on the ligand (Figure 3.17), the observed *m/z* values are consistent with the data calculated for cyclic macromolecules $[C_4H_6SO]_n$ (Figure 3.13). Another indirect support for the formation of cyclic (*vs.* linear) polymers arises from thermal studies, as in Appendices (for theoretical considerations see: the properties of cyclic polymer; experimental results *vide infra*).

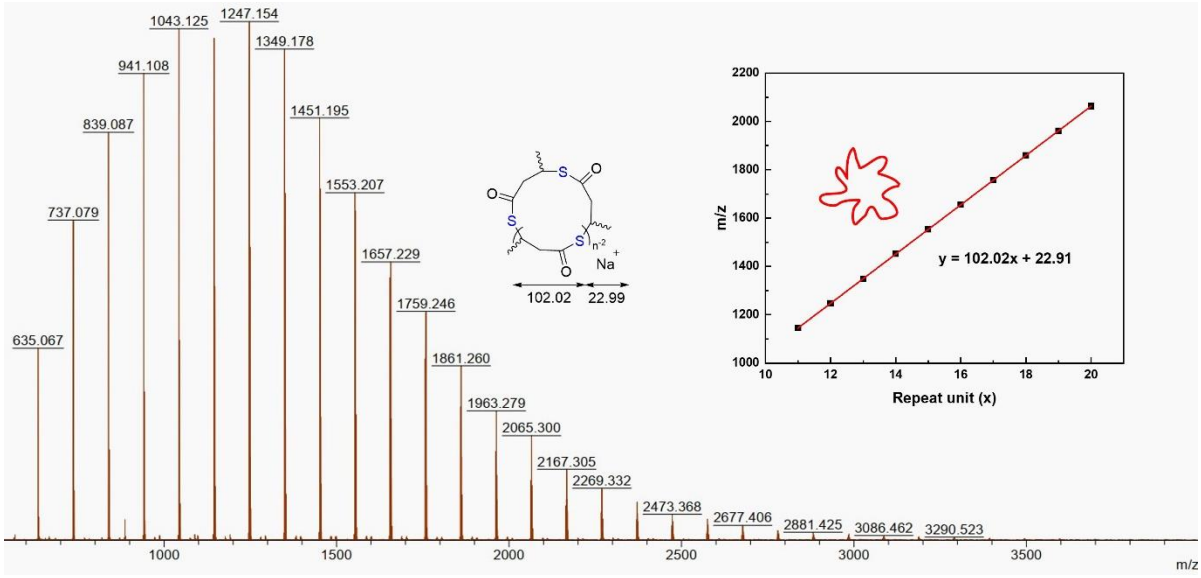

Figure 3.12. MALDI-ToF mass spectrum of a cyclic P3TB produced by Y{ONNO^{tBu2}}{N(SiHMe$_2$)$_2$}(THF) (**5a**) in toluene in the absence of a co-initiator (Table 3.2, HL337), with a plot of experimental *m/z* values vs. theoretical number of TBL repeating units.

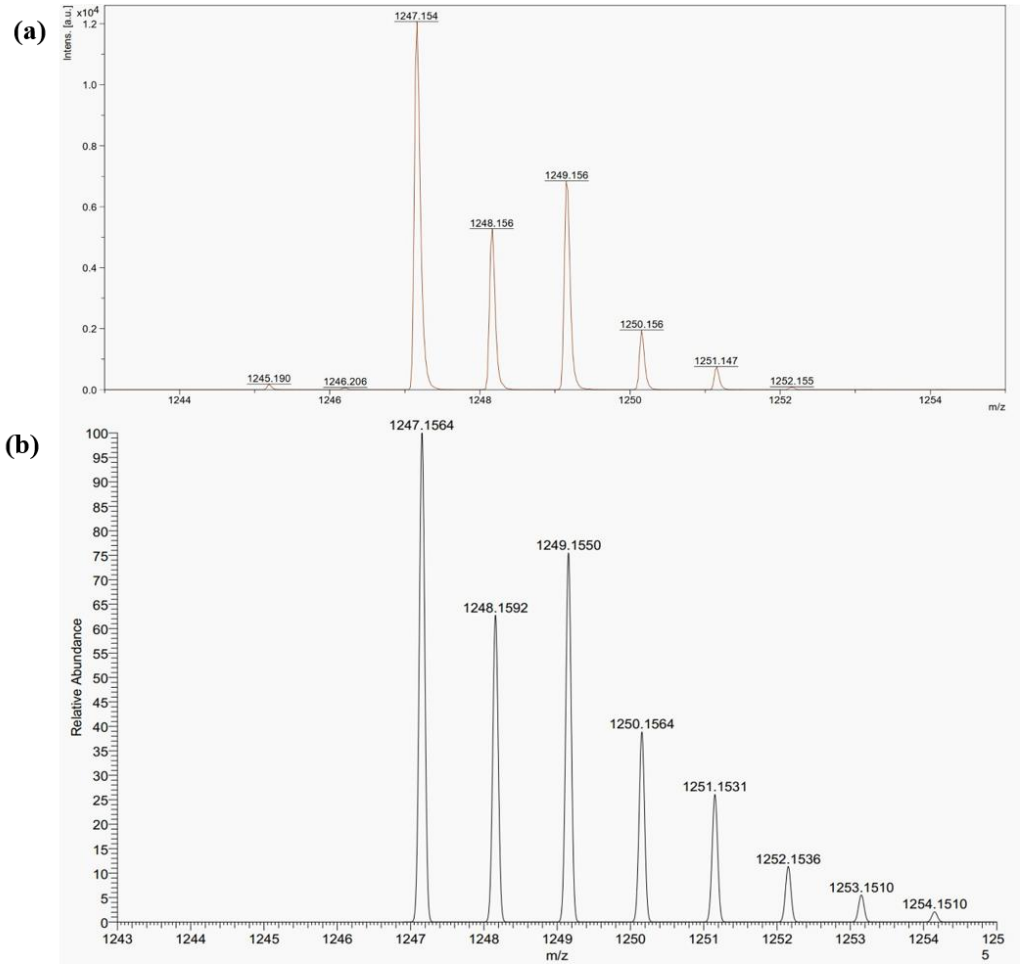

Figure 3.13. a) Zoomed region of the MALDI-ToF mass spectrum of a cyclic P3TB when *n* = 12, {$(C_4H_6SO)_n + Na^+$} (Table 3.2, entry HL337) from Figure 3.12; b) simulated spectrum of a cyclic P3TB when *n* = 12, {$(C_4H_6SO)_n + Na^+$}.

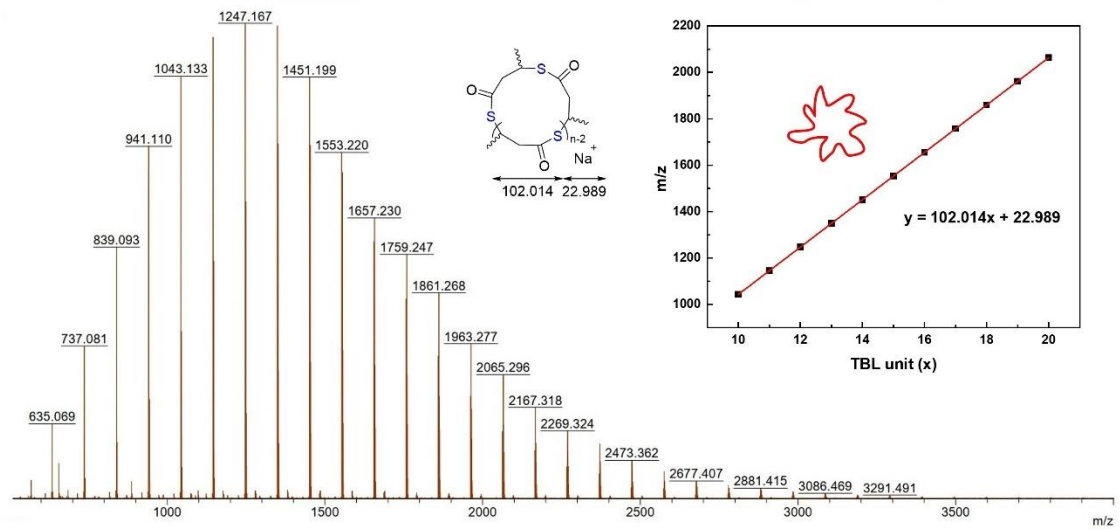

Figure 3.14. MALDI-ToF mass spectrum of a cyclic P3TB produced by the system Y{ONNO^{tBu2}}{N(SiHMe$_2$)$_2$}(THF) (**5a**)/*i*PrOH (1:1) in toluene (Table 3.2, HL350/574), with a plot of experimental *m*/*z* values *vs.* theoretical number of TBL repeating units.

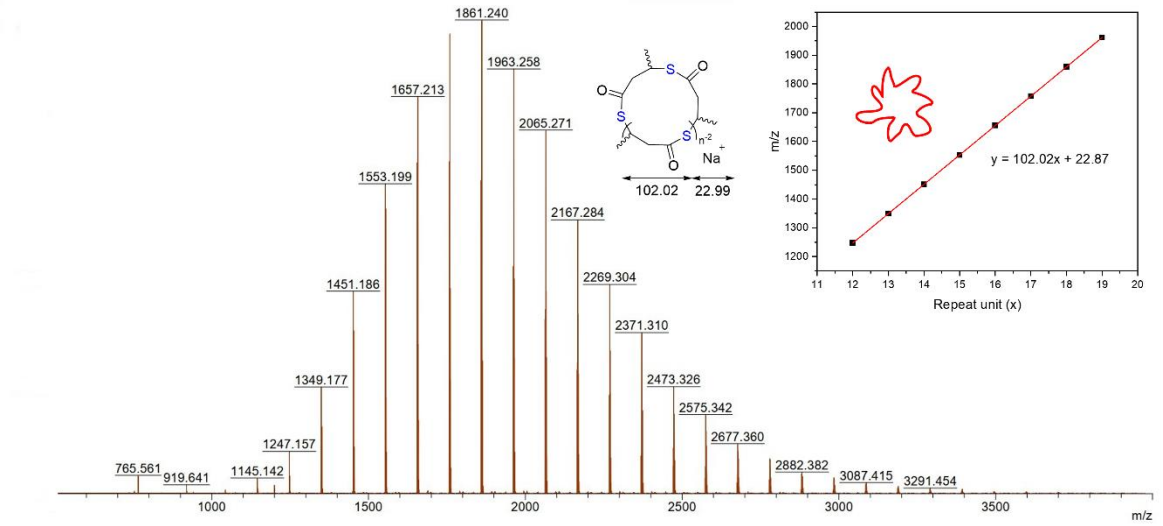

Figure 3.15. MALDI-ToF MS spectrum of a pure cyclic P3TB produced by Y{ONNO^{tBu2}}{N(SiHMe$_2$)$_2$}(THF) (**5a**) in toluene at room temperature in the presence of *i*PrSH (Table 3.2, HL498).

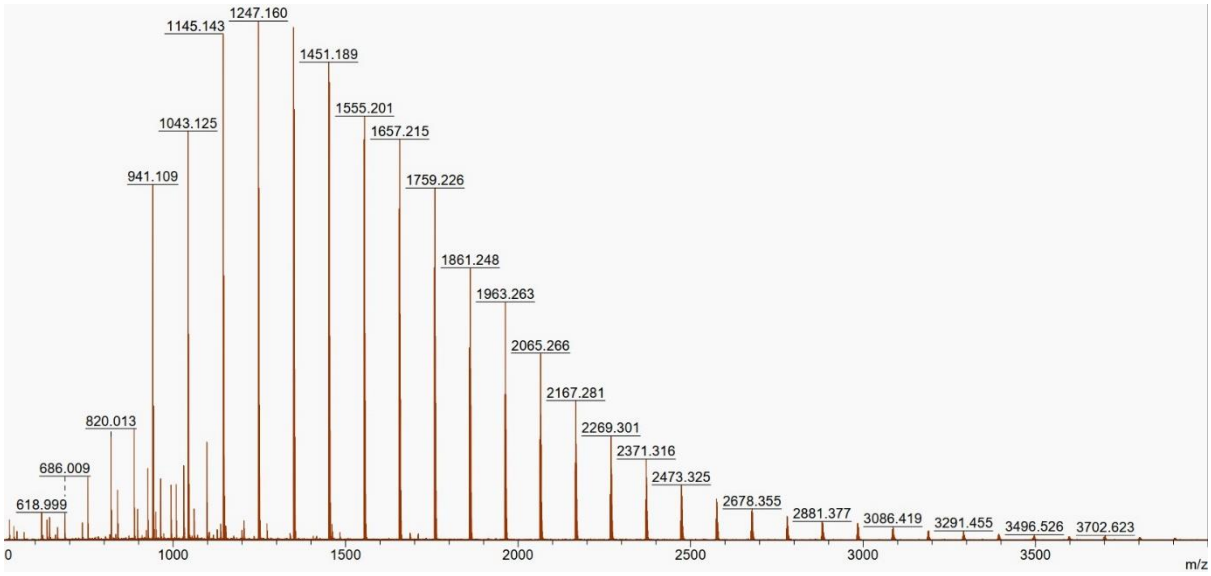

Figure 3.16. MALDI-ToF mass spectrum of a cyclic P3TB produced by Y{ONNO^{tBu2}}{N(SiHMe$_2$)$_2$}(THF) (**5a**) in THF in the absence of co-initiator (25:1:0, at r.t., in THF, 1 min, conv. = 99%). For n = 12, m/z exp = 1247.160 *vs.* m/z theo = 1247.156 for $[[C_4H_6OS]_{12}+Na]^+$.

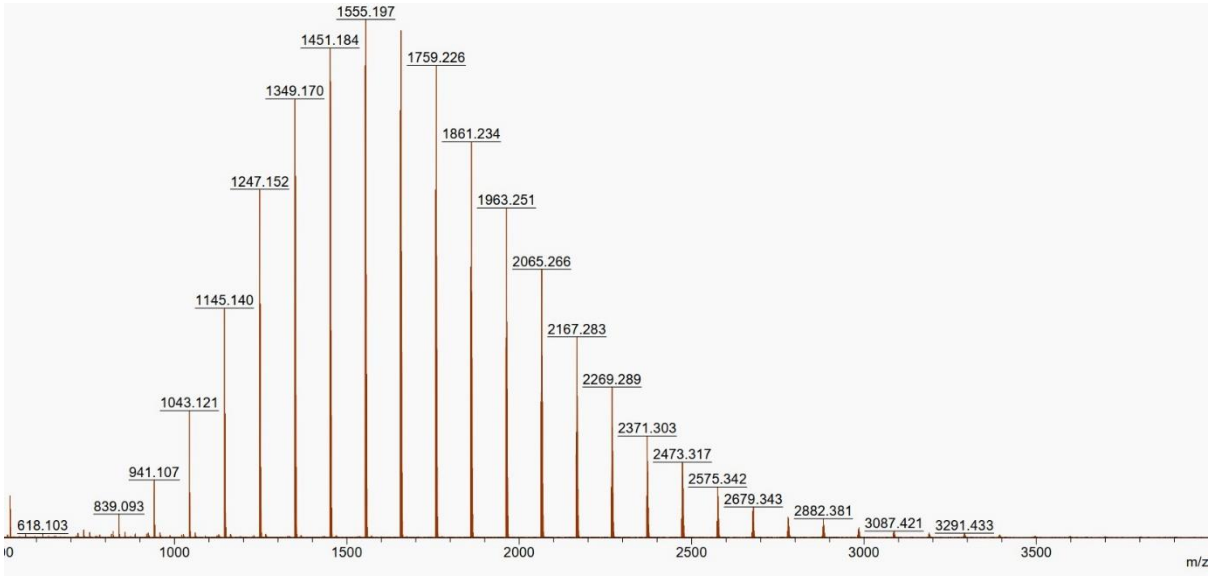

Figure 3.17. MALDI-ToF mass spectrum of a cyclic P3TB produced by Y{ONNO^{Cl2}}{N(SiHMe$_2$)$_2$}(THF) (**5k**) in THF in the absence of co-initiator (25:1:0, at r.t., 1 min, conv. = 99%, $M_{n,SEC}$ = 4100, $Đ_M$ = 1.72). For n = 15, m/z exp = 1553.194 *vs.* m/z theo = 1553.198 for $\{[C_4H_6OS]_{15}+Na\}^+$.

Several groups have reported that ROP by metal catalyst/initiator enable to access cyclic and linear polymers, depending on the [monomer]$_0$/[catalyst]$_0$/[initiator]$_0$ ratios. Chen and coworkers reported that the ROP of γ-butyrolactone at a high concentration (10 M or without solvent) at low temperature (−40 °C) using the lanthanum amide La[N(SiMe$_3$)$_2$]$_3$ in the absence of co-initiator, led to the formation of poly(γ-butyrolactone) with cyclic topology.[19] Upon addition of a co-initiator, *e.g.*, BnOH, *i*PrOH, Ph_2CHCH_2OH, to this catalytic system, the topology of the resulting polymer shifted from a predominantly cyclic one to a mixture of cyclic and linear structures to a primarily linear structure as the feed ratio changed from 100:1:1 to 100:1:2 to 100:1:3, respectively. The authors proposed that the

formation of the cyclic polyester results from back-biting and that this pathway is favored within chains initiated by –$N(SiMe_3)_2$, a better leaving group.[19] Du and coworkers reported that the ROP of β-butyrolactone mediated by amido-oxazolinate zinc complexes yielded cyclic P3HBs with high molar mass (M_n up to 197 kg mol^{-1}) and dispersity $Đ_M$ in the range 1.08−1.98.[20] In comparison, the zinc-catalyzed ROP of β-butyrolactone in the presence of a mono- or bifunctional coinitiator, *e.g.*, EtOH or 1,4-cyclohexanediol, led to the formation of strictly linear P3HBs. Xu and coworkers reported a synthetic strategy for the formation of cyclic poly(*O*-carboxyanhydride) through the ROP of *O*-carboxyanhydride.[13] Using $La[N(SiMe_3)_2]_3$ in the absence of co-initiator yielded a cyclic polymer, while $Zn[N(SiMe_3)_2]_2$ favored the formation of a linear polymer in the presence of BnOH. Other prior studies have noted that the co-initiator, to some extent, has a significant effect on the topology of the resulting polymer regarding ring-expansion polymerization of cyclic monomer by metal catalyst/initiator, especially on NHC-catalyzed ROP of cyclic esters.[21,22] However, in our studies, despite the variable nature of co-initiator groups used, such as −$N(SiHMe_2)_2$, −O*i*Pr, −SCH_2Ph, and −S*i*Pr, the ROP of *rac*-TBL mediated by complexes related to **5a** always gave pure cyclic P3TBs.

In fact, back-biting occurs to a significant extent during the ROP of *rac*-TBL promoted by these yttrium-based catalysts. Due to the intrinsically reactive dynamic thioester bonds within the P3TB main chain and the increased nucleophilicity of thiols versus alcohols, intramolecular transthioesterification occurs more readily than transesterification.[23-25] We assumed that thiolates attached to the yttrium metal center in the propagating species attack internal thioester groups at any site within the growing polymer chain, leading to the observed formation of cyclic P3TBs. A simple representation of the typical coordination-insertion putative mechanism at play in the ROP of cyclic (thio)esters for initiation and propagation steps, as well as dynamic processes that lead to the formation of cyclic P3TB and ring-expansion, are depicted in Figure 3.18. In this model, high molar mass P3TBs are formed, implying a propagation rate significantly faster than the cyclization rate ($k_p >> k_c$). On the other hand, common to chain-growth polymerizations, chain transfer processes, such as back-biting, can compete with chain propagation to enlarge the dispersity of the resulting polymer. It is worth reminding that the dispersity of the P3TBs recovered from such yttrium-promoted ROP reactions ($Đ_M$ = 1.42–1.66) is definitively larger than those observed ($Đ_M$ = 1.05–1.30) for P3HB recovered from the ROP of *rac*-β-butyrolactone under similar conditions.[17]

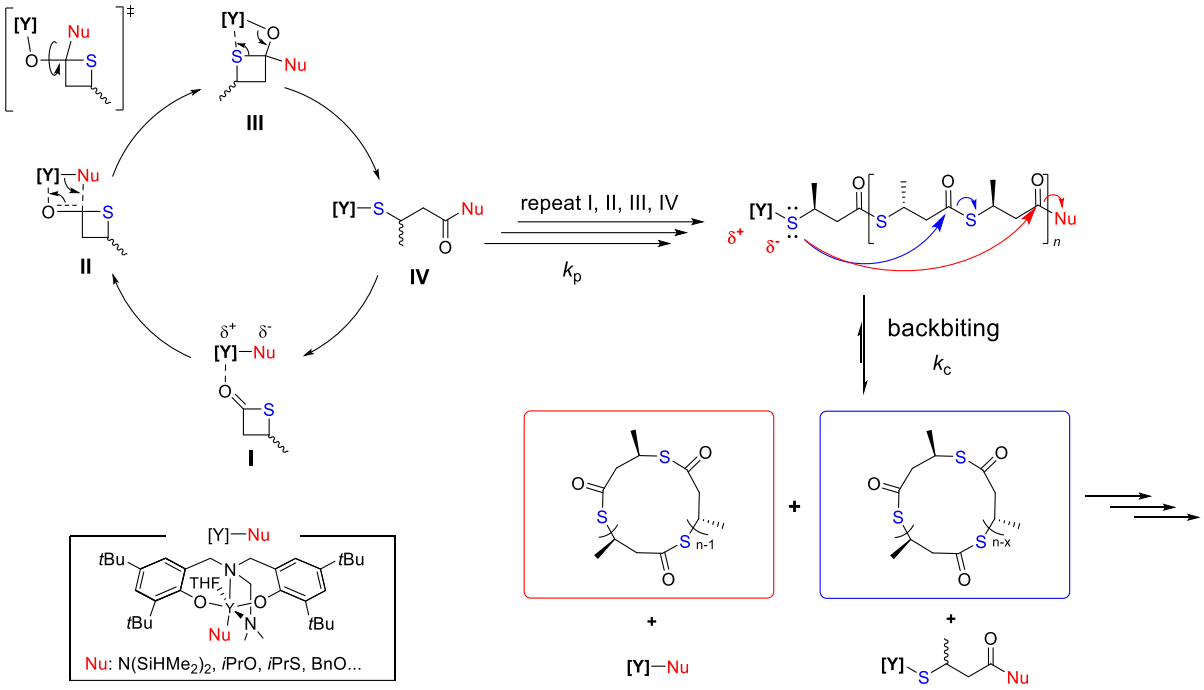

Figure 3.18. Proposed mechanism for the ROP of *rac*-TBL promoted by complex **5a** with initiation, propagation, back-biting, and ring-expansion steps.

In contrast, the anionic ROP of *rac*-TBL initiated by NaOMe, gave either linear P3TB or a mixture of cyclic and linear P3TBs (Figure 3.9, Figure 3.10, and Figure 3.11), largely depending on the reaction conditions and to some extent, the repetition of the reaction. We attributed this to the several propagating species existing in this system, that is tight ion pair, loose ion pair, and free ion pair, which coexist in equilibrium with each other (Figure 3.19).[26] The identity of ion pair largely depends on the particular reaction conditions and/or arguably the Lewis acidity of the counterion, which has large effect in ionic polymerization since different types of propagating species have different reactivities. Moreover, the higher charge density of a small counterion (*e.g.*, Na^+) results in stronger electrostatic attractive forces between the propagating center and counterion. In this regard, increase of the reaction temperature (such as 35 °C, Table 3.2, entry HL669) and change of the reaction medium, the equilibrium probably shifted towards right direction, *e.g.*, loose ion pair, or even free ion, which, led to, to some extent, back-biting reactions, giving the mixture of linear and cyclic P3TBs.

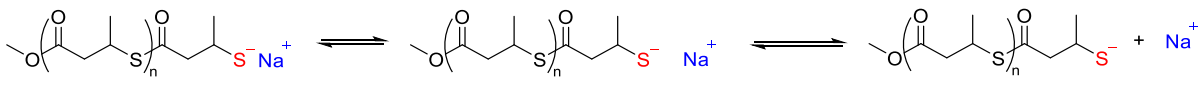

Figure 3.19. Possible propagating species exist in the NaOMe initiated *rac*-TBL system.

Another indication of easy transthioesterification is provided by the narrowing of dispersity values of P3TBs upon running the ROP of *rac*-TBL at low temperatures (typically $Đ_M = M_w/M_n$ = 1.3–1.7 at r.t. *vs.* 1.15−1.35 at $T_p \leqslant -70$ °C; *vide infra*, Table 3.3, entries HL406, HL444, HL510, HL532 and

HL581). Similar observations have been typically made in the ROP of lactones with highly reactive metal-alkoxide catalyst systems. Moreover, extending the polymerization time, the dispersities of the P3TBs obtained became broader (Table 3.2, entries HL350, HL344 *vs.* HL574), showing the pronounced transesterification side reaction over the course of polymerization.

3.5 Tacticity Control of Poly(3-Thiobutyrate)

The chemical shifts of some carbon atoms in a polymer chain are sensitive to the relative stereochemistry of nearby stereocenters, which proves to be of particular importance for investigating the microstructure of polymers.[27] The tacticity in the various isolated P3TBs can be appreciated by one-dimensional $^{13}C\{^{1}H\}$ NMR spectroscopy, which is one of the most common techniques for analyzing synthetic polymer tacticity, especially from the carbonyl and methyl regions; in fact; at 125 MHz, the methine and methylene regions do not display resolved resonances. The carbonyl region of regular P3TBs $^{13}C\{^{1}H\}$ NMR spectra (δ *ca.* 195.7 ppm) essentially features two broad, yet well-resolved resonances, the most downfield of which was assigned to a *meso* (*m*, isotactic) dyad and the most upfield one to the *racemo* (*r*, syndiotactic) dyad (Figure 3.22). In some of the $^{13}C\{^{1}H\}$ NMR spectra, four resonances can be identified in the carbonyl region, yet they cannot be deconvoluted confidently.

^{13}C projections of band selective HMBC analysis of the carbonyl region enabled to resolve the triad stereosequences of P3TB then assigned to the corresponding four triads *mm*, *rm*, *mr* and *rr*, from downfield to upfield, respectively (Figure 3.20). Deconvolution and analysis of these four resonances returned P_m/P_r values ($P_r = 1 - P_m$) fully consistent with those determined from the two *m* and *r* dyads of regular $^{13}C\{^{1}H\}$ NMR spectra and also from the triads in the methyl region (see Appendices Table S1 and Table S2, Determination of Tacticity of P3TB by Band Selective HMBC and HSQC).

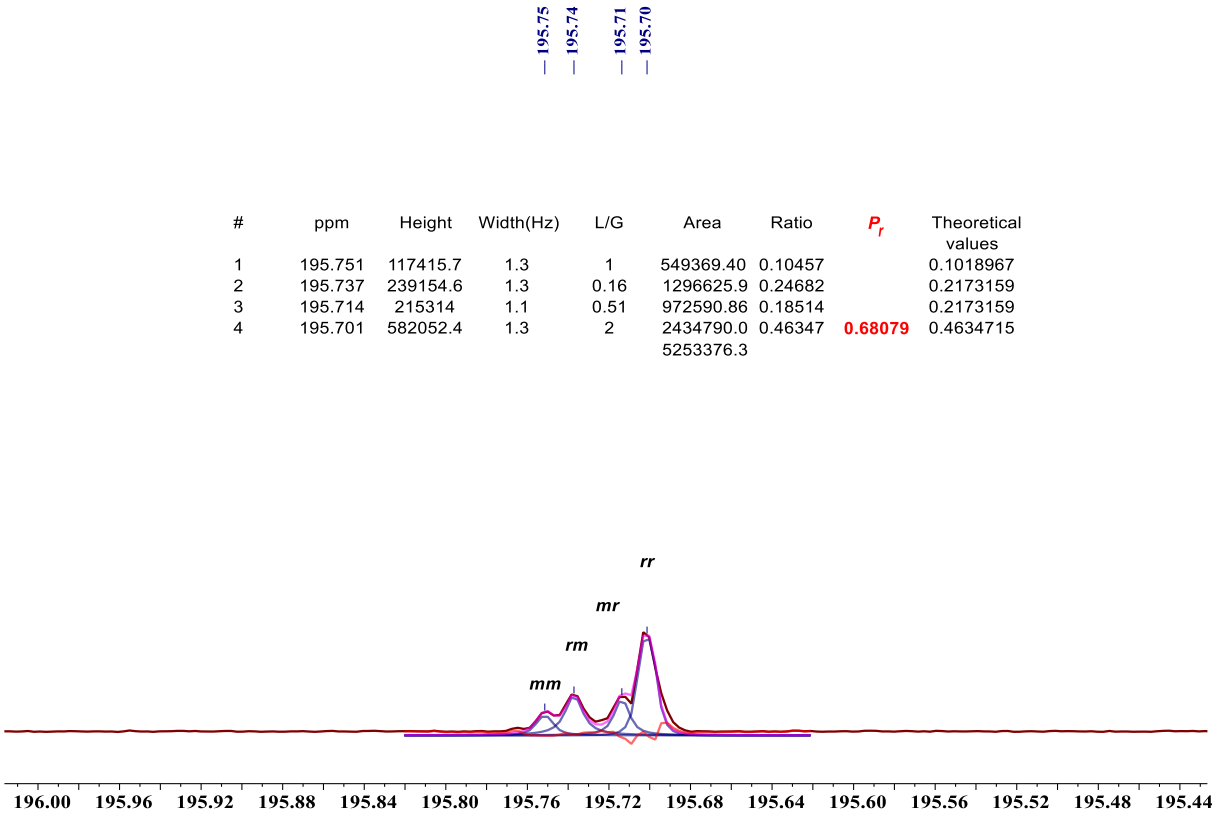

#	ppm	Height	Width(Hz)	L/G	Area	Ratio	P_r	Theoretical values
1	195.751	117415.7	1.3	1	549369.40	0.10457		0.1018967
2	195.737	239154.6	1.3	0.16	1296625.9	0.24682		0.2173159
3	195.714	215314	1.1	0.51	972590.86	0.18514		0.2173159
4	195.701	582052.4	1.3	2	2434790.0	0.46347	**0.68079**	0.4634715
					5253376.3			

Figure 3.20. ^{13}C projection extracted from band selective HMBC spectrum of a syndiotactic cyclic P3TB (Table 3.2, HL637) by summing columns between δ ^{1}H 2.60 and 3.00 ppm.

The methyl region of regular ^{13}C{^{1}H} NMR spectra (δ *ca.* 20.3- 20.5 ppm) is better resolved and shows four resonances corresponding to the triads; they actually form two (essentially non-overlapping) groups of two (partly overlapping) resonances, which are assigned, from high-to-low field, to the four triads *mm*, *rm*, *mr*, and *rr*, respectively. A similar triads distribution was also observed in the methine region (δ *ca.* 68.4- 68.8 ppm) of the parent PMLA^{R}s. Careful deconvolution of these four resonances allows extracting P_m values in good agreement with those determined from the carbonyl resonances, hence validating their assignment (Figure 3.21). Definitive confirmation of these assignments was gained from the ^{13}C NMR spectrum of a pure isotactic P3TB, independently prepared from the ROP of the enantiopure (*S*)-TBL prepared (see the experimental section, Figure 3.48).

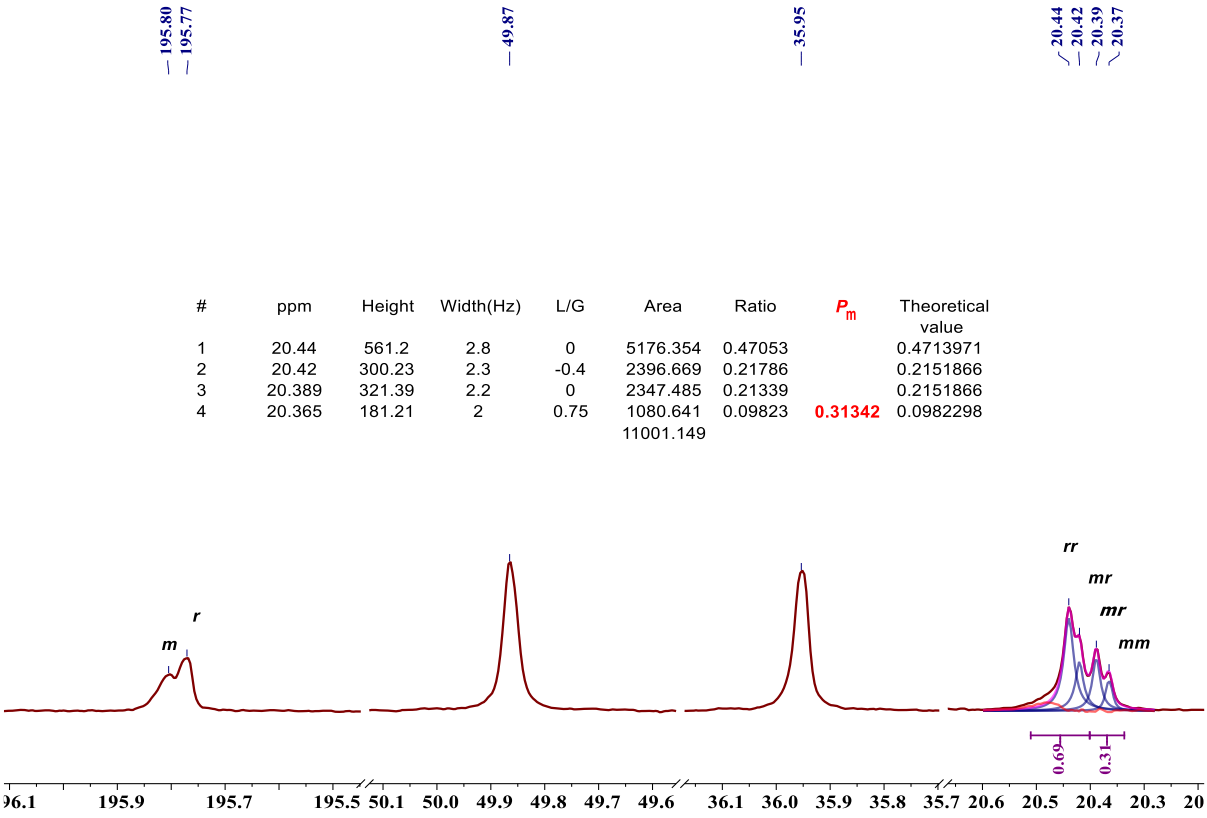

#	ppm	Height	Width(Hz)	L/G	Area	Ratio	P_m	Theoretical value
1	20.44	561.2	2.8	0	5176.354	0.47053		0.4713971
2	20.42	300.23	2.3	-0.4	2396.669	0.21786		0.2151866
3	20.389	321.39	2.2	0	2347.485	0.21339		0.2151866
4	20.365	181.21	2	0.75	1080.641	0.09823	**0.31342**	0.0982298
					11001.149			

Figure 3.21. Carbonyl, methine, methylene and methyl regions of the "regular" $^{13}C\{^1H\}$ NMR spectrum (125 MHz, $CDCl_3$, 25 °C) of a syndiotactic cyclic P3TB (Table 3.2, HL637).

Following the preliminary study of the ROP of *rac*-TBL promoted by (pre)catalyst **5a** (Table 3.2), the impact of the catalyst structure on the tacticity of P3TBs was further investigated with a set of ligands **a**-**l** well established for the stereoselective ROP of *racemic* β-lactones (*rac*-BL, *rac*-MLA^R, *rac*-BPL^{OR}),[28] *trans*-cyclohexyl-ring-fused γ-butyrolactone,[29] and *rac*-lactide.[30-32] Representative polymerization results are summarized in Table 3.3. All the yttrium catalysts, regardless of the nature of the substituents installed on the ligand, are quite active for the ROP of *rac*-TBL, thus allowing near quantitative conversion of up to 400 equiv. of *rac*-TBL within 2 min at ambient temperature. Even upon decreasing the reaction temperature down to −80 °C, the ROP reaction proceeded smoothly. This contrasts with the ROP of functional β-lactones for which a decrease of the reaction temperature makes the activity of the same catalytic system drop dramatically under similar conditions. Moreover, the molar mass measured by SEC increased monotonously with the [*rac*-TBL]$_0$/[Cat.**5c**]/[I]$_0$ feed ratio ranging from 100:1:1 to 400:1:1 (Table 3.3, entries HL382, HL398, HL457, and HL687, respectively). However, due to the occurrence of transthioesterification over the course of the polymerization, M_n values of the resulting P3TBs cannot be predicted by the feed ratio. Noteworthy is the minor influence of the solvent on the level of activity, with a little decrease observed when the polymerizations are carried out in THF instead of toluene; in many ROP of lactones, THF proved to be a deleterious solvent, likely because of concurrently coordination of the monomer onto the catalyst. As mentioned above, the use of a co-initiator, such as *i*PrOH, *i*PrSH or BnSH, does not affect the stereoselectivity of the

polymerizations; only the nature of the ligand's substituents, of course of the reaction temperature, and, in some of cases, of the solvent, drive the tacticity of the produced P3TB.

Table 3.3. Stereoselective ROP of *rac*-TBL mediated by yttrium complexes **5*a*–*k***.

Ref.	Cat.	$[M]_0/[Cat.]_0/[I]_0$[a]	Reaction temp. (°C)	Solvent	$[M]_0$ (mol/L)	Reaction time[b] (min)	Conv.[c] (%)	$M_{n,theo}$[d] (kg/mol)	$M_{n,SEC}$[e] (kg/mol)	$Đ_M$[e]	P_m[f]
HL574	***5 a***	50:1:1	r.t.	Tol	0.5	1	>99	5.1	3.8	1.42	0.34
HL345	***5 a***	100:1:1	r.t.	Tol	0.65	6	99	10.2	18.7	1.43	0.38
HL436	***5 a***	100:1:1	-70	Tol	0.5	10	90	9.0	40.7	1.40	0.42
HL444	***5 a***	100:1:1	-70	Tol	0.5	16	99	10.2	46.5	1.14	0.42
HL527	***5 a***	25:1:1	r.t.	Me-THF	0.5	2	93	2.4	13.3	1.20	0.46
HL528	***5 a***	50:1:1	r.t.	Me-THF	0.5	2	91	4.6	16.5	1.11	0.43
HL529	***5 a***	100:1:1	r.t.	Me-THF	0.5	2	92	9.2	13.4	1.20	0.48
HL379	***5 b***	100:1:1	r.t.	Tol	1	1	99	10.2	7.6	1.39	0.48
HL338	***5 c***	50:1:0	r.t.	Tol	0.5	5	99	5.1	4.9	1.47	0.38
HL412	***5 c***	100:1:0	r.t.	Tol	1	1	99	10.2	42.7	1.68	0.32
HL382	***5 c***	100:1:0	r.t.	Tol	1	1.5	99	10.2	7.6	1.53	0.39
HL398	***5 c***	150:1:1	r.t.	Tol	1	2	99	15.4	25.0	1.58	0.35
HL457	***5 c***	200:1:1	r.t.	Tol	1	1	99	20.4	30.2	1.59	0.35
HL687	***5 c***	400:1:1	r.t.	Tol	1	2	99	40.8	59.2	1.68	0.34
HL397	***5 c***	100:1:1	-50	Tol	0.5	15	98	10.0	31.9	1.50	0.30
HL416	***5 c***	100:1:1	-70	Tol	0.5	30	50	5.1	21.9	1.37	0.32
HL501	***5 d***	50:1:1	r.t.	Tol	0.5	1	99	5.1	8.0	1.62	0.47
HL353	***5 d***	100:1:1	r.t.	Tol	0.65	5	99	10.2	7.2	1.42	0.52
HL547	***5 e***	50:1:1	r.t.	Tol	0.5	1	99	5.1	21.4	1.31	0.41
HL538	***5 f***	50:1:1	r.t.	Tol	0.5	2	99	5.1	13.3	1.67	0.52
HL358	***5 g***	75:1:1	r.t.	Tol	0.5	2	99	7.6	6.8	1.42	0.58
HL399	***5 g***	100:1:1	-70	Tol	0.5	2	69	7.2	24.3	1.22	0.73
HL583	***5 g***	50:1:0	r.t.	THF	0.5	1	99	5.1	4.9	1.80	0.53
HL584	***5 g***	50:1:0	-50	THF	0.5	40	99	5.1	43.4	1.62	0.63
HL406	***5 g***	100:1:0	-70	THF	0.5	11	50	5.1	23.0	1.28	0.87
HL510	***5 g***	50:1:0	-80	THF	0.5	45	83	4.2	21.4	1.22	0.89
HL364	***5 h***	100:1:1	r.t.	Tol	1	5	99	10.2	2.5	1.24	0.54
HL454	***5 h***	100:1:1	r.t.	Tol	1	5	99	10.2	32.5	1.59	0.57
HL552	***5 h***	50:1:1	r.t.	THF	0.5	1	99	5.1	3.2	1.28	0.55

HL566	***5 h***	50:1:1	-20	THF	0.5	60	99	5.1	4.2	1.48	0.65
HL561	***5 h***	50:1:1	-50	THF	0.5	450	26	1.3	n.d.	n.d.	0.73
HL600	***5 i***	100:1:1	r.t.	Tol	1	1	41	4.1	1.9	1.21	0.54
HL546	***5 i***	50:1:1	r.t.	THF	0.5	1	99	5.1	14.5	1.48	0.57
HL558	***5 i***	50:1:1	r.t.	THF	0.5	1	99	5.1	4.6	1.47	0.63
HL587	***5 i***	50:1:0	r.t.	THF	0.5	1	99	5.1	4.8	1.61	0.58
HL589	***5 i***	50:1:0	-80	THF	0.5	95	99	5.1	5.9	1.79	0.69
HL541	***5 j***	50:1:1	r.t.	THF	0.5	1	99	5.1	10.8	1.22	0.54
HL588	***5 j***	50:1:0	r.t.	THF	0.5	1	99	5.1	4.5	1.42	0.58
HL590	***5 j***	50:1:0	-50	THF	0.5	60	99	5.1	5.9	1.65	0.75
HL593	***5 k***	50:1:0	r.t.	Tol	0.5	1	99	5.1	4.2	1.48	0.55
HL360	***5 k***	75:1:1	r.t.	Tol	0.65	1	99	7.6	5.3	1.17	0.57
HL361	***5 k***	75:1:1	r.t.	Tol	0.65	1	97	7.2	5.3	1.19	0.57
HL400	***5 k***	100:1:0	r.t.	Tol	0.5	2	99	10.2	22.5	1.55	0.51
HL591	***5 k***	50:1:0	r.t.	THF	0.5	1	99	5.1	4.8	1.53	0.57
HL592	***5 k***	50:1:0	-50	THF	0.5	34	99	5.1	5.2	1.37	0.72
HL532	***5 k***	50:1:0	-80	THF	0.5	45	76	3.9	25.0	1.28	0.90
HL420	***5 l***	50:1:1	r.t.	Tol	1	1	88	9.0	18.2	1.83	0.58
HL581	***5 l***	50:1:1	-80	Tol	0.5	30	90	4.6	5.1	1.21	0.83
HL586	***5 l***	50:1:0	-80	Tol	0.5	40	99	5.1	3.4	1.38	0.75
HL585	***5 l***	50:1:0	-80	THF	0.5	40	29	1.5	6.3	1.33	0.63

[a] co-initiator = *i*PrOH; [b] the reaction times were not necessarily optimized; [c] conversion of *rac*-TBL as determined by ^{1}H NMR analysis of the crude polymerization mixture (refer to the ESI); [d] molar mass calculated according to $M_{n,theo} = [TBL]_0/[I]_0 \times Conv._{TBL} \times M_{TBL}$; [e] number-average molar mass ($M_{n,SEC}$) and dispersity ($Đ_M$) as determined by SEC analysis in THF at 30 °C *vs.* polystyrene standards (uncorrected values); [f] P_m is the probability of *meso* enchainment between TBL units as determined by ^{13}C{^{1}H} NMR analysis of the isolated P3TBs.

As expected from previous works on the ROP of *rac*-BL and related functional β-lactones, the catalyst systems based on complexes **5a** and **5c** with bulky R^1 substituents (*t*Bu or cumyl groups) installed on the *ortho*-positions of the phenolate rings generated syndiotactic-biased P3TBs ($P_m \approx$ 0.32- 0.38) from the ROP of *rac*-TBL performed at ambient temperature in toluene. Decreasing the temperature down to –70 °C did not improve the syndioselectivity. Surprisingly enough, installation of a very bulky R^1 trityl substituent (−CPh$_3$), such as in **5l**, reversed the trend, as the resulting P3TB produced in toluene at ambient temperature featured a slight isotactic bias (P_m = 0.58, Table 3.3, entry HL420); the isoselectivity of this latter system improved significantly upon lowering the temperature down to –80 °C (P_m = 0.83, Table 3.3, entry HL581).

On the other hand, significant differences were observed depending on the nature of the X donor group in the "capping" moiety of the $\{ONXO^{R2}\}^{2-}$ ligand (X = CH_2OMe, CH_2NMe_2, CH_2NEt_2, 2-pyridyl). This pendant group X in the side arm of the ligand may affect the catalyst's electronics and/or sterics, and thus the catalytic activity and stereoselectivity in ROP reactions. In the ROP of *rac*-TBL, changing the side arm donor from β−NMe_2 in **5a** or **5c** to β−OMe as in **5b** or **5d**, respectively, reduced drastically the catalyst syndioselectivity and returned atactic P3TBs (P_m = 0.38, 0.32 *vs.* 0.48, 0.52, Table 3.3, entries HL345, 412 *vs.* HL379 and HL353, respectively). The β−NEt_2 system **5e** performed similarly to the β−NMe_2 system **5b**, in contrast to the pyridyl one (**5f**) which also produced atactic P3TB under these same conditions (Table 3.3, entries HL547, HL379, HL538).

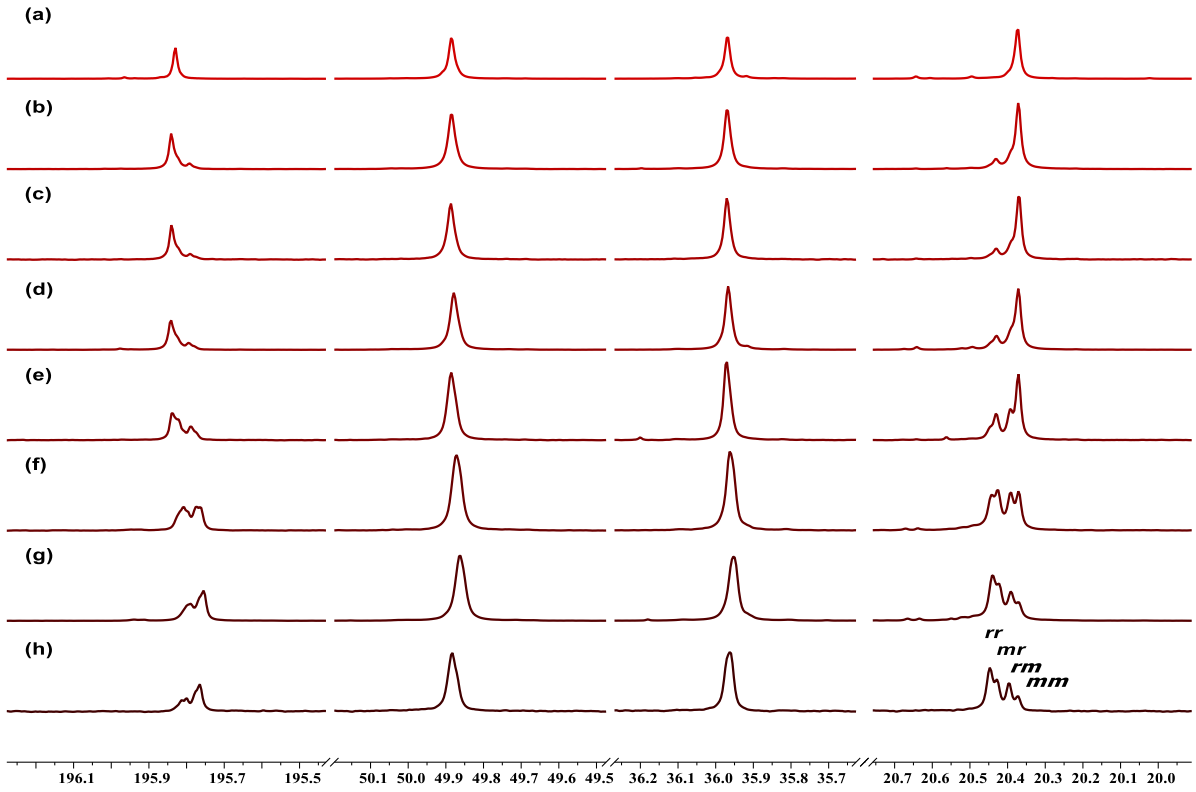

Figure 3.22. Carbonyl, methine, methylene and methyl regions of the $^{13}C\{^1H\}$ NMR spectra (125 MHz, $CDCl_3$, 25 °C) of: a) a highly isotactic P3TB (P_m > 0.95, M_n = 3.2 kg mol^{-1}, $Đ_M$ = 1.52) prepared from the ROP of enantiopure (*S*)-TBL (with the **5a**/*i*PrOH (1:1) system); and isotactic-, syndiotactic-enriched P3TBs prepared from the ROP of *rac*-TBL mediated by: b) complex **5k** ($[TBL]_0/[\mathbf{5}]/[co\text{-}init.]$ = 50:1:0, –80 °C, THF, P_m = 0.90, Table 3.3, entry HL532); c) complex **5g** (50:1:0, –80 °C, THF, P_m = 0.89, Table 3.3, entry HL510); d) system **5l**/*i*PrOH (50:1:1, −80 °C, toluene, P_m = 0.83, Table 3.3, entry HL 581); e) system **5g**/^{i}PrOH (100:1:1, −70 °C, toluene, P_m = 0.73, Table 3.3, entry HL399); f) system **5d**/*i*PrOH (100:1:1, r.t., toluene, P_m = 0.51, Table 3.3, entry HL353); g) system **5a**/*i*PrOH (50:1:1, r.t., toluene, P_m = 0.34, Table 3.3, entry HL574); h) system **5c**/*i*PrOH (100:1:1, −50 °C, toluene, P_m = 0.30, Table 3.3, entry HL397).

Also unexpected and to our knowledge unprecedented in the field of ROP of lactones, yttrium complexes bearing non-bulky substituents, namely the *o*,*p*-dimethyl-substituted systems **5g**−**5j** gave isotactic-enriched P3TBs. At ambient temperature in toluene or THF, these catalysts are highly active

for the ROP of *rac*-TBL, however with only a mild preference for isoselectivity (P_m = 0.53–0.58). Upon lowering the polymerization temperature down to - 70 or - 80 °C, isotacticity increased in toluene (P_m = 0.73, Table 3.3, entry HL399), and improved even more significantly in THF (P_m up to 0.89; Table 3.3, entry HL510). Also, the X capping moiety affected the performance in this series of *o,p*-dimethyl-substituted catalysts and the best isotacticity was again observed with the NMe_2-capped complex **5g**. The *o,p*-dichloro-substituted complex **5k** had the same behavior as its dimethyl-substituted analogue **5g** (P_m up to 0.90 in THF at - 80 °C; Table 3.3, entry HL532); this suggests that, in the ROP of *rac*-TBL, methyl and chloro substituents apparently similarly behave as a non-bulky group (and without electronic contribution for Cl); this is reminiscent of the results obtained in the ROP of *rac*-β-malolactonates, which yet offered syndiotactic $PMLA^R$s in contrast to the present isotactic P3TBs. The high activity of the *o,p*-dichloro-substituted system **5k**, even at low temperature (TOF > 3,000 h^{-1} at r.t. and 88 h^{-1} at –50 °C), is also noteworthy, as it contrasts strikingly with the ROP of *rac*-BL where only alkyl/aryl-substituted complexes are highly active, while "Y{$ONOO^{Cl2}$}" catalysts proved poorly active (TOF = 12 h^{-1} at r.t.). This further testifies of the high intrinsic reactivity of *rac*-TBL, and its singular behavior as compared to parent β-lactones.

Table 3.4. Influence of the solvent on the stereoselective ROP of *rac*-TBL promoted by complex **5k** without a co-initiator.[a]

Ref.	[TBL]/[**5k**]	Solvent	Dielectric constant	$[TBL]_0$ mol/L	Reaction time (min)[b]	*Conv.* (%)[c]	$M_{n,theo}$ (kg/mol)[d]	$M_{n,SEC}$ (kg/mol)[d]	$Đ_M$[e]	P_m[f]
HL582	100:1	*n*-Hexane	1.89	0.2	1	67	10.2	5.5	1.46	0.53
HL579	100:1	1.4-Dioxane	2.21	0.5	1	>99	10.2	5.3	1.61	0.50
HL575	100:1	Toluene	2.38	0.5	1	93	9.4	4.3	1.41	0.55
HL577	100:1	Me-THF	6.75	0.5	1	>99	10.2	4.9	1.55	0.53
HL576	100:1	THF	7.52	0.5	1	68	7.0	4.4	1.42	0.57
HL578	100:1	DCM	9.0	0.5	1	>99	10.2	4.4	1.34	0.53
HL659	100:1	Acetonitrile	36.64	0.5	1	21	2.1	*n.d.*	*n.d.*	*n.d.*

[a] Polymerizations performed at ambient temperature (15–20 °C); [b] the reaction times were not necessarily optimized; [c] conversion of *rac*-TBL as determined by ^1H NMR analysis of the crude polymerization mixture; [d] molar mass calculated according to $M_{n,theo} = [TBL]_0/[Cat.]_0 \times Conv._{TBL} \times M_{TBL}$; [e] number-average molar mass ($M_{n,SEC}$) and dispersity ($Đ_M$) of isolated P3TBs as determined by SEC analysis in THF at 30 °C *vs.* polystyrene standards (uncorrected values); [f] P_m is the probability of *meso* enchainment between TBL units as determined by $^{13}C\{^1H\}$ NMR analysis of isolated P3TBs.

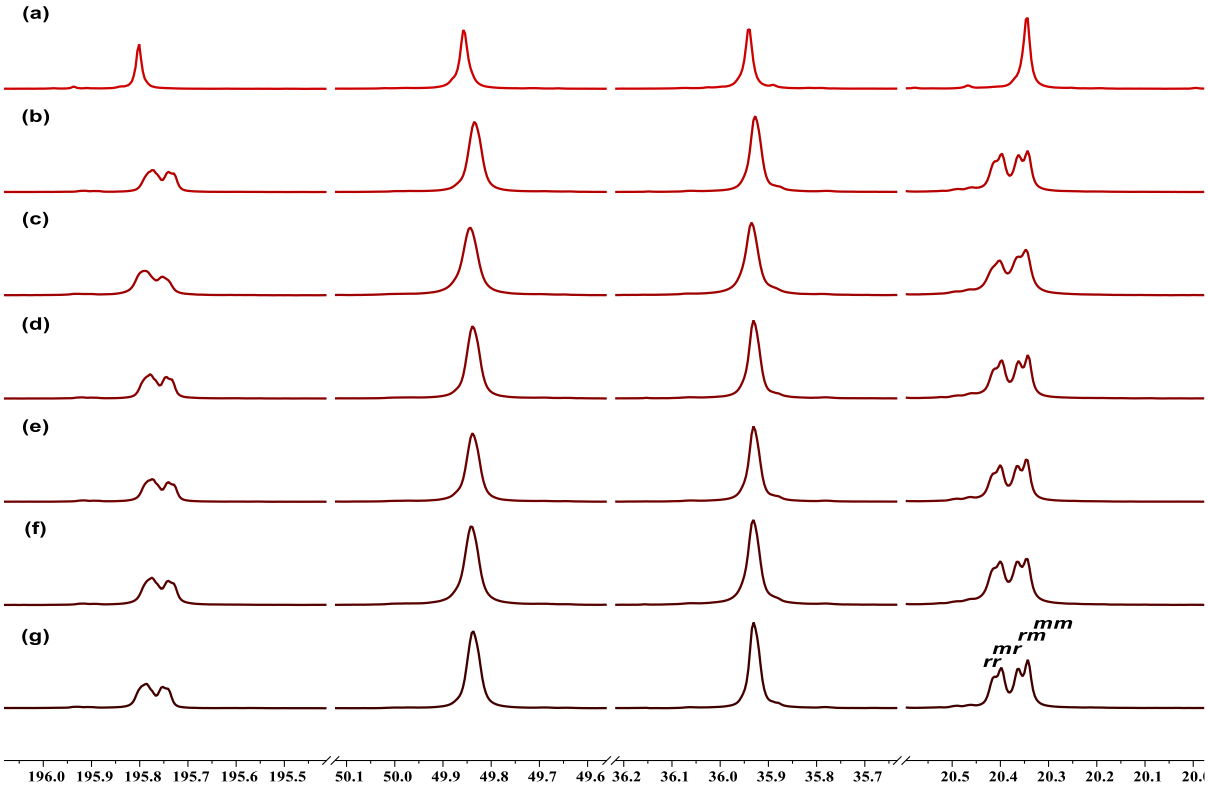

Figure 3.23. Carbonyl, methine, methylene and methyl regions of the $^{13}C\{^{1}H\}$ NMR spectra (125 MHz, $CDCl_3$, 20 °C) of isolated cyclic P3TBs produced in different solvents by the system **5k** (Table 3.4): a) a highly isotactic P3TB ($P_m > 0.95$, $M_n = 3.2$ kg mol^{-1}, $Đ_M = 1.52$) prepared from the ROP of enantiopure (*S*)-TBL; b) dichloromethane, $P_m = 0.53$; c) THF, $P_m = 0.57$; d) Me-THF, $P_m = 0.53$; e) toluene, $P_m = 0.55$; f) 1,4-dioxane, $P_m = 0.50$; g) *n*-hexane, $P_m = 0.53$.

The aforementioned positive influence of THF on the isoselective ROP of *rac*-TBL mediated by **5g** and **5k** prompted us to explore in a more systematic manner the influence of the solvent. A variety of solvents from low to high polarity (*n*-hexane, 1.4-dioxane, toluene, 2-MeTHF, THF, dichloromethane, acetonitrile) was investigated using both the isoselective catalyst **5k** (Table 3.4) and the syndioselective catalyst **5c** (Table 3.5). Yet, at ambient temperature, no significant difference and further possible improvements of stereoselectivity were noted. Only THF seemed to have a differentiated behavior, making non-stereoselective the catalyst **5c** otherwise syndioselective in other solvents (Figure 3.24 and Figure 3.23). We speculate this may be due to the aforementioned THF coordination (in apparent contrast to the more sterically crowded 2-MeTHF) onto the active site of the propagating species. This is in agreement with our previous observations with *rac*-lactide, in view of the high heteroselectivity displayed by the yttrium initiators in THF, whereas propagating species in toluene generate nearly atactic materials.[32]

Table 3.5. Influence of the solvent on the stereoselective ROP of *rac*-TBL promoted by complex **5c** /*i*PrOH.[a]

Ref.	[TBL]/[**5c**] /[I]	Solvent	Dielectric constant	$[TBL]_0$ mol/L	Reaction time (min)[b]	*Conv.* (%)[c]	$M_{n,theo}$ (kg/mol)[d]	$M_{n,SEC}$ (kg/mol)[d]	$Đ_M$[e]	P_m[f]
HL425	100:1:1	*n*-Hexane	1.89	0.2	1	>99	10.2	21.9	1.37	0.37
HL422	100:1:1	1.4-Dioxane	2.21	1	1	>99	10.2	19.0	1.16	0.39
HL346	100:1:1	Toluene	2.38	1	1	>99	10.2	13.8	1.19	0.38
HL502	100:1:1	2-MeTHF	6.75	1	1	>99	10.2	10.3	1.10	0.35
HL375	100:1:1	THF	7.52	1	2	>99	10.2	6.7	1.26	0.58
HL417	100:1:1	DCM	9.0	1	1	>99	10.2	35.0	1.48	0.35
HL433	100:1:1	Acetonitrile	36.64	1	2	>99	10.2	28.9	1.52	0.34

[a] Polymerizations performed at ambient temperature (15–20 °C); [b] the reaction times were not necessarily optimized; [c] conversion of *rac*-TBL as determined by ^{1}H NMR analysis of the crude polymerization mixture; [d] molar mass calculated according to $M_{n,theo} = [TBL]_0/[Cat.]_0 \times Conv._{TBL} \times M_{TBL}$; [e] number-average molar mass ($M_{n,SEC}$) and dispersity ($Đ_M$) of isolated P3TBs as determined by SEC analysis in THF at 30 °C *vs.* polystyrene standards (uncorrected values); [f] P_m is the probability of *meso* enchainment between TBL units as determined by $^{13}C\{^1H\}$ NMR analysis of isolated P3TBs.

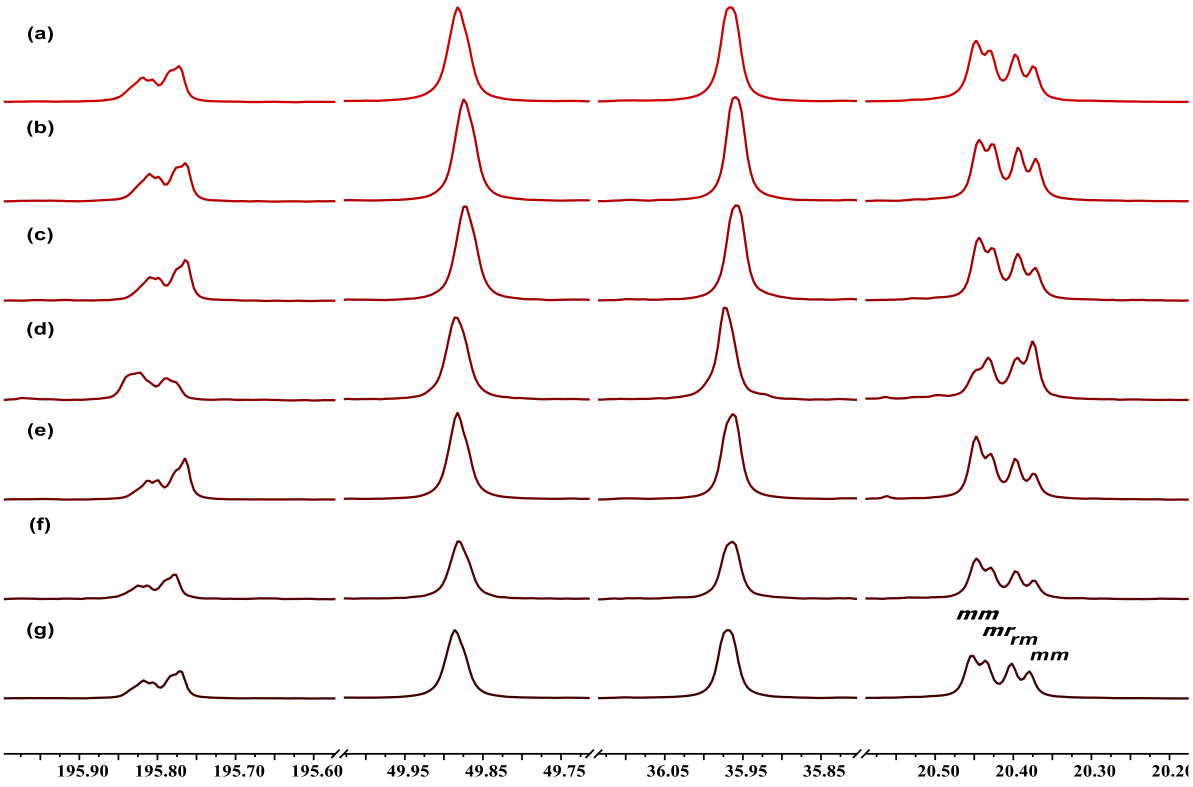

Figure 3.24. Carbonyl, methine, methylene and methyl regions of the $^{13}C\{^1H\}$ NMR spectra (125 MHz, $CDCl_3$, 25 °C) of isolated cyclic P3TBs produced in different solvents by the system **5c**/*i*PrOH (1:1) (Table 3.5): a) acetonitrile, P_m = 0.34; b) 1,4-dioxane, P_m = 0.39; c) Me-THF, P_m = 0.35; d) THF, P_m = 0.58; e) dichloromethane, P_m = 0.35; f) toluene, P_m = 0.38; g) *n*-hexane, P_m = 0.37.

The polymer stereosequence distributions obtained by NMR analysis are often analyzed by statistical propagation models to gain insight into the propagation mechanism. Propagation models exist for both catalyst site control and polymer chain-end control. The *Bernoullian* model (also referred to as the *zero-order Markov* model; only the last monomer unit in the propagating chain-end is important in determining polymer stereochemistry) and the *first-order Markov* model (the penultimate unit is important in determining subsequent stereochemistry) describe polymerization where stereochemistry is determined by polymer chain-end control; a more sophisticated *second-order Markov* model will not be discussed herein. The Bernoullian model requires *triad* data as a minimum for testing, while the first-order Markov model requires *tetrad* data. In the case of P3TB, only triad data are available for testing.

Analysis of the triad stereosequence distribution in both syndio- and iso-enriched P3TBs evidenced that it agrees well with Bernoullian statistics for a chain-end stereocontrol. In fact, the Bernoulli model triad test, B = (*mm*)(*rr*)/(*rm*)(*mr*), returned values very close to 1, usually in the range 0.8–1.35 (see Appendices Table S3, Propagation Statistics), which falls within an acceptable range due to errors in deconvoluting the four respective triad signals. This indicates that, in agreement with the achiral nature of these yttrium catalysts, the stereocontrol in this *rac*-TBL ROP process is a consequence of either (1) interactions between the last two TBL units in the P3TB chain (penultimate control) or (2) interactions between the last TBL unit in the chain and the next incoming monomer (ultimate control).

3.6 Thermal Signature of Poly(3-Thiobutyrate)s

Preliminary studies were conducted to determine the thermal behavior of P3TBs by thermal gravimetric analysis (TGA) and differential scanning calorimetry (DSC). Typical TGA curves of P3TB samples are shown in Figure 3.25 and Figure 3.26. A cyclic atactic P3TB produced by complex **5a** features a degradation temperature (T_d, defined as the temperature for 5% weight loss) of *ca.* 198 °C, which is 12 °C higher than the corresponding value for a linear (as assessed by MALDI-ToF MS; see Figure 3.10) atactic P3TB produced with NaOMe system with a comparable molar mass (M_n = 3.9 kg mol^{-1}) (Figure 3.25a). Also, the degradation extent at higher temperature is significantly more pronounced on the linear than on the cyclic polymer (*e.g.*, at 300 °C, 83.5% vs. 66% weight loss). This higher thermal stability can be accounted for by the extra energy needed to break cyclic polymers as compared to linear ones, as reported recently for other polyesters.[33-35] This behaviour is believed to primarily be a consequence of the fact that the first bond broken does not change the molar mass, but changes only the topology from cyclic to linear.[33]

A noticeable enhancement of the degradation temperature of cyclic P3TBs from T_d = 195 to 230 °C was observed when the monomer-to-initiator ratio increased from 50:1 to 150:1, thus presumably with a P3TB of higher molar mass (Figure 3.25b). On the other hand, the stereochemistry of cyclic P3TBs with similar molar mass, with P_m varying in the range 0.35 to 0.90, had a negligible influence on the thermal stability (Figure 3.26). This is in line with the weak tacticity effect noted on the thermal stability

of syndio- and isotactic polystyrenes,[36] but contrasts with previous studies on hetero-, syndio- and isotactic PLAs where $T_{d\,(5\%)}$ values spanned over a rather broad range (258–323 °C).[37]

Overall, this provides a valuable thermal processing window of more than 80 °C for highly stereoregular P3TBs (above the T_m (*vide infra*) and below the T_d), while the melting temperature of *i*-P3HB is very close to its decomposition temperature.

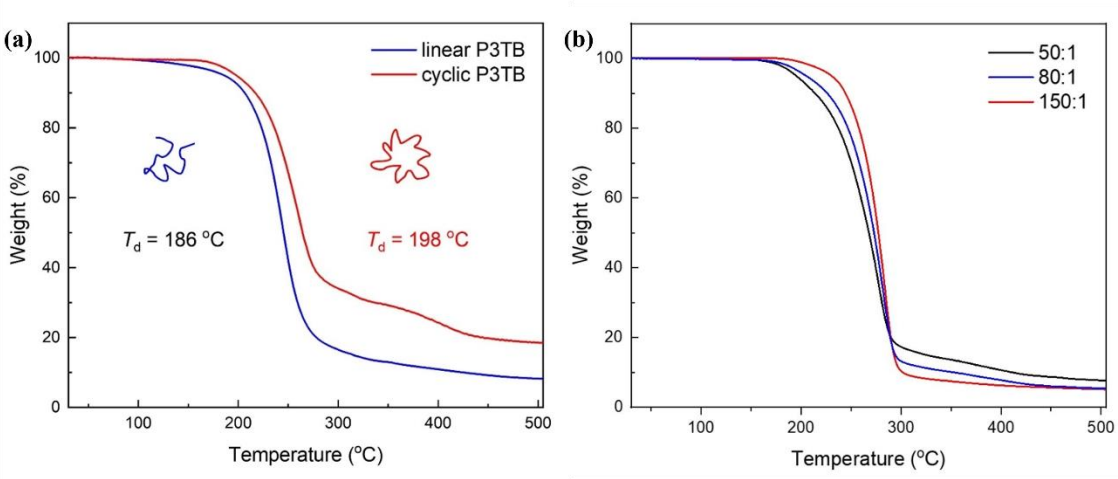

Figure 3.25. (a) TGA thermograms of P3TBs with different topologies: an essentially linear P3TB produced from NaOMe (blue line, $M_{n,SEC}$ = 3.9 kg mol^{-1} P_m = 0.50, Table 3.2, entry HL506) and a cyclic P3TB produced from complex **5a** (red line, $M_{n,SEC}$ = 4.9 kg mol^{-1}, P_m = 0.37, Table 3.2, HL337); (b) TGA thermograms of P3TBs produced from complex **5a** in toluene at room temperature as a function of the monomer-to-initiator ratio (T_d = 195 °C (50:1, P_m = 0.32; Table 3.2, entry HL350), 205 °C (80:1, P_m = 0.34; entry HL614), 230 °C (150:1, P_m = 0.35; Table 3.3, entry HL398). Heating rate = 10 °C min^{-1} in both cases.

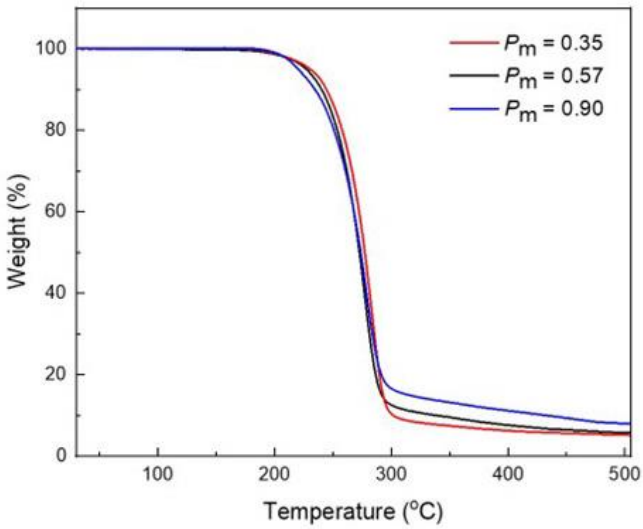

Figure 3.26. TGA thermogram of syndiotactic, atactic, isotactic cyclic P3TB samples with different stereoregularity but comparable molar mass (Table 3.3, entries HL398, HL454, and HL532). Heating rate = 10 °C min^{-1}.

The DSC curve of a cyclic isotactic P3TB sample (M_n = 25.0 kg mol^{-1}, P_m = 0.90; Table 3.3, entry HL532) features a glass-transition temperature (T_g) of 4 °C (Figure 3.27), which is 4 °C lower than that

reported for microbial P3TB (T_g = 8 °C) and is higher than that of oxo analogue (T_g = 4 °C).[2] In addition, a single exothermic transition with a crystallization temperature (T_c) of 95 °C and a single endothermic transition with a melting-transition temperature (T_m) of 101 °C are observed. The latter T_m value is very close to that reported for P3TB prepared with *E. coli* (T_m = 100 °C),[2] indirectly corroborating that the latter material is indeed also highly (purely) isotactic. The semi-crystalline isotactic P3TB produced by ROP of *rac*-TBL has a notably lower T_m than isotactic P3HB (T_m *ca.* 170 °C),[2] highlighting that the introduction of the sulfur atom into the backbone of P3HB significantly impacts chain folding and packing into the crystal lattice.

On the other hand, the perfectly isotactic P3TB (prepared by ROP of enantiopure TBL, P_m > 0.95) displayed an endothermic peak at T_m = 102 °C (ΔH = 33.8 J g^{-1}, Figure 3.28) on the DSC first heating scan; however, it showed no crystallization temperature (T_c) or T_m even upon cooling followed by a second heating rates at 5 °C min^{-1}, similar to perfectly isotactic poly(3-hydroxy-4-phenylbutyrate).[38] This suggests that perfectly P3TB could be crystalline but with a very slow crystallization rate. It is reported that the polythioester family displays a much lower crystallizability than the PHA family.[2] When sulfur replaces oxygen atom in the chain backbone, the material's crystallization may be hindered, as the Pauling electronegativity of sulfur (2.58), which is the same as that of carbon (2.55), is much lower than that of oxygen (3.44). In the case of PHAs, dipolar interactions associated to ester dipoles play a crucial role in stabilizing its helical conformation, while polythioesters probably lack this same stabilizing influence.

P3TBs with lower isotacticity (P_m < 0.73), as well as atactic and syndiotactic (P_r up to 0.70) ones, do not feature semi-crystallinity, as revealed by DSC. On the other hand, the stereoregularity of cyclic P3TB has a negligible influence on their T_g values.

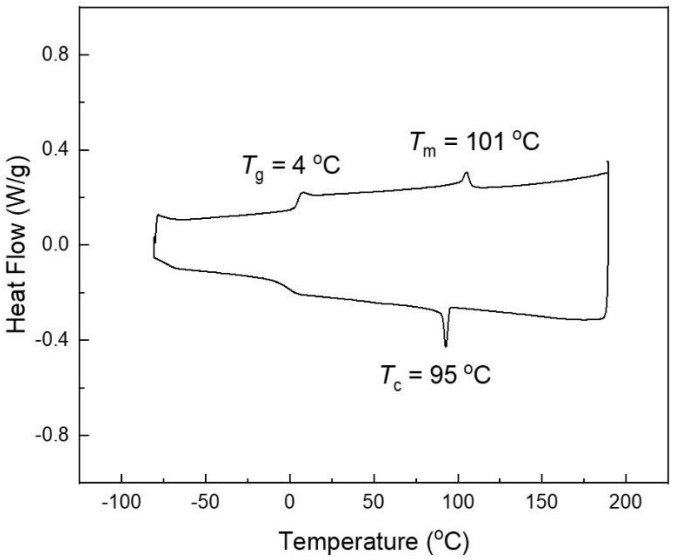

Figure 3.27. DSC curve of a highly isotactic P3TB produced from complex **5k** in toluene at room temperature (P_m = 0.90, Table 3.3, entry HL532) (heating rate = 10 °C min^{-1}, cooling rate = 5 °C min^{-1}).

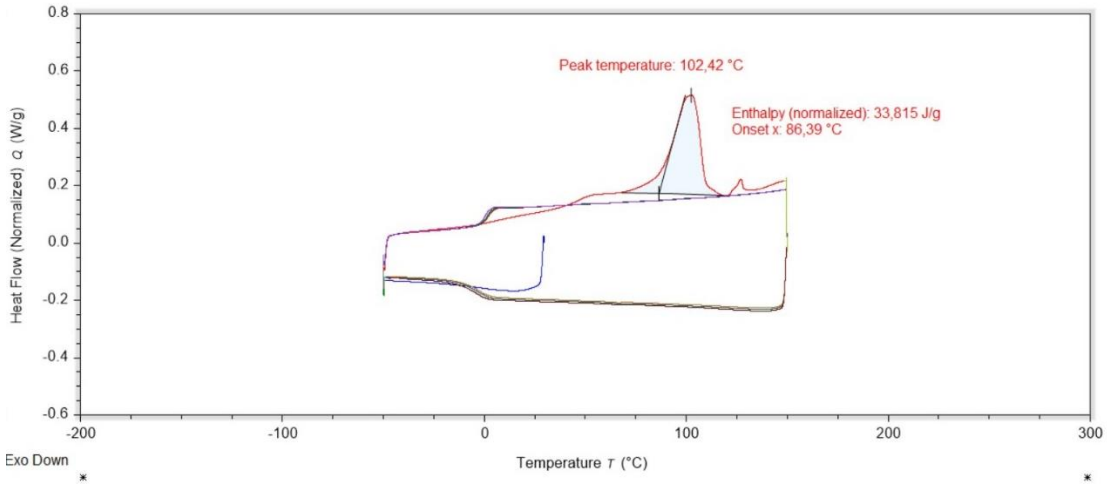

Figure 3.28. DSC curve of a perfectly isotactic P3TB produced from complex **5a** in toluene at room temperature (P_m > 0.95) (heating rate = 10 °C min^{-1}, cooling rate = 5 °C min^{-1}).

3.7 Attempts at Ring-Opening Copolymerization (ROCOP) of *rac*-β-Butyrolactone (*rac*-BL) and *rac*-β-Thiobutyrolactone (*rac*-TBL)

Isotactic poly(3HB-*co*-3TB) is an attractive class of microbial copolymer, for the melting point of poly(3HB-*co*-3TB) is much higher (T_m = 225 °C when the content of 3TB is 61%) than those of the corresponding homopolymers (175 °C for P3HB and 100 °C for P3TB), as reported by Steinbuchel and coworkers.[39] X-ray diffraction and ^{13}C cross-polarization/magic angle spinning NMR spectroscopic

analysis revealed that a separate crystalline phase in the solid state is formed. However, when the content of 3TB increased to 72.2%, the copolymer is completely amorphous.

The random ROCOP of *rac*-TBL and *rac*-BL was initially attempted with the cumyl-substituted yttrium complex "Y{ONNO^{cumyl2}}(N(SiHMe$_2$)$_2$)(THF)" in the presence of one equivalent of *i*PrOH in toluene at room temperature (Figure 3.29). These conditions were selected based on our previous work on both the ROP of *rac*-BL and *rac*-TBL.[1] The catalytic system was very active, allowing complete consumption of both monomers within less than 1 min at a [*rac*-BL]$_0$/[*rac*-TBL]$_0$/[Y]$_0$/[*i*PrOH]$_0$ feed ratio of 50:50:1:1 (Table 3.6, entry HL376); this is in line with the high activities observed in homopolymerization of *rac*-TBL and *rac*-BL. Due to the high activity of both monomers toward this catalytic system, detailed kinetic monitoring of the reaction was precluded at this stage.

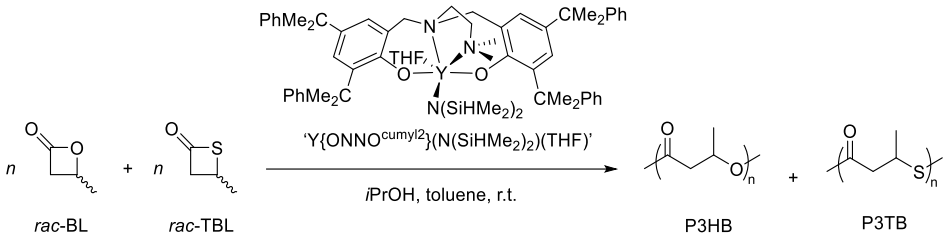

Figure 3.29. Attempted ROCOP of *rac*-TBL and *rac*-BL promoted by an yttrium complex.

Table 3.6. Preliminary attempts of random and sequential ROCOP of *rac*-BL and *rac*-TBL by yttrium complex.[a]

Entry	[BL]$_0$/[TBL]$_0$ /[Y]$_0$/[*i*PrOH]	Time (s)[b]	Conv.$_{BL}$ (%)[c]	Conv.$_{TBL}$ (%)[c]	$M_{n,theo}$[d] kg mol^{-1}	$M_{n,SEC}$[e] kg mol^{-1}	$Đ_M$[e]	P_r[f]
HL376[h]	50:50:1:1	60	>99	>99	9.4	*n.s.*[g]	*n.s.*[g]	0.85/0.60
HL679[h]	25:25:1:1	30	>99	>99	4.7	*n.s.*	*n.s.*	0.84/0.61
HL676[i]	25:25:1:1	30+30	>99	>99	4.7	*n.s.*	*n.s.*	0.89/0.59

[a] Polymerization conditions: [M]$_0$ = 1 M, toluene as solvent, at room temperature; [b] reaction time was not optimized; [c] the conversions of *rac*-TBL and *rac*-BL were calculated from ^{1}H NMR spectrum; [d] molar mass calculated according to $M_{n,theo}$ = [TBL]$_0$/[Y]$_0$ × *Conv.*$_{TBL}$ × M_{TBL} + [BL]$_0$/[Y]$_0$ × *Conv.*$_{TB}$ × M_{BL} + M_{iPrOH}; [e] number-average molar mass ($M_{n,SEC}$) and dispersity ($Đ_M$) determined by SEC analysis in THF at 30 °C *vs.* polystyrene standards (uncorrected values); [f] P_r is the probability of *racemic* enchainment between BL/TBL units as determined by ^{13}C{^{1}H} NMR analysis of the isolated polymer; [g] not soluble (*n.s.*) in THF; [h] random copolymerization; [i] sequential addition (TBL was added in the second loading).

Since *rac*-TBL is a far more reactive monomer than *rac*-BL with the present yttrium catalysts, one might expect to observe the rapid consumption of *rac*-TBL initially in the random ROCOP of *rac*-BL and *rac*-BL, followed by a slow consumption of *rac*-BL, affording a copolymer with a blocky microstructure. To verify this hypothesis, the isolated polymer was subjected to ^{13}C NMR studies (Figure 3.30 (d)). The ^{13}C{^{1}H} NMR spectrum clearly displayed the characteristic signals corresponding to both the BL (denoted as B) and TBL (denoted as T) repeating units. Yet, the chemical shifts of the resulting polymer did not change at all compared with those of their homopolymers, P3HB

(Figure 3.30 (a)) and P3TB (Figure 3.30 (b)), respectively, suggesting the formation of the mixture of P3HB and P3TB (at this stage blocky copolymer cannot be completely ruled out). This was further demonstrated by comparing the chemical shifts of a physical blend of syndiotactic P3HB and syndiotactic P3TB with the polymer obtained from the random copolymerization attempt (Figure 3.30 (c) and (d)).

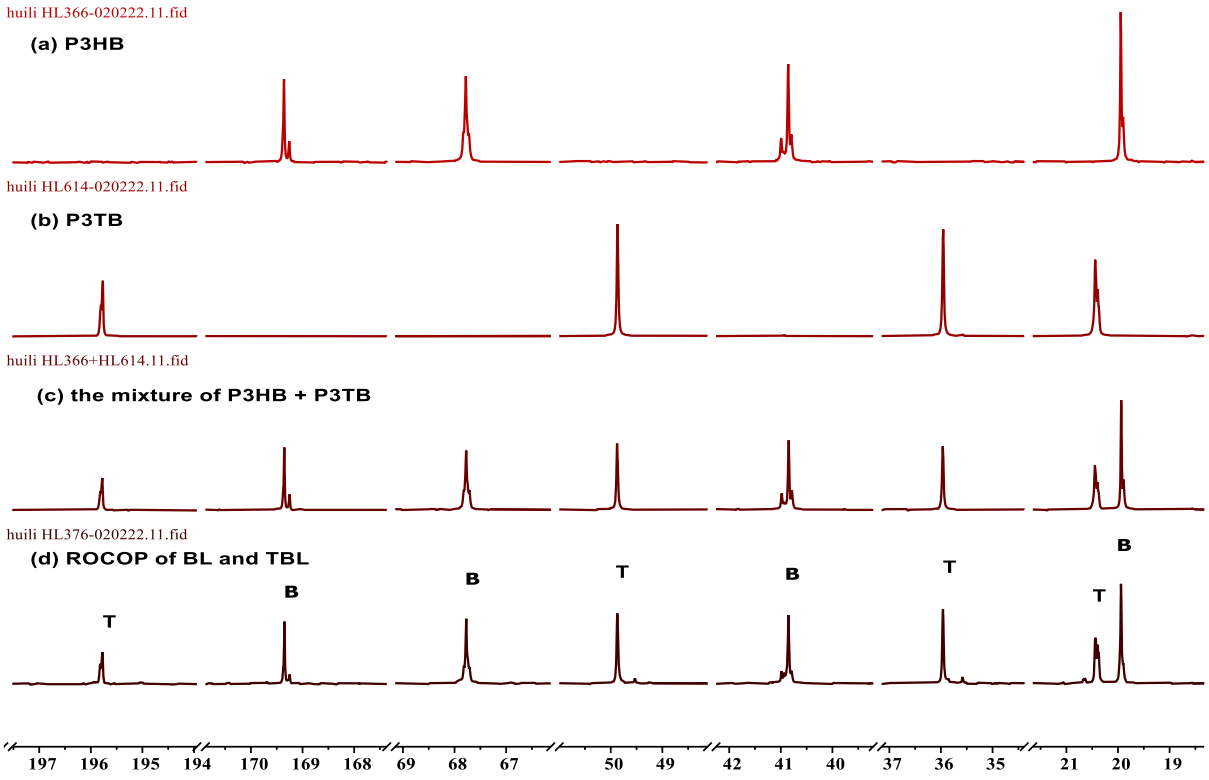

Figure 3.30. $^{13}C\{^{1}H\}$ NMR (100 MHz, $CDCl_3$, 25 °C) spectra of: (a) syndiotactic P3HB prepared by ROP of *rac*-BL mediated by "Y{ONNO^{tBu2}}" at room temperature in toluene; (b) syndiotactic-enriched P3TB prepared by ROP of *rac*-TBL promoted by "Y{ONNO^{tBu2}}" in toluene at room temperature; (c) the mixture of syndiotactic P3HB and P3TB individually prepared by ROP of *rac*-BL and *rac*-TBL, respectively; (d) polymer resulting from the attempted ring-opening copolymerization (ROCOP) of *rac*-BL and *rac*-TBL in toluene at ambient temperature (random polymerization).[1]

Further support of the macromolecular structure of the mixture of P3TB and P3HB was gained from MALDI-ToF mass spectrometry analysis. The key feature of the MALDI technique is the laser irradiation of the sample dispersed in an ultraviolet absorbing matrix. Although, to some extent, the cationizing agent and the laser power play essential roles in the ionization of the molecules and consequently should influence the appearance of the mass spectra, the proper choice of the matrix is one of the crucial factors for obtaining informative MALDI-ToF mass spectra. Yet, we have not found the best matrix to obtain a MS spectrum thus far; only linear P3HB macromolecules were detected, *e.g.*, n = 15, m/z_{exp} = 1373.588 *vs.* m/z_{theo} = 1373.60 for $\{i\text{PrO}-[C_4H_6O_2]_{15}-\text{H}+\text{Na}\}^+$ (Figure 3.31). We assume that the matrix chosen, namely *trans*-2-[3-(4-*tert*-butylphenyl)-2-methyl-2-

propenylidene]malononitrile (DCTB), did not allow co-crystallization of P3TB macromolecules in significant amounts, and/or the energy transfer from the matrix which had absorbed the exciting laser light to the P3TB failed due to the existence of impurities absorbing the energy efficiently.

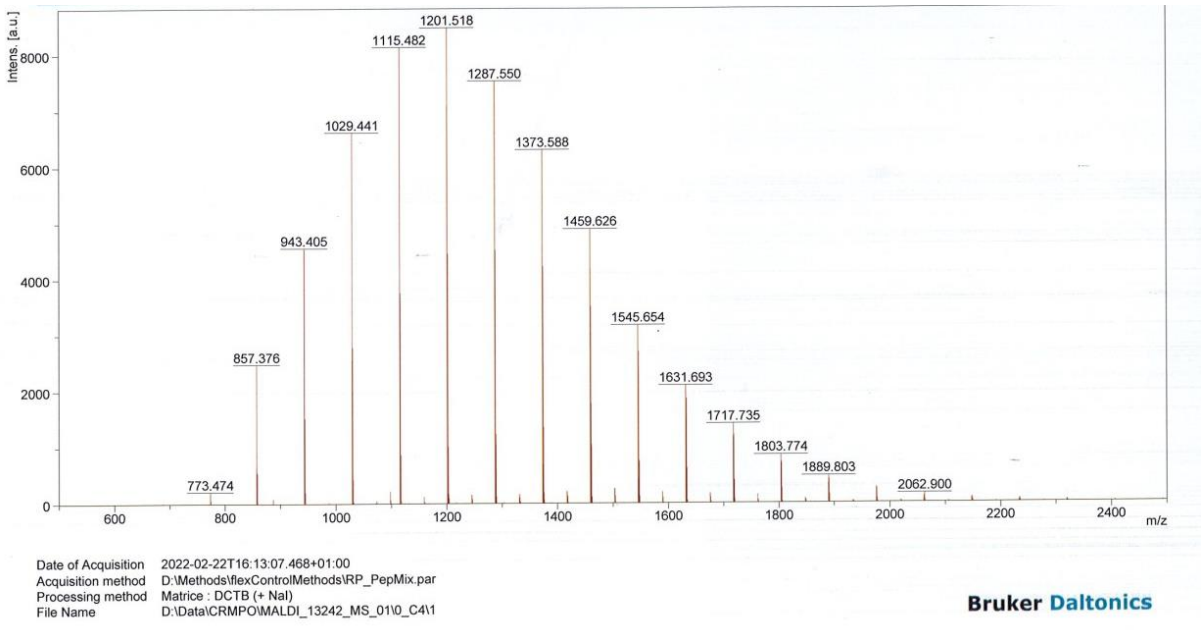

Figure 3.31. MALDI-ToF mass spectrum of the polymer obtained by simultaneous ROP of *rac*-TBL and *rac*-BL by the system Y{ONNO^{cumyl2}}{N(SiHMe$_2$)$_2$}(THF) / *i*PrOH (1:1) in toluene (Table 3.6, HL679), with a plot of experimental *m/z* values *vs.* theoretical number of BL repeat units. For $n = 15$, $m/z_{exp} = 1373.588$ *vs.* $m/z_{theo} = 1373.60$ for $\{i\text{PrO}–[C_4H_6O_2]_{15}–H+Na\}^+$.

The sequential polymerization of *rac*-BL and *rac*-TBL was performed under identical conditions as the random polymerization (Table 3.6, entry HL676). Again, both monomers were fully converted within less than 30 s, indicating the high activity of this system. Unfortunately, all the polymers formed (both of random and sequential ROCOP) remained insoluble in THF and poorly soluble in $CDCl_3$; thus, precluding the determination of the molar mass by SEC and their characterization by NMR analysis. We attributed this to the possible cocrystallization between the P3TB segments and the P3HB segments. In comparison, the microbial (isotactic) P3TB is poorly soluble in chloroform due to, to some extent, its high molar mass (typically $M_n > 150$ kg mol^{-1}), while the microbial isotactic poly(3HB-*co*-3TB) is soluble in chloroform (500 kg mol^{-1} < $M_{n,SEC}$ < 900 kg mol^{-1}).

Regarding the sequential ROCOP of *rac*-BL and *rac*-TBL, due to the occurrence of side reactions such as back-biting, transesterification ractions, it is reasonable to assume the formation of a mixture of linear P3HB and cyclic P3TB. After the full consumption of *rac*-BL, the active center of the polymer chain, *i*PrO-(3HB)$_n$-Y, mediated the *rac*-TBL polymerization when *rac*-TBL was added into the system. Subsequently, the newly formed thiolate-Y bonds attack the thioester bonds at any site of the P3TB segment along the active polymer chain, forming the cyclic P3TB and *i*PrO-(3HB)$_n$-Y. Eventually, the mixture of linear P3HB and cyclic P3TB was obtained after workup. Again, the NMR and MALDI-

ToF MS spectra (Figure 3.32) were similar to those of the random ROCOP of *rac*-BL and *rac*-TBL, *i.e.*, evidencing the presence only of macromolecules of P3HB, without any TBL unit inserted within.

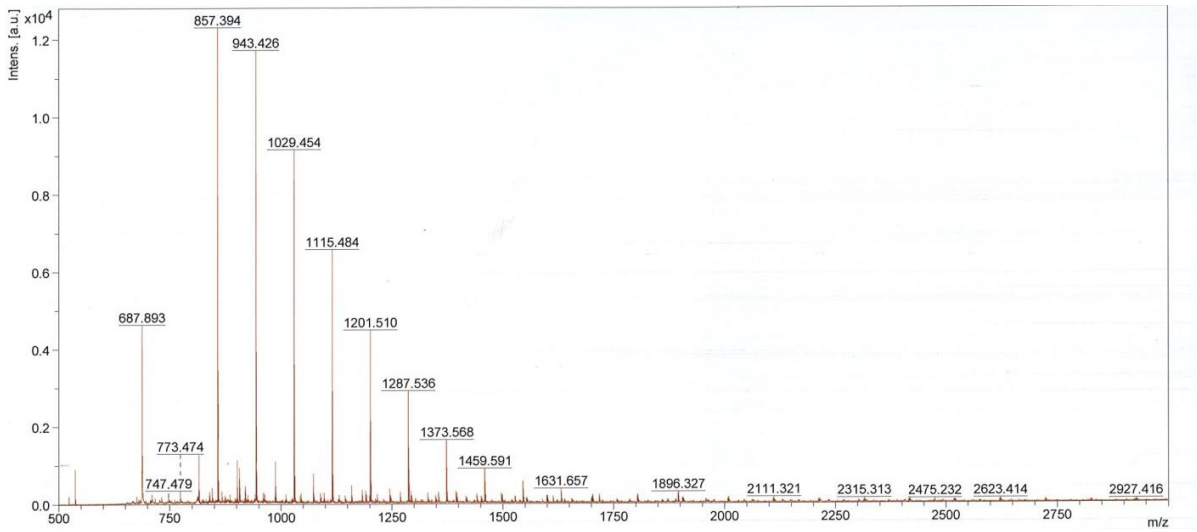

Figure 3.32. MALDI-ToF mass spectrum of the polymer obtained by sequential ROP of *rac*-TBL and *rac*-BL by the system Y{ONNO^{cumyl2}}{N(SiHMe$_2$)$_2$}(THF) / *i*PrOH (1:1) in toluene (Table 3.6, HL676), with a plot of experimental *m/z* values *vs.* theoretical number of BL repeating units. For n = 15, m/z_{exp} = 1373.588 *vs.* m/z_{theo} = 1373.60 for {*i*PrO−[C$_4$H$_6$O$_2$]$_{15}$−H+Na}$^+$.

The microstructure of polymers obtained from random or sequential ROCOP, a mixture of P3HB and P3TB in both cases, was evaluated by $^{13}C\{^1H\}$ NMR analysis (Figure 3.33, Figure 3.34, and Figure 3.35). On the basis of prior ^{13}C NMR assignment of the carbonyl and methylene region of P3HB, the sequential copolymerization of *rac*-BL and *rac*-TBL in toluene at room temperature gave P3HB with a P_r value of 0.89, which is consistent with the homopolymerization of *rac*-BL under the same conditions,[1] while the random copolymerization gave P3HB with essentially the same (85%) syndiotactic enchainment. Also, the microstructure of (putatively cyclic) P3TB obtained in the mixture for both cases is nearly the same (P_r *ca.* 0.6), which is somewhat lower than that of homopolymerization of *rac*-TBL under identical conditions (P_r typically ranging from 0.66 to 0.68).

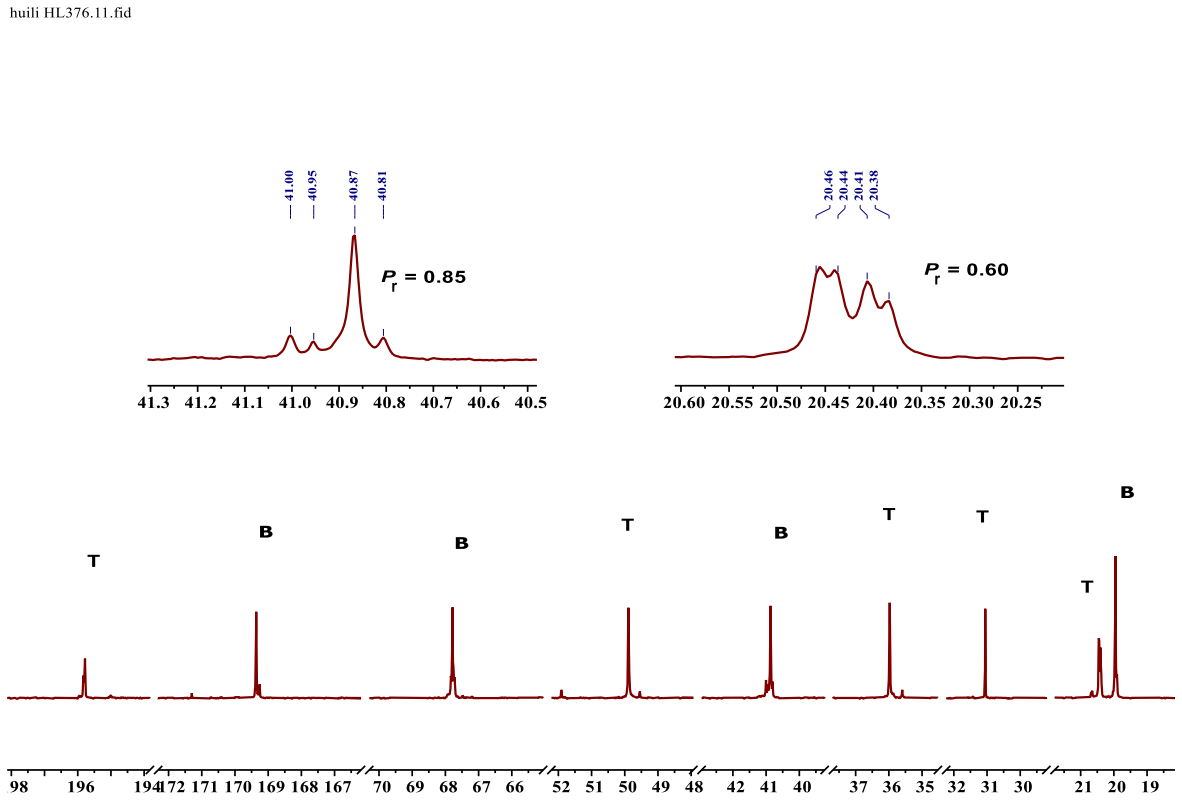

Figure 3.33. $^{13}C\{^{1}H\}$ NMR (125 MHz, $CDCl_3$, 25 °C) spectrum of the polymer prepared by simultaneous polymerization of *rac*-BL and *rac*-TBL (Table 3.6, entry HL376).

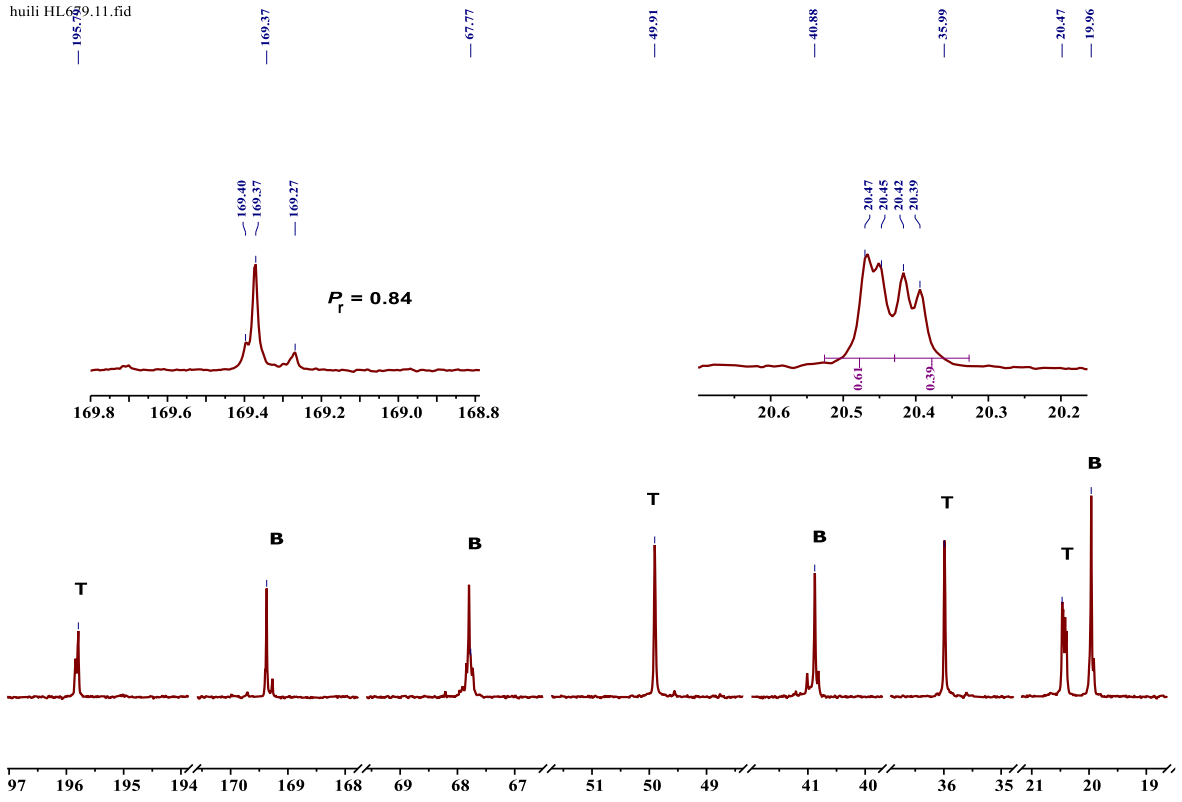

Figure 3.34. $^{13}C\{^{1}H\}$ NMR (125 MHz, $CDCl_3$, 25 °C) spectrum of the polymer produced by sequential polymerization (Table 3.6, entry HL679).

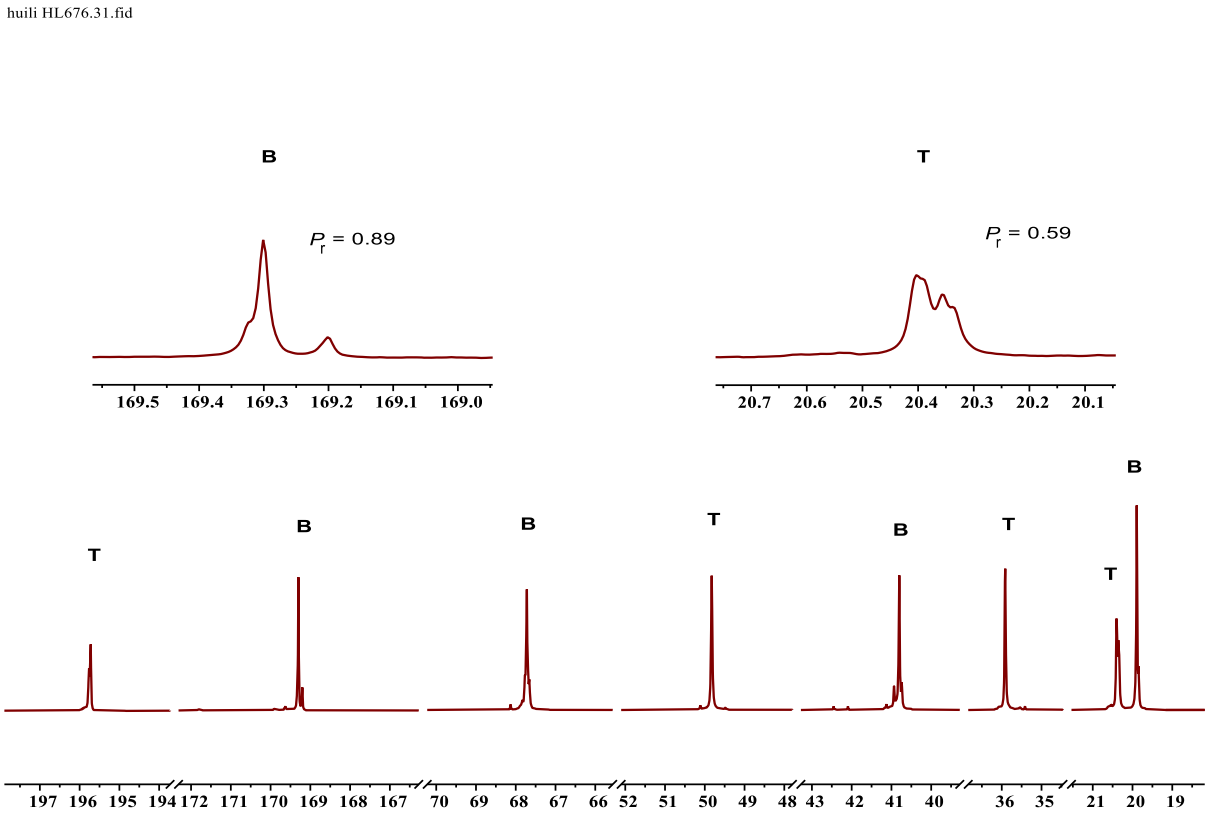

Figure 3.35. $^{13}C\{^1H\}$ NMR (100 MHz, $CDCl_3$, 25 °C) spectrum of the polymer produced by sequential polymerization (Table 3.6, entry HL676).

3.8 Conclusion

In summary, we have reported herein an efficient chemical synthesis of P3TB, initially biosynthesized from a recombinant strain of *E. coli*, via ROP of the corresponding racemic β-thiobutyrolactone (*rac*-TBL). A variety of well-established metal-based catalysts/initiators was investigated in the ROP of *rac*-TBL, allowing complete conversion of the TBL monomer to the desired polythioester with relatively high molar mass and narrow dispersity. Among them, the most promising results were obtained with yttrium complexes stabilized by tetradentate bis(phenolate) yttrium complexes "Y{ON(X)O^{R1,R2}}", giving rise to cyclic polymers, most likely as a result of easy intra-transthioesterification (back-biting). The cyclic polymer topology was evidenced by MALDI-ToF MS and NMR analyses, and also supported by TGA. As expected, these cyclic polymers display higher thermal properties than their linear counterparts.

Interestingly, using a *single family of achiral catalysts*, upon simple tuning of the substituents on the bis(phenolate) platform, the stereoselectivity of the ROP of *rac*-TBL can be switched from highly isoselective to syndioselective. The complexes incorporating "moderately bulky" *tert*-butyl or cumyl-substituted ligands afford syndiotactic P3TB, while the catalysts bearing the smaller substituents on the ligand, such as chloro or methyl, and the system with the larger trityl-substituted ligand, enable reaching isotactic P3TB. At this stage of our studies, we cannot elaborate confidently on the origin of this isotactic stereocontrol; neither can we state on the exact nature of isotactic P3TB: it could be a racemic

mixture of two isotactic homopolymers, a stereoblock copolymer, or a tapered blocked copolymer, which can be evaluated by detailed kinetic studies in conjunction with chiral HPLC or specific rotation.

On the other hand, probably due to the considerable difference in reactivity between *rac*-BL and *rac*-TBL, preliminary attempts at performing the copolymerization (ROCOP) of *rac*-BL and *rac*-TBL promoted by yttrium complex, "Y{ONNO^{cumyl2}}(N(SiHMe$_2$)$_2$)(THF)", gave rise to mixtures of homopolymers, namely cyclic P3TB and linear P3HB, as evidenced by NMR and MALDI-ToF MS analysis. We may consider the ROCOP of *rac*-TBL and *rac*-BL mediated by organic species as an alternative to access such copolymers.

We anticipate that this yttrium-catalyzed stereoselective ROP of the simplest, prototypical four-membered *racemic*-β-thiolactone may open up opportunities for efficiently converting a family of functional β-thiolactones, commonly accessible by organocatalysis, into new sustainable polymers with a wide range of enhanced properties and potential applications. The biodegradation and the mechanical properties of P3TB also remain to be established.

Experimental Section

General Considerations. All syntheses and manipulations of air- and moisture-sensitive materials were carried out in flame-dried Schlenk-type glassware on a vacuum dual-manifold Schlenk line or in an argon-filled glovebox. HPLC-grade organic solvents were first purged extensively with nitrogen during filling 20 L-solvent reservoirs and then dried by passage through activated alumina [for dichloromethane] and through Q-5 supported copper catalyst [for toluene] stainless steel columns. *n*-Hexane, 1,4-dioxane, 2-methyl-tetrahydrofuran (2-MeTHF), tetrahydrofuran (THF), acetonitrile and toluene were degassed and dried over sodium/benzophenone followed by distillation under argon. *iso*-Propanol (*i*PrOH), benzyl alcohol (BnOH), isopropyl mercaptan (*i*PrSH), benzyl mercaptan (BnSH) were purified by distillation from CaH_2. (SalBinam)AlO^iPr {SalBinam = *N*,*N*′-bis(salicylidene)-1,1′-binaphthyl-2,2′-diamine} (**1**), (BDI)ZnN(SiMe$_3$)$_2$ (**2a**), {Zn{N(SiMe$_3$)$_2$}$_2$ (**2b**), the amido yttrium-salan complex **4**, bisphenol {ONXO^{R2}}H_2 proligands ***a-l*** and yttrium amide precursors were synthesized according to the methods reported in the literature (see Appendices).

^{1}H (500, 400 and 300 MHz), ^{13}C{^{1}H} (125 and 100 MHz) and two-dimensional (2D) NMR spectra were recorded on Bruker Avance III HD 500, Av III 400 or Av III 300 spectrometers at 25 °C, fitted with a direct broadband 5 mm probehead (BBO) carefully tuned on both ^{1}H and ^{13}C channels. 1D ^{13}C spectra were acquired using Bruker standard zgpg30 sequence, acquisition time was 1.05 s and relaxation delay D1 5.00 s. Two-dimensional NMR experiments were acquired using standard pulse sequences (hsqcedetgpsisp2.3 for band-selective HSQC experiments; shmbcctetgpl2nd for band-selective HMBC experiments), 2D spectra were processed using Topspin software (Bruker Biospin, Billerica, MA, USA) and analyzed in MestReNova 14.2.0 (Mestrelab Research S.L). The ^{13}C projections were prepared in Topspin software by extracting F1 traces from the 2D HMBC and HSQC spectra across the peaks of interest.

Number and weight average molar mass ($M_{n,SEC}$ and $M_{w,SEC}$) and dispersity ($Đ_M = M_w/M_n$) values of the polymers were determined by size-exclusion chromatography (SEC) in THF at 30 °C (flow rate = 1.0 mL min^{-1}) on a Polymer Laboratories PL50 apparatus equipped with a refractive index detector and a set of two ResiPore PLgel 3 μm MIXED-D 300 × 7.5 mm columns. The polymer samples were dissolved in THF (2 mg mL^{-1}). All elution curves were calibrated with polystyrene standards (M_n range = 580 – 126,000 g mol^{-1}); the $M_{n,\,SEC}$ values of the P3TB reported in all Tables are uncorrected for the possible difference in hydrodynamic radius *versus* that of polystyrene.

High resolution Matrix Assisted Laser Desorption Ionization – Time of Flight (MALDI-ToF) mass spectra were recorded using an ULTRAFLEX III TOF/TOF spectrometer (Bruker Daltonik Gmbh, Bremen, Germany) in positive ionization mode at Centre Régional de Mesures Physiques de l'Ouest (CRMPO, ScanMAT UAR2025 CNRS, Université de Rennes 1). Spectra were recorded using reflectron mode and an accelerating voltage of 25 kV. A mixture of a freshly prepared solution of the polymer in CH_2Cl_2 (HPLC grade) and DCTB (*trans*-2-(3-(4-*tert*-butylphenyl)-2-methyl-2-

propenylidene) malononitrile in CH_2Cl_2 (HPLC grade, 10 mg mL^{-1}) , and a MeOH or CH_2Cl_2/CH_3CN (50/50, *v*/*v*) solution of the cationizing agent (NaI, 10 mg mL^{-1}) were prepared. The solutions were combined in a 1:1:1 (*v*/*v*/*v*) ratio of matrix-to-sample-to-cationizing agent. The resulting solution (0.25–0.5 µL) was deposited onto the sample target (Prespotted AnchorChip PAC II 384/96 HCCA) and air or vacuum dried. High resolution mass spectrum of *rac*-TBL was performed using a time-of-flight Maxis 4G (Bruker Daltonik Gmbh, Bremen,Germany) in ASAP (direct introduction, desorption temperature: 45°C) positive mode at the Centre Régional de Mesures Physiques de l'Ouest (CRMPO, ScanMAT, Université de Rennes1).Melting-transition (T_m) and glass-transition (T_g) temperatures were measured by differential scanning calorimetry (DSC) on a DSC2500, TA Instrument. All T_m and T_g values were obtained from the second heating run. The first heating rate was 10 °C min^{-1}, while the cooling rate was 10 °C min^{-1} and the second heating rate was 10 °C min^{-1}. The onset decomposition temperatures (T_d, defined as the temperature for 5% weight loss) of the polymers were measured by thermal gravimetric analysis (TGA) on a Mettler-Toledo TGA-DSC-1 apparatus under dry nitrogen flow, TA Instrument. Polymer samples were heated from ambient temperatures to 500 °C at a rate of 10 °C min^{-1}.

General Polymerization Procedure. In the glovebox, a Schlenk flask was charged with $[Y(N(SiHMe_2)_2)_3](THF)_2$ (6.3 mg, 10 µmol) and the desired $\{ONXO^{R2}\}H_2$ proligand (10 µmol), and toluene (0.88 mL) was added. To this solution, in the glove box, *i*PrOH (10 µmol, 38 µL of a 2% (*v*/*v*) solution in toluene) was added under stirring at 14 °C. After 5 min, *rac*-TBL (102 mg, 1.0 mmol, 100 *equiv.* vs. Y) was added rapidly. After the desired period, the polymerization was quenched by addition of benzoic acid (0.5 mL of 10 mg mL^{-1} solution in $CHCl_3$). An aliquot (0.1 mL) of the reaction mixture was used to determine the monomer conversion by ^1H NMR analysis. The resulting mixture was then concentrated to dryness under vacuum, and the resulting crude polymer was subsequently dissolved in CH_2Cl_2 (*ca.* 2 mL) and precipitated in pentane (*ca.* 50 mL, not cooled), filtered, and dried in a vacuum oven at room temperature till constant weight. The P3TB polymer was recovered as a white powder, and analyzed by NMR spectroscopy and SEC. Pure isotactic P3TB was prepared from ROP of (*R*)-TBL (50 equiv.) with the **5a**/*i*PrOH (1:1) system in toluene at room temperature (P_m > 0.95, M_n = 3.2 kg mol^{-1}, $Đ_M$ = 1.52).

Synthesis of *rac*-β-thiobutyrolactone (*rac*-TBL). The synthesis of *rac*-TBL relies on the cyclization of b-thiobutyric acid, initially prepared by the addition reaction of crotonic acid with thioacetic acid (Scheme 3.7), following optimization of literature procedures (*vide infra*).

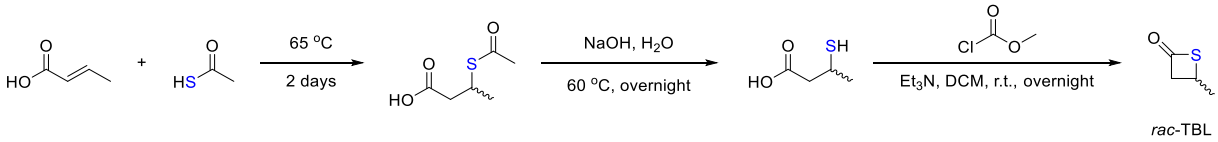

Scheme 3.7. Synthesis of *rac*-β-TBL.

Synthesis of 3-thiobutyric acid. Crotonic acid (Thermo Fisher Scientific, 84 g, 1.0 mol) and thioacetic acid (TCI, 83.6 g, 1.1 mol) were placed in a flask (1 L). The resulting mixture was heated up to 65 °C for 2 days. The crude product containing 3-acetylthiobutyric acid was treated with NaOH (500 mL of a 3 M aqueous solution, 1.5 mol) overnight. The resulting solution was acidified with HCl (300 mL of a 2.5 M aqueous solution, 0.75 mol) until pH = 3 and extracted with diethyl ether (2 × 500 mL). The organic phase was dried over anhydrous Na_2SO_4, the solvent was removed under reduced pressure, and the residue was purified by distillation under vacuum (*ca*. 400 mTorr) at 95 °C, to give 3-thiobutyric acid, as a yellowish liquid (96.9 g, 81% yield).

^{1}H NMR (300 MHz, $CDCl_3$, 25 °C, Figure 3.36): δ (ppm) 11.35 (s, 1H, COO*H*), 3.30–3.44 (dq, *J* = 14 and 7 Hz, 1H, C*H*), 2.58–2.73 (m, 2H, CH_2), 1.86 (d, *J* = 7 Hz, 1H, S*H*), 1.41 (d, *J* = 7 Hz, 3H, CH_3).

^{13}C{^{1}H} NMR (100 MHz, $CDCl_3$, 25 °C, Figure 3.37): δ (ppm) 177.83 (*C*O), 45.72 (*C*H_2), 30.97 (*C*H), 24.92 (*C*H_3).

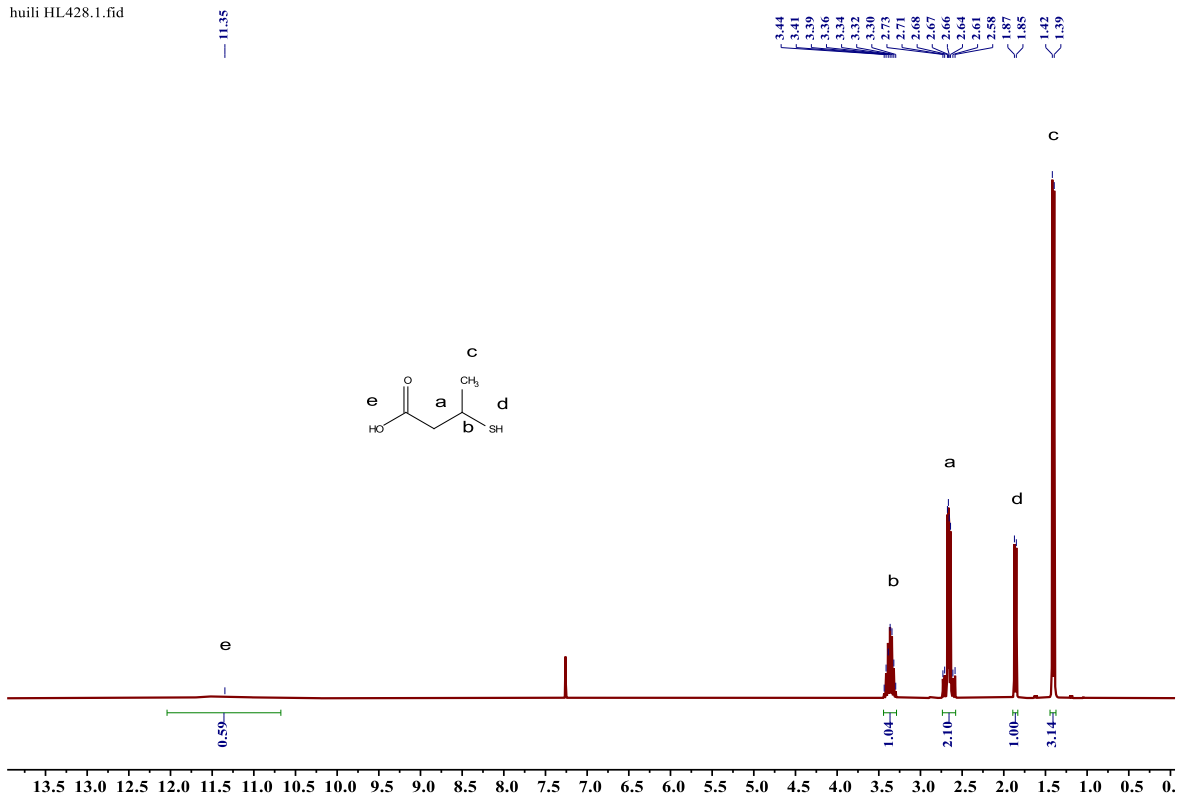

Figure 3.36. ^{1}H NMR spectrum (300 MHz, $CDCl_3$, 25 °C) of 3-mecaptobutyric acid (3MBA) (HL428).

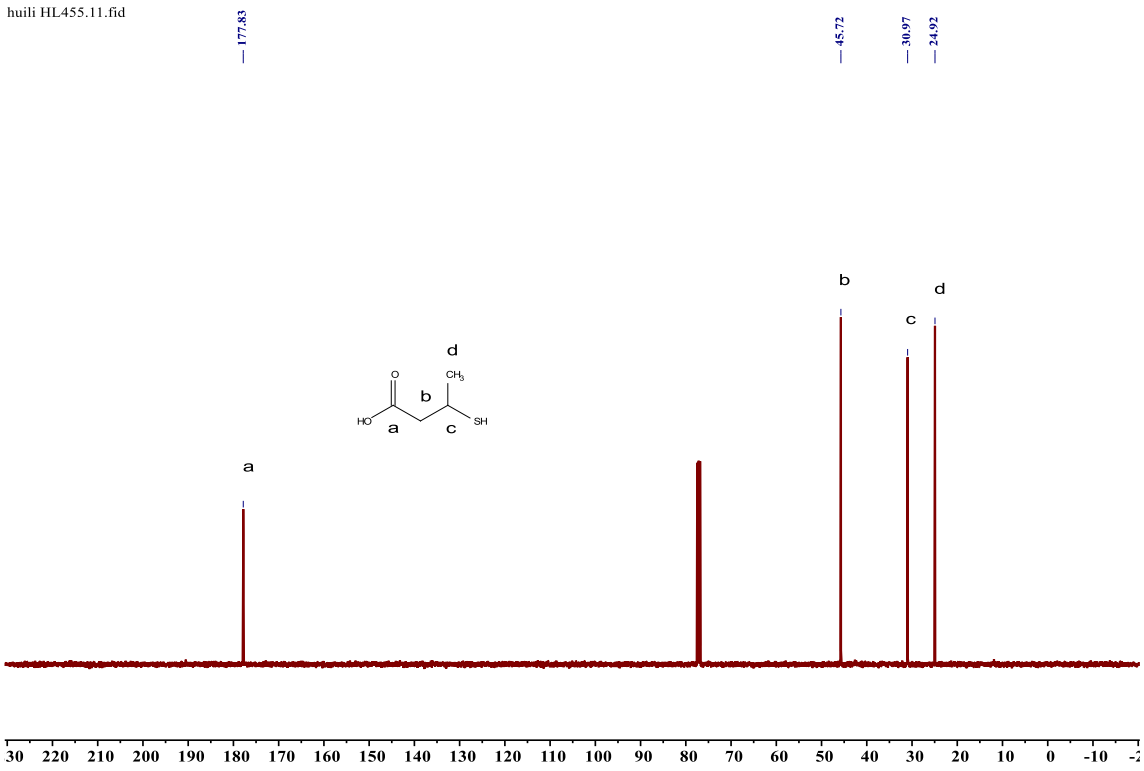

Figure 3.37. ^{13}C NMR spectrum (100 MHz, $CDCl_3$, 25 °C) of 3-mecaptobutyric acid (3MBA) (HL455).

Synthesis of *rac*-β-thiobutyrolactone (*rac*-TBL). Racemic β-thiobutyrolactone (*rac*-TBL) was then synthesized using a modified (optimization of the purification procedure) literature procedure. Methyl chloroformate (21.5 mL, 0.275 mol) was added dropwise at 0 °C to a solution of 3-thiobutyric acid (26.4 mL, 0.25 mol) and triethylamine (38.4 mL, 0.275 mol) in dry dichloromethane (350 mL). Once the addition was completed, the reaction mixture was warmed to room temperature and stirred until evolution of CO_2 ceased. The resulting mixture was washed with water (2 × 100 mL), saturated $NaHCO_3$ (250 mL), brine (250 mL) and the separated organic layer was dried over $MgSO_4$ and rotavapored under reduced pressure. The residue was purified by distillation using the Glass Oven B-585 under vacuum twice (35 °C, 500 mTorr) to give pure *rac*-TBL as a colorless liquid (6.5 g, 26% yield, Caution: *rac*-TBL will degrade or polymerize spontaneously if purified by column chromatography on silica or neutral alumina).

^{1}H NMR (400 MHz, $CDCl_3$, 25 °C, Figure 3.38): δ (ppm) 4.10 (dd, *J* = 17 and 7 Hz, 1H, C*H*H), 3.72 (pd, *J* = 7 and 4 Hz, 1H, C*H*), 3.52 (dd, *J* = 17 and 4 Hz, 1H, CH*H*), 1.67 (d, *J* = 7 Hz, 3H, CH_3).

^{13}C{^{1}H} NMR (125 MHz, $CDCl_3$, 25 °C, Figure 3.39): δ (ppm) 190.43 (*C*O), 62.88 (*C*H_2), 28.10 (*C*H), 23.78 (*C*H_3).

HRMS (ESI, Figure 3.40): calculated for C_4H_6SO $[M]^+$ *m/z* = 103.0212; found: 103.0212.

e.e. value (50%) of *rac*-TBL was depicted in Figure 3.41.

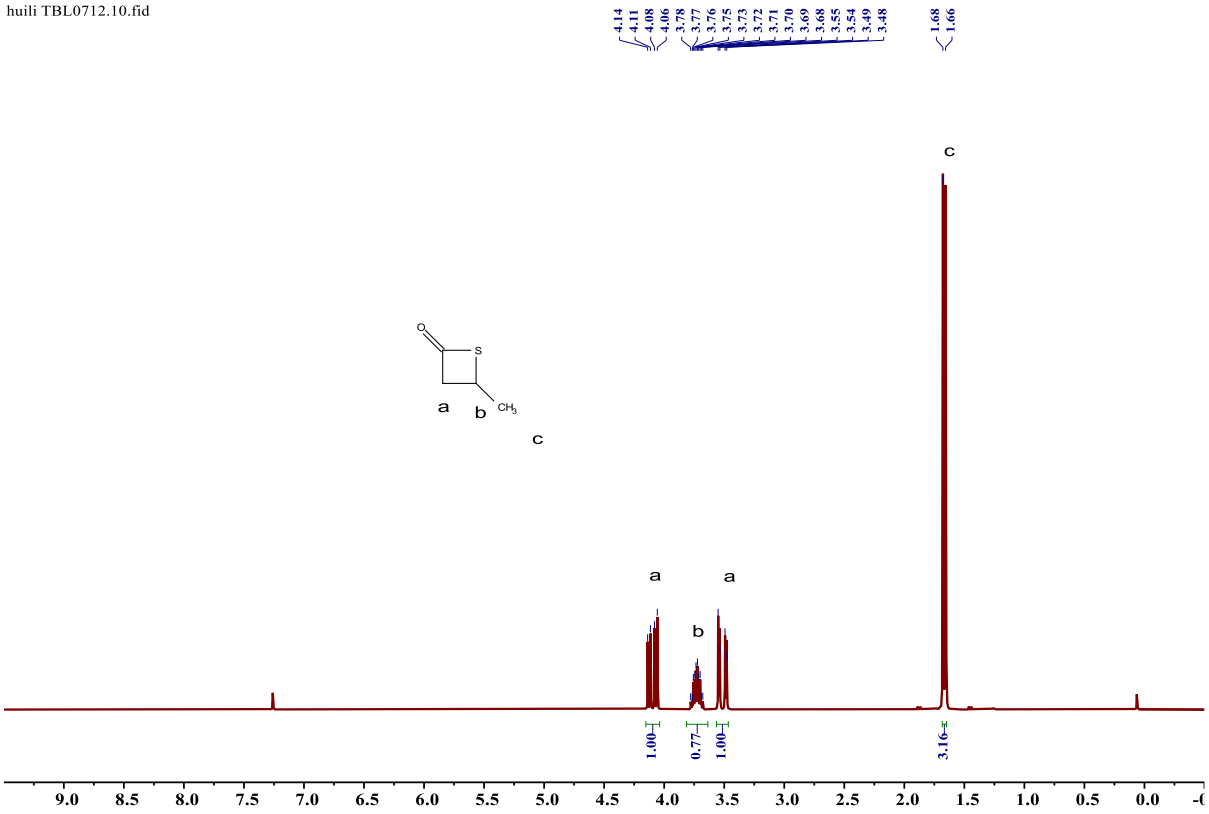

Figure 3.38. ^{1}H NMR spectrum (300 MHz, $CDCl_3$, 25 °C) of *rac*-β-thiobutyrolactone (*rac*-TBL); the weak signal at 0.06 ppm is silicone grease.

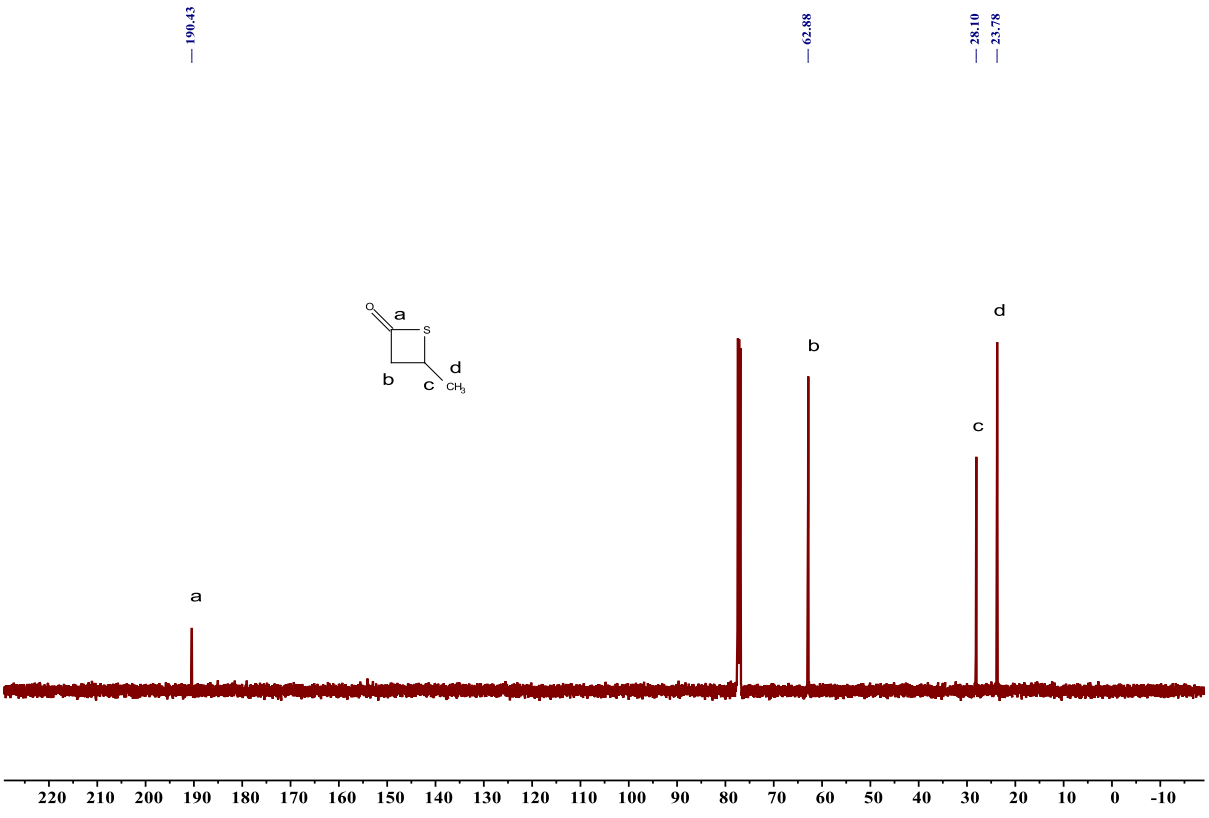

Figure 3.39. ^{13}C{^{1}H} NMR spectrum (125 MHz, $CDCl_3$, 25 °C) of *rac*-β-thiobutyrolactone (*rac*-TBL).

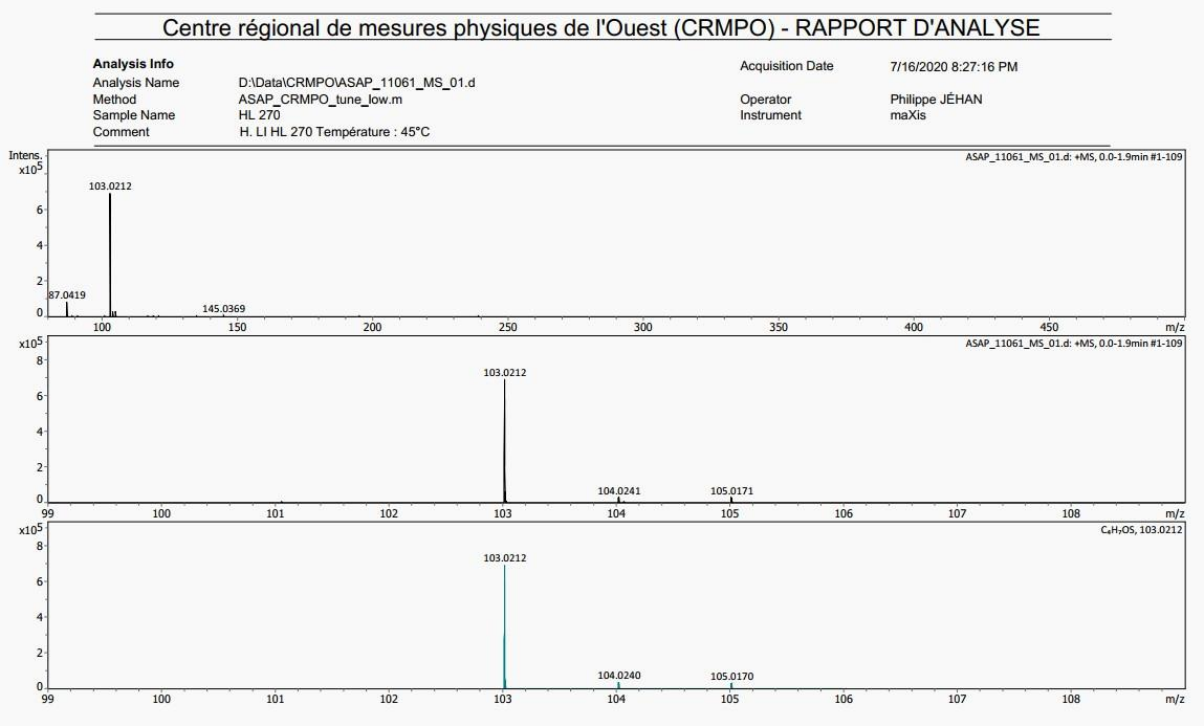

Figure 3.40. HRMS spectra of *rac*-TBL. Top: ESI mass spectrum of *rac*-TBL; middle: zoomed spectrum of top spectrum (*ca.* 104 *m/z*); bottom: simulated spectrum of *rac*-TBL.

Chromatogram and Results

General informations	
Sequence Name:	**2022-02-22**
Instrument:	**U3000**
Logiciel used:	**Chromeleon**
Column used:	**CHIRALPAK IC-3 DAICEL**

Injection Details			
Injection Name:	**HL-RAC-TBL-1mgmL-d1/4HEXANE-IC3-2022-02-22-**	*Run Time:*	**60.00 min**
Instrument Method:	**90-10-Hexane-DCM-60min-20°C-254nm**	*Injection Volume:*	**1.00 µL**
Injection Date/Time:	**22/févr./22 12:56**	*Channel:*	**UV_VIS_1**
		Wavelength:	**254 nm**

Instrument Method Details			
Instrument Method:	**90-10-Hexane-DCM-60min-20°C-254nm**		
%A **Dichloromethane**	**10 %**		
%B **Hexane**	**90 %**	*Température du four:*	**20.0 °C**
Débit:	**1.000 mL/min**	*Pression:*	**75 bars**

Chromatogram

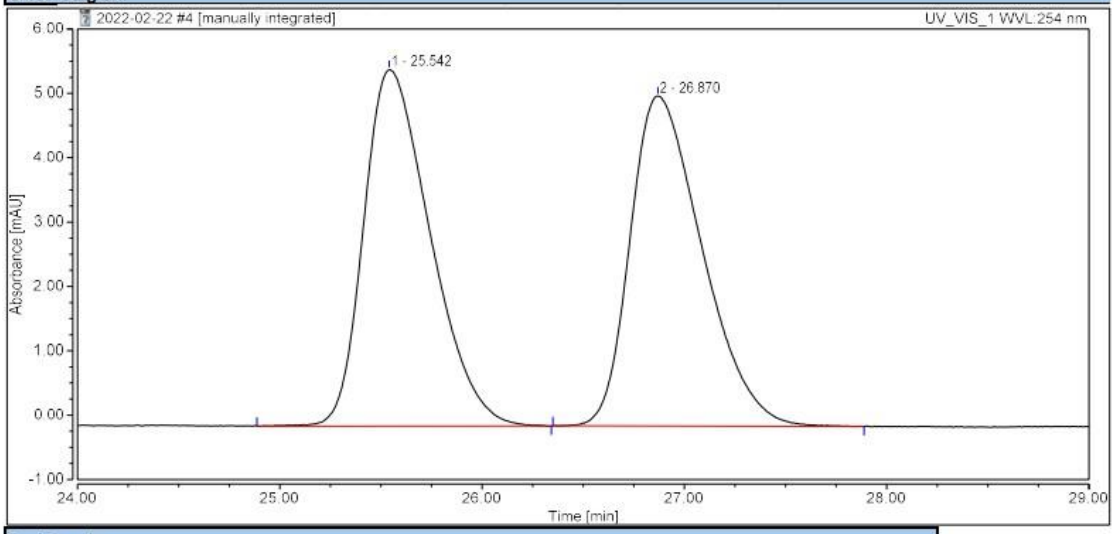

Peak Results

No.	Peak Name	Retention Time min	Width (50%) min	Resolution (EP)	Asymmetry (EP)	Plates (EP)
1		25.542	0.355	2.12	1.39	28614
2		26.870	0.385	n.a.	1.41	27044

Integration Results

No.	Peak Name	Retention Time min	Area mAU*min	Height mAU	Relative Area %
1		25.542	2.112	5.542	49.96
2		26.870	2.116	5.127	50.04
Total:			**4.228**	**10.669**	**100.00**

Figure 3.41. Chiral HPLC chromatogram (column Chiralcel-OD DAICEL; 250 mm × 4.6 mm, 5µm; 20 °C with a UV detector at 254 nm) of *rac*-TBL (hexane/DCM 90/10; 1 mL min^{-1}, 75 bars).

Synthesis of (*S*)-β-thiobutyrolactone ((*S*)-TBL). The fundamental steps involved in the synthesis of monomer (*S*)-TBL are depicted in Scheme 3.8. It relies on the cyclization of enantiomerically pure b-thiobutyric acid, initially prepared from (*R*)-β-butyrolactone.

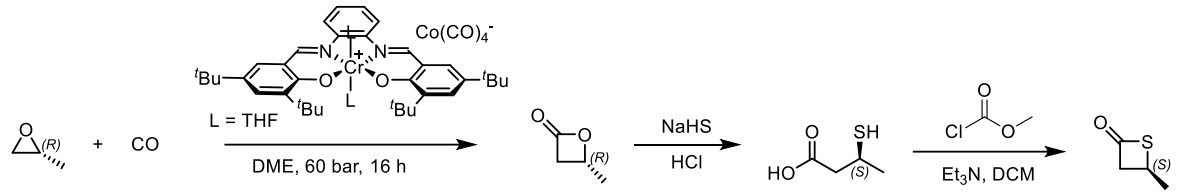

Scheme 3.8. Synthesis of enantiomerically pure (*R*)-TBL.

Synthesis of (R)-β-butyrolactone ((*R*)-BL): (*R*)-β-Butyrolactone was synthesized using a modified literature procedure (reaction conducted at higher pressure, *i.e.*, 60 bars instead of 1 bar). In the glovebox, a Schlenk flask was charged with $[salph(Cr(THF)_2)]^+[Co(CO)_4]^-$ (520 mg, 0.57 mmol). On a Schlenk line, dry DME (10 mL) was syringed into the reaction flask and the resulting solution was cannulated into a degassed high-pressure reactor which was then pressurized with carbon monoxide to 30 bars, followed by stirring for 15 min before depressurization. A solution of (*R*)-propylene oxide (Acros Organics, 98% *ee*, 15 mL, 0.22 mol) in dry DME (5 mL) was then transferred into the reactor which was then pressurized with CO to 60 bars. The reaction mixture was stirred overnight at 23 °C. The reactor was vented to atmospheric pressure, volatiles were removed under vacuum and the crude product was purified by distillation at 40 °C to afford (*R*)-BL as a colorless viscous liquid (4.6 g, 26 % yield).

^{1}H NMR (400 MHz, $CDCl_3$, 25 °C, Figure 3.42): δ (ppm) 4.74–4.67 (m, 1H, C*H*), 3.60–3.54 (m, 1H, C*H*H), 3.06 (dd, J = 16 and 4 Hz, 1H, CH*H*), 1.57 (d, J = 6 Hz, 3H, CH_3).

^{13}C{^{1}H} NMR (100 MHz, $CDCl_3$, 25 °C, Figure 3.43**):** δ (ppm) 168.17 (*C*O), 68.02 (*C*H_2), 44.43 (*C*H), 20.71 (*C*H_3).

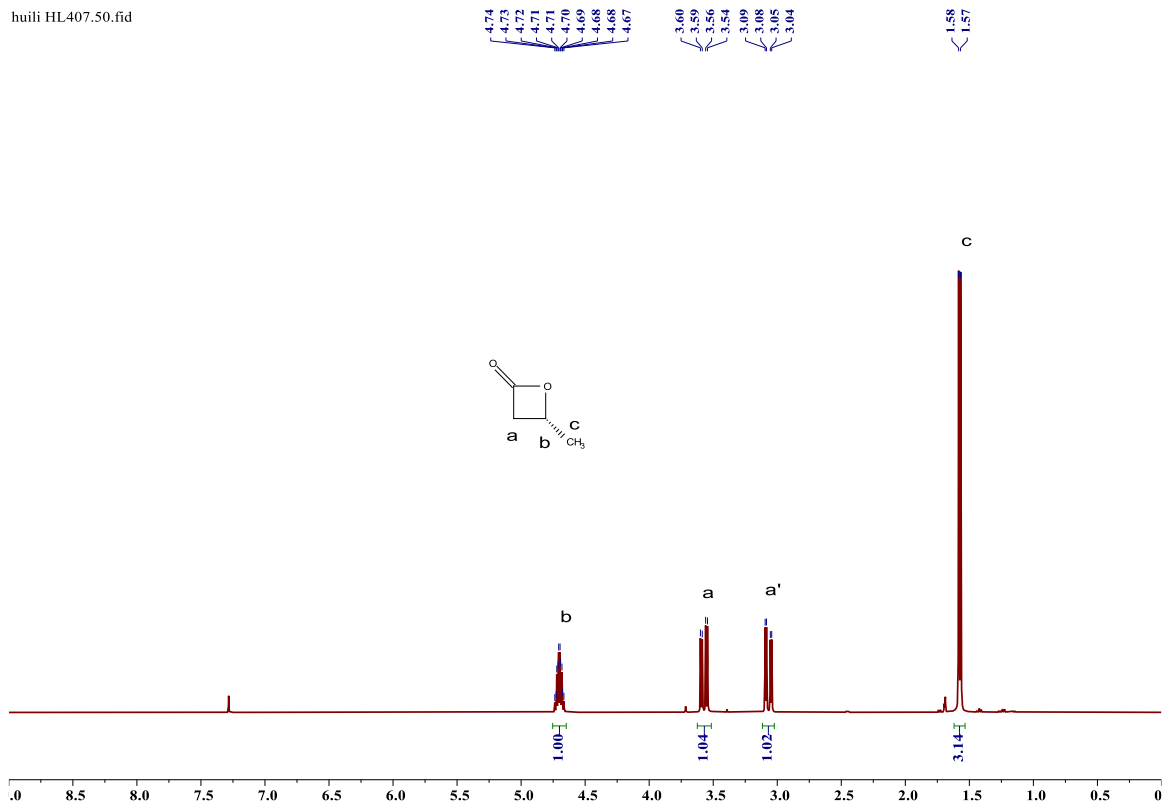

Figure 3.42. ^{1}H NMR spectrum (400 MHz, $CDCl_3$, 25 °C) of (*R*)-β-butyrolactone (HL407).

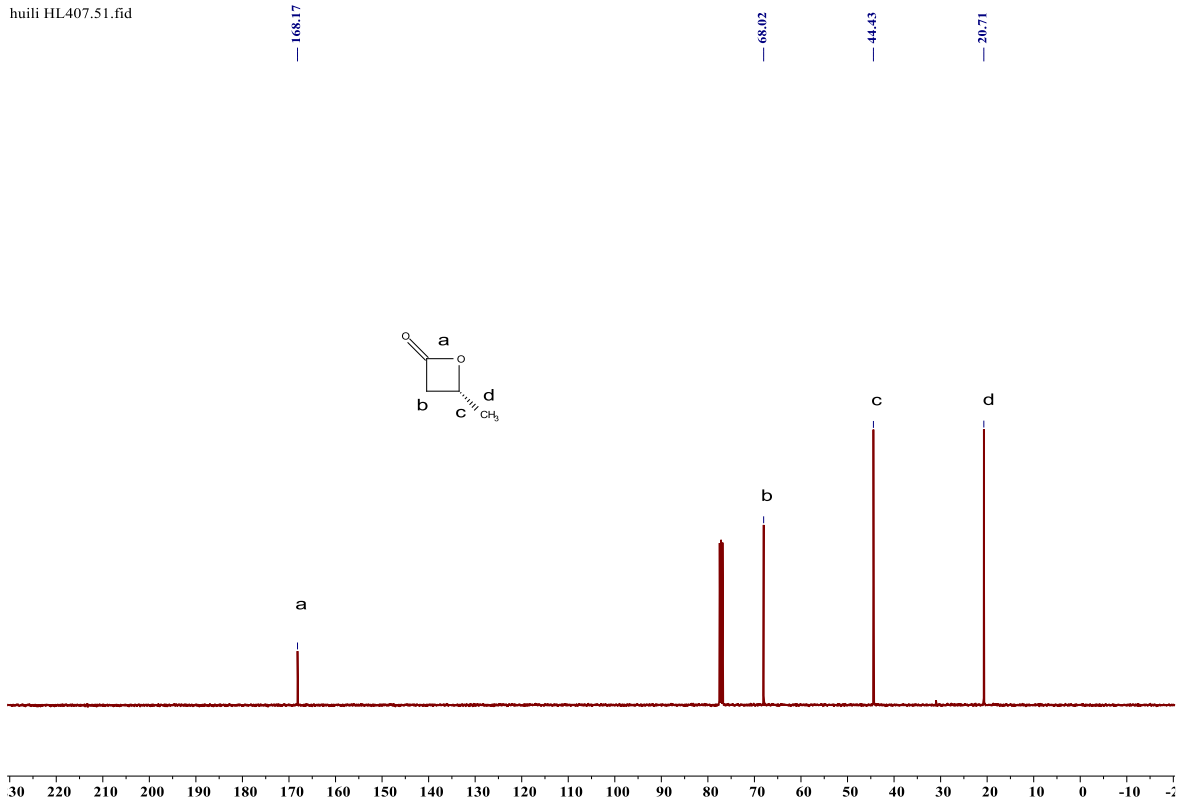

Figure 3.43. ^{13}C NMR spectrum (100 MHz, $CDCl_3$, 25 °C) of (*R*)-β-butyrolactone (HL407).

Synthesis of (*S*)-β-thiobutyrolactone ((*S*)-TBL). (*S*)-3-Thiobutyric acid was synthesized using a literature procedure. (*R*)-BL (7.54 g, 87.6 mmol) was added dropwise at 0 °C to a solution of NaSH ¶H_2O (5.06 g, 90.2 mmol) in water (90 mL). The mixture was then stirred for 1 h at 0 °C and for 24 h at 23 °C. Then, HCl (2.4 N aqueous solution) was added to adjust the pH ≈ 2 and the mixture was extracted with Et_2O (3 × 150 mL). The resulting organic phase was dried over $MgSO_4$, the solvent was removed under reduced pressure and the residue was distilled to give a ca. 2:1 mixture of (*S*)-3TBA and (*R*)-3HBA isolated as a colorless liquid (3.90 g, *ca.* 38% yield). This mixture of the two compounds was dissolved in a solution of triethylamine (3.6 mL, 0.036 mol) in dry dichloromethane (50 mL), and methyl chloroformate (2.8 mL, 0.036 mol) was then added dropwise at 0 ℃. Once the addition was completed, the reaction mixture was warmed to room temperature and stirred until evolution of CO_2 ceased. The resulting mixture was washed with water (2 × 30 mL), saturated $NaHCO_3$ (50 mL), brine (50 mL); the separated organic layer was dried over $MgSO_4$ and rotavapored under reduced pressure. Ultimately, (*S*)-TBL was isolated as described above for *rac*-TBL and recovered as a colorless liquid (335 mg, 3.3 mmol, 10% yield); NMR characteristics are identical to those of *rac*-TBL.

^{1}H NMR (400 MHz, $CDCl_3$, 25 °C, Figure 3.44): δ (ppm) 4.10 (dd, *J* = 17 and 7 Hz, 1H, C*H*H), 3.72 (pd, *J* = 7 and 4 Hz, 1H, C*H*), 3.52 (dd, *J* = 17 and 4 Hz, 1H, CH*H*), 1.67 (d, *J* = 7 Hz, 3H, CH_3).

e.e. value of (*S*)-TBL was depicted in Figure 3.45.

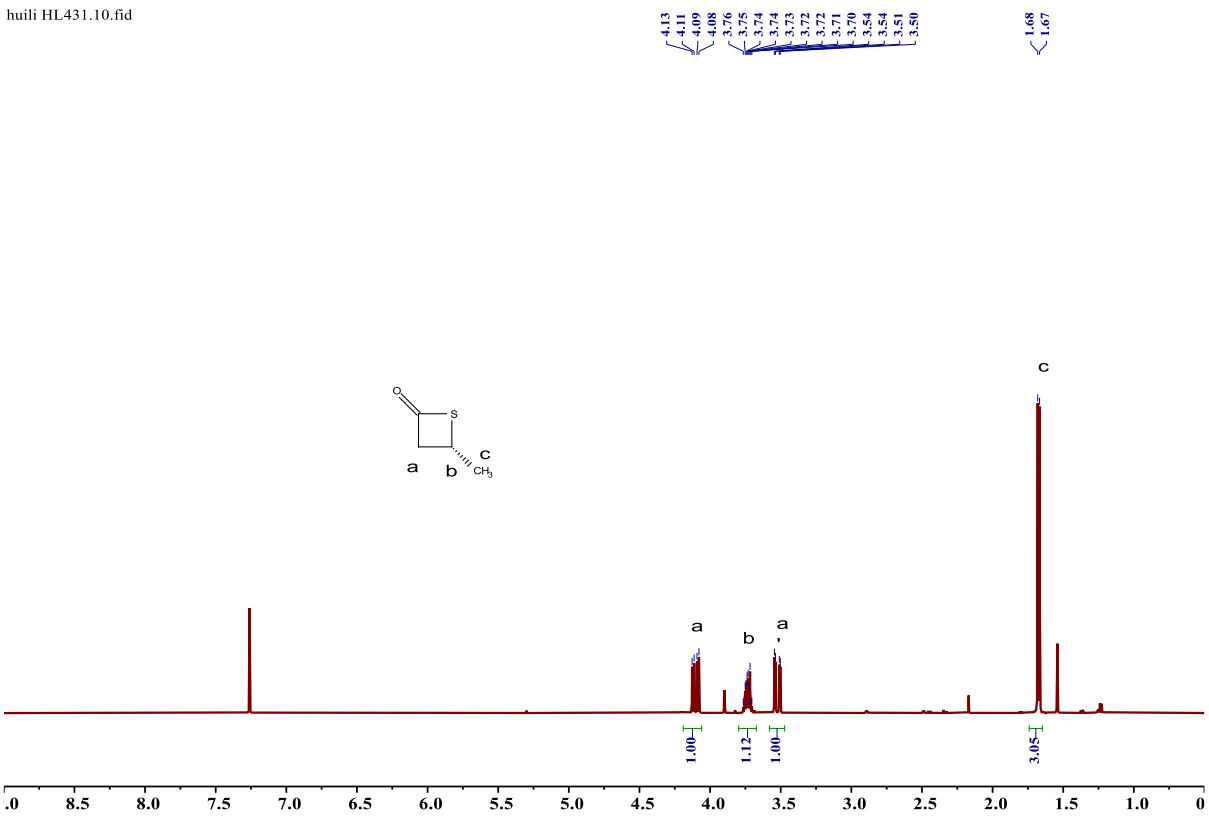

Figure 3.44. ^{1}H NMR spectrum (500 MHz, $CDCl_3$, 25°C) of (*R*)-TBL; the peaks at *d*2.18 and *d*1.56 ppm correspond to residual acetone and water, respectively).

Chromatogram and Results

General informations

Sequence Name:	**2022-02-22**
Instrument:	**U3000**
Logiciel used:	**Chromeleon**
Column used:	**CHIRALPAK IC-3 DAICEL**

Injection Details

Injection Name:	**HL-S-TBL-1mgmL-d1/20HEXANE-IC3-2022-02-22-9(**	*Run Time:*	**30.00 min**
Instrument Method:	**90-10-Hexane-DCM-30min-20°C-254nm**	*Injection Volume:*	**2.00 µL**
Injection Date/Time:	**22/févr./22 15:29**	*Channel:*	**UV_VIS_1**
		Wavelength:	**254 nm**

Instrument Method Details

Instrument Method:	**90-10-Hexane-DCM-30min-20°C-254nm**		
%A **Dichloromethane**	**10 %**		
%B **Hexane**	**90 %**	*Température du four:*	**20.0 °C**
Débit:	**1.000 mL/min**	*Pression:*	**75 bars**

Chromatogram

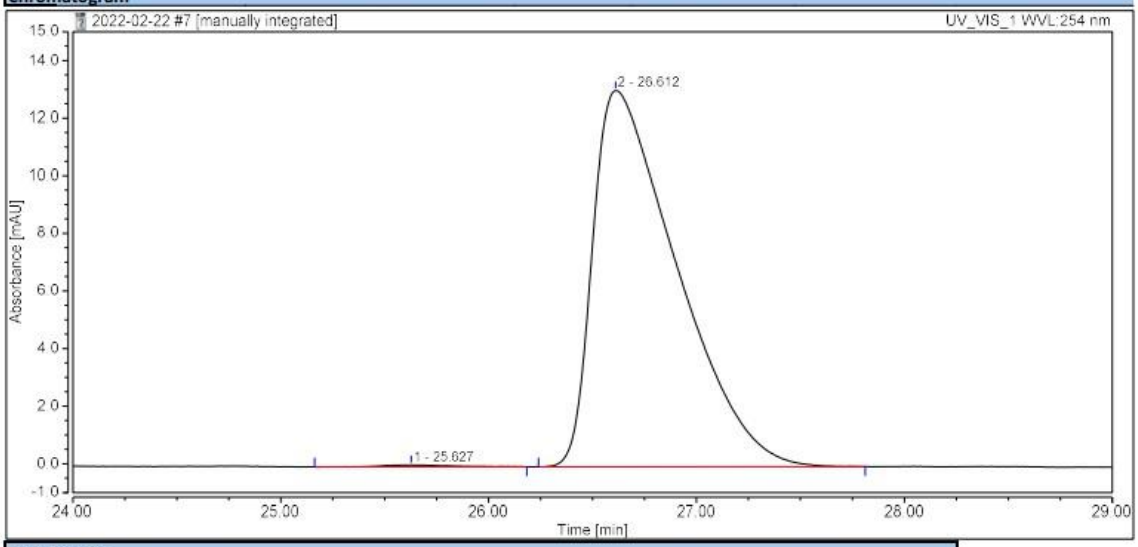

Peak Results

No.	Peak Name	Retention Time min	Width (50%) min	Resolution (EP)	Asymmetry (EP)	Plates (EP)
1		25.627	0.273	1.64	1.45	48832
2		26.612	0.437	n.a.	2.10	20508

Integration Results

No.	Peak Name	Retention Time min	Area mAU*min	Height mAU	Relative Area %
1		25.627	0.026	0.069	0.42
2		26.612	6.112	13.064	99.58
Total:			**6.138**	**13.133**	**100.00**

Figure 3.45. Chiral HPLC chromatogram (column Chiralcel-OD DAICEL; 250 mm × 4.6 mm, 5µm; 20 °C with a UV detector at 254 nm) of (*S*)-TBL (hexane/DCM 90/10; 1 mL min^{-1}, 75 bars).

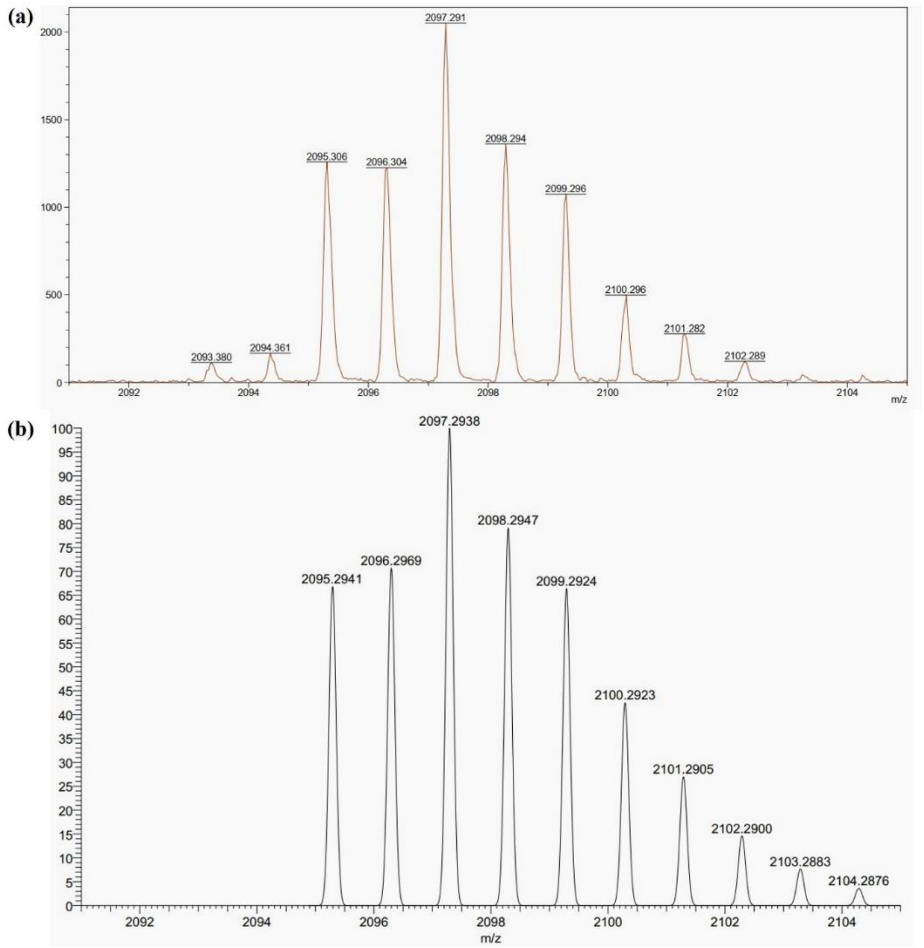

Figure 3.46. Details (isotopic distribution) of the MALDI-ToF mass spectrum of a linear P3TB produced by NaOMe in C_6D_6, showing the isotopic distribution for macromolecules {MeO-$[C_4H_6SO]_{20}$-H+Na}$^+$: a) experimental spectrum (Table 3.2, entry HL506); b) simulated spectrum.

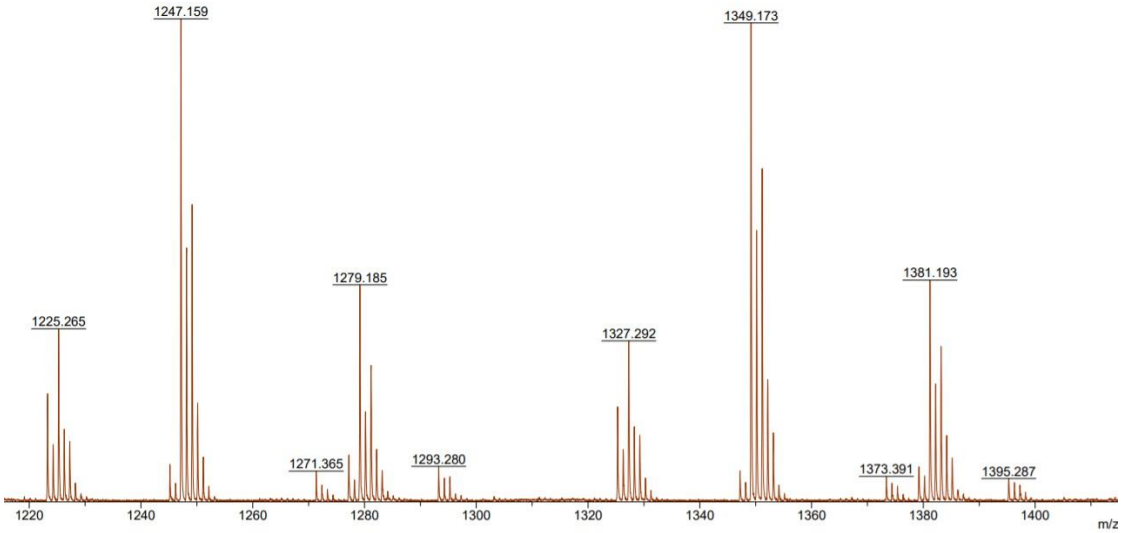

Figure 3.47. Details of the MALDI-ToF MS spectrum of a mixture of cyclic (major) and linear (minor) P3TB produced by the ROP of *rac*-TBL with NaOMe in toluene (40:1, toluene, 30 °C, 1 h, Table 3.2, entry HL669). One of the two minor populations corresponds to linear {MeO-$[TBL]_n$-H+Na}$^+$ macromolecules; for instance, for n = 12, *m/z* obser = 1279.185 *vs.* *m/z* calcd = 1279.183 for MeO-$[C_4H_6SO]_nH+Na^+$; the second one could not be unambiguously identified.

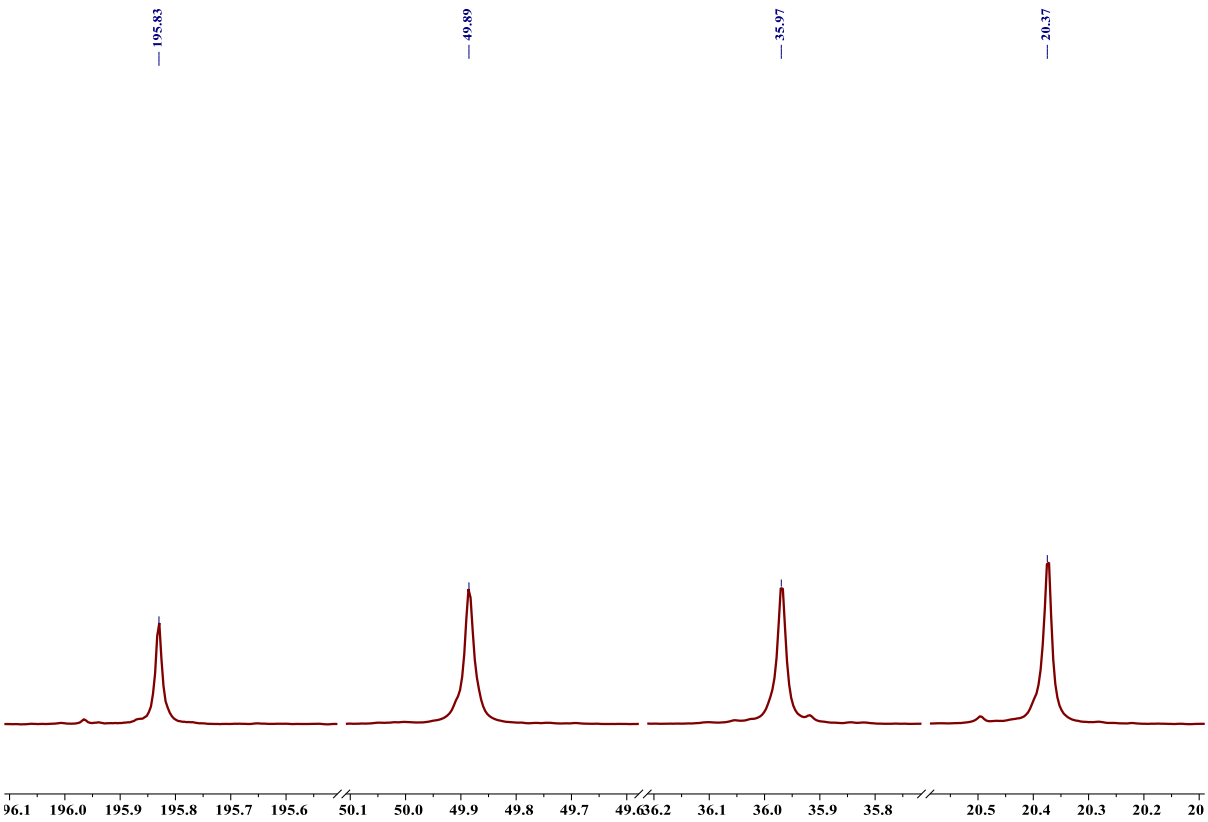

Figure 3.48. ^{13}C NMR spectrum (125 MHz, $CDCl_3$, 25 °C) of perfectly isotactic P3TB.

References

[1] A. Amgoune, C. M. Thomas, S. Ilinca, T. Roisnel, J.-F. Carpentier, Highly Active, Productive, and Syndiospecific Yttrium Initiators for the Polymerization of Racemic β-Butyrolactone. *Angew. Chem. Int. Ed.* **2006**, *45*, 2782-2784.

[2] T. Lutke-Eversloh, A. Fischer, U. Remminghorst, J. Kawada, R. H. Marchessault, A. Bogershausen, M. Kalwei, H. Eckert, R. Reichelt, S. J. Liu, A. Steinbuchel, Biosynthesis of Novel Thermoplastic Polythioesters by Engineered *Escherichia Coli*. *Nat. Mater*. **2002**, *1*, 236-240.

[3] M. G. Lin'kova, N. D. Kuleshova, I. L. Knunyants, Thiolactones. *Russ. Chem. Rev.* **1964**, *33*, 493-507.

[4] M. G. Lin'kova, I. L. Knunyants, Preparation and Properties of α-Methyl-β-Propiothiolactone. *Bull. Acad. Sci. USSR, Div. Chem. Sci.* **1968**, *17*, 1796-1797.

[5] A. Griesbeck, D. Seebach, Herstellung enantiomerenreiner Derivate von 3-Amino- und 3-Mercaptobuttersäure durch SN2-Ringöffnung des β-Lactons und eines 1,3-Dixoanons aus der 3-Hydroxybuttersä ure. *Helv. Chim. Acta* **1987**, *70*, 1326-1332.

[6] J. W. Kramer, E. B. Lobkovsky, G. W. Coates, Practical β-Lactone Synthesis: Epoxide Carbonylation at 1 atm. *Org. Lett.* **2006**, *8*, 3709-3712.

[7] M. Hong, E. Y.-X. Chen, Towards Truly Sustainable Polymers: A Metal-Free Recyclable Polyester from Biorenewable Non-Strained γ-Butyrolactone. *Angew. Chem. Int. Ed.* **2016**, *55*, 4188-4193.

[8] V. Hardouin Duparc, R. M. Shakaroun, M. Slawinski, J.-F. Carpentier, S. M. Guillaume, Ring-Opening (Co)Polymerization of Six-Membered Substituted δ-valerolactones with Alkali Metal Alkoxides. *Eur. Polym. J.* **2020**, *134*, 109858.

[9] L. R. Rieth, D. R. Moore, E. B. Lobkovsky, G. W. Coates, Single-Site β-Diiminate Zinc Catalysts for the Ring-Opening Polymerization of β-Butyrolactone and β-Valerolactone to Poly(3-hydroxyalkanoates). *J. Am. Chem. Soc.* **2002**, *124*, 15239-15248.

[10] B. M. Chamberlain, M. Cheng, D. R. Moore, T. M. Ovitt, E. B. Lobkovsky, G. W. Coates, Polymerization of Lactide with Zinc and Magnesium β-Diiminate Complexes: Stereocontrol and Mechanism. *J. Am. Chem. Soc.* **2001**, *123*, 3229-3238.

[11] M. Cheng, A. B. Attygalle, E. B. Lobkovsky, G. W. Coates, Single-Site Catalysts for Ring-Opening Polymerization: Synthesis of Heterotactic Poly(lactic acid) from rac-Lactide. *J. Am. Chem. Soc.* **1999**, *121*, 11583-11584.

[12] M. Cheng, E. B. Lobkovsky, G. W. Coates, Catalytic Reactions Involving C_1 Feedstocks: New High-Activity Zn(II)-Based Catalysts for the Alternating Copolymerization of Carbon Dioxide and Epoxides. *J. Am. Chem. Soc*. **1998**, *120*, 11018-11019.

[13] Y. Wang, T.-Q. Xu, Topology-Controlled Ring-Opening Polymerization of O-Carboxyanhydride. *Macromolecules* **2020**, *53*, 8829-8836.

[14] Y. Lu, J. H. Swisher, T. Y. Meyer, G. W. Coates, Chirality-Directed Regioselectivity: An Approach for the Synthesis of Alternating Poly(Lactic-co-Glycolic Acid). *J. Am. Chem. Soc.* **2021**, *143*, 4119-4124.

[15] T. M. Ovitt, G. W. Coates, Stereoselective Ring-Opening Polymerization of *meso*-Lactide: Synthesis of Syndiotactic Poly(lactic acid). *J. Am. Chem. Soc.* **1999**, *121*, 4072-4073.

[16] J. W. Kramer, D. S. Treitler, E. W. Dunn, P. M. Castro, T. Roisnel, C. M. Thomas, G. W. Coates, Polymerization of Enantiopure Monomers Using Syndiospecific Catalysts: A New Approach to Sequence Control in Polymer Synthesis. *J. Am. Chem. Soc.* **2009**, *131*, 16042-16044.

[17] M. Bouyahyi, N. Ajellal, E. Kirillov, C. M. Thomas, J.-F. Carpentier, Exploring Electronic versus Steric Effects in Stereoselective Ring-Opening Polymerization of Lactide and β-Butyrolactone with Amino-alkoxy-bis(phenolate)-yttrium Complexes. *Chem. Eur. J.* **2011**, *17*, 1872-1883.

[18] P. Yuan, Y. Sun, X. Xu, Y. Luo, M. Hong, Towards High-Performance Sustainable Polymers via Isomerization-Driven Irreversible Ring-Opening Polymerization of Five-Membered Thionolactones. *Nat. Chem.* **2022**, *14*, 294-303.

[19] M. Hong, E. Y.-X. Chen, Completely Recyclable Biopolymers with Linear and Cyclic Topologies via Ring-Opening Polymerization of γ-Butyrolactone. *Nat. Chem.* **2016**, *8*, 42-49.

[20] M. Shaik, J. Peterson, G. Du, Cyclic and Linear Polyhydroxylbutyrates from Ring-Opening Polymerization of β-Butyrolactone with Amido-Oxazolinate Zinc Catalysts. *Macromolecules* **2018**, *52*, 157-166.

[21] Y. A. Chang, R. M. Waymouth, Recent Progress on the Synthesis of Cyclic Polymers via Ring-Expansion Strategies. *J. Polym. Sci. Part A: Polym. Chem.* **2017**, *55*, 2892-2902.

[22] H. A. Brown, R. M. Waymouth, Zwitterionic Ring-Opening Polymerization for the Synthesis of High Molecular Weight Cyclic Polymers. *Acc. Chem. Res.* **2013**, *46*, 2585-2596.

[23] M. D. Konieczynska, J. C. Villa-Camacho, C. Ghobril, M. Perez-Viloria, K. M. Tevis, W. A. Blessing, A. Nazarian, E. K. Rodriguez, M. W. Grinstaff, On-Demand Dissolution of a Dendritic Hydrogel-based Dressing for Second-Degree Burn Wounds through Thiol-Thioester Exchange Reaction. *Angew. Chem. Int. Ed.* **2016**, *55*, 9984-9987.

[24] C. N. Bowman, C. J. Kloxin, Covalent Adaptable Networks: Reversible Bond Structures Incorporated in Polymer Networks. *Angew. Chem. Int. Ed.* **2012**, *51*, 4272-4274.

[25] C. Ghobril, K. Charoen, E. K. Rodriguez, A. Nazarian, M. W. Grinstaff, A Dendritic Thioester Hydrogel Based on Thiol-Thioester Exchange as a Dissolvable Sealant System for Wound Closure. *Angew. Chem. Int. Ed.* **2013**, *52*, 14070-14074.

[26] S. Liu, C. Ren, N. Zhao, Y. Shen, Z. Li, Phosphazene Bases as Organocatalysts for Ring-Opening Polymerization of Cyclic Esters. *Macromol. Rapid Commun.* **2018**, *39*, e1800485.

[27] E. Caytan, R. Ligny, J.-F. Carpentier, S. M. Guillaume, Evaluation of Band-Selective HSQC and HMBC: Methodological Validation on the Cyclosporin Cyclic Peptide and Application for Poly(3-hydroxyalkanoate)s Stereoregularity Determination. *Polymers* **2018**, *10*, 533-546.

[28] R. Ligny, M. M. Hanninen, S. M. Guillaume, J.-F. Carpentier, Steric *vs.* Electronic Stereocontrol in Syndio- or Iso-selective ROP of Functional Chiral β-Lactones Mediated by Achiral Yttrium-Bisphenolate Complexes. *Chem. Commun.* **2018**, *54*, 8024-8031.

[29] J. B. Zhu, E. Y.-X. Chen, Catalyst-Sidearm-Induced Stereoselectivity Switching in Polymerization of a Racemic Lactone for Stereocomplexed Crystalline Polymer with a Circular Life Cycle. *Angew. Chem. Int. Ed.* **2019**, *58*, 1178-1182.

[30] J.-F. Carpentier, Rare-Earth Complexes Supported by Tripodal Tetradentate Bis(phenolate) Ligands: A Privileged Class of Catalysts for Ring-Opening Polymerization of Cyclic Esters. *Organometallics* **2015**, *34*, 4175-4189.

[31] C. X. Cai, A. Amgoune, C. W. Lehmann, J.-F. Carpentier, Stereoselective Ring-Opening Polymerization of Racemic Lactide Using Alkoxy-Amino-Bis(phenolate) Group 3 Metal Complexes. *Chem. Commun.* **2004**, 330-331.

[32] A. Amgoune, C. M. Thomas, T. Roisnel, J.-F. Carpentier, Ring-Opening Polymerization of Lactide with Group 3 Metal Complexes Supported by Dianionic Alkoxy-Amino-Bisphenolate Ligands: Combining High Activity, Productivity, and Selectivity. *Chem. Eur. J.* **2005**, *12*, 169-179.

[33] F. M. Haque, S. M. Grayson, The Synthesis, Properties and Potential Applications of Cyclic Polymers. *Nat. Chem.* **2020**, *12*, 433-444.

[34] P. B. Yang, M. G. Davidson, K. J. Edler, S. Brown, Synthesis, Properties, and Applications of Bio-Based Cyclic Aliphatic Polyesters. *Biomacromolecules* **2021**, *22*, 3649-3667.

[35] C. Chen, T. Weil, Cyclic Polymers: Synthesis, Characteristics, and Emerging applications. *Nanoscale Horiz.* **2022**, *7*, 1121-1135.

[36] K. Chen, K. Harris, S. Vyazovkin, Tacticity as a Factor Contributing to the Thermal Stability of Polystyrene. *Macromol. Chem. Phys.* **2007**, *208*, 2525-2532.

[37] L.-E. Chile, P. Mehrkhodavandi, S. G. Hatzikiriakos, A Comparison of the Rheological and Mechanical Properties of Isotactic, Syndiotactic, and Heterotactic Poly(lactide). *Macromolecules* **2016**, *49*, 909-919.

[38] A. H. Westlie, E. Y.-X. Chen, Catalyzed Chemical Synthesis of Unnatural Aromatic Polyhydroxyalkanoate and Aromatic-Aliphatic PHAs with Record-High Glass-Transition and Decomposition Temperatures. *Macromolecules* **2020**, *53*, 9906-9915.

[39] T. Lutke-Eversloh, J. Kawada, R. H. Marchessault, A. Steinbuchel, Characterization of microbial polythioesters: physical properties of novel copolymers synthesized by Ralstonia eutropha. *Biomacromolecules* **2002**, *3*, 159-166.

Chapter 4

Preliminary Studies on the Organomediated Ring-Opening Polymerization of *rac*-Thiobutyrolactone

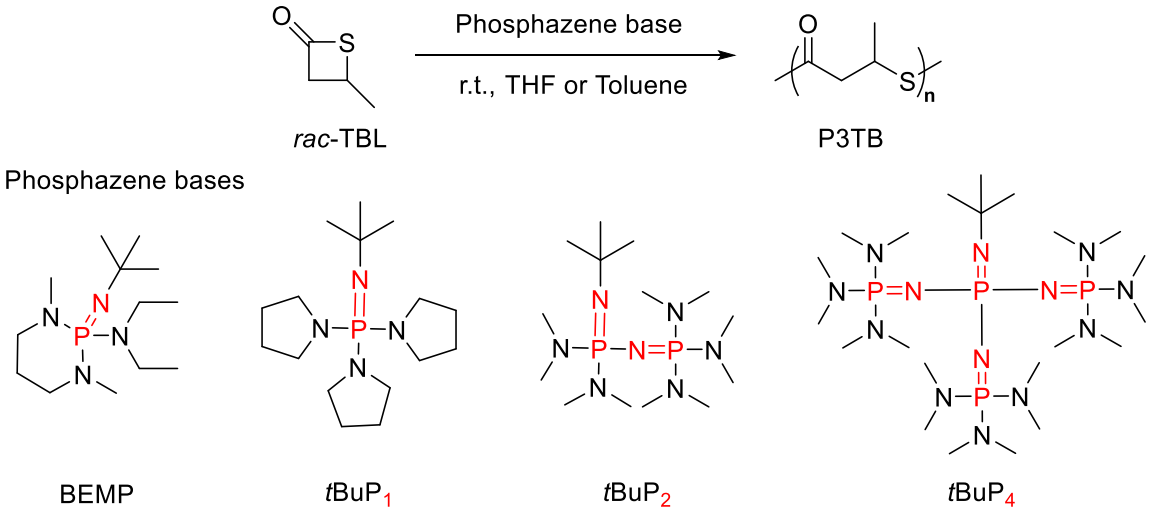

4.1 Introduction

The replacement of metal-based catalysts with small organic molecules has emerged as another appealing polymerization process within the context of plastics designed for microelectronics, or pharmaceutical and biomedical devices.[1] Organocatalysts are of interest for their high chemical stability, relatively low cost, ease of handling and, for some of them, relative innocuity towards living organisms, which have brought about the rapid evolution of metal-free polymerization techniques, especially in the field of biocompatibility and (bio)degradable polymers.

A wide range of organic molecules is available for ring-opening polymerization (ROP) of heterocyclic monomers, such as sulfonic and phosphoric acids, *N*-heterocyclic carbenes (NHCs), amidines, guanidines, phosphines, and phosphazene bases.[2-7] Among these, phosphazene bases, due to their high basicity, non-nucleophilic nature, and good solubility in various organic solvents, have been widely investigated for ROP and ring-opening copolymerization of different types of monomers, such as epoxides, cyclic esters, cyclic carbonates (Figure 4.1).[8] It is worth noting that the performance of phosphazene bases highly depends on their molecular structures and basicity. It was reported that higher basicity is able to improve polymerization rate, yet along with undesirable side reactions, such as chain-transfer, that is inter- and intra-transesterification reactions, which broaden the dispersity of the resulting polymers.[8] Therefore, a judicious choice of phosphazene base with suitable basicity matching the target monomer, to some extent, is critical for the achievement of a controlled polymerization. These phosphazene bases are largely used to convert exogenous protic reagents, such as alcohol, thiol, into nucleophilic initiators through the deprotonation or activation of weak nucleophiles.

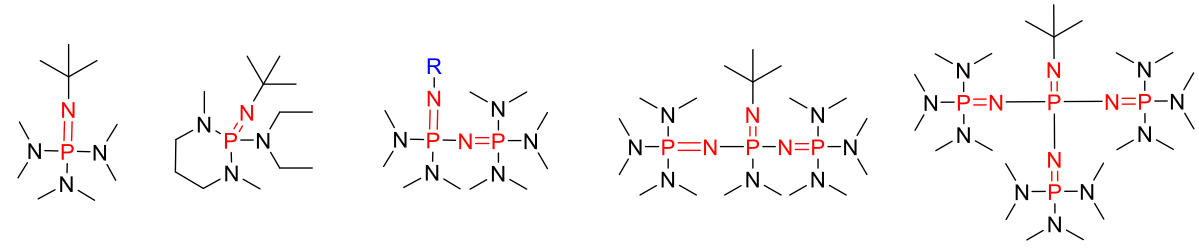

Figure 4.1. Common phosphazene bases used in ROP and their pK_a values measured in MeCN (in parenthesis).[8]

A variety of organocatalysts have been investigated in the ROP of β-lactones.[6] Our group demonstrated that 2-*tert*-butylimino-2-diethylamino-1,3-dimethylperhydro-1,3,2-diazaphosphorine (BEMP) can act as a nucleophilic initiator in the ROP of racemic β-butyrolactone (*rac*-BL) or racemic benzyl β-malolactone (*rac*-MLA^{Bn}) at 60 °C in bulk (neat) conditions. These reactions gave rise to the corresponding α-phosphazene,ω-crotonate telechelic polymers in a controlled manner, as suggested by NMR spectroscopy and MALDI-ToF MS analyses (Figure 4.2).[9,10]

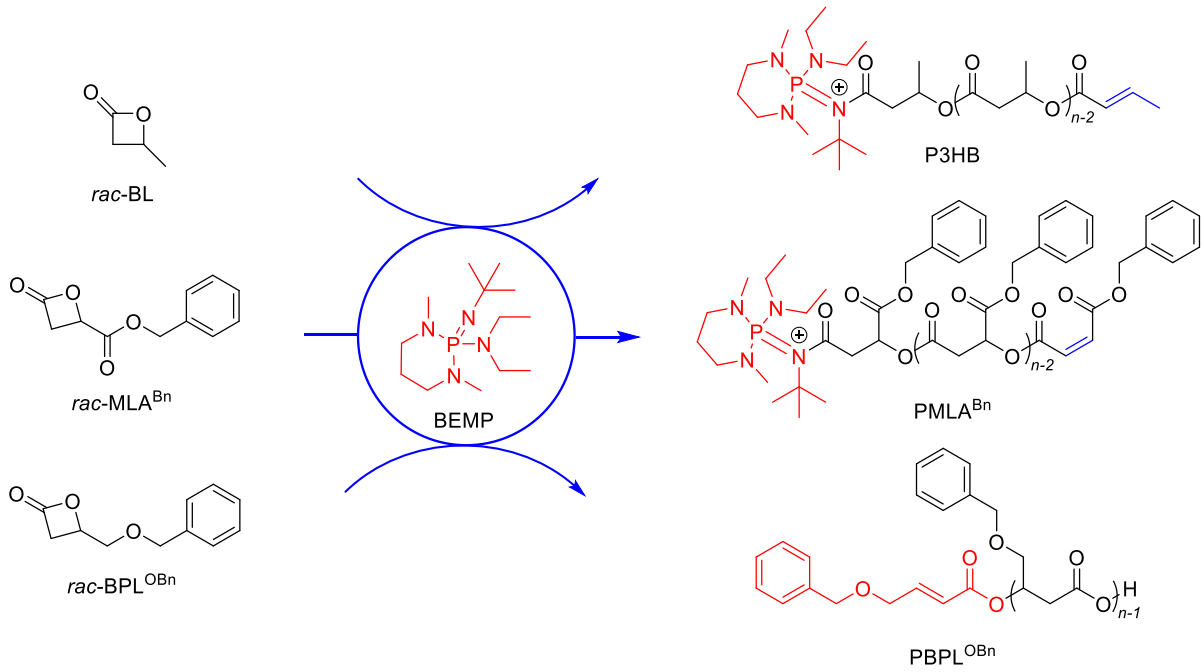

Figure 4.2. Ring-opening polymerization of *rac*-BL and its higher derivatives mediated by BEMP in bulk.[9,10]

However, a recent contribution reported by our group on the ROP of racemic 4-alkoxymethylene-β-propiolactones (*rac*-BPL^{OR}, R = −Me, −Bn, −SiMe$_2$*t*Bu, *etc.*) initiated by BEMP, revealed that this organocatalyst acts as a basic pre-initiator that abstracts one of the methylene hydrogen in α-position of the *rac*-BPL^{OR} monomer, thereby leading to the formation of an α,β-unsaturated carboxylate species as the "real" initiator, which propagates via *O*-alkyl cleavage of the monomer units to be inserted. Ultimately, (ROCH$_2$CH=CHC(O)O)−(BPL^{OR})$_n$−H chains formed upon quenching reactions.[11] It is important to stress that, as illustrated in the aforementioned examples with different β-lactones, the polymerization mechanism at play in organocatalyzed ROP strongly depends on the chemical nature of the monomer and catalyst/initiator and, also quite importantly, on the reaction conditions.

Based on our previous work about organocatalyzed ROP of *rac*-BL and its higher functional derivatives, we have sought at extending this chemistry to the ROP of *rac*-TBL. We have focused our studies on the following phosphazene bases: BEMP, *t*BuP$_1$, *t*BuP$_2$, and *t*BuP$_4$ (Figure 4.3). Preliminary attempts revealed that the polymerization rates increase with the basicity of the phosphazene bases. In addition, the formation of crotonate-capped poly(3-thiobutyrate) (P3TB) was evidenced by NMR analysis. We formulated the following hypothesis to address the challenge of the synthesis of pure linear P3TB due to the occurrence of back-biting reactions (see Chapter 3): phosphazene bases can directly generate highly active species upon reaction with *rac*-TBL in the absence of any co-initiating component, thereby forming conjugated phosphazenium cations which can stabilize the active propagating center of to suppress the back-biting side reaction occurring.

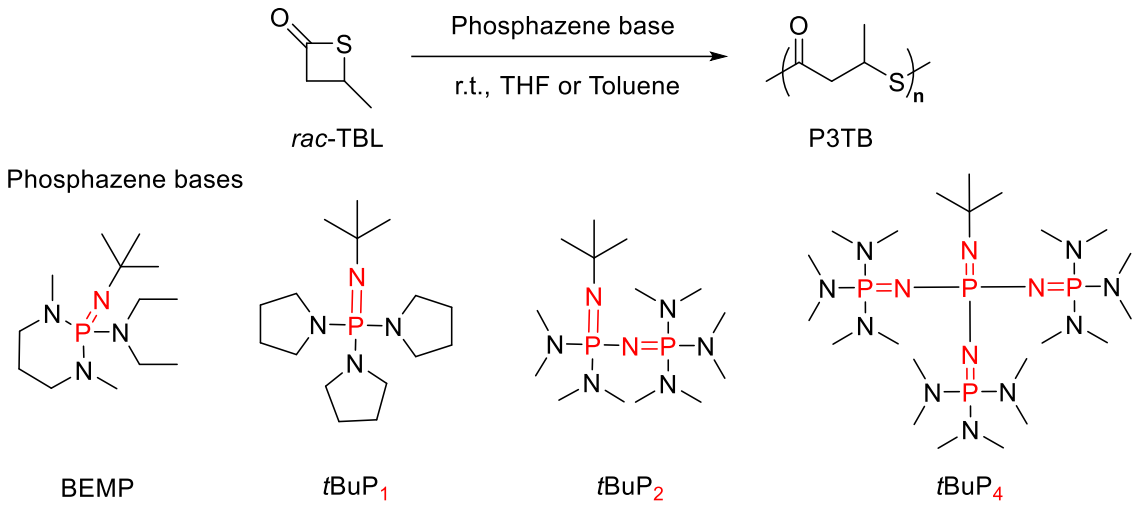

Figure 4.3. Phosphazene bases used in ROP of *rac*-TBL in this study.

4.2 Results and Discussion

Initially, the ROP of *rac*-TBL was initiated by BEMP (Figure 4.2), a common phosphazene base (pK_a = 26.9 in CH_3CN) used in ROP of β-lactones,[9] at the $[TBL]_0/[BEMP]_0$ feed ratio of 40:1 at 60 °C in bulk (neat) conditions (Table 4.1, entry HL692); this base and these initial conditions were selected based on previous work in our group on organopolymerization of *rac*-BPL^{OR}.[11] The ROP reaction reached 99% conversion of TBL within less than 3 h; this is a higher activity than that observed with *rac*-BPL^{OR}, regardless of the nature of the ether moiety of the CH_2OR group. At this stage, a more detailed kinetic monitoring under these conditions has not been established. Yet, we can assume that the reaction should achieve high conversion within less than 30 min, as the ROP of 50 equiv. of *rac*-BL was completed in less than 30 min under identical conditions,[9] which should be in line with our early findings summarized in Chapter 3, that is, *rac*-TBL is a much more reactive monomer than its oxo analog.[12] Upon lowering the temperature to room temperature, the reaction proceeded to 52% conversion after 7 h at the feed ratio of 50:1 in toluene (Table 4.1, entry HL479). In both cases, the molar mass measured by SEC (uncorrected values) were much higher than the theoretical ones and the dispersity was broad ($Đ_M$ = 1.51 and 1.79, respectively); this is indicative of a poor, slow initiation efficiency, and/or undesirable side-reactions.

Table 4.1. Preliminary results on the ROP of *rac*-TBL promoted by phosphazene bases.[a]

Ref.	[I][b]	Co-init.[c]	$[M]_0/[I]_0$ /[co-init.]$_0$	T_p[d] (°C)	Solvent	Reaction time[e] (h)	TBL Conv.[f] (%)	$M_{n,theo}$[g] (kg mol^{-1})	$M_{n,NMR}$[h] (kg mol^{-1})	$M_{n,SEC}$[i] (kg mol^{-1})	$Đ_M$[i]
HL692	BEMP	-	40:1:0	60	bulk	3	> 99	4.1	20.6	12.5	1.51
HL479	BEMP	-	50:1:0	r.t.	Tol.	7	52	2.6	18.0	8.7	1.79
HL482	*t*BuP$_1$	-	50:1:0	r.t.	Tol.	7	59	3.0	9.0	9.2	1.68
HL480	*t*BuP$_2$	-	50:1:0	r.t.	Tol.	7	66	3.4	6.8	7.5	1.88
HL697	*t*BuP$_4$	-	25:1:0	r.t.	Tol.	5	90	2.3	8.8	8.9	2.03
HL481	*t*BuP$_4$	-	50:1:0	r.t.	Tol.	7	90	4.6	9.5	8.2	1.60
HL553	*t*BuP$_4$	-	50:1:0	r.t.	Tol.	7.5	92	4.7	26.7	7.5	1.65
HL698	*t*BuP$_4$	-	100:1:0	r.t.	Tol.	17.5	94	9.6	22.4	12.4	1.64
HL699	*t*BuP$_4$	-	25:1:0	r.t.	THF	4	93	2.4	5.2	*n.d.*[j]	*n.d.*
HL683	*t*BuP$_4$	-	50:1:0	r.t.	THF	8	89	4.6	4.9	6.8	1.46
HL701	*t*BuP$_4$	-	100:1:0	r.t.	THF	17	94	9.6	16.4	*n.d.*	*n.d.*
HL685	*t*BuP$_4$	BnOH	25:1:1	r.t.	THF	4	78	2.1	3.6	5.8	1.51
HL682	*t*BuP$_4$	BnOH	50:1:1	r.t.	THF	8	95	4.9	6.7	8.4	1.49
HL686	*t*BuP$_4$	BnOH	100:1:1	r.t.	THF	16	89	9.1	8.5	10.6	1.43
HL702	*t*BuP$_4$	BnSH	50:1:1	r.t.	THF	8	93	4.8	24.5	*n.d.*	*n.d.*
HL514	*t*BuP$_4$	BnSH	50:1:1	r.t.	Tol.	7	73	3.8	5.0	8.2	1.58
HL449	*t*BuP$_4$	BnSH	100:1:1	r.t.	Tol.	14.2	65	6.7	9.2	14.9	1.58
HL450	*t*BuP$_4$	BnSH	100:1:1	r.t.	Tol.	17.5	73	7.5	6.7	13.2	1.31
HL378	*t*BuP$_4$	*i*PrOH	50:1:1	r.t.	Tol.	3.25	45	2.3	--	5.3	1.58

[a] Polymerization conditions: $[TBL]_0$ = 1.0 M; [b] initiator denoted as [I]; [c] co-initiator/co-reagent; [d] polymerization temperature (T_p); [e] reaction time (t); [f] conversion of *rac*-TBL as determined by ^{1}H NMR analysis of the crude polymerization mixture; [g] molar mass calculated according to $M_{n,theo} = [M]_0/[I]_0 \times Conv._{TBL} \times M_{w,TBL}$; [h] molar mass determined from ^{1}H NMR; [i] number-average molar mass ($M_{n,SEC}$) and dispersity ($Đ_M$) determined by SEC analysis in THF at 30 °C *vs.* polystyrene standards (uncorrected values); [j] *n.d.* = not determined.

Switching to *t*BuP$_1$, another phosphazene with a similar basicity (pK_a = 28.6 in CH_3CN), the ROP of 50 equiv. of *rac*-BL at room temperature in toluene proceeded in 59% conversion within 7 h (Table 4.1, entry HL482). When the ROP of *rac*-TBL was operated with a more basic phosphazene, *t*BuP$_2$ (pK_a = 33.5 in CH_3CN), a slight improvement in conversion was noted (*ca.* 66%; Table 4.1, entry HL480). The use of the *t*BuP$_4$ phosphazene superbase (pK_a = 42.7 in CH_3CN) allowed 90% monomer conversion under the same reaction conditions (Table 4.1, entry HL481). Hence, the polymerization rate appears to increase monotonously with the basicity of the phosphazene as BEMP ~ *t*BuP$_1$ < *t*BuP$_2$ < *t*BuP$_4$. This reactivity trend suggests that initiation of the ROP proceeds by abstraction of the relatively acidic proton from the monomer to eventually generate a carboxylate initiating/chain-propagating species (Figure 4.4, bottom). Possibly, the other phosphazene bases, *i.e.*, BEMP, *t*BuP$_1$, with less

basicity may trigger polymerization through nucleophilic attack of the carbonyl group of *rac*-TBL in a more controlled manner (Figure 4.4, top).[13,14] For most experiments conducted with phosphazenes *t*BuP$_n$ (n = 1,2,4) in toluene, the molar mass values obtained from SEC are similar to that calculated from the ^{1}H NMR analysis (*vide infra*), yet still with a relatively broad dispersity ($Đ_M$ = 1.68-1.88).

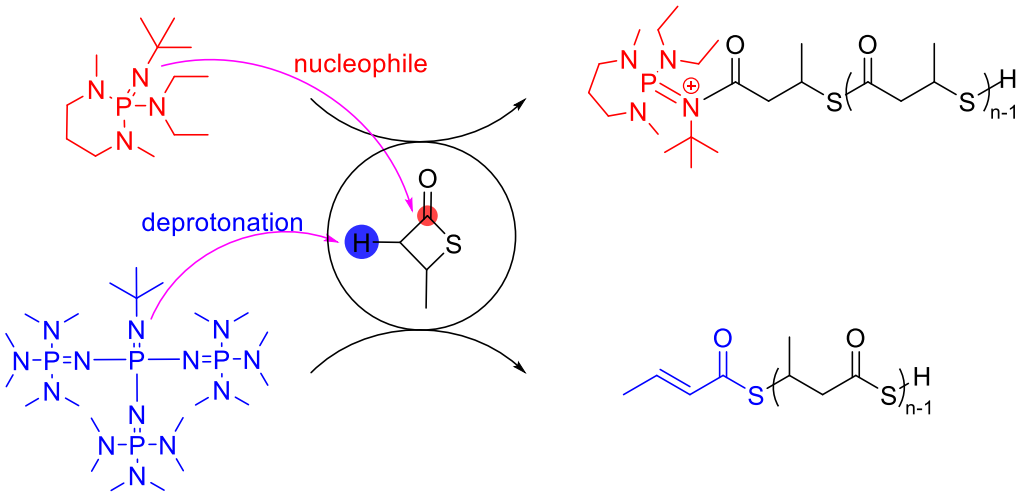

Figure 4.4. Plausible initiating steps in ROP of *rac*-TBL promoted by different phosphazene bases.

The ROP of *rac*-TBL mediated by *t*BuP$_4$ carried out in THF, a more polar solvent (ε = 7.39 vs. 2.38 for toluene), resulted in an apparently more controlled reaction, as appreciated from the molar mass values as determined by SEC and NMR and also by the reduced dispersity value (Table 4.1, entry HL683). Moreover, in THF, the molar mass of the resulting P3TB could be better controlled tuned by altering the [*rac*-TBL]$_0$/[*t*BuP$_4$]$_0$ feed ratio. For example, with the [*rac*-TBL]$_0$/[*t*BuP$_4$]$_0$ feed ratios of 25:1 and 100:1, the resulting polymers have high M_n values of 5.2 and 16.4 kg mol^{-1}, respectively (Table 4.1, entries HL699 and HL701). We assume this is because the more polar solvent better stabilizes the ion pair of the active species (*vide infra*).[8,15,16]

The polymerization was apparently more effective when *t*BuP$_4$ was premixed with BnOH at room temperature, followed by the addition of *rac*-TBL. Thus, when the feed ratio increased from [*rac*-TBL]$_0$/[*t*BuP$_4$]$_0$/[BnOH]$_0$ = 25:1:1 to 100:1:1 (Table 4.1, entries HL685, HL682 and HL686), the molar mass of the resulting P3TB increased from low $M_{n,SEC}$ = 5.8 kg mol^{-1} to $M_{n,SEC}$ = 10.6 kg mol^{-1}. However, when the ROP of *rac*-TBL in toluene was performed by *t*BuP$_4$ in the presence of benzyl mercaptan (BnSH) instead of BnOH, the polymerization rate did not improve compared with the *rac*-TBL polymerization without coinitiator (Table 4.1, entries HL514 and HL618)

To gain insight into the macromolecular topology (linear and/or cyclic) and also into the chain end-groups, the resulting P3TB were analyzed by matrix-assisted laser desorption ionization-time of flight mass spectrometry analysis (MALDI-ToF MS). As mentioned in Chapter 3, the key feature of the MALDI technique is the laser irradiation of the sample dispersed in an ultraviolet absorbing matrix; this requires the analyte molecules to be embedded throughout the matrix so that they are completely

isolated from one another, and also, intense laser pulses ablate the bulk portions of this 'solid solution' over a short duration to induce sublimation of the matrix. In this regard, we chose the matrix, namely *trans*-2-[3-(4-*tert*-butylphenyl)-2-methyl-2-propenylidene]malononitrile (DCTB) which revealed effective toward P3TBs produced by yttrium catalysts (see Chapter 3). However, for the present P3TB samples made from organocatalysts *t*BuP$_4$, *t*BuP$_2$ and BEMP, no signal (apart from that attributed to the protonated phosphazene base) was observed, even upon increasing the power of laser to a very high level. As a control experiment, a cyclic P3TB sample prepared by yttrium catalyst (Table 4.1, entry HL337) was mixed with a small quantity (*ca.* 1%) of BEMP, and the resulting sample was subjected to MALDI-ToF MS analysis: again, the MS signal of macromolecules completely vanished. Obviously, phosphazene bases are highly detrimental to obtain MALDI-ToF mass spectra of P3TB samples. Hence, thus far, this technique proved ineffective for obtaining the macromolecular structures of P3TBs prepared by phosphazene bases. Only in the case of a P3TB sample prepared by *t*BuP$_1$, the MALDI-ToF MS spectrum returned signals for several populations, among which cyclic P3TB was unambiguously identified (Table 4.1, entry HL482; Figure S36 and Figure S37). However, in our opinion, the latter population may well be overexpressed as compared to the population of crotonate end-capped P3TB, which is clearly observed in the NMR spectrum (see Figure 4.8).

The microstructure of the resulting P3TBs was then evaluated by ^{1}H, ^{13}C{^{1}H} and Diffusion-Ordered Spectroscopy (DOSY) NMR analyses to probe the nature of the end-capping groups of the P3TB, the number of populations in an attempt to suggest the possible corresponding ROP mechanism(s). All the ^{1}H and ^{13}C{^{1}H} NMR spectra clearly displayed the characteristic signals corresponding to the TBL repeating units, consistent with our previous work in Chapter 3.[12] The nature of one of the end-groups of P3TB, that is, a crotonate moiety, produced by phosphazene bases without any exogenous protic initiator (Table 4.1, entries HL698, HL480, HL482, HL481), was obviously observed: *e.g.* the ^{1}H NMR spectra (Figures 4.5, 4.8 and 4.9), featured resonances at δ 6.86 ppm (CH$_3$C*H*=CH−), 6.04 ppm (CH$_3$CH=C*H*−), and 1.85 ppm (C*H*$_3$CH=CH−).

A DOSY analysis was performed on an isolated P3TB (Figure 4.7, Table 4.1, entry HL698). The measurement of the diffusion coefficient allows one to check if the crotonate group and the TBL repeating units are on the same macromolecule (or if it is a mixture of two distinct compounds). Indeed, in the former case, they will have the same diffusion coefficient, whereas in the latter case, two diffusion coefficients will be detected. The DOSY analysis shows that the TBL repeating units (bottom part) and the crotonate group ((Figure 4.7, small figure inside) have the same diffusion coefficient, indicating the crotonate group is associated with the P3TB chain. More interestingly, the DOSY spectrum revealed the presence of another species, {*t*BuP$_4$H$^+$}, suggesting that *t*BuP$_4$ alone polymerizes *rac*-TBL through deprotonation of the acidic hydrogen of *rac*-TBL.

To further probe this hypothesis, we next investigated the stoichiometric reaction between *t*BuP$_4$ and *rac*-TBL in C$_6$D$_6$ at room temperature (Figure 4.9). This reaction was monitored by ^{31}P NMR (Figure 4.9) and actually revealed the formation of the phosphazenium cation ({*t*BuP$_4$H$^+$}, the ^{1}H NMR

spectrum of {*t*BuP$_4$H$^+$} featured resonances at δ 1.64 ppm (***Me***$_2$N−P) 1.25 ppm (***t*Bu**−N=P); Figure 4.5), which is in line with the findings of Chen on ring-opening polymerization of γ-butyrolactone promoted by *t*BuP$_4$ without co-initiator.[14] However, the nature of the other end-capping group remains to be established.

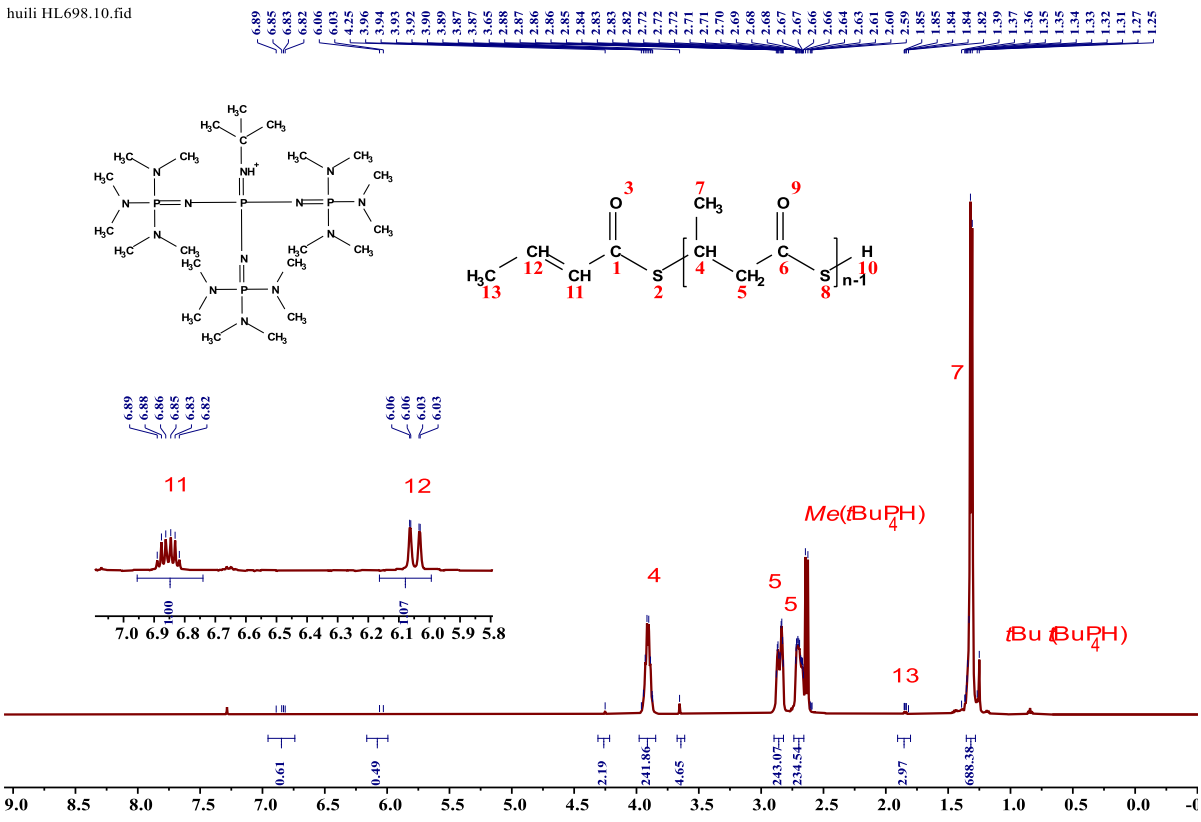

Figure 4.5. ^{1}H NMR (500 MHz, $CDCl_3$, 25 °C) spectrum of a P3TB prepared with *t*BuP$_4$ in toluene without co-initiator (Table 4.1, entry HL698).

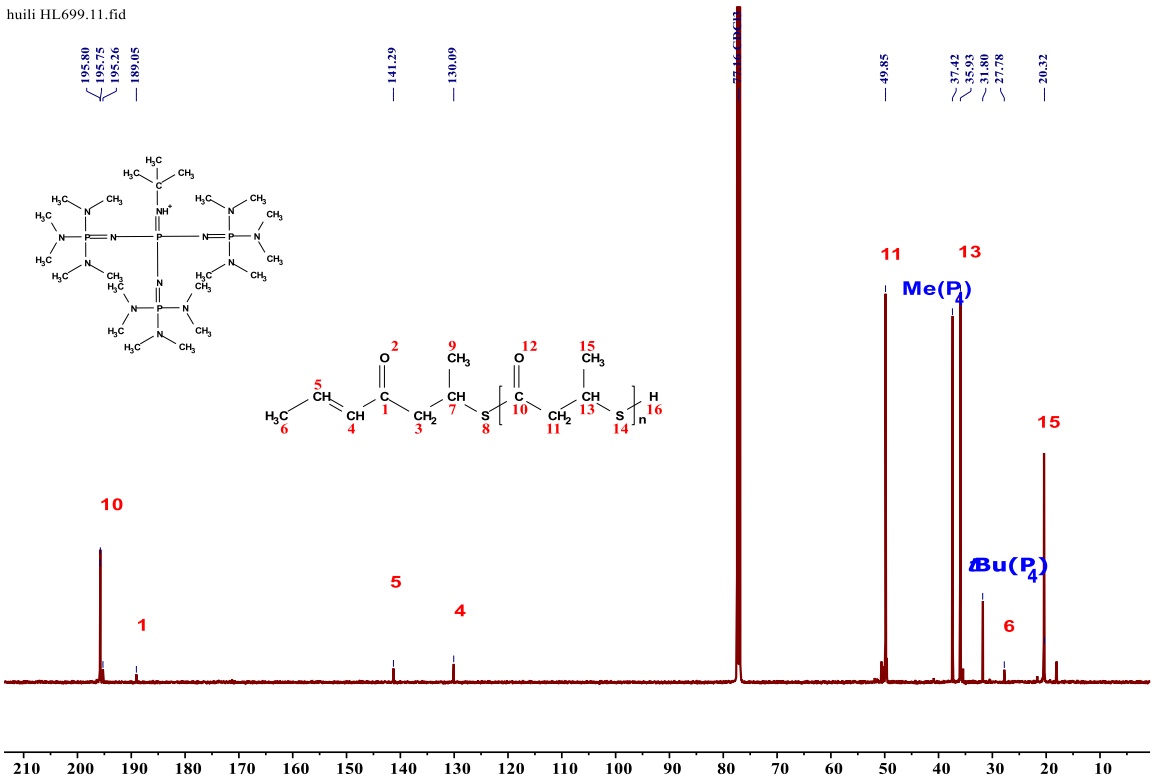

Figure 4.6. $^{13}C\{^{1}H\}$ NMR (125 MHz, $CDCl_3$, 25 °C) spectrum of a P3TB prepared with *t*BuP_4 in toluene without co-initiator (Table 4.1, entry HL699).

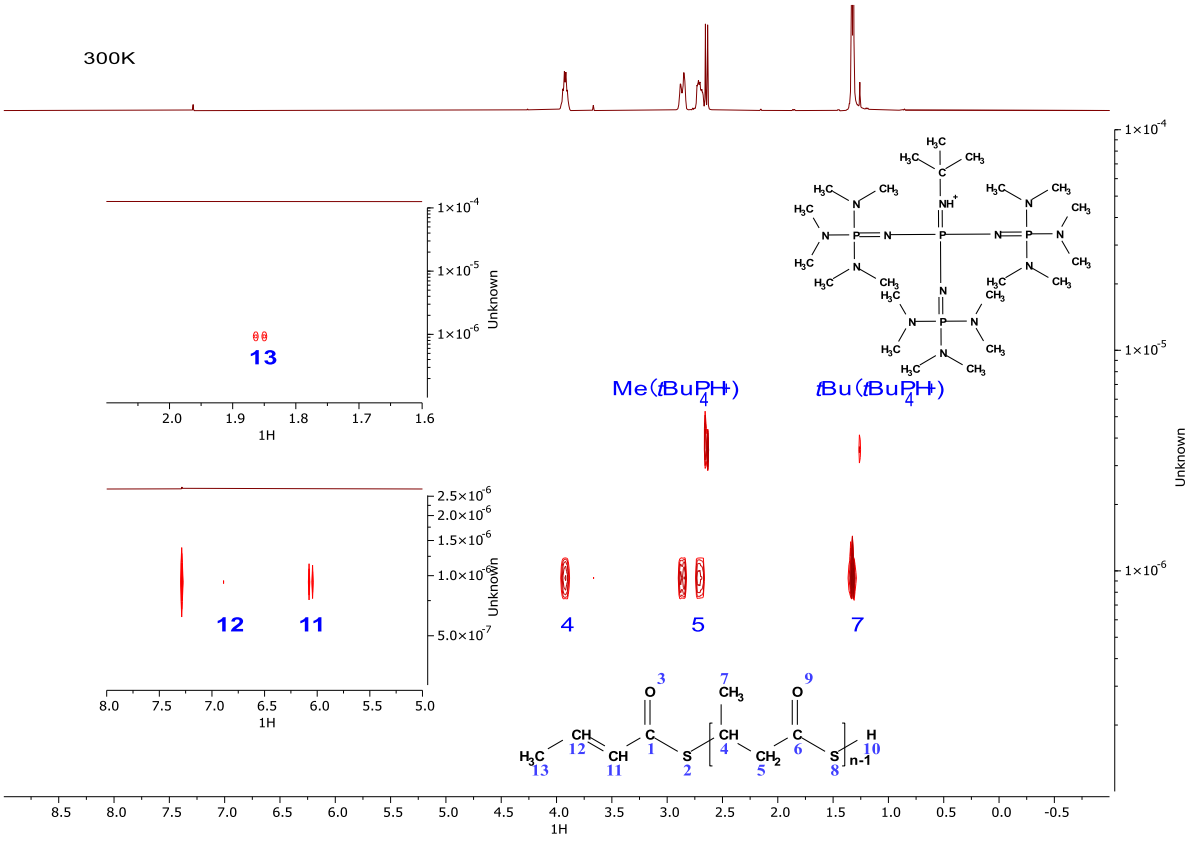

Figure 4.7. DOSY NMR spectrum (500 MHz, $CDCl_3$, 25 °C) of a P3TB prepared with *t*BuP_4 in toluene without co-initiator (Table 4.1, entry HL698).

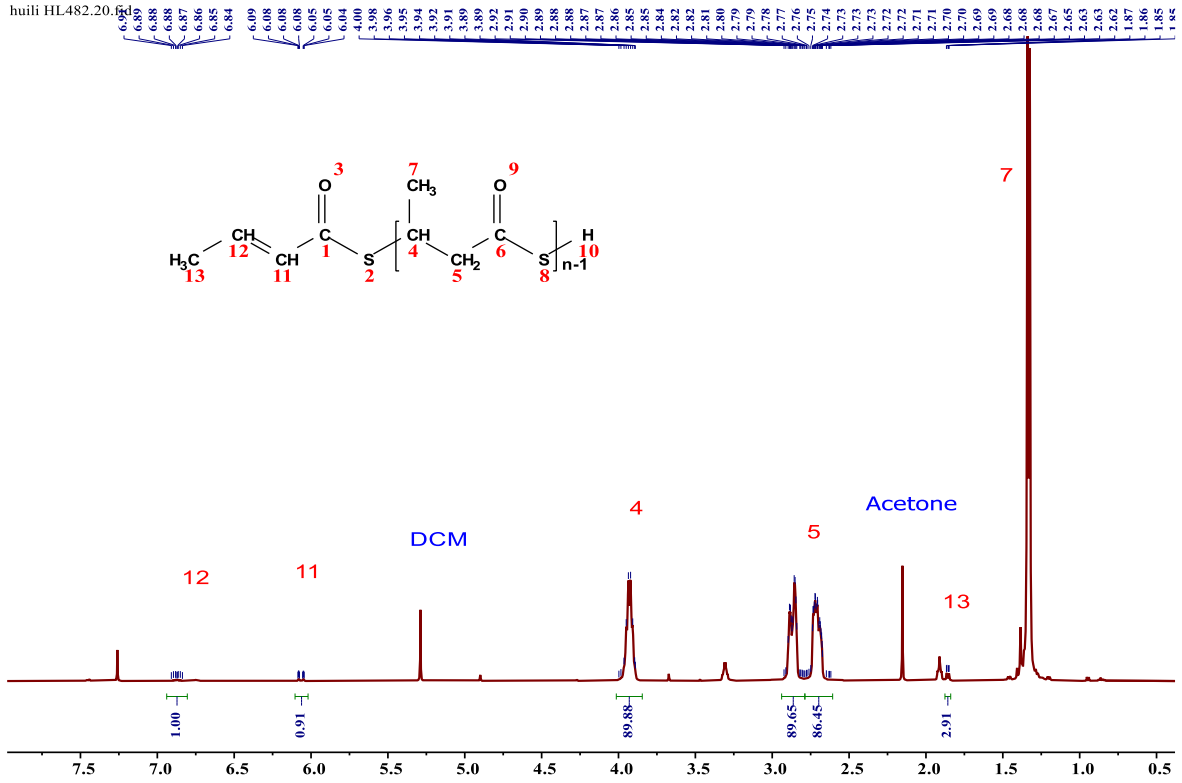

Figure 4.8. ^{1}H NMR (500 MHz, $CDCl_3$, 25 °C) spectrum of a P3TB prepared with *t*BuP_1 without co-initiator (Table 4.1, entry HL482).

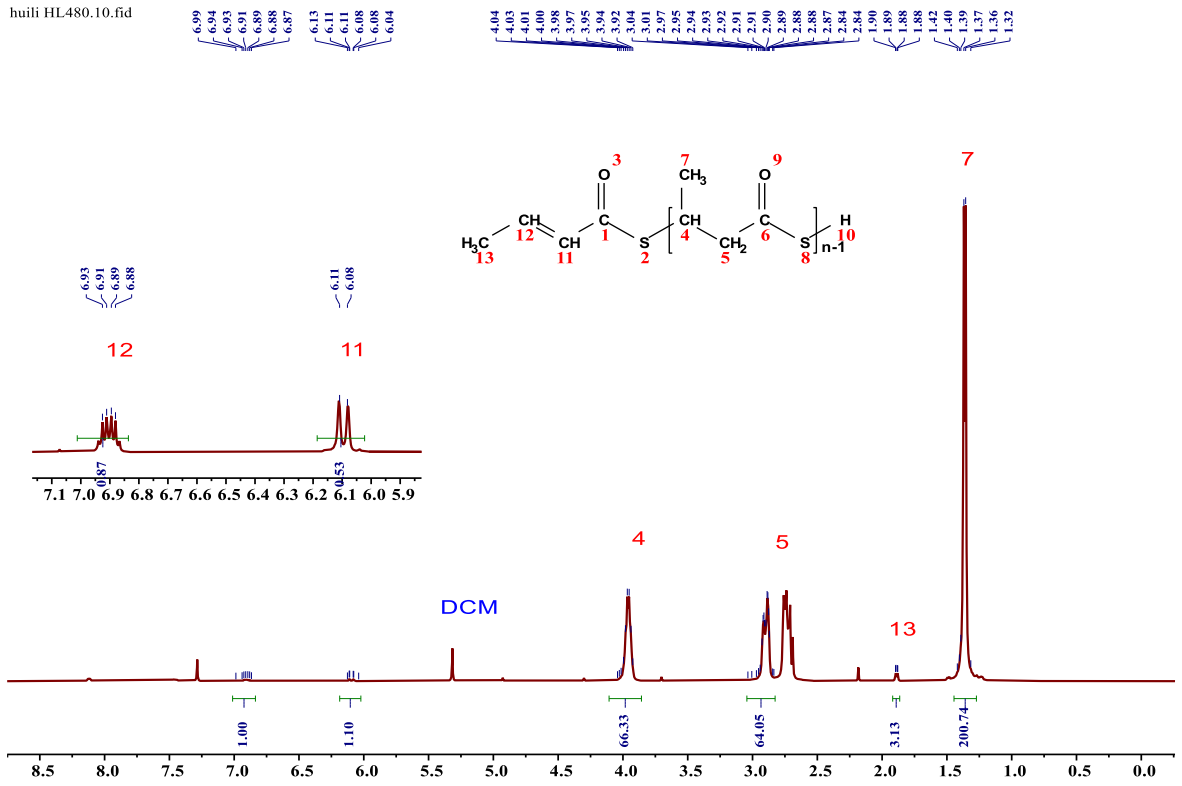

Figure 4.9. ^{1}H NMR (500 MHz, $CDCl_3$, 25 °C) spectrum of a P3TB prepared with *t*BuP_2 without co-initiator (Table 4.1, entry HL480).

As evidenced by DOSY analysis, the ROP of *rac*-TBL promoted by *t*BuP$_4$ in toluene at room temperature gives only one population of macromolecules, the crotonate-capped P3TB. Based on the relative intensity of the crotonate signals, the molar mass value of the resulting P3TBs can be easily determined by ^{1}H NMR ($M_{n,NMR}$). For example, the ROP of *rac*-TBL promoted by *t*BuP$_4$ at a $[TBL]_0/[t\text{BuP}_4]_0$ feed ratio of 50:1 in toluene, gave the corresponding P3TB with a molar mass value determined by NMR of 9,500 g mol^{-1}, to some extent close to of the (uncorrected) value measured by SEC (8,200 g mol^{-1}), yet the double of that expected based on a fully efficient initiation (Table 4.1, entry HL481).

4.3 Conclusion

Preliminary attempts on the ROP of *rac*-TBL mediated by phosphazene bases of different basicity, namely BEMP, *t*BuP$_1$, *t*BuP$_2$, and *t*BuP$_4$, were documented herein. The formation of linear P3TB was suggested by NMR analysis, especially those produced by *t*BuP$_4$ in the absence of a co-initiator. Yet, a clear pattern of the mechanism at play has not been established, and further work will focus on the initiating step for different phosphazene bases. Subsequently, the properties of the high molar mass linear P3TBs shall be compared with those of cyclic P3TBs.

Experimental Section

General Considerations. All syntheses and manipulations of air- and moisture-sensitive materials were carried out in flame-dried Schlenk-type glassware on a vacuum dual-manifold Schlenk line or in an argon-filled glovebox. HPLC-grade organic solvents were first purged extensively with nitrogen during filling 20 L-solvent reservoirs, and then dried by passage through Q-5 supported copper catalyst [for toluene] stainless steel columns. Tetrahydrofuran (THF) and toluene (Tol.) were degassed and dried over sodium/benzophenone followed by distillation under argon. *iso*-Propanol (*i*PrOH), benzyl alcohol (BnOH), benzyl mercaptan (BnSH) were purified by distillation from CaH_2. 2-*tert*-Butylimino-2-diethylamino-1,3-dimethylperhydro-1,3,2-diazaphosphorine (BEMP, 1.0 M in hexane); *tert*-butylimino-tri(pyrrolidino)phosphorane (*t*BuP$_1$); 1-*tert*-butyl-2,2,4,4,4-pentakis(dimethylamino)-2λ^5,4λ^5-catenadi(phosphazene) (*t*BuP$_2$, 2.0 M in THF); 1-*tert*-butyl-4,4,4-tris(dimethylamino)-2,2-bis-[tris(dimethylamino)phosphoranylidenamino]-2λ^5,4λ^5-catenadi(phosphazene) (*t*BuP$_4$, 0.8 M in hexane) were purchased from Aldrich Chemical Co. and the solvents were removed in vacuo prior to use. *rac*-Thiobutyrolactone (*rac*-TBL) was synthesized according to the procedure reported before (see Chapter 3).

^{1}H (500, 400 and 300 MHz), ^{13}C{^{1}H} (125 and 100 MHz), ^{31}P{^{1}H} (202 MHz) and two-dimensional (2D DOSY, 500 MHz) NMR spectra were recorded on Bruker Avance III HD 500, Av III 400 or Av III 300 spectrometers at 25 °C, fitted with a direct broadband 5 mm probe head (BBO) carefully tuned on both ^{1}H and ^{13}C channels. 1D ^{13}C spectra were acquired using Bruker standard zgpg30 sequence, acquisition time was 1.05 s and relaxation delay D1 5.00 s.

Number and weight average molar mass ($M_{n,SEC}$ and $M_{w,SEC}$) and dispersity ($Đ_M = M_w/M_n$) values of the polymers were determined by size-exclusion chromatography (SEC) in THF at 30 °C (flow rate = 1.0 mL min^{-1}) on a Polymer Laboratories PL50 apparatus equipped with a refractive index detector and a set of two ResiPore PLgel 3 μm MIXED-D 300 × 7.5 mm columns. The polymer samples were dissolved in THF (2 mg mL^{-1}). All elution curves were calibrated with polystyrene standards (M_n range = 580 – 126,000 g mol^{-1}); the $M_{n,SEC}$ values of the P3TB reported in all Tables are uncorrected for the possible difference in hydrodynamic radius *versus* that of polystyrene.

High resolution Matrix Assisted Laser Desorption Ionization – Time of Flight (MALDI-ToF) mass spectrometry analyses were performed using an ULTRAFLEX III TOF/TOF spectrometer (Bruker Daltonik Gmbh, Bremen, Germany) in positive ionization mode at Centre Régional de Mesures Physiques de l'Ouest (CRMPO, ScanMAT UAR 2025 CNRS, Université de Rennes 1). Spectra were recorded using reflectron mode and an accelerating voltage of 25 kV. A mixture of a freshly prepared solution of the polymer in CH_2Cl_2 (HPLC grade) and DCTB (*trans*-2-(3-(4-*tert*-butylphenyl)-2-methyl-2-propenylidene) malononitrile in CH_2Cl_2 (HPLC grade, 10 mg mL^{-1}), and a MeOH or CH_2Cl_2/CH_3CN (50:50, *v*/*v*) solution of the cationizing agent (NaI, 10 mg mL^{-1}) were prepared. The solutions were combined in a 1:1:1 (*v*/*v*/*v*) ratio of matrix-to-sample-to-cationizing agent. The resulting solution (0.25–

0.5 µL) was deposited onto the sample target (Prespotted AnchorChip PAC II 384/96 HCCA) and air or vacuum dried. High resolution mass spectrum of *rac*-TBL was performed using a time-of-flight Maxis 4G (Bruker Daltonik Gmbh, Bremen,Germany) in ASAP (direct introduction, desorption temperature: 45 °C) positive mode at the Centre Régional de Mesures Physiques de l'Ouest (CRMPO, ScanMAT, Université de Rennes1).

General Polymerization Procedures. Polymerizations were performed either in 5 mL glass vial inside the inert glovebox for room temperature runs or 10-mL flame-dried Schlenk flasks interfaced to the dual-manifold Schlenk line for runs using an external temperature bath. The vial was charged with a predetermined amount of phosphazene base (with or without initiator) and solvent. For runs at RT, the polymerization was initiated by rapid addition of a predetermined amount of monomer via a gastight syringe. For runs using an external temperature bath, the reactor was sealed, taken out of the glovebox, and then immersed in the external temperature bath under the predetermined temperature. After equilibration at the desired polymerization temperature, the polymerization was initiated by the rapid addition of a predetermined amount of monomer via a gastight syringe. After a desired period of time, the polymerization was quenched by addition of 0.5 mL of 'wet' commercial-grade hexanes. A 0.1 mL aliquot was taken from the reaction mixture and prepared for ^{1}H NMR analysis to obtain the percent monomer conversion data. The quenched mixture was then decanted into a vessel containing 100 mL of commercial-grade hexanes. After all of the viscous polymers precipitated at the bottom of the vessel, the supernatant liquid was decanted off. The remaining polymer was redissolved in DCM and reprecipitated to remove all of the unreacted monomer, and then dried in a vacuum oven at room temperature.

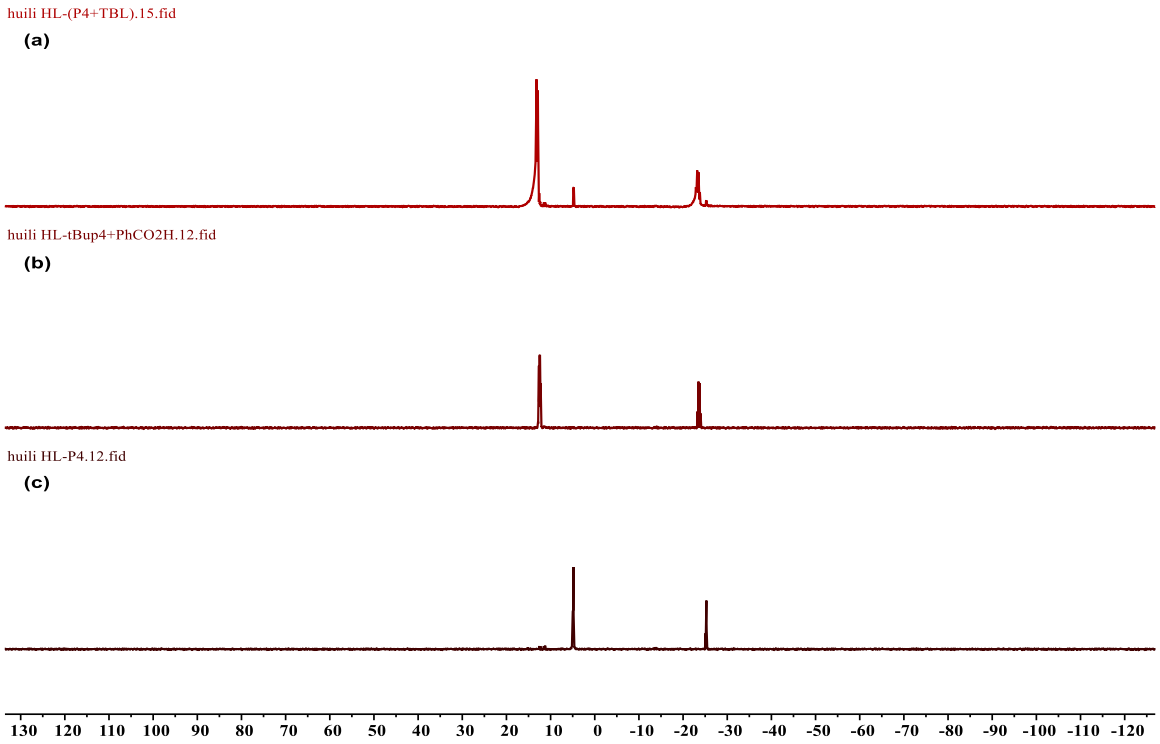

Figure 4.9. ^{31}P NMR (202 MHz, C_6D_6, 25 °C) spectra of: (a) 1:1 mixture of *t*BuP$_4$ and *rac*-TBL; (b) 1:1 mixture of *t*BuP$_4$ and benzoic acid; (c) *t*BuP$_4$.

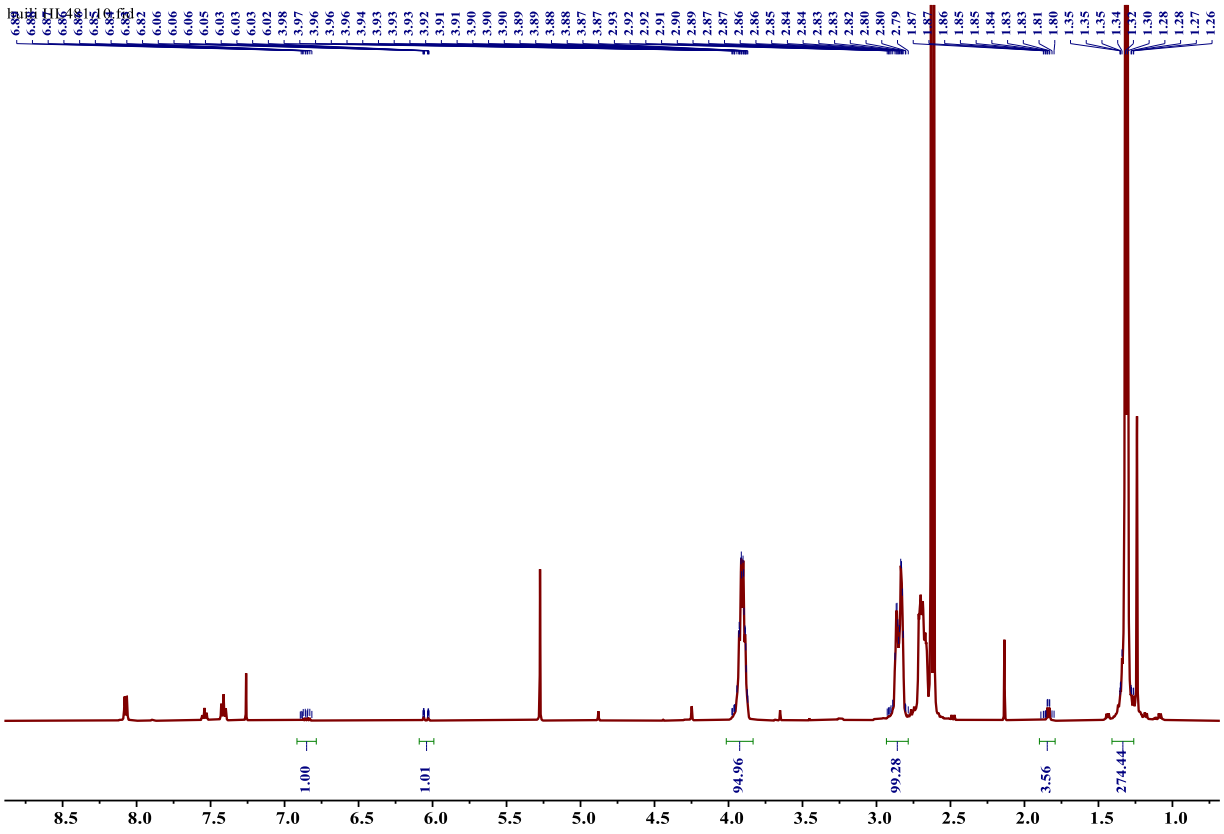

Figure 4.10. ^{1}H NMR (500 MHz, $CDCl_3$, 25 °C) spectrum of a P3TB prepared with *t*BuP$_4$ (Table 4.1, entry HL481).

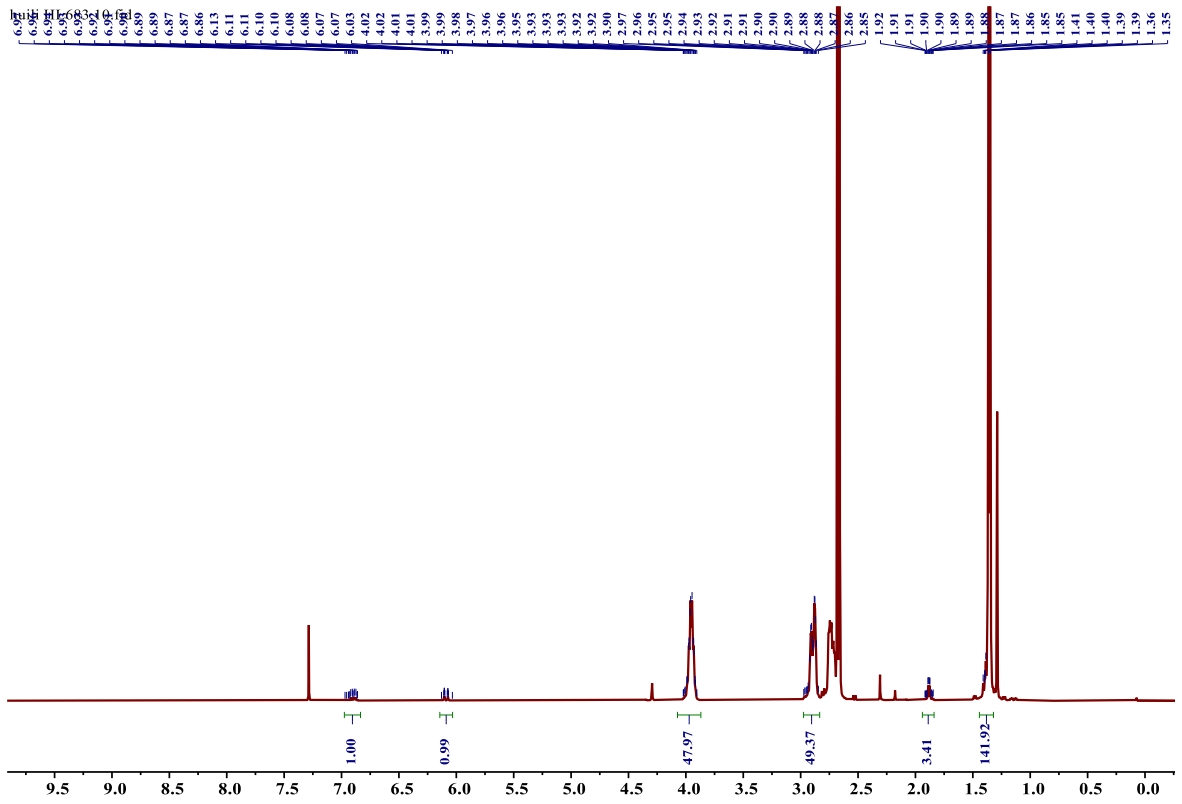

Figure 4.11. ^{1}H NMR (500 MHz, $CDCl_3$, 25 °C) spectrum of a P3TB prepared with *t*BuP_4 (Table 4.1, entry HL683).

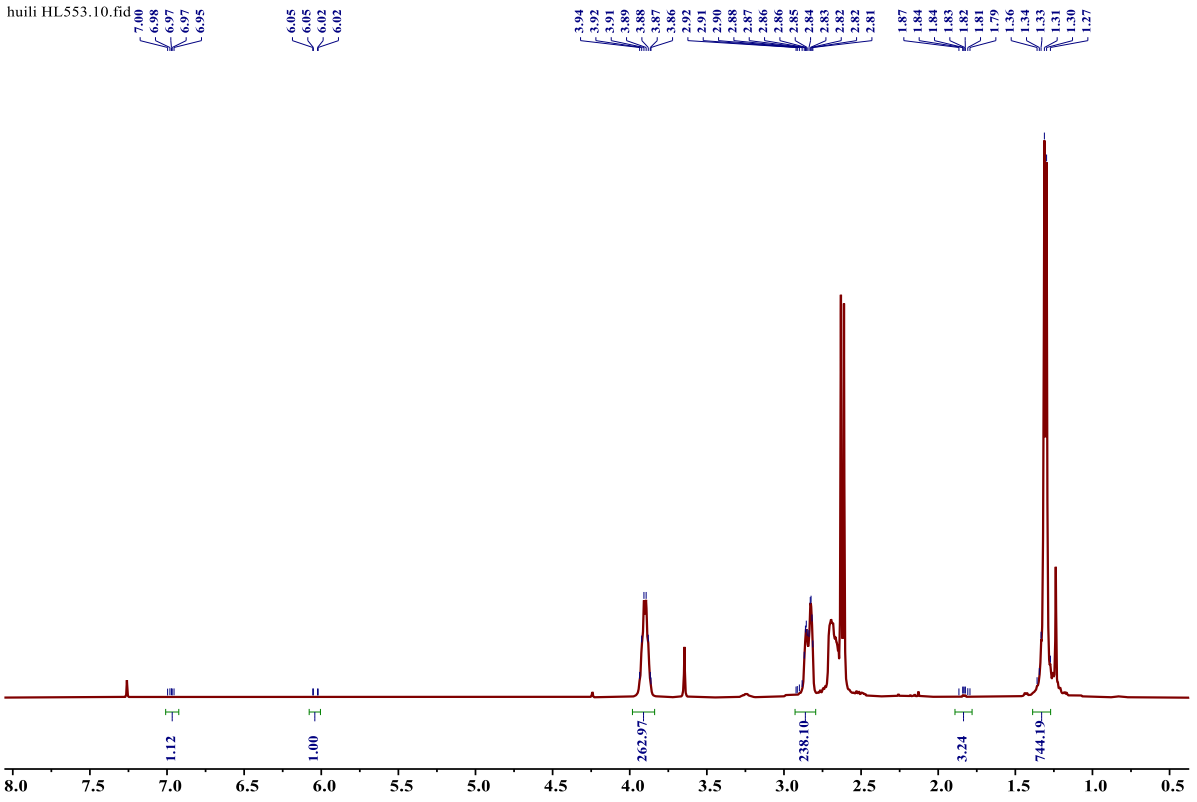

Figure 4.12. ^{1}H NMR (500 MHz, $CDCl_3$, 25 °C) spectrum of a P3TB prepared with *t*BuP_4 (Table 4.1, entry HL553).

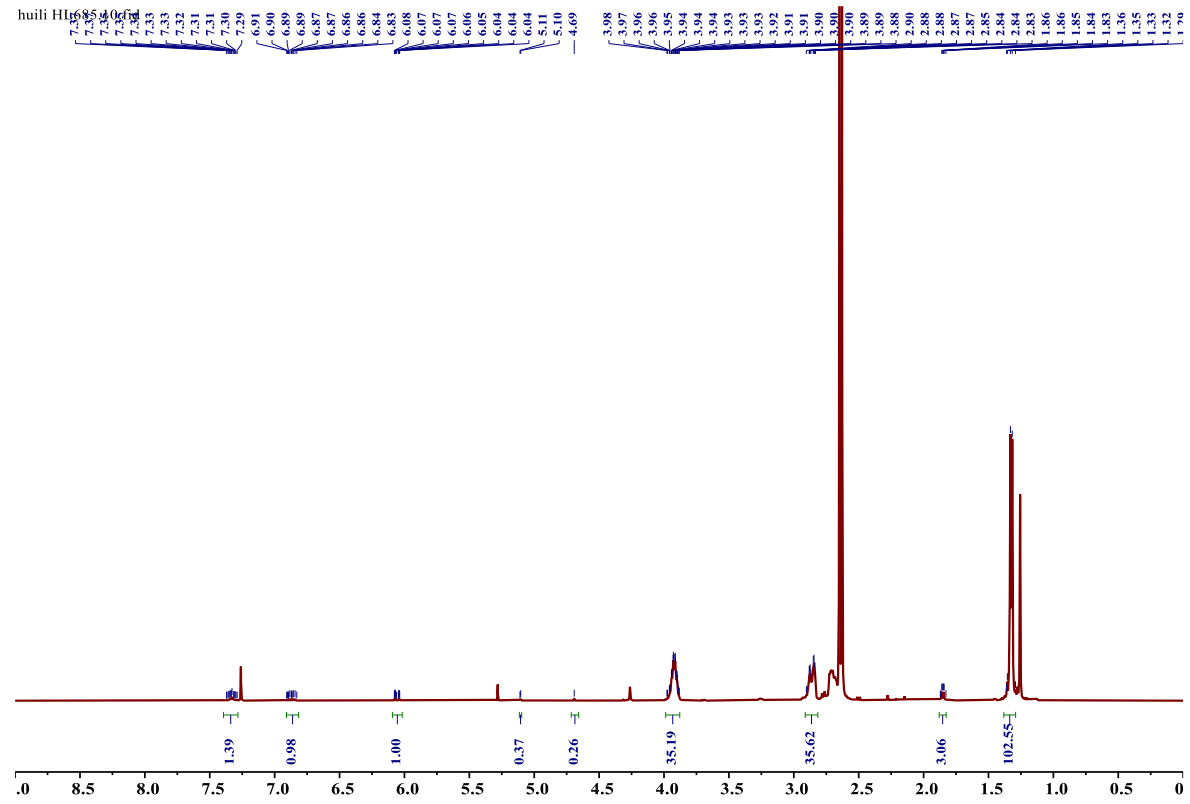

Figure 4.13. ^{1}H NMR (500 MHz, $CDCl_3$, 25 °C) spectrum of a P3TB prepared with *t*BuP_4 in the presence of BnOH (Table 4.1, entry HL685).

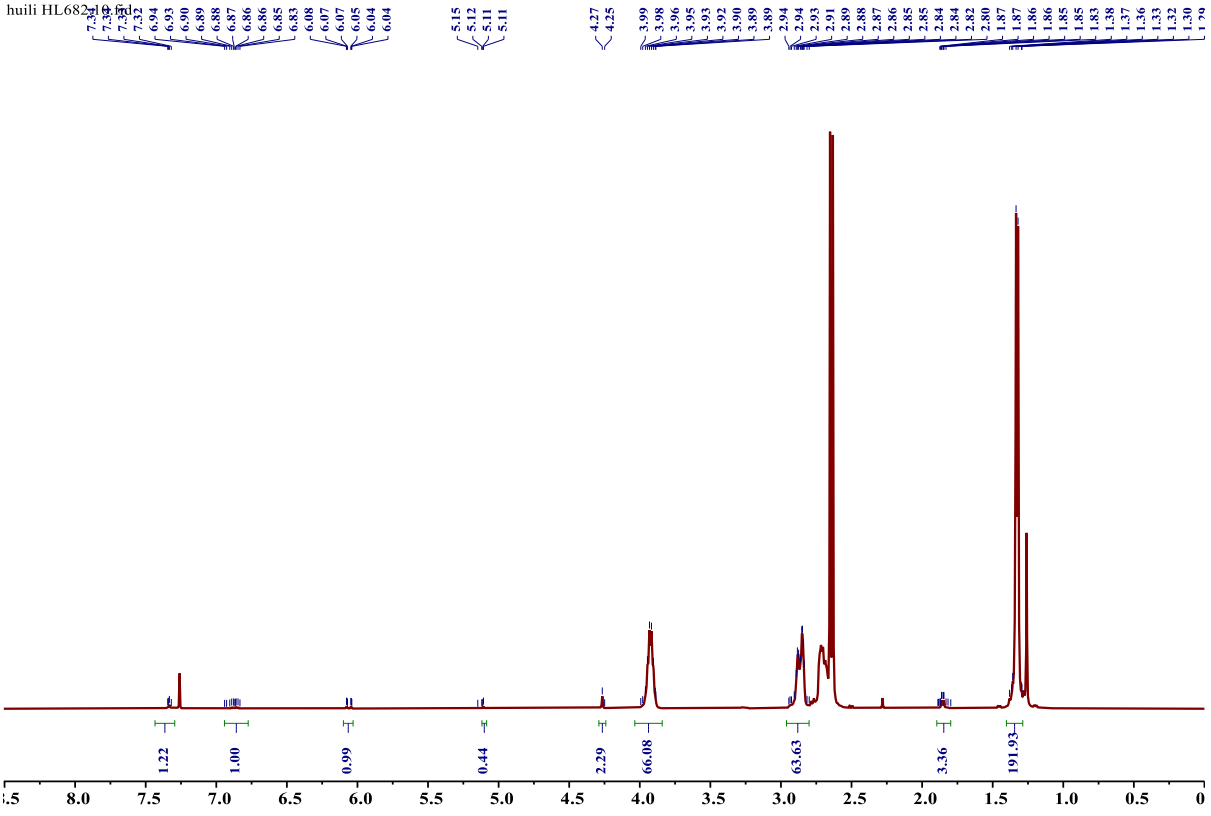

Figure 4.14. ^{1}H NMR (500 MHz, $CDCl_3$, 25 °C) spectrum of a P3TB prepared with *t*BuP_4 in the presence of BnOH (Table 4.1, entry HL682).

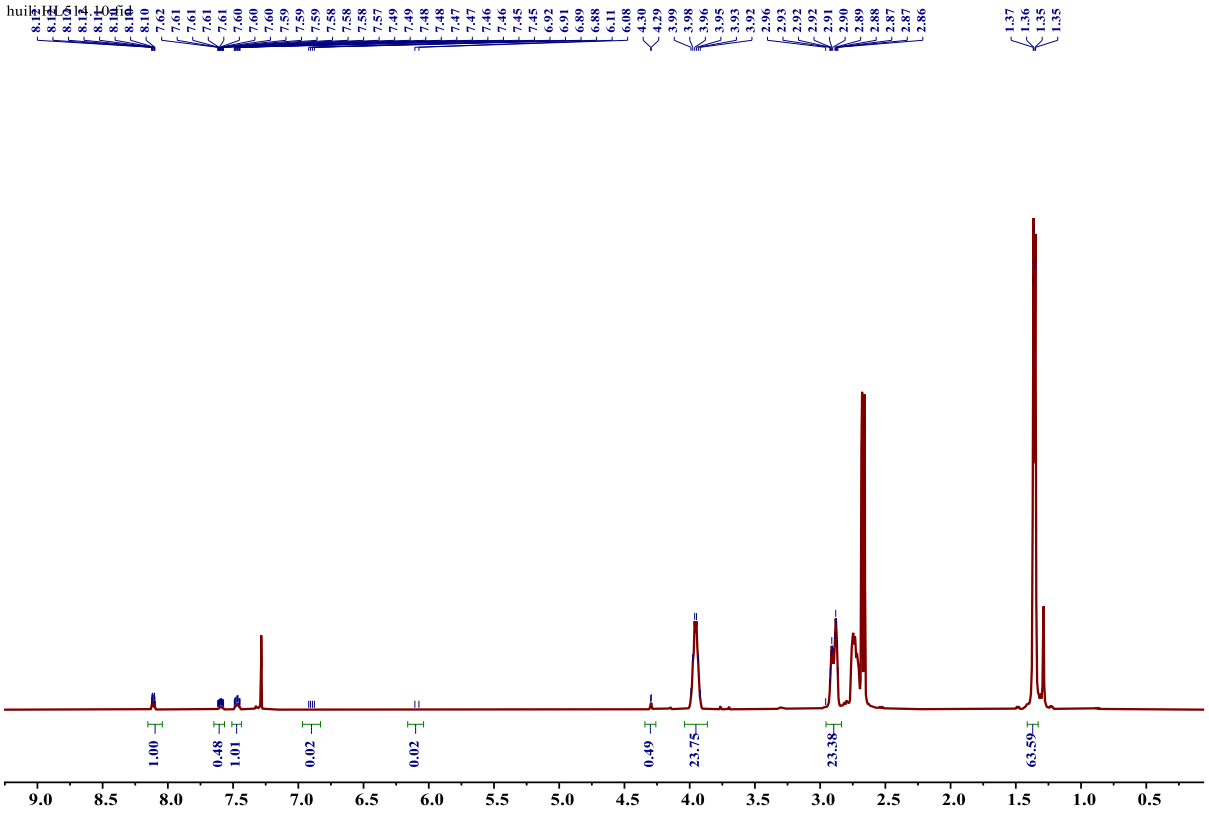

Figure 4.15. ^{1}H NMR (500 MHz, $CDCl_3$, 25 °C) spectrum of a P3TB prepared with *t*BuP_4 in the presence of BnSH (Table 4.1, entry HL514).

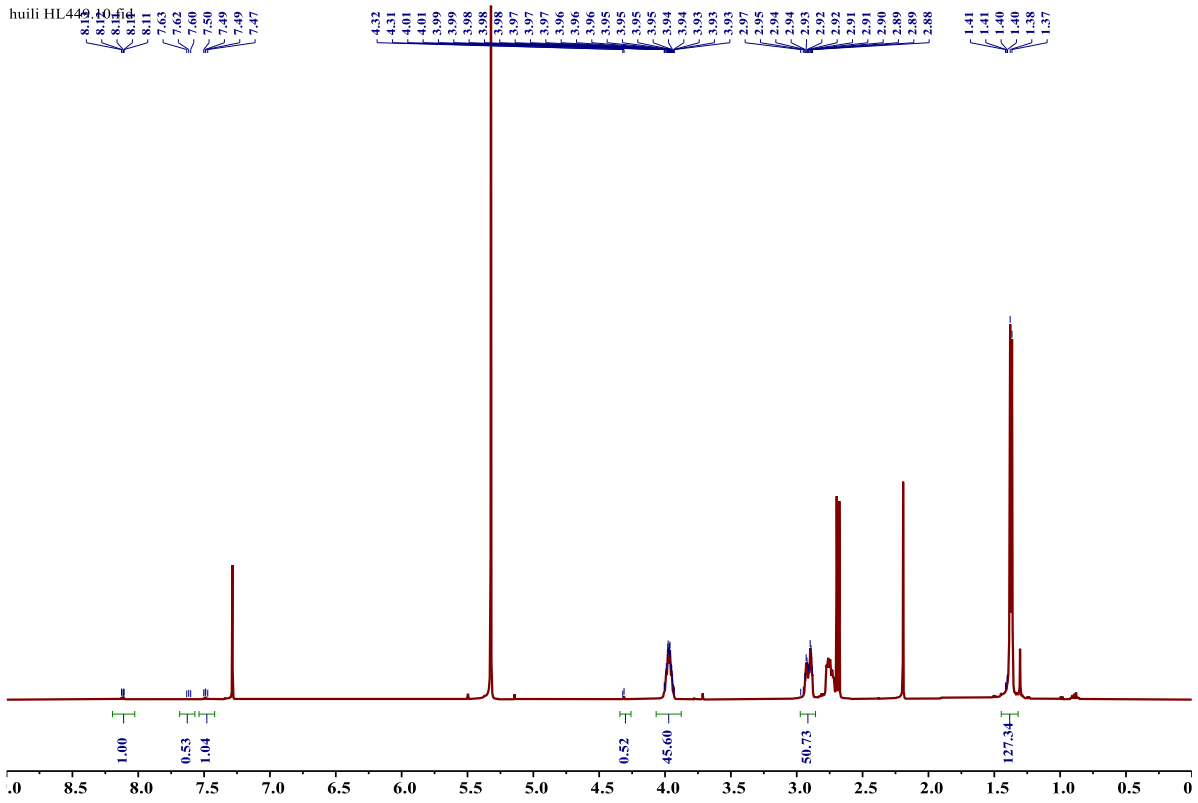

Figure 4.16. ^{1}H NMR (500 MHz, $CDCl_3$, 25 °C) spectrum of a P3TB prepared with *t*BuP_4 in the presence of BnSH (Table 4.1, entry HL449).

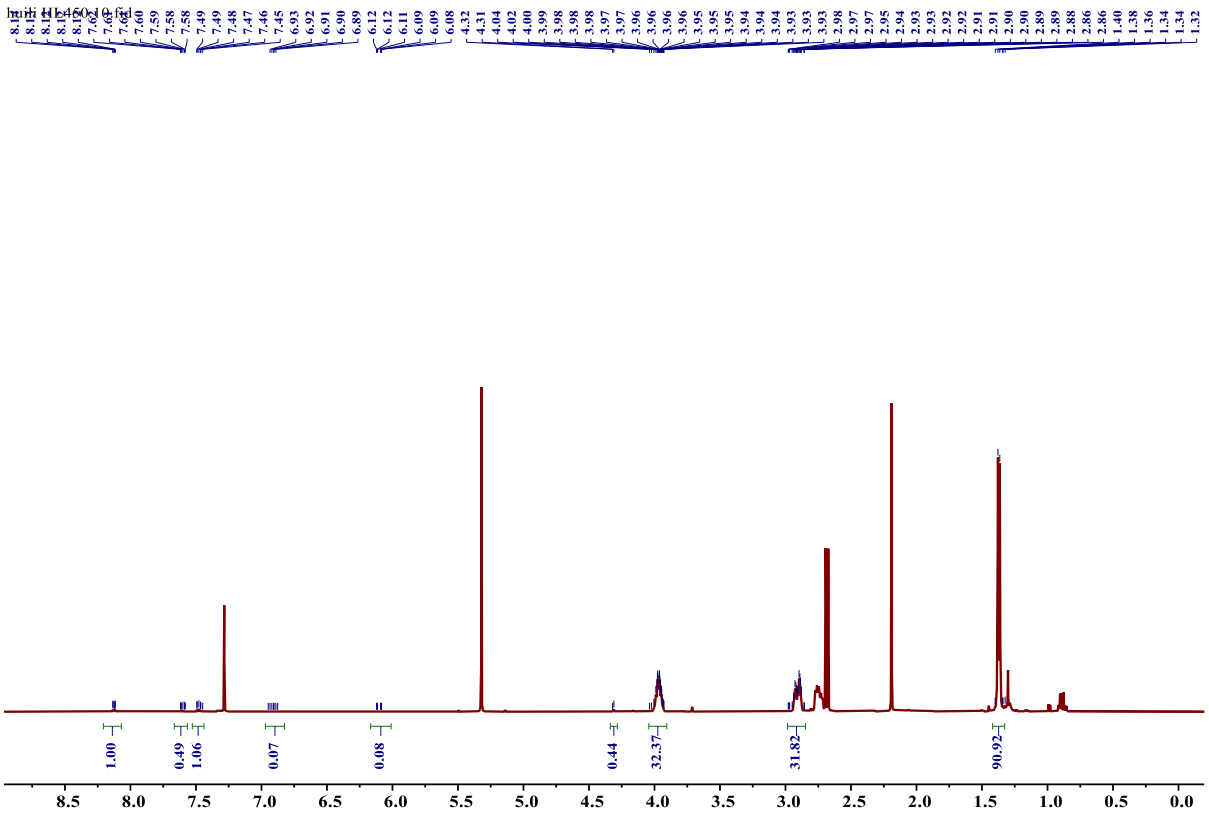

Figure 4.17. ^{1}H NMR (500 MHz, $CDCl_3$, 25 °C) spectrum of a P3TB prepared with *t*BuP_4 in the presence of BnSH (Table 4.1, entry HL450).

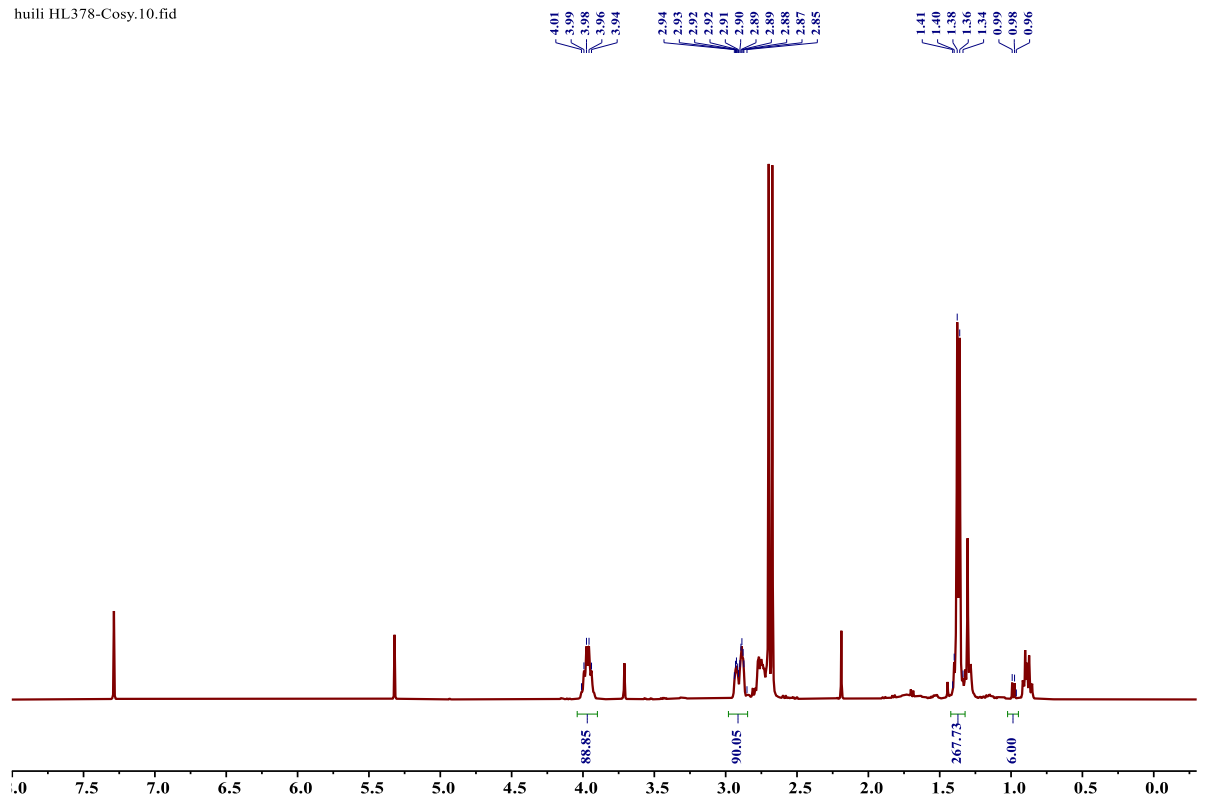

Figure 4.18. ^{1}H NMR (500 MHz, $CDCl_3$, 25 °C) spectrum of a P3TB prepared with *t*BuP_4 in the presence of *i*PrOH (Table 4.1, entry HL378).

References

[1] X. Zhang, M. Fevre, G. O. Jones, R. M. Waymouth, Catalysis as an Enabling Science for Sustainable Polymers. *Chem. Rev.* **2018**, *118*, 839-885.

[2] W. N. Ottou, H. Sardon, D. Mecerreyes, J. Vignolle, D. Taton, Update and Challenges in Organo-Mediated Polymerization Reactions. *Prog. Polym. Sci.* **2016**, *56*, 64-115.

[3] N. E. Kamber, W. Jeong, R. M. Waymouth, R. C. Pratt, B. G. Lohmeijer, J. L. Hedrick, Organocatalytic Ring-Opening Polymerization. *Chem. Rev.* **2007**, *107*, 5813-5840.

[4] M. K. Kiesewetter, E. J. Shin, J. L. Hedrick, R. M. Waymouth, Organocatalysis: Opportunities and Challenges for Polymer Synthesis. *Macromolecules* **2010**, *43*, 2093-2107.

[5] M. Fevre, J. Pinaud, Y. Gnanou, J. Vignolle, D. Taton, N-Heterocyclic Carbenes (NHCs) as Organocatalysts and Structural Components in Metal-Free Polymer Synthesis. *Chem. Soc. Rev.* **2013**, *42*, 2142-2172.

[6] A. Khalil, S. Cammas-Marion, O. Coulembier, Organocatalysis Applied to the Ring-Opening Polymerization of β-Lactones: A Brief Overview. *J. Polym. Sci., Part A: Polym. Chem.* **2019**, *57*, 657-672.

[7] L. Mespouille, O. Coulembier, M. Kawalec, A. P. Dove, P. Dubois, Implementation of Metal-Free Ring-Opening Polymerization in the Preparation of Aliphatic Polycarbonate Materials. *Prog. Polym. Sci.* **2014**, *39*, 1144-1164.

[8] S. Liu, C. Ren, N. Zhao, Y. Shen, Z. Li, Phosphazene Bases as Organocatalysts for Ring-Opening Polymerization of Cyclic Esters. *Macromol. Rapid Commun.* **2018**, *39*, e1800485.

[9] C. G. Jaffredo, J. F. Carpentier, S. M. Guillaume, Controlled ROP of β-Butyrolactone Simply Mediated by Amidine, Guanidine, and Phosphazene Organocatalysts. *Macromol. Rapid Commun.* **2012**, *33*, 1938-1944.

[10] C. G. Jaffredo, J.-F. Carpentier, S. M. Guillaume, Organocatalyzed Controlled ROP of β-Lactones towards Poly(hydroxyalkanoate)s: From β-Butyrolactone to Benzyl β-Malolactone Polymers. *Polym. Chem.* **2013**, *4*, 3837-3850.

[11] R. M. Shakaroun, P. Jéhan, A. Alaaeddine, J.-F. Carpentier, S. M. Guillaume, Organocatalyzed Ring-Opening Polymerization (ROP) of Functional β-Lactones: New Insights into the ROP Mechanism and Poly(hydroxyalkanoate)s (PHAs) Macromolecular Structure. *Polym. Chem.* **2020**, *11*, 2640-2652.

[12] H. Li, J. Ollivier, S. M. Guillaume, J.-F. Carpentier, Tacticity Control of Cyclic Poly(3-Thiobutyrate) Prepared by Ring-Opening Polymerization of Racemic β-Thiobutyrolactone. *Angew. Chem. Int. Ed.* **2022**, *61*, e202202386.

[13] S. Liu, C. Ren, N. Zhao, Y. Shen, Z. Li, Phosphazene Bases as Organocatalysts for Ring-Opening Polymerization of Cyclic Esters. *Macromol. Rapid. Commun.* **2018**, *39*, e1800485.

[14] M. Hong, E. Y.-X. Chen, Towards Truly Sustainable Polymers: A Metal-Free Recyclable Polyester from Biorenewable Non-Strained γ-Butyrolactone. *Angew. Chem. Int. Ed.* **2016**, *55*, 4188-4193.

[15] C. Shi, M. L. McGraw, Z. C. Li, L. Cavallo, L. Falivene, E. Y. Chen, High-Performance Pan-Tactic Polythioesters with Intrinsic Crystallinity and Chemical Recyclability. *Sci. Adv.* **2020**, *6*, eabc0495.

[16] S. Liu, H. Li, N. Zhao, Z. Li, Stereoselective Ring-Opening Polymerization of *rac*-Lactide Using Organocatalytic Cyclic Trimeric Phosphazene Base. *ACS Macro Lett.* **2018**, *7*, 624-628.

Conclusion & Perspectives

Polyhydroxyalkanoates (PHAs) are biocompatible polyesters that can (bio)degrade under ambient conditions either in managed or unmanaged environments.[1] They have gained increasing attention as suitable alternatives to fossil resources-based non-degradable plastics because they hold great potential to offer a practical solution to address the plastics pollution crisis. However, the relative lack of functional diversity and limited thermo-mechanical performance of PHAs limit their broader applications as commodity plastics.

Similar to other classes of polymers, thermal and mechanical properties of PHAs can generally be tuned by manipulating the microstructure, in particular tacticity, and pendant group structure. In this context, based on previous contributions from our group, to gain further insights into the factors that control the stereoselectivity of the ROP of functional, chiral racemic β-lactones mediated by yttrium complexes. we designed another functional β-lactone, namely 4-(2-(benzyloxy)ethyl)oxetan-2-one (*rac*-BPL^{CH2CH2OBn}). New functional polyBPL^{CH2CH2OBn} homopolymers with a good control of stereoselectivity have been successfully prepared from the ROP of *rac*-BPL^{CH2CH2OBn}. The best catalytic activities were reached using the yttrium complexes with the "crowded" substituents installed on the bisphenolate ligand (*e.g.*, *t*Bu, CMe_2Ph), which also gave syndiotactic-enriched polyBPL^{CH2CH2OBn} (P_r up to 0.86). On the other hand, the yttrium complexes incorporating halogenated "uncrowded" ligand, such as the Cl-substituted one, gave rise to atactic polyBPL^{CH2CH2OBn}, suggesting "non-covalent interactions" were not at play during polymerization in contrast to what was observed in the synthesis of PBPL^{OBn}; this is possibly due to a different conformation in the monomer/active species interactions, and/or due to the decrease in acidity of the methylene moiety (–C***H***$_2$CH$_2$OBn) of the side-chain, ultimately weakening the "noncovalent interactions" and leading to the loss of isoselectivity to afford atactic polymers.

The combination (secondary interactions) of the metal's ligand framework featuring appropriate R^1 substituents in the *ortho*-position of the phenolates with the chemical functionality of β-lactones is the key to achieve high isoselectivity.[2] Previous results from the group in the production of highly isotactic PBPL^{OR} shed light on the nature of secondary interactions, attractive interactions between moieties within the propagating polymer chain and substituents on the ancillary ligand nearby (Chart 4);[3] apparently, the strength of such attractive interactions must be high enough, otherwise such yttrium-catalysed polymerization evolves into the "regular" syndiotactic stereoselectivity, which proceeds under chain-end control by steric interactions between the last inserted monomer unit in the growing polymer chain and the new incoming monomer unit. Many challenges still exist in such secondary interactions' chemistry, yet the major one will be to understand and rationalize these

noncovalent interactions, so as to be able to implement them for preparing “at will” highly isoselective ROP of functional β-lactones.

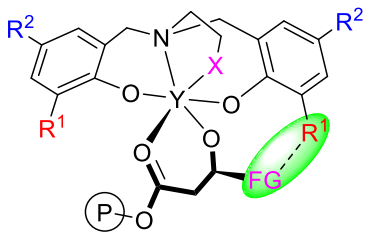

Chart 4. Illustration of tentative secondary interactions at work in highly stereo(iso)selective ROP of functional racemic β-lactones.

In order to further tune the performance of PHAs, another strategy was proposed, that is, the modification of the backbone of PHAs, which might endow polymers with differentiated, sometimes enhanced properties, such as improved thermal and mechanical properties. Hence, poly(3-thiobutyrate) (P3TB), is of great potential interest due to its biocompatibility and degradability properties. We were the first to investigate the chemical synthesis of P3TB via ROP of the racemic β-thiobutyrolactone (*rac*-TBL) with anionic-type initiators/catalysts. Among the latter, the most promising results were obtained with yttrium complexes, leading to well-defined P3TBs characterized by NMR and MALDI-ToF MS analyses, and which revealed quite unexpectedly to be purely *cyclic* polymers. It is worth noting here that this is a rare example of generation of cyclic polymers generated by yttrium complexes. We assume that thiolates attached to the yttrium metal center attack labile thioester bonds at any site within the growing polymer chain, that is back-biting reactions occur to a significant extent, leading to the formation of purely cyclic P3TBs. The properties of cyclic polymers generally differ broadly from their linear counterparts, although we only analyzed this briefly in our studies on P3TBs. Contrastingly, this yttrium catalyst family favors the formation of linear polyesters when applied to the parent oxo-β-lactones, which testifies the singular behavior of β-thiolactone/thiolate moieties. It could be interesting to assess whether the introduction of few thioester bonds into P3HB (via copolymerization, Chart 5), to form poly(3HB-*co*-3TB) allows the formation of cyclic copolymers via transesterification/back-biting reactions.

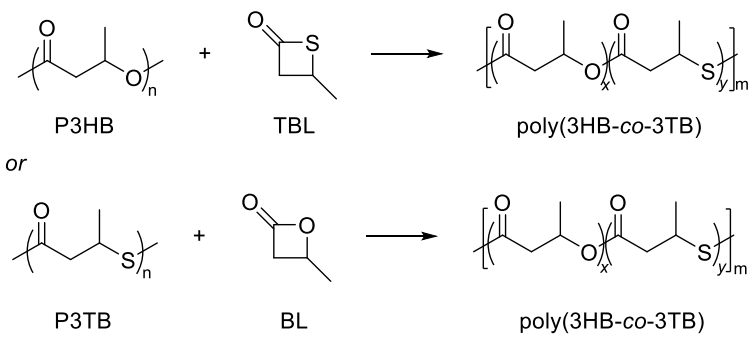

Chart 5. Proposed synthetic pathway towards poly(3HB-*co*-3TB) by transesterification reactions.

Interestingly, upon simple tuning of the substituents on the bis(phenolate) platform, the stereoselectivity of the ROP of *rac*-TBL can be switched from highly isoselective to syndioselective. In fact, the complexes incorporating "moderately bulky" *tert*-butyl or cumyl-substituted ligands afford *syndiotactic* cyclic P3TB (P_r up to 0.70), while the catalysts bearing the smaller substituents on the ligand, such as chloro or methyl, and the system with the larger trityl-substituted ligand, enable reaching *isotactic* cyclic P3TB (P_m up to 0.90). To our knowledge, this isotacticity is quite a rare feature in ROP catalysis which was observed previously only for *rac*-lactide with aluminium complexes supported by tetradentate aminophenoxide ligands and for *rac*-BPL^{OR} (R = Me, allyl, benzyl) monomers with the same yttrium complexes as those used in this study. However, its origin has not been established, though it is, to some extent, under chain-end control mechanism in the light of statistical propagation models analysis.

In addition, probably due to the considerable difference in reactivity between racemic β-butyrolactone (*rac*-BL) and *rac*-TBL, preliminary attempts at performing the copolymerization of *rac*-BL and *rac*-TBL promoted by yttrium complex, led to mixtures of homopolymers.

Within the context of polyesters that target sensitive applications in microelectronics and biomedical devices and also based on our previous work about organocatalyzed ROP of *rac*-BL and its higher functional derivatives, we extended our studies to the organocatalyzed polymerization of *rac*-TBL. The latter was evaluated with various phosphazene bases, such as BEMP, *t*BuP$_1$, *t*BuP$_2$, and *t*BuP$_4$. Preliminary attempts revealed that polymerization rates increase with the basicity of the phosphazene base. The formation of crotonate end-capped poly(3-thiobutyrate) (P3TB) was evidenced by NMR analysis. We formulate the hypothesis that the superbase, such as *t*BuP$_4$, abstracts one of the methylene hydrogens in α-position of the *rac*-TBL, thereby leading to the formation of an α,β-unsaturated carbothiolate species ((C=O)−S$^-$) as the "real" initiator, which propagates via *S*-alkyl cleavage of the monomer units to be inserted. Further detailed mechanistic studies are necessary to further assess our assumptions.

As we have summarized in Chapter 1, only a limited range of chiral racemic β-lactones have been successfully implemented in the stereoselective ROP towards stereoregular PHAs. Most of these chiral β-lactones feature a substituent at the β-position. Rare examples were reported regarding the synthesis of PHAs based on β-lactones with α,β-disubstituted groups or a ring fused at both α- and β-positions, particularly, in comparison with poly(4-hydroxyalkanoate)s. In this regard, a new type of chiral racemic β-lactone fused with an eight-membered ring at α- and β-positions, namely 9-oxabicyclo[6.2.0]decan-10-one, respectively (Chart 6b), would be worth to be investigated. These can be easily obtained by carbonylation of the corresponding cyclooctene oxide.[4] The introduction of a fused ring in the backbone limits the flexibility of the polymer chain, thereby altering the thermal properties of the resulting PHAs. In fact, ROP of the five-membered ring fused *cis*-β-lactone mediated by an yttrium catalyst gave the corresponding *cis*-PHA with a melting point of 185 °C which is close to that of the naturally-occurring P3HB (Chart 6a).[5] Overall, we anticipate that the stereoselective ROP of these

ring-fused β-lactones will open up unique opportunities for the formation of robust PHAs with a wide range of notable properties and potential applications.

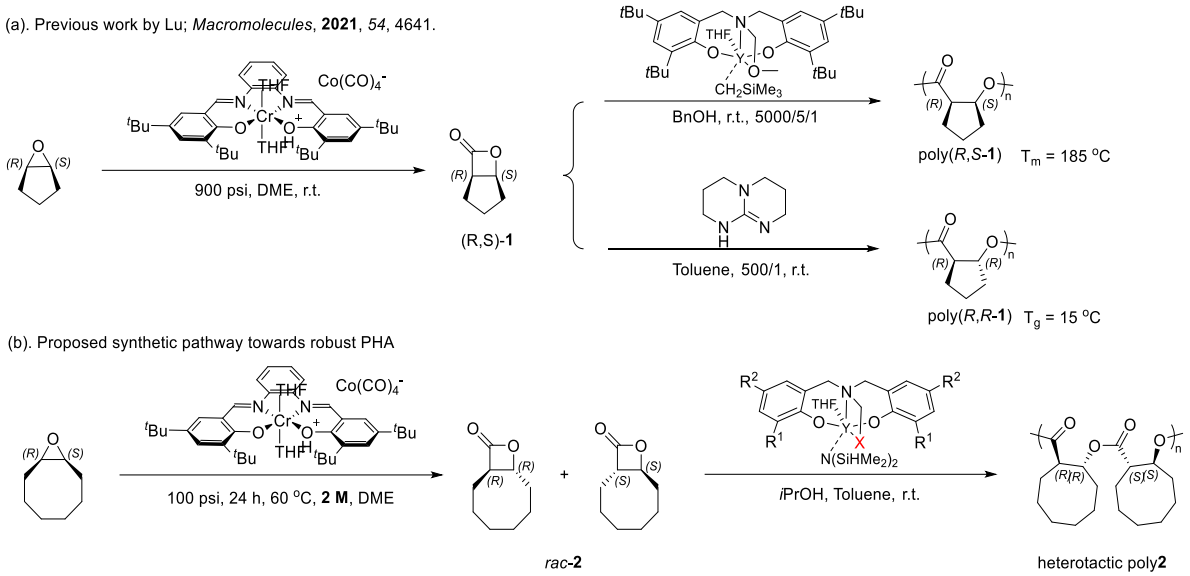

Chart 6. (a). Previous study reported in the literature about ROP of a ring-fused β-lactone;[5] (b). proposed chiral racemic β-lactone used for stereoselective ROP in future work.

On the other hand, due to the significant side reactions, *e.g.*, back-biting, inter- and intra-transesterification reactions, the finely controlled polymerization in terms of molar mass towards *rac*-TBL by well-defined metal-based complexes is still challenging thus far. The catalytic efficiency of hydrogen-bonding organocatalysts,[6] such as Takemoto's catalyst (Chart 7), may encourage us to employ them in place of metal-based complexes in the area of β-thiolactones realizing better molar mass control. All H-bonds involved in ROP promoted by such catalyst are weak (lower activity than some nucleophilic organocatalysts) which, to some extent, might prevent significant transesterification reactions.

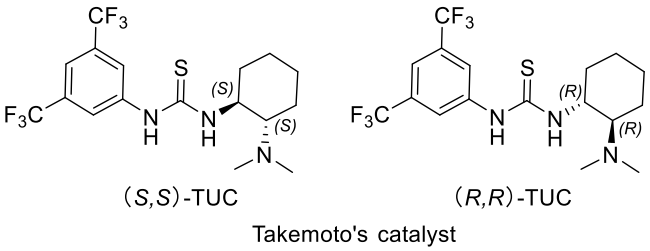

Chart 7. Chemical structure of Takemoto's catalyst.[7-9]

References

[1] A. H. Westlie, E. C. Quinn, C. R. Parker, E. Y. X. Chen, Synthetic Biodegradable Polyhydroxyalkanoates (PHAs): Recent Advances and Future Challenges. *Prog. Polym. Sci.* **2022**, *134*, 101608.

[2] R. Ligny, M. M. Hanninen, S. M. Guillaume, J. F. Carpentier, Steric vs. Electronic Stereocontrol in Syndio- or Iso-Selective ROP of Functional Chiral β-Lactones Mediated by Achiral Yttrium-Bisphenolate Complexes. *Chem. Commun.* **2018**, *54*, 8024-8031.

[3] H. Li, R. M. Shakaroun, S. M. Guillaume, J. F. Carpentier, Recent Advances in Metal-Mediated Stereoselective Ring-Opening Polymerization of Functional Cyclic Esters towards Well-Defined Poly(hydroxy acid)s: From Stereoselectivity to Sequence-Control. *Chem. Eur. J.* **2020**, *26*, 128-138.

[4] J. W. Kramer, E. B. Lobkovsky, G. W. Coates, Practical β-Lactone Synthesis: Epoxide Carbonylation at 1 atm. *Org. Lett.* **2006**, *8*, 3709-3712.

[5] Y.-T. Li, H.-Y. Yu, W.-B. Li, Y. Liu, X.-B. Lu, Recyclable Polyhydroxyalkanoates via a Regioselective Ring-Opening Polymerization of α,β-Disubstituted β-Lactone Monomers. *Macromolecules* **2021**, *54*, 4641-4648.

[6] C. Thomas, B. Bibal, Hydrogen-Bonding Organocatalysts for Ring-Opening Polymerization. *Green Chem.* **2014**, *16*, 1687-1699.

[7] M. S. Zaky, A. L. Wirotius, O. Coulembier, G. Guichard, D. Taton, Reaching High Stereoselectivity and Activity in Organocatalyzed Ring-Opening Polymerization of Racemic Lactide by the Combined Use of a Chiral (Thio)Urea and a N-Heterocyclic Carbene. *ACS Macro Lett.* **2022**, *11*, 1148-1155.

[8] M. S. Zaky, A. L. Wirotius, O. Coulembier, G. Guichard, D. Taton, A Chiral Thiourea and a Phosphazene for Fast and Stereoselective Organocatalytic Ring-Opening-Polymerization of Racemic Lactide. *Chem. Commun.* **2021**, *57*, 3777-3780.

[9] B. Orhan, M. J. L. Tschan, A.-L. Wirotius, A. P. Dove, O. Coulembier, D. Taton, Isoselective Ring-Opening Polymerization of *rac*-Lactide from Chiral Takemoto's Organocatalysts: Elucidation of Stereocontrol. *ACS Macro Lett.* **2018**, *7*, 1413-1419.

Appendices

General Information on Stereocontrol

One of the major developments in macromolecular science has been the elucidation of the occurrence of stereoisomerism in polymers. Stereoisomeric polymers have the same atom connectivity but differ in their absolute or relative configurations of the stereogenic centres.

The Definition of Tacticity

The regularity in the relative configurations of successive stereocenters determines the tacticity of the polymer chain. Two basic ordered structures can occur: *isotactic* and *syndiotactic* (Figure S1). An isotactic microstructure occurs when the stereocenter in each repeating unit in the polymer chain has the same configuration. A syndiotactic polymer structure occurs when the configurations of the stereocenters perfectly alternate from one repeating unit to the next one. Oppositely, if the stereocenters are randomly distributed on the polymer chain, the polymer does not have particular tacticity and is termed *atactic*. More complex tacticities can be defined such as hemiisotacticity but won't be considered in the following. It is worth noting here that, if the monomer possesses two stereocenters (such as *rac*-lactide), *heterotactic* polymer in which the stereocenters doubly alternate *i.e.*, *-SSRRSSRR-* can be obtained.

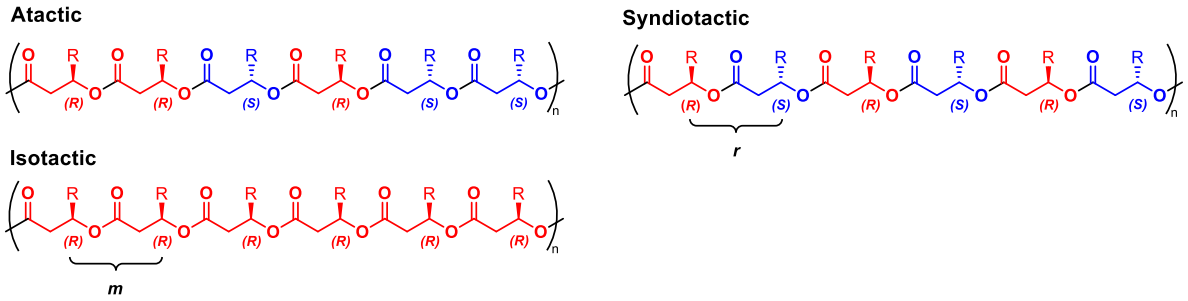

Figure S1. Basic tacticities of poly(hydroxyalkanoate)s (PHAs).

Polymers with isotactic or syndiotactic structures, referred to as stereoregular polymers, usually are crystalline and have improved thermal and mechanical properties relative to those of atactic polymers.

The Origin of Stereoselectivity

Many metal-based catalysts have been developed over the past three decades to promote ROP reactions of cyclic esters. As customary of molecular catalysis, the ancillary ligands often play an important role in ROP catalysis to fine-tune the sterics and electronics of the metal complex and to

control eventually the polymerization process. Remarkably, unlike the catalytic synthesis of small molecules, in polymerization catalysis the growing polymer chain (most often) remains coordinated onto the metal centre after each monomer insertion; hence, the polymer chain itself constitutes another genuine component that affects the properties of the catalytically active, propagating organometallic species. The chain growth propagation typically proceeds by a coordination–insertion mechanism. Taking the ROP of *rac*-lactide as an example, the insertion of a single lactide unit into a metal–polymeryl bond is described in Figure S2, along with the numeral assignment of the five (possible) stereogenic centres, that is the incoming lactide monomer (#1 and #2), the metal site (#3), and the last inserted lactidyl unit (#4 and #5). Among these (possible) chiral centres, three are "proximal" ones (#1, #3, and #4), thereby either the growing polymer chain or ancillary ligands of a catalyst can influence the stereo-preference of the monomer to be inserted when chiral racemic cyclic ester is used.

The strength of these interactions determines the type of stereocontrol in the ROP: a dominant interaction between the proximal stereogenic centre of the incoming monomer and the stereogenic metal site (#1 and #3) is termed "enantiomorphic-site control" and results in homochiral enchainment preference. On the other hand, a dominant interaction between the proximal stereogenic centre of the incoming monomer and the proximal centre of the last inserted monomer unit (#1 and #4) is termed "chain-end control" and results in either heterochiral (most common) or homochiral (quite rare) enchainment preferences and hence, in syndiotactic or isotactic polymers, respectively.

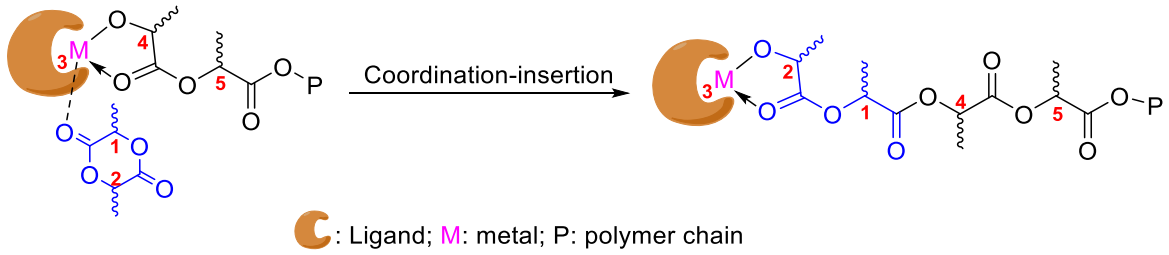

Figure S2. Lactide insertion into a metal–polymeryl bond with the numbering of stereogenic centers.

Chain-End Control

The stereogenic centre from the last-inserted monomer unit influences the stereochemistry of the next monomer to be inserted; if this influence is significant or dominant, the mode of stereochemical regulation is referred to as the "chain-end control" (CEC) mechanism. This is generally associated with sterically hindered but achiral catalyst systems.

ROP reactions that are controlled by such CEC mechanism usually proceed *via* minimization of steric interactions between the last inserted monomer unit in the growing polymer chain and the next monomer unit to be inserted. Hence, this often leads to the alternation of monomer units with opposite configuration, and in turn, these reactions give a syndiotactic polymer. The initiating step occurs without enantiomeric differentiation of the racemic monomer, thereby giving rise to the chirality incorporated into the propagating chain-end (Figure S3). The monomer with the opposite chirality of

the inserted monomer is preferentially incorporated into the propagating chain-end. Once a monomer with the same chirality is mistakenly incorporated, the monomer with the opposite chirality of the mismatched monomer turns into a matched monomer in the next propagation step. It should be noted here that, in some rare instances, more than one stereogenic centre of the polymer chain can play a significant role in stereoregulation.[1]

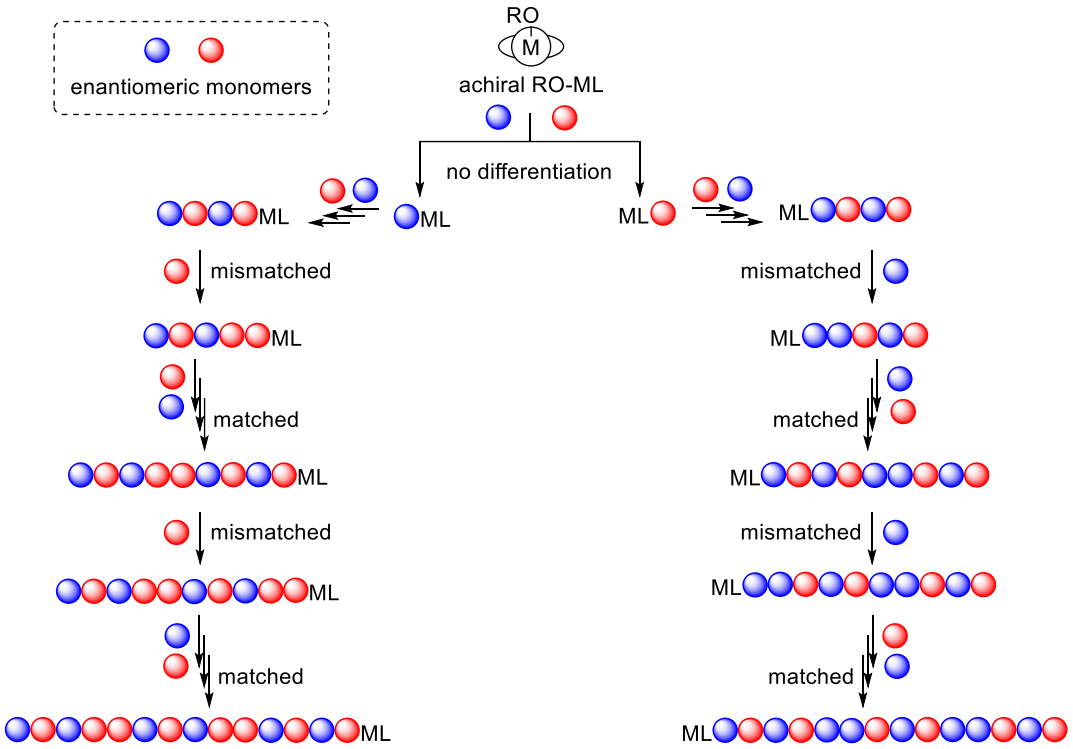

Figure S3. Syndioselective polymerization by chain-end control mechanism.

An isoselective ROP of chiral cyclic esters that dominates by a CEC mechanism, is less common (Figure S4). The initiating step occurs without enantiomeric differentiation of the racemic monomer, leading to the chirality incorporated into the propagating chain-end. Subsequently, the monomer with the same chirality as that of the inserted monomer is preferentially incorporated into the propagating chain-end. Once a monomer with opposite chirality is mistakenly incorporated, the monomer with the same chirality as that of the mismatched monomer turns into a matched monomer in the next propagation step. In fact, isoselective ROP governed by the CEC mechanism affords a multiblock stereocopolymer due to several inversions of the chirality of the incorporated monomer in most cases.

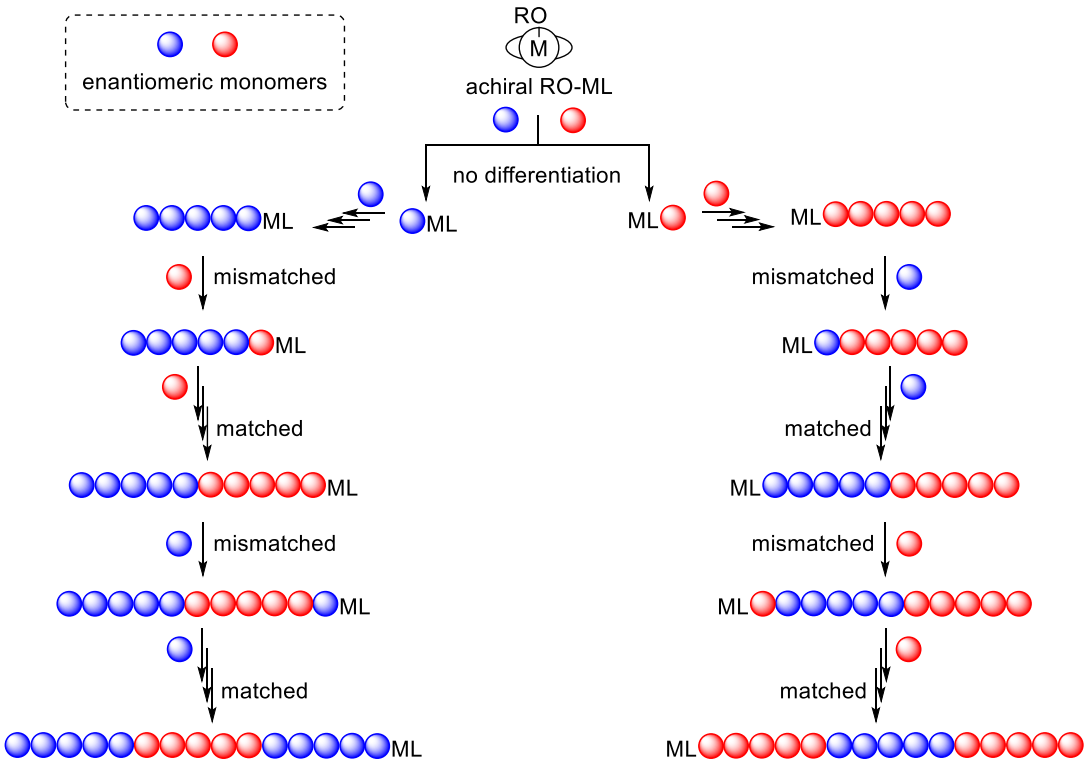

Figure S4. Isoselective polymerization by chain-end control mechanism.

Enantiomorphic Site Control

If the ligand set is chiral and overrides the influence of the polymer chain-end, the mechanism of stereochemical direction is termed "enantiomorphic-site control" (ESC); that is, the chirality of the catalyst dictates the chirality of the next insertion.[1] The complex has a chiral environment dominated by the ligand around the metal centre and can consistently differentiate and react preferentially with one enantiomer from the other one. In a ROP reaction controlled by the ESC mechanism, once a monomer with opposite chirality is mistakenly incorporated, a correction occurs immediately in the subsequent insertion since the ligands direct the stereochemical events (Figure S5). Coates has shown that macromolecules (*e.g.*, polylactides) produced by ESC have often multiblock stereosequences due to polymer exchange when the mismatched monomer is incorporated (*see below*).[2]

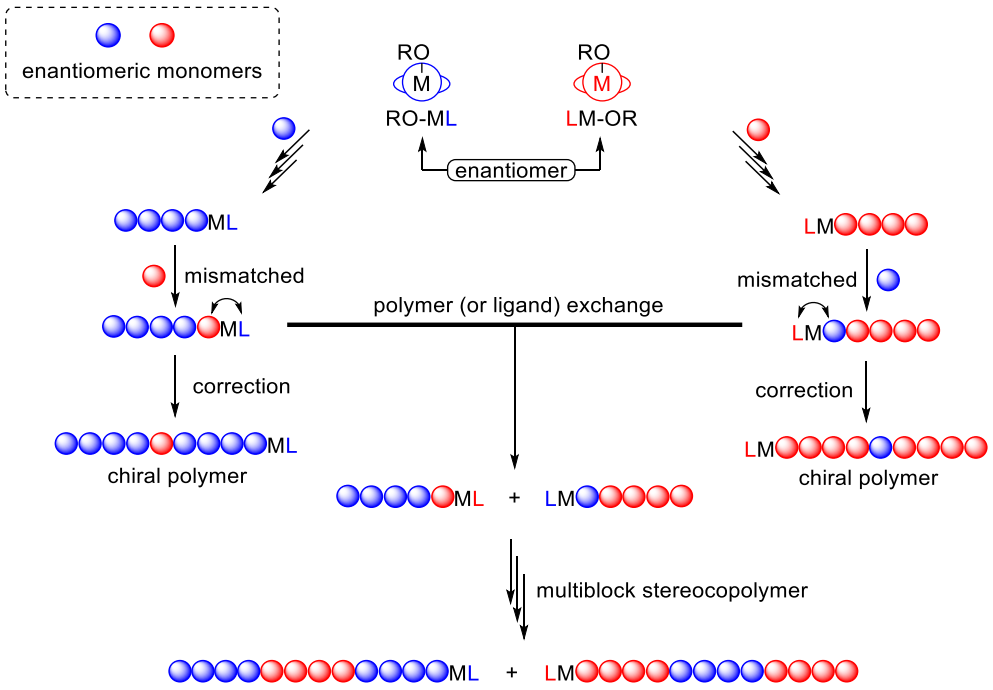

Figure S5. Isoselective polymerization by enantiomorphic site control.

However, it is crucial to mention that using a chiral catalytic system does not necessarily imply a site control mechanism for stereoselective systems, even if enantioselective discrimination towards the *racemic* monomer is observed during the polymerization.

Determination of the Tacticity of Polymers

The parameters that are used to describe the stereoselectivity of the monomer enchainment process are depicted in Figure S6. For chain-end control, the parameters P_m and P_r refer to the probability of *meso* and *racemic* enchainments, respectively (the Bovey formalism is a convenient way to describe polymer tacticity, with "*m*" for *meso*, and "*r*" for *racemic* relationships between adjacent stereogenic centers).[1] In the ROP of chiral cyclic monomers, P_m is the probability of forming a new *m* dyad, while P_r is equal to probability of generating a next *r* dyad (obviously $P_m + P_r = 1$). $P_r = P_m = 0.50$ describes a completely atactic polymer; $P_m = 1.00$ (*i.e.*, $P_r = 0.00$) and $P_m = 0.00$ (*i.e.*, $P_r = 1.00$) describe perfectly isotactic and syndiotactic polymers, respectively. Chain-end control mechanism will produce perfectly isotactic/syndiotactic polymer as long as there are no misinsertion. However, the difference in energy between insertion of (*R*)-monomer and (*S*)-monomer is fairly small in most cases, leading to the presence of stereoerrors; the result is a stereoblock structure with one isolated *r* defect, *mmmrmmm*, or with one isolated *m* defect, *rrrmrrr*. The signature for a chain-end control mechanism is therefore the presence of the *mr* and *rm* triad in a 1:1 ratio in the ^{13}C NMR spectroscopy (Figure S6).

For enantiomorphic site-control mechanisms, the parameter α represents the degree of enantiotopic selectivity of the enchainment. When α is either 1 or 0, an isotactic polymer forms, while an α parameter of 0.5 produces an atactic polymer. Since the structure of the catalyst (metal center and ligands)

determines the enantiotopic selectivity of the *racemic* monomer, the microstructure of the resulting polymer synthesized under enantiomorphic site-control is different from the microstructure resulting from chain-end control. A mistaken monomer insertion with the opposite chirality does not change the enantiotopic preference of the following insertion and the occurrence of an *r* dyad resulting from misinsertion is not propagated. Rather, the catalyst "corrects" itself by generating a second *r* dyad to generate a *mmmrrmmm* sequence (Figure S6).

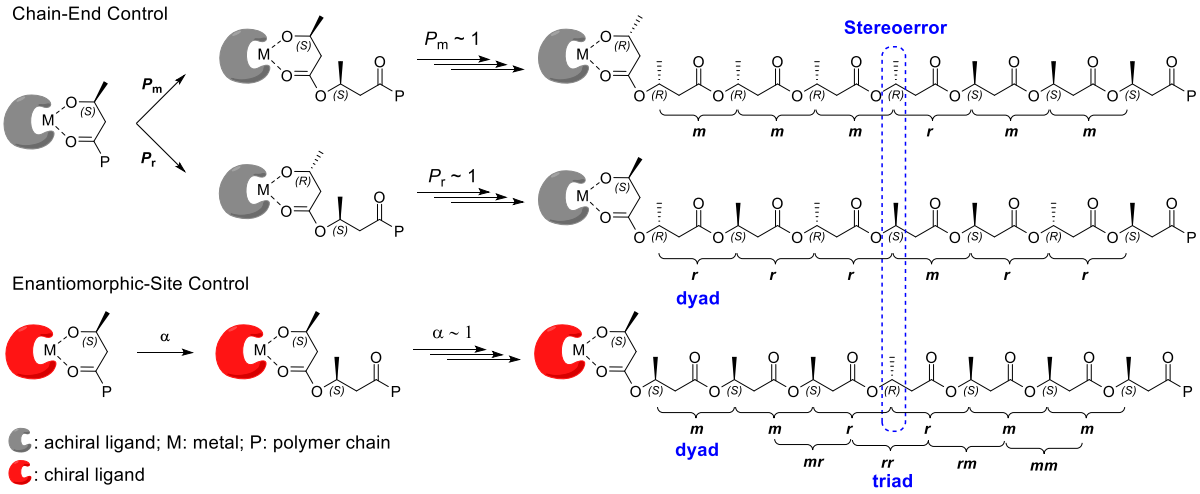

Figure S6. Impact on error insertion as exemplified in the synthesis of poly(hydroxybutyrate)s.[1]

The most important tool for assessing the stereochemistry of a polymer chain is the quantitative ^{13}C NMR spectrum (or the deconvoluted homonuclear decoupled ^{1}H NMR spectrum). Taken poly(hydroxybutyrate)s as example, the chemical shift of carbonyl carbons at *ca.* 169.3 ppm (or other carbons) is sensitive to the relative stereochemistry of neighboring methyl carbons, which shows four peaks that could assign at the triad level. There are a total of four possible triads, that is *mm*, *mr*, *rr*, *rm*, respectively. The carbonyl carbon of the triad at 169.29 ppm described as *rr* resonates, while the carbonyl carbon of the triad at 169.20 ppm described as *mm* resonates as shown in Figure S7. It is worth noting that *mr* and *rm* are described as stereo-defects at 169.32, 169.20 ppm, respectively. Since two of these are roughly coincident at 100 MHz, three peaks are typically observed at this NMR frequency. Generally, a ^{13}C NMR spectrum with one predominant carbonyl signal at 169.20 ppm (*mm*) is considered isotactic (compared with perfectly isotactic polymer prepared from enantiopure monomer; (*mm*) = 100 %, perfectly isotactic polymer) and a ^{13}C NMR spectrum with one predominant carbonyl at 169.29 ppm (*rr*) is considered syndiotactic ((*rr*) = 100 % perfectly syndiotactic polymer). When (*rr*) = (*mm*) = (*rm*) = (*mr*) = 25 %, such polymer is atactic. On the other hand, the methyl region shows essentially two signals that correspond to dyad sensitivity; these are actually two groups of resonances, but the limited resolution at 100 MHz does not allow to further discriminate at a higher than dyad level.

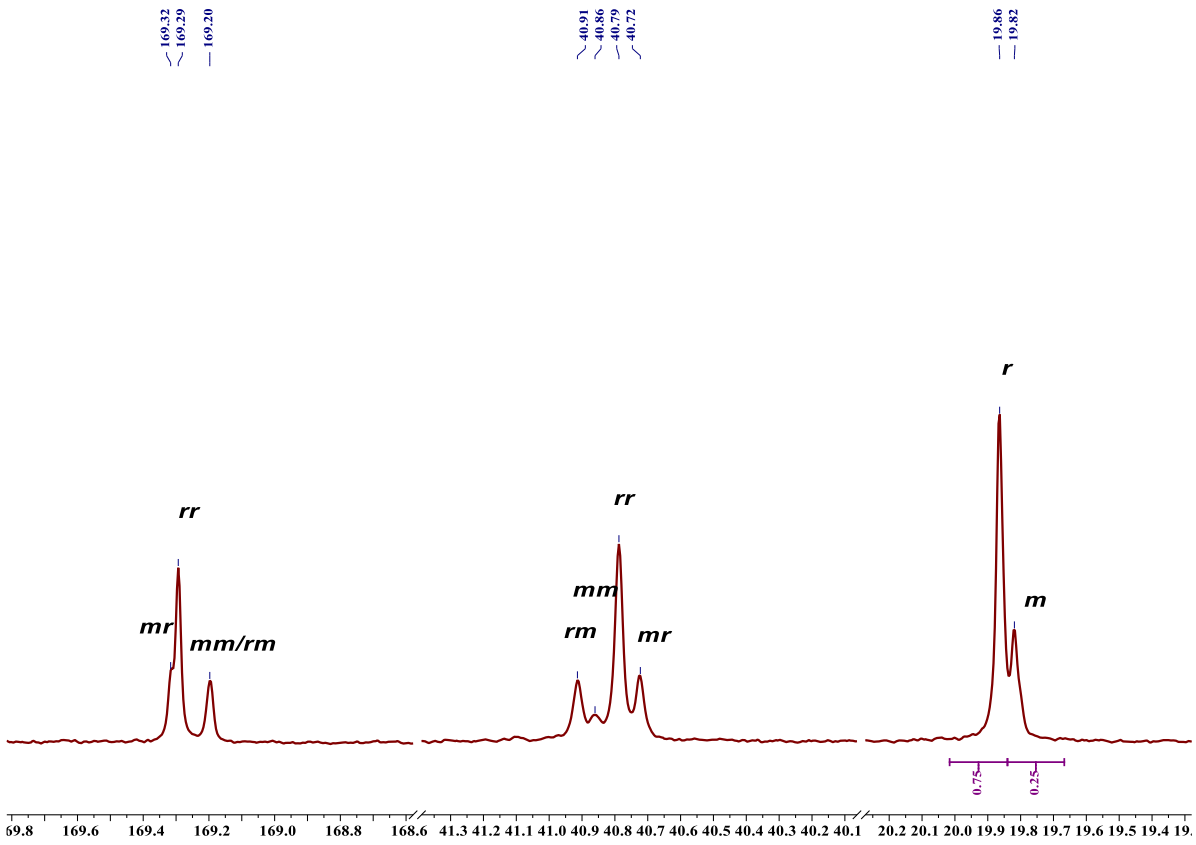

Figure S7. ^{13}C NMR (100 MHz, $CDCl_3$, 25 ℃) spectrum of a syndiotactic-biased poly(hydroxybutyrate) (P_r = 0.75) produced by chain-end control mechanism (polymer prepared from ROP of rac-BL mediated by tripodal tetradentate bis(phonate) yttrium complex bearing tBu substituents in toluene at room temperature).[3]

The Properties of Cyclic Polymer

Cyclic polymers have a ring-like structure, and all repeating units are chemically and physically equivalent. In contrast to linear polymers, cyclic polymers are unable to reptate, which fundamentally changes their mode of movement and entanglement, thereby leading to unique physical properties in thin films, solutions and bulk; for example, the radius of gyration, intrinsic viscosity, critical solution temperature, refractive index, density, dipole moment, glass transition temperature, thermostability.[4]

The ratio of the mean square of the radius of gyration of a random coil linear polymer to that of a cyclic polymer, which can be calculated under Gaussian statistics, theoretically should be equal to 2 in the absence of a volume effect in the case of polymers with the same molar mass, indicating that cyclic polymers possess smaller hydrodynamic volumes. A difference in volume between cyclic and linear polymers leads to different solution properties of the cyclic polymers compared to the linear polymers, such as, higher gel permeation chromatography (GPC) elution volume, which can be used to separate them from their linear analogues by preparative GPC and cyclic purity is able to be accurately analysed by size exclusion chromatography.[5]

The lack of free end groups in cyclic polymers, suggesting fewer entanglement, leads to less viscous than their corresponding linear counterparts. The difference in viscosity ($[\eta]_{cyclic}/[\eta]_{linear}$) is

often used as evidence for successful synthesis, yet the viscosity date cannot rule out the presence of a small amount of linear polymer. For instance, Waymouth and coworkers reported that ROP of LA catalyzed by *N*-heterocyclic carbenes in the presence of an alcohol initiator and in the absence of alcohol gave rise to purely linear and cyclic PLAs, respectively.[6] Viscosity measurements with a light-scattering detector coupled to a viscometer showed that the ratio $[h]_{cyclic}/[h]_{linear}$ obtained from the Mark−Houwink plot (double logarithm plots of intrinsic viscosity ([h]) versus M_w) is approximately 0.7, which is in good agreement with theoretical predictions and is also consistent with a cyclic structure, as the intrinsic viscosities of cyclic polymers are less than those for linear polymers of the same molar mass.

Due to the absence of chain ends and the topological constraint, cyclic polymers possess a more compact structure and smaller free volume than their linear chains of equivalent molar mass, resulting in a higher *glass transition temperature* (T_g), which is usually, in practice, around 5 °C; yet the difference is more pronounced for low molar mass polymers. An example of this difference was demonstrated by poly(vinyl ether)s, that is, cyclic poly(vinyl ether)s carrying bulky tricyclic alkane pendant exhibited higher T_gs than their linear counterparts of similar molar mass. Interestingly, cyclic poly(vinyl ether)s showed a much weaker molar mass dependence for the T_g than their linear analogues, which was attributed to the relatively smaller free volume of cyclic polymers.[7] Analogous and complementary behaviours of increased *melting temperature* and *crystallization temperature* of the cyclic polymer have also been found for polybutadiene and poly(ε-caprolactone), respectively.[8,9]

Owing to the extra energy needed to break the cycle about thermal degradation, cyclic polymers also exhibit more stability compared to their linear counterparts.[10] This behaviour is believed to primarily be a consequence of the fact that the first bond broken does not change the molar mass, but changes only the topology from cyclic to linear. The best evidence of this extent is the work on γ-butyrolactone, in which the cyclic polymer displayed a much higher onset degradation temperature (*ca.* 72 °C) than the linear polymer with a similar molar mass. Moreover, TGA analysis is often used to distinguish between cyclic and linear forms due to this noticeable difference.

The cyclic polymers have also shown profound differences from the linear polymer in other properties, including higher density, melt viscosity (greater at low molar mass but smaller at high molar mass), and higher refractive index.

Synthesis of Proligands

Synthesis of 6,6'-(*N,N*-dimethylethylenediamine) bis(methylene) bis(2,4-dichlorophenol), $\{ONNO^{Cl2}\}H_2$[11]

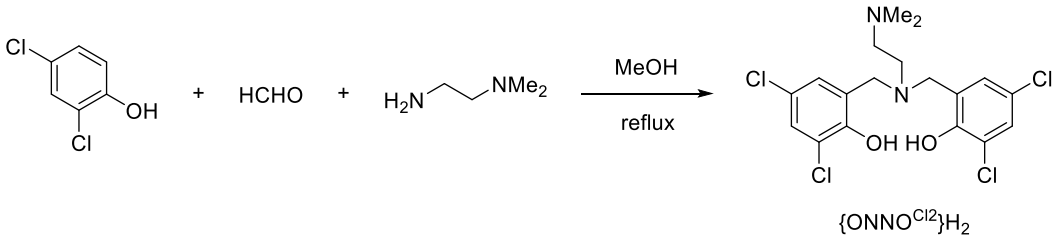

Scheme S1. The synthetic pathway towards proligand {ONNO^{Cl2}}H_2.[11]

In a round bottom flask, a solution of 2,4-dichlorophenol (20.00 g, 122.70 mmol), *N,N'*-dimethylethylenediamine (6.48 mL, 61.35 mmol) and formaldehyde (9.96 g of a 37% solution, 122.70 mmol) in methanol (60 mL) was refluxed for 3 days. The reaction mixture was cooled to room temperature and the ligand precipitated. The white precipitate (22.60 g, 84%) was collected by filtration, washed with cold ethanol and dried under vacuum.

^{1}H NMR (500 MHz, $CDCl_3$, Figure S8): δ 10.51 (s, 2H), 7.26 (d, J = 2.4, 2H), 6.91 (d, J = 2.6, 2H), 3.63 (s, 4H), 2.62 (s, 4H), 2.36 (s, 5H).

^{13}C NMR (126 MHz, $CDCl_3$, Figure S9): δ 151.92, 129.73, 128.38, 124.52, 123.57, 122.78, 77.16, 56.27, 55.87, 49.33, 45.03.

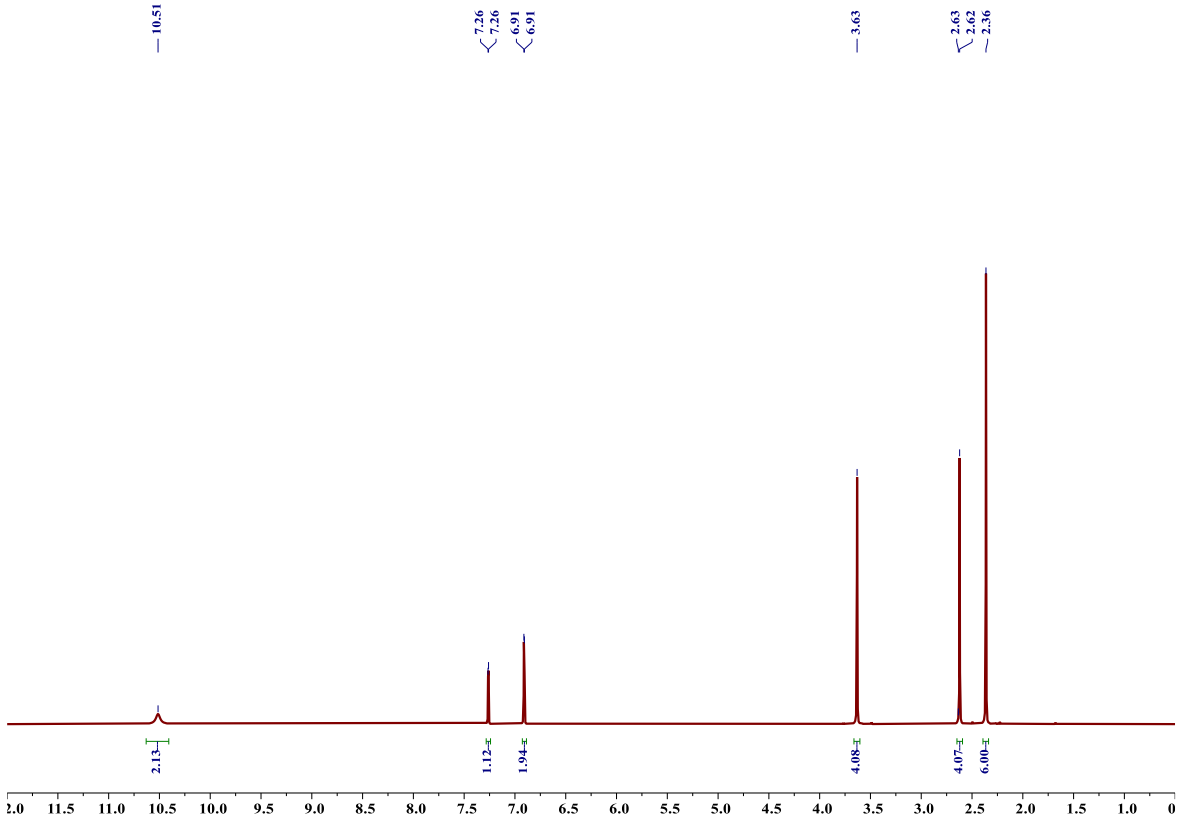

Figure S8. ^{1}H NMR spectrum (500 MHz, $CDCl_3$, 25 °C) of proligand {ONNO^{Cl2}}H_2.

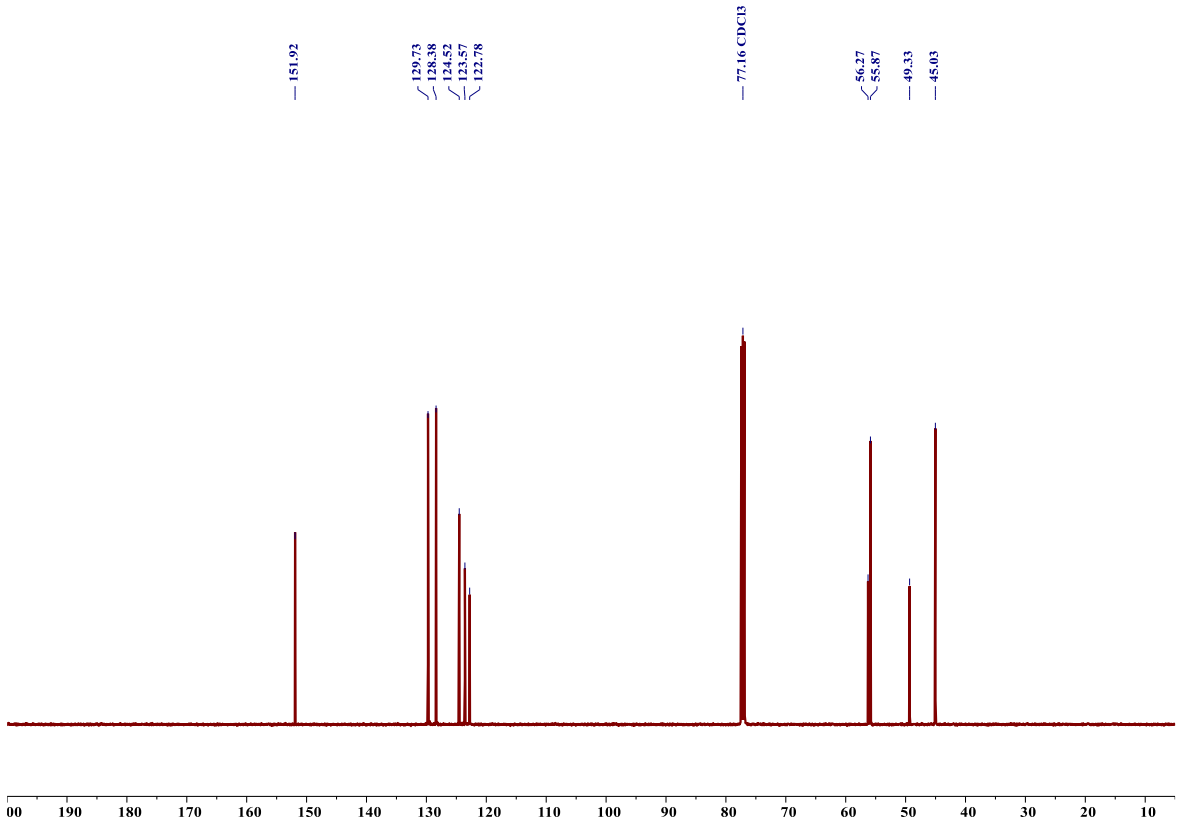

Figure S9. ^{13}C NMR spectrum (125 MHz, $CDCl_3$, 25 °C) of proligand {ONNO^{Cl2}}H_2.

Synthesis of 6,6'-(((2-methoxyethyl)azanediyl)bis(methylene))bis(2,4-dimethylphenol), {ONOO^{Me2}}H_2[12]

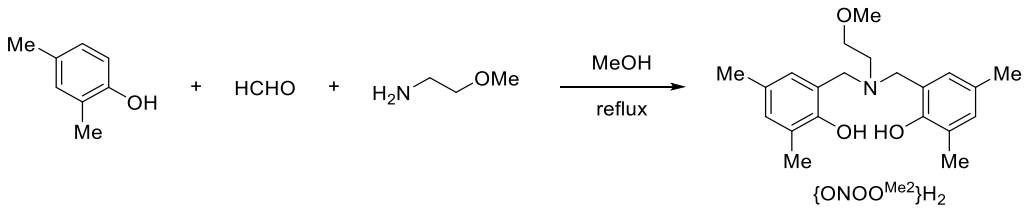

Scheme S2. The synthetic pathway towards proligand {ONOO^{Me2}}H_2.[12]

In a round bottom flask, a solution of 2,4-di-methylphenol (15.70 g, 128.7 mmol), 2-methoxyethylamine (4.3 mL, 49.5 mmol), and formaldehyde (9.5 mL of a 37% solution, 131.6 mmol) in methanol (35 mL) was heated at reflux for 3 days. Cooling the mixture gave a white crystal which was filtered and washed with cold ethanol to afford {ONOO^{Me2}}H_2.

^{1}H NMR (500 MHz, $CDCl_3$, Figure S10) δ 8.41 (s, 2H), 6.87 (d, J = 2.2, 2H), 6.68 (d, J = 2.2, 2H), 3.73 (s, 4H), 3.59 (t, J = 5.2, 2H), 3.47 (s, 3H), 2.71 (t, J = 5.1, 2H), 2.22 (s, 6H), 2.21 (s, 6H).

^{13}C NMR (126 MHz, $CDCl_3$, Figure S11) δ 152.46, 131.35, 128.57, 128.07, 125.28, 121.29, 77.16, 71.68, 59.17, 57.18, 51.01, 20.51, 16.16.

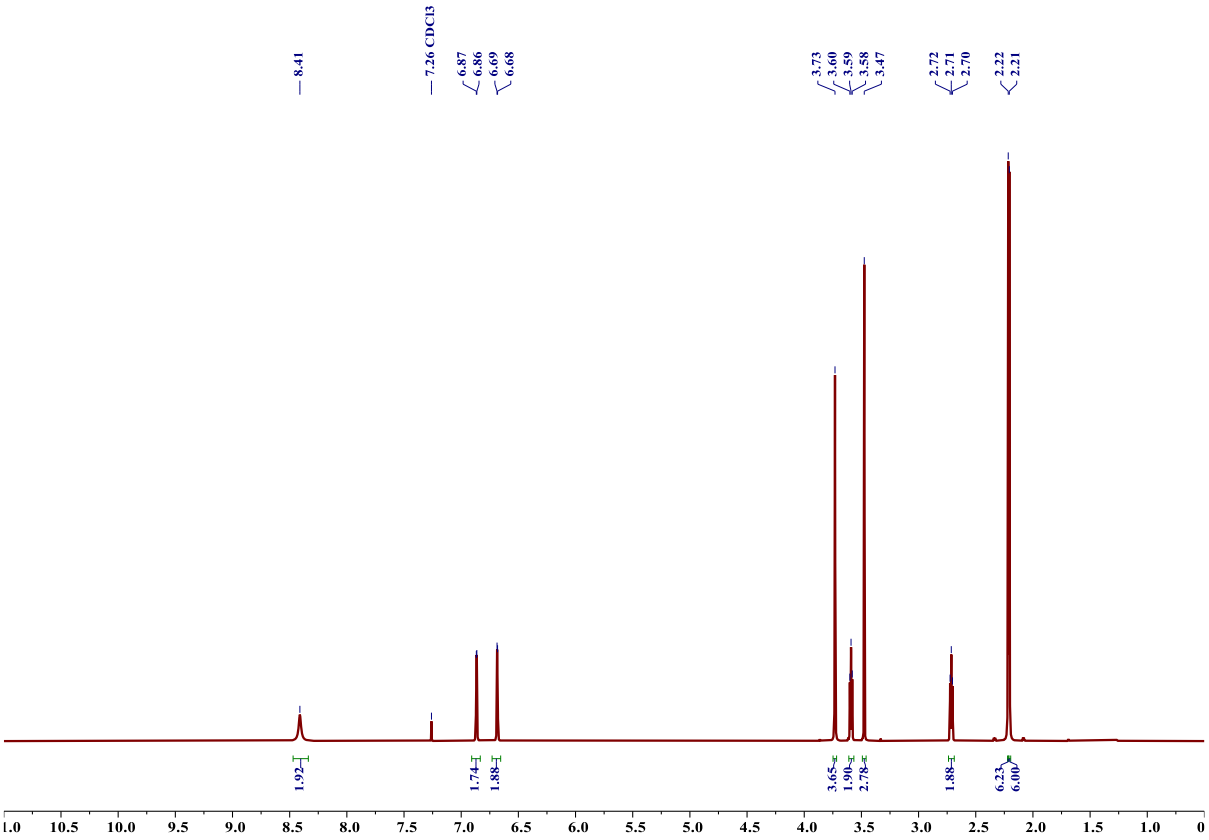

Figure S10. ^{1}H NMR spectrum (500 MHz, $CDCl_3$, 25 °C) of proligand $\{ONOO^{Me2}\}H_2$.

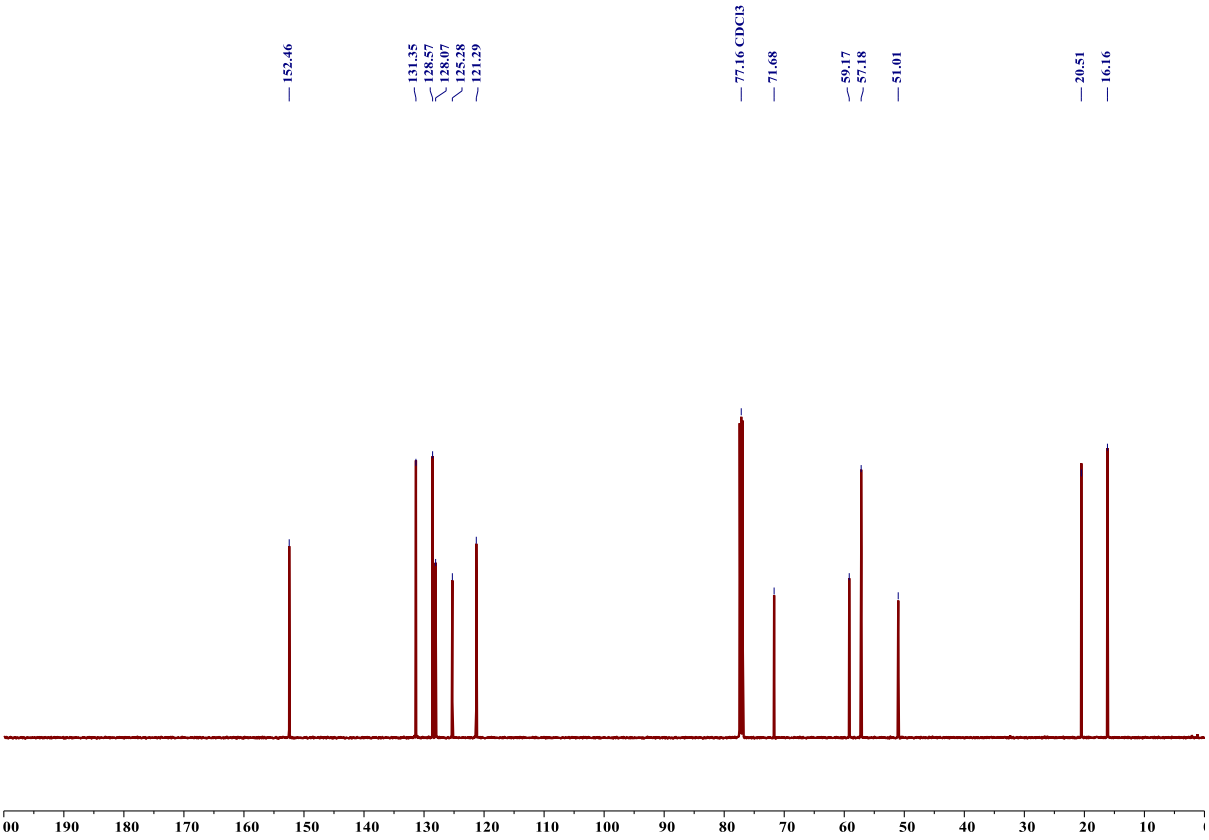

Figure S11. ^{13}C NMR spectrum (125 MHz, $CDCl_3$, 25 °C) of proligand $\{ONOO^{Me2}\}H_2$.

Synthesis of 6,6'-(((2-(dimethylamino)ethyl)azanediyl)bis(methylene))bis(2,4-dimethylphenol), {ONNO^{Me2}}H$_2$[12]

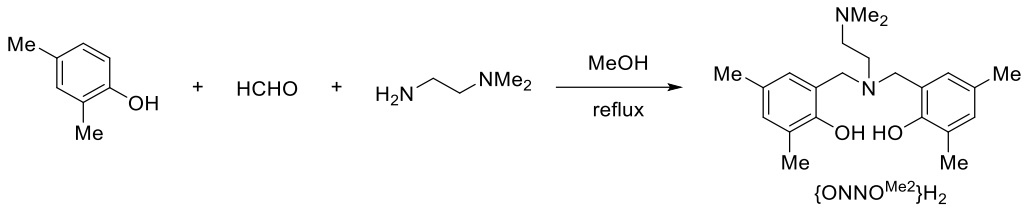

Scheme S3. The synthetic pathway towards proligand {ONNO^{Me2}}H$_2$.[12]

In a round bottom flask, a solution of 2,4-di-*tert*-butylphenol (15.85 g, 129.95 mmol), *N*,*N'*-dimethylethylenediamine (5.45 mL, 49.98 mmol) and formaldehyde (9.5 mL of a 37% solution, 131.59 mmol) in methanol (34 mL) was heated at reflux for 2 days. Cooling of the mixture gave a white precipitate which was filtered and washed with cold ethanol to give {ONNO^{Me2}}H$_2$ as a white powder (84% yield, 42.20 mmol).

^{1}H NMR (500 MHz, $CDCl_3$, Figure S12): δ 9.47 (s, 2H), 6.91 – 6.87 (m, 2H), 6.71 (d, J = 2.3, 2H), 3.61 (s, 4H), 2.59 (s, 4H), 2.34 (s, 6H), 2.24 (s, 12H).

^{13}C NMR (126 MHz, $CDCl_3$, Figure S13): δ 152.74, 131.28, 128.42, 127.61, 125.50, 121.68, 77.16, 56.49, 55.97, 49.20, 45.08, 20.49, 16.27.

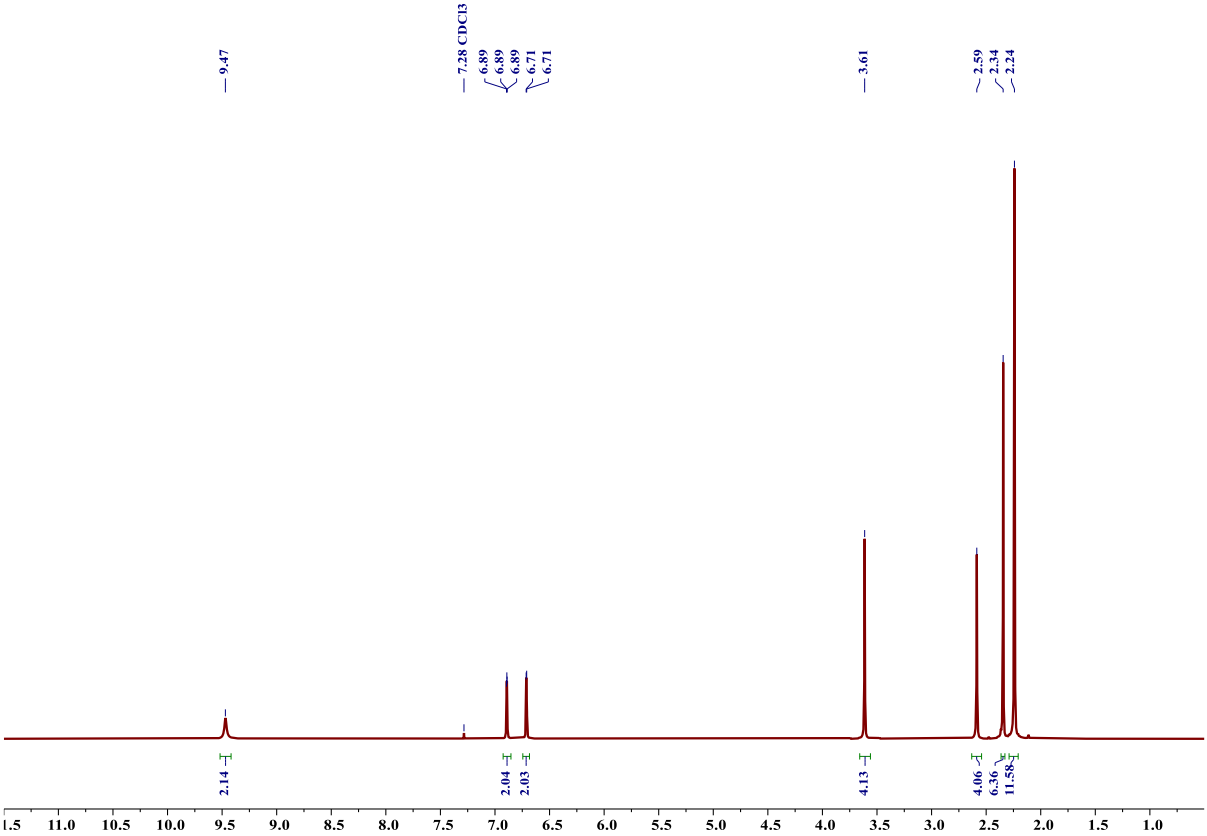

Figure S12. ^{1}H NMR spectrum (500 MHz, $CDCl_3$, 25 °C) of proligand {ONNO^{Me2}}H$_2$.

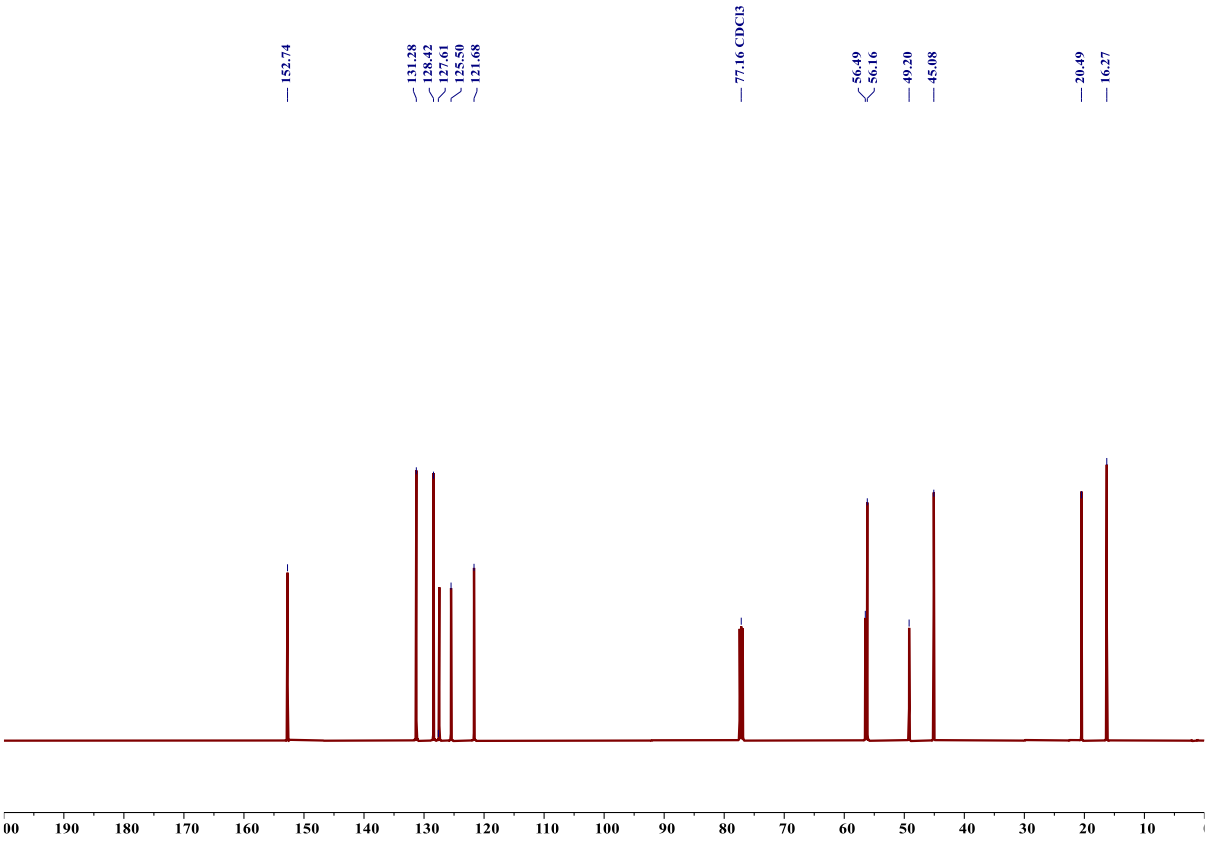

Figure S13. ^{13}C NMR spectrum (125 MHz, $CDCl_3$, 25 °C) of proligand $\{ONNO^{Me2}\}H_2$.

Synthesis of 6,6'-(2-methoxyethylazanediyl)bis(methylene)bis(2,4-di-*tert*butylphenol), $\{ONOO^{tBu2}\}H_2$[12]

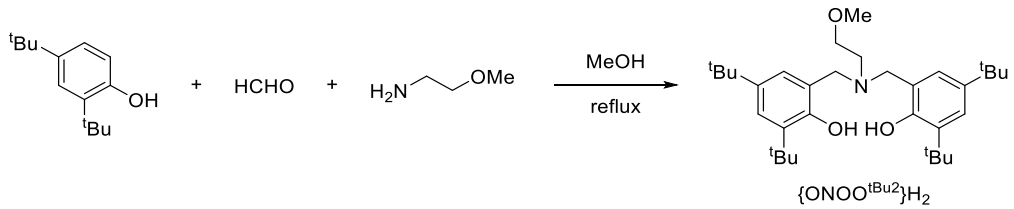

Scheme S4. The synthetic pathway towards proligand $\{ONOO^{tBu2}\}H_2$.[12]

In a round bottom flask, a solution of 2,4-di-*tert*-butylphenol (15.41 g, 74.81 mmol), 2-methoxyethylamine (3.24 mL, 37.32 mmol), and formaldehyde (9.25 mL of a 37% solution, 128.09 mmol) in methanol (30 mL) was heated at reflux for 7 days. The mixture was cooled and decanted. Following removal of the solution, the remaining oil was dissolved in methanol and refluxed for 4 h. Cooling the mixture gave a white precipitate which was filtered and washed with cold ethanol to afford $\{ONOO^{tBu2}\}H_2$ as white powder in 37% yield (13.67 mmol).

^{1}H NMR (500 MHz, $CDCl_3$, Figure S14): δ 8.48 (s, 2H), 7.21 (d, J = 2.5, 2H), 6.89 (d, J = 2.5, 2H), 3.74 (s, 4H), 3.56 (t, J = 5.2, 2H), 3.47 (s, 3H), 2.75 (t, J = 5.2, 2H), 1.41 (s, 18H), 1.27 (s, 18H).

^{13}C NMR (126 MHz, $CDCl_3$, Figure S15): δ 153.05, 140.94, 136.22, 125.04, 123.62, 121.78, 71.61, 59.01, 58.23, 51.54, 35.14, 34.99, 34.27, 31.83, 29.74.

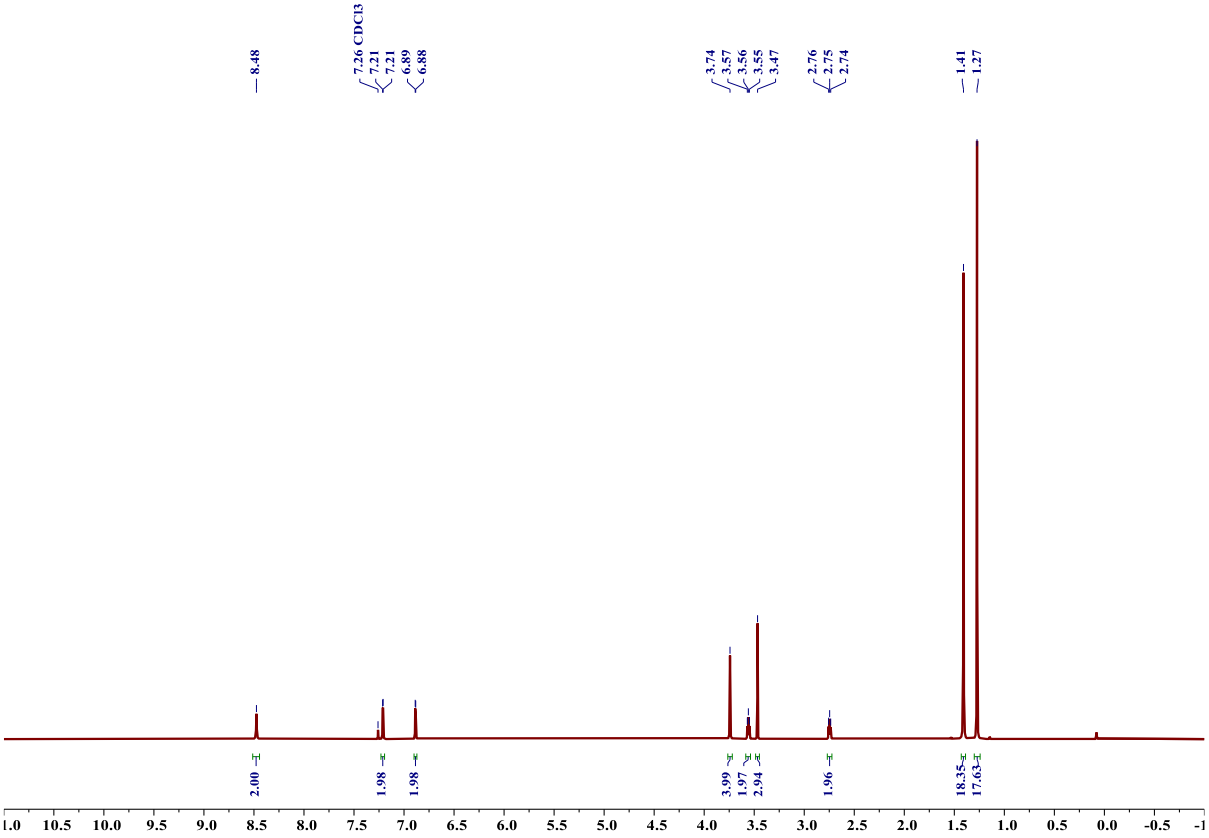

Figure S14. ^{1}H NMR spectrum (500 MHz, $CDCl_3$, 25 °C) of proligand $\{ONOO^{tBu2}\}H_2$.

Figure S15. ^{1}H NMR spectrum (125 MHz, $CDCl_3$, 25 °C) of proligand $\{ONOO^{tBu2}\}H_2$.

Synthesis of 6,6'-(*N*,*N*-dimethylethylenediamine)bis(methylene)bis(2,4-di-*tert*-butylphenol), ({ONNO^{tBu2}}H$_2$[12]

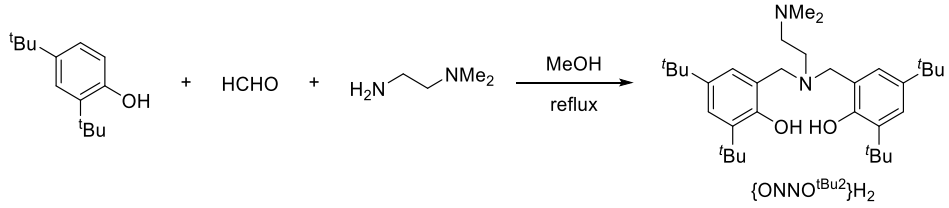

Scheme S5. The synthetic pathway towards proligand {ONNO^{tBu2}}H$_2$.

In a round bottom flask, a solution of 2,4-di-*tert*-butylphenol (15.02 g, 72.89 mmol), *N*,*N'*-dimethylethylenediamine (3.12 mL, 29.03 mmol) and formaldehyde (5.25 mL of a 37% solution, 72.82 mmol) in of methanol (30 mL) was heated at reflux for 6 days. Cooling of the mixture gave a white precipitate which was filtered and washed with cold ethanol to give {ONNO^{tBu2}}H$_2$ as a white powder (86% yield, 25.00 mmol).

^{1}H NMR (400 MHz, $CDCl_3$, Figure S16): δ 9.79 (s, 2H), 7.20 (d, J = 2.5, 2H), 6.88 (d, J = 2.4, 2H), 3.61 (s, 4H), 2.59 (tt, J = 5.9, 3.0, 4H), 2.32 (s, 6H), 1.40 (s, 18H), 1.28 (s, 18H).

^{13}C NMR (126 MHz, $CDCl_3$, Figure S17): δ 153.45, 140.30, 136.23, 124.96, 123.49, 121.77, 77.16, 56.74, 56.09, 49.21, 45.02, 35.17, 34.23, 31.87, 29.71.

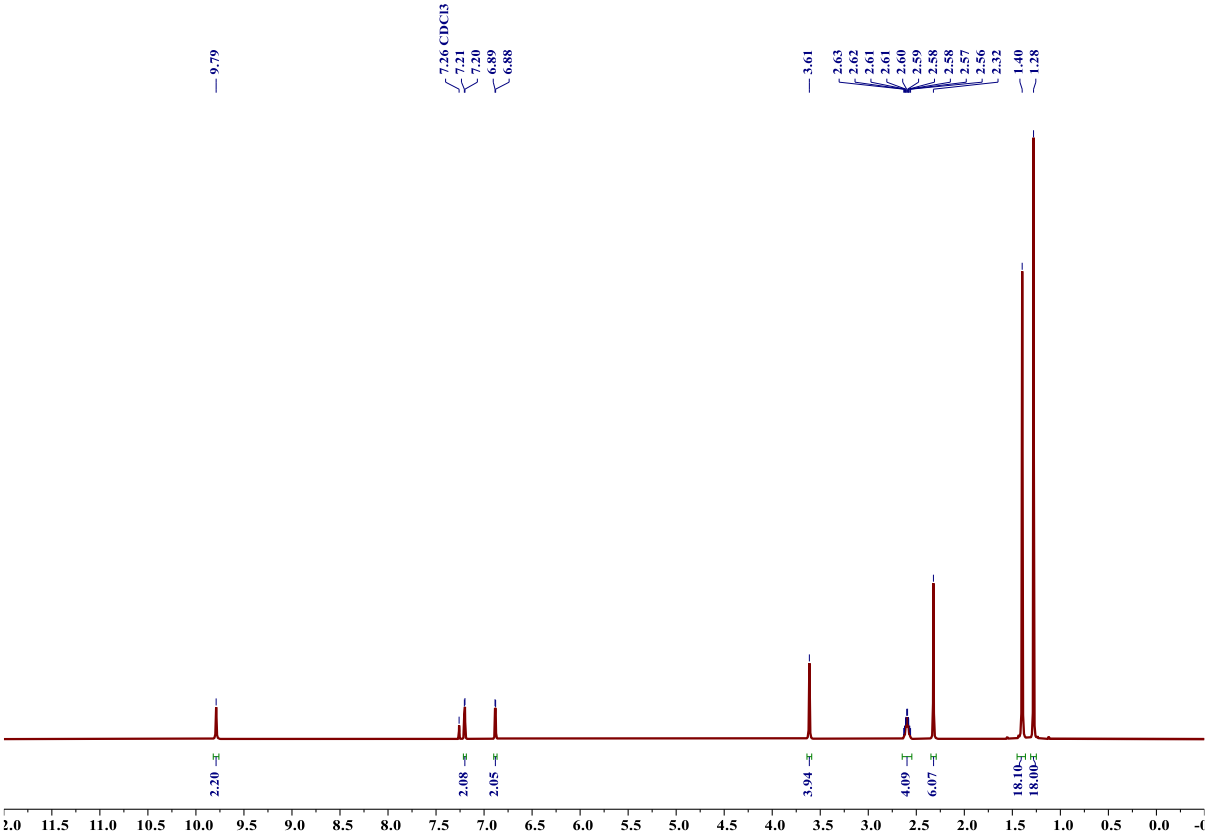

Figure S16. ^{1}H NMR spectrum (400 MHz, $CDCl_3$, 25 °C) of proligand $\{ONNO^{tBu2}\}H_2$.

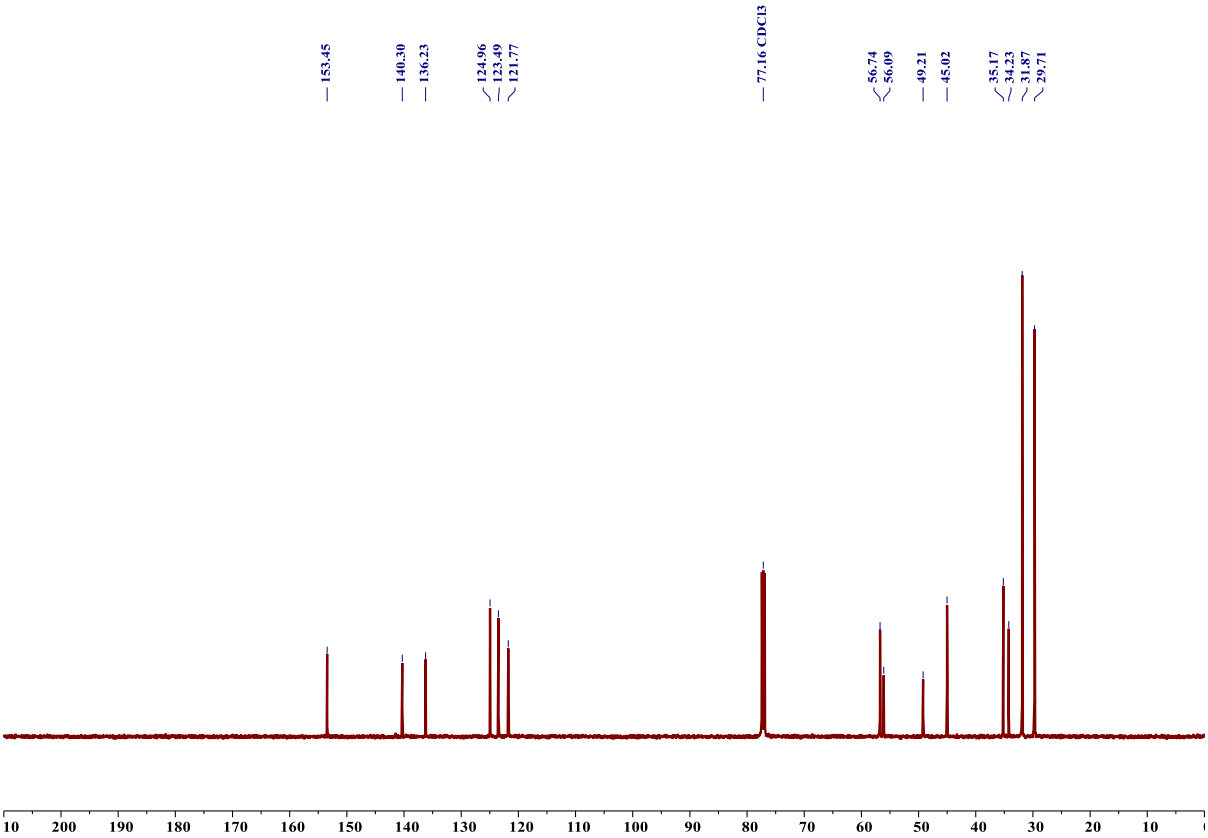

Figure S17. ^{1}H NMR spectrum (125 MHz, $CDCl_3$, 25 °C) of proligand $\{ONNO^{tBu2}\}H_2$.

Synthesis of 6,6'-(2-methoxyethylazanediyl)bis(methylene)bis(2,4-dicumylphenol), {ONOO^{cuml2}}H$_2$[12]

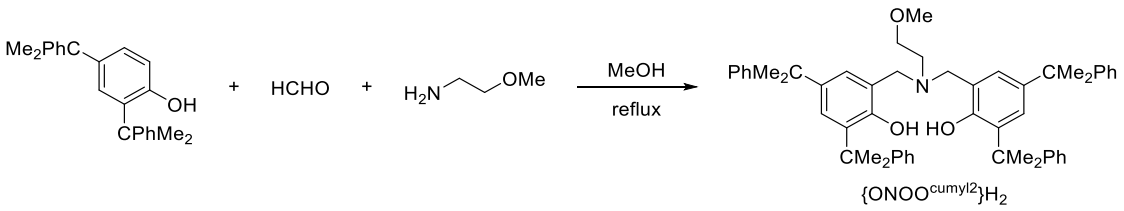

Scheme S6. The synthetic pathway towards proligand {ONOO^{cumyl2}}H$_2$.[12]

In a round bottom flask (25 mL), a solution of 2,4-dicumylphenol (5.00 g, 15.18 mmol), 2-methoxyethylamine (0.5 mL, 5.76 mmol) and formaldehyde (1.12 mL of a 37% aq. solution, 15.51 mmol) in MeOH (4 mL) was refluxed for 3 days. The reaction mixture was cooled and decanted. Following removal of the supernatant solution, the remaining oil was dissolved in MeOH and refluxed for 24 h. Cooling the mixture to give a white precipitate which was filtered and washed with cold ethanol to afford {ONOO^{cumyl2}}H$_2$ (27% yield, 1.53 mmol).

^{1}H NMR (400 MHz, $CDCl_3$, Figure S18): δ 7.73 (s, 2H), 7.36 – 7.10 (m, 22H), 6.78 (d, J = 2.3, 2H), 3.52 (s, 4H), 3.02 (t, J = 5.7, 2H), 2.97 (s, 3H), 2.42 (t, J = 5.7, 2H), 1.69 (s, 11H), 1.64 (s, 12H).

^{13}C NMR (101 MHz, $CDCl_3$, Figure S19): δ 152.42, 151.44, 150.73, 140.54, 135.47, 128.00, 127.15, 126.89, 126.04, 125.53, 125.36, 125.04, 122.64, 71.03, 58.56, 56.92, 51.21, 42.59, 42.16, 31.19, 29.54.

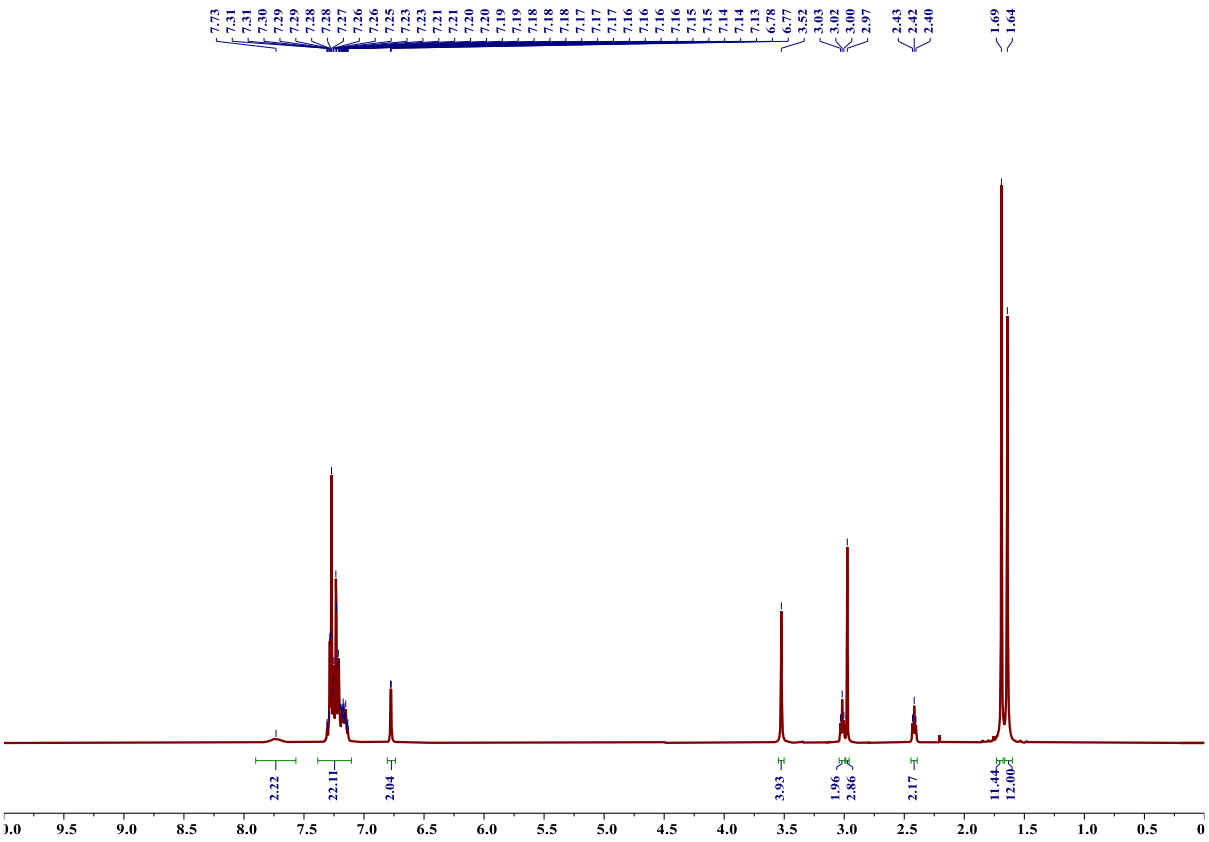

Figure S18. ^{1}H NMR spectrum (400 MHz, $CDCl_3$, 25 °C) of proligand $\{ONOO^{cumyl2}\}H_2$.

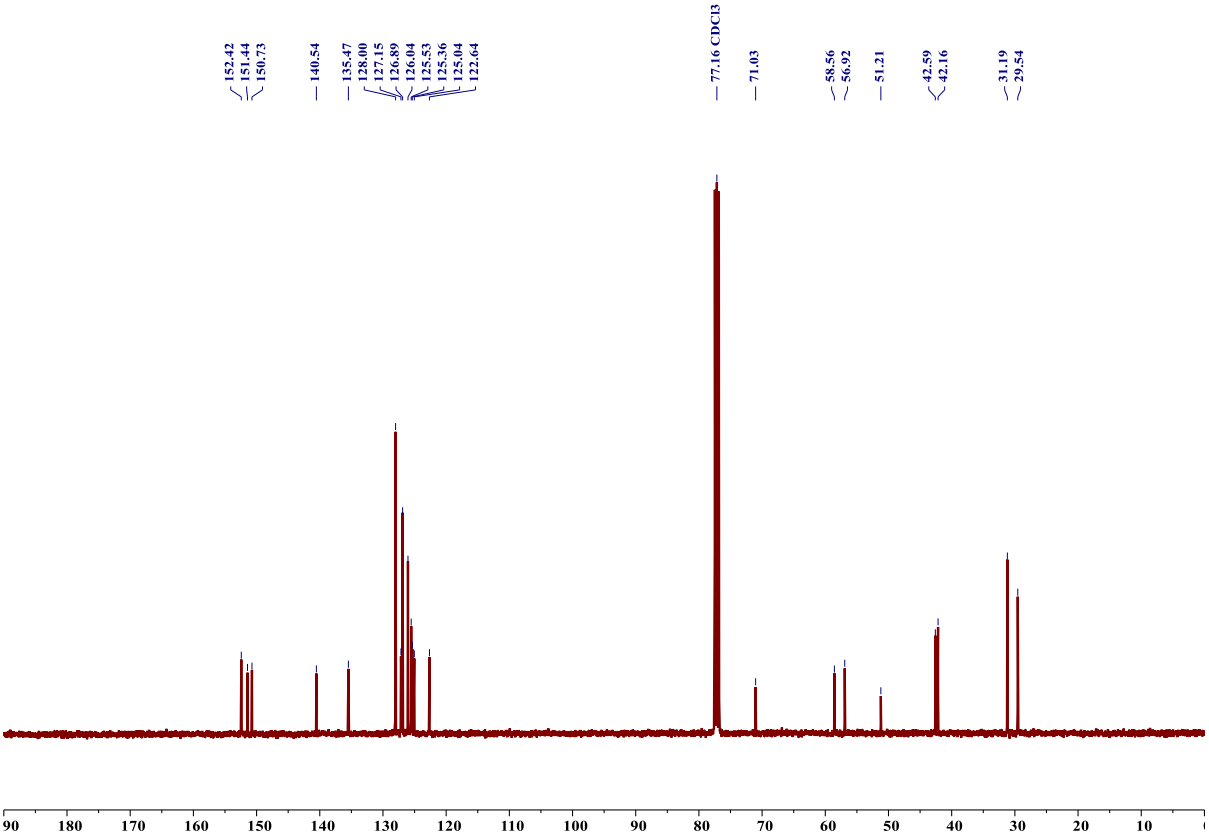

Figure S19. ^{13}C NMR spectrum (125 MHz, $CDCl_3$, 25 °C) of proligand $\{ONOO^{cumyl2}\}H_2$.

Synthesis of 6,6'-(*N*,*N*-dimethylethylenediamine)bis(methylene)bis(2,4-dicumylphenol), {ONNO^{cuml2}}H$_2$[13]

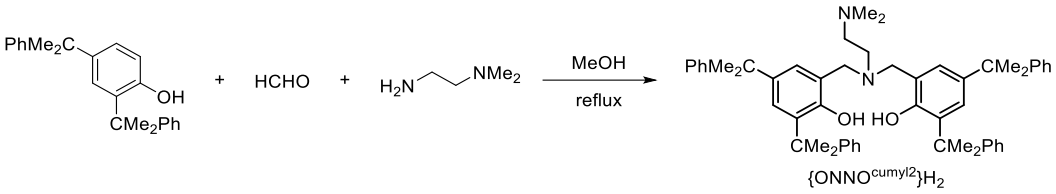

Scheme S7. The synthetic pathway towards proligand {ONNO^{cumyl2}}H$_2$.[13]

In a 25 mL round bottom flask, a solution of 2,4-dicumylphenol (16.50 g, 50 mmol), *N*,*N*'-dimethylethylenediamine (2.21 g, 25 mmol) and formaldehyde (10.5 mL of a 37% solution, 50 mmol) in methanol (25 mL) was refluxed for 48 h, during which a white precipitate was formed. Filtration and washing of the solid with cold ethanol afforded {ONNO^{cumyl2}}H$_2$ as a white powder in 99% yield.

^{1}H NMR (500 MHz, $CDCl_3$, Figure S20): δ 9.45 (s, 2H), 7.25 (d, J = 4.3, 8H), 7.21 – 7.12 (m, 13H), 7.07 (hept, J = 4.0, 2H), 6.71 (d, J = 2.4, 2H), 3.38 (s, 4H), 2.29 (t, J = 5.9, 2H), 2.11 (t, J = 5.9, 2H), 1.67 (s, 12H), 1.65 (s, 5H), 1.63 (s, 12H).

^{13}C NMR (126 MHz, $CDCl_3$, Figure S21): δ 153.07, 151.66, 151.63, 139.51, 135.93, 127.96, 127.51, 127.00, 126.92, 126.07, 125.46, 125.33, 124.63, 122.07, 77.16, 56.65, 56.17, 48.78, 44.38, 42.55, 42.20, 31.24, 29.40.

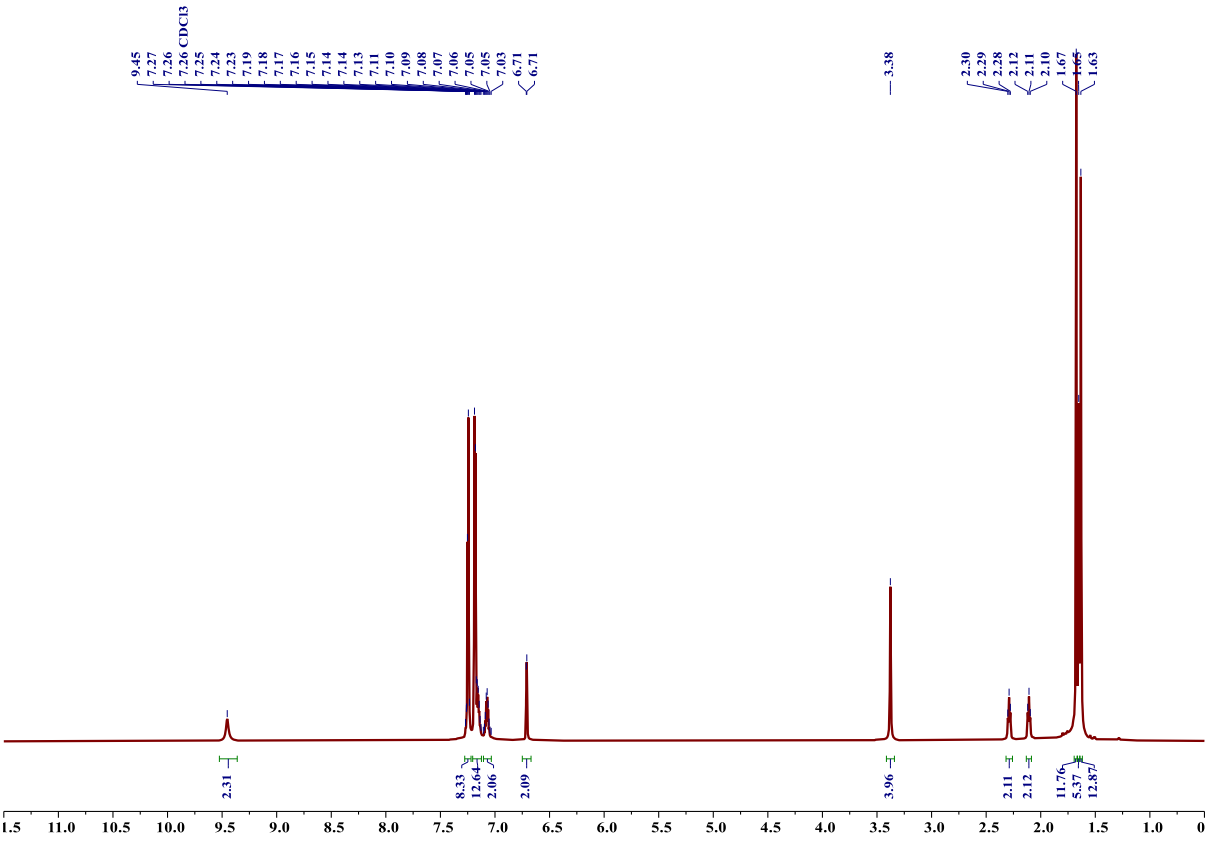

Figure S20. ^{1}H NMR spectrum (500 MHz, $CDCl_3$, 25 °C) of proligand {ONNO^{cumyl2}}H$_2$.

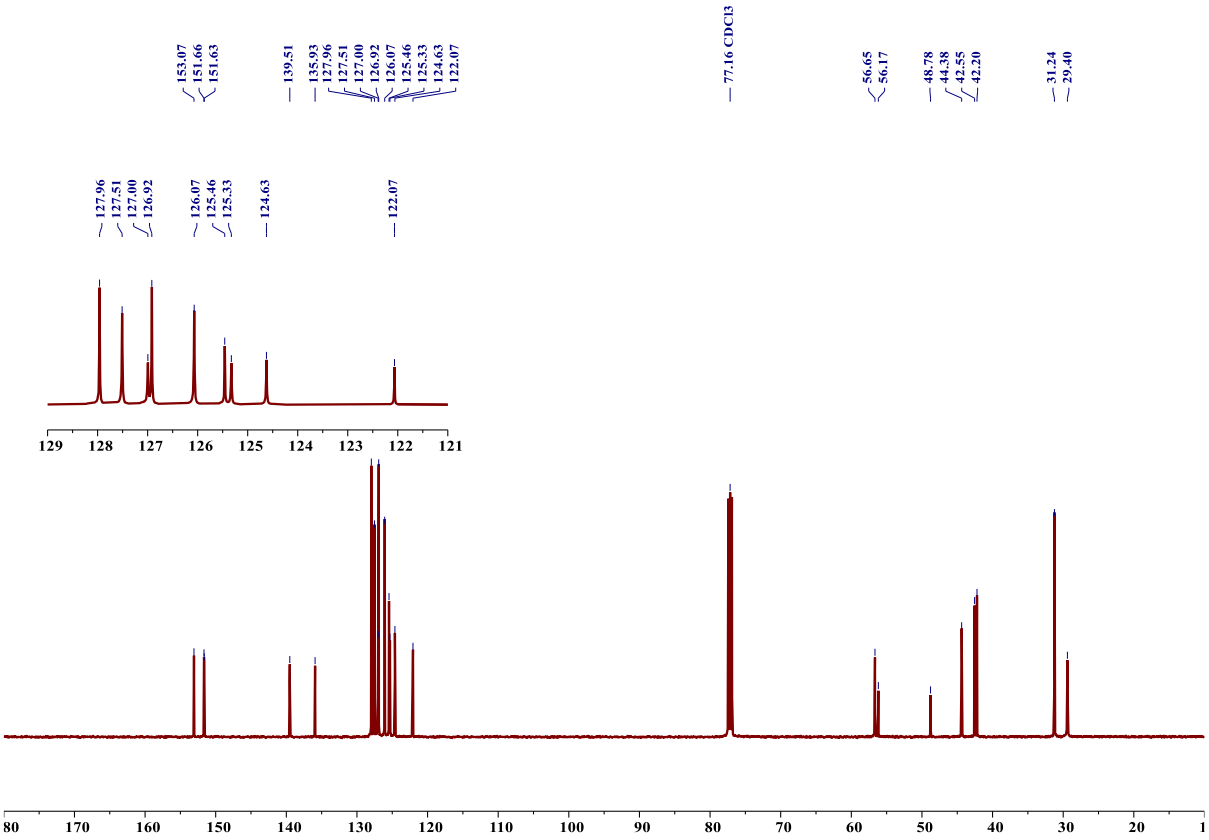

Figure S21. ^{13}C NMR spectrum (125 MHz, $CDCl_3$, 25 °C) of proligand {ONNO^{cumyl2}}H_2.

Synthesis of *N*-(2-Pyridylmethyl)-*N*,*N*-bis(2'-hydroxy-3',5'-dimethylbenzyl)amine {ONN^{Py}O^{Me2}}H_2[14]

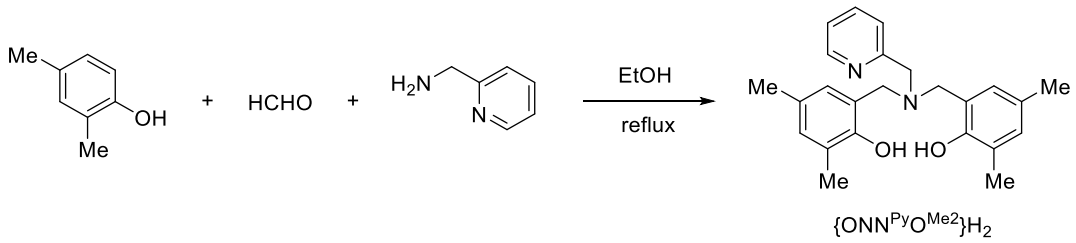

Scheme S8. The synthetic pathway towards proligand {ONN^{Py}O^{Me2}}H_2.[14]

2-Aminomethylpyridine (2.70 g, 24.9 mmol), 2,4-dimethylphenol (6.10 g, 49.9 mmol), and paraformaldehyde (1.50 g, 49.9 mmol) were dissolved in absolute ethanol (50 mL) in a thick-walled ampule equipped with a Rotaflo valve. The mixture was stirred at 110 °C for 3 days. The volatiles were subsequently removed under reduced pressure to leave an orange oil. This oil was triturated with 30 mL of absolute ethanol to yield a white powder (4.80 g, 51% yield), which was isolated by filtration and drying.

^{1}H NMR (500 MHz, $CDCl_3$, Figure S22): δ 10.44 (s, 1H), 8.71 (d, J = 4.7, 1H), 7.70 (td, J = 7.7, 1.8, 1H), 7.28 (ddd, J = 7.6, 5.0, 1.2, 1H), 7.12 (d, J = 7.9, 1H), 6.88 (s, 2H), 6.72 (s, 2H), 3.85 (s, 2H), 3.76 (s, 3H), 2.23 (d, J = 2.9, 12H).

^{13}C NMR (126 MHz, $CDCl_3$, Figure S23): δ 156.35, 153.26, 148.41, 137.58, 131.58, 128.62, 127.67, 125.66, 123.86, 122.63, 120.91, 56.56, 55.60, 20.51, 16.36.

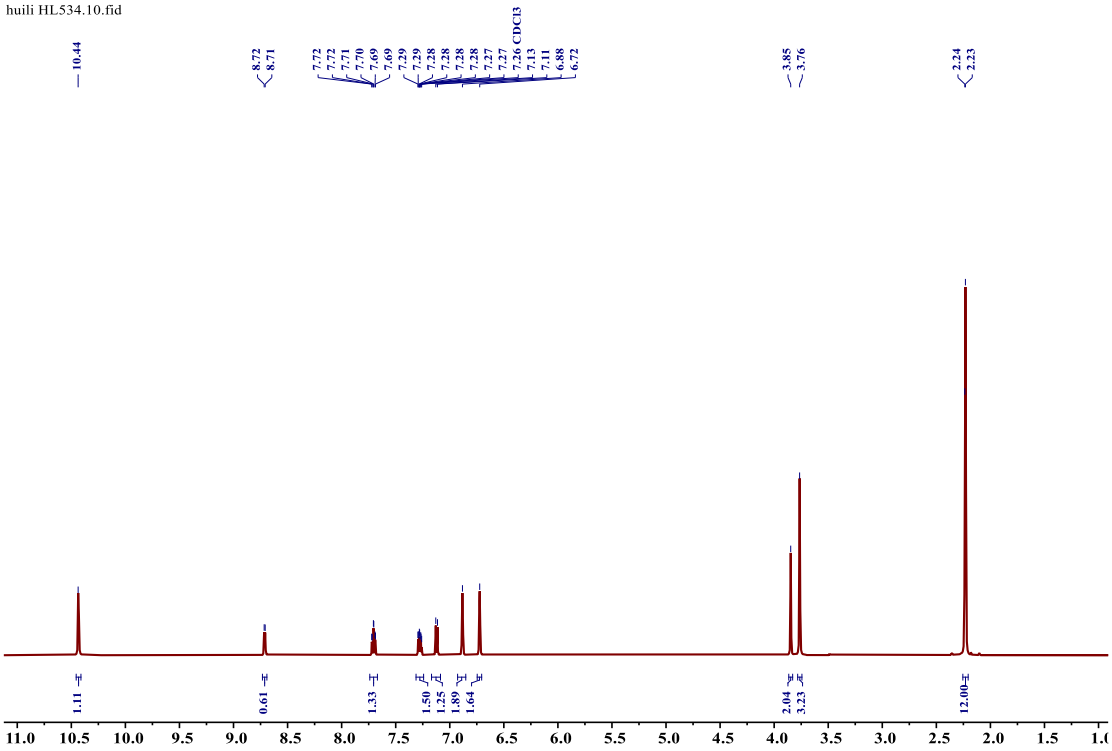

Figure S22. ^{1}H NMR spectrum (500 MHz, $CDCl_3$, 25 °C) of proligand $\{ONN^{Py}O^{Me2}\}H_2$.

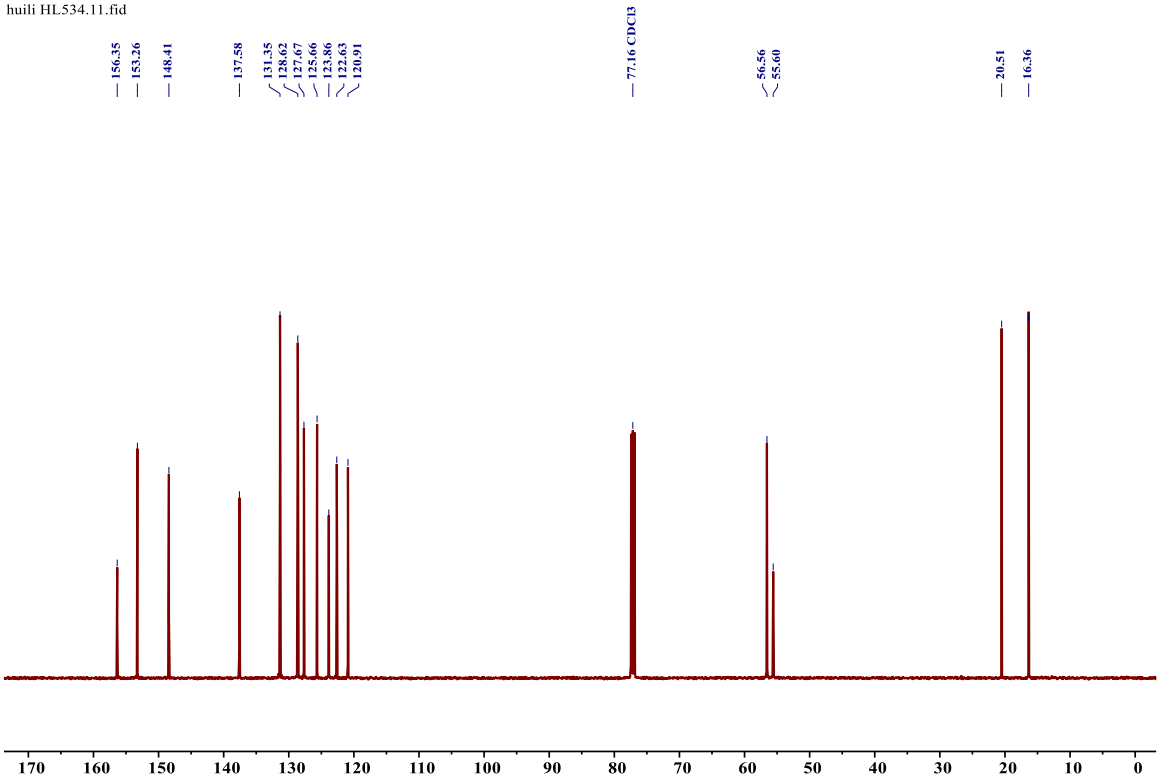

Figure S23. ^{13}C NMR spectrum (125 MHz, $CDCl_3$, 25 °C) of proligand $\{ONN^{Py}O^{Me2}\}H_2$.

Synthesis of Catalyst Precursors

Synthesis of lithium bis(dimethylsilyl)amide, {LiN(SiHMe$_2$)$_2$}

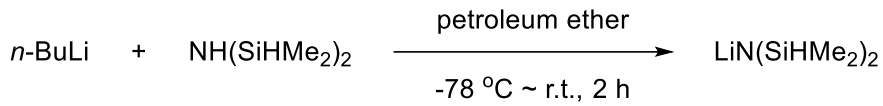

Scheme S9. The synthetic pathway towards LiN(SiHMe$_2$)$_2$.

1,1,3,3-Tetramethyldisilazane (7.66 g, 57.45 mmol) was placed in a 250 mL flask, dissolved in petroleum ether (75 mL) and cooled down to - 78 °C. Then *n*-butyllithium (22 mL of a 2.5 M solution of in *n*-hexane, 55.0 mmol) was added over a period of 15 min under vigorous stirring. After complete addition, the white suspension was allowed to warm up to ambient temperature, stirred for another 2 h period, and evaporated to dryness, leaving lithium bis(dimethylsilyl)amide as a white powder (7.62 g, 98% yield).

The synthesis of Y(N(SiHMe$_2$)$_2$)$_3$(THF)$_2$[15]

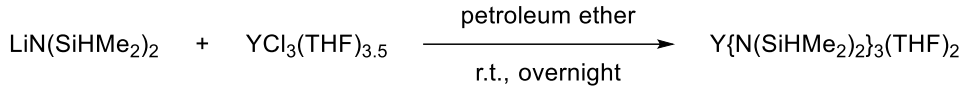

Scheme S10. The synthetic pathway towards Y{N(SiHMe$_2$)$_2$}$_2$(THF)$_2$.[15]

YCl$_3$ (4.00g, 20.49mmol) in THF (60 mL) was charged in a 100 mL flask under an inert atmosphere and heated to reflux for 1.5h, the mixture was cooled to ambient temperature. Evaporated to dryness to give white powder. Lithium bis(dimethylsilyl)amide (1.47 g, 10.06 mmol) was added slowly to a suspension of this white power (1.58 g, 3.50 mmol) in petroleum ether (60 mL). After stirring for 12 h at ambient temperature, the reaction mixture was filtered and the white residue was washed with petroleum ether (2 × 40 mL). The petroleum ether phases were combined and the volatiles were removed *in vacuo*. After recrystallized in hexane at -30 °C, a white powder Y{N(SiHMe$_2$)$_2$}$_2$(THF)$_2$ was obtained (1.67 g, 79.5% yield).

^{1}H NMR (400 MHz, C_6D_6. Figure S24): δ 4.99 (hept, J = 3.0, 6H), 3.86 – 3.76 (m, 8H), 1.39 – 1.31 (m, 8H), 0.39 (d, J = 3.1, 36H).

^{13}Li NMR (Figure S25)

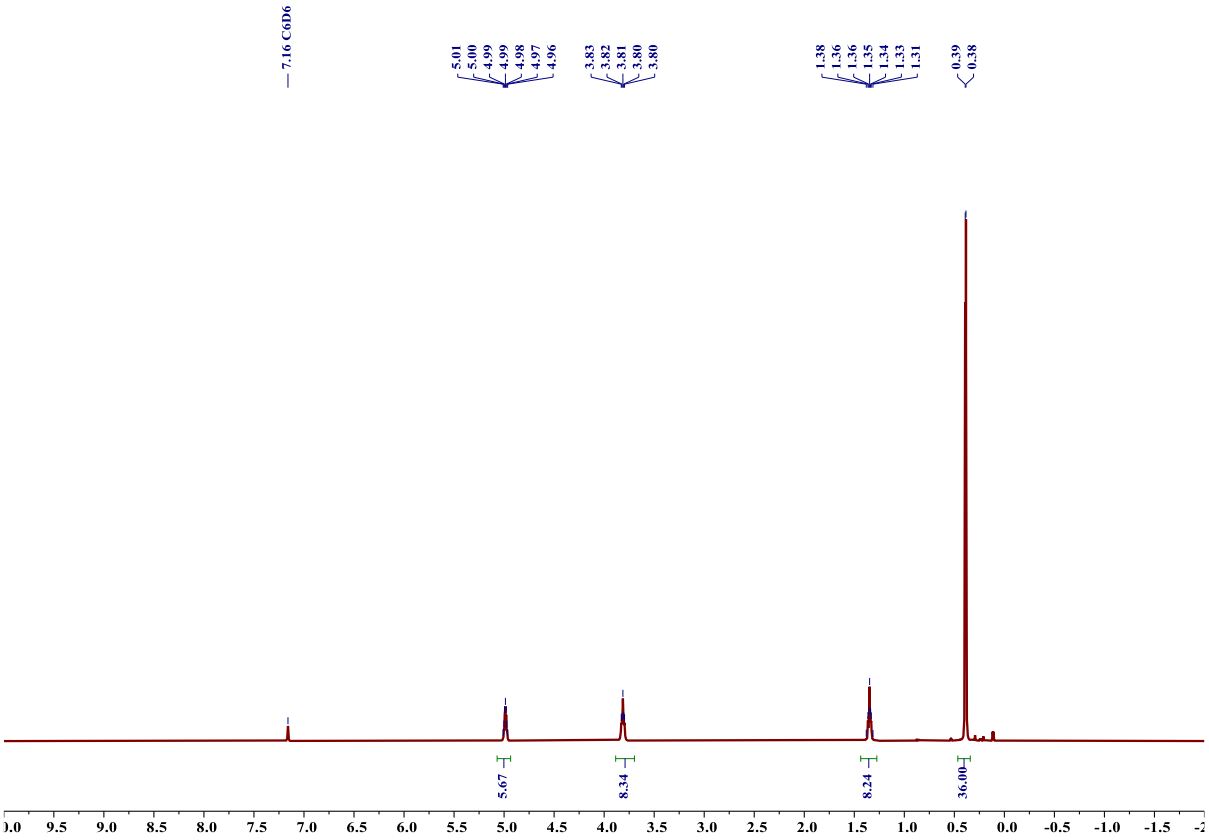

Figure S24. ^{1}H NMR spectrum (400 MHz, C_6D_6, 25 °C) of $Y\{N(SiHMe_2)_2\}_2(THF)_2$.

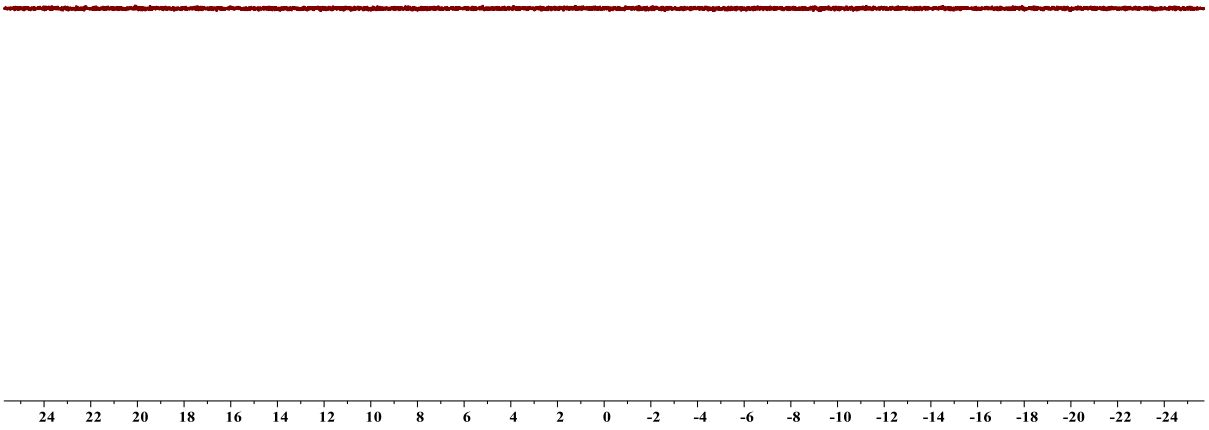

Figure S25. ^{7}Li NMR spectrum (194 MHz, C_6D_6, 25 °C) of $Y\{N(SiHMe_2)_2\}_2(THF)_2$.

The synthesis of {ONOO^{tBu2}}Y(N(SiHMe$_2$)$_2$)(THF)[12]

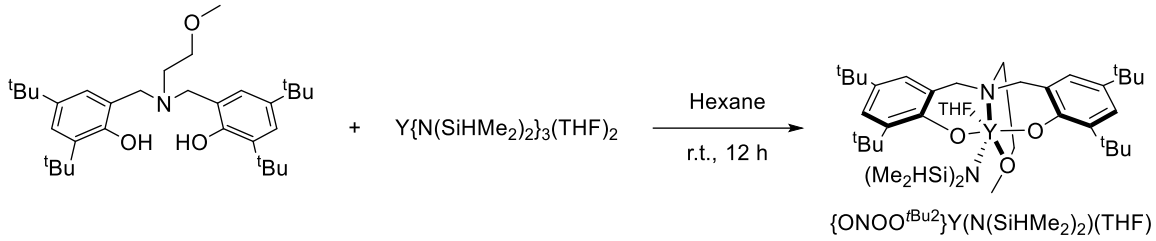

Scheme S11. Synthetic pathway towards yttrium complex "Y{ONOO^{tBu2}}(N(SiHMe$_2$)$_2$)(THF)".[12]

A solution of {ONOO^{tBu2}}H$_2$ (0.809 g, 1.58 mmol) in hexane (15 mL) was added at room temperature to a stirred solution of Y{N(SiHMe$_2$)$_2$}$_3$(THF)$_2$ (1.00 g, 1.58 mmol) in hexane (10 mL). After the mixture had been stirred for 21 h at room temperature, a white precipitate had formed. The solid was then filtered out, yielding "Y{ONOO^{tBu2}}(N(SiHMe$_2$)$_2$)(THF)" as a white powder (0.85 g, 67%).

^{1}H NMR (400 MHz, C_6D_6, Figure S26): δ 7.60 (d, J = 2.6, 2H), 7.09 (d, J = 2.6, 2H), 5.18 – 5.11 (m, 2H), 3.80 (s, 6H), 3.01 (d, J = 12.6, 2H), 2.85 (s, 3H), 2.72 (t, J = 5.5, 2H), 2.31 (t, J = 5.5, 2H), 1.78 (s, 18H), 1.46 (s, 18H), 1.22 (s, 4H), 0.49 (d, J = 3.0, 12H).

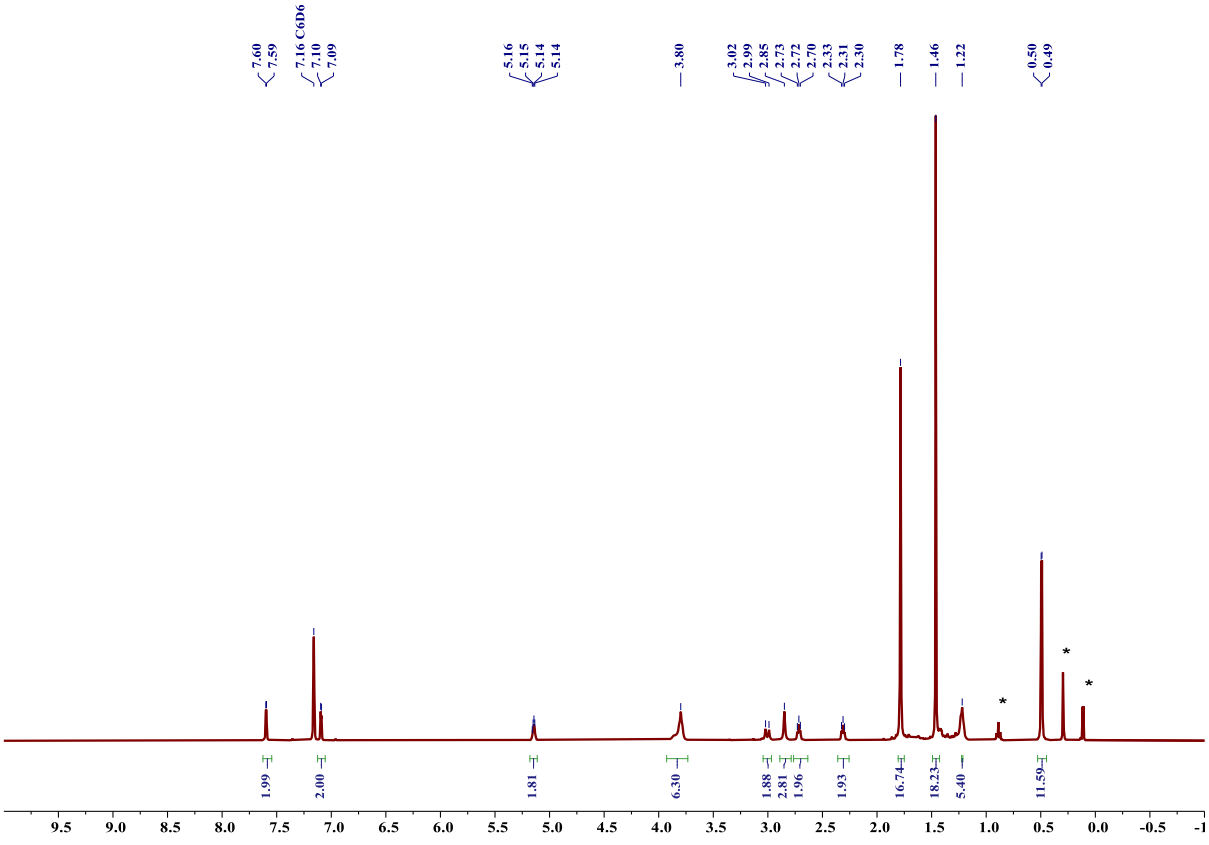

Figure S26. ^{1}H NMR spectrum (400 MHz, C_6D_6, 25 °C) of {ONOO^{tBu2}}Y(N(SiHMe$_2$)$_2$)(THF).

Synthesis of (BDI)ZnN(TMS)$_2$[16]

Synthesis of (BDI)H

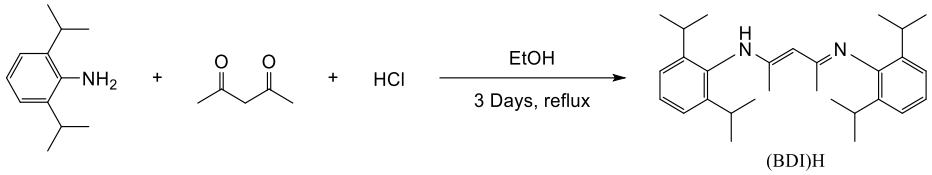

Figure S27. Synthetic pathway towards (BDI)H.

Concentrated HCl (1.2 mL, 14.42 mmol) was added to a solution of 2,4-pentanedione (1.50 mL 14.71 mmol) and 2,6-diisopropylaniline (5.88 g; 33.0 mmol) in ethanol (60 mL). The reaction mixture was heated at reflux for 3 days and then concentrated to a brown residue. The crude product was extracted with 30 mL of methylene chloride. After stirring with 60 mL saturated sodium carbonate, compound was extracted into methylene chloride. Evaporation of solvent and recrystallization from methanol afforded (BDI)H as a white crystalline solid (2.74 g, 45 %).

^{1}H NMR (400 MHz, $CDCl_3$, Figure S28): δ 12.13 (s, 1H), 7.18 – 7.09 (m, 6H), 4.88 (s, 1H), 3.13 (p, J = 6.9, 4H), 1.73 (s, 6H), 1.23 (d, J = 6.9, 11H), 1.13 (d, J = 6.9, 12H).

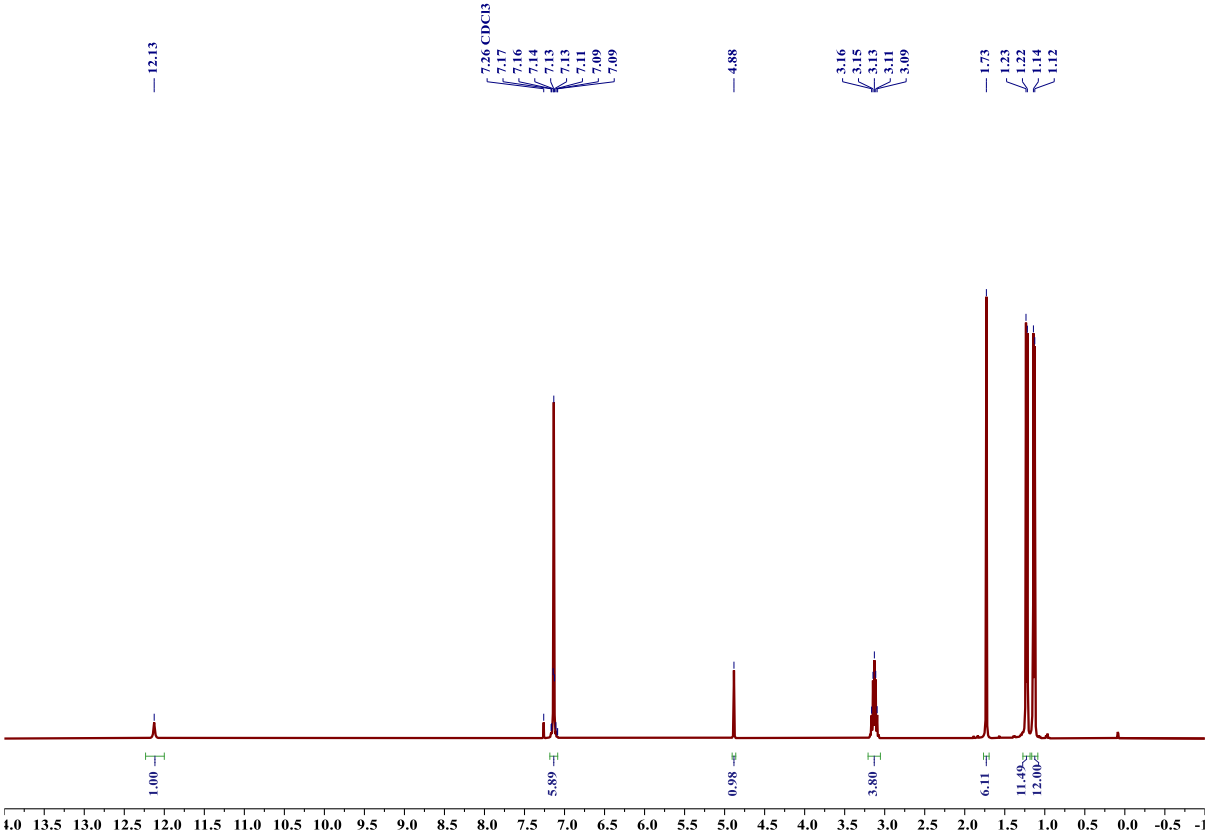

Figure S28. ^{1}H NMR spectrum (400 MHz, $CDCl_3$, 25 °C) of (BDI)H.

Synthesis of zinc bis[bis(trimethylsilyl)amide], {Zn(N(TMS)$_2$)$_2$}

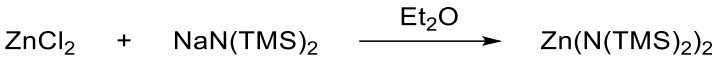

Scheme S12. Synthetic pathway towards zinc bis[bis(trimethylsilyl)amide].

To a 250-mL three-necked flask equipped with magnetic stirrer, reflux condenser, and dropping funnel and connected to the inert gas supply of a vacuum line are added sodium amide (5.2 g, 0.133 mol) and toluene (100 mL). 1,1,1,3,3,3-Hexamethyldisilazane (29 mL, 0.137 mol) is added dropwise to the stirred suspension at room temperature over a period of 40 min. The reaction mixture is then refluxed for 6 h and allowed to cool to room temperature; the solvent is then removed in vacuo to give $NaN(TMS)_2$ as a white residue which is dried in vacuo for 2 h, yielding 23.8 g (0.130 mol, 98%). This compound is dissolved in diethyl ether (100 mL), cooled to – 78°C, and anhydrous $ZnCl_2$, (7.62 g, 56 mmol) is added. The stirred mixture is allowed to warm to room temperature, refluxed for 1 h, and filtered, and the white residue is washed with diethyl ether (2 x 50 mL). The combined filtrates are evaporated in vacuo and the pale-yellow liquid residue is distilled to give $Zn(N(TMS)_2)_2$, as a colourless liquid (15.1 g, 39 mmol, 70% yield).

^{1}H NMR (400 MHz, $CDCl_3$, Figure S29): δ 0.10 (s, 36H).

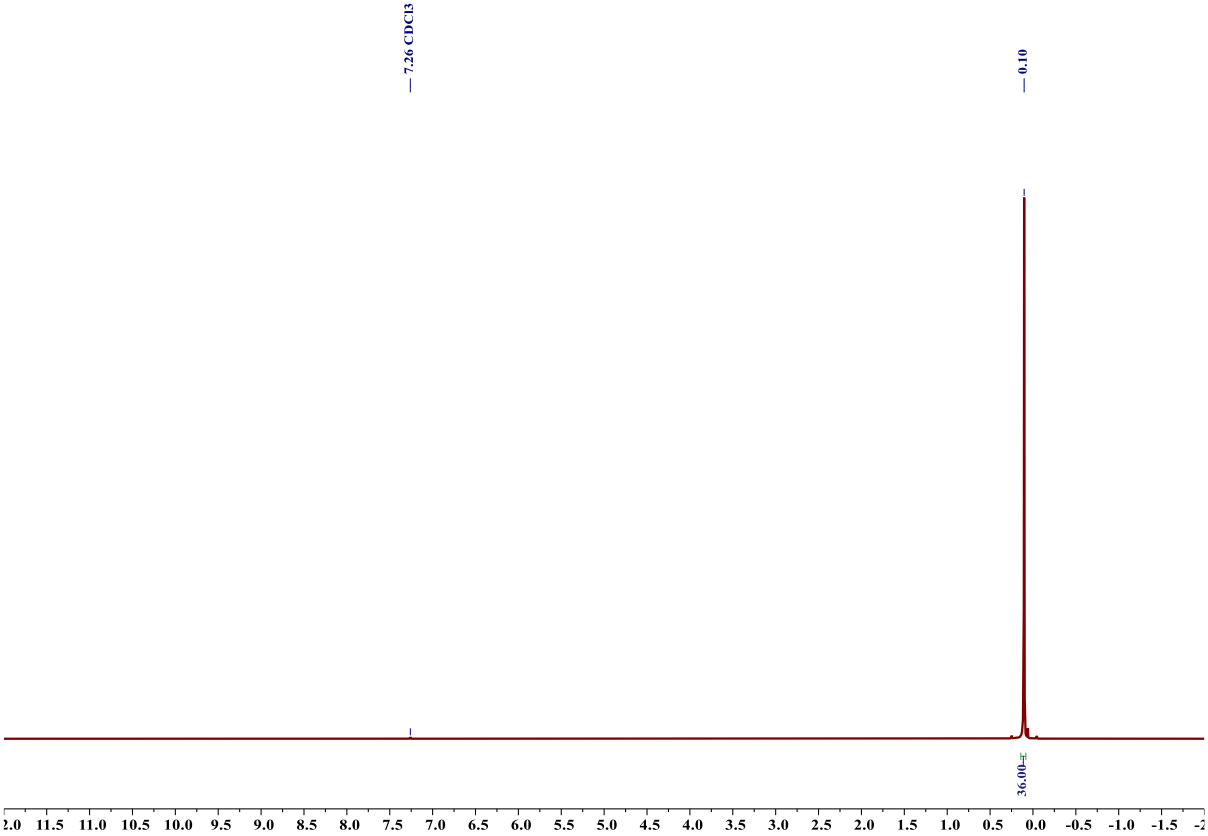

Figure S29. ^{1}H NMR spectrum (400 MHz, $CDCl_3$, 25 °C) of $Zn(N(TMS)_2)_2$.

Synthesis of (BDI)ZnN(TMS)$_2$

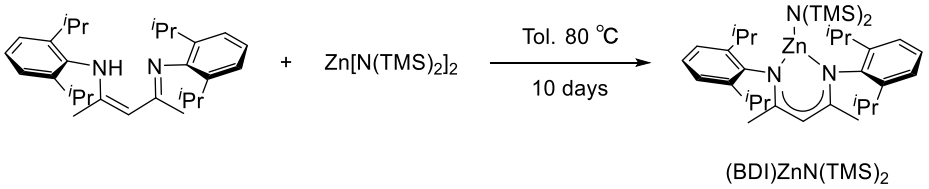

Scheme S13. Synthetic pathway towards (BDI)ZnN(TMS)$_2$.

A solution of (BDI)H (1.52 g, 3.65 mmol) in toluene (7.5mL) was added into Zn(N(TMS)$_2$)$_2$ (1.5 mL, 3.6 mmol)in toluene (2.5 mL) at room temperature. After stirring for 10 days at 80 ℃, the clear, yellow green solution was dried in vacuum, giving (BDI)ZnN(TMS)$_2$ in quantitative yield**.** The light-yellow solid was recrystallized from toluene (5 mL) at −30 °C.

^{1}H NMR (400 MHz, C_6D_6, Figure S30): δ 7.15 (s, 6H), 4.88 (s, 1H), 3.26 (hept, J = 6.9, 4H), 1.68 (s, 6H), 1.39 (d, J = 6.8, 12H), 1.14 (d, J = 6.7, 12H), 0.01 (s, 18H).

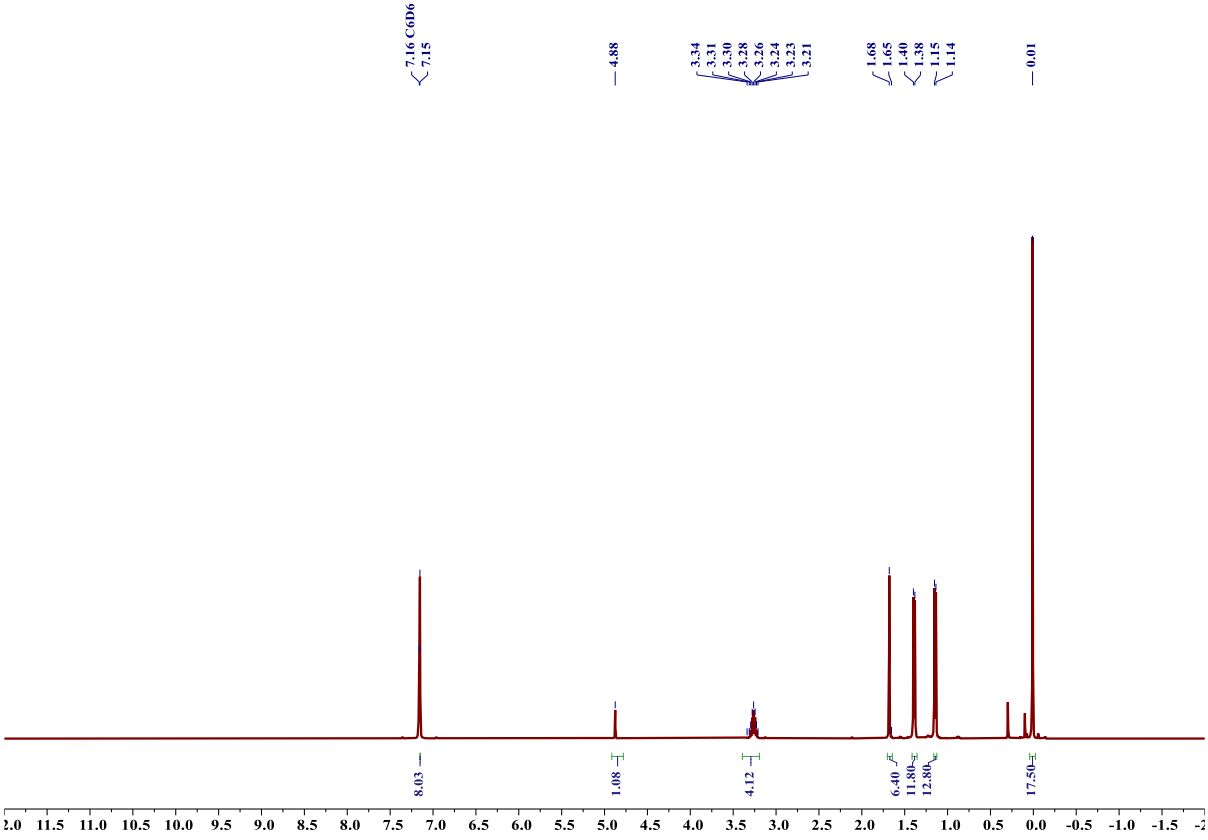

Figure S30. ^{1}H NMR spectrum (400 MHz, C_6D_6, 25 °C) of (BDI)ZnN(TMS)$_2$.

Synthesis of [(salph)Cr(THF)$_2$][Co(CO)$_4$][17]

Synthesis of (salph)H$_2$

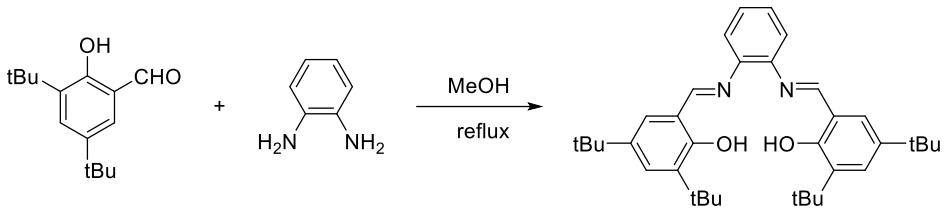

Scheme S14. Synthetic pathway towards (Salph)H_2.

3,5-Di-*tert*-butylsalicylaldehyde(18.48 g, 81.4 mmol) and 1,2-diaminobenzene (4 g, 37 mmol) were refluxed in methanol (400 mL) for 20 h. The solution was allowed to cool to room temperature. The precipitate was filtered off and washed with ethanol (200 mL). The product was dried under high vacuum to yield (salph)H_2 (12.58 g, 63%) as yellow crystals.

^{1}H NMR (400 MHz, $CDCl_3$, Figure S31): δ 13.53 (s, 2H), 8.66 (s, 2H), 7.44 (d, J = 2.5, 2H), 7.32 (dd, J = 5.9, 3.4, 2H), 7.25 – 7.19 (m, 4H), 1.44 (s, 18H), 1.32 (s, 18H).

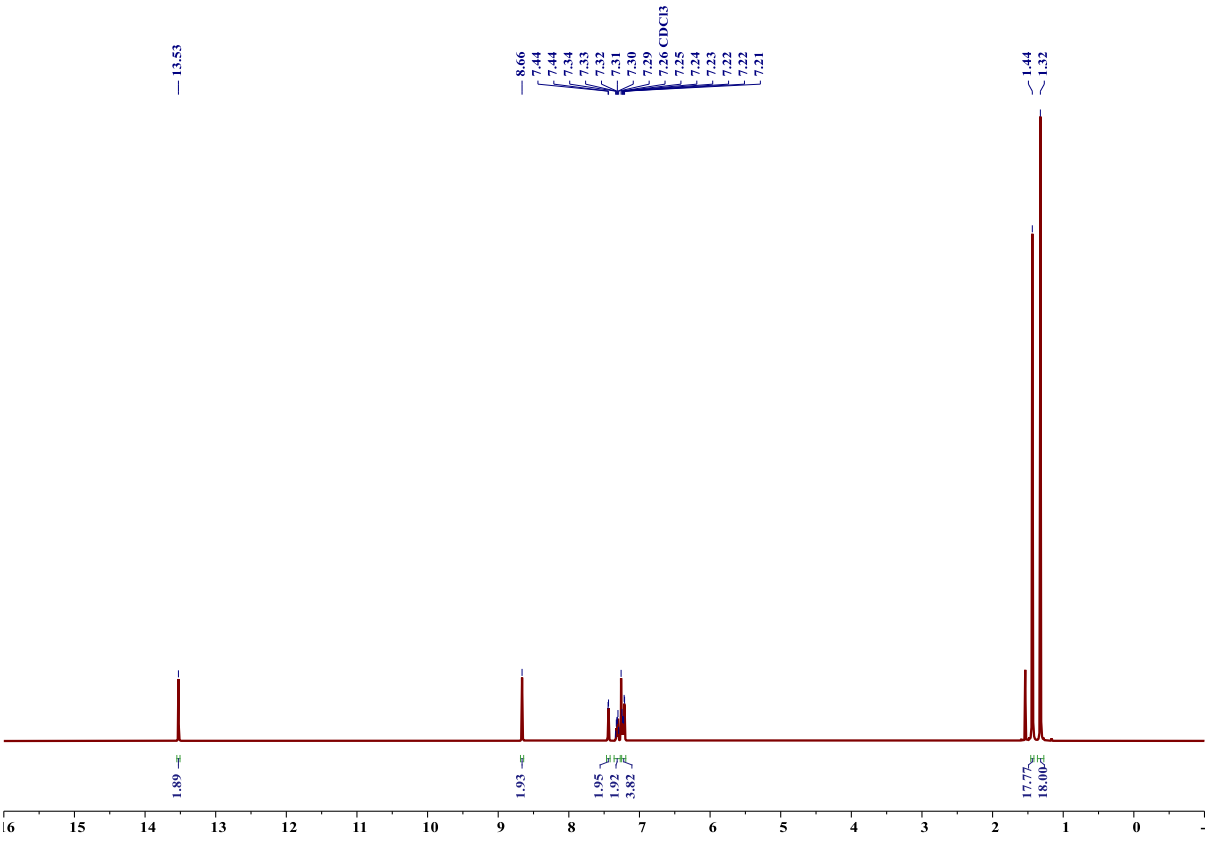

Figure S31. ^{1}H NMR spectrum (400 MHz, $CDCl_3$, 25 °C) of (salph)H_2.

Synthesis of (salph)CrCl

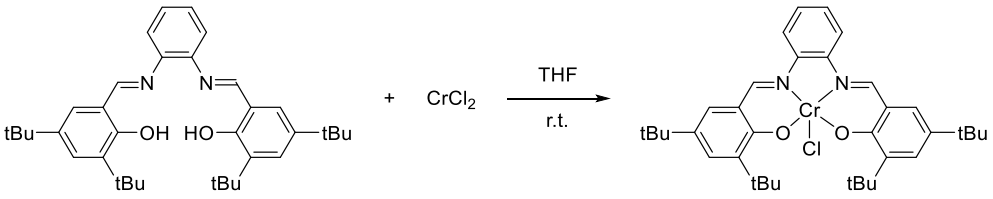

Scheme S15. Synthetic pathway towards (salph)CrCl.

In a glove box, (salph)H_2 (3.0 g, 5.5 mmol) and $CrCl_2$ (0.77 g, 6.3 mmol) were combined in an oven-dried Schlenk tube. Dry, degassed THF (150 mL) was added to the flask with stirring at room temperature to afford an immediate colour change from orange to dark red. After stirring for 3 h under nitrogen, the flask was opened to air and allowed to stir overnight. The reaction was diluted with 200 mL diethyl ether and washed twice with sat. $NH_4Cl_{(aq.)}$ and three times with sat. $NaCl_{(aq.)}$. The organic phase was then dried over Na_2SO_4 and the solvent was removed under reduced pressure to afford a red powder. The residue can be recrystallized from hot acetonitrile by cooling to –20 °C overnight to yield dark red crystals of (salph)CrCl (2.1 g, 53%).

Synthesis of $NaCo(CO)_4$

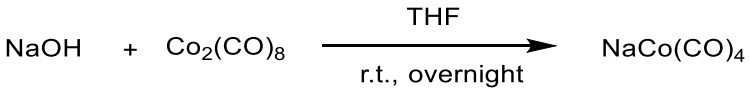

Scheme S16. Synthetic pathway towards $NaCo(CO)_4$.

In a glovebox, 1.66 g of $Co_2(CO)_8$ and 3.0 g of NaOH were combined in a Schlenk tube. Caution! Then 40 mL of THF was added slowly. The solution was stirred maintaining inert atmosphere. After 2 h, the colour of the solution change from dark red to yellow solution. Then the yellow solution was filtered to a Schlenk flask, and evaporated the solvent under vacuum obtaining a white salt (1.2 g).

Synthesis of $[(salph)Cr(THF)_2]^+[Co(CO)_4]^-$

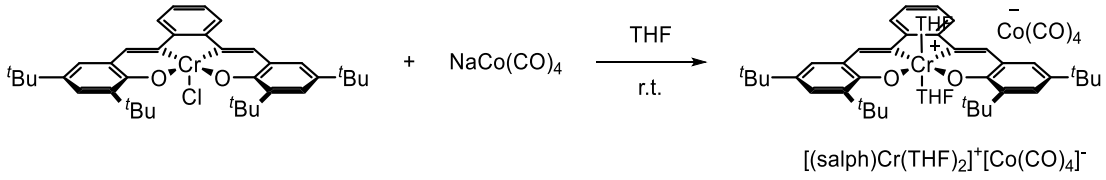

Scheme S17. Synthetic pathway towards $[(salph)Cr(THF)_2]^+[Co(CO)_4]^-$

$NaCo(CO)_4$ (0.57 g, 2.9 mmol) and (salph)CrCl (2.2 g, 2.9 mmol) were dissolved in 100 mL THF and stirred at room temperature overnight. The red solution was filtered to remove NaCl, reduced to 50 mL, and layered with 100 mL hexane. Within days, large crystals formed and the supernatant was removed. The red crystals were washed three times with hexanes and dried under vacuum to afford $[(salph)Cr(THF)_2]^+[Co(CO)_4]^-$ (1.9 g, 71%).

Determination of Tacticity of P3TB by Band Selective HMBC and HSQC

Some deconvolutions-calculations were also performed on the carbonyl ^{13}C projection extracted from the band-selective HMBC spectrum. For instance, for entry HL637 (Table 3.2, see spectra below), the normalized intensity of the *rr* triad accounts for 0.463, *i.e.*, P_r = *ca.* 0.68 ($P_m = 1 - P_r = 0.32$). From this experimental value, one can calculate the theoretical value of the triad distribution, and then compare it to the experimental ones.

Table S1. Statistical analysis of the carbonyl resonances of a syndiotactic P3TB (Table , entry HL637) made from integration determined by ^{13}C projection extracted from band-selective HMBC spectrum.

Theoretical values	Experimental values
$(mm) = (m)(m) = 0.102$	$(mm) = (m)(m) = 0.104$
$(rr) = (r)(r) = 0.463$	$(rr) = (r)(r) = 0.463$
$(rm) = (mr) = (m)(r) = 0.217$	$(rm) = (mr) = (m)(r) = 0.216$*

* Average experimental value = [0.247 + 0.185]/2. Bernoulli model triad test, B = $(mm)(rr)/(rm)(mr)$ = 1.03

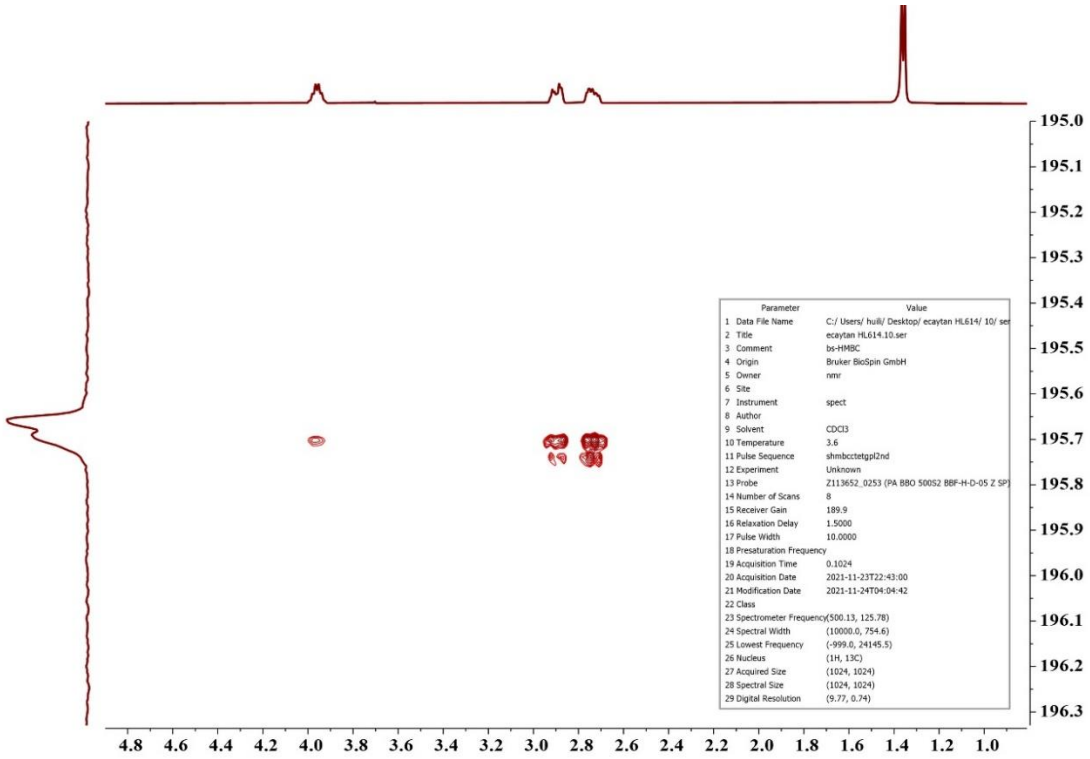

Figure S32. Band-selective HMBC spectrum of a syndiotactic cyclic P3TB (Table , entry HL637). The ^{1}H NMR (500 MHz) spectrum is plotted on the F2 axis and the ^{13}C NMR (125 MHz) spectrum is plotted on the F1 axis.

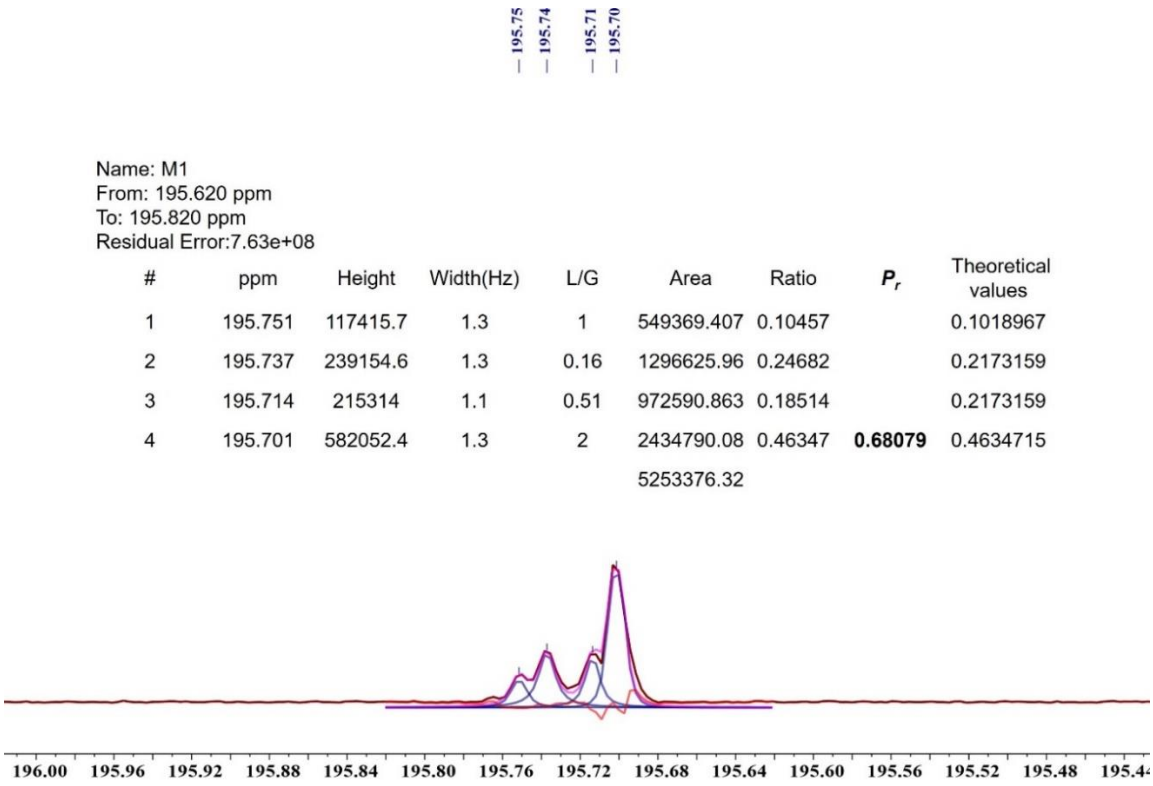

Figure S33. ^{13}C projection extracted from the band-selective HMBC of a syndiotactic cyclic P3TB (Table 3.2, entry HL637) by summing F1 slices between δ ^{1}H 2.60 and 3.00 ppm.

The same deconvolutions-calculations can be performed on the methyl ^{13}C projection extracted from the band-selective HSQC spectrum. For instance, for entry HL637 (Table 3.2, see spectra below), the normalized intensity of the *mm* triad accounts for 0.100, *i.e.*, P_m = *ca.* 0.32 (P_r = 1 – P_m = 0.68). From this experimental value, one can calculate the theoretical value of the triad distribution, and then compare it to the experimental ones (Table S2).

Table S2. Statistical analysis of the methyl resonances of a syndiotactic-enriched P3TB (Table 3.2, entry HL637) made from integration determined by ^{13}C projection extracted from band-selective HSQC spectrum.

Theoretical values	Experimental values
(*mm*) = (*m*)(*m*) = 0.100	(*mm*) = (*m*)(*m*) = 0.100
(*rr*) = (*r*)(*r*) = 0.467	(*rr*) = (*r*)(*r*) = 0.454
(*rm*) = (*mr*) = (*m*)(*r*) = 0.216	(*rm*) = (*mr*) = (*m*)(*r*) = 0.216

Bernoulli model triad test, B = (*mm*)(*rr*)/(*rm*)(*mr*) = 0.97.

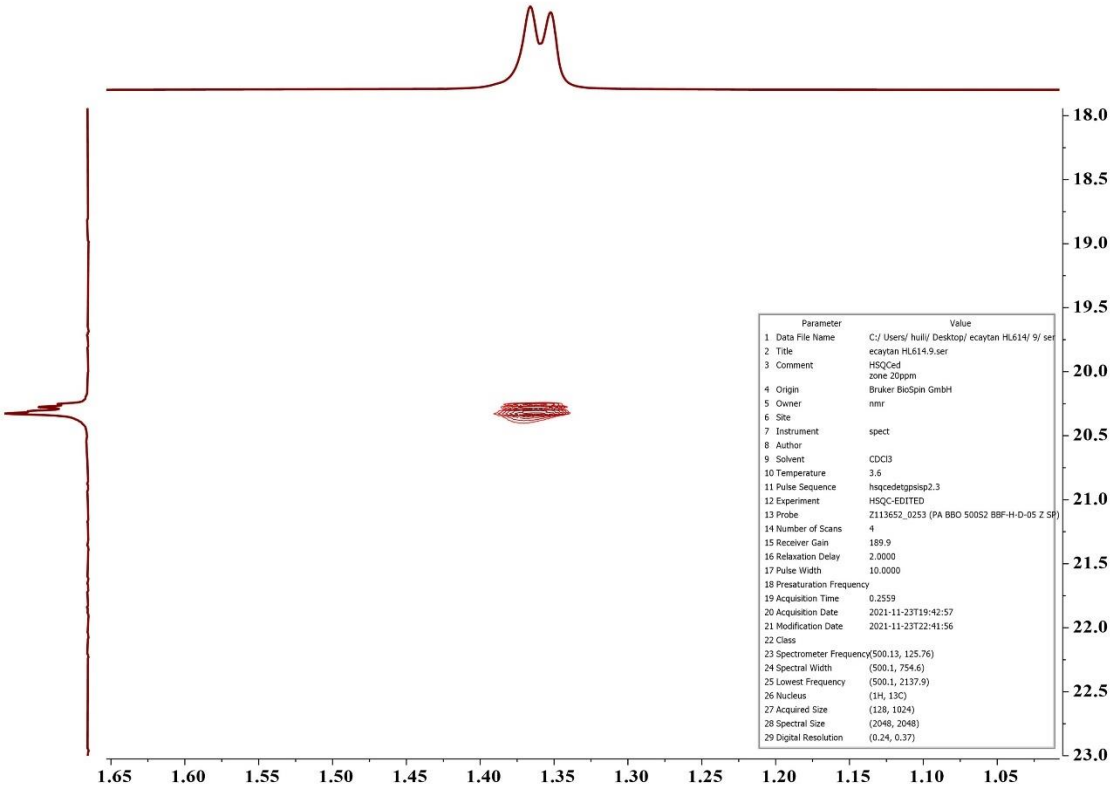

Figure S34. Band-selective HSQC spectrum of a syndiotactic-enriched cyclic P3TB (Table 3.2, entry HL637). The ^{1}H NMR (500 MHz) spectrum is plotted on the F2 axis and the ^{13}C NMR (125 MHz) spectrum is plotted on the F1 axis.

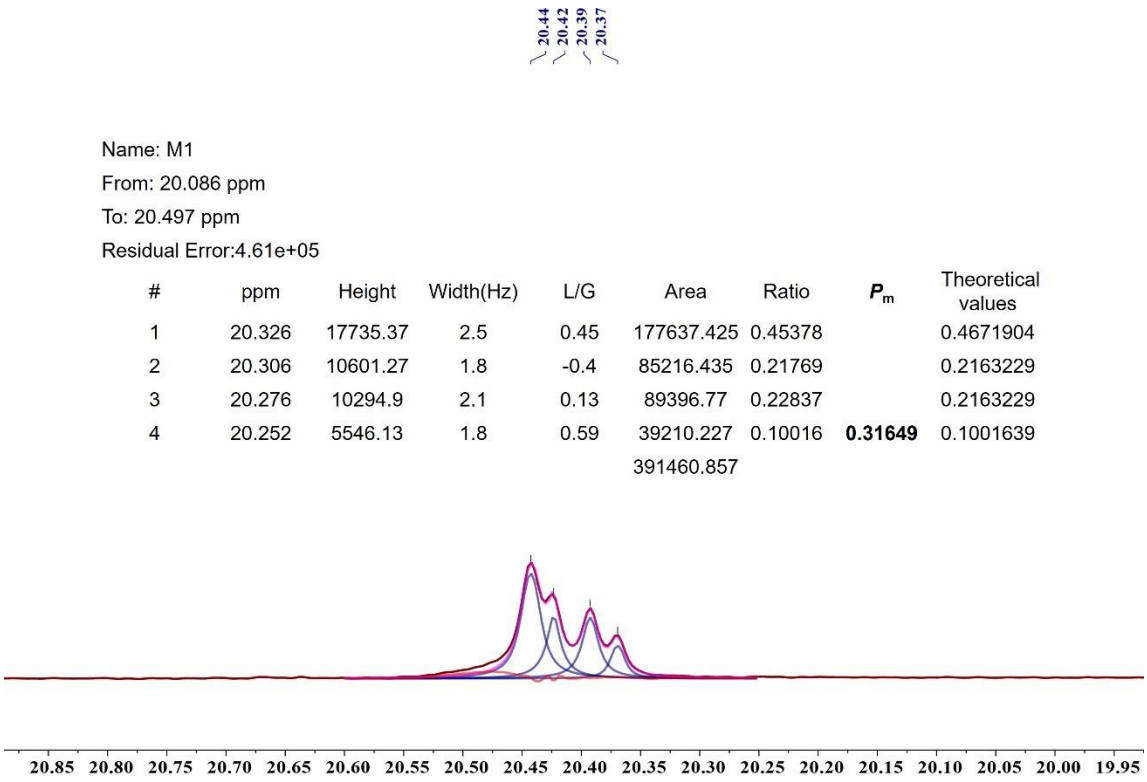

#	ppm	Height	Width(Hz)	L/G	Area	Ratio	P_m	Theoretical values
1	20.326	17735.37	2.5	0.45	177637.425	0.45378		0.4671904
2	20.306	10601.27	1.8	-0.4	85216.435	0.21769		0.2163229
3	20.276	10294.9	2.1	0.13	89396.77	0.22837		0.2163229
4	20.252	5546.13	1.8	0.59	39210.227	0.10016	**0.31649**	0.1001639
					391460.857			

Figure S35. ^{13}C projection extracted from the band-selective HSQC of a syndiotactic-enriched cyclic P3TB (Table 3.2, entry HL637) by summing F1 slices between δ ^{1}H 1.30 and 1.45 ppm.

Propagation Statistics

Table S3. Bernoulli model triad test B = (*mm*)(*rr*)/(*rm*)(*mr*)

Entry	B
Table 3.3, entry HL510 (P_m = 0.89), cat. ***5 g***	1.28
Table 3.3, entry HL406 (P_m = 0.87), cat. ***5 g***	1.77
Table 3.3, entry HL581 (P_m = 0.83), cat. ***5 l***	1.37
Table 3.3, entry HL399 (P_m = 0.73), cat. ***5 g***	1.35
Table 3.3, entry HL592 (P_m = 0.72), cat. ***5 k***	0.53
Table 3.2, entry HL637 (P_m = 0.32), cat. ***5 a***	1.03
Table 3.2, entry HL573 (P_m = 0.32), cat. ***5 a***	0.81
Table 3.3, entry HL397 (P_m = 0.30), cat. ***5 c***	0.84

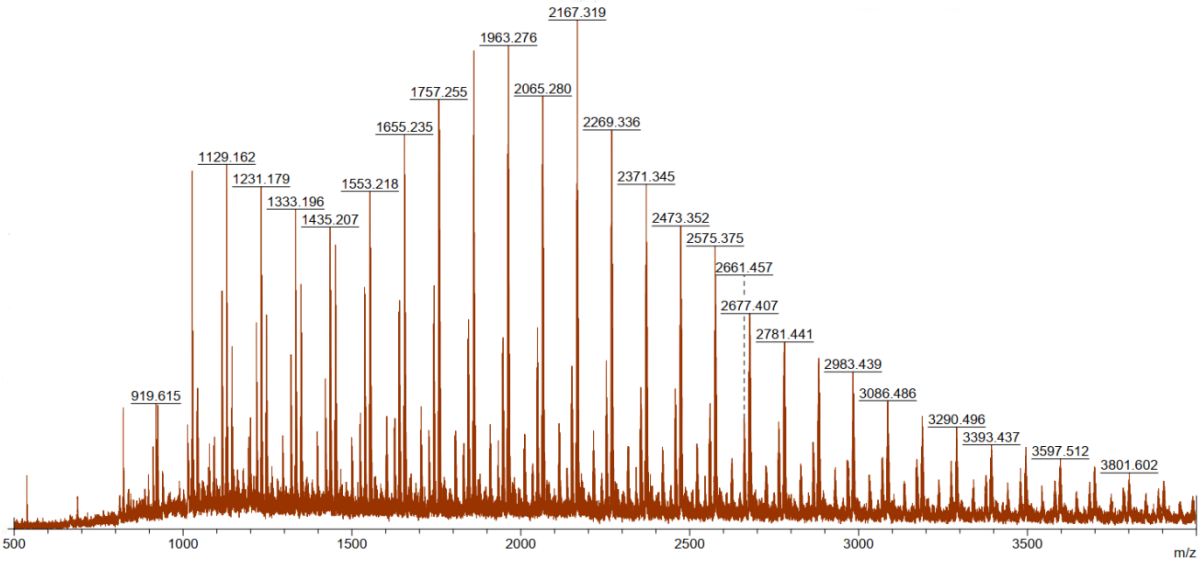

Figure S36. MALDI-ToF mass spectrum of a mixture of several populations of P3TB, produced by the ROP of *rac*-TBL with *t*BuP$_1$ in toluene (Table 4.1, entry HL482).

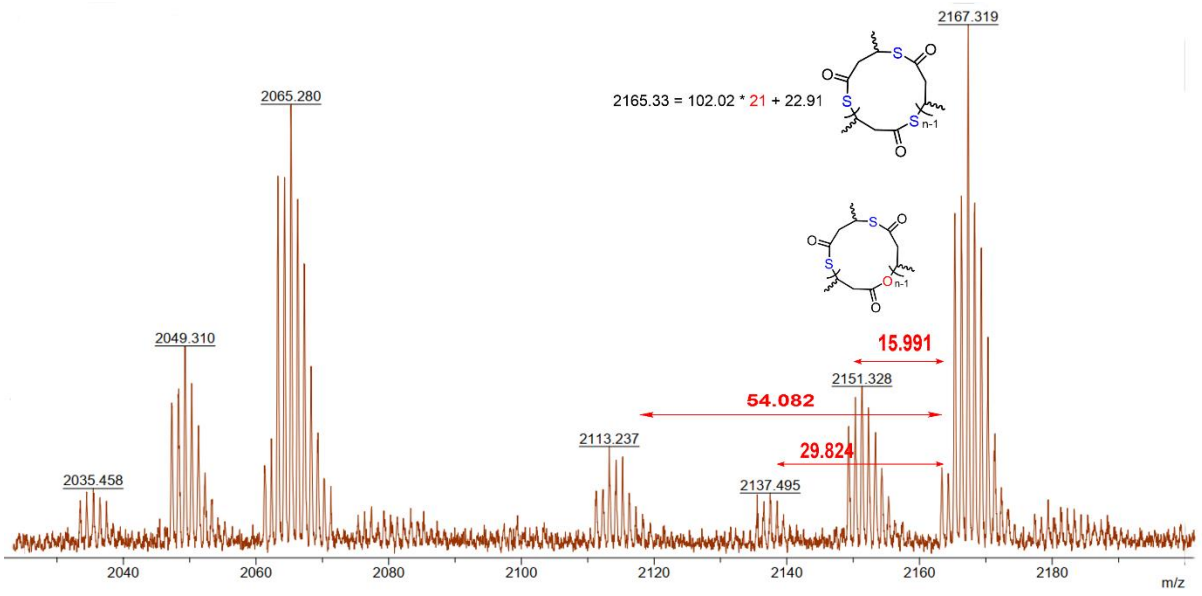

Figure S37. Details of the MALDI-ToF MS spectrum of a mixture of P3TB produced by the ROP of *rac*-TBL with *t*BuP$_1$ in toluene without co-initiator (Table 4.1, entry HL482).

References

[1] G. W. Coates, Precise Control of Polyolefin Stereochemistry Using Single-Site Metal Catalysts. *Chem. Rev.* **2000**, *100*, 1223-1252.

[2] T. M. Ovitt, G. W. Coates, Stereochemistry of Lactide Polymerization with Chiral Catalysts: New Opportunities for Stereocontrol Using Polymer Exchange Mechanisms. *J. Am. Chem. Soc.* **2002**, *124*, 1316-1326.

[3] M. Bouyahyi, N. Ajellal, E. Kirillov, C. M. Thomas, J.-F. Carpentier, Exploring Electronic versus Steric Effects in Stereoselective Ring-Opening Polymerization of Lactide and β-Butyrolactone with Amino-alkoxy-bis(phenolate)-yttrium Complexes. *Chem. Eur. J.* **2011**, *17*, 1872-1883.

[4] F. M. Haque, S. M. Grayson, The Synthesis, Properties and Potential Applications of Cyclic Polymers. *Nat. Chem.* **2020**, *12*, 433-444.

[5] Y. Shi, S.-P. R. Chen, Z. Jia, M. J. Monteiro, Analysis of Cyclic Polymer Purity by Size Exclusion Chromatography: A Model System. *Polym. Chem.* **2020**, *11*, 7354-7361.

[6] D. A. Culkin, W. Jeong, S. Csihony, E. D. Gomez, N. P. Balsara, J. L. Hedrick, R. M. Waymouth, Zwitterionic Polymerization of Lactide to Cyclic Poly(Lactide) by Using N-Heterocyclic Carbene Organocatalysts. *Angew. Chem. Int. Ed.* **2007**, *119*, 2681-2684.

[7] H. Kammiyada, M. Ouchi, M. Sawamoto, A Study on Physical Properties of Cyclic Poly(vinyl ether)s Synthesized via Ring-Expansion Cationic Polymerization. *Macromolecules* **2017**, *50*, 841-848.

[8] J. Wang, Z. Li, R. A. Pérez, A. J. Müller, B. Zhang, S. M. Grayson, W. Hu, Comparing Crystallization Rates Between Linear and Cyclic Poly(epsilon-caprolactones) via Fast-Scan Chip-Calorimeter Measurements. *Polymer* **2015**, *63*, 34-40.

[9] C. W. Bielawski, D. Benitez, R. H. Grubbs, An "Endless" Route to Cyclic Polymers. *Science* **2002**, *297*, 2041-2044.

[10] P. B. Yang, M. G. Davidson, K. J. Edler, S. Brown, Synthesis, Properties, and Applications of Bio-Based Cyclic Aliphatic Polyesters. *Biomacromolecules* **2021**, *22*, 3649-3667.

[11] R. Ligny, M. M. Hanninen, S. M. Guillaume, J.-F. Carpentier, Highly Syndiotactic or Isotactic Polyhydroxyalkanoates by Ligand-Controlled Yttrium-Catalyzed Stereoselective Ring-Opening Polymerization of Functional Racemic β-Lactones. *Angew. Chem. Int. Ed.* **2017**, *56*, 10388-10393.

[12] A. Amgoune, C. M. Thomas, T. Roisnel, J.-F. Carpentier, Ring-Opening Polymerization of Lactide with Group 3 Metal Complexes Supported by Dianionic Alkoxy-Amino-Bisphenolate Ligands: Combining High Activity, Productivity, and Selectivity. *Chem. Eur. J.* **2005**, *12*, 169-179.

[13] J. B. Zhu, E. Y.-X. Chen, Catalyst-Sidearm-Induced Stereoselectivity Switching in Polymerization of a Racemic Lactone for Stereocomplexed Crystalline Polymer with a Circular Life Cycle. *Angew. Chem. Int. Ed.* **2019**, *58*, 1178-1182.

[14] T. Toupance, S. R. Dubberley, N. H. Rees, B. R. Tyrrell, P. Mountford, Zirconium Complexes of Diamine−Bis(phenolate) Ligands: Synthesis, Structures, and Solution Dynamics. *Organometallics* **2002**, *21*, 1367-1382.

[15] R. Anwander, O. Runte, J. Eppinger, G. Gerstberger, E. Herdtweck, M. Spiegler, Synthesis and Structural Characterisation of Rare-Earth Bis(dimethylsilyl)amides and Their Surface Organometallic Chemistry on Mesoporous MCM-41†. *J. Chem. Soc., Dalton Trans.* **1998**, 847-858.

[16] M. Cheng, A. B. Attygalle, E. B. Lobkovsky, G. W. Coates, Single-Site Catalysts for Ring-Opening Polymerization: Synthesis of Heterotactic Poly(lactic acid) from rac-Lactide. *J. Am. Chem. Soc.* **1999**, *121*, 11583-11584.

[17] J. W. Kramer, E. B. Lobkovsky, G. W. Coates, Practical β-Lactone Synthesis: Epoxide Carbonylation at 1 atm. *Org. Lett.* **2006**, *8*, 3709-3712.

Polymérisation Stéréosélective par Ouverture de Cycle de β-Lactones Fonctionnelles: Accès à des Polyhydroxyalcanoates Originaux

De nos jours, les polymères synthétiques jouent un rôle important dans tous les aspects de notre vie quotidienne, mais la majorité de ces polymères dérivés du pétrole/gaz/charbon ne sont pas (bio)dégradables.[1] Ainsi, les polymères (bio)dégradables ont récemment suscité un grand intérêt en tant qu'alternative aux matériaux conventionnels à base de pétrole. Parmi les polymères biodégradables, les poly(hydroxyalcanoates) (PHA), qui combinent les propriétés de barrière aux films des polyesters avec (dans une certaine mesure) les performances mécaniques du polyéthylène et du polypropylène dérivés du pétrole, présentent un intérêt particulier.[2] Parmi la grande variété de PHA, le poly(3-hydroxybutyrate) (P3HB) se distingue. Lorsqu'il est préparé par fermentation de sucres naturels dérivés de la biomasse (par exemple, le saccharose, le glucose) avec des micro-organismes, il s'agit d'un polyester thermoplastique purement (*R*)-isotactique, hautement cristallin, qui ressemble dans une certaine mesure au polypropylène isotactique. Cependant, la température de fusion du (*R*)-P3HB est très proche de sa température de décomposition, ce qui entraîne une dégradation thermique par pyrolyse de l'ester lors du traitement à l'état fondu, rendant ainsi difficile le traitement des produits finaux.

Plusieurs paramètres ont été signalés comme influençant les propriétés thermomécaniques des PHA; l'un des déterminants les plus critiques des propriétés physiques et mécaniques d'un polymère est sa tacticité, c'est-à-dire la régularité des configurations relatives des stéréocentres adjacents le long de la chaîne polymère.[3] Deux structures ordonnées de base peuvent apparaître: les structures isotactiques, dans lesquelles les configurations des stéréocentres voisins sont les mêmes, et les structures syndiotactiques, dans lesquelles les stéréocentres adjacents ont des configurations alternées. Si les groupes *R* de deux stéréocentres successifs sont distribués de manière aléatoire le long de la chaîne polymère, celle-ci est dite atactique (Schéma 1). Les polymères à structure isotactique ou syndiotactique, appelés polymères stéréoréguliers, sont généralement cristallins et présentent des performances thermiques et mécaniques améliorées par rapport à celles des polymères atactiques. Il y a donc un grand intérêt à développer des stratégies qui permettent un contrôle de la masse molaire et de la stéréochimie.[4]

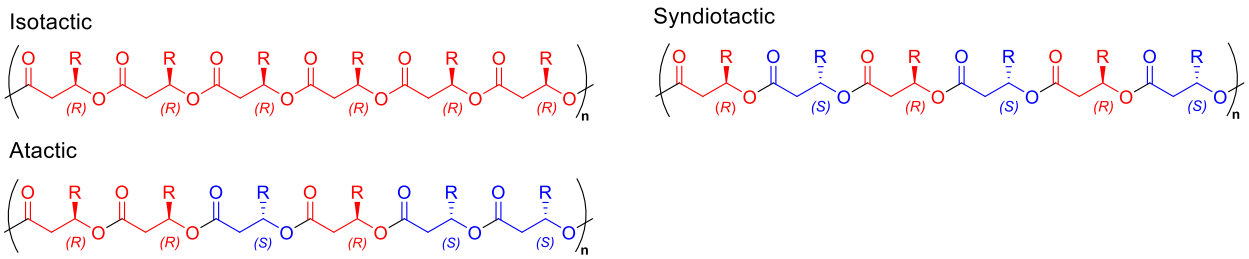

Schéma 1. Tactiques de base des poly(hydroxyalkanoate) (PHA).

L'une des voies de synthèse les plus pratiques et les plus prometteuses pour obtenir un P3HB hautement contrôlé est la polymérisation par ouverture de cycle (ROP) de la β-butyrolactone (BL) ou du diolide correspondant, où le soulagement de la contrainte de cycle est la force motrice de la polymérisation.[2,5] Le (*R*)- ou (*S*)-P3HB hautement isotactique peut être obtenu lorsque le (*R*)- ou (*S*)-BL optiquement pur est utilisé, tandis que l'utilisation d'un mélange racémique de BL peut donner lieu à des matériaux atactiques, isotactiques ou syndiotactiques, selon la nature du catalyseur utilisé (Schéma 2). Les principaux avantages du ROP sont le contrôle fin de la masse molaire, de la dispersion, des groupes terminaux et, le cas échéant, de la stéréosélectivité. Pourtant, relativement peu de catalyseurs/initiateurs permettent le ROP du *rac*-BL, et encore moins abordent la stéréosélectivité.[6]

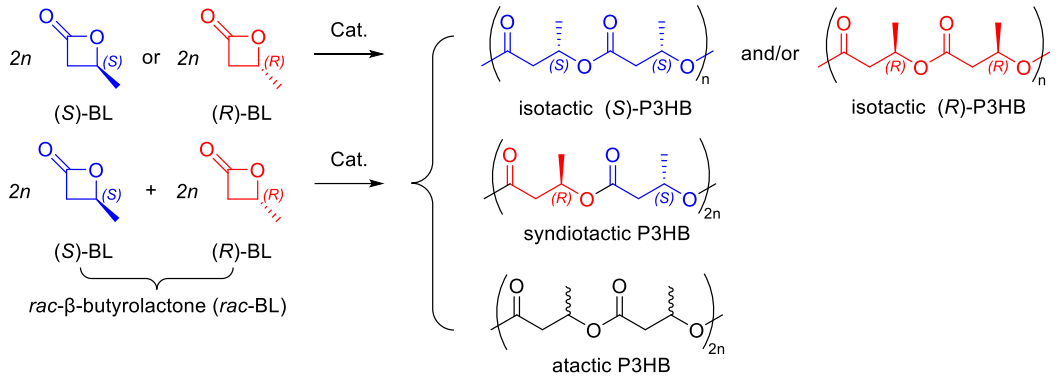

Schéma 2. Stéréoconfigurations possibles du P3HB préparé par ROP de différentes β-butyrolactones.

Notre groupe a rapporté que les catalyseurs à l'yttrium stabilisés par des ligands bis(phénolate) tétradentés $\{ONXO^{R1,R2}\}^{2-}$ (X = O, N) permettent d'accéder à des P3HB hautement syndiotactiques avec des P_r allant jusqu'à 0,96,* à condition que des substituants R^1 volumineux contenant des groupes aryle soient installés en position *ortho* de la plate-forme phénolate. Cette catalyse ROP stéréosélective à base d'yttrium a été étendue aux 4-alkoxycarbonyl-β-propiolactones, (*rac*-MLA^R; R = allyle, benzyle; Schéma 3). De manière assez surprenante, pour cette dernière classe de β-lactones, seuls les catalyseurs à l'yttrium avec un ligand ortho-substitué non encombré, par exemple, R^1 = Me ou Cl, ont permis des polymérisations hautement syndiotactiques (P_r > 0,95). Les catalyseurs avec des R^1 alkyl/aryl *ortho*-substitués encombrés stériquement sur l'ancillaire $\{ONXO^{R1,R2}\}^{2-}$ n'ont permis qu'une modeste syndiosélectivité.

* Dans le ROP des monomères cycliques chiraux, le degré de stéréorégularité est couramment exprimé comme la probabilité d'enchaînement racémique ou méso (probabilité de former une nouvelle diade *racémique* (syndiotactique) ou *méso* (isotactique)), P_r et P_m ($P_m = 1 - P_r$), respectivement. $P_r = P_m = 0{,}50$ décrit un polymère complètement atactique; $P_m = 1{,}00$ (c'est-à-dire $P_r = 0{,}00$) et $P_m = 0{,}00$ (c'est-à-dire $P_r = 1{,}00$) décrivent des polymères parfaitement isotactiques et syndiotactiques, respectivement. Ces paramètres peuvent être calculés à partir des spectres homonucléaires déconvolués de RMN ^{1}H et/ou de RMN ^{13}C quantitatifs.

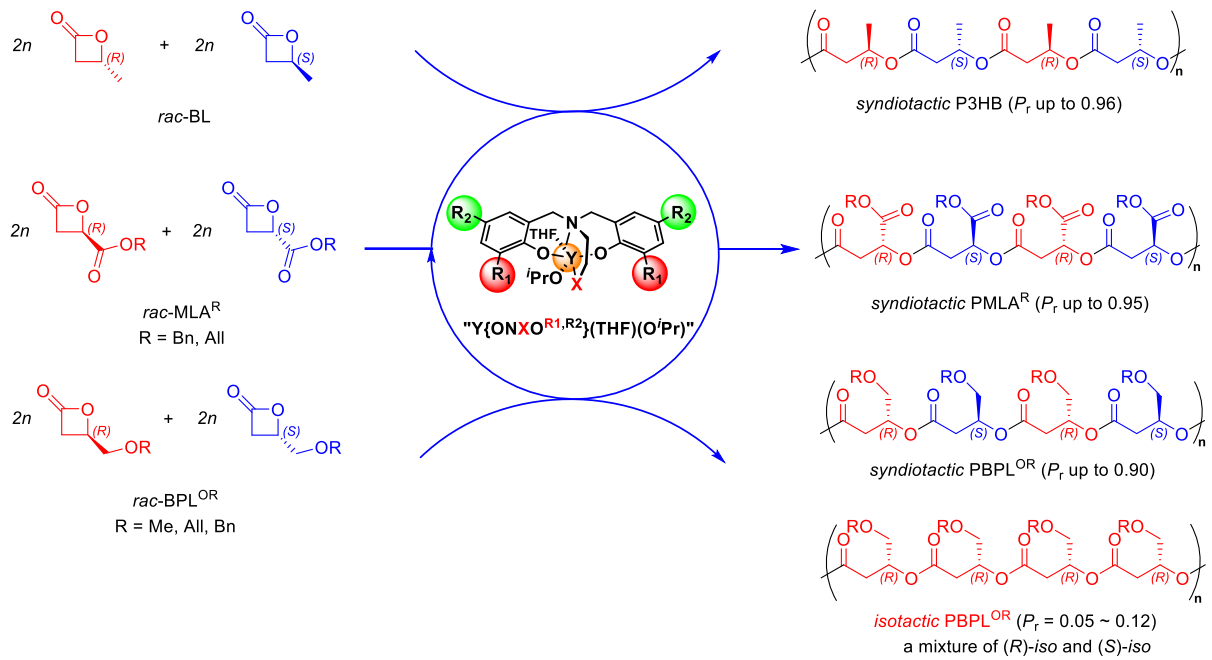

Schéma 3. Polymérisation stéréosélective par ouverture de cycle (ROP) de *rac*-BL et de ses dérivés supérieurs.[7]

En 2017, notre groupe a rapporté la première ROP stéréosélective de *rac*-4-alkoxyméthylène-β-propiolactones (*rac*-BPL^{OR}s) par des complexes d'yttrium, présentant à la fois une excellente activité catalytique et un haut degré de contrôle des masses molaires des PBPL^{OR}s résultants (Schéma 3).[7c] Il a été démontré qu'une simple modification des substituants R^1 et R^2 sur la plate-forme $\{ONXO^{R1,R2}\}^{2-}$ du catalyseur à l'yttrium, induit un changement complet de la polymérisation syndiosélective à la polymérisation isosélective de cette classe spécifique de *rac*-BPL^{OR}s. Plus précisément, le complexe d'yttrium portant un ligand *o,p*-dichloro-substitué a généré des polyesters hautement isotactiques (P_m jusqu'à 0,95), tandis que les complexes avec des ligands substitués par *t*Bu et *cumyl* ont donné des polyesters syndio-enrichis (P_r jusqu'à 0,90). Les calculs DFT ont suggéré que l'origine de l'isosélectivité était liée à de fortes interactions C-H···Cl ("interactions non covalentes") entre l'hydrogène du groupe alcoxyméthylène dans le monomère à cycle ouvert de la chaîne en croissance et les substituants chloro du ligand (Schéma 4).[6a]

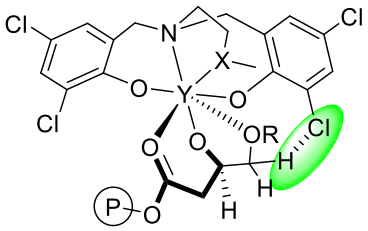

Schéma 4. "Interactions non covalentes" à l'œuvre dans la ROP stéréosélective du *rac*-BPL^{OR}.[7c]

Sur la base des travaux antérieurs de notre laboratoire, nous avons conçu un nouveau type de rac-β-lactone fonctionnelle, à savoir la 4-(2-(benzyloxy)éthyl)oxétan-2-one (*rac*-BPL^{CH2CH2OBn}, Schéma 5), qui diffère "simplement" de l'ancien monomère *rac*-BPL^{OBn} par le remplacement du groupe latéral (exocyclique) du méthylène par une fraction éthylène, ce qui nous a permis d'évaluer l'influence de la longueur du bras sur le processus de ROP catalytique. En effet, il est beaucoup plus probable que cela affecte l'interaction entre le groupe du bras latéral (-CH_2OR) avec le catalyseur.[8]

Project 1: Influence of the Exocyclic Side-Group in the Stereoselective Ring-Opening Polymerization of Functional β-Lactones: ROP of 4-Ethylenylalkoxy vs. Methylenealkoxy-β-Butyrolactones

Le *rac*-BPL^{CH2CH2OBn} et l'énantiopure (*S*)-BPL^{CH2CH2OBn} ont été préparés avec des rendements modérés à partir de la réaction de carbonylation des époxydes correspondants *rac*-, (*S*)-2-[2-(benzyloxy)éthyl]oxirane, initialement préparés à partir de 3-buten-1-ol, respectivement, qui ont été entièrement caractérisés par RMN, MS et analyse HPLC chirale (Schéma 5).

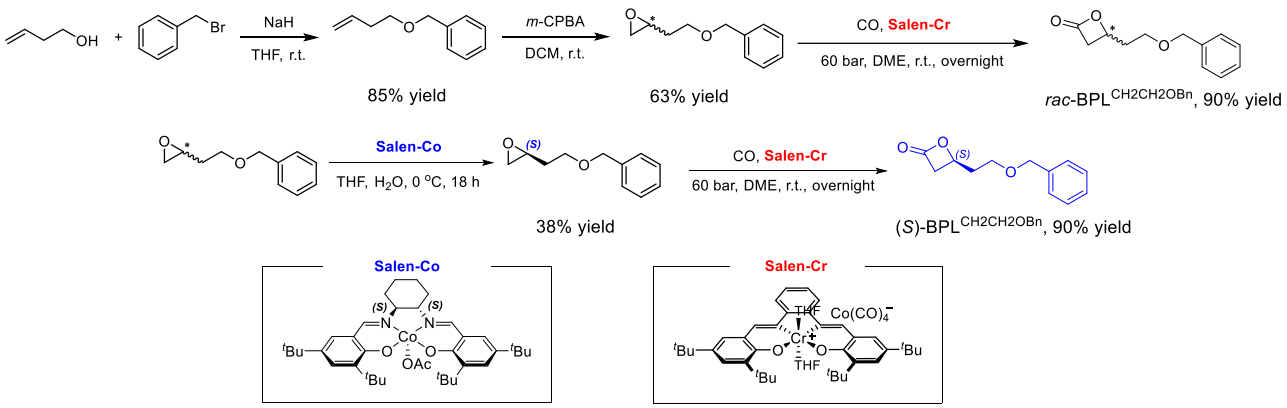

Schéma 5. La voie de synthèse vers *rac*-BPL^{CH2CH2OBn} et (*S*)-BPL^{CH2CH2OBn}.[8]

Par la suite, la *rac*-BPL^{CH2CH2OBn} obtenue a été soumise à une ROP stéréosélective médiée par des complexes d'yttrium (***a-g***) avec 1 équivalent d'*i*PrOH à température ambiante dans le toluène (Schéma 6), qui a été choisie sur la base de nos travaux précédents sur la ROP stéréosélective de la *rac*-BPL^{OBn}, donnant lieu aux polyBPL^{CH2CH2OBn} correspondants bien définis. Les études cinétiques ont révélé que les activités des complexes d'yttrium "encombrés" (TOF ~ 1 000 h^{-1}), tels que ***d***, ***e***, ***f*** et ***g***, sont beaucoup plus actives que celles des complexes "non encombrés" (TOF ~ 1,4 h^{-1}), tels que ***a***, ***b*** et ***c***, quelle que soit la nature du groupe de coiffage (le groupe donneur X pendant). Ceux-ci ont donné des polyBPL^{CH2CH2OBn} bien définis avec une dispersité étroite (typiquement $Đ_M$ = 1,05-1,19) et des valeurs de masse molaire prévisibles (M_n jusqu'à 29 800 g mol^{-1}) dictées par le rapport d'alimentation monomère/initiateur (jusqu'à 150:1:1) ; de plus, les valeurs de M_n ont également montré une relation linéaire avec la conversion des monomères ainsi qu'une

dispersion étroite ($Đ_M$ < 1. 20), tout ceci soutenant le caractère vivant contrôlé de la ROP catalysée par l'yttrium de *rac*-BPL^{CH2CH2OBn}.

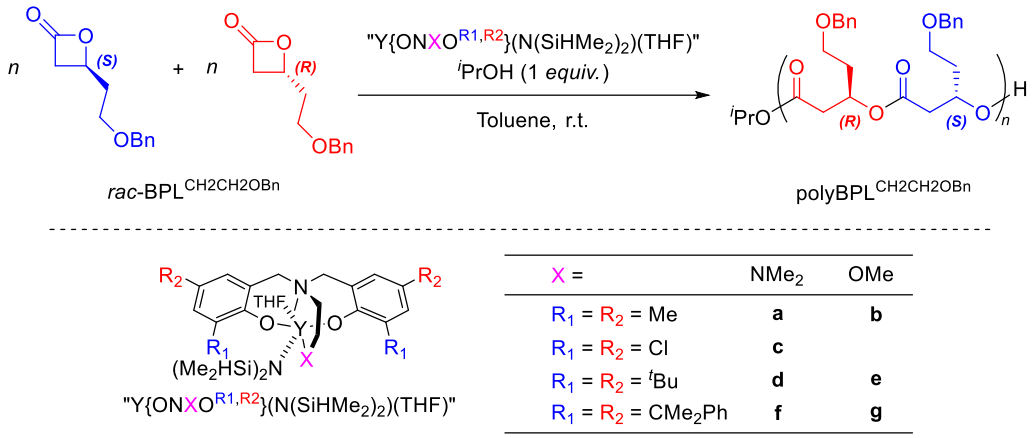

X =	NMe_2	OMe
R_1 = R_2 = Me	**a**	**b**
R_1 = R_2 = Cl	**c**	
R_1 = R_2 = ^{t}Bu	**d**	**e**
R_1 = R_2 = CMe_2Ph	**f**	**g**

Schéma 6. ROP stéréosélective de *rac*-BPL^{CH2CH2OBn} promue par des complexes d'yttrium.[8]

La tacticité des polyBPL^{CH2CH2OBn} récupérés a ensuite été évaluée à partir de l'analyse des spectres RMN ^{13}C (par comparaison avec le spectre correspondant du polyBPL^{CH2CH2OBn} parfaitement isotactique préparé à partir du monomère énantiopur) en relation étroite avec la nature de la charpente du ligand phénolate substitué des complexes d'yttrium (***a***~***g***). En accord avec nos résultats précédents,[7c] les complexes d'yttrium qui portent des substituants R^1, *t*Bu et *cumyl*, très encombrants stériquement sur le ligand et qui se sont avérés si efficaces dans le ROP syndiosélectif de *rac*-BPL^{OBn} (valeur P_r jusqu'à 0,90), n'ont offert que des polyBPL^{CH2CH2OBn} syndio-enrichis (valeur P_r jusqu'à 0,86). De manière inattendue et très frappante, l'utilisation d'un ligand substitué en *ortho*-dichloro en ***c*** a donné des polyBPL^{CH2CH2OBn} atactiques (P_r = 0,49), par rapport aux PBPL^{OBn} isotactiques (P_r = 0,10). La partie éthylène dans le groupe pendant (exocyclique) de *rac*-BPL^{CH2CH2OBn} semble nuire au contrôle stéréologique promu par ***c***. Nous supposons que cela est peut-être dû à une conformation différente dans les interactions monomère/espèce active et/ou à la diminution de l'acidité des méthylènes adjacents à la méthine de la chaîne latérale dans -CH_2CH_2OBn vs. -CH_2OBn, affaiblissant finalement les "interactions non covalentes" et conduisant à la perte du contrôle stéréologique, permettant ainsi d'obtenir un polyBPL^{CH2CH2OBn} atactique.

Il est bien connu que l'introduction d'atomes de soufre dans le squelette des PHA peut conférer aux polythioesters résultants des propriétés thermiques, optiques et mécaniques différenciées, parfois améliorées, élargissant ainsi leur polyvalence et leur utilisation.

Project 2: Stereoregular Cyclic Poly(3-thiobutyrate)s by Ligand-Controlled Yttrium-Catalyzed Stereoselective Ring-Opening Polymerization of Racemic β-Thiolactone

Le poly(3-thiobutyrate) (P3TB), l'analogue thioester de l'omniprésent P3HB, est un homopolymère microbien dont le squelette comporte des liaisons thioester et qui a été isolé pour la première fois il y a vingt ans à partir d'une souche recombinante de E. coli cultivée avec des acides thioalcanoïques.[9] Cette approche de fermentation génère du P3TB avec une masse molaire élevée (M_n = environ 175 kg mol^{-1}) et une dispersité modérément large ($Đ_M$ = 1,9);[9] cependant, la composition, la microstructure (vraisemblablement hautement isotactique) et la performance thermomécanique du P3TB microbien sont difficiles à ajuster. A notre connaissance, la synthèse chimique de polythioesters par ROP de β-thiolactones n'a jusqu'à présent impliqué que des organocatalyseurs et des PTE retournés atactiques, à moins de partir de monomères énantiomériquement purs. Dans ce contexte, nous rapportons ici la synthèse chimique de P3TB avec une tacticité contrôlée et une topologie sans précédent via la ROP stéréosélective de rac-thiobutyrolactone (*rac*-TBL) promue par des complexes à base de métal.[10]

Une variété de catalyseurs/initiateurs à base de métaux bien établis a été étudiée dans la ROP du *rac*-TBL (Schéma 7).[10] Les résultats les plus prometteurs ont été obtenus avec des complexes d'yttrium, "Y{ON(X)O^{R1,R2}}" établis par notre groupe il y a deux décennies.[11] La ROP du *rac*-TBL dans le toluène promue par le complexe **5a**, un complexe prototypique de cette famille flanqué de substituants *t*Bu simples, se déroule très rapidement à température ambiante (TOF > 3,000 h^{-1}). Des études microstructurelles par spectroscopie RMN ^{13}C ont montré que tous les P3TBs formés présentent des microstructures syndio-enrichies (P_m = 0,31-0,37). Les P3TBs également caractérisés par analyse MALDI-ToF MS, ont révélé de manière assez inattendue la formation de polymères purement cycliques. Quel que soit le solvant (toluène ou THF) et la nature du co-initiateur (*i*PrOH, *i*PrSH ou BnSH, 1 équiv. par rapport à Y), les valeurs *m*/*z* expérimentales correspondent aux données isotopiques calculées pour $[C_4H_6SO]_n$.

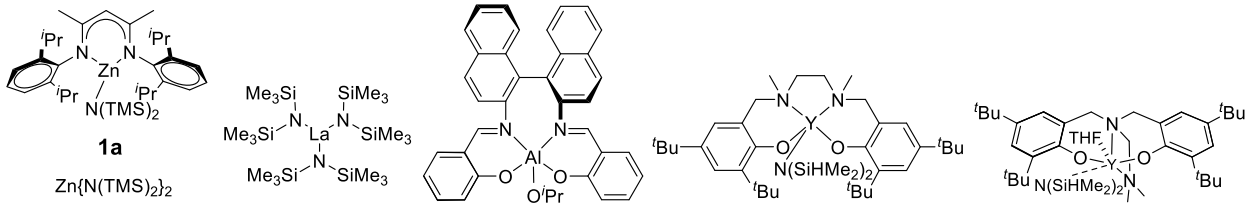

Schéma 7. Structure chimique des catalyseurs/initiateurs utilisés pour le ROP du *rac*-TBL.[10]

Nous supposons que le back-biting se produit dans une large mesure pendant le ROP du *rac*-TBL promu par ces catalyseurs à base d'yttrium. En fait, en raison de la nature dynamique intrinsèquement réactive des liaisons thioester dans la chaîne principale des P3TB, et de la nucléophilie accrue des thiols par rapport aux alcools, la transthioestérification intramoléculaire se produit plus facilement que la

transestérification.[12] Comme illustré dans le Schéma 8, nous avons supposé que les thiolates attachés au centre métallique de l'yttrium attaquent les groupes thioester internes à n'importe quel endroit de la chaîne polymère en croissance, ce qui conduit à la formation de P3TB cycliques et à l'expansion du cycle. Dans ce modèle, des P3TB de masse molaire élevée sont formés, ce qui implique une vitesse de propagation significativement plus rapide que la vitesse de cyclisation (k_p >> k_c, Schéma 8).

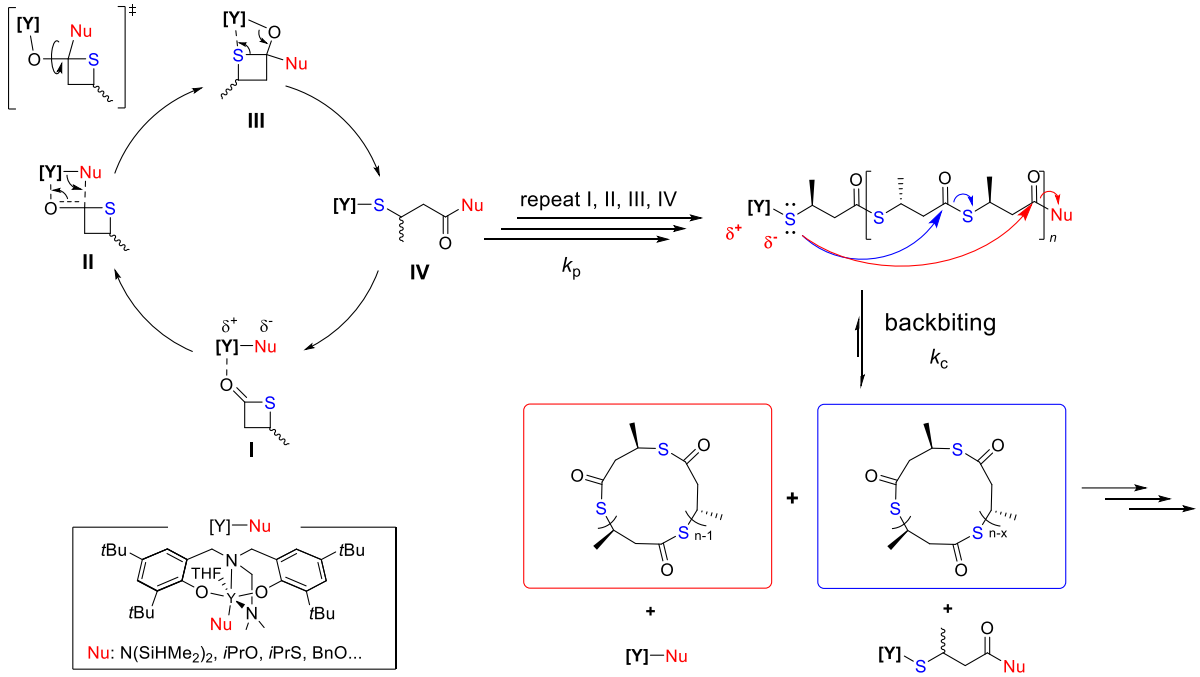

Schéma 8. Mécanisme proposé pour le ROP du *rac*-TBL promu par le complexe **5a** avec les étapes d'initiation, de propagation, de retour en arrière et d'expansion du cycle.[10]

La caractéristique la plus unique et la plus précieuse des complexes "Y{ON(X)O^{R1,R2}}" est leur capacité à ajuster finement le contrôle stéréoscopique de la ROP des esters cycliques.[6,13] Ceci peut être fait en changeant simplement la nature des substituants R^1, R^2 sur les moitiés phénolate et en manipulant le bras latéral du ligand (c'est-à-dire le groupe donneur X pendant) (Schéma 9). Ce réglage a permis d'accéder à des P3TB avec des niveaux de tacticité très différents, avec des valeurs de P_m comprises entre 0,30 et 0,90. Les complexes d'yttrium avec des ligands modérément volumineux substitués par un *tert*-butyle ou un *cumyle* donnent des P3TB syndiotactiques, ce qui est en accord avec les travaux précédents sur le *rac*-BL parent et les dérivés apparentés.[6a] De manière inattendue, le système catalytique avec le ligand substitué par un *trityle* significativement plus grand a donné des P3TB enrichis en isotactique (P_m = 0,58 à température ambiante, P_m = 0,83 à -80°C). De manière plus inattendue, les catalyseurs portant les plus petits substituants sur le ligand ont également permis d'accéder au P3TB isotactique. Ainsi, les simples catalyseurs

substitués par un diméthyle ou un dichloro "non encombré " ont offert un P3TB hautement isotactique lors de l'exécution du ROP dans le THF à basse température (P_m jusqu'à 0,90).

Les polymères cycliques sont une classe spéciale de macromolécules ; en raison des contraintes de la topologie cyclique et de l'absence d'extrémités de chaîne, les propriétés de ces macromolécules diffèrent de celles de leurs homologues linéaires ; par exemple, elles présentent généralement une densité plus élevée, une température de transition vitreuse et un point de fusion plus élevés, une viscosité intrinsèque plus faible, un taux de cristallisation plus élevé.[14] A cet égard, le P3TB linéaire avec une masse molaire élevée est hautement souhaité, les propriétés thermomécaniques de celui-ci seront comparées à celles du P3TB cyclique préparé ci-dessus.

Project 3: Preliminary Attempts on Organomediated Ring-Opening Polymerization of *rac*-Thiobutyrolactone

Étant donné que divers catalyseurs/initiateurs à base de métaux bien établis ont donné des P3TB mal définis ou cycliques dans les travaux précédents,[10] nous nous tournons vers l'organocatalyse. La plupart des organocatalyseurs sont tolérants à l'eau et à l'air, donnant des polymères exempts de contaminants métalliques résiduels, qui sont devenus des alternatives attrayantes aux catalyseurs organométalliques, comme les applications électroniques. Une variété de bases organiques, telles que le 8-diazabicyclo(5.4.0)undec-7-ène (DBU), la 4-diméthylaminopyridine (DMAP), la triéthylamine (TEA), le 1,5,7-triazabicyclo[4.4.0]dec-5-ène (TBD), et les bases phosphazènes, ont été criblées pour le ROP du *rac*-TBL, mais toutes ont conduit à des P3TB atactiques. Parmi eux, le *t*Bu-P4, avec ou sans coinitiateur protique, était l'initiateur le plus actif pour la polymérisation du rac-TBL (TOF > 5,5 h^{-1}, Schéma 7). De plus, une augmentation du ratio monomère/amorceur a conduit à des P3TBs linéaires avec une augmentation monotone de leurs masses molaires. Cependant, le mécanisme de la formation des P3TBs linéaires, en particulier l'étape d'initiation, n'a pas été établi.

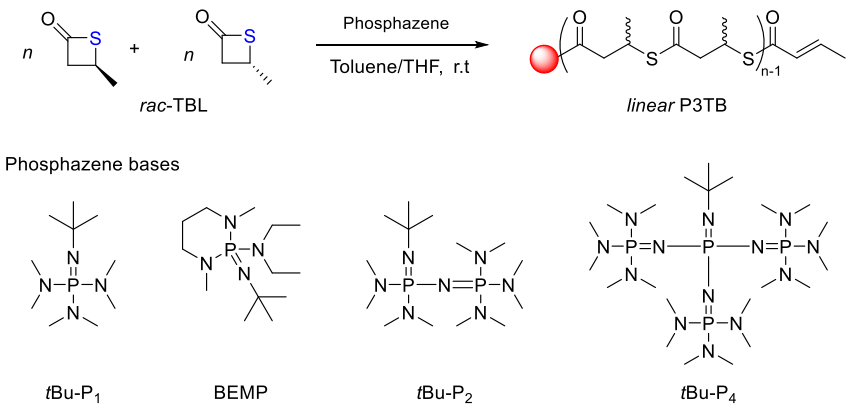

Schéma 7. ROP organocatalysé de *rac*-TBL vers des P3TBs linéaires.

References

[1] (a) C. Jehanno, J. W. Alty, M. Roosen, S. De Meester, A. P. Dove *et al.*, *Nature* **2022,** *603*, 803-814; (b) F. M. Haque, J. S. A. Ishibashi, C. A. L. Lidston, H. Shao, F. S. Bates *et al.*, *Chem. Rev.* **2022,** *122*, 6322-6373.

[2] L. R. Rieth, D. R. Moore, E. B. Lobkovsky, G. W. Coates, *J. Am. Chem. Soc.* **2002,** *124*, 15239-15248.

[3] J. Fang, M. J. L. Tschan, T. Roisnel, X. Trivelli, R. M. Gauvin *et al.*, *Polym. Chem.* **2013,** *4*, 360-367.

[4] Q. Feng, L. Yang, Y. Zhong, D. Guo, G. Liu *et al.*, *Nat. Commun.* **2018,** *9*, 1559.

[5] (a) X. Tang, A. H. Westlie, E. M. Watson, E. Y.-X. Chen, *Science* **2019,** *366*, 754-758; (b) X. Tang, E. Y.-X. Chen, *Nat. Commun.* **2018,** *9*, 2345; (c) X. Tang, A. H. Westlie, L. Caporaso, L. Cavallo, L. Falivene *et al.*, *Angew. Chem. Int. Ed.* **2020,** *59*, 7881-7890.

[6] (a) R. Ligny, M. M. Hanninen, S. M. Guillaume, J.-F. Carpentier, *Chem. Commun.* **2018,** *54*, 8024-8031; (b) H. Li, R. M. Shakaroun, S. M. Guillaume, J.-F. Carpentier, *Chem. Eur. J.* **2020,** *26*, 128-138.

[7] (a) A. Amgoune, C. M. Thomas, S. Ilinca, T. Roisnel, J.-F. Carpentier, *Angew. Chem. Int. Ed.* **2006,** *45*, 2782-2784; (b) C. G. Jaffredo, Y. Chapurina, S. M. Guillaume, J.-F. Carpentier, *Angew. Chem. Int. Ed.* **2014,** *53*, 2687-2691; (c) R. Ligny, M. M. Hanninen, S. M. Guillaume, J.-F. Carpentier, *Angew. Chem. Int. Ed.* **2017,** *56*, 10388-10393.

[8] R. M. Shakaroun, H. Li, P. Jéhan, M. Blot, A. Alaaeddine *et al.*, *Polym. Chem.* **2021,** *12*, 4022-4034.

[9] T. Lutke-Eversloh, A. Fischer, U. Remminghorst, J. Kawada, R. H. Marchessault *et al.*, *Nat. Mater.* **2002,** *1*, 236-240.

[10] H. Li, J. Ollivier, S. M. Guillaume, J.-F. Carpentier, *Angew. Chem. Int. Ed.* **2022,** *61*, e202202386.

[11] (a) C.-X. Cai, L. Toupet, C. W. Lehmann, J.-F. Carpentier, *J. Organomet. Chem.* **2003,** *683*, 131-136; (b) C. X. Cai, A. Amgoune, C. W. Lehmann, J.-F. Carpentier, *Chem. Commun.* **2004**, 330-331; (c) A. Amgoune, C. M. Thomas, T. Roisnel, J.-F. Carpentier, *Chem. Eur. J.* **2005,** *12*, 169-179.

[12] S. Aksakal, R. Aksakal, C. R. Becer, *Polym. Chem.* **2018,** *9*, 4507-4516.

[13] J. S. Klitzke, T. Roisnel, E. Kirillov, O. d. L. Casagrande, J.-F. Carpentier, *Organometallics* **2013,** *33*, 309-321.

[14] (a) P. B. Yang, M. G. Davidson, K. J. Edler, S. Brown, *Biomacromolecules* **2021,** *22*, 3649-3667; (b) F. M. Haque, S. M. Grayson, *Nat. Chem.* **2020,** *12*, 433-444.